

Studies on the Synthesis of Marine Natural Product (-)-Zampanolide and its Analogues

By

Jingjing Wang

*A thesis submitted to Victoria University of Wellington in
fulfilment of the requirements for the degree of
Doctor of Philosophy*



School of Chemical and Physical Sciences

2016

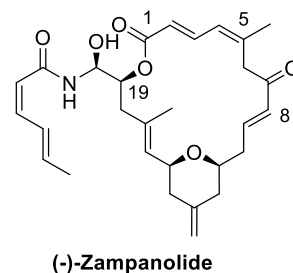
Dedicated to my dear husband and best friend,

Marcus Sheerin

for your love and support

Abstract

(-)-Zampanolide is a microtubule-stabilising marine natural product, with promise as a cancer drug candidate. The potential therapeutic application of zampanolide has fuelled worldwide interest in its total synthesis, but few analogue studies have been reported. Analogues afford the possibility of examining the structure-activity relationships with a view to optimising for potency and medicinal viability. This project seeks to devise a new route to zampanolide and generate a series of analogues for bioactivity evaluation.



The initial approach to zampanolide and a number of designed analogues was through disconnections at C20 by an *N*-aldol reaction, at C1 by Yamaguchi esterification, at C8-C9 by metathesis and at C15-C16 by alkynylation. During the development of fragment syntheses, problems were encountered with protection of the secondary hydroxyl group at C19 and establishment of an aldehyde at C15. Useful natural and analogue fragments were generated during this exploratory phase.

The order of connections was revised, and effort has been put towards the improvement of the synthetic efficiency. A three-component reaction involving (triphenylphosphoranylidene)-ketene, also known as Bestmann ylide, as a linchpin was envisaged to provide the dienolate of zampanolide. This is an expanded application of Bestmann ylide and therefore the scope of this linchpin reaction was investigated using simple alcohols and aldehydes. Success in the scoping study fortified this approach, and the coupling of the C3-C8 and C16-C20 fragments of zampanolide proceeded with good yields and stereoselectivity of the *E,Z*-geometry.

The planned late stage connections were tested on model substrates. The side arm attachment by a chiral boron reagent-promoted aza-aldol reaction failed to produce desired product on a simple model. However, model substrates that better account for the functionality of the zampanolide macrocycle are proposed for subsequent studies. In case these also do not succeed,

reliable alternative methods described in the literature would be used. Several methods were scanned for the asymmetric alkynylation required for the C15-C16 bond connection. That involving ProPhenol and diethylzinc produced an excellent yield with a model alkyne. Although the stereoselectivity of the alkynylation is yet to be optimized, it was also tested on the full zampanolide fragment generated from the Bestmann ylide reaction. A small amount of the desired product was isolated, establishing 16 out of the 18 carbons of the macrocycle. Formation of a macrocycle is close at hand.

Acknowledgements

Doing a PhD is one of the best decisions I have made in my life. I enjoyed the highs and the lows of research, and the tricky balance of life and work. During it, the awesome people I have met made this journey of PhD so much more exciting, memorable and fulfilling.

First, I want to give my greatest thanks to my primary supervisor Dr. Joanne Harvey for the guidance and support through the years. There is never a day I remembered Joanne with a low spirit. Her enthusiastic attitude is captivating, and helped me to stay optimistic and motivated, especially when things were not going smooth. Her extensive knowledge on organic chemistry guided me to find solutions in research. Additionally, thanks to Joanne's in-depth editing and comments, it has helped me to improve my writing skill. Joanne not only helped me to learn so much more organic chemistry, but also has been a role model that I can look up to.

I would also like to thank my secondary supervisor Dr. Paul Teesdale-Spittle for his help. I am so fortunate to have worked in such a great research group. We shared knowledge to solve problems, joy for success and great times outside the lab. These are treasured memories. I would like to thank the past and current group members: Sophie Geyrhofer, Thomas Bevan, Sam Ting, Dr. Kalpani Somarathne, Dr. Hemi Cumming, Dr. Mark Bartlett, Peter Moore, Amira Brackovic, Loïc Lassueur, Sarah Brown, Ben Durrant, Dan Phipps, Chris Orme, José Pinedo Rivera, Claire Turner, Dylan Davies, Scott Riordan, Jasmin Riesterer. I especially thank Sophie Geyrhofer, Peter Moore, Chris Hasenöhrl and Chris Orme for proof-reading, Claudia Gray and Sam Ting for all the preliminary work, and Sophie Geyrhofer again for running all my MS samples this years and carrying on the zampanolide project.

The School of Chemical and Physical Sciences at Victoria University of Wellington has been a great place to work, and I would like to thank everybody for the amazing experience I had. In particular, Ian Vorster and Rob Keyzers often helped me with NMR and MS. I do apologise for all the weekend emails and after-hour calls to Ian for NMR problems. I also thank Teresa

Gen for letting me borrow solvents when the chemical store was closed, and Peter Northcote for useful comments on purification and spectroscopic data. I am extremely grateful for the PhD scholarship from New Zealand Health Research Council, travel and conference grants from VUW, New Zealand Institute of Chemistry, Centre of Biodiscovery, and the thesis submission scholarship from Faculty of Graduate Research. Without the financial support this thesis would not be possible.

Friends and family have also given me huge support. The person deserves the biggest thank you is my husband Marcus Sheerin. He has been taking such good care of me, so that I could concentrate on my work. Without his love and support, especially all the delicious lunches and dinners he cooked for me, I would not have achieved nearly as much or stayed healthy during the time of thesis writing. Sharing a life with Marcus is the best thing in my life. I also want to thank Marcus' bosses Rob, Mike and Fay for arranging Marcus to work from home, so that we could be together in Wellington. My parents and Marcus's family have given us great help. Marcus and I got married during my PhD. Thanks to everybody in Marcus' family, especially Rowene, Brian, David, Alana, Nat and Sharolyn, our wedding was perfect, and I would not have wanted anything different.

Fourteen years ago, my parents Zhigang and Huixia made the decision to use their lifesavings to send me to New Zealand for better education. Because of this decision, I had the chance to experience this very exciting life in New Zealand: finding a passion for chemistry and mountains, meeting Marcus, making lifetime friends and so much more. This achievement is not mine alone, but builds on the years of care, support and guidance from my parents.

Table of contents

Abstract	i
Acknowledgements	iii
List of contents	v
Abbreviations	ix
Chapter 1: Introduction	1
1.1 A brief history of marine natural products	1
1.2 Microtubule-targeting agents and paclitaxel	2
1.3 (-)-Zampanolide and (+)-dactylolide	7
1.4 Published total synthesis of zampanolide	10
1.4.1 Synthetic methods for formation of the pyran fragment	12
1.4.2 Synthetic methods of macrocyclization	15
1.4.3 Synthesis of <i>N</i> -acyl hemiaminal linkage	16
1.5 Published total synthesis of dactylolide	18
1.5.1 Synthetic methods for formation of the pyran fragment	19
1.5.2 Other methods for the formation of dactylolide macrocycle	21
1.6 Analogue studies	23
1.7 Efficiency of total synthesis: linchpin synthesis	26
1.8 References	32
Chapter 2: Aim and preliminary work	37
2.1 Aim	37
2.2 Preliminary work	38

2.2.1 Preliminary work on side-arm variants	38
2.2.2 Preliminary work on fragment synthesis	40
2.3 References	43
Chapter 3: First generation and fragment synthesis	45
3.1 Retrosynthetic analysis	45
3.2 Proposed synthesis of C1-C8 fragment	47
3.2.1 Synthesis of the natural C1-C8 fragment	48
3.2.2 Synthesis of the des-methyl C1-C8 analogue fragment	52
3.3 Synthesis of C16–C20 fragment	57
3.4 Proposed synthesis of C9-C15 fragment	63
3.4.1 Synthesis of the natural C9-C15 fragment	64
3.4.2 Synthesis of C9-C15 analogue fragments	68
3.5 Experimental data	74
3.6 References	92
Chapter 4: Second generation synthesis and Bestmann ylide linchpin	97
4.1 Second generation retrosynthetic analysis	97
4.2 Bestmann ylide	98
4.3 Scope of the Bestmann ylide cascade in the synthesis of $\alpha,\beta,\gamma,\delta$ -unsaturated esters	102
4.4 Applying the Bestmann ylide linchpin to macrocycle fragments	107
4.5 Experimental data	113
4.6 References	129

Chapter 5: Exploration of late-stage connections	131
5.1 Formation of <i>N</i> -acyl hemiaminal	131
5.2 Model study of C20 oxidation	141
5.3 Asymmetric alkynylation of aldehydes for C15-C16 connection	142
5.4 Summary	156
5.5 Experimental data	157
5.6 References	169
Chapter 6: Summary and Future work	173
6.1 Alternatives to the acrolein-dependent C3-C8 fragment	174
6.2 A new strategy involving a dithiane at C15	175
6.3 References	177
Appendix: NMR spectra	179

Abbreviations

(S)-TRIP	(S)-3,3'-Bis(2,4,6-triisopropylphenyl)-1,1'-binaphthyl-2,2'-diyl hydrogenphosphate
Ac	Acetic
Ad	Adamantyl
aq.	Aqueous
Asn	Asparagine
ATR	Attenuated total reflectance
BAIB	1,1-Diacetateiodobenzene
BINOL	1,1'-Bi-2-naphthol
Bn	Benzyl
Boc ₂ O	Di- <i>tert</i> -butyl dicarbonate
BSA	<i>N,O</i> -Bis(trimethylsilyl)acetamide
Bz	Bezoyl
CIGAR	Constant time inverse-detection gradient accordion rescaled
COSY	Correlation spectroscopy
Cp	1,3-Cyclopentadiene
CSA	Camphorsulphonic acid
DBU	1,8-Diazabicycloundec-7-ene
DCE	1,2-Dichloroethane
DCM	Dichloromethane
DDQ	2,3-Dichloro-5,6-dicyano-1,4-benzoquinone
DIBAL-H	Di- <i>iso</i> -butylaluminum hydride
DIP-chloride	Chlorodiisopinocampheylborane
DMAP	4-(<i>N,N</i> -Dimethylamino)pyridine
DME	1,2-dimethoxyethane
DMF	Dimethylformamide
DMP	Dess-Martin periodinane
DMSO	Dimethyl sulfoxide
EDCI	<i>N</i> -(3-Dimethylaminopropyl)- <i>N'</i> -ethylcarbodiimide hydrochloride
ee	Enantiomeric excess
Et	Ethyl
FCC	Flash column chromatography
FT-IR	Fourier transform infrared spectroscopy
GI	Growth inhibition concentration
Grubbs II	Grubbs 2nd generation catalyst
HBTU	<i>O</i> -(Benzotriazol-1-yl)- <i>N,N,N',N'</i> -tetramethyluronium hexafluorophosphate
His	Histidine
HMBC	Heteronuclear multiple-bond correlation
HRMS	High resolution mass spectrometry
HSQC	Heteronuclear single quantum coherence spectroscopy

HWE	Horner-Wadsworth-Emmons
IBX	2-Iodoxybenzoic acid
IC ₅₀	Half maximal inhibitory concentration
Imid.	Imidazole
LiHMDS	Lithium bis(trimethylsilyl)amide
MDA	Microtubule-destabilizing agents
Me	Methyl
MIDA	<i>N</i> -Methyliminodiacetic acid
MOM	Methoxymethyl
MRP	Multidrug resistance-associated proteins
MS	Molecular sieve
MSA	Microtubule-stabilizing agents
MTA	Microtubule-targeting agent
MTPA	α -Methoxy- α -trifluoromethylphenylacetic acid
MTT	3-(4,5-Dimethylthiazol-2-yl)-2,5-diphenyltetrazolium bromide
NaHMDS	Sodium bis(trimethylsilyl)amide
NHC	<i>N</i> -Heterocyclic carbene
NMR	Nuclear magnetic resonance
NOESY	Nuclear Overhauser effect spectroscopy
ox.	Oxidation
PCC	Pyridinium chlorochromate
PG	Protecting group
Piv	Pivaloyl
PMB	<i>para</i> -Methoxybenzyl
PMP	<i>para</i> -Methoxyphenyl
PPTS	Pyridinium <i>p</i> -toluenesulfonate
ProPhenol	2,6-Bis[2-(hydroxydiphenylmethyl)-1-pyrrolidinyl-methyl]-4-methylphenol
Py	Pyridine
r.t.	Room temperature
RCM	Ring-closing metathesis
ROESY	Rotating frame Overhauser effect spectroscopy
SAR	Structure-activity relationship
TBAF	Tetra- <i>n</i> -butylammonium fluoride
TBAI	Tetra- <i>n</i> -butylammonium iodide
TBDPS	<i>tert</i> -Butyldiphenylsilyl
TBHP	<i>tert</i> -Butyl hydroperoxide
TBS	<i>tert</i> -Butyldimethylsilyl
TCBC	2,4,6-Trichlorobenzoylchloride
TEMPO	2,2,6,6-Tetramethyl-1-piperidinyloxy free radical
TEOC	Trimethylsilylethylcarboxy
TES	Triethylsilyl
Tf	triflate
TFA	Trifluoroacetic acid
TfO	Triflic

THF	Tetrahydrofuran
TLC	Thin layer chromatography
TMEDA	Tetramethylethylenediamine
TMS	Trimethylsilyl
TPPO	Triphenylphosphine oxide
XTT	2,3-Bis-(2-methoxy-4-nitro-5-sulfophenyl)-2H-tetrazolium-5-carboxanilide

Chapter 1: Introduction

1.1 A brief history of marine natural products

Historically, natural products have played an important role in drug development. From the herbal medicines used in ancient times and traditional medicines to industrially produced pharmaceuticals in modern days, nature has provided us with a rich mine of potential drugs with enormous diversity in structure and biochemical activities. The boom of marine natural product chemistry came with the invention of SCUBA. Prior to SCUBA, only shallow water species had been accessible. Isolation of natural products from marine organisms has proven to be a great source of pharmaceuticals. The first isolated marine products were the nucleosides spongothymidine (**1**) and spongouridine (**2**), discovered in 1951 (**Figure 1.1**).¹ Since then, the field of marine natural products has attracted increasing attention, resulting in the discovery of a vast number of marine products, that could be used in fighting numerous diverse illnesses, for example fungal infections, tumour growth, cancer and Alzheimer's disease.

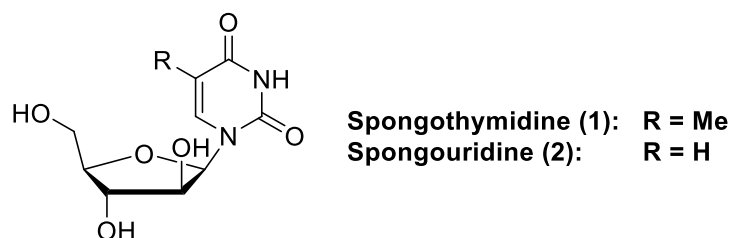


Figure 1.1: Structure of spongothymidine (**1**) and spongouridine (**2**).

Marine natural products are commonly secondary metabolites, which evolved for the natural defence of the organisms. Unlike vertebrates, marine sponges, corals and algae are sessile, meaning they don't have mobility; they also generally don't have external fighting facilities to defend themselves. Their defence is totally chemical and thus dependent on these secondary metabolites. The nature of their defence system determines that these metabolites have to be potent in order to be effective because, once released, they are diluted instantly by sea water. One example of current medicines that are derived from marine organisms is the breast cancer drug eribulin (**3**) (**Figure 1.2**). It is the simplified and

optimized analogue of halichondrin B (**4**), which was isolated from the marine sponge, *Halichondria okadai*.²

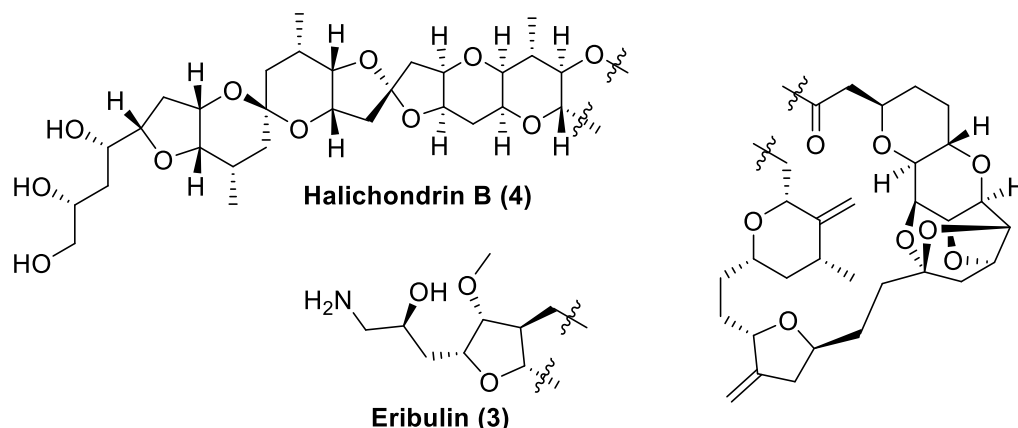


Figure 1.2: Structures of eribulin (**3**) and halichondrin B (**4**).

1.2 Microtubule-targeting agents and paclitaxel

Eribulin (**3**) is an example of the microtubule-targeting agents (MTAs), a group of largely nature-derived drugs or candidates that affect cell function by influencing the microtubules. They have been identified as good candidates for cancer treatment, and a number of such anti-cancer drugs are already in regular clinical use, such as vinorelbine (**5**), estramustine (**6**) and ixabepilone (**7**) (**Figure 1.3**).³ This success can be attributed to the important roles that microtubules play in cells, especially in proliferation and growth regulation. The first MTAs discovered were the vinca alkaloids.⁴ Their effect on microtubules was observed as the development of honeycomb-shaped crystals under the electron microscope, which were identified as abnormally large tubules resulting from the binding of vinca alkaloids. Since then a large number of such natural products have been reported, and enormous effort has been put towards better understanding of these compounds and their effects on microtubules.

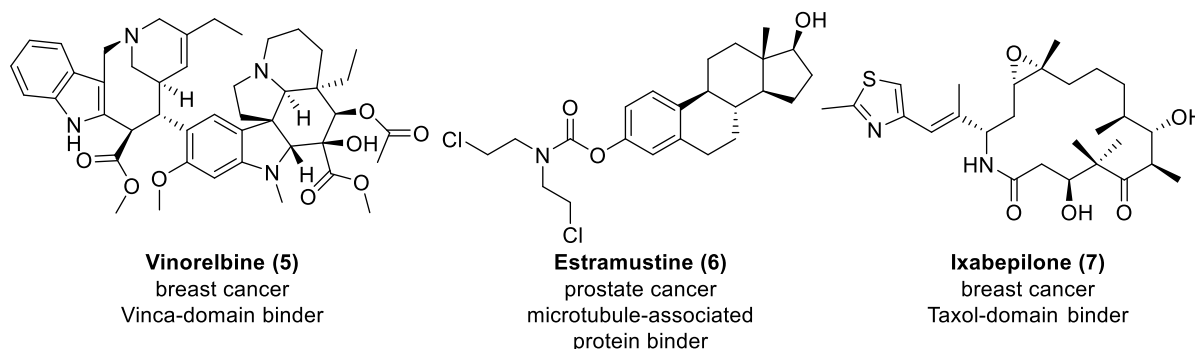
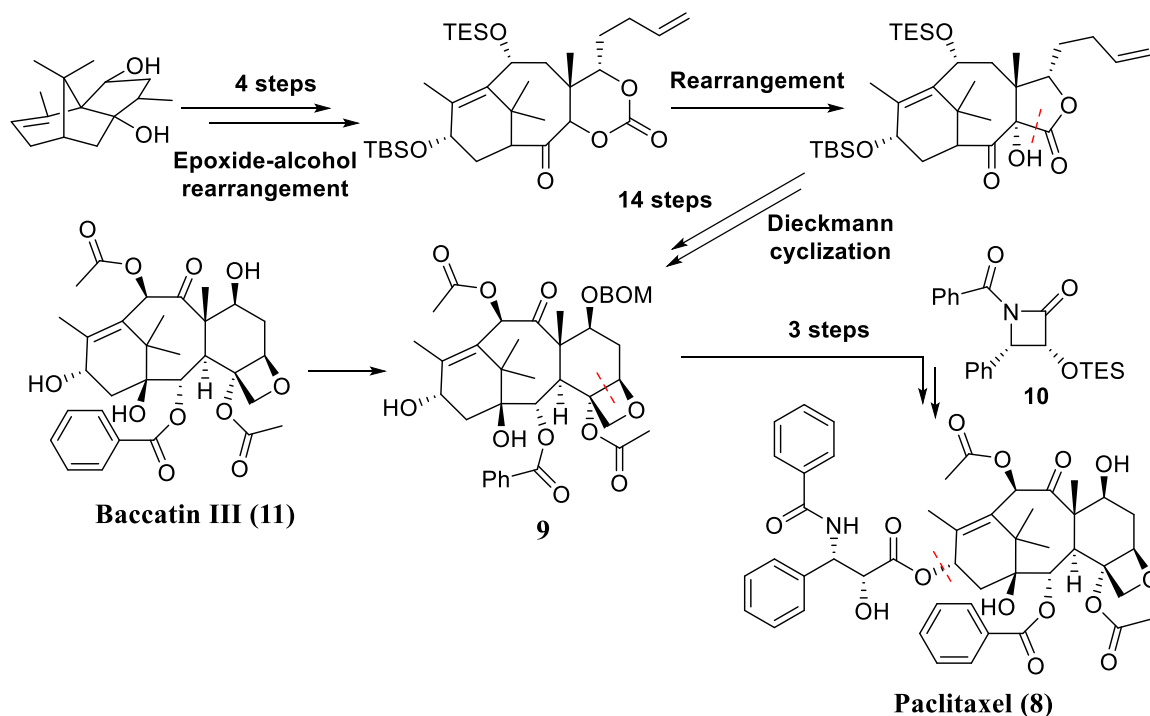


Figure 1.3: Examples of approved microtubule-targeting drugs.

Microtubule-targeting agents can affect microtubules through different mechanisms. Microtubule formation is a dynamic process, such that both assembly and disassembly of tubule monomers occur simultaneously. By maintaining a healthy equilibrium, normal function of microtubules, such as cell division and proliferation, can be carried out. Interruption of either end of the equilibrium can be disruptive or lethal for cells. Most MTAs disturb this dynamic by binding directly to microtubules, but some were also found to bind to microtubule-associated proteins, whose function is to regulate microtubule dynamics.⁵ Generally, MTAs are classified into two categories according to their outcomes: microtubule-destabilizing agents (MDAs) and microtubule-stabilizing agents (MSAs). Compounds that bind to the vinca domain (at the end of microtubules) or colchicine domain (soluble tubulin dimers) are MDAs. This type of binding disrupts polymerization of microtubules, and as a result the microfibers essential to pull cells apart cannot be formed, thus cell proliferation is halted. Vinca-domain binders include drugs such as eribulin (**3**), vinorelbine (**5**), vinblastine and romidepsin. Colchicine-domain binders are a smaller group, and contain the potential drugs fosbretabulin, verubulin and ombrabulin that are currently in clinical trials. On the other hand, those that bind to the paclitaxel domain (inner surface of microtubules) are MSAs. In this case, microtubule disassembly is interrupted and multiple asters are often formed, resulting in cell lysis. Although MSAs were discovered later, they have become a more active area of research than the MDAs.

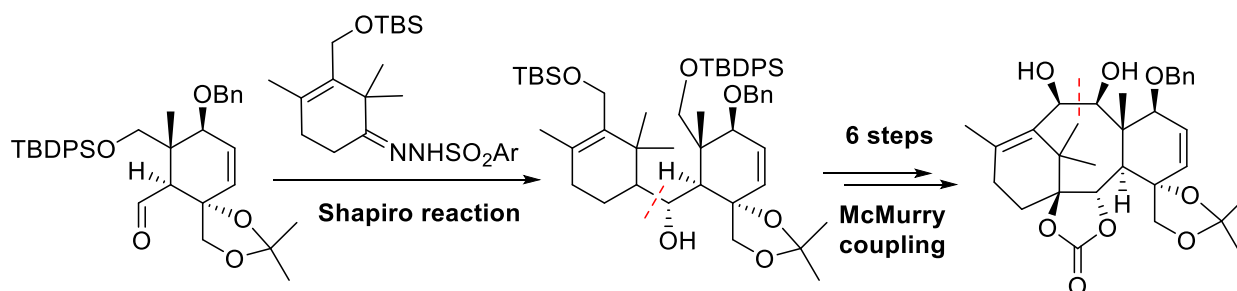
The most well-known example of a microtubule-stablizing drug is paclitaxel (**8**), trade-marked as Taxol. It is one of the most successful anti-cancer drugs on the market. Discovered in the late 1960's,⁶⁻⁷ paclitaxel's biological activity was extensively studied during the following decade,⁸ and it was finally approved for treatment of ovarian and breast cancer in 1992 and 1994, respectively. Because the natural source of paclitaxel (**8**), the Pacific yew tree (*Taxus brevifolia*), is highly scarce, isolation alone cannot meet the demand of the clinic. During the 1990s, the structure of paclitaxel (**8**) attracted around 30 groups worldwide towards its total synthesis,⁹ which contains a core 6-8-6 tricyclic ring system with appended hydroxyls, esters and a fused oxetane (**Scheme 1.1**). In addition to the tricyclic ring system, the existence of multiple quaternary and stereocenters makes the synthesis of **8** very challenging. In 1994, two of these total syntheses were published. Holton's synthesis utilized an epoxide-alcohol rearrangement strategy for the core synthesis (**Scheme 1.1**),^{10,11} which was developed by their group in 1988 to synthesize a similar taxane, taxusin.¹² The saturated six-membered ring in **9** was formed *via* Dieckmann cyclization and the side-arm was sourced from Ojima's β -lactam (**10**). Holton's synthesis also included a route starting from baccatin III (**11**), which was also

isolated from the Pacific yew tree. Although this could increase the production of paclitaxel (**8**), it is still far from meeting the market demand.



Scheme 1.1: Holton's synthesis of paclitaxel (**8**).

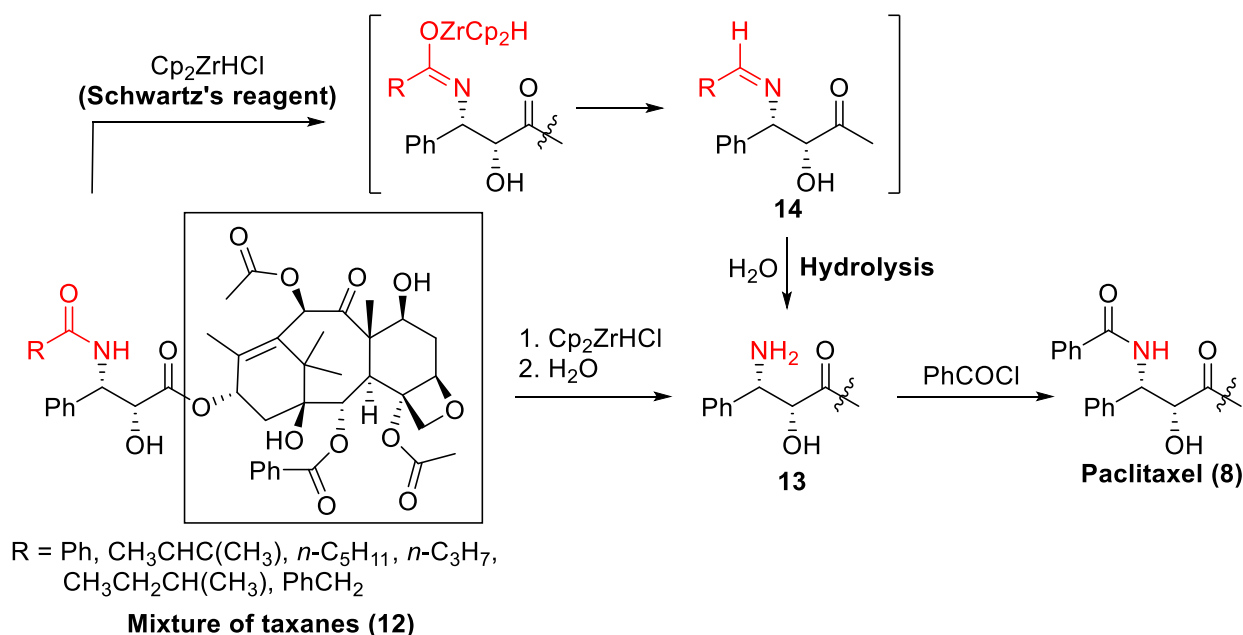
Nicolaou's synthesis used the same β -lactam **10** for the side-arm, but the core structure was constructed around the central 8-membered ring, *via* Shapiro and McMurry coupling reactions (**Scheme 1.2**).¹³ Due to the complexity of the structure, a total synthesis approach would be too expensive for industry-scale production. Nevertheless, Holton and Nicolaou's research was a valuable development in synthetic methodology, and researchers continued to find more methods and reliable sources for mass production of paclitaxel (**8**).



Scheme 1.2: Key steps of Nicolaou's synthesis of paclitaxel (**8**).

The source problem was resolved by Bristol-Myers Squibb. They re-discovered paclitaxel from the leaves of ornamental yew tree in a mixture with related taxanes (**12**) that differ at the amide

on the side-arm (**Scheme 1.3**). Compared to the 100-200 years growth cycle needed to harvest paclitaxel from the bark of the Pacific yew trees, the leaves of ornamental yew trees only need 3-4 years to regenerate.¹⁴ A sequence was developed to convert the mixture of taxanes (**12**) to **8** in two simple steps, owing to a previously reported method of imine synthesis with Schwartz's reagent^{15,16} (**Scheme 1.3**). The amide on the side-arm was converted to an amine (**13**) *via* hydrido-zirconation to produce imine (**14**), followed by hydrolysis. The subsequent esterification afforded taxol (**8**). This method of production allows industry-scale manufacture



Scheme 1.3: Bristol-Myers Squibb's synthesis of paclitaxel (**8**).

of paclitaxel (**8**) for commercialization, which also enables derivatives of paclitaxel (**8**) to be accessed readily and studied. Fruitfully, a few related drugs have since been developed and approved by FDA for various types of cancer, for example docetaxel (**15**), cabazitaxel (**16**) (**Figure 1.4**) and nanoparticle albumin-bound paclitaxel (nab-paclitaxel). The derivatization of paclitaxel (**8**) is still a very active area of study.¹⁷

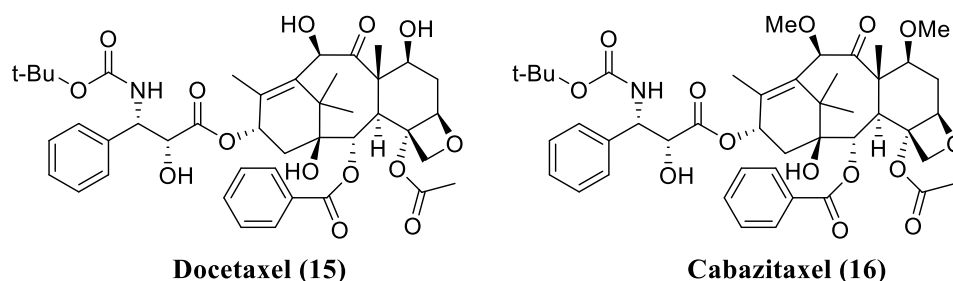


Figure 1.4: Structure of docetaxel (**15**) and cabazitaxel (**16**).

During the clinical application of those drugs, some patients were found to be developing resistance. The first cause for this resistance was identified as an overexpression of P-glycoprotein efflux pumps.¹⁸⁻²¹ This mechanism is part of the energy-dependant transport of small molecules through the cell membrane, and provides the cell's natural defence against toxins. It has the ability to remove toxins, in this case drugs, from the cell, resulting in ineffective chemotherapy.²² Elevated P-glycoprotein level is the most common cause of drug-resistance amongst many cell lines, and against various small-molecule drugs.¹⁸ Later, another resistance pathway was observed, involving multidrug resistance-associated proteins (MRP). The first MRP was isolated from drug-resistant lung cancer cells with normal P-glycoprotein levels,²³ and six more members of the MRP family were subsequently discovered.²⁴ Both P-glycoprotein and MRP are validated targets for overcoming the problem of drug resistance. Research targeting these mechanisms include suppression of these small-molecule efflux pumps by inhibitors and reducing the toxicity of drugs to allow higher application dose.²⁰ There is also a potential solution offered by microtubule-stabilizing agents that bind covalently to microtubules. In 2005, Hamel's study on the previously isolated natural product cyclostreptin (**17**), also known as FR182877 (**Figure 1.5**),²⁵⁻²⁷ produced a puzzling outcome:²⁸ although cyclostreptin (**17**) was 7- and 12-fold less potent than paclitaxel (**8**) against cell lines MCF-7 (breast cancer) and 1A9 (ovarian cancer) respectively, its cytotoxicity was less affected by paclitaxel-resistant cell lines (1A9PTX10, 1A9PTX22). While the effectiveness of paclitaxel was reduced by 33/34-fold against its resistant strains, that of cyclostreptin (**17**) was only reduced 2-fold. A follow-on study ascribed the cause of this observation to covalent binding between **17** and microtubules.²⁹ This finding shed light on the problem of drug-resistance through small-molecule transporter channels: if the drug binds to microtubules irreversibly, the cell can no longer "pump" it out. In 2008, another group of natural products, taccalonolides,³⁰⁻³⁷ was confirmed to covalently bind to microtubules.^{38,39} Six members of this family of compounds demonstrated cytotoxicity, with taccalonolide AJ (**18**) leading the chart (**Figure 1.5**).⁴⁰ However, all of taccalonolides and cyclostreptin (**17**) have relatively weak cytotoxicity, with their IC₅₀ values only at μ M-scale.^{28,38} Even against the paclitaxel-resistant strains, they are less or only marginally more potent than paclitaxel (**8**). It wasn't until the discovery of another two marine natural products, (-)-zampanolide (**19**) and (+)-dactylolide (**20**), which are covalently binding microtubule-stabilizing agents, that new hope was found for this potential solution to drug-resistance.

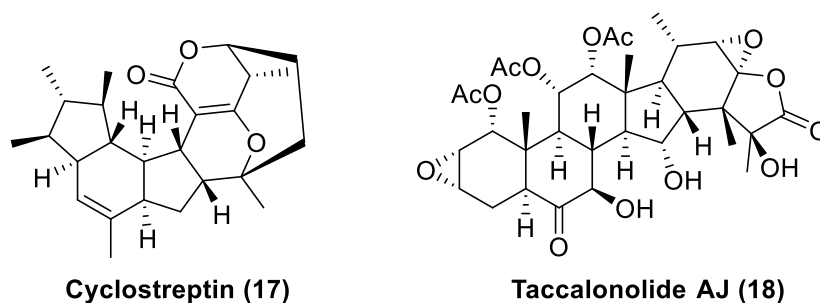


Figure 1.5: Structure of cyclostreptin (**17**) and taccalonolide AJ (**18**).

1.3 (-)-Zampanolide and (+)-dactylolide

(-)-Zampanolide (**19**) was first isolated in 1996 from a marine sponge called *Fasciospongia rimosa*, which was discovered at Cape Zampa in Japan (**Figure 1.6**).⁴¹ Its unique structure consists of an 18-membered macrolactone with an unusual *N*-acyl hemiaminal substituent at C19. The macrolide core is highly unsaturated and bears an embedded pyran with an *exo*-methylene motif. The stereochemistry at C20 was not defined in the isolation paper and was later determined through the total synthesis by Smith, Safonov and Corbett.⁴²

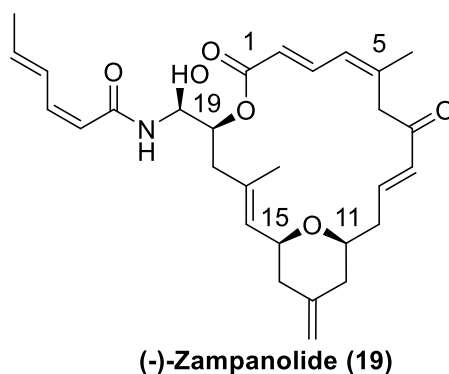
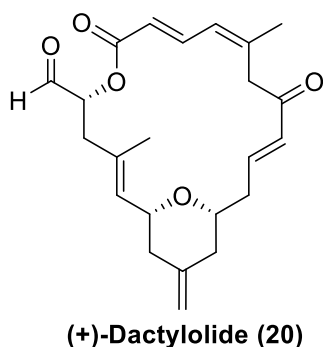


Figure 1.6: The structure of (-)-zampanolide (**19**).

(-)-Zampanolide (**19**) was found to exhibit potent anticancer activity comparable with the widely used cancer chemotherapy drug paclitaxel (**8**) (see **Figure 1.4**).⁴³ It also displays a similar biochemical mode of action to paclitaxel (**8**), both being microtubule stabilizing agents.⁴⁴ A detailed mechanistic study of (-)-zampanolide (**19**) has been reported by researchers at Victoria University of Wellington.⁴³ The cytotoxicity was determined as a half maximal inhibitory concentration (IC₅₀), which is the concentration required to inhibit normal function of 50% of the cells in the assay. In this case, the inhibited cells can be evaluated by an MTT

dye reduction assay. The IC_{50} values of (-)-zampanolide (**19**) were 4.3 ± 1.1 nM and 14.3 ± 2.4 nM against HL-60 (human promyelocytic leukemia) and 1A9 (human ovarian carcinoma) cells respectively. More remarkably, the cytotoxicity of (-)-zampanolide (**19**) was similar against the parental strain A2780 or the paclitaxel-resistant human ovarian cancer cell line A2780AD, with an IC_{50} value of 7.5 ± 0.6 nM against A2780AD, which is over 50-fold more potent than paclitaxel (**8**).⁴³ Studies have found that (-)-zampanolide (**19**) causes the stabilization of microtubule bundles at interphase and multiple asters during mitosis; as a result, the cell is divided unevenly into three or more non-viable daughter cells.⁴³

In 2001, a similar natural product dactylolide (**20**) was isolated and identified by Cutignano (**Figure 1.7**).⁴⁵ Uenishi's thermolysis and degradation study of (-)-zampanolide (**19**) found that, although (+)-**20** could be produced by thermolysis of (+)-**19**, no (-)-**20** was observed subjecting (-)-**19** to Riccio's isolation conditions. Therefore dactylolide (**20**) was thought not to be the decomposition product of (-)-zampanolide (**19**) from the isolation process, but a distinct natural product.⁴⁶ Surprisingly, the core macrocyclic structure of dactylolide (**20**) was initially proposed to have the same structure, but opposite configuration to (-)-zampanolide (**19**) based on optical rotation data of isolated and synthetic samples.⁴⁵ However, evidence has since accumulated from the optical rotation values of synthetic dactylolide (**20**) to suggest that the opposite sign of optical rotation of isolated dactylolide is merely due to contamination of the natural sample by a highly absorbing species with a positive rotatory effect on plane polarised light (**Figure 1.7**).⁴⁷ The structural similarity of zampanolide and dactylolide indicates that they are likely to be synthesized by the same biosynthetic pathways, yet they were isolated from different sponges. It would be unusual for the configuration of a metabolite to be inverted at a late stage of a biosynthesis. However, the hypothesis of contamination has not been proved yet. Like (-)-zampanolide (**19**), dactylolide (**20**) is a microtubule stabilizing agent, but has much lower potency. The cytotoxicity of **20** was reported together with the isolation. The inhibition percentages of dactylolide (**20**) at 3.2 μ g/mL were 63% for the L1210 cell line (lymphatic leukaemia of mice) and 40% for SK-OV-3 (carcinoma of the ovaries).⁴⁵



Isolated: $\alpha_D = +30$ ($c = 1.0$, MeOH)
 (-)-Synthetic: $\alpha_D = -128$ to -258 ($c = 0.11$ to 1.2 , MeOH)
 (+)-Synthetic: $\alpha_D = -128$ to -258 ($c = 0.07$ to 0.52 , MeOH)

Figure 1.7: The structure and optical rotation data of dactylolide (**20**).

More insight into the protein binding sites of (-)-zampanolide (**19**) was provided by a report in July 2012, which included (-)-dactylolide (**20**) for comparison.⁴⁴ High resolution mass spectrometry (HRMS) and nuclear magnetic resonance (NMR) data indicated that both compounds bind to the luminal site on β -tubulin, adjacent to the paclitaxel-binding site, and thus disrupt the function of microtubule. More excitingly, the binding is covalent and irreversible, and the binding of (-)-zampanolide (**19**) is at least 8 times faster than the binding of (-)-dactylolide (**20**). The irreversible binding could mean low drug dosage and application frequency if (-)-zampanolide (**19**) were eventually commercialised. The HRMS study showed that the covalent binding is either between an Asn amide and C3, or a His and C9 of the zampanolide ring (**Figure 1.8**), which are the result of conjugate additions of the nucleophilic side-arms on the amino acids to the electrophilic α,β -unsaturated carbonyl moieties. For (-)-zampanolide (**19**), significant hydrogen bonding interaction was also seen between tubulin and the *N*-acyl hemiaminal linkage. In addition, hydrogen bonding from tubulin to the carbonyl at C7 also occurs, and the exocyclic methylene group at C13 interacts hydrophobically with its resident protein pocket. Interestingly, modelling study indicated that the orientation of (-)-dactylolide (**20**) in the binding site is reversed relative to **19**, yet the covalent bonds form at the same positions. The ester and aldehyde provide the major hydrogen bonding in (-)-**20**, and the eastern side of (-)-dactylolide (**20**) occupies the pocket where the side-arm of (-)-**19** resides. A hydrophobic interaction of the methylene still occurs, but with a hydrophobic pocket adjacent to the one involved in the (-)-zampanolide (**19**) binding.⁴⁴

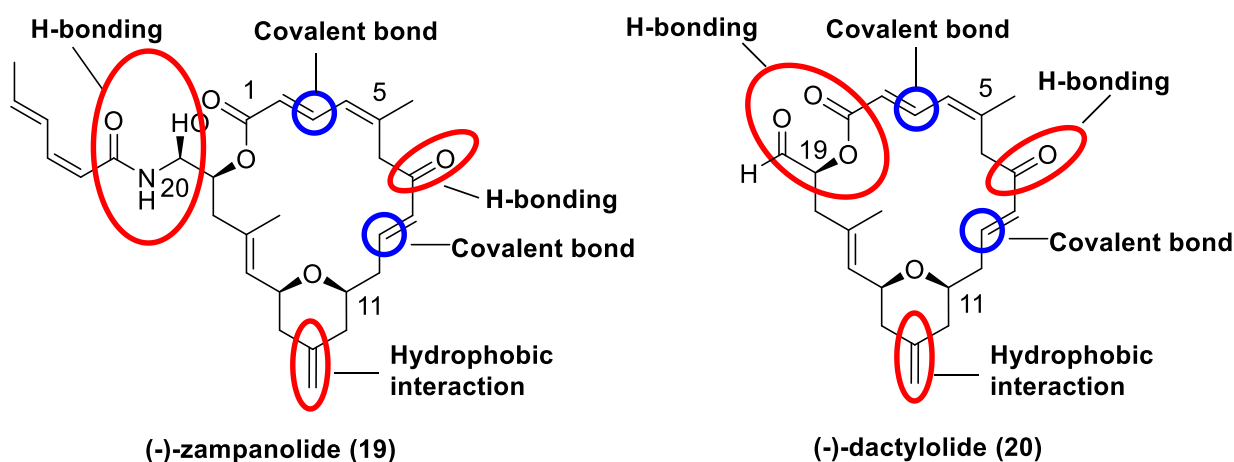


Figure 1.8: Binding of (-)-zampanolide (**19**) and (-)-dactylolide (**20**).

In 2013, the high resolution X-ray crystallography of zampanolide (**19**) complexed with $\alpha\beta$ -tubulin was published,⁴⁸ which agreed with most of the findings from the HRMS study, and the covalent binding between His and C9 was confirmed. The most recently published study on zampanolide (**19**) binding resorted to computational methods, using molecular docking and dynamics stimulation to calculate the orientation and binding of zampanolide (**19**) in the taxane pocket.⁴⁹ It concluded that the C3 binding should be major, because of the short distance between C3 and the His nitrogen (3.667 Å) leading to the preferred nucleophilic attack. Although the major site for covalent binding interaction is still debatable, it is certain that the covalent binding between **19** and the taxane binding pocket enhances the cytotoxicity of zampanolide (**19**) and makes it a good anti-cancer drug candidate.

1.4 Published total syntheses of zampanolide

The potential for zampanolide (**19**) to become an effective anti-cancer drug has motivated research groups around the globe to target its total synthesis and obtain a better understanding of its mode of action.⁴⁷ A number of total syntheses of zampanolide (**19**) have been published since 2001 (**Table 1.1**), as well as the total syntheses of dactylolide (**20**) and formal synthesis of **19**, which will be described in section 1.5. A few analogues of **19** were also generated, which provided some structure-activity relationships. However, more insightful information on the tubulin binding of **19** was obtained from the mode of action studies.^{43,44,48,49} The structural complexity of the compound sets many challenges for its synthesis, especially the pyran ring synthesis, the macrocyclization step and formation of the *N*-hemiaminal linkage.

Table 1.1: Timeline of published zampanolide (**19**) syntheses and mode of action studies.

Year	Authors	Major finding
2001	Smith, A. B.; Safonov, I. G.; Corbett, R. M. ^{42,50}	Synthesis of (+)- 19
2003	Hoye, T. R.; Hu, M. ⁵¹	Synthesis of (-)- 19
2009	Field, J. J.; Singh, A. J.; Kanakkanthara, A.; Halafihi, T.; Northcote, P. T.; Miller, J. H. ⁴³	19 identified as a microtubule-stabilizing agent
2009	Uenishi, J.; Iwamoto, T.; Tanaka, J. ⁴⁶	Synthesis of (-)- 19
2012	Field, J. J.; Pera, B.; Calvo, E.; Canales, a.; Zurwerra, D.; Trigili, C.; Rodriguez-Salarichs, J.; Matesanz, R.; Kanakkanthara, A.; Wakefield, J.; Singh, J.; Jimenez-Barbero, J.; Northcote, P.; Miller, J. H.; Lopez, J. A.; Hamel, E.; Barasoain, I.; Altmann, K-H.; Diaz, J. F. ⁴⁴	Binding site of 19 to tubulin determined
2012	Ghosh, A. K.; Cheng, X.; Bai, R.; Hamel, E. ⁵²	Synthesis of (-)- 19
2012	Zurwerra, D.; Glaus, F.; Betschart, L.; Schuster, J.; Gertsch, J.; Ganci, W.; Altmann, K-H. ⁵³	Synthesis of (-)- 19
2013	Prota, A. E.; Bargsten, K.; Zurwerra, D.; Field, J. J.; Diaz, J. F.; Altmann, K. H.; Steinmetz, M. O. ⁴⁸	X-ray crystallography structure of zampanolide-tubulin complex
2014	Liao, S. Y.; Mo, G. Q.; Chen, J. C.; Zheng, K. C. ⁴⁹	Computational study of 19 binding mode on tubulin.

The disconnections dictating the retrosynthetic strategies of the previous total syntheses are summarised in **Figure 1.9**. Although each total synthesis has its unique features, there are a few retrosynthetic disconnections that are popular strategies: in the forward direction, all of the total syntheses of zampanolide (**19**) have the formation of the *N*-acyl hemiaminal group as the last step; a majority adopt esterification or macrolactonization at C1, with either Mitsunobu or Yamaguchi condition; alkenes are generally chosen as major disconnection points, due to the

abundance of well-established olefination methods, such as the Horner-Wadsworth-Emmons reaction (HWE), Wittig reaction, ring-closing metathesis (RCM) with Grubbs' catalyst and Julia-Kocienski olefination. On the other hand, the synthetic methods diverge with respect to the pyran motif.

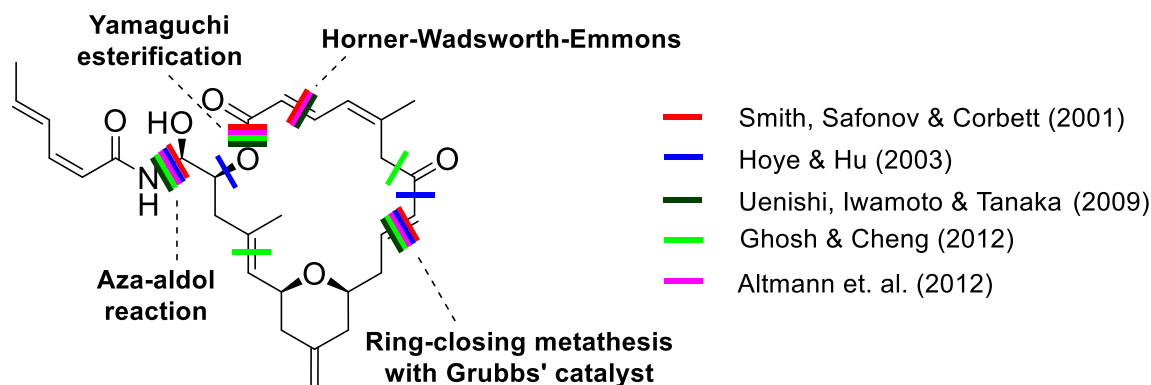
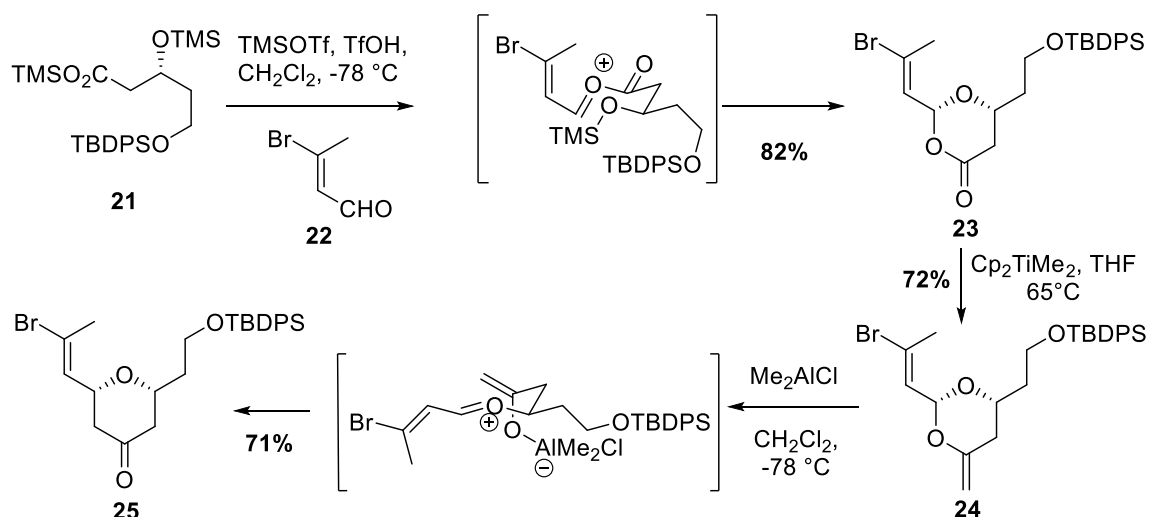


Figure 1.9: Reported major disconnections for (-)-zampanolide (**19**).

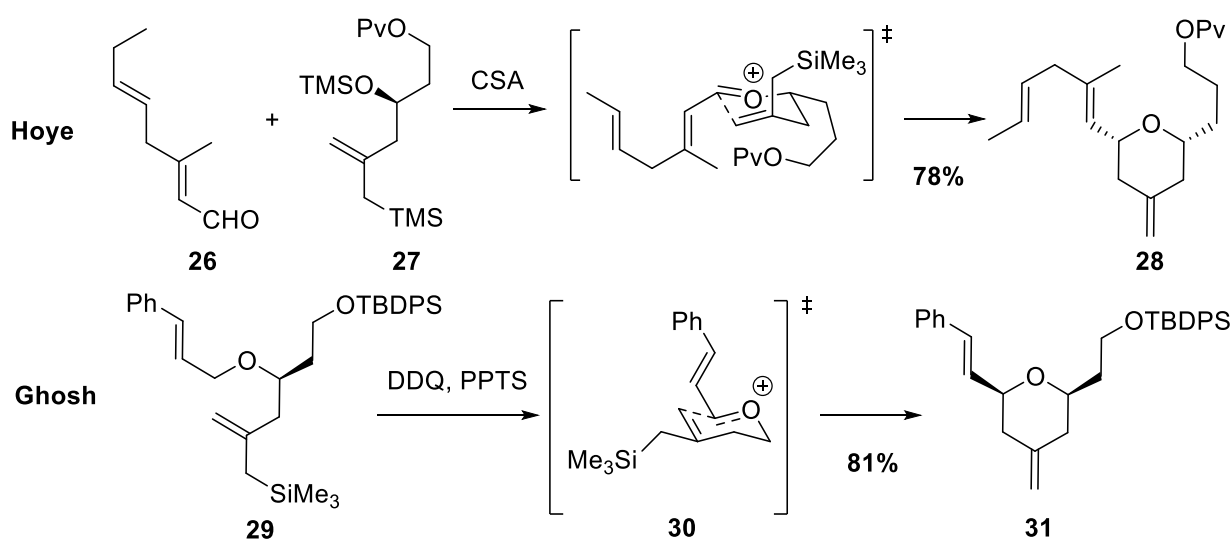
1.4.1 Synthetic methods for formation of the pyran fragment

In Smith's seminal total synthesis of the unnatural enantiomer, (+)-**19**, the C9-C17 pyran fragment was constructed by dioxanone formation, followed by a Petasis-Ferrier rearrangement (**Scheme 1.4**).^{42,50} This acid-promoted cyclization of trimethylsilyl (TMS) ester **21** with (*E*)-3-bromo-but-2-enal (**22**) can be carried out with triflic acid generated *in situ* from trimethylsilyl triflate (TMSOTf), but the addition of a catalytic amount of triflic acid (5 to 10 mol%) was essential in scaled-up reactions to initiate the reaction. The subsequent Petasis-Ferrier reaction sequence involves methylenation of the dioxanone **23** by Cp_2TiMe_2 to produce **24**, which then transformed to an aluminum enolate and rearranged in Ferrier-fashion. The pyran **25** was produced with the correct *cis*-configuration, which agrees with the prediction based on the substituent pattern.⁵⁴



Scheme 1.4: Smith's Petasis-Ferrier rearrangement.

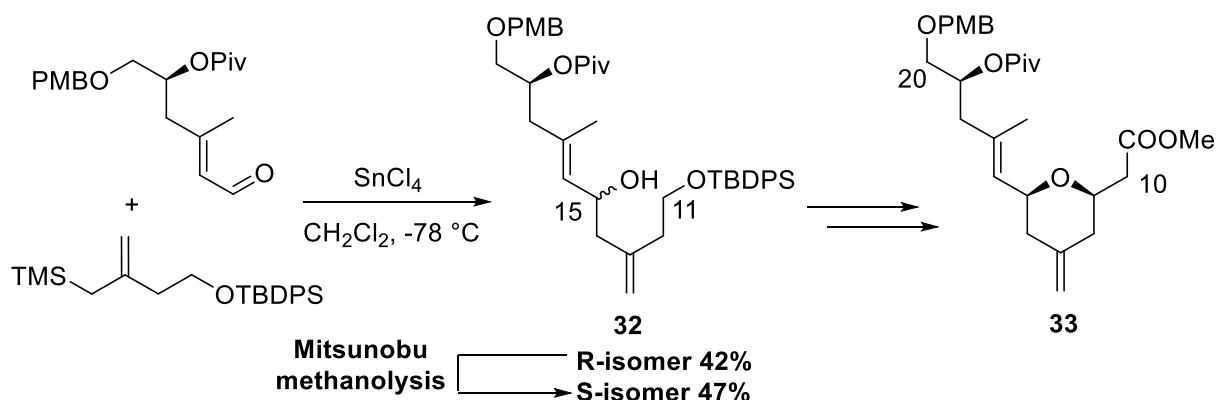
Although Smith's method produced the pyran with the correct stereochemistry in a satisfying yield, some other syntheses have chosen to use one-step methods for the pyran synthesis. Hoyo and Ghosh both used an acid-catalyzed Sakurai-type reaction to produce the pyran with an *exo*-methylene in one step (Scheme 1.5).^{51,52} This reaction is driven by the β -silicon effect.⁵⁵ The electron deficient carbocation that forms at the β -position to the silyl is stabilized by the molecular orbitals of the trimethylsilyl group, which promotes the nucleophilic addition to the oxonium intermediate. Hoyo used camphorsulfonic acid (CSA) to catalyze the union of the two fragments **26** and **27**, and the product **28** was obtained with a good yield (78%) and exclusively



Scheme 1.5: Hoyo and Ghosh's Sakurai-type reactions.

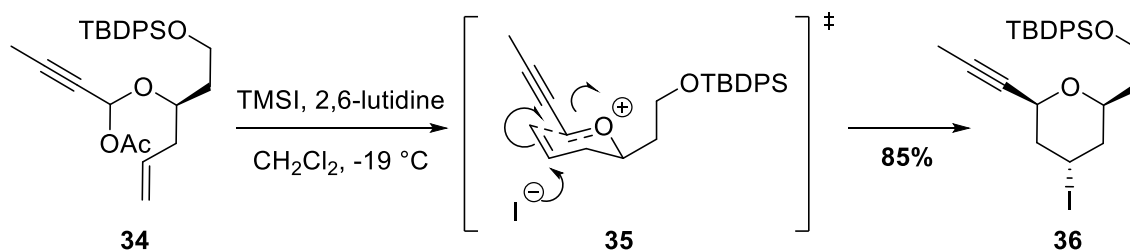
in the desired configuration.⁵¹ Ghosh achieved the pyran cyclization of **29** via an oxidative and intramolecular Sakurai-type reaction. An oxocarbenium intermediate (**30**) was generated by 2,3-dichloro-5,6-dicyano-1,4-benzoquinone (DDQ) in the presence of a weak Lewis acid (PPTS) that enhances the oxidative ability of DDQ (**Scheme 1.5**).⁵²

Uenishi also used a Sakurai-type reaction in the pyran synthesis, in conjunction with an *O*-Michael cyclization, producing the pyran fragment C9-C20 (**Scheme 1.6**).⁴⁶ No stereoselectivity was observed for this Hosomi-Sakurai reaction, and a mixture of *R*- and *S*-**32** was obtained. Fortunately, the two isomers were separable, and the undesired *R*-isomer was converted to the *S*-isomer in 65% yield over a two-step process involving Mitsunobu reaction and methanolysis. This inversion of the configuration at C15 proceeded mechanistically through a S_N2-type nucleophilic substitution of the activated alcohol followed by deacetylation to afford the inverted alcohol. After establishing a conjugated unsaturated methyl ester at C11, an intramolecular *O*-Michael addition was performed to complete the pyran (**33**) formation.



Scheme 1.6: Hosomi-Sakurai reaction and *O*-Michael addition in Uenishi's synthesis.

In Altmann's synthesis, a Prins cyclization was used to construct the pyran. The starting material **34** proceeded through a six-membered transition state **35** similar to Ghosh's Sakurai-type transition state to produce the pyran **36** with an appending iodide (**Scheme 1.7**). The iodide was transformed to a methylene via substitution by acetate, saponification, oxidation and Wittig reaction.



Scheme 1.7: Prins cyclization in Altmann's synthesis.

1.4.2 Synthetic methods of macrocyclization

Most of the total syntheses of **19** used well-established chemistry for macrocyclization. The most common ones are Yamaguchi esterification at C1,⁵⁶ Horner-Wadsworth-Emmon reaction to form alkene C2-C3⁵⁰ and ring-closing metathesis to link C8 to C9^{51,52,57} (**Figure 1.10**).

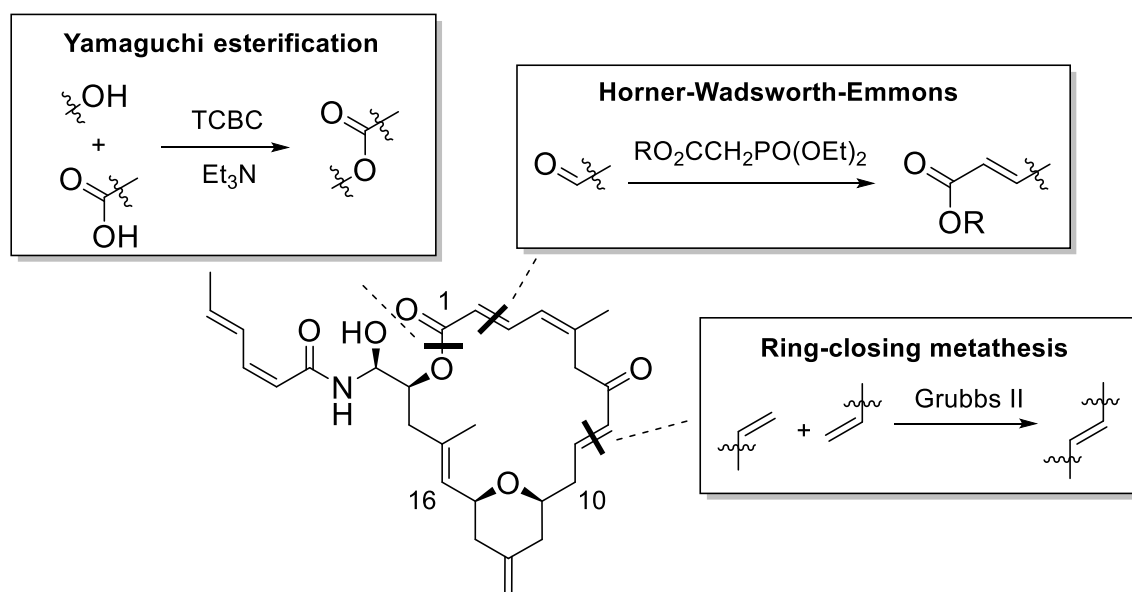
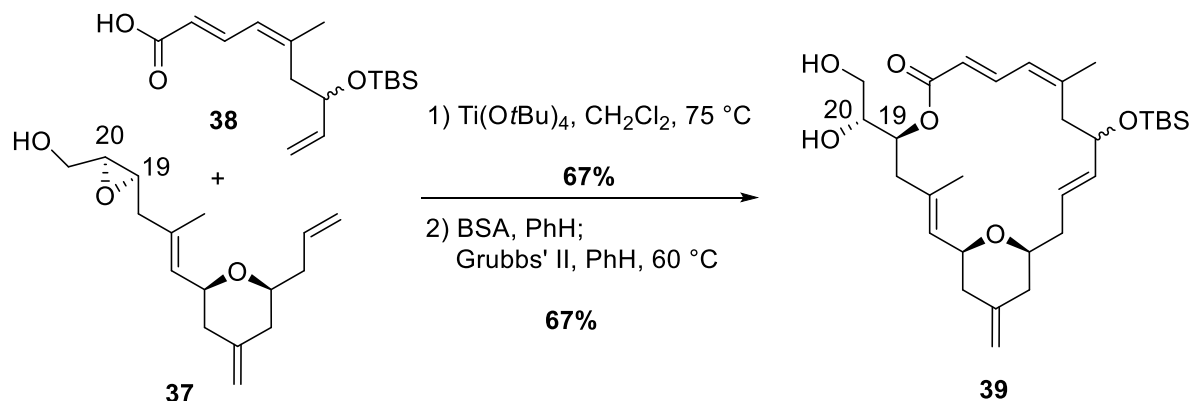


Figure 1.10: Common macrocyclization methods.

Hoye's synthesis planned to use a unique epoxide opening as their final macrolactonization step.⁵¹ However, the reaction had poor regioselectivity and lactonization at C20 became a problem. Therefore, this strategy was revised, and ring-closing metathesis was chosen as the final macrocyclization, after intermolecular epoxide opening (**Scheme 1.8**). The tetra(*tert*-butoxy)titanium-catalyzed epoxide opening of **37** by carboxylic acid **38** created the desired

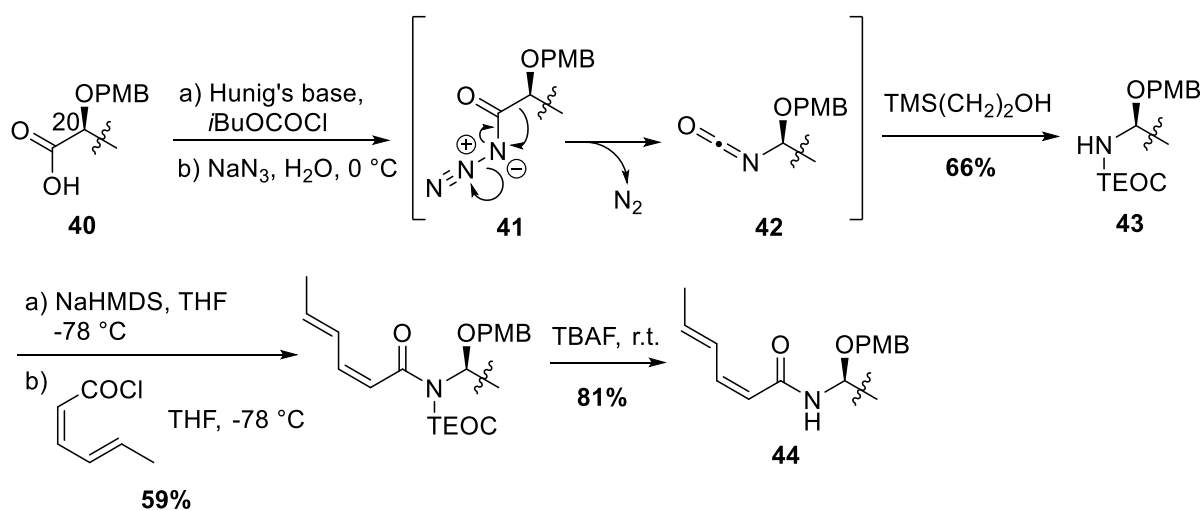
stereochemistry at C19, and the product was subjected to RCM to macrocycle **39**, which proceeded through to produce (-)-dactylolide (**20**) and zampanolide (**19**) (**Scheme 1.8**).



Scheme 1.8: Hoyer's tetra(*tert*-butoxy)titanium-catalyzed epoxide opening.

1.4.3 Synthesis of *N*-acyl hemiaminal linkage

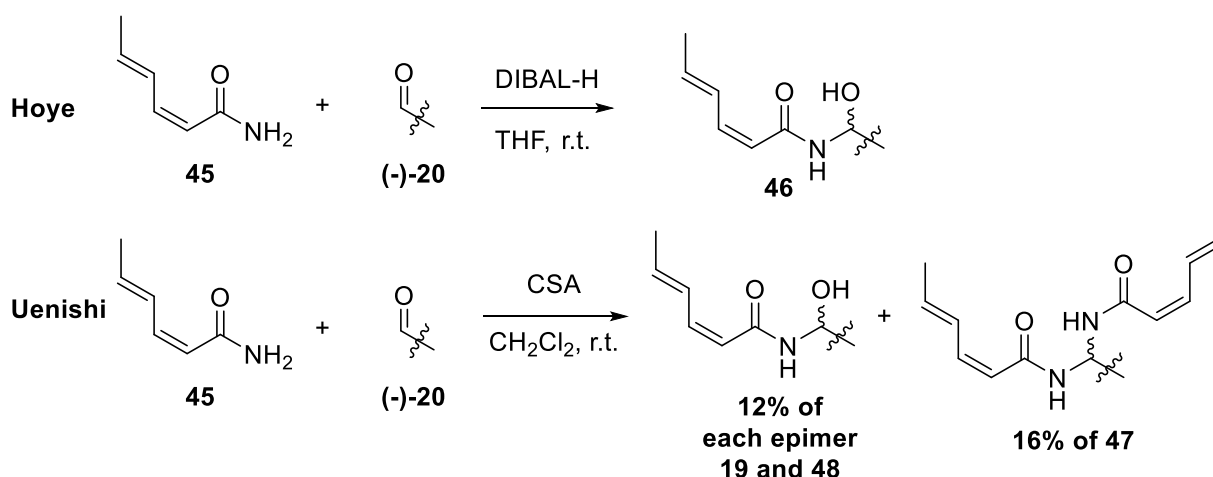
The *N*-acyl hemiaminal functionality is more common within ring structures, and scarcely found in the linear form within natural products, thus little research has previously been done on the construction of groups such as that in the zampanolide side-arm. Smith's connection of the *N*-acyl hemiaminal side-arm to the core was achieved with Curtius rearrangement of **40** and acylation in good yield (**Scheme 1.9**).⁴² The Curtius rearrangement begins with a rearrangement of the acyl azide intermediate (**41**) to produce an isocyanate (**42**), which then



Scheme 1.9: Smith's *N*-acyl hemiaminal formation by Curtius rearrangement.

reacts with trimethylsilylethyl alcohol to afford the trimethylsilylethyl carboxy (TEOC)-protected amine (**43**). Upon coupling with an acyl chloride and deprotection, the desired *N*-acyl hemiaminal (**44**) structure was formed.

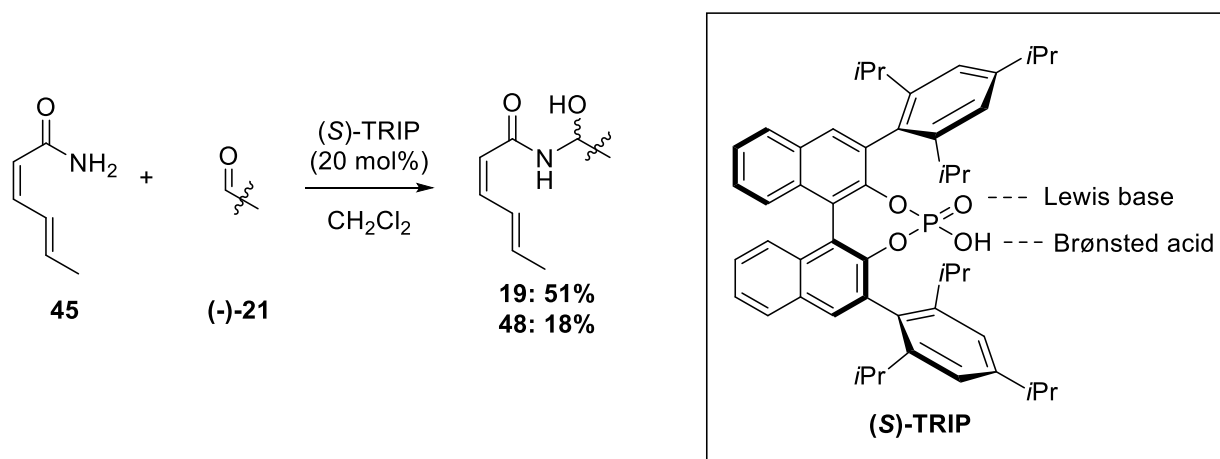
Hoye and Uenishi chose to attach the side-arm with aza-aldol reactions, which were promoted by di-*i*-butylaluminum hydride (DIBAL-H) and camphorsulfonic acid (CSA), respectively (**Scheme 1.10**).⁵¹ In both cases the desired product was formed from (-)-**20** and *Z,E*-hex-2,4-dienamide (**45**), but no stereoselectivity was observed. Hoye's 1:1 mixture of the two C20-epimers (**46**) was not separated, and no yield was reported. Uenishi only achieved a poor yield of 12% (Scheme 1.8).⁴⁶ The low yield of zampanolide (**19**) was attributed primarily to incompleteness of the reaction (35% recovery of (-)-**20**), disubstitution by the amide **45** to form **47** (16%) and the lack of stereoselectivity (12% of C20-epimer (**48**)).



Scheme 1.10: Hoye and Uenishi's aza-aldol reactions for connection of the side-arm.

The most efficient method so far reported is the amidation employed in Ghosh's total synthesis.⁵² This amidation was catalyzed by a chiral Brønsted acid, (*S*)-TRIP (**Scheme 1.11**). This catalyst is one of the chiral cyclic phosphoric acids derived from BINOL, which have found use in asymmetric catalysis only within the last ten years. They have succeeded in catalyzing a number of processes, such as Mannich-type, Pictet-Spengler, Friedel-Crafts-type and aza-Diels-Alder reactions.⁵⁸ The phosphoric acid motif in the promoter is bifunctional, containing both Lewis basic and Brønsted acidic parts. In this reaction, both aldehyde and amide substrates are thought to be activated by hydrogen bonding with the phosphoric acid.

Dictated by the BINOL scaffold, the hydrogen bonding also brings the two substrates into close proximity. The stereoselectivity was provided by the relative positions of the two 2,4,6-tri(*i*-propyl)phenyl groups. This reaction totally eliminated the formation of the disubstituted product **47**, and the desired product **19** and its C20 epimer (**48**) were produced in a 3:1 ratio.



Scheme 1.11: Ghosh's *N*-acyl hemiaminal connection.

1.5 Published total syntheses of dactylolide

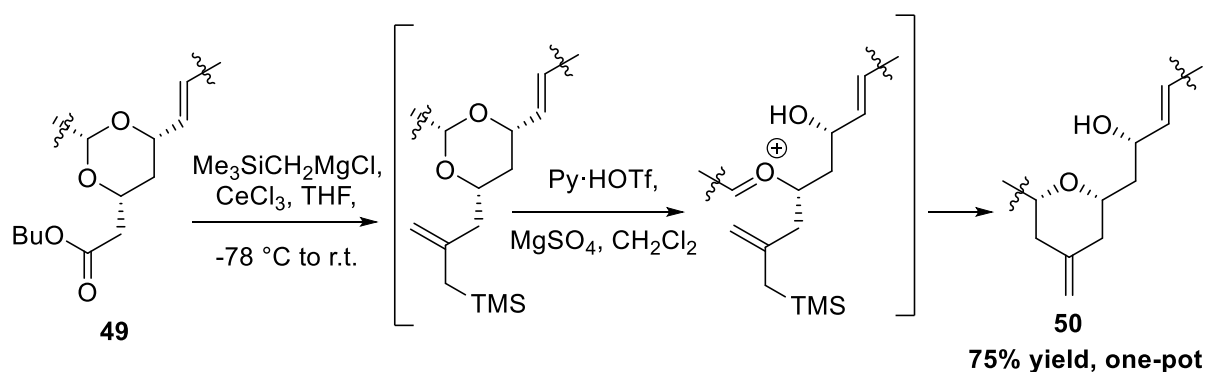
Due to the high structural similarity of dactylolide (**20**) and zampanolide (**19**), examination of the total syntheses of dactylolide (**20**) can provide good guidance to the macrolide core synthesis. In fact, all (-)-zampanolide (**19**) syntheses go *via* (-)-dactylolide (**20**) as an intermediate. A number of total syntheses of both (+)-**20** and (-)-**20** have been published (**Table 1.2**), including Smith *et. al.* and Altmann *et. al.* who also used their strategy to complete the total synthesis of (-)-zampanolide (**19**).^{53,56,59-62}

Table 1.2: Timeline of published dactylolide (**20**) syntheses.

Year	Authors
2002	Smith, A. B.; Safonov, I. G. ⁵⁹
2005	Aubele, D. L.; Wan, S. Y.; Floreancig, P. E. ⁵⁶
2005	Sanchez, C. C.; Keck, G. E. ⁶⁰
2006	Louis, I.; Hungerford, N. L.; Humphries, E. J.; McLeod, M. D. ⁶¹
2008	Ding, F.; Jennings, M. P. ⁶³
2010	Yun, S. Y.; Hansen, E. C.; Volchkov, I.; Cho, E. J.; Lo, W. Y.; Lee, D. ⁶⁴
2010	Zurwerra, D.; Gertsch, J.; Altmann, K. H. ⁶²
2012	Lee, K.; Kim, H.; Hong, J. Y. ⁶⁵

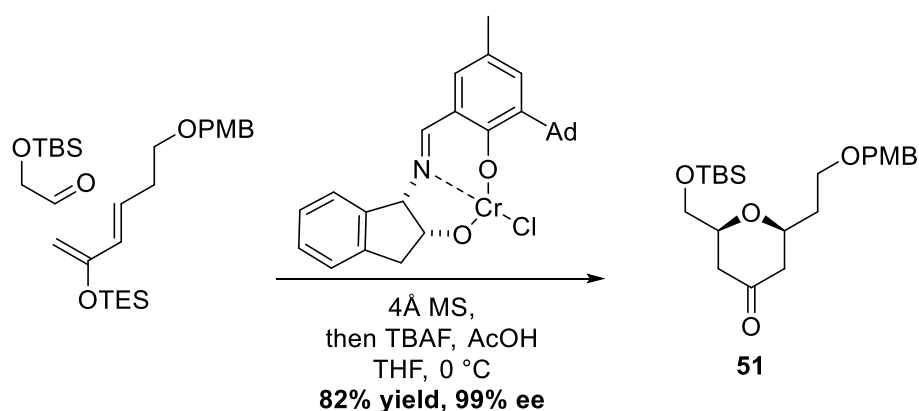
1.5.1 Synthetic methods for formation of the pyran fragment

The strategies for the major disconnections in total syntheses of dactylolide (**20**) are similar to those of zampanolide (**19**), with Horner-Wadsworth-Emmon reaction followed by esterification to construct the dienolate and ring closing metathesis between C8 and C9 commonly used. As in the zampanolide (**19**) syntheses, the methodology for formation of the pyran in dactylolide (**20**) is diversified, and some very good methods with high yields and stereoselectivities were found. Floreancig's pyran synthesis from **49** used excess trimethylsilylmethylmagnesium chloride and cerium(III) chloride to form the substrate for Peterson olefination and Prins cyclization *in situ*, which smoothly produced **50** in a multi-step, one-pot reaction (**Scheme 1.12**).⁵⁶



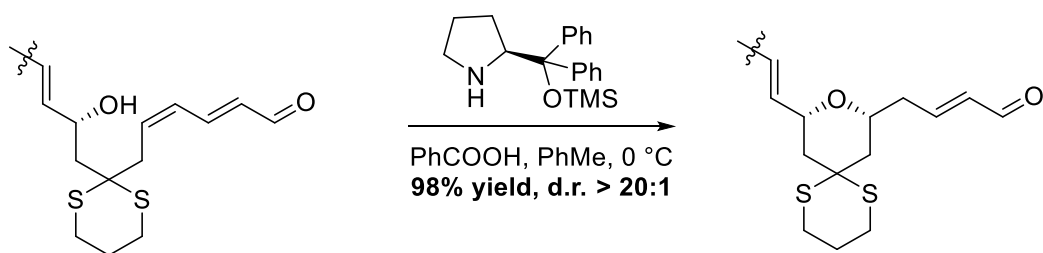
Scheme 1.12: Floreancig's pyran synthesis.

McLeod used a hetero-Diels-Alder reaction catalyzed by a chiral Lewis acid to construct the pyran motif. Upon desilylation, the pyranone **51** was produced with excellent yield and ee (**Scheme 1.13**).⁶¹ The Lewis acid catalyst was Jacobsen's chiral tridentate chromium(III) Schiff's base complex, containing an adamantyl (Ad) group for steric shielding, and was made conveniently in three steps. It provided excellent regio- and stereoselectivity in the formation of **51**.⁶⁶



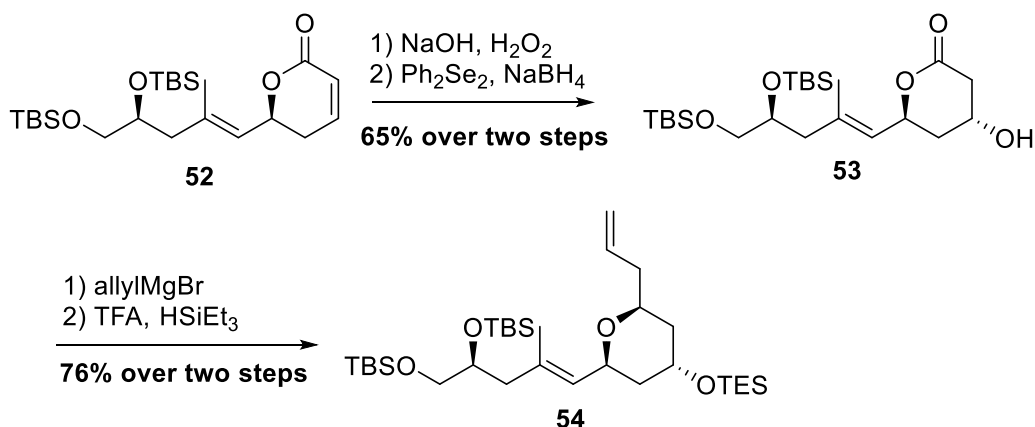
Scheme 1.13: McLeod's hetero-Diels-Alder reaction in pyran synthesis.

Hong employed an *O*-Michael addition with a chiral proline-derived catalyst (**Scheme 1.14**).⁶⁴ This type of reactions usually proceed through an iminium intermediate resulted from the aldehyde. Although the chiral directing groups on the catalyst are further away from the reacting carbon in this 1,6-conjugate addition, excellent yield and diastereoselectivity were still obtained. Deprotection of the dithiane to a ketone sets up for the subsequent Wittig reaction to produce the *exo*-cyclic methylene.



Scheme 1.14: Hong's *O*-conjugate addition in pyran synthesis.

Jennings' method proceeds *via* an α,β -unsaturated lactone (**52**) (Scheme 1.15).⁶³ A diastereoselective epoxidation controlled by the configuration of the substrate **52** followed by epoxide ring-opening afforded the β -hydroxy lactone (**53**) as a single diastereoisomer. Allyl addition to the carbonyl and deoxygenation then established the terminal alkene (**54**) for macrocyclic RCM.

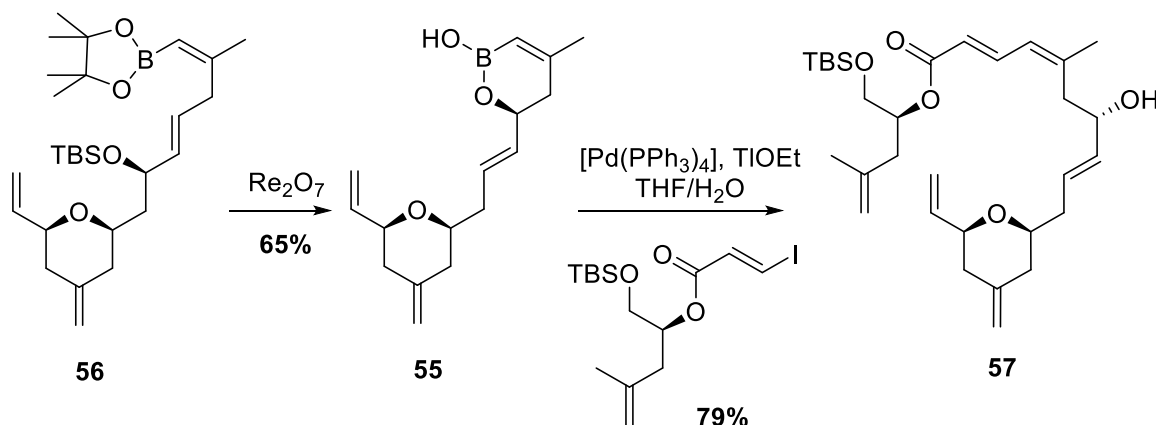


Scheme 1.15: Jennings' lactone method.

1.5.2 Other methods for the formation of dactylolide macrocycle

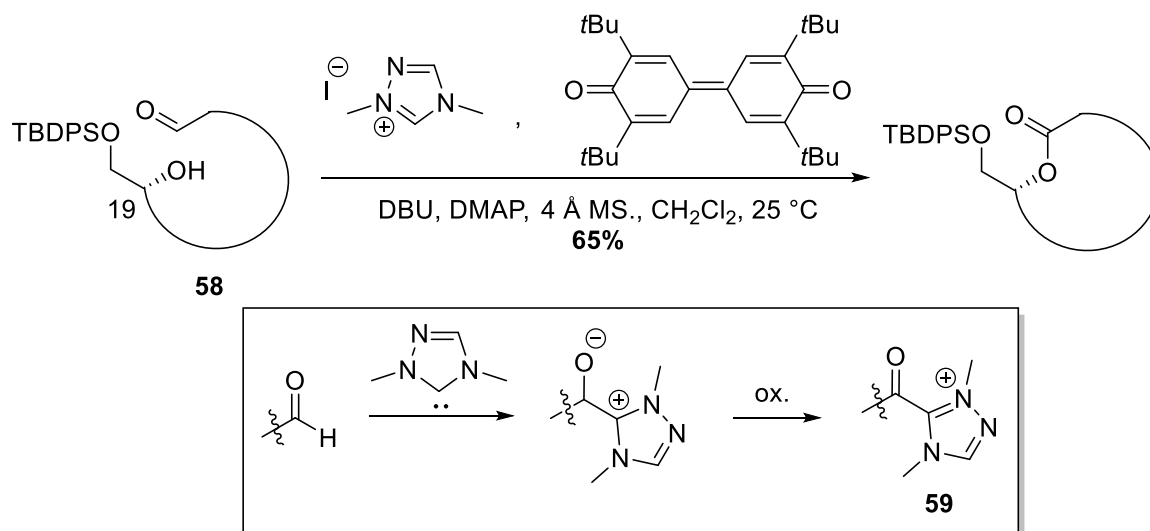
While the conjugated diene moiety is commonly made by Horner-Wadsworth-Emmons or Wittig reactions, in Yun's synthesis a Suzuki cross-coupling reaction was used (Scheme 1.16).⁶⁴ Formation of a cyclic boronic acid **55** from boronate **56** was achieved by [1,3]-transposition of the allylic oxygen.⁶⁷ The cyclic boronic acid **55** then underwent a Pd-mediated Suzuki reaction to provide the precursor for macrocyclization by RCM, *viz.* **57**. Despite the

complexity of functional groups in the structure, the two steps proceeded with a satisfactory combined yield of 51%.



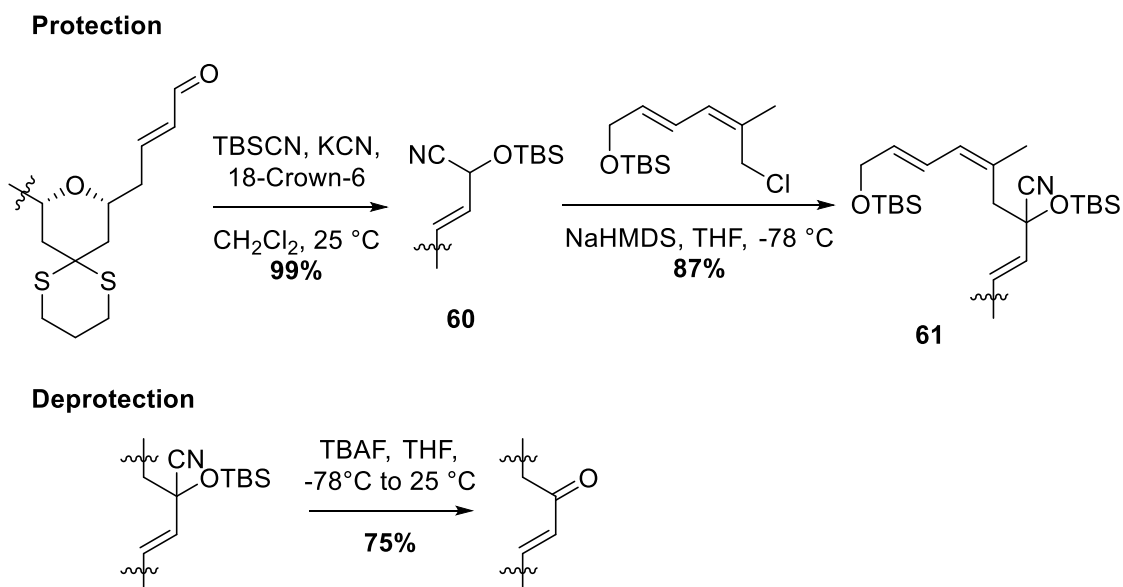
Scheme 1.16: Yun's Suzuki reaction.

Hong's *N*-heterocyclic carbene (NHC)-catalyzed oxidative macrolactonization is also quite unique (**Scheme 1.17**).⁶⁵ In this interesting redox process, the aldehyde in **58** is activated by nucleophilic addition of the NHC formed by deprotonation of triazonium, and then oxidized to acyl azolium ion (**59**) by 3,3',5,5'-tetra-*tert*-butyl-diphenylquinone (inset box). It was observed that, without *N,N*-dimethylaminopyridine (DMAP), a very low yield was obtained for this reaction, thus activation of the carbonyl by DMAP may be required for the addition of NHC.



Scheme 1.17: Hong's macrolactonization.

Hong's synthesis included the protection of C7 ketone with TBS-cyanide (**Scheme 1.18**).⁶⁵ The TBS-protected cyanohydrin **60**, upon deprotonation at the geminally substituted carbon, serves as an acyl anion equivalent to achieve α -alkylation with the C1-C6 fragment. An excellent yield of 86% was obtained over two steps to produce **61**. Conveniently, the protected cyanohydrin was inert to several subsequent transformations, and was later deprotected to afford the ketone after macrocyclization in a good yield (75%).



Scheme 1.18: Lee's TBSCN protection and deprotection.

1.6 Analogue studies

Although the total syntheses of zampanolide (**19**) and dactylolide (**20**) have been hotly contested, not many analogues have been reported. All of the analogues were reported before the publication of Field's paper that describes the covalent binding of (-)-zampanolide (**19**) and (-)-**20** to β -tublin,⁴⁴ and the main purpose for analogue formation was to perform structure-activity relationship (SAR) studies by determining the regions in the molecule that are important for its cytotoxicity. The structural similarity of **19** and **20** means that they can be considered as analogues of each other, and the fact that (-)-**19** is about one thousand-fold more potent than **20** suggests that both the *N*-acyl hemiaminal side-arm and the configuration of the macrolide are crucial to its activity.

The first unnatural analogue was published by Ding and Jennings, and they concentrated on altering the absolute configuration of the macrolide. Their synthesized (-)-**20** displayed slightly more potent cytotoxicity than (+)-**20**,⁶³ but it is still not comparable with (-)-zampanolide (**19**) (Table 1.3). This result confirmed the importance of the side-arm for the cytotoxicity of zampanolide (**19**).

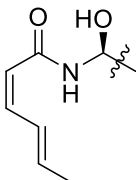
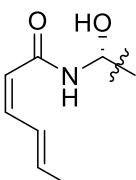
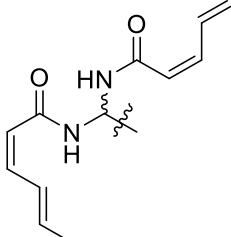
Table 1.3: IC₅₀ and GI values of (-)-zampanolide (**19**), (-)- and (+)-dactylolide (**20**).^{41,43,45,63}

Cell line	(-)-zampanolide (19)	(-)-dactylolide (20)	(+)-dactylolide (20) ^c
A549 (lung)	3.2 nM ^a	301 nM ^a	
HCT116 (colon)	7.2 nM ^a	0.133 µg/mL (GI ₅₀) ^b	
MCF-7 (breast)	6.5 nM ^a	0.076 µg/mL (GI ₅₀) ^b	
SK-OV-3 (ovary)		1.8 µg/mL (GI ₅₀) ^b	3.2 µg/mL (GI ₅₀) ^c
L1210 (leukemia)			3.2 µg/mL (GI ₄₀) ^c

^a Methylene blue staining, IC₅₀ value; ^b MTT assay, GI₅₀ value; ^c XTT assay, and GI value with inhibition percentage indicated.

The next two analogues were side products obtained from the CSA-catalyzed aza-aldol reaction in Uenishi's total synthesis of (-)-zampanolide (**19**).⁴⁶ One of them is the C20 epimer of (-)-zampanolide (**48**), which is 10-fold less active than (-)-zampanolide (**19**) (Table 1.4). The other one is the disubstitution product (**47**), which is 500-fold less active. These two analogues provided some information about the importance of the side-arm. It was suggested that the stereochemistry at C20 has some significance in the cytotoxicity, and a bulkier group at C20 was not favorable.

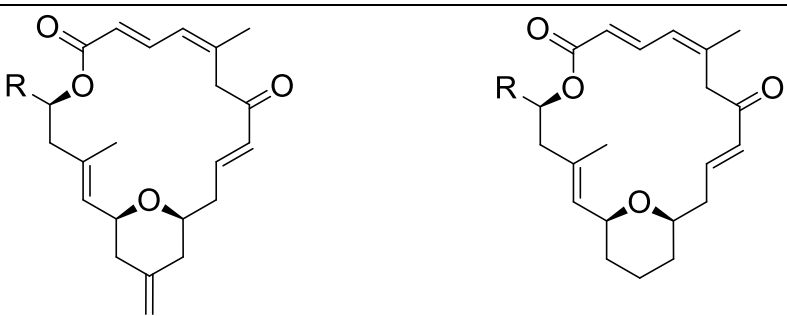
Table 1.4: IC₅₀ values^a (nM) of Uenishi's analogues.

Cell line			
	(-)-zampanolide (19)	C20 epimer (48)	Disubstitution product (47)
SKM-1 (leukemia)	1.1	10	490
U937 (lymphoma)	2.9	27	950

^a MTT assay.

Another study of analogues used (-)-dactyloide (**20**) as a model, in order to study the requirement of both the carbonyl at C20 and the methylene substituent on the tetrahydrofuran ring.⁶² Four analogues were produced and studied by Altmann *et al.* (**Table 1.5**). By comparing the IC₅₀ values of compounds **20** and **63**, it can be seen that removal of the methylene at C13 from **20** has little effect on the inhibition concentration, if anything, enhancing it by 0.5 to 1.5 fold. The effect of a hydroxyl group at C20 is not clear. While **62** displayed a lower inhibitory concentration against cell lines A549 and MCF-7, the cytotoxicity against HCLT116 was slightly increased. In comparison, analogue **64**, having both no *exo*-cyclic methylene and a hydroxyl group improved on the cytotoxicity of **20**.

Table 1.5: IC₅₀ values^a (nM) of compounds **20** to **64**.

				
Cell line	20	62	63	64
	R = CHO	R = CH ₂ OH	R = CHO	R = CH ₂ OH
A549 (lung)	301.5	149.0	127.5	189.0
MCF-7 (breast)	247.6	68.0	106.0	114.4
HCLT116 (colon)	210.4	249.5	155.8	74.1

^a MTT assay.

1.7 Efficiency of total synthesis: linchpin synthesis

In recent years, chemists have placed increasing importance on chemical efficiency and the “greenness” of a chemical process. Many renowned chemists have published accounts on different aspects of this matter,⁶⁸⁻⁷³ which Anastas and Eghbali summarized as the 12 principles of green chemistry. Poliakoff *et. al.* further concentrated the 12 principles as the acronym “PRODUCTIVELY” (**Figure 1.11**).⁷⁴⁻⁷⁶ Synthetic chemists have also envisaged better chemical efficiency in total synthesis. Trost developed the concept of atom economy in 1995,⁶⁹ and Nicolaou published an account, “Tandem reactions, cascade sequences and biomimetic strategies in total synthesis” in 2003, which illustrated the use of these methods to reduce the number of synthetic steps, increase yields and minimize the amount of waste.⁷⁰ In 2008, Wender introduced the function-oriented synthesis, where simplified analogues of complex natural products were designed to retain the functionalities important for bioactivity, while

reducing the synthetic effort and increasing efficiency.⁷⁷ Following these concepts, many syntheses of natural products with excellent efficiency have been developed.⁷⁸

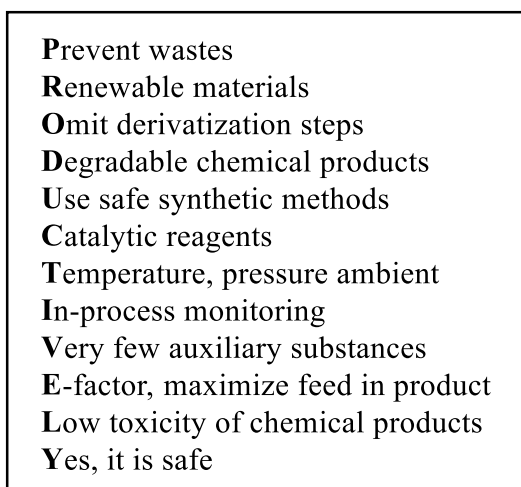
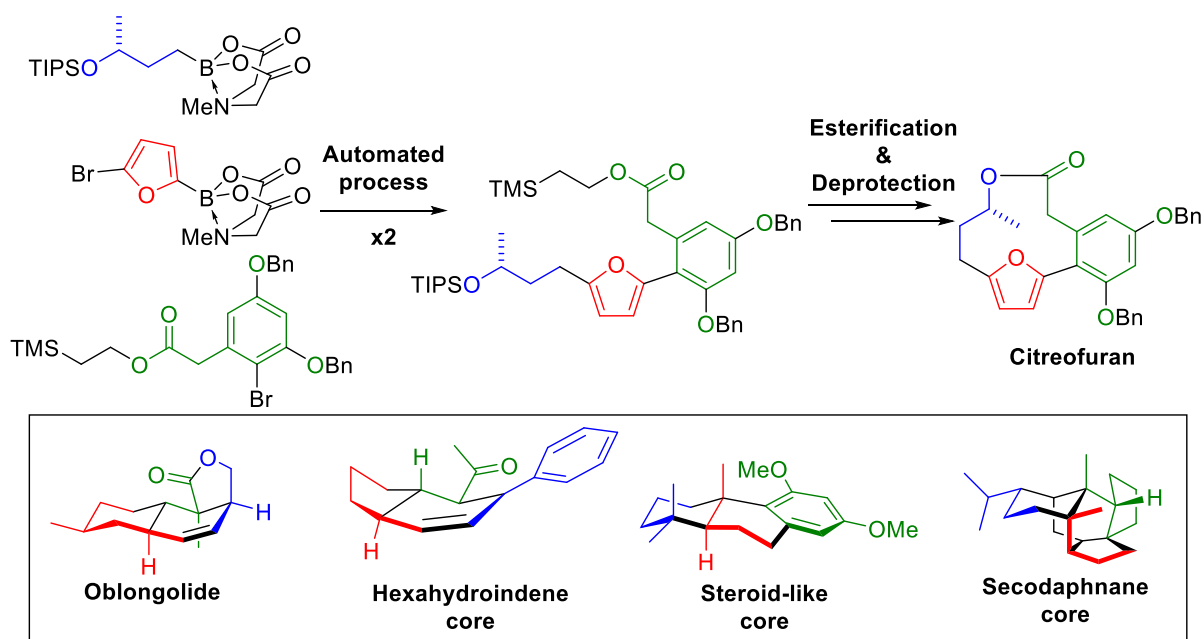


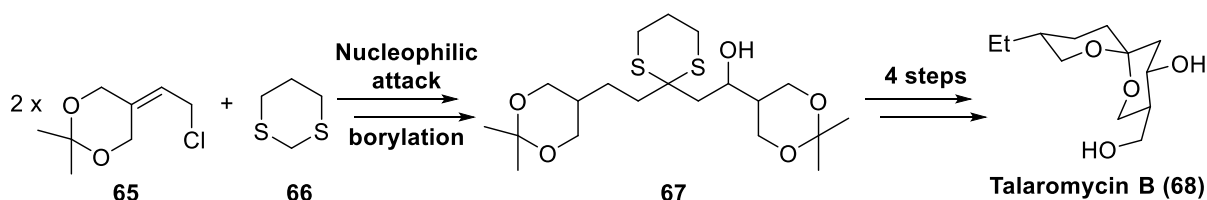
Figure 1.11: 12 principles of green chemistry.

One of the most frequently considered aspects of multistep syntheses is the convergence of the sequence. While in a linear synthesis, small building blocks are assembled in sequential order, a convergent synthesis builds larger fragments from the building blocks, and joins the fragments at a later stage. Linear synthesis has its own advantages, especially for highly repetitive molecules with well-established and reliable chemistry, in which case the synthesis can be automated. Examples are the routinely used peptide⁷⁹⁻⁸⁴ and oligonucleotide⁸⁵⁻⁸⁷ synthesizers, and the recent development of a small molecules synthesizer by Burke. Burke's initial study claimed that, with an iterative Suzuki-Miyaura reaction and 12 alkene-based building blocks, most of the polyene natural products can be made by an automated or semi-automated synthesis.⁸⁸ The potential of expanding this process to more areas of natural product synthesis was then explored. This library of building blocks, now known as *N*-methyliminodiacetic acid (MIDA) boronates, has been extended to include aryl, alkyl, alkynyl, and cyclic functionalities and a list of over 160 MIDA boronates are commercially available. With these building blocks, Burke's group produced precursors that can be converted to structures such as polycyclic natural products in a few steps (**Scheme 1.19**).⁸⁹



Scheme 1.19: Burke's semi-automated syntheses of natural products.⁸⁹

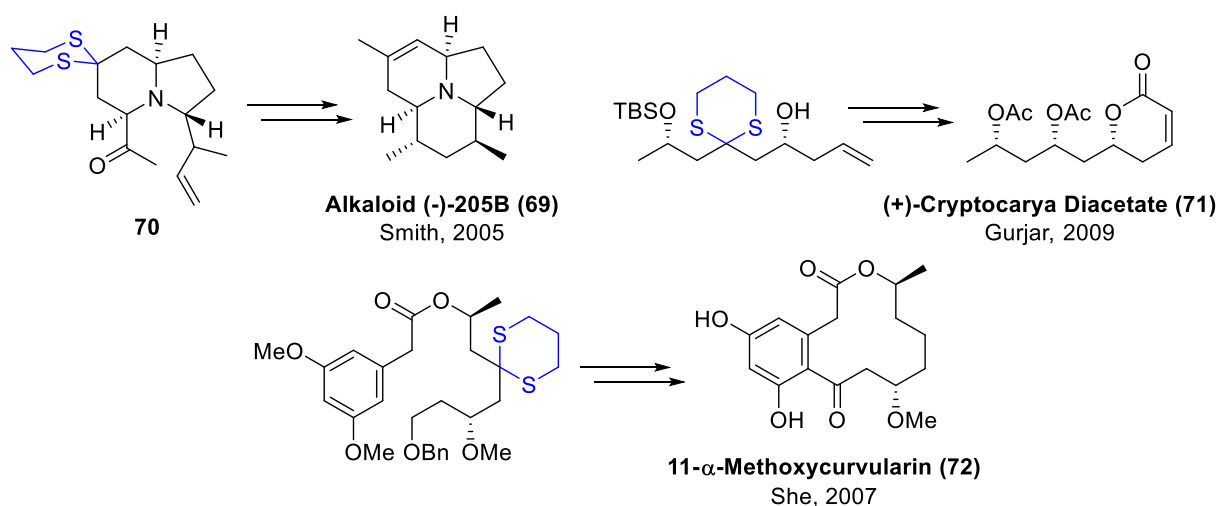
For complex and diversified structures, convergent synthesis has more advantages: shortened longest linear sequence; comparably better yield; easier diversification. This strategy has been widely applied to the synthesis of dendrons and dendrimers,^{90,91} polycyclic ethers⁹² and alkaloid natural products⁹³⁻⁹⁹. One useful synthetic tool in convergent synthesis of natural product is the use of "linchpin".¹⁰⁰⁻¹⁰⁴ The term "linchpin" was first used for total synthesis in 1983, to describe the use of the dithiane (**66**) to link two 5-carbon units in the form of the allylic chloride **65**, producing the 11-carbon precursor **67** of the spiroketal natural product **68** (Scheme 1.20).¹⁰⁵



Scheme 1.20: Use of a dithiane linchpin in the total synthesis of talaromycin B (**68**).

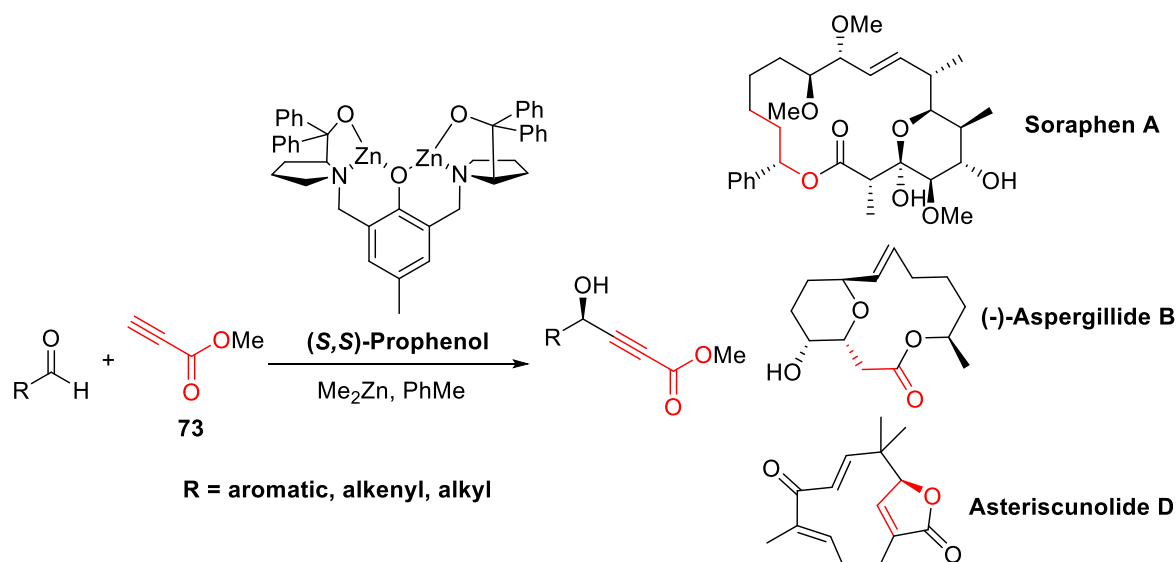
This linchpin approach is a crafty strategy for total syntheses: linking two fragments with a small fragment is a good way to build up molecular weight fast. Chemists have developed various small fragments to serve as linchpins. Dithiane has been proven to be a valuable one-

carbon linchpin. Not only does the acidic methylene facilitate nucleophilic addition, dithiane is often used as a protecting group for carbonyls, thereby providing easy access to carbonyls in the product; alternatively, it can be simply removed reductively by desulfurization. In Smith's synthesis of alkaloid (-)-205B (**69**), the dithiane linchpin was used to form the linear precursor of the di-cyclic product **70** (Scheme 1.21). At a late stage, the dithiane provided access to the tri-substituted alkene upon deprotection to a ketone, Wittig reaction and bond migration.¹⁰⁶ Dithiane linchpin has also been used in the synthesis of small and macrocyclic lactones, for example (+)-cryptocarya diacetate (**71**) and 11- α -methoxycurvularin (**72**). After assisting the construction of larger fragments, the dithiane was converted to an acetate in **71** and simply removed in **72**.^{107,108}



Scheme 1.21: Dithiane in natural product syntheses.¹⁰⁶⁻¹⁰⁸

Unlike dithiane, the majority of the linchpins are bifunctional small fragments. The design of linchpins is often tied with advancement of methodology. With the development of the Zn/Prophenol-catalyzed alkynylation of aldehyde by Trost, methyl propiolate (**73**) has become a useful linchpin (Scheme 1.22).¹⁰⁹ Alkynylation is a powerful way to form C-C bonds, and the resulting propargylic alcohol is also highly versatile synthetically. The ester end can either be saponified to a carboxylic acid or reduced to an alcohol or aldehyde, all of which are well-established synthetic handles for further elaboration. Using this methodology, Trost's group has successfully synthesized several natural products including soraphen A,¹⁰³ aspergillide B¹⁰¹ and asteriscunolide D.¹¹⁰



Scheme 1.22: Trost's asymmetric alkynylation and examples in natural product synthesis.

Another linchpin that relies on alkyne chemistry is a phosphonium salt connected to a silylated alkyne (**74**), where the phosphonium is set up for a Wittig reaction, and the silylated alkyne is readily deprotected for further connection through alkynylation (**Figure 1.12**). The potential of this linchpin hasn't been explored fully, however, it has been used to produce *E,E*-dienes upon reduction of alkyne, which further went through a Diels-Alder cyclization to produce the octahydronaphthalene structure in Marshall's kijanolide subunit (**75**) synthesis.¹¹¹ Later, Rizzacasa's group used this linchpin **74** to produce the *E,Z,E,E*-tetraene motif in resolvin D2 (**76**).¹¹²

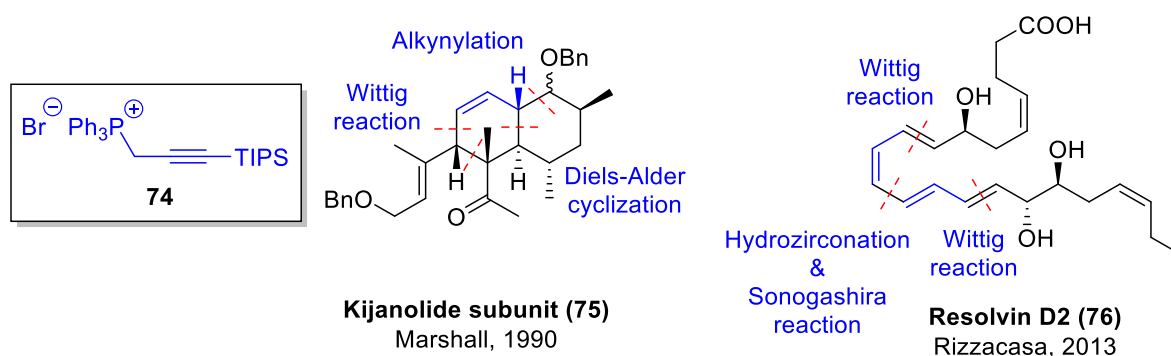


Figure 1.12: Phosphonium salt **74** in natural product synthesis.

Although the term “linchpin” is not very often used in literature, linchpin-type strategies are well-established in natural product synthesis and relevant to this thesis, in macrolactone synthesis. Looking at several recently published syntheses of macrolactones, many of them contain linchpin-type fragments (**Figure 1.13**).¹¹³⁻¹¹⁶ However, the assembly of fragments with the aid of a linchpin often takes multiple steps, because protection, deprotection, and/or conversion of functional groups are often required. This does not utilize the full potential efficiency of the linchpin strategy and, arguably, is not truly a linchpin strategy. An efficient linchpin should be easy to prepare, have reasonable stability, and require mild reaction conditions that are compatible to various functional groups. Furthermore, it should ideally react with the fragments in a multi-component fashion in a single step, without additional manipulation between the reactions at each reacting site of the linchpin. In this project, a three-component linchpin method that meets the above criteria was explored and applied to the synthesis of a major portion of the (-)-zampanolide (**19**) and the (-)-dactylolide (**20**) macrocycle after difficulty with the first generation synthetic plan, which will be described in chapter two.

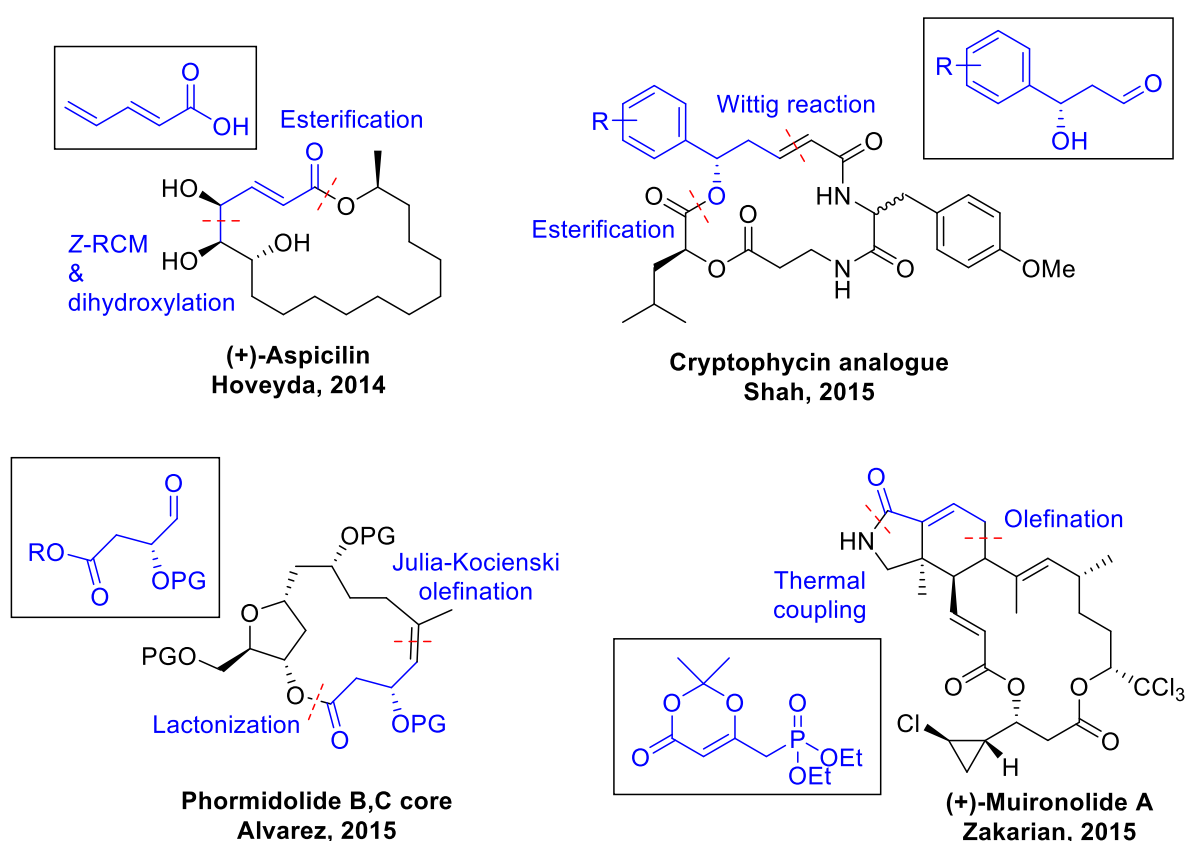


Figure 1.13: Recent examples of linchpins (in box) in total synthesis of macrolactones.

1.8 References

- (1) Bergmann, W.; Feeney, R. J. *J. Org. Chem.* **1951**, *16*, 981.
- (2) Hirata, Y.; Uemura, D. *Pure Appl. Chem.* **1986**, *58*, 701.
- (3) Dumontet, C.; Jordan, M. A. *Nat. Rev. Drug Discov.* **2010**, *9*, 587.
- (4) Bensch, K. G.; Malawista, S. E. *Nature* **1968**, *218*, 1176.
- (5) Stearns, M. E.; Wang, M.; Tew, K. D.; Binder, L. I. *J. Cell Biol.* **1988**, *107*, 2647.
- (6) Wani, M. C.; Taylor, H. L.; Wall, M. E.; Coggon, P.; McPhail, A. T. *J. Am. Chem. Soc.* **1971**, *93*, 2325.
- (7) Wani, M. C.; Horwitz, S. B. *Anti-Cancer Drug* **2014**, *25*, 482.
- (8) Schiff, P. B.; Fant, J.; Horwitz, S. B. *Nature* **1979**, *277*, 665.
- (9) Hall, N. *Chem. Commun.* **2003**, 661.
- (10) Holton, R. A.; Somoza, C.; Kim, H. B.; Liang, F.; Biediger, R. J.; Boatman, P. D.; Shindo, M.; Smith, C. C.; Kim, S.; Nadizadeh, H.; Suzuki, Y.; Tao, C.; Vu, P.; Tang, S.; Zhang, P.; Murthi, K. K.; Gentile, L. N.; Liu, J. H. *J. Am. Chem. Soc.* **1994**, *116*, 1597.
- (11) Holton, R. A.; Somoza, C.; Kim, H. B.; Liang, F.; Biediger, R. J.; Boatman, P. D.; Shindo, M.; Smith, C. C.; Kim, S.; Nadizadeh, H.; Suzuki, Y.; Tao, C.; Vu, P.; Tang, S.; Zhang, P.; Murthi, K. K.; Gentile, L. N.; Liu, J. H. *J. Am. Chem. Soc.* **1994**, *116*, 1599.
- (12) Holton, R. A.; Juo, R. R.; Kim, H. B.; Williams, A. D.; Harusawa, S.; Lowenthal, R. E.; Yogai, S. *J. Am. Chem. Soc.* **1988**, *110*, 6558.
- (13) Nicolaou, K. C.; Yang, Z.; Liu, J. J.; Ueno, H.; Nantermet, P. G.; Guy, R. K.; Claiborne, C. F.; Renaud, J.; Couladouros, E. A.; Paulvannan, K.; Sorensen, E. J. *Nature* **1994**, *367*, 630.
- (13) Ganem, B.; Franke, R. R. *J. Org. Chem.* **2007**, *72*, 3981.
- (14) Schedler, D. J. A.; Godfrey, A. G.; Ganem, B. *Tetrahedron Lett.* **1993**, *34*, 5035.
- (15) Schedler, D. J. A.; Li, J.; Ganem, B. *J. Org. Chem.* **1996**, *61*, 4115.
- (17) Yared, J. A.; Tkaczuk, K. H. R. *Drug Des. Dev. Ther.* **2012**, *6*, 371.
- (18) Juliano, R. L.; Ling, V. *Biochim. Biophys. Acta* **1976**, *455*, 152.
- (19) Debenham, P. G.; Kartner, N.; Siminovitch, L.; Riordan, J. R.; Ling, V. *Mol. Cell. Biol.* **1982**, *2*, 881.
- (20) Persidis, A. *Nature Biotechnol.* **1999**, *17*, 94.

- (21) Riordan, J. R.; Ling, V. *J. Biol. Chem.* **1979**, *254*, 2701.
- (22) Sharom, F. J. *J. Membr. Biol.* **1997**, *160*, 161.
- (23) Cole, S. P.; Bhardwaj, G.; Gerlach, J. H.; Mackie, J. E.; Grant, C. E.; Almquist, K. C.; Stewart, A. J.; Kurz, E. U.; Duncan, A. M.; Deeley, R. G. *Science* **1992**, *258*, 1650.
- (24) Borst, P.; Evers, R.; Kool, M.; Wijnholds, J. *Biochim. Biophys. Acta* **1999**, *1461*, 347.
- (25) Yoshimura, S.; Sato, B.; Kinoshita, T.; Takase, S.; Terano, H. *J. Antibiot.* **2000**, *53*, 615.
- (26) Sato, B.; Nakajima, H.; Hori, Y.; Hino, M.; Hashimoto, S.; Terano, H. *J. Antibiot.* **2000**, *53*, 204.
- (27) Sato, B.; Muramatsu, H.; Miyauchi, M.; Hori, Y.; Takase, S.; Hino, M.; Hashimoto, S.; Terano, H. *J. Antibiot.* **2000**, *53*, 123.
- (28) Edler, M. C.; Buey, R. M.; Gussio, R.; Marcus, A. I.; Vanderwal, C. D.; Sorensen, E. J.; Diaz, J. F.; Giannakakou, P.; Hamel, E. *Biochemistry* **2005**, *44*, 11525.
- (29) Buey, R. M.; Calvo, E.; Barasoain, I.; Pineda, O.; Edler, M. C.; Matesanz, R.; Cerezo, G.; Vanderwal, C. D.; Day, B. W.; Sorensen, E. J.; Lopez, J. A.; Andreu, J. M.; Hamel, E.; Diaz, J. F. *Nature Chem. Biol.* **2007**, *3*, 117.
- (30) Chen, Z.-l.; Wang, B.-D.; Chen, M.-Q. *Tetrahedron Lett.* **1987**, *28*, 1673.
- (31) Chen, Z.-L.; Wang, B.-D.; Shen, J.-H. *Phytochemistry* **1988**, *27*, 2999.
- (32) Li, Z.; Upadhyay, V.; DeCamp, A. E.; DiMichele, L.; Reider, P. J. *Synthesis* **1999**, 1453.
- (33) Shen, J.; Chen, Z.; Gao, Y. *Chin. J. Chem.* **1991**, *9*, 92.
- (34) Shen, J.; Chen, Z.; Gao, Y. *Phytochemistry* **1996**, *42*, 891.
- (35) Yang, J.-Y.; Zhao, R.-H.; Chen, C.-X.; Ni, W.; Teng, F.; Hao, X.-J.; Liu, H.-Y. *Helv. Chim. Acta* **2008**, *91*, 1077.
- (36) Mühlbauer, A.; Seip, S.; Nowak, A.; Tran, V. S. *Helv. Chim. Acta* **2003**, *86*, 2065.
- (37) Huang, Y.; Liu, J.-K.; Mühlbauer, A.; Henkel, T. *Helv. Chim. Acta* **2002**, *85*, 2553.
- (38) Risinger, A. L.; Jackson, E. M.; Polin, L. A.; Helms, G. L.; LeBoeuf, D. A.; Joe, P. A.; Hopper-Borge, E.; Luduena, R. F.; Kruh, G. D.; Mooberry, S. L. *Cancer Res.* **2008**, *68*, 8881.
- (39) Tinley, T. L.; Randall-Hlubek, D. A.; Leal, R. M.; Jackson, E. M.; Cessac, J. W.; Quada, J. C., Jr.; Hemscheidt, T. K.; Mooberry, S. L. *Cancer Res.* **2003**, *63*, 3211.
- (40) Risinger, A. L.; Riffle, S. M.; Lopus, M.; Jordan, M. A.; Wilson, L.; Mooberry, S. L. *Molec. Cancer* **2014**, *13*, 41.
- (41) Tanaka, J.; Higa, T. *Tetrahedron Lett.* **1996**, *37*, 5535.
- (42) Smith, A. B.; Safonov, I. G.; Corbett, R. M. *J. Am. Chem. Soc.* **2002**, *124*, 11102.

- (43) Field, J. J.; Singh, A. J.; Kanakkanthara, A.; Halafihi, T.; Northcote, P. T.; Miller, J. H. *J. Med. Chem.* **2009**, *52*, 7328.
- (44) Field, J. J.; Pera, B.; Calvo, E.; Canales, A.; Zurwerra, D.; Trigili, C.; Rodriguez-Salarichs, J.; Matesanz, R.; Kanakkanthara, A.; Wakefield, J.; Singh, J.; Jimenez-Barbero, J.; Northcote, P.; Miller, J. H.; Lopez, J. A.; Hamel, E.; Barasoain, I.; Altmann, K.-H.; Diaz, J. F. *Chem. Biol.* **2012**, *19*, 686.
- (45) Cutignano, A.; Bruno, I.; Bifulco, G.; Casapullo, A.; Debitus, C.; Gomez-Paloma, L.; Riccio, R. *Eur. J. Org. Chem.* **2001**, 775.
- (46) Uenishi, J.; Iwamoto, T.; Tanaka, J. *Org. Lett.* **2009**, *11*, 3262.
- (47) Chen, Q. H.; Kingston, D. G. *Nat. Prod. Rep.* **2014**, *31*, 1202.
- (48) Prota, A. E.; Bargsten, K.; Zurwerra, D.; Field, J. J.; Diaz, J. F.; Altmann, K. H.; Steinmetz, M. O. *Science* **2013**, *339*, 587.
- (49) Liao, S. Y.; Mo, G. Q.; Chen, J. C.; Zheng, K. C. *J. Mol. Model.* **2014**, *20*, 2070.
- (50) Smith, A. B.; Safonov, I. G.; Corbett, R. M. *J. Am. Chem. Soc.* **2001**, *123*, 12426.
- (51) Hoye, T. R.; Hu, M. *J. Am. Chem. Soc.* **2003**, *125*, 9576.
- (52) Ghosh, A. K.; Cheng, X. *Org. Lett.* **2011**, *13*, 4108.
- (53) Zurwerra, D.; Glaus, F.; Betschart, L.; Schuster, J.; Gertsch, J.; Ganci, W.; Altmann, K. H. *Chem.-Eur. J.* **2012**, *18*, 16868.
- (54) Petasis, N. A.; Lu, S. P. *Tetrahedron Lett.* **1996**, *37*, 141.
- (55) Kelsi, P. S. *Organic reactions and their mechanisms*; 2nd ed.; Tunbridge Wells, UK: New Age Science, 1996.
- (56) Aubele, D. L.; Wan, S. Y.; Floreancig, P. E. *Angew. Chem. Int. Ed.* **2005**, *44*, 3485.
- (57) Ding, F.; Jennings, M. P. *Org. Lett.* **2005**, *7*, 2321.
- (58) Akiyama, T. *Chem. Rev.* **2007**, *107*, 5744.
- (59) Smith, A. B.; Safonov, I. G. *Org. Lett.* **2002**, *4*, 635.
- (60) Sanchez, C. C.; Keck, G. E. *Org. Lett.* **2005**, *7*, 3053.
- (61) Louis, I.; Hungerford, N. L.; Humphries, E. J.; McLeod, M. D. *Org. Lett.* **2006**, *8*, 1117.
- (62) Zurwerra, D.; Gertsch, J.; Altmann, K. H. *Org. Lett.* **2010**, *12*, 2302.
- (63) Ding, F.; Jennings, M. P. *J. Org. Chem.* **2008**, *73*, 5965.
- (64) Yun, S. Y.; Hansen, E. C.; Volchkov, I.; Cho, E. J.; Lo, W. Y.; Lee, D. *Angew. Chem. Int. Ed.* **2010**, *49*, 4261.
- (65) Lee, K.; Kim, H.; Hong, J. Y. *Angew. Chem. Int. Ed.* **2012**, *51*, 5735.
- (66) Dossetter, A. G.; Jamison, T. F.; Jacobsen, E. N. *Angew. Chem. Int. Ed.* **1999**, *38*, 2398.
- (67) Hansen, E. C.; Lee, D. S. *J. Am. Chem. Soc.* **2006**, *128*, 8142.

- (68) Sheldon, R. A. *Chem. Commun.* **2008**, 3352.
- (69) Trost, B. M. *Angew. Chem. Int. Ed.* **1995**, 34, 259.
- (70) Nicolaou, K. C.; Montagnon, T.; Snyder, S. A. *Chem. Commun.* **2003**, 551.
- (71) Mermolia, W.; Steinkam, J.; Vogel, K. *Nachrichtentech. Z.* **1969**, 22, 133.
- (72) Curzons, A. D.; Constable, D. J. C.; Mortimer, D. N.; Cunningham, V. L. *Green Chem.* **2001**, 3, 1.
- (73) Sheldon, R. A. *Pure Appl. Chem.* **2000**, 72, 1233.
- (74) Kuntiyong, P.; Lee, T. H.; Kranemann, C. L.; White, J. D. *Org. Biomol. Chem.* **2012**, 10, 7884.
- (75) Tang, S. Y.; Bourne, R. A.; Poliakoff, M.; Smith, R. L. *Green Chem.* **2008**, 10, 268.
- (76) Tang, S. L. Y.; Smith, R. L.; Poliakoff, M. *Green Chem.* **2005**, 7, 761.
- (77) Wender, P. A.; Verma, V. A.; Paxton, T. J.; Pillow, T. H. *Acco. Chem. Res.* **2008**, 41, 40.
- (78) Newhouse, T.; Baran, P. S.; Hoffmann, R. W. *Chem. Soc. Rev.* **2009**, 38, 3010.
- (79) Gauthier, M. A.; Klok, H. A. *Chem. Commun.* **2008**, 2591.
- (80) Hurevich, M.; Seeberger, P. H. *Chem. Commun.* **2014**, 50, 1851.
- (81) Lukas, T. J.; Prystowsky, M. B.; Erickson, B. W. *Proc. Natl. Acad. Sci. USA* **1981**, 78, 2791.
- (82) Merrifield, R. B. *Science* **1965**, 150, 178.
- (83) Merrifield, R. B.; Stewart, J. M. *Nature* **1965**, 207, 522.
- (84) Merrifield, R. B. *Endeavour* **1965**, 24, 3.
- (85) Joshi, R.; Jha, D.; Su, W.; Engelmann, J. *J. Pept. Sci.* **2010**, 17, 8.
- (86) Pfundheller, H. M.; Sorensen, A. M.; Lomholt, C.; Johansen, A. M.; Koch, T.; Wengel, J. *Methods Mol. Biol.* **2005**, 288, 127.
- (87) Caruthers, M. H. *Science* **1985**, 230, 281.
- (88) Woerly, E. M.; Roy, J.; Burke, M. D. *Nat. Chem.* **2014**, 6, 484.
- (89) Lang, R. W.; Hansen, H. J. *Helv. Chim. Acta* **1980**, 63, 438.
- (90) Konkolewicz, D.; Monteiro, M. J.; Perrier, S. *Macromolecules* **2011**, 44, 7067.
- (91) Grayson, S. M.; Frechet, J. M. J. *Chem. Rev.* **2001**, 101, 3819.
- (92) Fuwa, H.; Sasaki, M. *Curr. Opin. Drug Discov.* **2007**, 10, 784.
- (93) Reddy, B. V. S.; Babu, R. A.; Reddy, B. J. M.; Sridhar, B.; Murthy, T. R.; Pranathi, P.; Kalivendi, S. V.; Rao, T. P. *RSC Adv.* **2015**, 5, 27476.
- (94) Markad, S. B.; Argade, N. P. *Org. Lett.* **2014**, 16, 5470.

- (95) Borrero, N. V.; DeRatt, L. G.; Ferreira Barbosa, L.; Abboud, K. A.; Aponick, A. *Org. Lett.* **2015**, *17*, 1754.
- (96) Liu, X. Y.; Chen, D. Y. *Angew. Chem. Int. Ed.* **2014**, *53*, 924.
- (97) Chen, R.; Liu, H.; Chen, X. *J. Nat. Prod.* **2013**, *76*, 1789.
- (98) Bonazzi, S.; Cheng, B.; Wzorek, J. S.; Evans, D. A. *J. Am. Chem. Soc.* **2013**, *135*, 9338.
- (99) Chiba, H.; Sakai, Y.; Ohara, A.; Oishi, S.; Fujii, N.; Ohno, H. *Chemistry* **2013**, *19*, 8875.
- (100) Trost, B. M.; Michaelis, D. J.; Malhotra, S. *Org. Lett.* **2013**, *15*, 5274.
- (101) Trost, B. M.; Bartlett, M. J. *Org. Lett.* **2012**, *14*, 1322.
- (102) Trost, B. M.; Papillon, J. P. N. *J. Am. Chem. Soc.* **2004**, *126*, 13618.
- (103) Trost, B. M.; Sieber, J. D.; Qian, W.; Dhawan, R.; Ball, Z. T. *Angew. Chem. Int. Ed.* **2009**, *48*, 5478.
- (104) Trost, B. M.; Weiss, A. H. *Adv. Synth. Catal.* **2009**, *351*, 963.
- (105) Evans, D. A.; Kim, A. S.; Metternich, R.; Novack, V. J. *J. Am. Chem. Soc.* **1998**, *120*, 5921.
- (106) Smith, A. B., 3rd; Kim, D. S. *Org. Lett.* **2005**, *7*, 3247.
- (107) Gurjar, M. K.; Raghupathi, N.; Chorghade, M. S. *Heterocycles* **2009**, *77*, 945.
- (108) Liang, Q.; Sun, Y.; Yu, B.; She, X.; Pan, X. *J. Org. Chem.* **2007**, *72*, 9846.
- (109) Trost, B. M.; Bartlett, M. J.; Weiss, A. H.; Jacobi von Wangelin, A.; Chan, V. S. *Chem.-Eur. J.* **2012**, *18*, 16498.
- (110) Gharpure, S. J.; Shelke, Y. G.; Reddy, S. R. B. *RSC Adv.* **2014**, *4*, 46962.
- (111) Marshall, J. A.; Salovich, J. M.; Shearer, B. G. *J. Org. Chem.* **1990**, *55*, 2398.
- (112) Fortier-McGill, B.; Toader, V.; Reven, L. *Macromolecules* **2011**, *44*, 2755.
- (113) Zhang, H. M.; Yu, E. C.; Torker, S.; Schrock, R. R.; Hoveyda, A. H. *J. Am. Chem. Soc.* **2014**, *136*, 16493.
- (114) Kumar, A.; Kumar, M.; Sharma, S.; Guru, S. K.; Shushan, S.; Shah, B. A. *Eur. J. Med. Chem.* **2015**, *93*, 55.
- (115) Lorente, A.; Gil, A.; Fernandez, R.; Cuevas, C.; Albericio, F.; Alvarez, M. *Chem.-Eur. J.* **2015**, *21*, 150.
- (116) Xiao, Q.; Young, K.; Zakarian, A. *J. Am. Chem. Soc.* **2015**, *137*, 5907.

Chapter 2: Aims and preliminary work

2.1 Aims

The aim of this project is to advance towards the synthesis of (-)-zampanolide (**19**) and novel analogues in order to undertake structure-activity relationship (SAR) studies. Guided by the protein binding studies of (-)-zampanolide (**19**)¹ and the thus-far published analogues,²⁻⁴ the design of the analogues has been focused on alterations of the side-arm, pendant methyl groups and the pyran motif (**Figure 2.1**). The importance of the side-arm for binding to tubulin has been suggested by the different cytotoxicities of **19** and (-)-dactylolide (**20**), and the interaction with protein was confirmed by HRMS and X-ray crystallography studies. A range of side-arm alterations was explored prior to this project, including the synthesis of aromatic, alkyl and alternative alkenyl amide moieties. The sequential removal of the methyl groups on the macrocycle is proposed in order to facilitate the synthesis, which might also reduce steric hindrance and improve the affinity of **19** for the microtubule binding site. As for the pyran modifications, previous analogue studies by Altmann have shown that the removal of the *exo*-methylene has little effect on the cytotoxicity of (-)-**20**.⁴ Replacement of the *exo*-methylene with a carbonyl or hydroxyl group at this position might cause conformational change or

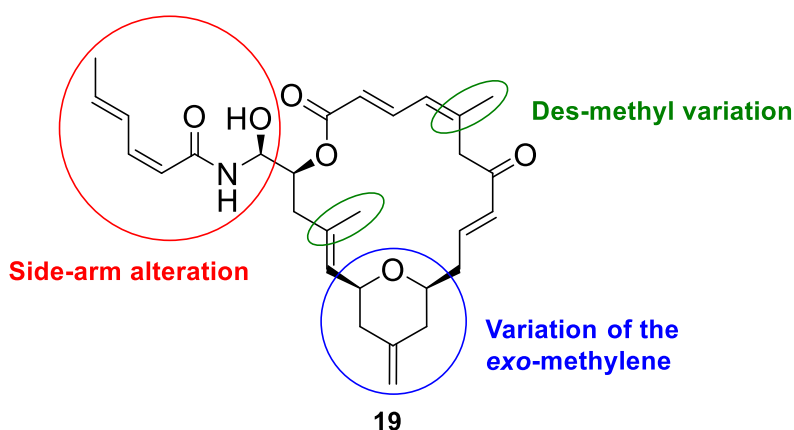


Figure 2.1: Proposed sites of modification.

encourage hydrogen bonding interactions, which could enhance the binding to the protein. In addition, monocyclic compounds lacking the pyran ring and with an hydroxy group in place of

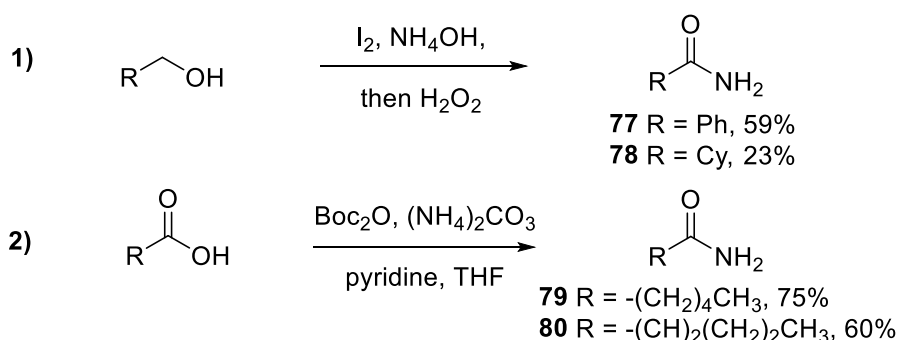
the pyran ether would certainly result in major conformational change. Nonetheless, if the microtubule activity can be sustained, a monocyclic analogue would significantly simplify the synthesis.

2.2 Preliminary work

The work of this thesis builds upon the preliminary work done by previous group members Samuel Ting and Claudia Gray. Ting's focus was on exploring synthetic routes to fragments making up the macrocyclic core,⁵ while Gray was working mostly on the synthesis of the analogue side-arms.⁶

2.2.1 Preliminary work on side-arm variants

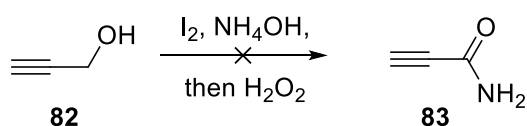
A preliminary study on the synthesis of simple amides as models of the side-arm of zampanolide (**19**) was undertaken by Claudia Gray prior to the commencement of this project (**Scheme 2.1**). The one-pot amidation of primary alcohols *via* oxidation with iodine and in the presence of ammonia, was found to provide a reasonable yield of an aromatic amide **77**, but the reaction of the saturated equivalent **78** was poor yielding (eq. 1).⁷ Therefore, a second method starting from carboxylic acids was explored, with di-*t*-butyl dicarbonate (Boc₂O) activating the acid by anhydride formation, and ammonium carbonate as a nitrogen source.⁸ This method provided a better result for the synthesis of alkyl amide **79**, and alkenyl amide **80** could also be prepared in a reasonable yield (eq. 2).



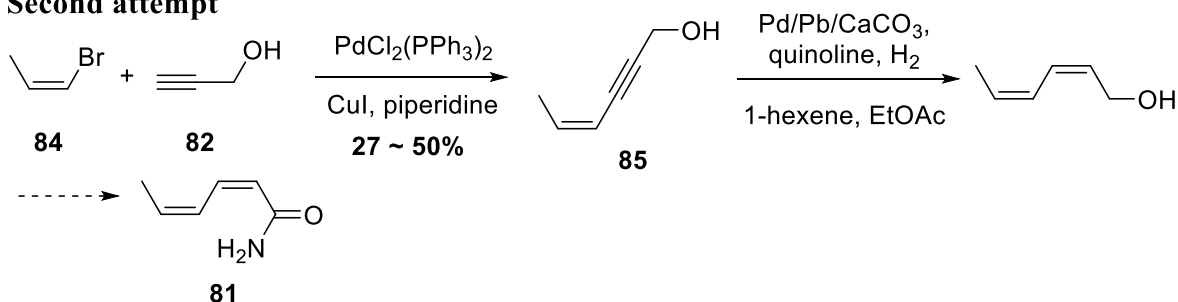
Scheme 2.1: Gray's synthesis of simple amides as models of the side-arm.

Claudia Gray also explored the synthesis of (Z,Z)-2,4-hexadienylamide (**81**) as side-arm from commercially available **82**. First, a sequence involving amidation, Sonogashira coupling⁹ and Lindlar hydrogenation was explored (**Scheme 2.2**). However, the oxidative amidation of propargyl alcohol (**82**) failed to produce the amide **83**. Reordering the sequence led to successful Sonogashira coupling of **82** and (Z)-1-bromopropene (**84**). The subsequent Lindlar hydrogenation of **85** caused some over-reduction, which was not prevented by the methods available, nor could the mixture of products be separated. Thus the subsequent amidation was not attempted.

First attempt

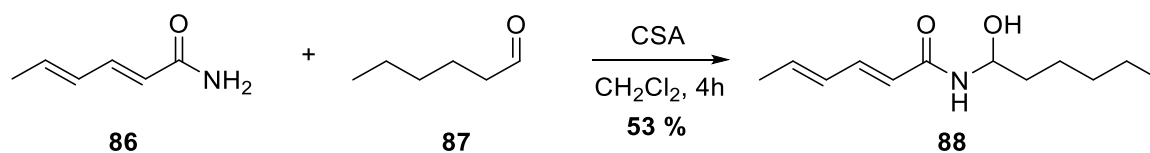


Second attempt



Scheme 2.2: Gray's attempts to synthesize (Z,Z)-2,4-hexadienylamide (**81**).

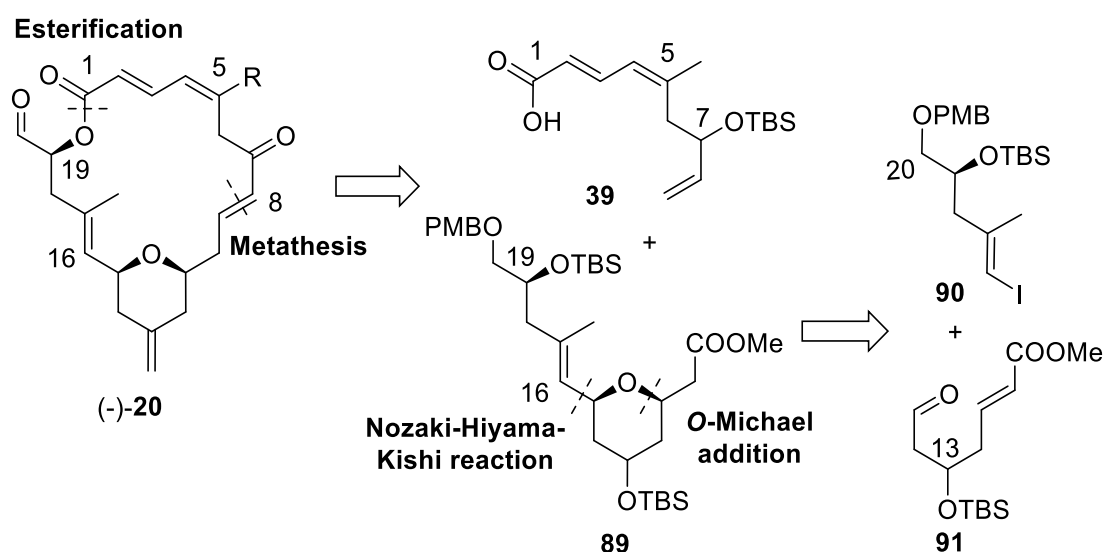
In the published total syntheses of zampanolide (**19**), reagents such as CSA, DIBAL-H, and the most successful (*S*)-TRIP have been used in aza-aldol reactions to construct *N*-acyl hemiaminal functionalities.^{2,10,11} Gray's attempt to reproduce the CSA-catalyzed aza-aldol reaction with sorbamide (**86**) as a model amide and *n*-pentanal (**87**) as a model aldehyde was successful (**Scheme 2.3**).⁶ The length of reaction was found to be crucial: a four-hour reaction produced the *N*-acyl hemiaminal **88** in 53% yield, while an overnight reaction only returned starting material in the crude reaction mixture. This was presumed to be due to the low stability of the product, as it could be sensitive to retro-aza-aldol hydrolysis.¹²



Scheme 2.3: Gray's *N*-acyl hemiaminal model reaction.

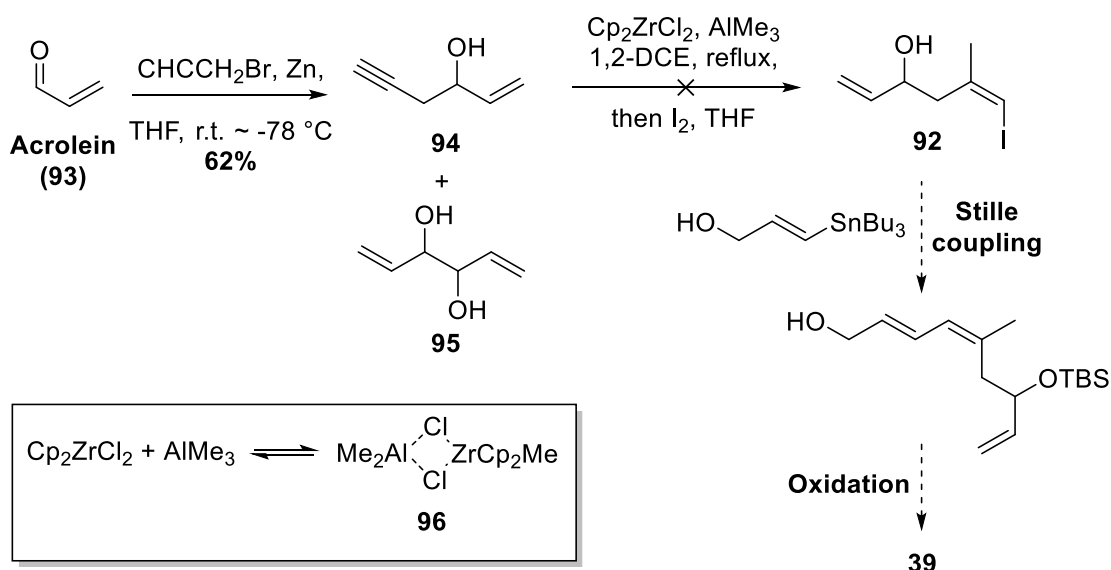
2.2.2 Preliminary work on fragment syntheses

Prior to this project, Sam Ting had investigated the synthesis of fragments of the zampanolide macrolactone ring. Ting's original retrosynthetic strategy of (-)-dactylolide (**20**) incorporated the well-established esterification at C1 and ring-closing metathesis at C8. An *O*-Michael addition was planned to synthesize the pyran in **89**, after a Nozaki-Hiyama-Kishi reaction to connect the western and southern fragments, **90** and **91** (Scheme 2.4).^{3,13,14}



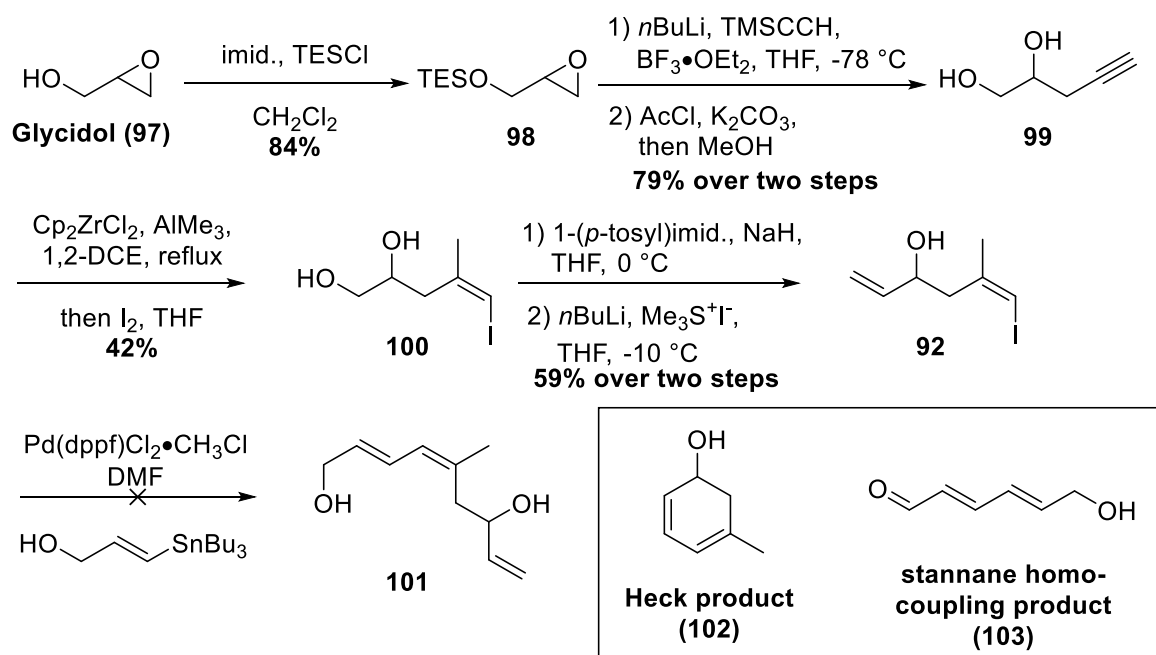
Scheme 2.4: Ting's retrosynthetic strategy.

The first synthetic route to build the northern fragment (**39**) proceeded by way of a Stille cross-coupling reaction (Scheme 2.5). Synthesis of the vinyl iodide **92**, the Stille precursor, was first attempted using acrolein (**93**) as starting material; the Barbier reaction of acrolein (**93**) proceeded with a satisfying 62% yield of **94** obtained, after a series of optimization reactions to eliminate the homocoupling by-product **95**. However, the following carboalumination¹⁵ was found to be unfruitful. This was proposed to be due to the quality of available trimethylaluminum, but the addition of excess trimethylaluminum was deemed too risky because the active aluminum-zirconium species **96** could also react with the terminal alkene.



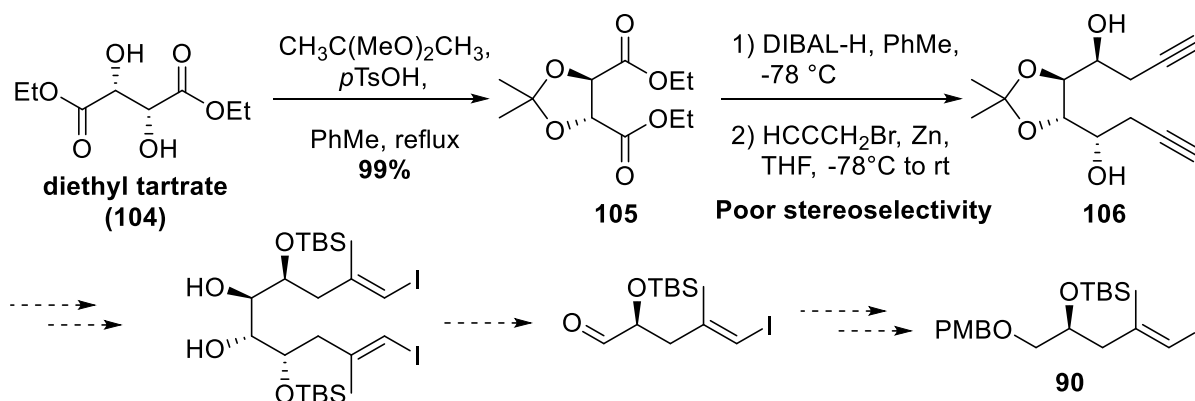
Scheme 2.5: Ting's first attempted synthesis of fragment **39**.

Ting then tried to establish the iodoalkene functional group before installation of the terminal alkene. After protecting glycidol (**97**) as the triethylsilyl (TES) ether **98**, the epoxide was opened by TMS-acetylene anion, and both of the silyl groups were then removed to produce diol **99** (Scheme 2.6). The ensuing carboalumination-iodination step progressed much more smoothly on this new substrate, leading to product **100**. The terminal alkene in **92** was subsequently installed by a Corey-Chaykovsky reaction, where the tosylated primary alcohol derived from **99** was substituted by the ylide prepared from trimethylsulfonium iodide, and underwent elimination in the presence of a base to form alkene **92**. However, when this vinyl iodide **92** was subjected to Stille coupling conditions, none of the desired diene **101** was formed. Instead, the product was a mixture of the unwanted Heck product **102**, resulting from intramolecular reaction of the vinyl iodide with the terminal alkene and the oxidized stannane homocoupled product **103**.



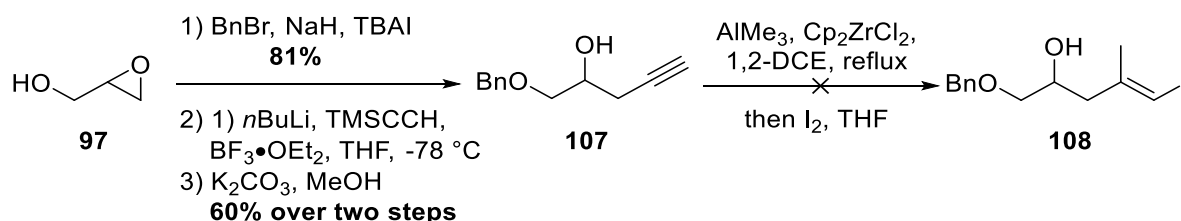
Scheme 2.6: Ting's second attempted synthesis of fragment **39**.

A strategy was planned for the synthesis of the western fragment **90**, using the existing configuration of diethyl tartrate (**104**) to provide stereocontrol at the desired chiral centre. The plan was to carry out functional group transformations at both ends simultaneously and symmetrically, and then cleave the dimer towards the end of this sequence to produce two equivalents of the desired fragment **90** (Scheme 2.7). The acetal formation and the reduction of the two esters in **105** were successful. However, this route was quickly abandoned, after insufficient stereoselectivity was obtained in propargylzinc addition to **105** to produce **106**. The best ratio of isomers was reported by Ting as 2:1, but he did not clarify the configuration of the isomers.



Scheme 2.7: Ting's first attempt to synthesize fragment **90**.

Ting then resorted to using glycidol (**97**) as a precursor in the synthesis of fragment **90**. The propargylic alcohol **107** was successfully made, but attempts to produce the vinyl iodide **108** following the same carboalumination/iodination procedure as before all failed (**Scheme 2.8**). Brief investigation into variations in temperature, solvent and order of addition did not promote the desired carboiodination.



Scheme 2.8: Ting's attempt to synthesize fragment **108** from **97**.

Because of the failed carboalumination-based synthesis of the northern fragment **39** and the difficulty in producing the NHK precursor **90**, this synthetic plan was abandoned. Modification of the northern fragment synthesis to proceed from acrolein (**93**), and employing asymmetric alkynylation in place of the NHK reaction led to the first generation retrosynthesis described in this thesis.

2.3 References

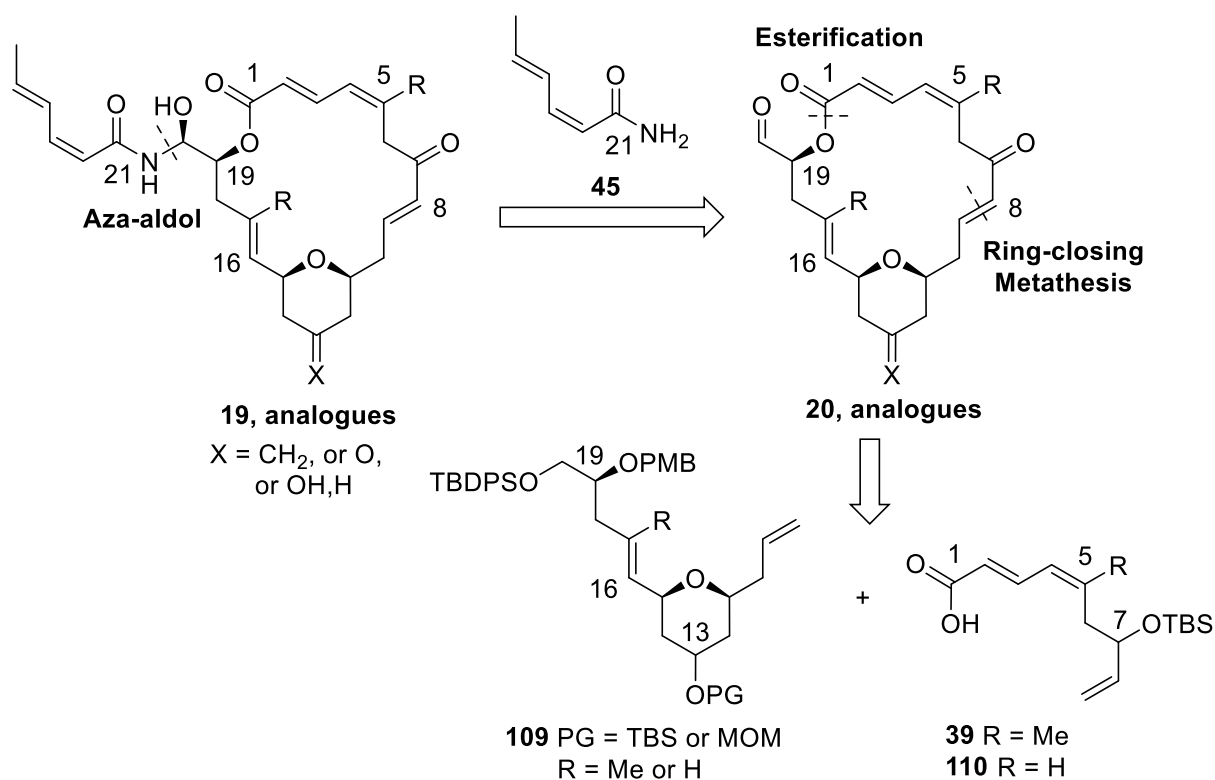
- (1) Zhao, M. Z.; King, A. O.; Larsen, R. D.; Verhoeven, T. R.; Reider, P. J. *Tetrahedron Lett.* **1997**, 38, 2641.
- (2) Uenishi, J.; Iwamoto, T.; Tanaka, J. *Org. Lett.* **2009**, 11, 3262.
- (3) Ding, F.; Jennings, M. P. *Org. Lett.* **2005**, 7, 2321.
- (4) Yun, S. Y.; Hansen, E. C.; Volchkov, I.; Cho, E. J.; Lo, W. Y.; Lee, D. *Angew. Chem. Int. Ed.* **2010**, 49, 4261.
- (5) Ting, S. Z. Y.; Harvey, J. E. Unpublished results, **2011**.
- (6) Gray, C. *Synthesis of side chain variants for (-)-zampanolide analogues*, Honours report, VUW **2011**.
- (7) Ohmura, R.; Takahata, M.; Togo, H. *Tetrahedron Lett.* **2010**, 51, 4378.
- (8) Patent WO 2008095058, TW **2008**.

- (9) Egger, M.; Pellett, P.; Nickl, K.; Geiger, S.; Graetz, S.; Seifert, R.; Heilmann, J.; König, B. *Chem.-Eur. J.* **2008**, *14*, 10978.
- (10) Ghosh, A. K.; Cheng, X. *Org. Lett.* **2011**, *13*, 4108.
- (11) Hoye, T. R.; Hu, M. *J. Am. Chem. Soc.* **2003**, *125*, 9576.
- (12) Gradillas, A.; Perez-Castells, J. *Angew. Chem. Int. Ed.* **2006**, *45*, 8086.
- (13) Ghosh, A. K.; Cheng, X.; Bai, R.; Hamel, E. *Eur. J. Org. Chem.* **2012**, 4130.
- (14) Zurwerra, D.; Glaus, F.; Betschart, L.; Schuster, J.; Gertsch, J.; Ganci, W.; Altmann, K. H. *Chem.-Eur. J.* **2012**, *18*, 16868.
- (15) Negishi, E.; Vanhorn, D. E.; Yoshida, T. *J. Am. Chem. Soc.* **1985**, *107*, 6639.

Chapter 3: First generation and fragment syntheses

3.1 Retrosynthetic analysis

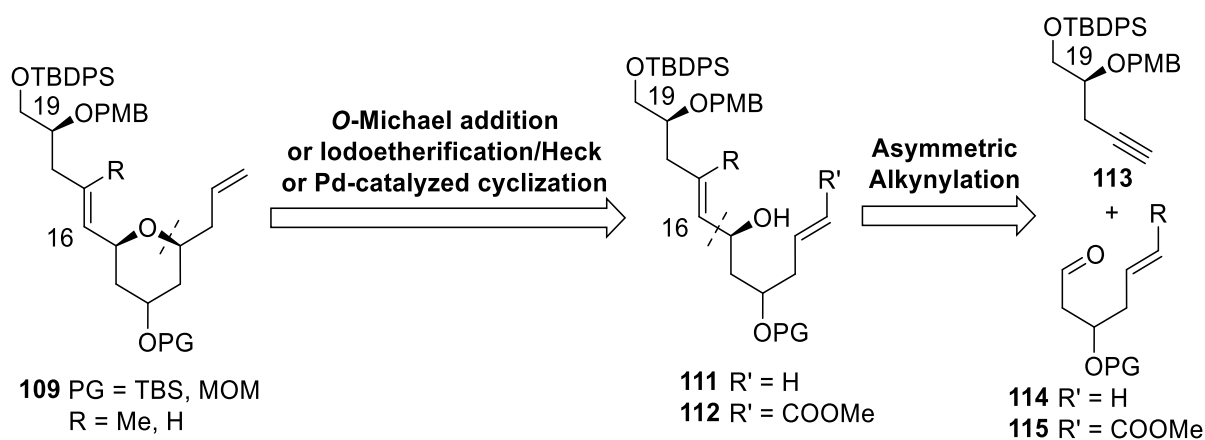
Target compounds of this thesis comprise the natural product (-)-zampanolide (**19**), the related compound (-)-**20** and analogues described in chapter 2, which include modifications at the side-arm, pyran region and the appended methyl groups at C5 and C17 on the macrocycle. Both natural and modified synthetic fragments will be needed for the target compounds. Due to the structural similarity amongst these compounds, a synthetic plan was developed allowing the synthesis of the proposed analogues to be carried out in parallel with the total syntheses of **19**. A first-generation retrosynthetic analysis is shown in **Scheme 3.1**. Dactylolide (**20**) can be converted to **19** through an aza-aldol reaction with fragment **45**. The major retrosynthetic disconnections of the macrocycle are ring-closing metathesis at C8-C9 and esterification at C1, leading back to fragments **109** and **39**, or the des-methyl analogue fragment **110**.



Scheme 3.1: First generation retrosynthetic analysis.

A protecting group strategy was developed to facilitate the synthesis, although it was realized that revisions might prove necessary. According to this synthetic plan, the hydroxyl group at C19 will be deprotected first in order to perform esterification. The hydroxyl groups at C7 and C13 can be deprotected and oxidized simultaneously to provide the C13 keto analogue and the natural product **19** in anticipation that the difference in electron deficiency at the two carbonyls will allow chemoselective Wittig olefination on the pyranone rather than the α,β -unsaturated ketone at C7. Finally, the hydroxyl group at C20 can be deprotected and oxidized to produce the aldehyde of **20**, and in preparation for the *N*-acyl hemiaminal synthesis to afford **19**. However, for the analogue with a hydroxyl group on the pyran motif instead of the methylene, the protecting group plan will need to be changed so that the hydroxyl group at C13 is deprotected last. In case the chemoselective Wittig reaction alluded to above fails, this can also serve as a backup plan for the total synthesis. Therefore, the first hydroxyl protection strategy chosen to assist the planned synthesis involved TBS at O7, TBS or methoxymethyl (MOM) at O13, *para*-methoxybenzyl (PMB) at O19 and TBDPS at O20 (**Scheme 3.1**).

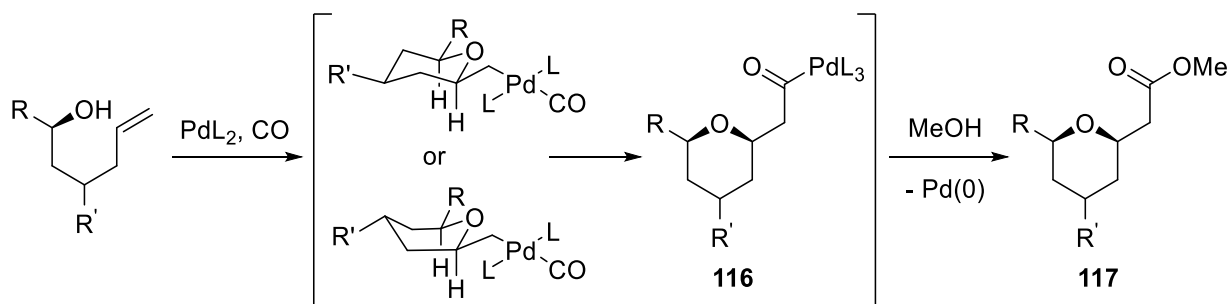
Fragment **109** contains a tetrahydropyran moiety, which is a privileged scaffold in natural products.¹⁻⁵ Extensive studies have been done to construct tetrahydropyrans, and the most commonly used methods are Prins-type cyclization,^{6,7} iodoetherification,⁸ *O*-Michael conjugate addition^{5,9-12} and metal-catalyzed heterocyclization.¹³⁻¹⁵ To achieve the tetrahydropyran with the required substituents in **109**, *O*-Michael addition, iodoetherification or palladium-catalyzed cyclization could be suitable for the current strategy, which leads to two related variations of the cyclization precursor, **111** and **112** (**Scheme 3.2**). Both



Scheme 3.2: Retrosynthetic analysis of the pyran fragment **109**.

tetrahydropyran precursors **111** and **112** can be synthesized *via* an asymmetric alkyne addition of **113** to aldehydes **114** or **115**, followed by either alkyne reduction or reductive methylation to afford natural or analogue fragments.

The iodoetherification would need to be accompanied by a two-carbon homologation, such as by a Heck reaction in order to establish the terminal alkene required for ring-closing metathesis. Such Heck reactions involve the activation of a sp^3 carbon by palladium (0), which is known to give an unstable intermediate prone to elimination and very few examples of related process have been published.^{16,17} A palladium-catalyzed cyclization could be coupled with a carbonylation step, producing intermediate **116** (Scheme 3.3). Upon treatment with methanol, **116** could be converted to an ester in **117**, and the ester functionality can be transformed to an alkene in two or three steps.¹⁸⁻²⁰ Palladium-catalyzed reactions are very sensitive to the choice of ligands and the catalyst loading, and lengthy optimization may be required. Therefore, the more reliable *O*-Michael addition of **112** will be attempted first. If this route proves unsuccessful, iodoetherification and palladium-catalyzed cyclization will be explored using the precursor **111**.

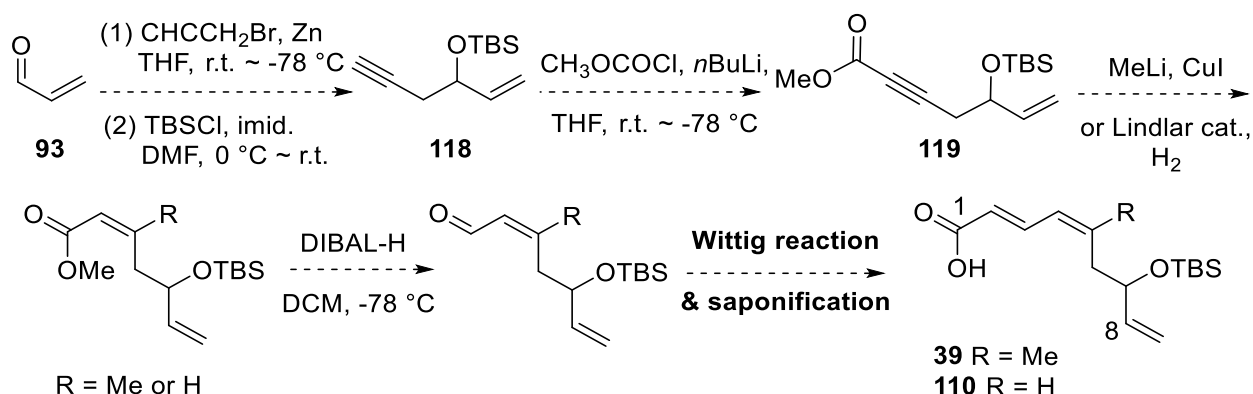


Scheme 3.3: Mechanism of the palladium-catalyzed cyclization-carbonylation cascade.

3.2 Proposed synthesis of C1-C8 fragment

Synthesis of the natural and modified variants of the C1-C8 fragment (*viz.* **39** and **110**) was proposed to start from acrolein (**93**) and pass through a Barbier reaction followed by TBS-protection to provide enyne **118**, and the subsequent alkyne substitution with methyl chloroformate forming ynoate **119** (Scheme 3.4). From this point, the fragment **39** will be achieved by reductive methylation, ester reduction, Wittig olefination and saponification. In

the synthesis of the analogue fragment **110**, the reductive methylation step will divert to a Z-selective reduction of alkyne in **119**, which will be attempted using the Lindlar hydrogenation.

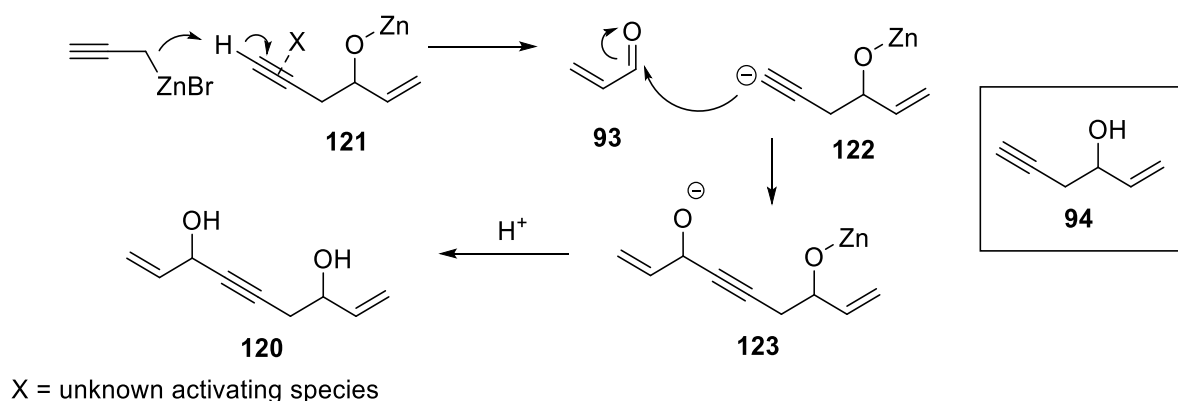


Scheme 3.4: Plan for fragments C1-C8 (**39** and **110**) synthesis.

3.2.1 Synthesis of the natural C1-C8 fragment

The Barbier reaction is often compared to the Grignard reaction, but it offers more advantages including wider substrate scope, more reliable preparation, more stable intermediate and milder reaction condition.^{21,22} Initial trials were carried out using commercially available zinc powder without activation. Following the reported procedure, in addition to the two equivalents each of propargyl bromide and zinc dust employed at the outset of the reaction to react with propargyl bromide, another 1 equivalent of zinc dust was added immediately before the addition of acrolein.²¹ The first attempt at the Barbier reaction did not achieve a satisfying result and a large amount of diol **120** (46%) was obtained alongside the desired product **94** (22% yield) (**Scheme 3.5**). A plausible mechanism was proposed to explain the formation of **120**. The excess zinc or an impurity present in the reaction mixture may have activated the terminal alkyne in the zinc alkoxide salt of the intermediate **121** to allow deprotonation by the excess propargylzinc bromide, or by proton transfer from alkyne to alkoxide. The resulting acetylenic anion **122** could then perform a nucleophilic attack on another molecule of acrolein (**93**), upon protonation of **123** producing the observed diol **120**. Due to the fact that acrolein (**93**) was the limiting reagent, the deprotonation of the terminal alkyne must be favored kinetically over the desired Barbier pathway. A trial with no additional equivalent of zinc dust at later stage of the reaction gave a poor yield (30%) of the product **94** and no by-product **120**. This result was attributed to incomplete reaction, because activation of the carbonyl by the third

equivalent of zinc powder was absent. However, the highly volatile acrolein (**93**, b.p. 51-53 °C) cannot be recovered to support this claim. The Barbier product **94** was also found to be volatile, so that exposure to a vacuum, such as by prolonged time on rotary evaporator, can cause loss of product.

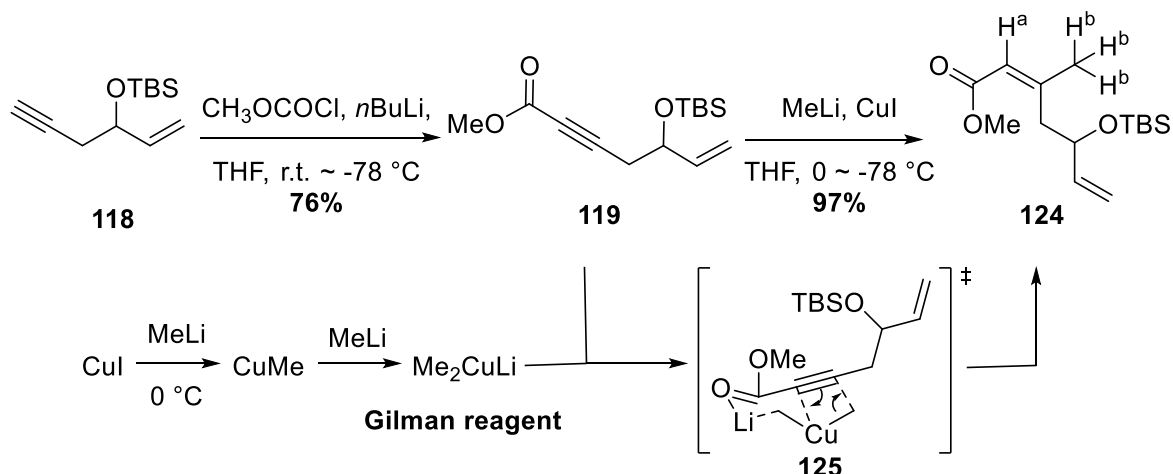


Scheme 3.5: Proposed mechanism for the formation of **120** in Barbier reaction.

Attention was turned to combining the Barbier reaction with TBS-protection of the resulting alcohol **94**. Activated zinc powder was also used. An initial attempt at subjecting the crude Barbier product to silyl protection did not succeed. Without purifying the alcohol **94**, no TBS-protection can occur. Next, the product of the Barbier reaction **94** was purified by a short silica plug. The elute was not reduced to dryness to avoid loss of **94**, which was then subjected to TBS-protection. With 2 equivalents of activated zinc dust, a reproducible 61~68% yield of **118** was obtained over the two-steps. The best yield, 81%, was obtained using a third equivalent of activated zinc dust and newly purchased propargyl bromide without purification. The by-product **120** was not observed, which suggested that the formation of the diol **120** was likely to be promoted by impurities present in the commercial zinc dust or propargyl bromide.

The carbonyl necessary for olefination was then established by a nucleophilic substitution of methyl chloroformate with alkyne **118**, and a reductive methylation using Gilman reagent was used to produce the tri-substituted alkene **124** (Scheme 3.6). The use of Gilman reagent in 1,4-addition to α,β -unsaturated carbonyls is well-precedented.^{23,24} The Gilman reagent was pre-formed by treating copper (I) iodide with two equivalents of methyllithium at 0 °C. A deep red colour, indicative of methylcopper (I), gradually developed during the addition of the first

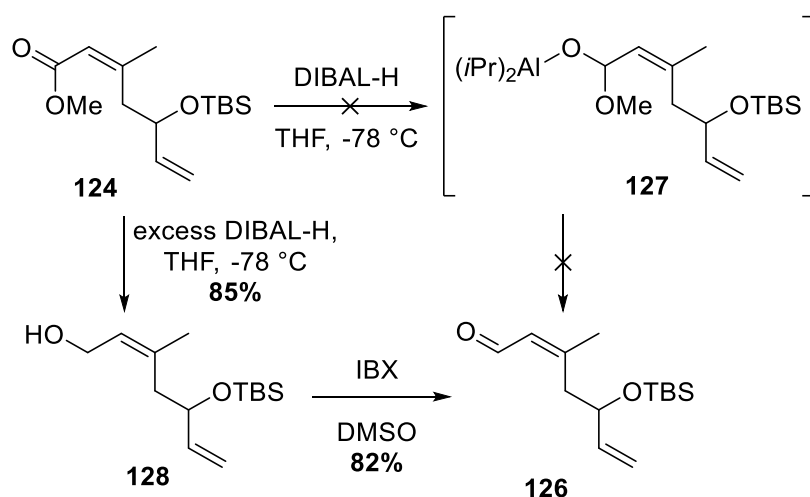
equivalent of methyllithium, which then disappeared slowly during the addition of the second equivalent, resulting in a colourless solution of the Gilman reagent, Me_2CuLi . The mechanism describing the regio-selectivity of the Gilman reagent is postulated to go through a bicyclic transition state **125**, where the lithium interacts with both the carbonyl oxygen and one of the methyl groups on Cu to direct the methyl addition to the γ -position; the following Cu-H exchange allowed the *cis*-selectivity (**Scheme 3.6**). The *cis*-configuration in product **124** was confirmed by a strong nuclear Overhauser effect spectroscopy (NOESY) correlation between the methyl protons H^b and the alpha proton H^a , which indicates a through-space interaction between these nuclei and their proximity. The alkyne substitution of **118** with methyl chloroformate and the subsequent reductive methylation of **119** both proceeded smoothly when good quality *n*-butyllithium, methyllithium and purified copper (I) iodide²⁵ were used, and high yields over the two steps were achieved.



Scheme 3.6: Alkyne homologation and subsequent reductive methylation.

Attempts to reduce the ester **124** to the aldehyde **126** with DIBAL-H were unsuccessful. This is always a challenging reaction, as it is very sensitive to temperature and the stability of the intermediate (**127** in this case) (**Scheme 3.7**). During the addition of DIBAL-H, the higher temperature of the droplets introduced to the cold reaction mixture can result in over-reduction. This is especially problematic for α,β -unsaturated esters.²⁶ To avoid over-reduction, 1.05 equivalent of DIBAL-H was added to a solution of ester **124** at -78°C slowly against the inner wall of the reaction vessel, but only starting material was recovered. The fact that no aldehyde or alcohol was observed at any stage of the reaction suggests that the DIBAL-H was of poor

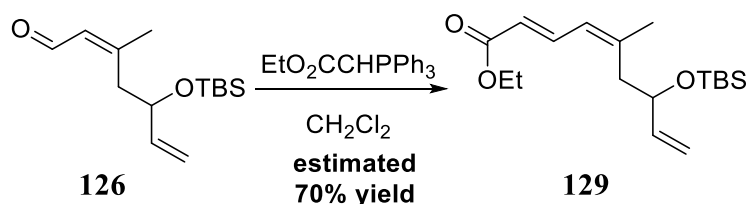
quality. Staged addition of DIBAL-H was then carried out, and the reaction was monitored by TLC analysis. No reaction was observed with 1.1 and 2.2 equivalents of DIBAL-H, but when 3.4 equivalents was added, the over-reduced product **128** was produced exclusively and isolated in good yield (85%). The amount of DIBAL-H necessary for reaction was later optimized to 2.8 equivalents. Therefore, a two-step reduction-oxidation process was undertaken to afford aldehyde **126**.



Scheme 3.7: Two-step reduction-oxidation process to aldehyde **126**.

Three oxidation methods were scanned for converting alcohol **128** to aldehyde **126**: Swern oxidation was observed to produce reasonable yields, about 50% with recovered starting material, but it was not very reliable; Parikh-Doering oxidation only gave a poor yield of 18%; employment of freshly prepared 2-iodoxybenzoic acid (IBX)²⁷ gave the best result. Frigerio reported that the purities of IBX prepared from iodobenzoic acid using 1.3 and 3.0 equivalents of oxone are $\geq 95\%$ and $\geq 99\%$ respectively.²⁷ It was found that the slight difference in the quality of IBX produced in these ways provided very different outcomes in the present work. The IBX prepared using 1.3 equivalents of oxone only provided up to 27% yield of **126**, while the sample made using 3.0 equivalents of oxone resulted in an excellent 82% yield of **126** (Scheme 3.7). The aldehyde **126** was then subjected to a Wittig reaction with ethyl (triphenylphosphoranylidene)acetate to produce dienoate **129** (Scheme 3.8). However, the Wittig reaction did not go to completion after 22 hours. The product **129** was contaminated by aliphatic compounds and starting material, which gave an estimated yield of **129** about 70%.

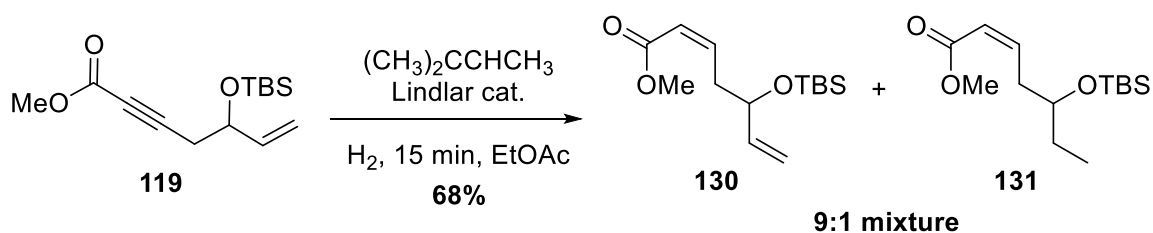
No further purification was carried out, and the Wittig reaction was not optimized, as a better route that bypasses this step was found, which will be discussed in chapter four.



Scheme 3.8: Wittig reaction in the synthesis of the C1-C8 fragment **129**.

3.2.2 Synthesis of the des-methyl C1-C8 analogue fragment

According to the planned synthetic route, preparation of the des-methyl analogue fragment **110** was initiated by reducing **119** using hydrogen gas in the presence of Lindlar's catalyst (see **Scheme 3.4**). A sacrificial alkene, 2-methylbut-2-ene, was used to avoid over-reduction of the alkenes in **130**. However, this reaction did not reach completion, and significant amounts of over-reduction occurred at the terminal alkene (**Scheme 3.9**). The over-reduced product **131** (present as 10% of the product mixture) was not separable from the desired product **130** by standard column chromatographic methods. Addition of extra portion of the sacrificial alkene did not make an improvement, and attempts to continue the reaction to completion resulted in 20 to 50% of over-reduction at the terminal alkene.



Scheme 3.9: Lindlar reduction of ynoate **119**.

This mixture of **130** and **131** was first observed as obscured minor and major multiplets with the same splitting pattern at 6.38 and 6.33 ppm in the ^1H nuclear magnetic resonance (NMR) spectrum, which correspond to β -protons. Only one set of the terminal alkene proton signals

(5.81, 5.20, 5.07 ppm) was observed (**Figure 3.1**). In addition, two sets of carbon signals were found for the ester and di-substituted alkene, while only one set of the terminal alkene signals was present. A close examination of the ^1H NMR spectrum with the assistance of correlation spectroscopy (COSY) found that both β -protons correlate to a complex multiplet between 2.76 and 2.94 ppm, which then correlates to the oxymethine proton signal at 4.29 ppm, as expected, as well as an obscured upfield multiplet at about 3.73 ppm (minor). The two corresponding oxymethine carbon signals were observed at 72.7 and 72.5 ppm in the ^{13}C NMR spectrum, respectively. The significant up-field shift of the oxymethine proton in the minor compound indicates that the allylic effect is not present. The structure of the over-reduction product **131** would agree with this observation. Moreover, the oxymethine proton with chemical shift around 3.73 ppm also correlates to an alkyl signal at 1.47 ppm, which accounts for two protons of the minor compound. In the ^{13}C NMR spectrum, two distinctive alkyl carbons signals of the over-reduced product **131** were found at 29.9 and 9.7 ppm.

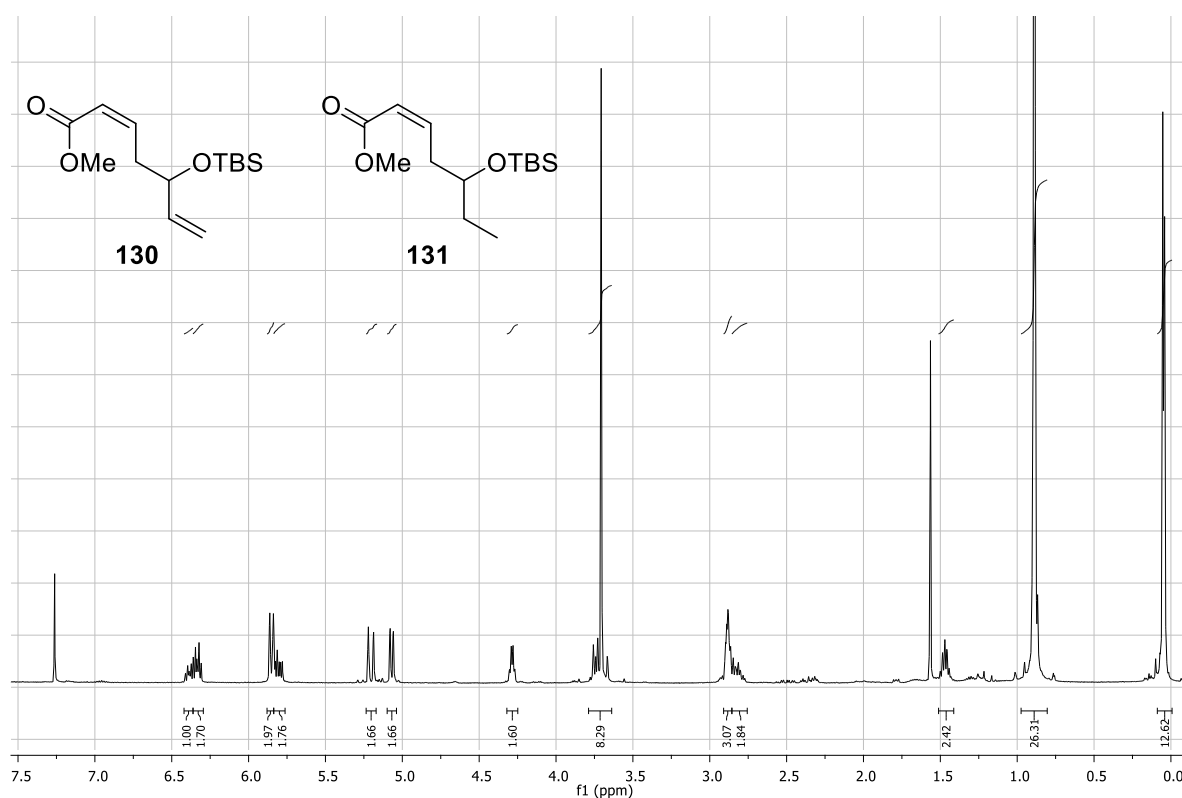
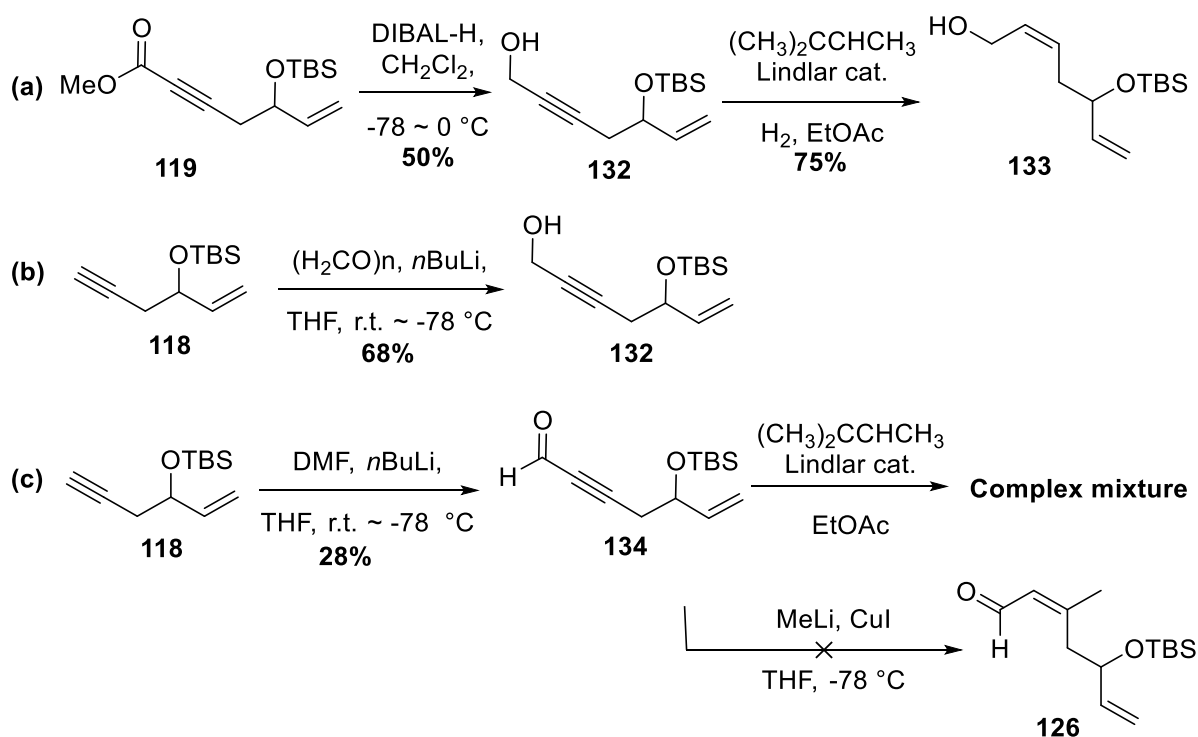


Figure 3.1: ^1H NMR spectrum of the mixture containing **130** and the over-reduced **131**.

The presence of the over-reduced product **131** and its lack of separation from the desired product **130** invoked a need to optimize the Lindlar process. In the hope that the propargylic

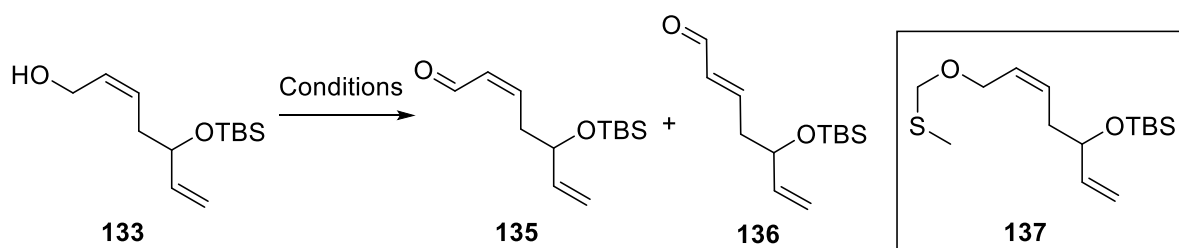
alcohol would be more electron rich than the conjugated ynoate, thus react significantly faster than alkene, the ester **119** was reduced to propargylic alcohol **132** by DIBAL-H prior to Lindlar reduction (Scheme 3.10, equation a). This reduction provided **132** in a moderate 50% yield. The initial attempt at the Lindlar reaction of **132** found that over-reduction occurred. It was thought that the sacrificial alkene 2-methylbut-2-ene could be too volatile (b.p. 36~40 °C) to last for the entire four hours reaction, therefore, an additional equivalent must be added during the reaction. This approach indeed solved the problem, with 75% yield of **133** obtained and no over-reduction (equation a). Experiments to shorten the sequence by installing the alcohol functional group directly to alkyne **118** and thus avoiding the ester-reduction step were also attempted. The addition of the anion of **118** to paraformaldehyde produced a reasonable 68% yield of propargylic alcohol **132** (equation b). Attempts to shorten the sequence even further by formylation of alkyne **118** using dimethylformamide (DMF) only achieved a low 28% yield of **134** (equation c). In the hope that the yield could be optimized later, **134** was tested in Lindlar reduction, but this resulted in a complex mixture of the desired product, the isomerized *E*-alkene, over-reduced product at either one of the two alkenes, as well as doubly over-reduced product. In an effort to avoid the reduction-oxidation steps in the sequence leading to the natural fragment **126**, reductive methylation on **134** was attempted, but only starting material was recovered.



Scheme 3.10: Lindlar reduction of alkyne substrates **132** and **134**.

With the allylic alcohol **133** in hand, its oxidation to aldehyde **135** was performed. Thermal isomerization of *Z*-alkenes to the less strained *E*-configuration can readily occur for 1,2-disubstituted alkenes at room temperature, catalyzed by the presence of acid. Hence, low temperature, basic oxidation methods like Swern reaction are often used to oxidize *Z*-allylic alcohols. Therefore, Swern oxidation was attempted first in order to minimize the formation of **136**, but no reaction was observed (Table 3.1, entry 1). To facilitate this reaction, freshly distilled reagents and additional equivalents of dimethylsulfoxide (DMSO) and oxalyl chloride were used, but still no reaction occurred. A step-wise elevation of temperature up to room temperature resulted in a 1:1 mixture of starting material and decomposed products (entry 2). A trace amount of the desired aldehyde **135** was also observed, which was too insignificant for isolation and purification. The decomposed products were not characterized, but it is well known that the standard sulfonium intermediate can go through an alternative pathway to a thioacetal **137** at high temperature, instead of the normal oxidation process.

Table 3.1: Results for the oxidation of **133**.



Entry	Conditions	Obtained ratios of starting material and products			
		133	135	136	Decomposition
1	DMSO, (COCl) ₂ , NEt ₃ , -78 °C	1	-	-	-
2	DMSO, (COCl) ₂ , NEt ₃ , -78 °C to r.t.	1	-	-	1
3	Commercially available MnO ₂ , r.t.	1	-	-	-
4	Prepared MnO ₂ , r.t., 3 h ^a	3	2	-	-
5	Prepared MnO ₂ , r.t., 5 h ^b		2	1	-

^a The reaction was carried out in air; ^b The starting material was a 3:2 mixture of **133** and **135**.

Manganese dioxide provides an oxidation method that is selective for α,β -unsaturated alcohols and is known to facilitate oxidation of *Z*-allylic alcohols without isomerization.^{28,29} A sample of commercial manganese dioxide did not promote any reaction, even after it was activated by heating at 130 °C for 18 hours (**Table 3.1**, entry 3). Freshly prepared manganese dioxide³⁰ (10 equivalents) was then used. As Gritter and Wallace reported that no difference in oxidation facility was observed whether under air or nitrogen atmosphere,³¹ the first trial with manganese dioxide was carried out without an inert atmosphere. This reaction converted about 40% of the alcohol **133** to aldehyde **135** after 3 hours, before the MnO₂ became apparently inactivated (entry 4). Future reactions involving MnO₂ were carried out under an atmosphere of nitrogen to prevent inactivation. Encouragingly, the aldehyde product from the above MnO₂ oxidation exclusively retained the *Z*-configuration of the precursor alcohol **133**. This unpurified mixture of 3:2 alcohol:aldehyde was treated with another 10 equivalents of MnO₂ and an additional 10 equivalents were added half-way through the reaction. After 5 hours, all starting material was consumed, but the product was obtained as a 7:3 mixture of *Z*:*E*-alkenes **135** and **136** (entry 5). In the ¹H NMR spectrum of the inseparable mixture, the signals for the internal alkene protons

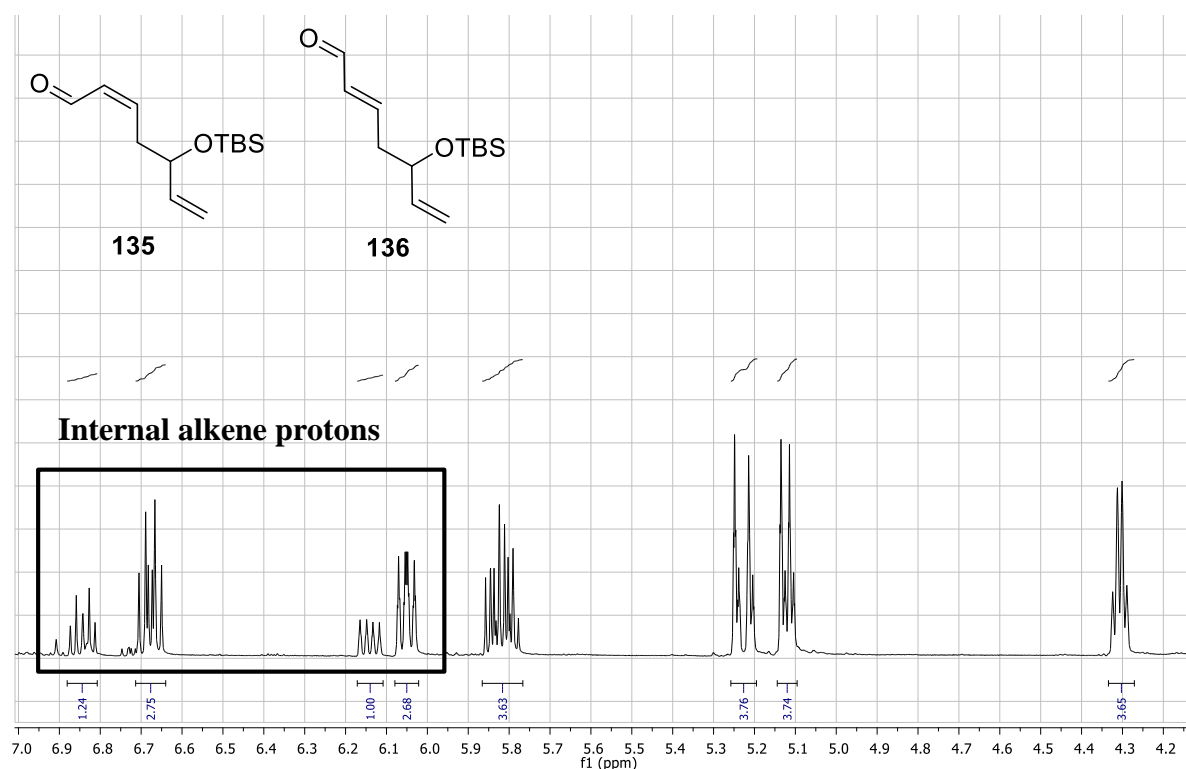
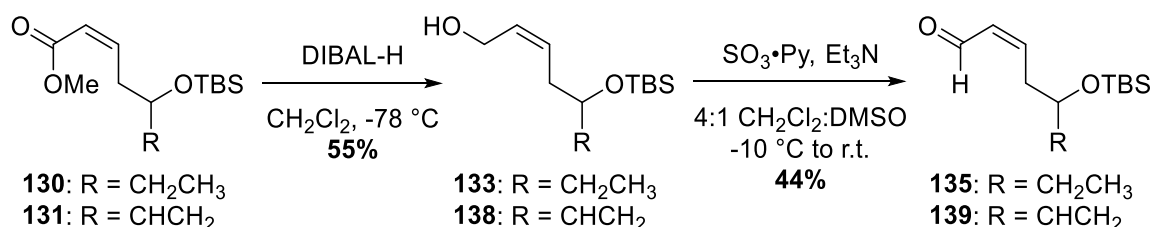


Figure 3.2: The alkene region of the ¹H NMR for the mixture of **135** and **136**.

are well-defined, and the vicinal coupling constants were measured as 11.1 and 15.5 Hz for the major and minor isomers, respectively, which are the typical values for *Z*- and *E*-alkenes

(**Figure 3.2**). Interestingly, although the oxymethine signal at 4.31 ppm is not differentiated for the two compounds, the terminal alkene proton signals at 5.82, 5.23 and 5.12 ppm all had slight upfield shifts in the minor *E*-isomer **136**. Thus, weak cross-talk must occur between the two alkenes in each compound. ^{13}C and 2D NMR experiments were conducted to assist the assignment of **135** and **135**. The prolonged reaction time was seen to provide a chance for the alkene to isomerize. There was literature precedent that the addition of sodium carbonate to neutralize any acid and lowering the reaction temperature to 0 °C can avoid the problem of isomerization,³² which can be investigated in future.

Parikh-Doering oxidation has not been a commonly used method for the oxidation of *Z*-allylic alcohols, because it is typically carried out at room temperature, which is prone to cause thermal isomerization. However, this method was still tested on a mixture of the alcohols **133** and **138** produced from DIBAL-H reduction of a 1:1 mixture of **130** and **131** (**Scheme 3.11**). To decrease the chance of isomerization, the reaction was quenched before it reached completion. Encouragingly, the product consisted of a 1:1 mixture of the two *Z*-products, **135** and **139**, and no isomerization was observed. Full NMR data were collected for characterization. Due to time constraints, Parikh-Doering oxidation on pure *Z*-allylic alcohol **133** was not performed.

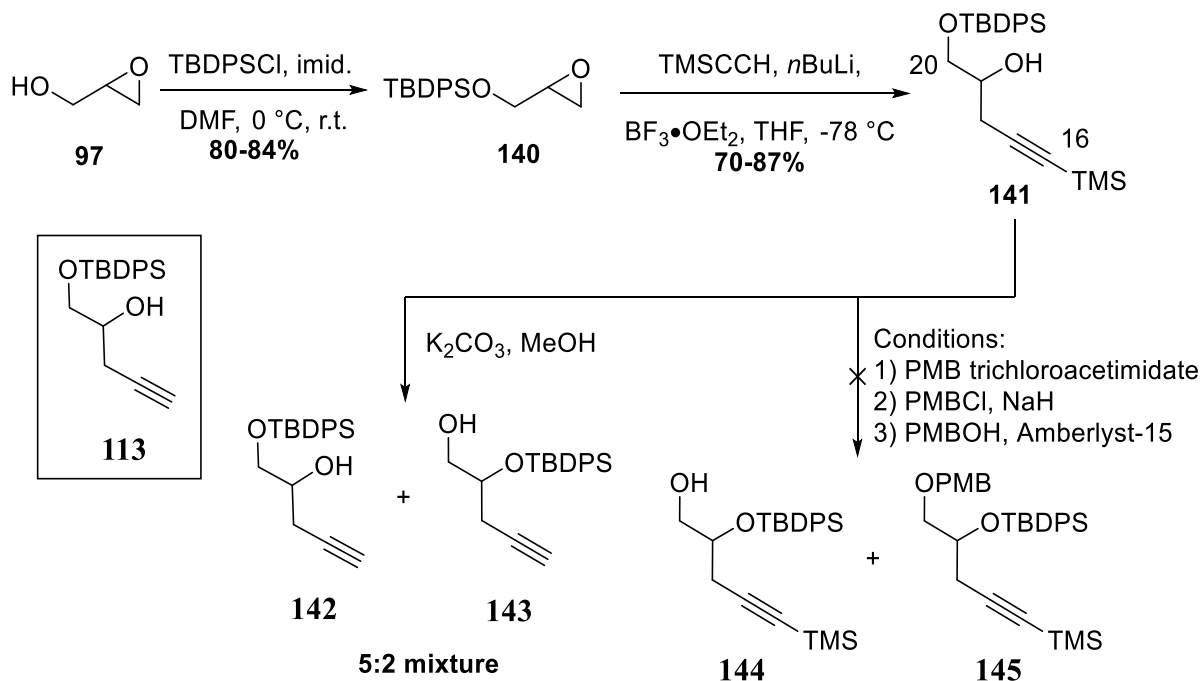


Scheme 3.11: Reduction and oxidation sequence on a 1:1 mixture of **130** and **131**.

3.3 Synthesis of C16–C20 fragment

According to the synthetic plan, the protection of the hydroxyl groups was sought with a TBDPS ether at C20 (see **Scheme 2.2**), and glycidol (**97**) was used as the starting material to synthesize the C16–C20 fragment **113**. To this end, the protection of **97** to afford **140** proceeded

in a consistently good yield (80~84%), as did the epoxide ring-opening with TMS-acetylide to afford **141** (70~87% yield) (**Scheme 3.12**). However, the acetylenic silyl deprotection produced an inseparable mixture of two products in a 5:2 ratio. While the TMS signal had disappeared, two sets of signals were observed in the oxygenated and propargylic regions of the ^1H NMR spectrum, and both closely resembled signals expected for the desired product **142**. This mixture was proposed to consist of a 5:2 mixture of desired **142** and its regioisomer **143**. To avoid silyl migration, this sequence was adjusted, such that removal of the acetylenic TMS protecting group could be accomplished after protection of the secondary alcohol in **141**, ideally as a *para*-methoxybenzyl (PMB) ether. Despite much effort, protection of the secondary alcohol with PMB was futile: both the well-established method using PMB-trichloroacetimidate³³ and a recent acid-catalyzed protection method using PMB-alcohol and Amberlyst-15³⁴ only returned starting material. The most common method involving deprotonation of alcohol **141** with NaH followed by substitution of PMBCl was also attempted but, not surprisingly, silyl-migration occurred under the basic conditions. The NMR evidence from the crude reaction mixture suggested that the product was mostly starting material **141** and the silyl-migrated material **144**, together with a small amount of C19-silyl,C20-PMB-protected product (**145**). Although this outcome is not desirable, it raised awareness that even

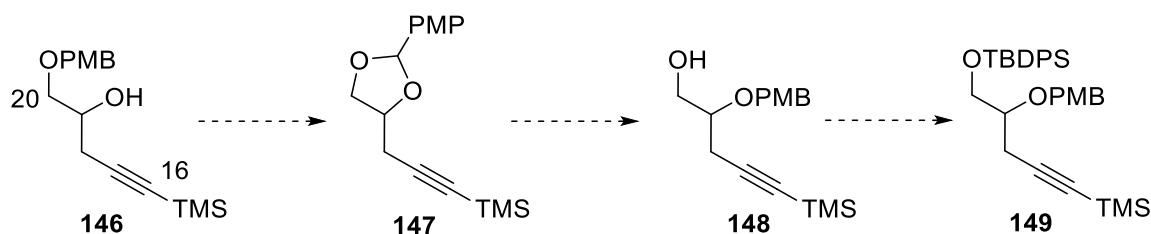


Scheme 3.12: The first attempt to synthesize C16-C20 fragment **113**.

with a bulky protecting group such as TBDPS on C19, protection of the primary alcohol at C20 is still possible. In contrast, protection of the secondary hydroxyl group in the presence of a

bulky C20 protecting group was deemed difficult, because of the higher steric hindrance around C19.

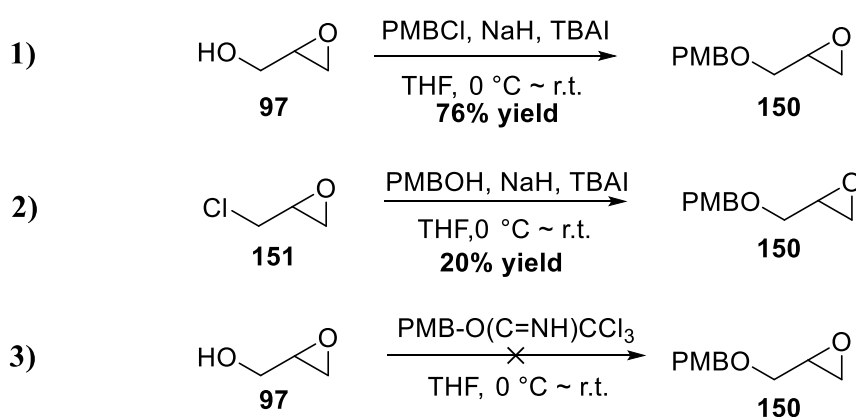
The previous findings evoked a new approach to this dual-protecting problem: a so-called “stepping stone” approach (**Scheme 3.13**). From the C20-PMB-protected fragment **146**, transfer of the PMB group on C20 to C19 via a *para*-methoxyphenyl (PMP) acetal **147** could allow the less hindered primary C20 alcohol in **148** to be protected with a silyl group, and thus achieves the sought differential protection. A lot of work has previously been done on the regioselective opening of benzylidene acetals.³⁵ The most commonly used DIBAL-H reduction method is expected to give the primary alcohol, because aluminum prefers to coordinate with the less hindered oxygen of the acetal, which then hydrolyzes during work-up to produce the primary alcohol.³⁶⁻³⁹ There are exceptions to the regioselectivity involving DIBAL-H, mainly due to unwanted additional chelation with other groups in those substrates, which should not occur with acetal **147**.^{40,41} To test this strategy, fragment **146** was required, which could be prepared from glycidol (**97**) following a similar strategy as for the C20-TBDPS-protected fragment **141**.



Scheme 3.13: “Stepping stone” approach to C16-C20 fragment **149**.

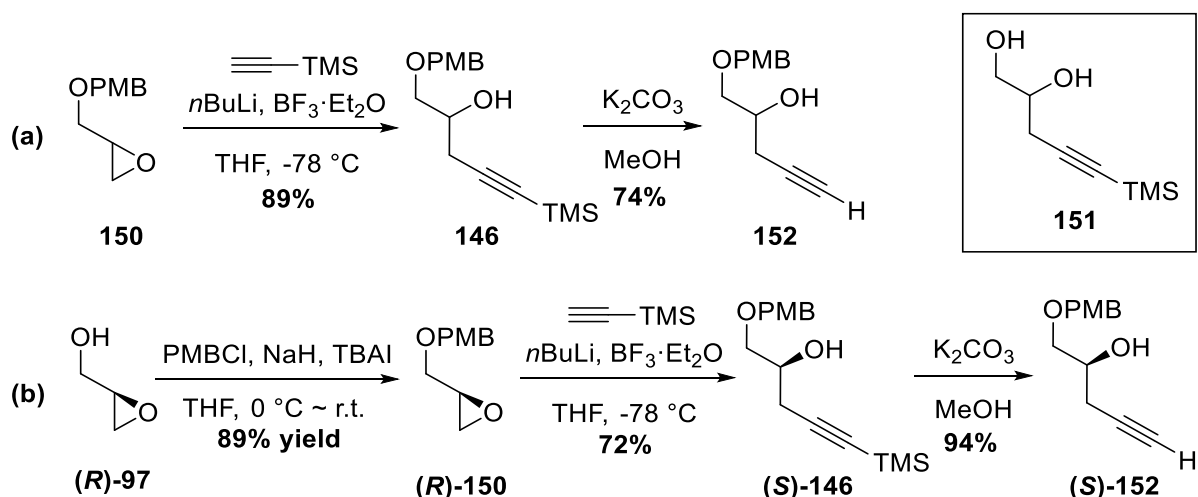
The first attempt to protect glycidol (**97**) with commercially available *p*-methoxybenzyl chloride (PMBCl) did not provide any reaction, presumed due to the quality of PMBCl. PMBCl can be freshly made from *p*-methoxybenzyl alcohol, following Luzzio and Chen’s sonication method.⁴² They reported that the quality of the prepared PMBCl was sufficient for use in reactions, after a simple separation of the aqueous layer, washing with water and drying with calcium chloride. However, the PMBCl prepared in that way also did not promote the desired protection, and mixtures of multiple degradation products were obtained, which were accompanied by disappearance of the epoxide signals in the ¹H NMR spectrum. The degradation could be resulted from the residual hydrochloric acid present in the prepared

PMBCl. An attempt to neutralize the PMBCl by washing it with an aqueous solution of sodium bicarbonate resulted in a mixture of about 1:1 PMBCl and PMBOH. The PMBCl was then purified by dilution with diethyl ether, washing thoroughly with large amounts of water, drying over calcium chloride and purging under high vacuum. The quality of this prepared PMBCl was proved sufficient to be used for protection, with a satisfying 76% yield of the PMB ether **150** achieved (**Scheme 3.14**, equation 1). Synthesis of the required PMB ether **149** was also attempted by substitution of epichlorohydrin (**151**) with *p*-methoxybenzyloxyde, or by reaction of glycidol (**97**) with freshly prepared PMB-trichloroacetimidate, but neither reaction provided satisfying results and insufficient conversions were obtained (equations 2 and 3).



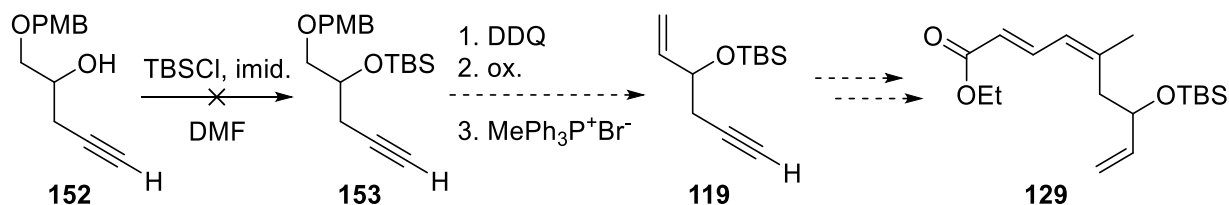
Scheme 3.14: Synthesis of PMB glycidyl ether **150**.

The epoxide opening of **150** by trimethylsilylacetylene was promoted by boron trifluoride diethyl etherate ($\text{BF}_3 \cdot \text{OEt}_2$). During the early trials, the available $\text{BF}_3 \cdot \text{OEt}_2$ had been stored under atmospheric condition for over ten years, and it was distilled over calcium hydride prior to the reaction. However, the majority of the product obtained using this $\text{BF}_3 \cdot \text{OEt}_2$ was the PMB-deprotected product **151**, which could be due to the presence of a strong acid. It is well known that $\text{BF}_3 \cdot \text{OEt}_2$ decomposes to a strong acid, tetrafluoroboric acid (BF_4H) in the presence of water, and it may not be removed fully by distillation.⁴³ With newly purchased $\text{BF}_3 \cdot \text{OEt}_2$, this reaction went smoothly without any deprotection (73~89% yield of **146**), even on a gram scale (**Scheme 3.15**, equation a). The following acetylenic trimethylsilyl (TMS) deprotection with potassium carbonate and methanol produced **152** in a good yield. The synthesis of the enantiomerically pure fragments (*S*)-**146** and (*S*)-**152** from (*R*)-glycidol was carried out in the same manner and proceeded cleanly with good yields (equation b).



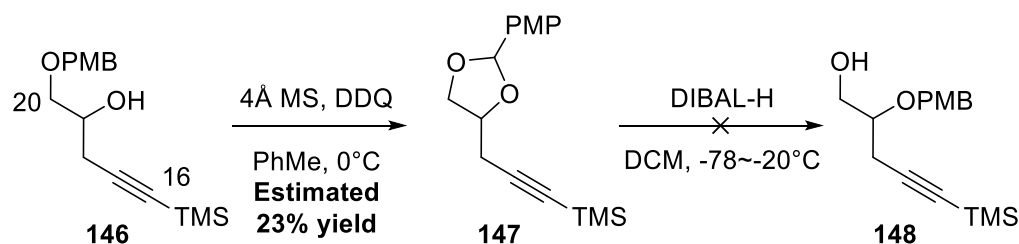
Scheme 3.15: Synthesis of the precursor to C16-C20 fragment **146** and **152**.

Protection of the secondary alcohol in **152** with TBS was attempted. Not only is TBS less bulky than TBDPS and similarly orthogonal to the primary PMB protection at the C20 hydroxyl, the resulting product **153** would also offer an alternative route to the C1-C8 fragment **129** (Scheme 3.16). Although the synthesis of the C1-C8 fragment (**129**) is efficient and high yielding, the starting material acrolein (**93**) possesses many environmental and safety hazards, and can be fatal through inhalation, contact and swallowing. In addition, most chemical suppliers have discontinued supply of acrolein (**93**) because of its toxicity and difficulty to transport. Therefore, there may be no long-term, reliable supply of acrolein (**93**). Once the dual-protected C16-C20 fragment **153** is made, it could be adapted for the C3-C8 fragment (**129**) in the following way: the PMB group on C20 could be selectively deprotected, oxidized and olefinated *via* a Wittig reaction to produce enyne **119**, a precursor to the C1-C8 fragment **129** as established earlier (see Scheme 3.4). However, the silyl protection did not proceed, even after 5 hours at 100 °C. The search for an alternative route to fragment **129** continues.



Scheme 3.16: Alternative synthetic plan for the C1-C8 fragment **129**.

The “stepping-stone” strategy for O19 protection was explored using **146** (Scheme 3.17). After a 14 h reaction with DDQ at 0 °C, the oxidative acetal formation did not reach completion, and the crude reaction mixture consisted of a 2:2:3 ratio of diastereomers of **147**: anisaldehyde: starting material **146**. The presence of anisaldehyde indicates that this reaction had not been kept thoroughly dry, so more care in drying the reagents and glassware was required in future. A sample of **147** was isolated as a mixture of diastereomers, as expected, but was contaminated with 10 mol% of anisaldehyde.



Scheme 3.17: Attempt to PMB-group transfer from O20 to O19.

The ^1H NMR spectrum of the mixture containing **147** diastereomers showed two sets of well-differentiated peaks for the methine H^a and the oxymethylene protons, H^b in **147** (Figure 3.3). Two singlets at 5.91 and 5.76 ppm were observed for the H^a acetal protons of the diastereomers

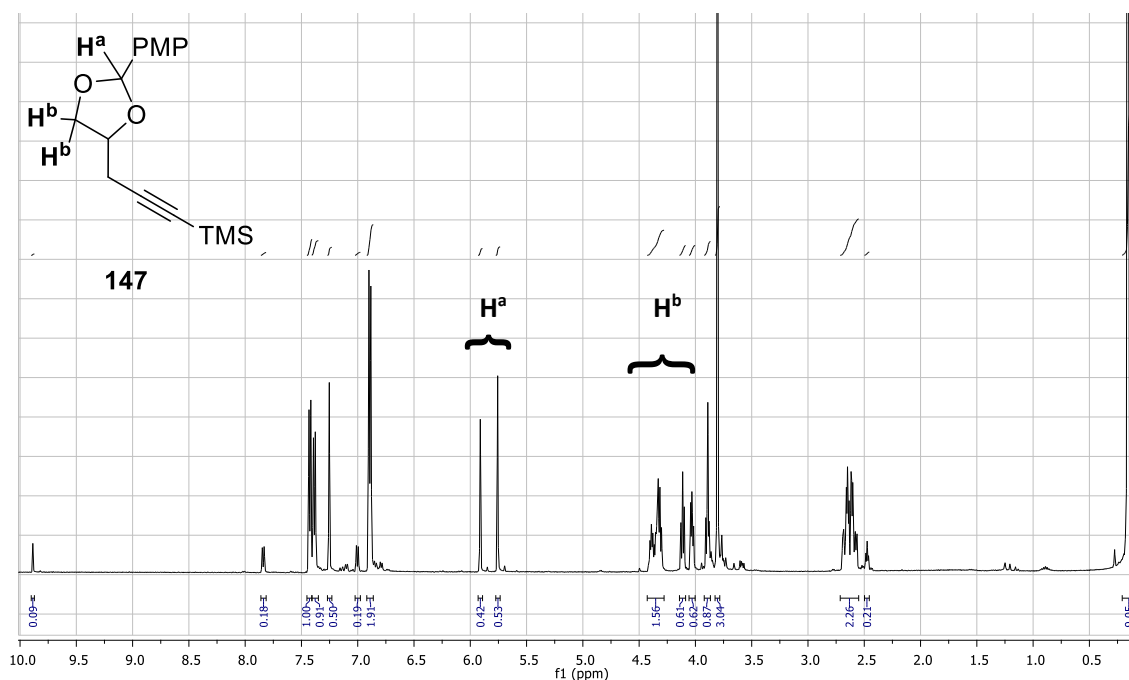


Figure 3.3: The ^1H NMR spectrum of the mixture containing diastereomeric **147**.

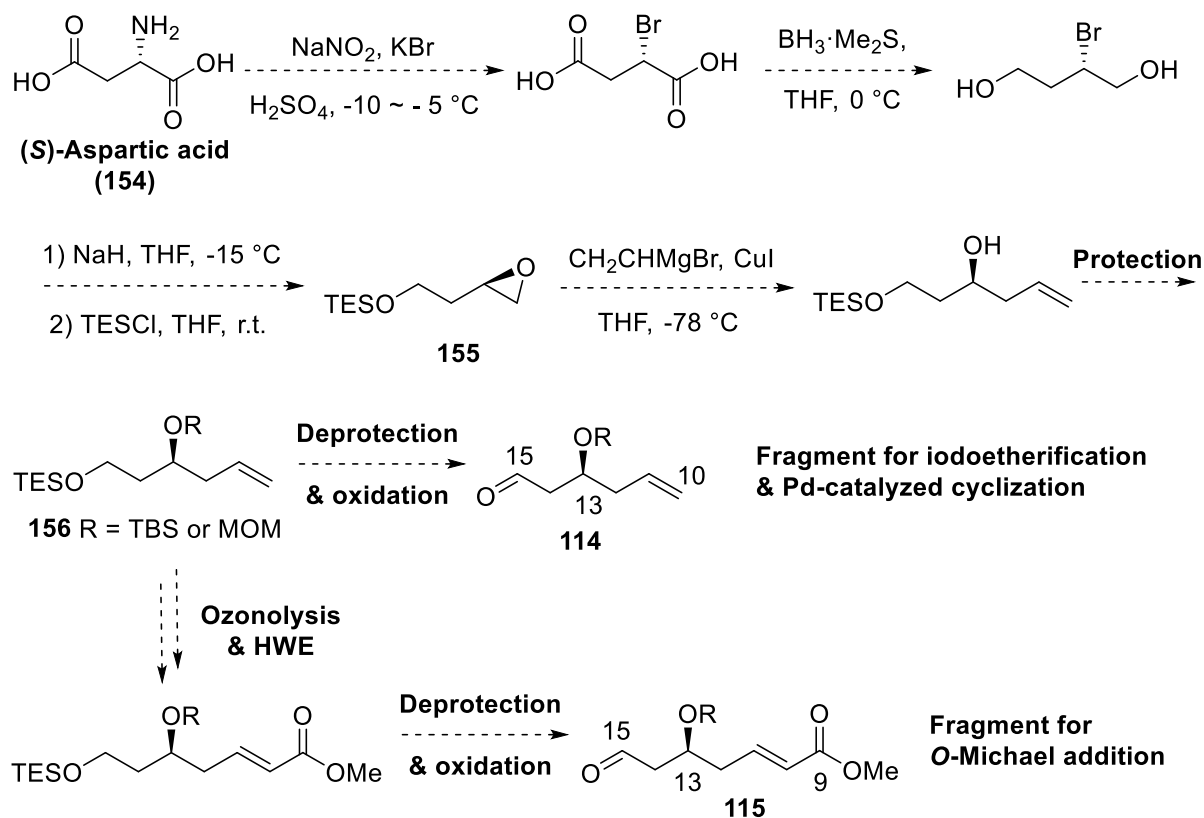
of **147**, while the oxymethylene protons H^b were in an ABM system with the oxymethine protons, thus vicinal coupling was observed, and the signals appeared as two pairs. One pair of signals have higher chemical shifts at 4.34 and 4.39 ppm, and the other pair was found at 3.90 and 3.88 ppm.

The mixture containing acetal **147** was subjected to treatment with DIBAL-H to test the regioselectivity of the reductive ring-opening (**Scheme 3.17**). An excess of DIBAL-H (2.5 equivalents) was used to compensate for the presence of anisaldehyde. After an overnight reaction at -19 °C, only the acetal starting material **147** was observed by TLC analysis and ¹H NMR spectroscopy. Other acetal-opening methods are available for future exploration, for example, the lithium aluminum hydride/ trichloroaluminum combination,⁴⁴ procedures involving borane^{40,45} and other boron-containing reagents^{46,47}. However, a more efficient approach that required the C19-hydroxyl to be unprotected was found, and thus effort was diverted to the new approach.

3.4 Proposed synthesis of C9-C15 fragment

Synthesis of the two variations of the C9-C15 subunit **115** and **116** (see **Scheme 3.2**) starts from (*S*)-aspartic acid (**154**) (**Scheme 3.18**). Firstly, the epoxide **155** can be formed stereoselectively *via* bromine substitution, reduction, epoxidation formation by intramolecular bromohydrin substitution and silyl protection. The preference for the oxirane over oxetane dictates exclusive formation of the desired epoxide **155**. The epoxide **155** can then be opened by the vinyl Grignard reagent, and the resulting alcohol would be protected to afford **156**. After the initial exploration of this method, a similar sequence was described in Altmann's publication of the total synthesis of (-)-zampanolide for production of the TBDPS equivalent of **155**, which became the C9-C14 fragment upon construction of the pyran through a Prins reaction.⁴⁸ In the present work, the secondary alcohol in **156** was protected with TBS or MOM groups for natural and analogue fragments. After selective deprotection of the silyl ether on the primary alcohol and oxidation, the substrate for pyran cyclization *via* iodoetherification or Pd-mediated cyclization (**114**) can be produced. Alternatively, the alkene in **156** can be ozonized followed by a Horner-Wadsworth-Emmons reaction to establish the α,β -unsaturated ester

required for the *O*-Michael cyclisation, upon deprotection and oxidation producing fragment **115**. Simplified fragments will also be synthesized to be used in model studies and to produce truncated analogues.

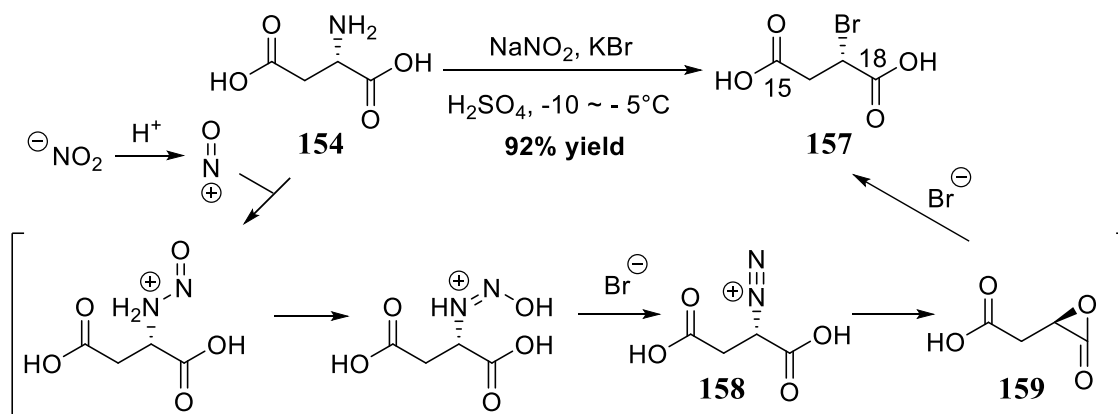


Scheme 3.18: Proposed synthesis of C9-C15 fragments **114** and **115**.

3.4.1 Synthesis of the natural C9-C15 fragment

This route had been explored by former colleague Sam Ting, although different protecting groups were planned to accommodate the current synthetic strategy. It proceeded with reasonable ease. The bromination to produce **157** is carried out *via* a Sandmeyer-type reaction,⁴⁹ wherein the amine in **154** is converted to diazonium salt **158** upon treatment with acidic sodium nitrite solution. Neighbouring group participation by the carboxylic acid facilitates the dissociation of diazonium in a $\text{S}_{\text{N}}2$ -type fashion, forming an intermediate lactone

159. Subsequent ring-opening by the bromide occurs, resulting in the double inversion, thus the stereochemistry at C17 is retained (**Scheme 3.19**).



Scheme 3.19: Bromination of **154** via Sandmeyer reaction.

This reaction should be maintained below -5°C , because diazonium salts are very unstable. Aromatic diazonium salts have been reported to dissociate to produce the corresponding phenol in the presence of acid and H_2O if temperature arises.^{50,51} A related problem was encountered when scaling up the reaction from 10 g of *S*-aspartic acid to 20 g: an unknown by-product was formed. Its presence was first noticed as a yield of over 100%. A closer examination revealed two peaks at 5.31 and 2.08 ppm in the ^1H NMR spectrum, which are typical chemical shifts for an oxymethine proton in an ester and hydroxyl group, respectively (**Figure 3.4**), or alternatively dichloromethane and acetone. Neither of these solvents was used during the reaction or work-up, but, regardless, the product was further purged under high vacuum. The two signals at 5.31 and 2.08 ppm did not disappear, consistent with them not being due to dichloromethane and acetone. The two peaks may suggest the formation of an alcohol by-product and esterification with the carboxylic acid. However, the mass spectrum showed a second major negative molecular ion at 414.8474 m/z as well as the product, and the isotope pattern indicated that it contains two bromines, which suggests instead that dimerization of the brominated product **157** or polymerization had occurred. However, no obvious polymerization products with the above characteristics match the molecular weight. Even though it seems a minor impurity, its presence interferes with the subsequent reduction reaction, resulting in reduced yields and product contaminated by inseparable impurities. A small amount of the contaminated sample of **157** was recrystallized from water to produce non-transparent crystals, but this did not make an improvement in subsequent reactivity.

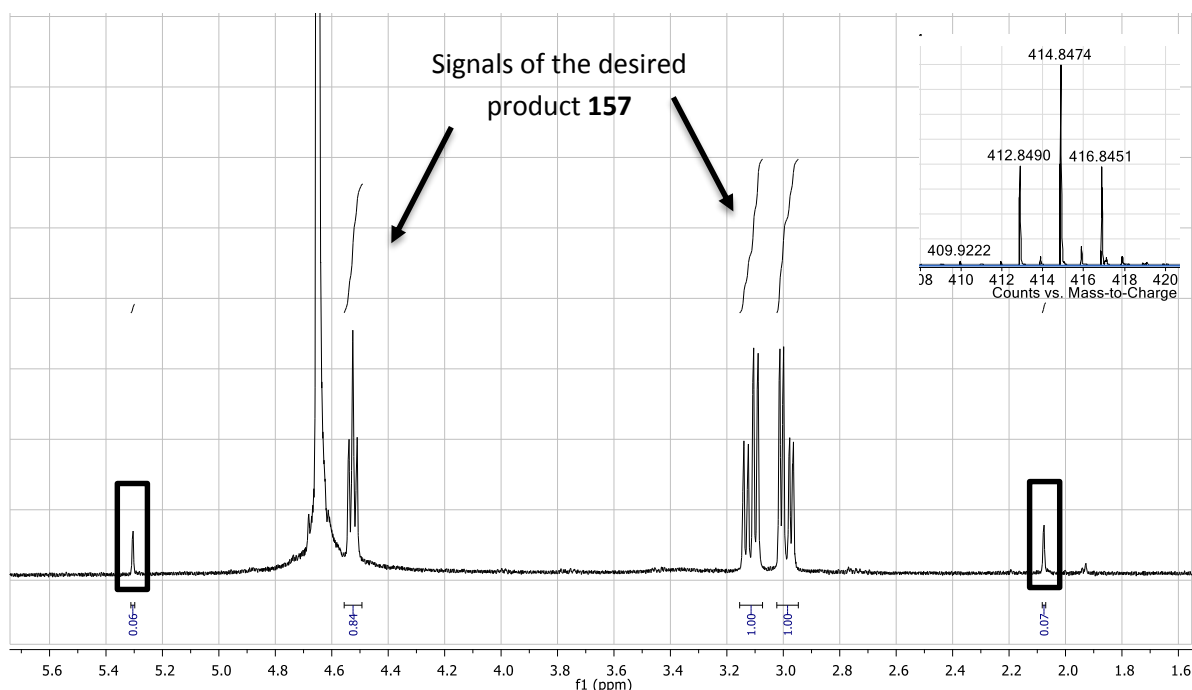
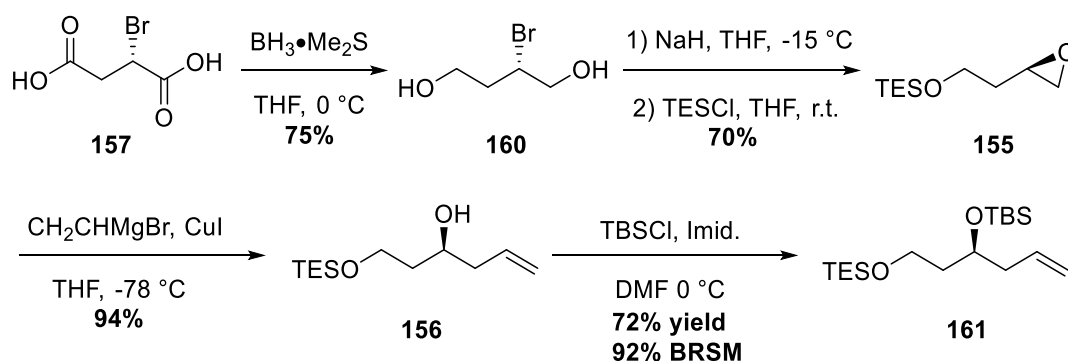


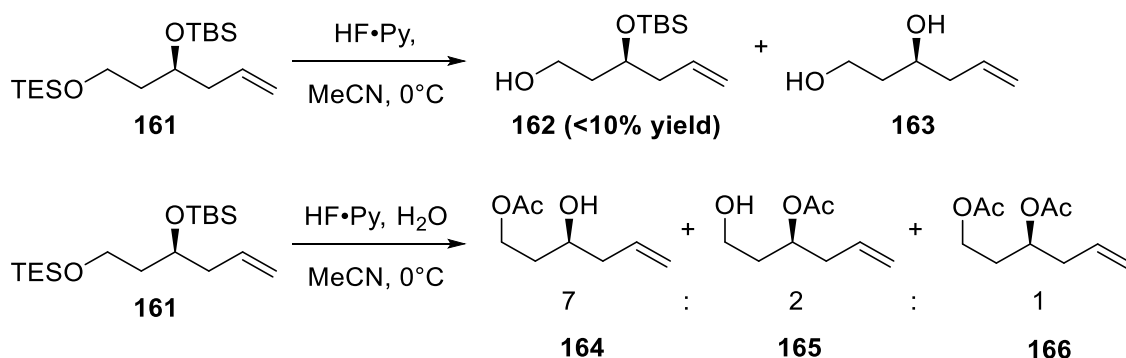
Figure 3.4: ^1H NMR and mass spectra of the unknown by-product from large-scale bromination.

The borane reduction of **157** to afford **160** was initially difficult to handle. Following the literature work-up,⁵² the reaction mixture turned into a hard gel upon warming to room temperature, even after quenching. This may have resulted from a borane-THF complexation or THF polymerization, but neither could be confirmed. Initially the reaction produced unsatisfyingly low yields. An attempt to switch the solvent from THF to toluene totally quenched the reactivity of borane and starting material was recovered. After more experiments the best yield (75%) was achieved with a Rochelle salt quench at 0 °C, slowly warming up to room temperature over an hour and vigorous stirring for a prolonged time (**Scheme 3.20**). The following one-pot epoxide formation and silyl protection to **155** is a very reliable reaction, and the epoxide opening with vinylmagnesium bromide also reached good yields when purified CuI and newly purchased Grignard reagent were used. According to the current protecting group strategy, this secondary alcohol in **156** was protected with TBS to afford bis-silylated product **161** with a 72% yield.



Scheme 3.20: Synthesis of C9-C15 fragment precursor **161**.

Deprotection of the TES ether in **161** with HF·Py to **162** was initially quite low yielding despite running the reaction overnight (Scheme 3.21). It was speculated that the prolonged reaction time promoted double deprotection to the diol **163**, and that shorter reaction times could avoid all or the majority of TES-deprotection. It was also found that the dryness of acetonitrile is essential. When analytical grade acetonitrile was used, both silyl groups were fully deprotected and either or both of the alcohols were found to be acetylated, producing inseparable mixtures of **164**, **165** and **166** in a ratio of 7:2:1, respectively. No direct acetylation source had been present.

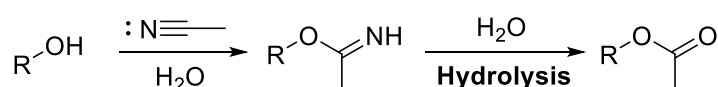


Scheme 3.21: Deprotection of TES ether in **161** with HF·Py.

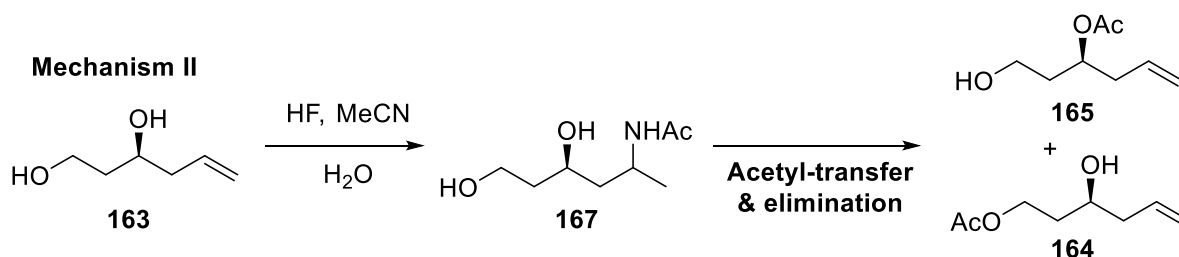
This puzzling phenomenon could be explained by an attack of the alcohol functionalities in doubly deprotected **163** on acetonitrile to produce an imine, which is then hydrolyzed in the presence of water to produce the acetates **164**, **165** and **166** (Scheme 3.22, mechanism I). This is only possible if the acetonitrile was protonated by HF in the presence of H₂O to become a better electrophile. Another possible mechanism was considered based on an observation

reported in 1970 by J. R. Norell. In that work, it was shown that hydrogen fluoride can fluorinate terminal alkenes at ambient temperatures (25~40°C), and the resulting fluoride reacts with acetonitrile in the presence of water to produce *N*-alkyl acetamides.⁵³ With this information, the acetyl may be sourced from the amide in **167** (Mechanism II). However, even though acetyl transfer to the secondary alcohol *via* a six-membered transition state is possible, the acetyl transfer to the primary alcohol *via* an eight-membered ring could be very difficult. In addition, to restore the terminal alkene, amine elimination must occur, which is highly unlikely under the reaction conditions.

Mechanism I



Mechanism II



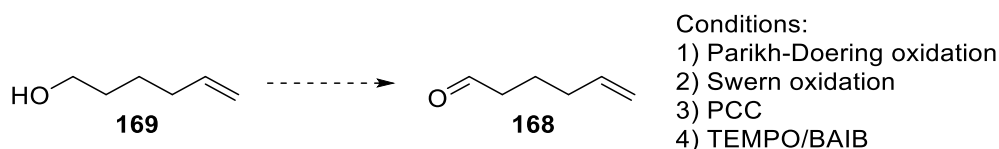
Scheme 3.22: Possible mechanisms for acetylation.

Current PhD student Sophie Geyrhofer confirmed the double deprotection of **161** to afford **163** occurs in overnight reactions, and successfully produced the TES-deprotected product **162** with a 61% yield after a 3 h reaction at 0 °C. Even with the short reaction time, 20% of the doubly deprotected diol **163** was also isolated, thus further optimization of this reaction is required. However, the synthetic strategy has been altered, and the TES protection was retained until a later stage.

3.4.2 Synthesis of C9-C15 analogue fragments

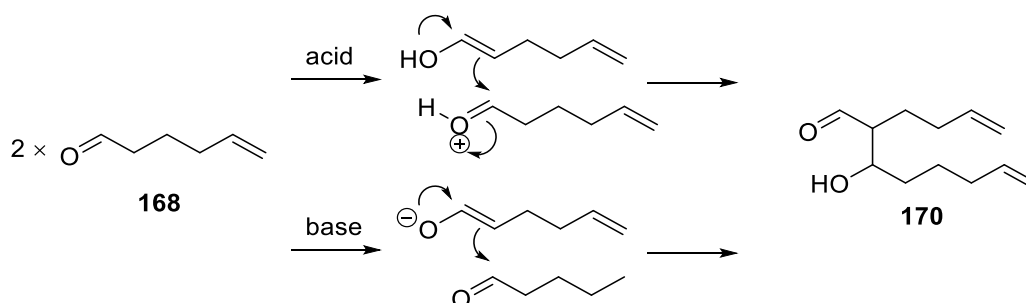
One aim of this project is to find simplified analogues of zampanolide (**19**) that can be synthesized by shorter sequences than for the natural product. As removal of the *exo*-methylene was found to be beneficial to retain the cytotoxicity,^{48,54} the use of 5-hexenal (**168**) as an

analogue fragment of C9-C16 was proposed, which avoids the lengthy process required to synthesize C9-C15 fragment (**115**). A good number of literature sources reported that **168** would be easily accessed by oxidation of the cheap and readily available 5-hexenol (**169**), and various oxidation methods could be used (**Scheme 3.23**).⁵⁵⁻⁵⁸



Scheme 3.23: Planned preparation of 5-hexenal (**168**) *via* oxidation.

Parikh-Doering oxidation was first attempted. By ¹H NMR spectroscopy, the crude mixture contained almost exclusively the desired aldehyde **168** and pyridinium compound. However, during column chromatography, the purified product decomposed. The ¹H NMR spectrum showed that nearly all aldehyde signals vanished and a new oxymethine signal appeared, which suggested that the aldehyde **168** might have polymerized. No effort was put towards the characterization of this product. Some fractions containing **168** was collected, but it was always contaminated by impurities. Preparation of 5-hexenal (**168**) was then attempted by using pyridinium chlorochromate (PCC). Attempts to purify the crude product with a Celite plug resulted in unsatisfying purification, and a silica plug again decomposed the desired **168**. However, the aldehyde functionality was conserved this time. This product was characterized, and identified as the dimerized product **170**. It is commonly known that aldehydes can dimerize *via* aldol reactions (**Scheme 3.24**), where the enol formation can be promoted by the presence of acid or base.



Scheme 3.24: Dimerization of 5-hexenal (**168**) *via* aldol reaction.

The dimerized product **170** was never obtained in pure form, but NMR, HRMS and IR evidence all support the assignment of the dimer structure. Interestingly the ^1H NMR spectrum of **170** shows the signals at 2.45 and 4.07 ppm as triplets (**Figure 3.5**), which are the protons α - and β - to the aldehyde (H^2 , H^3) respectively. The coupling constants indicate that there is no vicinal coupling between aldehyde and α -protons or α - and β -protons. According to the Karplus equation, vicinal coupling constant is proportional to $\cos^2\theta$, where θ is the dihedral angle. Thus, it can be assumed that free rotation is hindered and the α -proton must be approximately perpendicularly oriented to both aldehyde proton and β -proton.

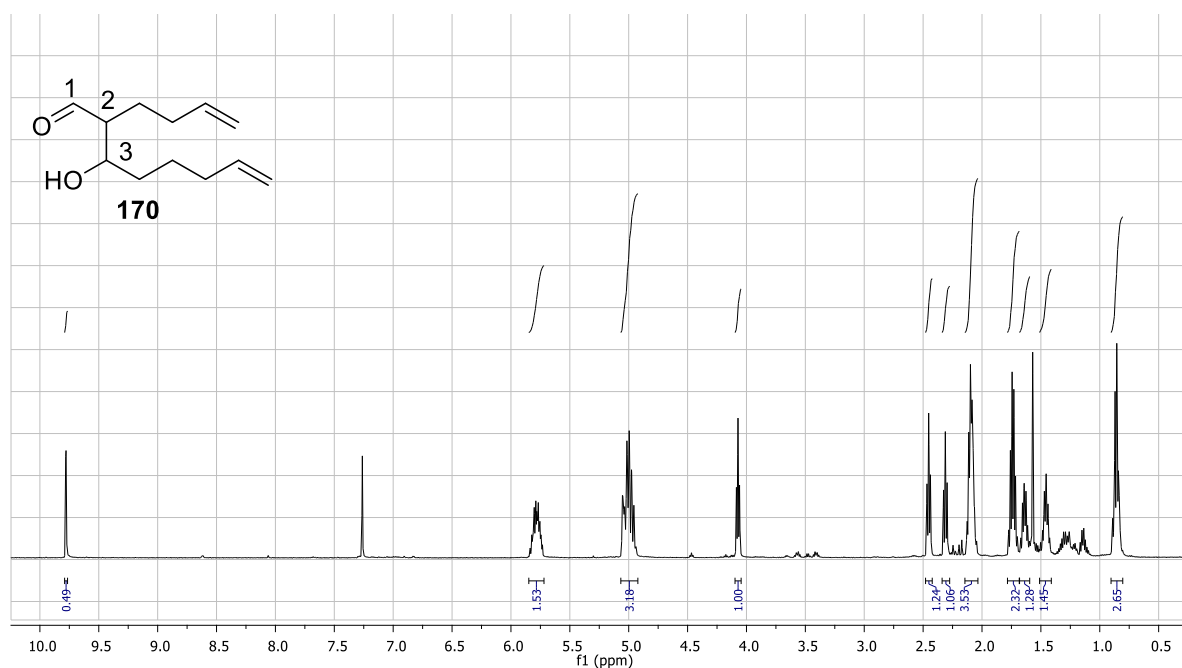


Figure 3.5: ^1H NMR spectrum of the dimerized aldehyde product **170**.

To have such geometry, hydrogen bonding between the hydroxy and aldehyde together with the steric hindrance of the long chains may be constraining **170** in a rigid six-membered ring such that there are *ca.* 90° angles between H^1 , H^2 and H^3 . The Newman projection of (2*R*,3*S*)-**170** is shown in **Figure 3.6** for demonstration.

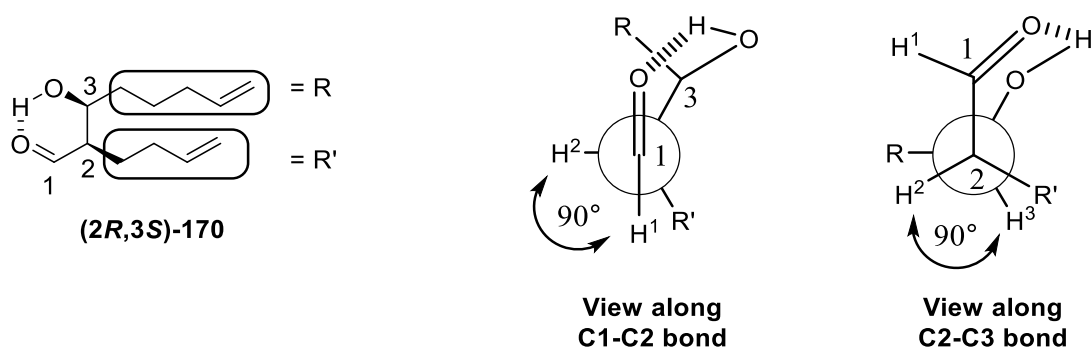
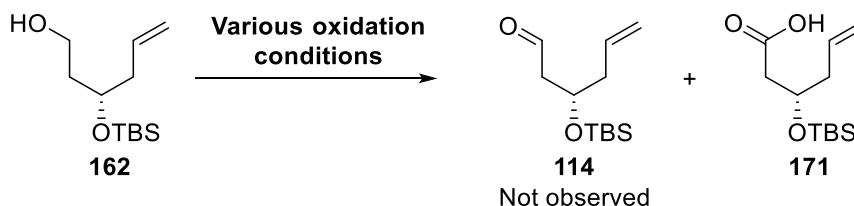


Figure 3.6: Proposed conformation of the dimerized product **170** based on proton coupling.

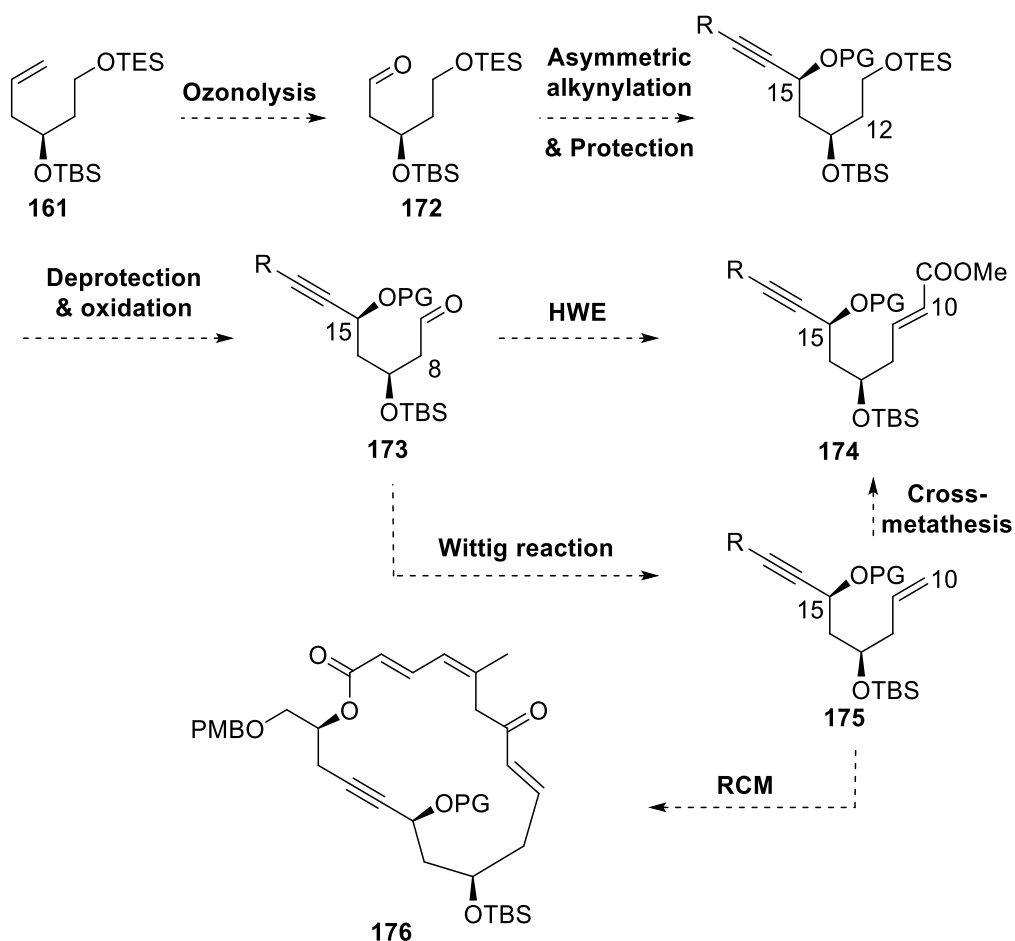
It was hypothesized that aldehyde **168** could be unstable in contact with the acidic silica or upon concentration. Swern oxidation of 5-hexenol (**169**) produced the cleanest sample of crude product **168**, which was hoped would allow purification without silica. After washing the reaction mixture thoroughly with water, the only contaminant left was triethylamine (Et_3N). However, the further attempt to remove Et_3N by washing with aqueous potassium bisulfate (KHSO_4) solution caused decomposition, and the aldehyde signal vanished on ^1H NMR spectrum. TEMPO/BAIB oxidation was also attempted. Theoretically, upon full conversion, the reaction mixture would contain mostly high boiling point species, and the relatively lower boiling point compounds would be the desired product **168** ($128\sim 129\text{ }^\circ\text{C}$)⁵⁹ and a low boiling solvent such as dichloromethane. Therefore, purification would be possible by distilling the reaction mixture to yield a solution of 5-hexenal (**168**) in dichloromethane. Vacuum distillation was initially investigated and yielded a dichloromethane solution of **168** enriched with iodobenzene. Atmospheric pressure distillation after dissolving the crude reaction mixture in diethyl ether indeed removed iodobenzene, but dimerization still occurred in the solution. Therefore, it is concluded that 5-hexenal (**168**) spontaneously dimerizes in pure form. A commercial source was also considered, but **168** is only available *via* custom synthesis, which is too expensive for this project. A careful review of the literature found that this aldehyde product **168** was often used without purification,⁶⁰⁻⁶³ but this is not an option for this project. The intended use of **168** is in a metal-promoted alkynylation reaction and such reactions are often very sensitive to impurities. Therefore, this model substrate was abandoned. Similar experiments to carry the C9-C15 fragment **162** to the aldehyde **114** were done by current PhD student Sophie Geyrhofer (**Scheme 3.25**). She found that the oxidation of TES-protected product **162** does not stop at the aldehyde, but demonstrated a high propensity to carry on to

the acid **171**. Various oxidation conditions were tested, including Dess-Martin periodinane, IBX, Swern, and TEMPO/BAIB oxidations.



Scheme 3.25: Geyrhofer's oxidation of alcohol **162**.

From the findings of both the model and real fragments, it was hypothesized that the terminal alkene might be interfering with the oxidation, thus the aldehyde should be formed in the absence of a terminal alkene. As described before, the fragment required for *O*-Michael addition (**115**) contains an α,β -unsaturated ester instead of the terminal alkene, thus the synthesis of fragment **115** could be explored (see **Scheme 3.18**). Alternatively, the alkene in **161** can be ozonized to produce the aldehyde **172**, and the C11 silyl ether can be cleaved after asymmetric alkynylation and protection of the resulting propargylic alcohol (**Scheme 3.26**). The primary alcohol is then revealed ready for oxidation to produce aldehyde **173**. A TES-protection can be used for the propargylic alcohol, as the primary TES ether can be deprotected selectively over the secondary, and TES is partially orthogonal to TBS for later transformations. The **173** can be transformed *via* a Horner-Wadsworth-Emmons reaction to afford the α,β -unsaturated methyl ester **174**, set up for *O*-Michael addition, or *via* a Wittig reaction to produce the precursor **175** for iodoetherification or Pd-catalyzed cyclization. The terminal alkene **175** could alternatively be subjected to cross metathesis with methyl acrylate to afford **174** or RCM to form **176**, precursor to a truncated monocyclic analogue.



Scheme 3.26: Alternative synthetic strategy for pyran fragment **174** and **175**.

A simple model aldehyde **177** was prepared in two steps *via* silyl protection of 5-hexenol (**169**) followed by ozonolysis. With only an aqueous work-up after the protection step, a good 95% yield of **177** was obtained over the two steps.



Scheme 3.27: Synthesis of model fragment **177**.

3.5 Experimental data

General experimental information

Unless otherwise stated, all reactions were carried out in oven-dried glassware under a positive pressure of nitrogen, delivered via a manifold, or argon from a balloon. Dry tetrahydrofuran, dichloromethane and toluene were obtained from a PureSolv MD 5 solvent purification system (Innovative Technology). Dry dimethylformamide was purchased from Acros and used without further purification. DMSO, triethylamine and oxalyl chloride were purified by distillation with calcium hydride as drying agent. Analytical grade solvents were used for aqueous work-up and column chromatography (petroleum ether, ethyl acetate, diethyl ether, dichloromethane and methanol). Column chromatography was performed on silica gel 60Å (Pure Science, 40–63 micron) with the eluent mixtures as stated in the corresponding procedures. Thin-layer chromatography was performed on silica-coated plastic plates (Macherey-Nagel, POLYGRAM® Sil G/UV₂₅₄). UV-active compounds were detected under UV irradiation ($\lambda = 254$ nm), while non-UV-active compounds were visualised with anisaldehyde or potassium permanganate staining solutions.

PMBCl was prepared freshly using the previously reported method.⁴² All other chemicals were purchased from Pure Science, Sigma-Aldrich, AK Scientific, Acros, Merck, British Drug House, Burkes Research, Thermo Fisher Scientific, Avocado, Panreac Riedel-de Haën and Apollo. Infra-red (IR) spectra were collected from liquid films on a Perkin Elmer Spectrum One FT-IR spectrometer or neat sample on an ALPHA FT-IR spectrometer (Bruker) fitted with attenuated total reflectance (ATR). The intensities of signals are defined as: br = broad, s = strong, m = medium, w = weak. Mass spectra were collected on an Agilent 6530 Accurate-Mass Q-TOF LC/MS high-resolution mass spectrometer (HRMS). The specific rotations were collected on an AUTOPOL II automatic polarimeter (Rudolph Research Analytical), and the reported values are an average of 10 measurements and concentrations are reported in g/100 mL.

Nuclear magnetic resonance (NMR) spectra were obtained in deuterated chloroform (CDCl₃) or deuterium oxide (D₂O) using Varian Inova instruments operating at 300 or 500 MHz for proton and 75 or 125 MHz for carbon. Proton and carbon chemical shifts are reported in parts per million (ppm) relative to residual CHCl₃ [$\delta(^1\text{H}) = 7.26$ ppm], H₂O [$\delta(^1\text{H}) = 4.66$ ppm], and CDCl₃ [$\delta(^{13}\text{C}) = 77.0$ ppm], respectively. Signals are defined as: s = singlet, d = doublet, t = triplet, q = quartet, quin = quintet, m = multiplet, app. = apparent, obs. = obscured peak, br. =

broad. Coupling constants (J) are reported in Hertz (Hz). Assignments were determined by two-dimensional NMR experiments (COSY, NOESY, HSQC and HMBC).

CuI purification:

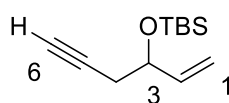
To a boiling aqueous solution of NaI (7.0 g, 47 mmol) in H₂O (5 mL, 9 M), CuI (1.00 g, 5.26 mmol) was added portionwise over 45 min. The solution progressively turned red with each addition. The solution was cooled down to r.t., and then 0 °C. H₂O was added to precipitate out CuI. The precipitate was filtered, washed with H₂O, ethanol, EtOAc, Et₂O and petroleum ether successively. The solid was further dried under high vacuum to yield CuI as a pale-pink powder (811 mg).

Activation of zinc powder:

To a suspension of zinc powder (3.1 g, 47 mmol) in H₂O (10 mL), an aqueous HCl solution (0.3 mL, 4 M) was added dropwise with shaking until the release of small gas bubbles was observed. The activated zinc powder was filtered, washed sequentially with H₂O, MeOH, EtOAc, Et₂O and petroleum ether, and dried under high vacuum to yield a pale grey powder (3.0 g).

Synthesis of C3-C8 fragment

(Hex-1-en-5-yn-3-yloxy)*tert*-butyldimethylsilane (118)



To a suspension of activated zinc powder (982 mg, 15.0 mmol) in THF (25 mL), a propargyl bromide solution (1.8 mL, 80 % w/w in toluene, 16 mmol) was added dropwise. The reaction mixture was stirred at r.t. for 1 h 30 min. After the addition of further equivalent of activated zinc powder (410 mg, 6.27 mmol), the reaction was cooled down to -78 °C. A solution of acrolein (**93**) (0.50 mL, 7.5 mmol) in THF (4.2 mL) was added dropwise at -78 °C. The reaction mixture was stirred at -78 °C for 1 h and at r.t. for 2 h. The reaction was quenched with sat. aq. NH₄Cl (20 mL) and filtered through a Celite pad. The filtrate was extracted with Et₂O (3×50 mL). The organic layers were combined, dried over MgSO₄, filtered and concentrated under reduced pressure. The yellow oil obtained was purified by column chromatography (silica, 3:1 Pet. ether/EtOAc, R_f = 0.27). The relevant fractions were partially concentrated to yield a solution of the desired intermediate alcohol in EtOAc. This mixture was combined with imidazole (620 mg, 9.11 mmol) and dissolved in DMF (9.0

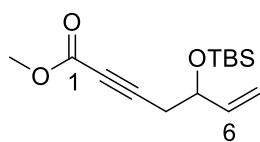
mL). After cooling down to 0 °C, a solution of TBSCl (1.32 g, 6.27 mmol) in DMF (9.0 mL) was added dropwise. The reaction was stirred at r.t. for 14 h, then diluted with Et₂O (50 mL), washed with H₂O (3×50 mL) and brine (50 mL), dried over MgSO₄, filtered and concentrated under reduced pressure. This crude product was purified by column chromatography (silica, 10:1 Pet. ether/EtOAc, R_f = 0.80) to yield **118** as a colourless oil (1.28 g, 81% yield).

¹H NMR (500 MHz, CDCl₃): δ 5.92 (ddd, *J* = 16.8, 10.8, 5.6 Hz, 1H, 2-CH), 5.26 (d, *J* = 17.1 Hz, 1H, one of 1-CH₂), 5.12 (d, *J* = 10.5 Hz, 1H, one of 1-CH₂), 4.27 (app. q, *J* = 5.6 Hz, 1H, 3-CH), 2.42 (ddd, *J* = 16.6, 6.1, 2.9 Hz, 1H, one of 4-CH₂), 2.33 (ddd, *J* = 16.6, 7.1, 2.4 Hz, 1H, one of 4-CH₂), 1.99 (t, *J* = 2.6 Hz, 1H, 6-CH), 0.91 (s, 9H, *t*Bu, TBS), 0.10 (s, 3H, Me, TBS), 0.07 (s, 3H, Me, TBS).

¹³C NMR (125 MHz, CDCl₃): δ 139.9 (CH, C2), 114.7 (CH₂, C1), 81.3 (C, C5), 72.2 (CH, C3), 69.9 (CH, C6), 28.3 (CH₂, C4), 25.8 (CH₃, *t*Bu, TBS), 18.2 (C, *t*Bu, TBS), -4.6 (CH₃, Me, TBS), -4.9 (CH₃, Me, TBS).

These data were consistent with those reported previously.⁶⁴

Methyl 5-*tert*-butyldimethylsilyloxy-6-hepten-2-ynoate (**119**)



To a solution of terminal alkyne **118** (905 mg, 4.30 mmol) in THF (43 mL) at -78 °C, *n*BuLi (2.6 mL, 1.8 M in cyclohexane, 4.68 mmol) was added dropwise. The reaction was stirred at -78 °C for 40 min. Methyl chloroformate (8.60 mmol, 0.66 mL) was added dropwise. After stirring for 2 h 30 min at -78 °C, the reaction was quenched with sat. aq. NH₄Cl (30 mL) and warmed up to r.t. The aqueous layer was separated and extracted with Et₂O (3 × 30 mL). The organic layers were combined, dried over MgSO₄, filtered and concentrated under reduced pressure. This crude product was purified by column chromatography (silica, 30:1 Pet. ether/EtOAc, R_f = 0.16) to yield the title compound **119** as a pale oil (875 mg, 76%).

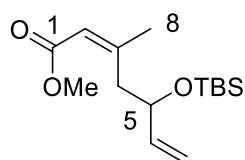
¹H NMR (500 MHz, CDCl₃): δ 5.87 (ddd, *J* = 16.7, 10.7, 5.9 Hz, 1H, 6-CH), 5.27 (d, *J* = 17.1 Hz, 1H, one of 7-CH₂), 5.14 (d, *J* = 10.5 Hz, 1H, one of 7-CH₂), 4.32 (app. q, *J* = 6.3 Hz, 1H, 5-CH), 3.76 (s, 3H, CH₃, OMe), 2.55 (dd, *J* = 16.9, 6.3 Hz, 1H, one of 4-CH₂), 2.47 (dd, *J* = 16.9, 6.3 Hz, 1H, one of 4-CH₂), 0.90 (s, 9H, *t*Bu, TBS), 0.10 (s, 3H, Me, TBS), 0.06 (s, 3H, Me, TBS).

¹³C NMR (125 MHz, CDCl₃): δ 154.1 (C, C1), 139.4 (CH, C6), 115.4 (CH₂, C7), 110.0 (C, C3), 86.5 (C, C2), 71.5 (CH, C5), 52.6 (CH₃, OMe), 28.6 (CH₂, C4), 25.7 (CH₃, *t*Bu, TBS), 18.2 (C, *t*Bu, TBS), -4.6 (CH₃, Me, TBS), -5.0 (CH₃, Me, TBS).

IR (neat) cm⁻¹: 2954 (m, C–H), 2930 (m, C–H), 2857 (m, C–H), 2241 (m, C≡C), 1716 (s, C=O), 1248 (s, C–O), 1073 (s, C–H), 930 (s, C–Si), 836 (s, C–Si), 777 (s, C–Si).

HRMS (ESI) *m/z*: found 286.1837, calcd for C₁₄H₂₈O₃SiN [M+NH₄]⁺ 286.1833 (Δ = 2.1 ppm).

(2*Z*)-Methyl 5-(*tert*-butyldimethylsilyloxy)-3-methyl-2,6-heptadienoate (**125**)



To a suspension of CuI (641 mg, 3.37 mmol) in THF (14 mL) at 0 °C, MeLi was added dropwise (2.4 mL, 2.8 M in Et₂O, 8.4 mmol). After stirring at 0 °C for 45 min, a solution of the ynoate **120** (600 mg, 2.24 mmol) in THF (3.2 mL) was added dropwise at -78 °C. The reaction mixture was stirred at -78 °C for 3 h. The reaction was quenched with sat. aq. NH₄Cl (30 mL) and warmed up to r.t. The aqueous layer was separated and extracted with Et₂O (3 × 50 mL). The organic layers were combined, dried over MgSO₄, filtered and concentrated under reduced pressure. This crude product was purified by column chromatography (silica, 36:1 Pet. ether/ Et₂O, R_f = 0.22) to yield **125** as a yellow oil (620 mg, 97% yield).

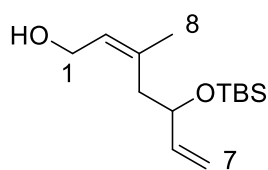
¹H NMR (500 MHz, CDCl₃): δ 5.86 (ddd, *J* = 16.4, 10.5, 5.9 Hz, 1H, 6-CH), 5.73 (s, 1H, 2-CH), 5.20 (d, *J* = 17.1 Hz, 1H, one of 7-CH₂), 5.03 (d, *J* = 10.3 Hz, 1H, one of 7-CH₂), 4.42 (m, 1H, 5-CH), 3.68 (s, 3H, CH₃, OMe), 2.88 (dd, *J* = 12.2, 4.6 Hz, 1H, one of 4-CH₂), 2.71 (dd, *J* = 12.6, 7.9 Hz, 1H, one of 4-CH₂), 1.95 (s, 3H, 8-CH₃), 0.88 (s, 9H, *t*Bu, TBS), 0.01 (s, 6H, Me, TBS).

¹³C NMR (125 MHz, CDCl₃): δ 166.7 (C, C1), 158.4 (C, C3), 141.3 (CH, C6), 116.9 (CH, C2), 113.7 (CH₂, C7), 73.6 (CH, C5), 50.8 (CH₃, OMe), 41.9 (CH₂, C4), 27.5 (CH₃, C8), 25.9 (CH₃, *t*Bu, TBS), 18.1 (C, *t*Bu, TBS), -4.5 (CH₃, Me, TBS), -4.9 (CH₃, Me, TBS).

IR (neat) cm⁻¹: 2952 (m, C–H), 2929 (m, C–H), 2857 (m, C–H), 1718 (s, C=O), 1645 (m, C=C), 1251 (s, C–O), 1196 (s, C–H), 1027 (s, C–H), 834 (s, C–Si), 775 (s, C–Si).

HRMS (ESI) *m/z*: found 285.1869, calcd for C₁₅H₃₂O₃SiN [M+NH₄]⁺ 285.1880 (Δ = 3.9 ppm).

(2Z)-3-Methyl-5-(tert-butyldimethylsilyloxy)hepta-2,6-dien-1-ol (128)



To a solution of the ester **125** (306 mg, 1.08 mmol) in CH_2Cl_2 (10.5 mL, 0.10 M) at $-78\text{ }^\circ\text{C}$, a solution of DIBAL-H (3.5 mL, 1.0 M in THF, 3.5 mmol) was added dropwise. The reaction was stirred at $-78\text{ }^\circ\text{C}$ for 30 min, followed by $0\text{ }^\circ\text{C}$ for 30 min and r.t. for 30 min. It was then quenched with a sat. aq. solution of Rochelle's salt (15 mL) and stirred vigorously for 1 h. The mixture was extracted with CH_2Cl_2 ($3 \times 15\text{ mL}$). The organic layers were combined and dried over MgSO_4 and concentrated under reduced pressure. This crude product was purified by column chromatography (silica, 5:1 Pet. ether/EtOAc, $R_f = 0.41$) to yield the product **128** as a yellow oil (229 mg, 85% yield).

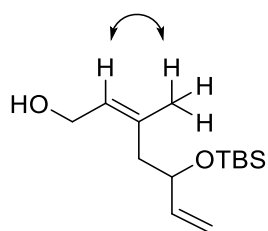
^1H NMR (500 MHz, CDCl_3): δ 5.83 (ddd, $J = 17.0, 10.5, 6.6\text{ Hz}$, 1H, 6-CH), 5.65 (t, $J = 7.1\text{ Hz}$, 1H, 2-CH), 5.17 (dd, $J = 17.3, 1.2\text{ Hz}$, 1H, one of 7- CH_2), 5.06 (dd, $J = 10.3, 1.0\text{ Hz}$, 1H, one of 7- CH_2), 4.25 (m, 1H, 5-CH), 4.19 (m, 1H, one of 1- CH_2), 4.00 (app. dt, $J = 12.1, 6.5\text{ Hz}$, 1H, one of 1- CH_2), 2.51 (dd, $J = 13.3, 8.7\text{ Hz}$, 1H, one of 4- CH_2), 2.10 (dd, $J = 13.4, 4.6\text{ Hz}$, 1H, one of 4- CH_2), 1.96 (t, $J = 5.4\text{ Hz}$, 1H, OH), 1.78 (s, 3H, 8- CH_3), 0.89 (s, 9H, *t*Bu), 0.05 (s, 3H, Me), 0.05 (s, 3H, Me).

^{13}C NMR (125 MHz, CDCl_3): δ 141.4 (CH, C6), 136.8 (C, C3), 127.1 (CH, C2), 114.1 (CH_2 , C7), 72.1 (CH, C5), 58.6 (CH_2 , C1), 41.0 (CH_2 , C4), 25.9 (CH_3 , *t*Bu), 23.9 (CH_3 , C8), 18.3 (C, *t*Bu), -4.5 (CH_3 , Me), -4.7 (CH_3 , Me).

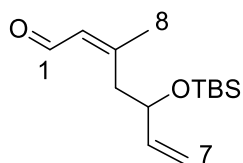
IR (film from CH_2Cl_2) cm^{-1} : 3410 (br, O-H), 2956 (s, C-H), 2930 (s, C-H), 2886 (s, C-H), 2857 (s, C-H), 1678 (s, C=C), 1472 (m, C-H), 1253 (s, C-O), 937 (s, C-H), 8345 (s, C-Si), 776 (s, C-Si).

HRMS (ESI) m/z : found 279.1756, calcd for $\text{C}_{14}\text{H}_{28}\text{O}_2\text{SiNa}$ $[\text{M}+\text{Na}]^+$ 279.1756 ($\Delta = 0.0\text{ ppm}$).

NOESY (600 MHz, CDCl_3):



(2Z)-3-Methyl-5-(*tert*-butyldimethylsilyloxy)hepta-2,6-dienal (126)



To a solution of the alcohol **128** (374 mg, 1.46 mmol) in DMSO (2.5 mL, 0.58 M) at r.t., a solution of IBX (1.23 g, 4.37 mmol) in DMSO (18.8 mL) was added dropwise. After stirring at r.t. for 17 h, EtOAc (20 mL) was added to the reaction mixture to precipitate out IBX. The mixture was filtered through Celite, and the filtrate was concentrated under reduced pressure. This crude product was purified by column chromatography (silica, 20:1 Pet. ether/ EtOAc, R_f = 0.38) to yield the aldehyde **126** as a colourless oil (306 mg, 82% yield).

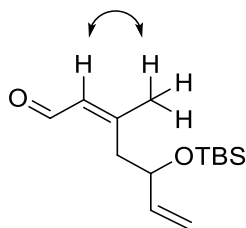
^1H NMR (500 MHz, CDCl_3): δ 9.90 (d, J = 8.1 Hz, 1H, 1-CH), 5.96 (d, J = 7.7 Hz, 1H, 2-CH), 5.83 (dddd, J = 17.9, 10.3, 6.4, 2.1 Hz, 1H, 6-CH), 5.22 (d, J = 17.3 Hz, 1H, one of 7-CH₂), 5.11 (d, J = 10.5 Hz, 1H, one of 7-CH₂), 4.32 (m, 1H, 5-CH), 2.91 (ddd, J = 13.0, 8.2, 1.5 Hz, 1H, one of 4-CH₂), 2.54 (ddd, J = 13.1, 4.3, 1.3 Hz, 1H, one of 4-CH₂), 2.02 (s, 3H, 8-CH₃), 0.86 (s, 9H, *t*Bu), 0.02 (s, 3H, Me), 0.01 (s, 3H, Me).

^{13}C NMR (125 MHz, CDCl_3): δ 191.5 (CH, C1), 159.8 (C, C3), 140.6 (CH, C6), 130.4 (CH, C2), 114.9 (CH₂, C7), 72.6 (CH, C5), 41.5 (CH₂, C4), 26.1 (CH₃, C8), 25.8 (CH₃, *t*Bu), 18.1 (C, *t*Bu), -4.5 (CH₃, Me), -4.9 (CH₃, Me).

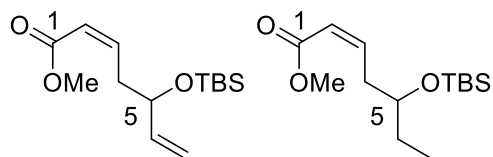
IR (neat) cm^{-1} : 2956 (m, C–H), 2930 (m, C–H), 2857 (m, C–H), 1676 (s, C=O), 1631 (w, C=C), 1609 (w, C=C), 1073 (s, C–O), 835 (s, C–Si), 775 (s, C–Si).

HRMS (ESI) m/z : found 255.1776, calcd for $\text{C}_{14}\text{H}_{27}\text{O}_2\text{Si}$ $[\text{M}+\text{H}]^+$ 255.1775 (Δ = 0.4 ppm).

NOESY (600 MHz, CDCl_3):



Mixture of (2Z)-methyl 5-(*tert*-butyldimethylsilyloxy)-2,6-heptadienoate (130**) and (2Z)-methyl 5-(*tert*-butyldimethylsilyloxy)-2-heptenoate (**131**) (3:2)**



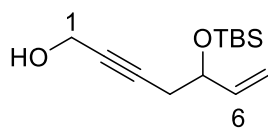
To a solution of **119** (50 mg, 0.186 mmol) and Lindlar's catalyst (10 mg) in EtOAc (1.3 mL, 0.14 M), was added 2-methylbutene (0.13 mL). H₂ gas was

bubbled through the solution for 2 h. The reaction mixture was filtered through a Celite pad, and rinsed with CH₂Cl₂. The filtrate was concentrated under reduced pressure. This crude product was purified by column chromatography (silica, 95:5 Pet. ether/EtOAc, R_f = 0.55) to yield **130** in a mixture with 40% of **131** (34 mg, 68% combined yield).

¹H NMR (500 MHz, CDCl₃) δ 6.39 (dt, *J* = 11.4, 7.2 Hz, 0.4H, 3-CH-**131**), 6.33 (dt, *J* = 11.6, 7.2 Hz, 0.6H, 3-CH-**130**), 5.85 (d, *J* = 11.7 Hz, 1H, 2-CH), 5.80 (ddd, *J* = 11.7, 10.5, 5.6 Hz, 0.6H, 6-CH-**130**), 5.21 (dd, *J* = 17.1, 1.4 Hz, 0.6H, one of 7-CH₂-**130**), 5.07 (dd, *J* = 10.4, 1.3 Hz, 0.6H, one of 7-CH₂-**130**), 4.29 (app. q, *J* = 5.6 Hz, 0.6H, 5-CH-**130**), 3.79–3.64 (obs. m, 0.4H, 5-CH-**131**), 3.71 (s, 3H, CH₃, OMe), 2.95–2.76 (complex m, 2H, 4-CH₂), 1.47 (app. quin, *J* = 7.3 Hz, 0.8H, 6-CH₂-**131**), 0.91–0.86 (complex m, 10.2H, CH₃, *t*Bu-TBS and 7-CH₃-**131**), 0.05 (s, 2.4H, CH₃, Me, TBS-**131**), 0.043 (obs. s, 1.8H, CH₃, Me, TBS-**130**), 0.041 (obs. s, 1.8H, CH₃, Me, TBS-**130**).

¹³C NMR (126 MHz, CDCl₃) δ 166.7 (C, C1), 147.3 (CH, C3-**131**), 146.4 (CH, C3-**130**), 140.7 (CH, C6-**130**), 120.5 (CH, C2-**130**), 120.2 (CH, C2-**131**), 114.2 (CH₂, C7-**130**), 72.7 (CH, C5-**131**), 72.5 (CH, C5-**130**), 67.9 (CH₃, OMe), 51.98 (), 51.95 (), 37.1 (CH₂, C4-**130**), 35.9 (CH₂, C4-**131**), 29.9 (CH₂, C6-**131**), 25.83 (CH₃, *t*Bu, TBS), 25.77 (CH₃, *t*Bu, TBS), 18.2 (C, *t*Bu, TBS), 18.1 (C, *t*Bu, TBS), 9.7 (CH₃, C7-**131**), -4.54 (CH₃, Me, TBS), -4.56 (CH₃, Me, TBS), -4.6 (CH₃, Me, TBS), -4.9 (CH₃, Me, TBS).

5-(*tert*-Butyldimethylsilyloxy)-6-hepten-2-yn-1-ol (132**)**



To a solution of ester **119** (100 mg, 0.475 mmol) in THF (1.0 mL, 0.5 M) at -78 °C, *n*BuLi (0.36 mL, 2.0 M in THF, 0.71 mmol) was added dropwise. After stirring at -78 °C for 35 min, paraformaldehyde (29 mg,

0.95 mmol) was added, and the mixture was warmed to r.t. and stirred for 20 h. The reaction was quenched with sat. aq. NH₄Cl solution (10 mL), and extracted with Et₂O (2 × 10 mL). The

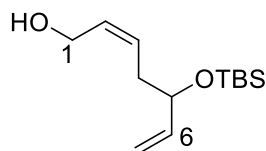
organic layers were combined, dried over MgSO_4 and concentrated under reduced pressure. This crude product was purified by column chromatography (silica, 5:1 Pet. ether/EtOAc, $R_f = 0.35$) to yield **132** as a colourless oil (77 mg, 68% yield).

^1H NMR (500 MHz, CDCl_3): δ 5.91 (ddd, $J = 16.3, 10.4, 5.5$ Hz, 1H, 6-CH), 5.25 (d, $J = 17.1$ Hz, 1H, one of 7- CH_2), 5.11 (d, $J = 10.4$ Hz, 1H, one of 7- CH_2), 4.28–4.22 (complex m, 3H, 1- CH_2 and 5-CH), 2.45 (dd, $J = 16.5, 6.3$ Hz, 1H, one of 4- CH_2), 2.36 (dd, $J = 16.5, 6.7$ Hz, 1H, one of 4- CH_2), 1.54 (t, $J = 5.5$ Hz, 1H, OH), 0.91 (s, 9H, *t*Bu, TBS), 0.09 (s, 3H, CH_3 , Me, TBS), 0.07 (s, 3H, CH_3 , Me, TBS).

^{13}C NMR (125 MHz, CDCl_3) δ 140.0 (CH, C6), 114.6 (C, C7), 83.3 (C, C3), 80.0 (C, C2), 72.3 (CH, C5), 51.4 (CH_2 , C1), 28.6 (CH_2 , C4), 25.8 (CH_3 , *t*Bu, TBS), 18.3 (C, *t*Bu), -4.6 (CH_3 , Me), -4.9 (CH_3 , Me).

HRMS (ESI) m/z : found 258.1884, calcd for $\text{C}_{13}\text{H}_{28}\text{O}_2\text{SiN}$ $[\text{M}+\text{NH}_4]^+$ 258.1884 ($\Delta = 0.0$ ppm).

2*E*-5-(*tert*-Butyldimethylsilyloxy)hepta-2,6-dien-1-ol (**133**)



To a solution of **132** (24 mg, 0.099 mmol) and Lindlar's catalyst (6 mg) in EtOAc (0.9 mL, 0.11 M), was added 2-methylbutene (0.08 mL). H_2 gas was bubbled through the solution for 6 h, with another portion of 2-methylbutene (0.08 mL) added at 2 h. The reaction mixture was filtered through a Celite pad, and rinsed with CH_2Cl_2 . The filtrate was concentrated under reduced pressure to yield **133** as a colourless oil (18 mg, 75% yield).

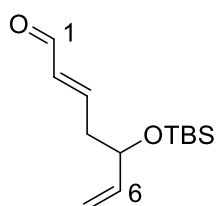
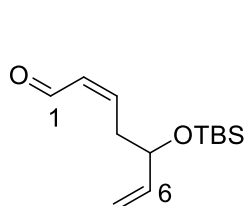
^1H NMR (500 MHz, CDCl_3): δ 5.82 (partially obs. ddd, $J = 16.9, 10.5, 6.1$ Hz, 1H, 6-CH), 5.77 (partially obs. dt, $J = 11.4, 6.9$ Hz, 1H, 2-CH), 5.59 (dt, $J = 11.0, 7.5$ Hz, 1H, 3-CH), 5.17 (d, $J = 17.1$ Hz, 1H, one of 7- CH_2), 5.07 (d, $J = 10.3$ Hz, 1H, one of 7- CH_2), 4.21–4.07 (complex m, 3H, 1- CH_2 & 5-CH), 2.37 (dt, $J = 13.9, 7.8$ Hz, 1H, one of 4- CH_2), 2.27 (m, 1H, one of 4- CH_2), 1.62 (t, $J = 5.6$ Hz, 1H, OH), 0.90 (s, 9H, CH_3 , *t*Bu, TBS), 0.06 (s, 3H, CH_3 , Me, TBS), 0.05 (s, 3H, CH_3 , Me, TBS).

^{13}C NMR (125 MHz, CDCl_3): δ 141.0 (CH, C6), 130.7 (CH, C2), 128.8 (CH, C3), 114.2 (CH_2 , C7), 73.2 (CH, C5), 58.5 (CH_2 , C1), 36.3 (CH_2 , C4), 25.9 (CH_3 , *t*Bu, TBS), 18.3 (C, *t*Bu, TBS), -4.5 (CH_3 , Me, TBS), -4.7 (CH_3 , Me, TBS).

IR (ATR) cm^{-1} : 3355 (br, O–H), 2931 (m, C–H), 2858 (m, C–H), 1462 (w, C–H), 1252 (m, C–O), 1026 (s, C–O), 834 (s, C–Si), 775 (s, C–Si).

HRMS (ESI) m/z : found 243.1777, calcd for $\text{C}_{13}\text{H}_{27}\text{O}_2\text{Si}$ $[\text{M}+\text{H}]^+$ 243.1775 ($\Delta = 0.8$ ppm).

Mixture of (2Z)-5-(tert-butyldimethylsilyloxy)hepta-2,6-dienal (135) and (2E) 5-(tert-butyldimethylsilyloxy)hepta-2,6-dienal (136) (7:3)



To a solution of **133** (18 mg, 0.074 mmol) in CH_2Cl_2 (0.7 mL, 0.01 M), freshly prepared MnO_2 (116 mg, 0.74 mmol) was added. After 7 h, the reaction mixture was filtered, and the filtrate was

concentrated to yield a mixture of 3:2 s.m.:desired Z-product. This mixture was dissolved in CH_2Cl_2 (0.5 mL), and MnO_2 (147 mg, 0.93 mmol) was added. After 3 h, additional MnO_2 (102 mg, 0.65 mmol) was added, and the reaction was stirred for a further 2 h 30 min. The reaction mixture was filtered, and the filtrate was concentrated to yield a colorless oil. This crude product was purified by column chromatography (silica, 10:1 Pet. ether/EtOAc, $R_f = 0.39$) to yield a mixture of 7:3 **135:136** as a colourless oil (9 mg, 50% combined yield).

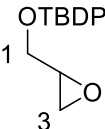
^1H NMR (500 MHz, CDCl_3) δ 10.03 (d, $J = 8.0$ Hz, 0.7H, 1-CH-**135**), 9.50 (d, $J = 7.9$ Hz, 0.3H, 1-CH-**136**), 6.84 (dt, $J = 15.8, 7.6$ Hz, 0.3H, 3-CH-**136**), 6.68 (dt, $J = 11.3, 8.1$ Hz, 0.7H, 3-CH-**135**), 6.14 (dd, $J = 15.7, 7.9$ Hz, 0.3H, 2-CH-**136**), 6.05 (ddt, $J = 11.0, 8.1, 1.4$ Hz, 0.7H, 2-CH-**135**), 5.82 (dd, $J = 17.0, 10.4, 6.1$ Hz, 0.7H, 6-CH-**135**), 5.85–5.77 (obs. m, 0.3H, 6-CH-**136**), 5.24 (dt, $J = 17.1, 1.3$ Hz, 0.7H, one of 7- CH_2 -**135**), 5.23 (dt, $J = 17.1, 1.3$ Hz, 0.3H, one of 7- CH_2 -**136**), 5.12 (dt, $J = 10.3, 1.2$ Hz, 0.7H, one of 7- CH_2 -**135**), 5.11 (dt, $J = 10.4, 1.2$ Hz, 0.3H, one of 7- CH_2 -**136**), 4.31 (app. q, $J = 5.9$ Hz, 1H, 5-CH), 2.88–2.73 (complex m, 1.4H, 4- CH_2 -**135**), 2.54 (app. ddt, $J = 7.2, 5.7, 1.4$ Hz, 0.6H, 4- CH_2 -**136**), 0.89 (s, 2.7H, CH_3 , *t*Bu, TBS-**136**), 0.89 (s, 6.3H, CH_3 , *t*Bu, TBS-**135**), 0.06 (s, 0.9H, CH_3 , Me, TBS-**136**), 0.05 (s, 2.1H, CH_3 , Me, TBS-**135**), 0.04 (s, 3H, CH_3 , Me, TBS-**135** and TBS-**136**).

^{13}C NMR (126 MHz, CDCl_3) δ 193.9 (C, C1-**136**), 191.2 (C, C1-**135**), 154.6 (CH, C3-**136**), 148.7 (CH, C3-**135**), 140.14 (CH, C6-**136**), 140.09 (CH, C6-**135**), 134.9 (CH, C2-**136**), 131.7 (CH, C2-**135**), 131.50, 115.1 (CH_2 , C7-**135**), 115.0 (CH_2 , C7-**136**), 72.4 (CH, C5-**135**), 72.3 (CH, C5-**136**), 41.3 (CH_2 , C4-**136**), 36.4 (CH_2 , C4-**135**), 25.77 (CH_3 , *t*Bu, TBS), 25.76 (CH_3 ,

*t*Bu, TBS), 18.2 (C, *t*Bu, TBS), -4.4 (CH₃, Me, TBS), -4.5 (CH₃, Me, TBS), -4.87 (CH₃, Me, TBS), -4.91 (CH₃, Me, TBS).

Synthesis of C16–C20 fragment

2-(*tert*-Butyldiphenylsilyloxy)methyloxirane (140**)**

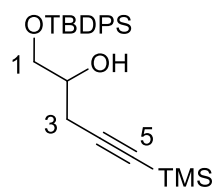
 To a solution of glycidol (**97**, 116 mg, 1.56 mmol) and imidazole (138 mg, 2.03 mmol) in DMF (2.2 mL, 0.71 M) at 0 °C, TBDPSCl (0.47 mL, 1.8 mmol) was added dropwise. After stirring at r.t. for 3 h 30 min, the reaction mixture was quenched with H₂O (10 mL) and diluted with Et₂O (15 mL). The organic layer was separated and washed sequentially with saturated aqueous NaHCO₃ solution (2 × 15 mL), H₂O (15 mL), brine (15 mL), and then dried over MgSO₄, filtered and concentrated under reduced pressure. This crude product was purified by column chromatography (silica, 50:1 Pet. ether/EtOAc, *R*_f = 0.18) to yield **140** as a colourless oil (396 mg, 84%).

¹H NMR (500 MHz, CDCl₃): δ 7.71–7.67 (complex m, 4H, CH, Ph, TBDPS), 7.46–7.37 (complex m, 6H, CH, Ph, TBDPS), 3.85 (dd, *J* = 11.7, 3.2 Hz, 1H, one of 1-CH₂), 3.71 (dd, *J* = 11.8, 4.8 Hz, 1H, one of 1-CH₂), 3.14 (m, 1H, 2-CH), 2.75 (t, *J* = 4.6 Hz, 1H, one of 3-CH₂), 2.62 (dd, *J* = 5.1, 2.7 Hz, 1H, one of 3-CH₂), 1.06 (s, 9H, CH₃, *t*Bu, TBDPS).

¹³C NMR (126 MHz, CDCl₃): δ = 135.61 (CH, Ph), 135.55 (CH, Ph), 133.26 (C, Ph), 133.24 (C, Ph), 129.74 (CH, Ph), 129.73 (CH, Ph), 127.72 (CH, Ph), 127.71 (CH, Ph), 64.3 (CH₂, C1), 52.3 (CH, C2), 44.5 (CH₂, C3), 26.7 (CH₃, *t*Bu), 19.2 (C, *t*Bu).

These data matched those reported previously.⁶⁵

1-(*tert*-Butyldiphenylsilyloxy)-5-trimethylsilyl-4-pentyn-2-ol (**141**)



To a solution of ethynyltrimethylsilane (375 mg, 3.82 mmol) in THF (12.7 mL, 0.30 M) at -78 °C, was added dropwise a solution of *n*BuLi (2.0 mL, 1.9 M in cyclohexane, 3.8 mmol). The reaction mixture was stirred at -78 °C for 50 min, before BF₃·Et₂O (0.48 mL, 3.81 mmol) was added dropwise.

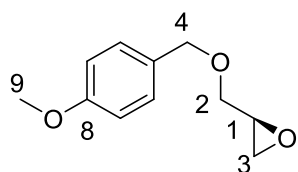
After 10 min stirring, a solution of epoxide **140** (991 mg, 3.17 mmol) in THF (4.0 mL, 0.79 M) was added dropwise. The reaction was stirred at -78 °C for 2 h 40 min, and then quenched with saturated aqueous NH₄Cl (15 mL), and extracted with Et₂O (3 × 40 mL). The organic layers were combined, dried over MgSO₄, filtered and concentrated under reduced pressure. This crude product was purified by column chromatography (silica, 20:1 Pet. ether/EtOAc, R_f = 0.23) to yield **141** a pale yellow oil (1.18 g, 91%).

¹H NMR (500 MHz, CDCl₃): δ 7.71–7.67 (complex m, 4H, CH, Ph, TBDPS), 7.44 (t, *J* = 7.2 Hz, 2H, CH, Ph, TBDPS), 7.41 (t, *J* = 7.2 Hz, 4H, CH, Ph, TBDPS), 3.88 (m, 1H, 2-CH), 3.76 (dd, *J* = 10.1, 4.3 Hz, 1H, one of 1-CH₂), 3.69 (dd, *J* = 10.0, 5.9 Hz, 1H, one of 1-CH₂), 2.54 (dd, *J* = 16.9, 6.3 Hz, 1H, one of 3-CH₂), 2.51 (dd, *J* = 17.3, 6.7 Hz, 1H, one of 3-CH₂), 1.07 (s, 9H, CH₃, *t*Bu, TBDPS), 0.11 (s, 9H, CH₃, TMS).

¹³C NMR (125 MHz, CDCl₃): δ 135.52 (CH, Ph, TBDPS), 135.51 (CH, Ph, TBDPS), 133.05 (C, Ph, TBDPS), 133.03 (C, Ph, TBDPS), 129.84 (CH, Ph, TBDPS), 129.83 (CH, Ph, TBDPS), 127.8 (CH, Ph, TBDPS), 102.6 (C, C4), 87.1 (C, C5), 70.2 (CH₂, C1), 66.4 (CH, C2), 26.9 (CH₃, *t*Bu, TBDPS), 24.7 (CH₂, C3), 19.3 (C, *t*Bu, TBDPS), 0.03 (CH₃, TMS).

These data matched those reported previously.⁶⁶

(*S*)-2-(*para*-Methoxybenzyl)methyloxirane (**150**)



To a suspension of NaH (725 mg, 60% w/w in mineral oil, 18.1 mmol) in DMF (11.0 mL, 1.6 M) at -70 °C, a solution of (*S*)-glycidol (**97**, 1.0 mL, 1.11 g, 14.8 mmol) in DMF (5.5 mL, 2.7 M) was added dropwise. The mixture was stirred for 30 min. PMBCl (2.87 g, 18.3

mmol, freshly prepared from PMBOH) was added dropwise, followed by TBAI (6 mg, 0.02 mmol). The reaction was stirred for 25 min at -70 °C before warming to r.t., and stirred for 5 h 25 min. Reaction was quenched with H₂O (40 mL), and then extracted with Et₂O (3 × 50 mL).

The organic layers were combined, dried over MgSO_4 and concentrated under reduced pressure. The crude product was purified by column chromatography (silica, 10:1 Pet. ether/EtOAc, $R_f = 0.14$) to yield **150** as a colourless oil (2.60 g, 89%).

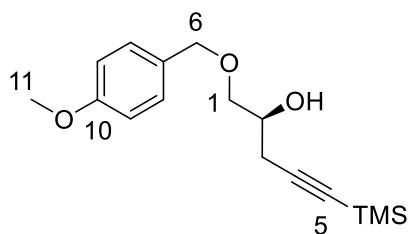
^1H NMR (500 MHz, CDCl_3): δ 7.28 (d, $J = 9.3$ Hz, 2H, 6-CH), 6.89 (d, $J = 8.5$ Hz, 2H, 7-CH), 4.55 (d, $J = 11.5$ Hz, 1H, one of CH_2 , 4- CH_2), 4.49 (d, $J = 11.5$ Hz, 1H, one of 4- CH_2), 3.81 (s, 3H, 9- CH_3), 3.73 (dd, $J = 11.4, 3.1$ Hz, 1H, one of 2- CH_2), 3.42 (dd, $J = 11.5, 5.9$ Hz, 1H, one of 2- CH_2), 3.18 (ddt, $J = 5.9, 4.1, 2.9$ Hz, 1H, 1-CH), 2.80 (dd, $J = 5.0, 4.3$ Hz, 1H, one of 3- CH_2), 2.61 (dd, $J = 5.1, 2.7$ Hz, 1H, one of 3- CH_2).

^{13}C NMR (125 MHz, CDCl_3): δ 159.3 (C, C8), 129.9 (C, C5), 129.4 (CH, C6), 113.8 (CH, C7), 73.0 (CH_2 , C4), 70.5 (CH_2 , C1), 55.3 (CH_3 , C9), 50.9 (CH, C2), 44.4 (CH_2 , C3).

Specific rotation: $[\alpha]_D^{25} = -1.04$ ($c = 1.34$, CH_2Cl_2). Lit.: $[\alpha]_D^{24} = -5.98$ ($c = 0.98$, CHCl_3).⁵⁴

These NMR data matched those reported previously.⁵⁴

(*S*)-1-(*para*-Methoxybenzyl)oxy-5-trimethylsilyl-4-pentyn-2-ol (**146**)



To a solution of ethynyltrimethylsilane (0.87 mL, 609 mg, 6.20 mmol) in THF (20.0 mL, 0.31 M) at -78°C , $n\text{BuLi}$ (3.2 mL, 1.9 M in cyclohexane, 6.18 mmol) was added dropwise. This solution was stirred for 50 min. $\text{BF}_3 \cdot \text{Et}_2\text{O}$ (0.78 mL, 6.18 mmol) was added dropwise. After 10 min, a solution of

151 (1.01 g, 5.20 mmol) in THF (5.0 mL, 1.0 M) was added dropwise. The reaction was stirred for 3 h 15 min at -78°C . The reaction was quenched with sat. aq. NH_4Cl solution, and then extracted with EtOAc (3×30 mL). The organic layers were combined, dried over MgSO_4 and concentrated under reduced pressure. The crude product was purified by column chromatography (silica, 5:1 Pet. ether/EtOAc, $R_f = 0.38$) to yield **146** as a pale yellow oil (1.08 g, 72%).

^1H NMR (500 MHz, CDCl_3): δ 7.27 (d, $J = 8.7$ Hz, 2H, 8-CH), 6.89 (d, $J = 8.8$ Hz, 2H, 9-CH), 4.51 (s, 2H, 6- CH_2), 3.98–3.91 (m, 1H, 2-CH), 3.81 (s, 3H, 11- CH_3), 3.58 (dd, $J = 9.6, 3.9$ Hz, 1H, one of 1- CH_2), 3.47 (dd, $J = 9.8, 6.5$ Hz, 1H, one of 1- CH_2), 2.51 (dd, $J = 16.8, 6.0$ Hz, 1H, one of 3- CH_2), 2.46 (dd, $J = 16.8, 6.8$ Hz, 1H, one of 3- CH_2), 2.42 (d, $J = 4.1$ Hz, 1H, OH), 0.14 (s, 9H, CH_3 , TMS).

¹³C NMR (125 MHz, CDCl₃): δ 159.3 (C, C10), 129.9 (C, C7), 129.4 (CH, C8), 113.8 (CH, C9), 102.5 (C, C4), 87.3 (C, C5), 73.1 (CH₂, C6), 72.4 (CH₂, C1), 68.8 (CH, C2), 55.3 (CH₃, C11), 25.0 (CH₂, C3), 0.03 (CH₃, TMS).

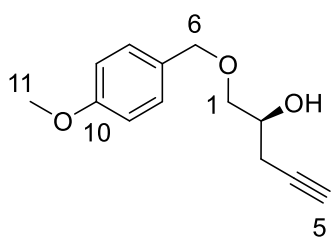
IR (neat) cm⁻¹: 3433 (br, OH), 2956 (m, C–H), 2921 (m, C–H), 2836 (m, C–H), 2179 (m, C≡C), 1612 (m, Ar C–C), 1247 (s, C–O), 1073 (br, C–O), 1033 (s, C–O), 839 (s, C–Si), 739 (m, C–H).

HRMS (ESI) *m/z*: found 293.1571, calcd for C₁₆H₂₅O₃Si [M+H]⁺ 293.1567 (Δ = 1.4 ppm).

Specific rotation: [α]_D²² = +13.9 (*c* = 1.14, CH₂Cl₂).

Only ¹H NMR data was reported previously, and the above ¹H NMR data matched those reported previously.⁶⁷

(*S*)-1-(*para*-Methoxybenzyl)oxy-4-pentyn-2-ol (**152**)



To a solution of **146** (114 mg, 0.390 mmol) in MeOH (2.6 mL, 0.15 M) at r.t., K₂CO₃ (26 mg, 1.95 mmol) was added. After 4 h 30 min of stirring, reaction was diluted with H₂O and extracted with Et₂O (3 × 40 mL). The organic layers were combined, dried over MgSO₄ and concentrated under reduced pressure. The crude product was purified by column chromatography (silica, 5:1 Pet. ether/EtOAc, followed by 1:1 Pet. ether/EtOAc, R_f = 0.10 in 5:1 Pet. ether/EtOAc) to yield **152** as a colourless oil (64 mg, 74%).

¹H NMR (500 MHz, CDCl₃): δ 7.27 (d, *J* = 8.1 Hz, 2H, 8-CH), 6.89 (d, *J* = 8.3 Hz, 2H, 9-CH), 4.51 (s, 2H, 6-CH₂), 3.97 (m, 1H, 2-CH), 3.81 (s, 3H, 11-CH₃), 3.59 (dd, *J* = 9.5, 3.7 Hz, 1H, one of 1-CH₂), 3.48 (dd, *J* = 9.4, 6.7 Hz, 1H, one of 1-CH₂), 2.51 (br. d, *J* = 6.2 Hz, 2H, 3-CH₂), 2.47 (d, *J* = 4.9 Hz, 1H, OH), 2.03 (br. s, 1H, 5-CH).

¹³C NMR (125 MHz, CDCl₃): δ 159.3 (C, C10), 129.9 (C, C7), 129.4 (CH, C8), 113.9 (CH, C9), 80.2 (C, C4), 73.1 (CH₂, C6), 72.5 (CH₂, C1), 70.6 (CH, C5), 68.7 (CH, C2), 55.3 (CH₃, C11), 23.5 (CH₂, C3).

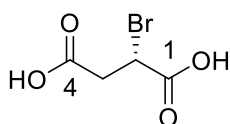
IR (neat) cm^{-1} : 3436 (br, OH), 3289 (m, C–H), 2911 (m, C–H), 2863 (m, C–H), 2180 (w, $\text{C}\equiv\text{C}$), 1612 (m, Ar C–C), 1245 (s, C–O), 1078 (m, C–O), 1031 (s, C–O), 817 (m, C–H), 638 (m, C–H).

HRMS (ESI) m/z : found 243.1000, calcd for $\text{C}_{13}\text{H}_{16}\text{O}_3\text{Na}$ $[\text{M}+\text{Na}]^+$ 243.0992 ($\Delta = 3.3$ ppm).

Specific rotation: $[\alpha]_D^{23} = +6.32$ ($c = 0.64$, CH_2Cl_2).

Fragment C9-C15

(S)-Bromosuccinic acid (157)



A solution of (*S*)-sspartic acid (**154**, 10.0 g, 75.1 mmol) and potassium bromide (40.7 g, 342 mmol) in sulfuric acid (195 mL, 2.5 M in H_2O) was cooled down to $-10\text{ }^\circ\text{C}$. A solution of sodium nitrite (9.25 g, 134 mmol) in water (17.8 mL, 7.54 M) was added slowly over 50 min, at such a rate to keep the temperature between -10 and $-5\text{ }^\circ\text{C}$. The fumes generated in the reaction were neutralized in a gas trap containing NaOH aqueous solution before releasing in the fumehood. The reaction was stirred at $-10\text{ }^\circ\text{C}$ for 2 h, and white precipitate was observed. The reaction mixture was warmed to r.t. and extracted with EtOAc (3×100 mL). The organic layers were combined, dried over MgSO_4 and concentrated under reduced pressure. The product obtained was further dried under high vacuum to yield **157** as a white powder (12.5 g, 84% yield).

^1H NMR (500 MHz, D_2O): δ 4.53 (dd, $J = 7.9, 6.5$ Hz, 1H, 2-CH), 3.11 (dd, $J = 17.5, 7.8$ Hz, 1H, one of 3- CH_2), 2.99 (dd, $J = 17.5, 6.5$ Hz, 1H, one of 3- CH_2).

^{13}C NMR (125 MHz, D_2O): δ 173.8 (C, C4), 172.9 (C, C1), 39.3 (CH_2 , C3), 39.0 (CH, C2).

IR (neat): 3009 (br, O–H), 2646 (br, C–H), 1702 (s, C=O), 1420 (s, C–H), 1306 (m, C–H), 1185 (s, C–O), 934 (s, O–H), 648 (s, C–Br) cm^{-1} .

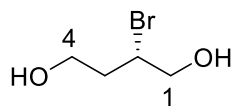
HRMS (ESI) m/z : found 194.9292, calcd for $\text{C}_4\text{H}_4\text{O}_4\text{Br}^{79}$ $[\text{M}-\text{H}]^-$ 194.9298 ($\Delta = 3.1$ ppm).

M.p.: $169.4 - 170.8\text{ }^\circ\text{C}$ (Lit. $166 - 167\text{ }^\circ\text{C}$).

Specific rotation: $[\alpha]_D^{27} = -41.8$ ($c = 1.11$, H_2O).

These NMR data are consistent with those reported in MeOH-d₄, and the IR and m.p. matched those reported previously.⁶⁸

(*S*)-2-Bromobutane-1,4-diol (**160**)



To a solution of (*S*)-bromosuccinic acid (**157**, 3.83 g, 19.4 mmol) in THF (23.0 mL, 0.84 M) at 0 °C, BH₃•Me₂S (29.1 mL, 2.0 M in THF, 58.2 mmol) was added drop-wise over 1 h 15 min. This reaction was stirred at 0 °C for 1 h, and then slowly warmed to r.t. over 20 min. A saturated aqueous solution of K₂CO₃ (10 mL) was added dropwise, at a rate that allowed the vigorous gas release to settle after each addition. This mixture was filtered through Celite and the filtrate was concentrated. The crude product was purified by column chromatography (silica, 50:1 EtOAc:MeOH, R_f = 0.44) to yield **160** as a colourless clear oil (2.47 g, 75% yield).

¹H NMR (500 MHz, CDCl₃): δ 4.37 (app. dt, *J* = 12.9, 5.6 Hz, 1H, 2-CH), 3.95–3.80 (complex m, 4H, 1-CH₂ & 4-CH₂), 2.68 (br., 2H, OH), 2.21–2.07 (m, 2H, 3-CH₂).

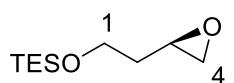
¹³C NMR (125 MHz, CDCl₃): δ 67.1 (CH₂, C4), 60.1 (CH₂, C1), 55.2 (CH, C2), 37.7 (CH₂, C3).

IR (neat) cm⁻¹: 3315 (br, O–H), 2932 (w, C–H), 2885 (w, C–H), 1420 (m, C–H), 1377 (w, C–H), 1051 (s, C–O), 1022 (s, C–O), 639 (m, C–Br), 533 (m, C–Br).

Specific rotation: [*a*]_D²⁵ = -32.8 (*c* = 1.00, CH₂Cl₂).

These data matched those reported previously.^{54,52}

(*R*)-Triethyl-3-(oxiranyl)ethoxysilane (**155**)



To a suspension of NaH (1.77 g, 60% w/w in mineral oil, 44.3 mmol) in THF (20 mL) at -15 °C under N₂ atm., a solution of (*S*)-2-bromobutane-1,4-diol (**160**, 2.47 g, 14.6 mmol) in THF (20 mL, 0.71 M) was added dropwise over 45 min. After stirring at temperatures between -9 and -15 °C for 30 min, chlorotriethylsilane (2.25 mL, 17.5 mmol) was added dropwise via a syringe, and THF (1.0 mL) was used to rinse the syringe. The reaction mixture was allowed to warm to r.t. over 10 min. After stirring at r.t. for 1 h, the

reaction was slowly quenched with sat. aq. NH_4Cl solution (30 mL), and a minimum amount of H_2O was added to dissolve any precipitate. The mixture was extracted with EtOAc (3×50 mL). The organic layers were combined, dried over MgSO_4 and concentrated under reduced pressure. The crude product was purified by column chromatography (silica, 5:1 Pet. ether:EtOAc, $R_f = 0.69$) to yield **155** as a colourless clear oil (2.08 g, 70% yield).

^1H NMR (500 MHz, CDCl_3): δ 3.78 (t, $J = 6.0$ Hz, 2H, 1- CH_2), 3.06 (m, 1H, 3-CH), 2.79 (app. t, $J = 4.6$ Hz, 1H, one of 4- CH_2), 2.52 (dd, $J = 5.1, 2.7$ Hz, 1H, one of 4- CH_2), 1.81 (dtd, $J = 13.9, 7.0, 5.0$ Hz, 1H, one of 2- CH_2), 1.71 (app. dq, $J = 13.9, 5.9$ Hz, 1H, one of 2- CH_2), 0.97 (t, $J = 8.1$ Hz, 9H, CH_3 , TES), 0.61 (q, $J = 8.1$ Hz, 6H, CH_2 , TES).

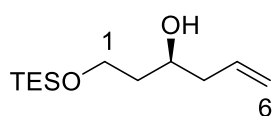
^{13}C NMR (125 MHz, CDCl_3): δ 59.7 (CH_2 , C1), 50.0 (CH, C3), 47.2 (CH_2 , C4), 35.9 (CH_2 , C2), 6.7 (CH_3 , TES), 4.4 (CH_2 , TES).

IR (neat) cm^{-1} : 2954 (m, C-H), 2913 (m, C-H), 2876 (m, C-H), 1459 (m, C-H), 1414 (m, C-H), 1238 (m, epoxide), 1096 (s, C-O), 1039 (s, C-O), 765 (m, epoxide), 727 (s, O-Si).

HRMS (ESI) m/z : found 241.1025, calcd for $\text{C}_{10}\text{H}_{22}\text{O}_2\text{SiK}$ $[\text{M}+\text{K}]^+$ 241.1021 ($\Delta = 1.7$ ppm).

Specific rotation: $[\alpha]_D^{25} = +1.35$ ($c = 1.06$, CH_2Cl_2).

(S)-Triethyl-(3-hydroxy)hex-5-enoxysilane (**156**)



A mixture of purified CuI (147 mg, 0.772 mmol) and vinyl magnesium bromide (15.4 mL, 1.0 M in THF, 15.4 mmol) was stirred at -78°C for 10 min, then a solution of **155** (1.56 g, 7.71 mmol) in THF was added dropwise. This reaction was stirred for 2 h, and slowly warmed to -50°C . A sat. aq. NH_4Cl solution (30 mL) was added to quench the reaction, followed by H_2O (10 mL) and aqueous ammonia solution (5 mL, 35% w/w), and the mixture was stirred at r.t. for a further 10 min. The mixture was extracted with EtOAc (2×30 mL). The organic layers were combined, dried over MgSO_4 and concentrated under reduced pressure. This crude product was purified by column chromatography (SiO_2 , 2:1 Pet. ether:EtOAc, $R_f = 0.66$) to yield **156** as a clear oil (1.67 g, 94% yield).

^1H NMR (500 MHz, CDCl_3): δ 5.85 (ddt, $J = 15.6, 8.8, 8.5$ Hz, 1H, 5-CH), 5.11 (d, $J = 15.6$ Hz, 1H, one of 6- CH_2), 5.08 (d, $J = 9.4$ Hz, 1H, one of 6- CH_2), 3.94–3.87 (complex m, 2H, 3-

CH and one of 1-CH₂), 3.87–3.78 (m, 1H, one of 1-CH₂), 3.47 (d, $J = 1.7$ Hz, OH), 2.33–2.18 (m, 2H, 4-CH₂), 1.68 (app. q, $J = 5.4$ Hz, 2H, 2-CH₂), 0.96 (t, $J = 7.9$ Hz, 9H, CH₃, TES), 0.62 (q, $J = 7.9$ Hz, 6H, CH₂, TES).

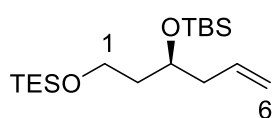
¹³C NMR (125 MHz, CDCl₃): δ 135.0 (CH, C5), 117.3 (CH₂, C6), 71.3 (CH, C1), 62.3 (CH₂, C3), 42.0 (CH₂, C4), 37.7 (CH₂, C2), 6.7 (CH₃, TES), 4.2 (CH₂, TES).

IR (neat) cm⁻¹: 3440 (br, O–H), 3077 (w, C–H), 2954 (s, C–H), 2912 (s, C–H), 2876 (s, C–H), 1641 (w, C=C), 1414 (m, C–H), 1239 (m, C–H), 1085 (s, C–O), 743 (s, O–Si).

HRMS (ESI) m/z : found 231.1770, calcd for C₁₂H₂₇O₂Si [M+H]⁺ 231.1775 ($\Delta = 2.2$ ppm).

Specific rotation: $[\alpha]_D^{20} = -9.03$ ($c = 1.20$, CH₂Cl₂).

(S)-1-Triethylsilyloxy-3-(*t*-butyldimethylsilyloxy)hex-5-ene (**161**)



To a solution of imidazole (629 mg, 9.24 mmol) and **156** (1.07 g, 4.64 mmol) in DMF (9.3 mL, 0.50 M) at 0 °C, a solution of TBSCl (1.09 g, 7.23 mmol) in DMF (8.5 mL, 0.9 M) was added dropwise. The reaction temperature was brought up to r.t. and stirred for 21 h. The reaction mixture was then diluted with EtOAc (30 mL) and washed with H₂O (30 mL). The aqueous layer was extracted with EtOAc (2 × 30 mL). The organic layers were combined, washed with H₂O (30 mL) and brine (2 × 30 mL), dried over MgSO₄ and concentrated under reduced pressure. The crude product was purified by column chromatography (SiO₂, 20:1 Pet. ether:EtOAc, $R_f = 0.56$) to yield **161** as a clear oil (1.16 g, 72% yield).

¹H NMR (500 MHz, CDCl₃): δ 5.88–5.76 (m, 1H, 5-CH), 5.04 (d, $J = 16.6$ Hz, 1H, one of 6-CH₂), 5.03 (d, $J = 11.0$ Hz, 1H, one of 6-CH₂), 3.87 (tt, $J = 12.5, 6.4$ Hz, 1H, 3-CH), 3.72–3.61 (m, 2H, 1-CH₂), 2.32–2.15 (m, 2H, 4-CH₂), 1.73–1.60 (m, 2H, 2-CH₂), 0.96 (t, $J = 7.9$ Hz, 9H, CH₃, TES), 0.89 (s, 9H, CH₃, TBS), 0.60 (q, $J = 7.8$ Hz, 6H, CH₃, TES), 0.05 (s, 3H, CH₃, TBS), 0.04 (s, 3H, CH₃, TBS).

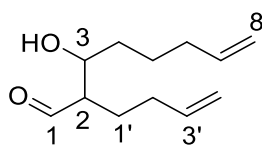
¹³C NMR (125 MHz, CDCl₃): δ 135.1 (CH, C5), 116.8 (CH₂, C6), 69.0 (CH, C3), 59.6 (CH₂, C1), 42.2 (CH₂, C4), 39.8 (CH₂, C2), 25.9 (CH₃, *t*Bu, TBS), 18.1 (C, *t*Bu, TBS), 6.8 (CH₃, TES), 4.4 (CH₂, TES), -4.7 (CH₃, Me, TBS), -5.3 (CH₃, Me, TBS).

IR (neat) cm^{-1} : 3077 (w, C–H), 2954 (s, C–H), 2877 (s, C–H), 1641 (w, C=C), 1471 (m, C–H), 1415 (m, C–H), 1253 (m, C–H), 1089 (s, C–O), 834 (s, O–Si), 773 (s, O–Si), 725 (s, O–Si).

HRMS (ESI) m/z : found 345.2643, calcd for $\text{C}_{18}\text{H}_{41}\text{O}_2\text{Si}_2$ $[\text{M}+\text{H}]^+$ 345.2640 ($\Delta = 0.9$ ppm).

Specific rotation: $[\alpha]_D^{22} = +12.0$ ($c = 0.87$, CH_2Cl_2).

2-(But-3'-enyl)-3-hydroxyoct-7-enal (170), Characterized from a mixture with unidentified by-product)



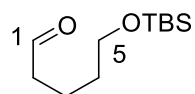
^1H NMR (500 MHz, CDCl_3): δ 9.78 (d, $J = 1.2$ Hz, 1H, 1-CH), 5.85–5.72 (complex m, 2H, 7-CH & 3'-CH), 5.07–4.92 (complex m, 4H, 8- CH_2 & 4'- CH_2), 4.07 (t, $J = 6.6$ Hz, 1H, 3-CH), 2.45 (t, $J = 7.3$ Hz, 1H, 2-CH), 2.14–2.04 (complex m, 4H, 6- CH_2 & 2'- CH_2), 1.74 (partially obs. dt, $J = 7.3$, 7.0 Hz, 2H, 1'- CH_2), 1.64 (app. quin, $J = 7.2$ Hz, 2H, 4- CH_2), 1.64 (app. quin, $J = 7.6$ Hz, 2H, 5- CH_2).

^{13}C NMR (125 MHz, CDCl_3): δ 202.5 (CH, C1), 138.3 (C, C7), 137.5 (C, C3'), 115.6 (CH_2 , C8), 114.8 (CH_2 , C4'), 64.2 (CH, C3), 43.1 (CH, C2), 33.06 (CH_2 , C6), 33.00 (CH_2 , C2'), 28.1 (CH_2 , C4), 25.2 (CH_2 , C5), 21.2 (CH_2 , C1').

IR (neat) cm^{-1} : 3437 (br, O–H), 3077 (w, C–H), 2933 (s, C–H), 2862 (m, C–H), 1735 (s, C=O), 1440 (s, C–H), 1244 (s, C–O), 1170 (s, C–O), 909 (s, C–H).

HRMS (ESI) m/z : found 197.1536, calcd for $\text{C}_{12}\text{H}_{21}\text{O}_2$ $[\text{M}+\text{H}]^+$ 197.1536 ($\Delta = 0.0$ ppm).

5-(*t*-Butyldimethylsilyloxy)pentanal (177)



To a solution of 5-hexenol (**169**, 508 mg, 5.08 mmol) and imidazole (419 mg, 6.16 mmol) in DMF (5.0 mL, 1.0 M) at 0 °C, a solution of TBSCl (937 mg, 6.22 mmol) in DMF (5.0 mL, 1.2 M) was added dropwise. The reaction was stirred at 0 °C for 10 min, then warmed to r.t. and stirred for 16 h. The reaction mixture was diluted with EtOAc (30 mL) and washed with H_2O (30 mL). The aqueous layer was extracted with EtOAc (2×30

mL). The organic layers were combined, dried over MgSO₄ and concentrated under reduced pressure. The crude mixture was filtered through a silica plug (5:1 Pet. Ether:EtOAc). The filtrate was concentrated to yield the TBS ether. The product was dissolved in CH₂Cl₂ (25 mL), and cooled down to -78 °C. Ozone gas was passed through the reaction until the solution turned pale blue. Triphenylphosphine (1.56 g, 5.74 mmol) was added, and the blue colour disappeared. The reaction was allowed to warm to room temperature and stirred overnight. The solvent was removed and the oil obtained was purified by column chromatography (SiO₂, 10:1 Pet. ether:EtOAc, R_f = 0.38) to yield **177** a clear colourless oil (1.05 g, 95% yield).

¹H NMR (500 MHz, CDCl₃): δ 9.76 (t, *J* = 1.6 Hz, 1H, 1-CH), 3.62 (t, *J* = 6.2 Hz, 2H, 5-CH₂), 2.45 (td, *J* = 7.3, 1.6 Hz, 2H, 2-CH₂), 1.69 (quin, *J* = 7.5 Hz, 2H, 3-CH₂), 1.61–1.49 (m, 2H, 4-CH₂), 0.88 (s, 9H, CH₃, *t*Bu, TBS), 0.04 (s, 6H, *t*Bu, TBS).

¹³C NMR (126 MHz, CDCl₃): δ 202.7 (CH, C1), 62.6 (CH₂, C5), 43.6 (CH₂, C2), 32.1 (CH₂, C4), 25.9 (CH₃, *t*Bu, TBS), 18.6 (C, *t*Bu, TBS), 18.3 (CH₂, C3), -5.4 (CH₃, Me, TBS).

These data matched those reported previously.⁶⁹

3.6 References

- (1) Lu, S.; Kurtan, T.; Yang, G. J.; Sun, P.; Mandi, A.; Krohn, K.; Draeger, S.; Schulz, B.; Yi, Y. H.; Li, L.; Zhang, W. *Eur. J. Org. Chem.* **2011**, 5452.
- (2) Kito, K.; Ookura, R.; Yoshida, S.; Namikoshi, M.; Ooi, T.; Kusumi, T. *Org. Lett.* **2008**, *10*, 225.
- (3) Wright, A. E.; Botelho, J. C.; Guzman, E.; Harmody, D.; Linley, P.; McCarthy, P. J.; Pitts, T. P.; Pomponi, S. A.; Reed, J. K. *J. Nat. Prod.* **2007**, *70*, 412.
- (4) Williams, D. E.; Roberge, M.; Van Soest, R.; Andersen, R. J. *J. Am. Chem. Soc.* **2003**, *125*, 5296.
- (5) Fuwa, H. *Heterocycles* **2012**, *85*, 1255.
- (6) Olier, C.; Kaafarani, M.; Gastaldi, S.; Bertrand, M. P. *Tetrahedron* **2010**, *66*, 413.
- (7) Xu, Y. J.; Yin, Z. P.; Lin, X. L.; Gan, Z. B.; He, Y. Y.; Gao, L.; Song, Z. L. *Org. Lett.* **2015**, *17*, 1846.
- (8) Minami, T.; Moriyama, A.; Hanaoka, M. *Synlett* **1995**, 663.

- (9) Fuwa, H.; Noguchi, T.; Noto, K.; Sasaki, M. *Org. Biomol. Chem.* **2012**, *10*, 8108.
- (10) Bates, R. W.; Song, P. *Synthesis* **2010**, 2935.
- (11) Banwell, M. G.; Bissett, B. D.; Bui, C. T.; Pham, H. T. T.; Simpson, G. W. *Aust. J. Chem.* **1998**, *51*, 9.
- (12) Gharpure, S. J.; Prasad, J. V. K.; Bera, K. *Eur J. Org. Chem.* **2014**, 3570.
- (13) Qian, H.; Han, X. Q.; Widenhoefer, R. A. *J. Am. Chem. Soc.* **2004**, *126*, 9536.
- (14) Sutivisedsak, N.; Dawadi, S.; Spilling, C. D. *Tetrahedron Lett.* **2015**, *56*, 3534.
- (15) Tietze, L. F.; Zinngrebe, J.; Spiegl, D. A.; Stecker, F. *Heterocycles* **2007**, *74*, 473.
- (16) Gharpure, S. J.; Shelke, Y. G.; Reddy, S. R. B. *RSC Adv.* **2014**, *4*, 46962.
- (17) Mao, J. G.; Zhang, S. Q.; Shi, B. F.; Bao, W. L. *Chem. Commun.* **2014**, *50*, 3692.
- (18) Semmelhack, M. F.; Bodurow, C. *Abstr. of Pap. Am. Chem. Soc.* **1983**, *186*, 87.
- (19) White, J. D.; Hong, J.; Robarge, L. A. *Tetrahedron Lett.* **1999**, *40*, 1463.
- (20) Kuntiyong, P.; Lee, T. H.; Kranemann, C. L.; White, J. D. *Org. Biomol. Chem.* **2012**, *10*, 7884.
- (21) Bohlmann, F.; Herbst, P. *Chem. Ber.-Recl.* **1959**, *92*, 1319.
- (22) Molle, G.; Bauer, P. *J. Am. Chem. Soc.* **1982**, *104*, 3481.
- (23) Gilman, H.; Jones, R. G.; Woods, L. A. *J. Org. Chem.* **1952**, *17*, 1630.
- (24) Normant, J. F. *Synth. Int. J. Methods* **1972**, 63.
- (25) Dieter, R. K.; Silks, L. A.; Fishpaugh, J. R.; Kastner, M. E. *J. Am. Chem. Soc.* **1985**, *107*, 4679.
- (26) Zakharkin, L. I.; Khorlina, I. M. *B. Acad. Sci. USSR Chem.* **1963**, *12*, 316.
- (27) Frigerio, M.; Santagostino, M.; Sputore, S. *J. Org. Chem.* **1999**, *64*, 4537.
- (28) Wei, X. D.; Taylor, R. J. K. *J. Org. Chem.* **2000**, *65*, 616.
- (29) Aoyama, T.; Sonoda, N.; Yamauchi, M.; Toriyama, K.; Anzai, M.; Ando, A.; Shioiri, T. *Synlett* **1998**, 35.
- (30) Carpino, L. A. *J. Org. Chem.* **1970**, *35*, 3971.
- (31) Gritter, R. J.; Wallace, T. J. *J. Org. Chem.* **1959**, *24*, 1051.
- (32) Xiao, X. Y.; Prestwich, G. D. *Synth. Commun.* **1990**, *20*, 3125.
- (33) Reddy, K. K.; Saady, M.; Falck, J. R.; Whited, G. *J. Org. Chem.* **1995**, *60*, 3385.
- (34) Chavan, S. P.; Harale, K. R. *Tetrahedron Lett.* **2012**, *53*, 4683.
- (35) Wuts, P. G. M.; Greene, T. W. *Greene's protective groups in organic synthesis*, 4th ed.; Wiley-Interscience Hoboken, N.J, **2007**.
- (36) Munakata, R.; Katakai, H.; Ueki, T.; Kurosaka, J.; Takao, K.; Tadano, K. *J. Am. Chem. Soc.* **2004**, *126*, 11254.

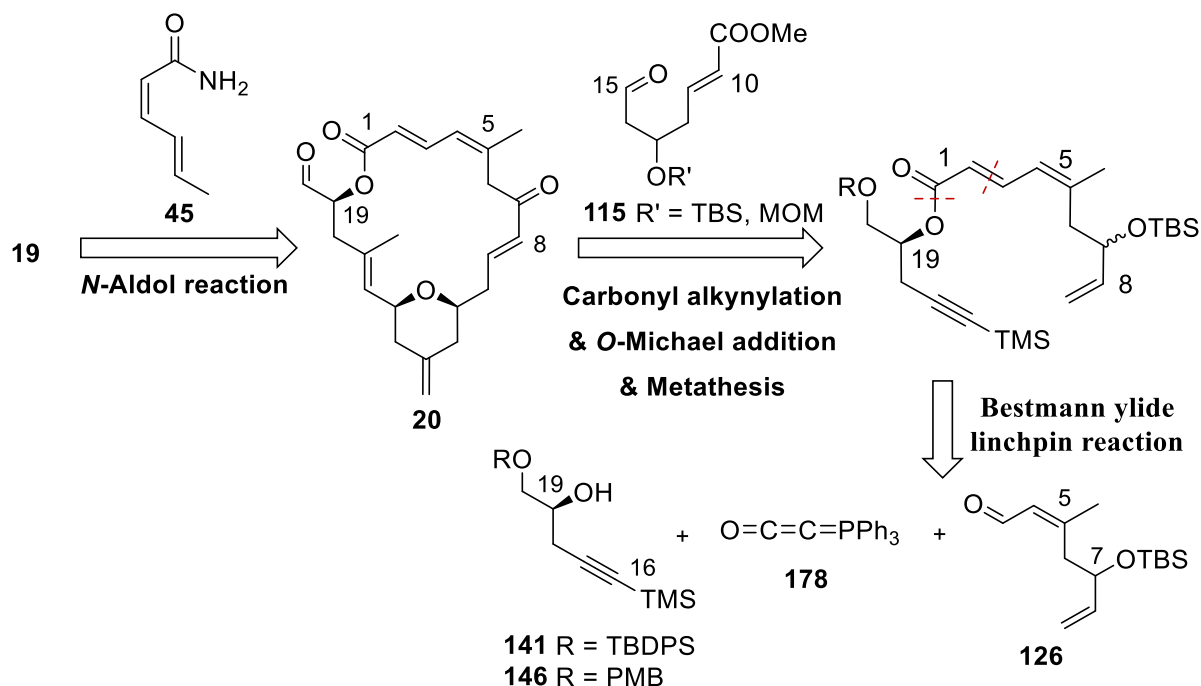
- (37) Fürstner, A.; Nagano, T.; Müller, C.; Seidel, G.; Müller, O. *Chemistry* **2007**, *13*, 1452.
- (38) Gille, A.; Hiersemann, M. *Org. Lett.* **2010**, *12*, 5258.
- (39) Bejjanki, N. K.; Venkatesham, A.; Balraju, K.; Nagaiah, K. *Helv. Chim. Acta* **2013**, *96*, 1571.
- (40) Tsuru, T.; Kamata, S. *Tetrahedron Lett.* **1985**, *26*, 5195.
- (41) Mulzer, J.; Mantoulidis, A.; Ohler, E. *J. Org. Chem.* **2000**, *65*, 7456.
- (42) Luzzio, F. A.; Chen, J. *J. Org. Chem.* **2008**, *73*, 5621.
- (43) Wamser, C. A. *J. Am. Chem. Soc.* **1951**, *73*, 409.
- (44) Sato, I.; Akahori, Y.; Iida, K.; Hiramata, M. *Tetrahedron Lett.* **1996**, *37*, 5135.
- (45) Hernandez-Torres, J. M.; Achkar, J.; Wei, A. *J. Org. Chem.* **2004**, *69*, 7206.
- (46) Evans, D. A.; Kim, A. S.; Metternich, R.; Novack, V. J. *J. Am. Chem. Soc.* **1998**, *120*, 5921.
- (47) Dilhas, A.; Bonnaffé, D. *Tetrahedron Lett.* **2004**, *45*, 3643.
- (48) Zurwerra, D.; Glaus, F.; Betschart, L.; Schuster, J.; Gertsch, J.; Ganci, W.; Altmann, K. *H. Chem.-Eur. J.* **2012**, *18*, 16868.
- (49) Li, J. J., *Name reactions for homologation, Part 1*. John Wiley & Sons: Hoboken, NJ, **2009**; p 685.
- (50) Hoffman, R. V. *Org. Synth.* **1981**, *60*, 121.
- (51) Pavia, D.; Kriz, G.; Lampman, G.; Engel, R. *A Small Scale Approach to Organic Laboratory Techniques*, 4th ed.; Cengage Learning: Boston, MA, **2015**.
- (52) Frick, J. A.; Klassen, J. B.; Bathe, A.; Abramson, J. M.; Rapoport, H. *Synthesis* **1992**, 621.
- (53) Norell, J. R. *J. Org. Chem.* **1970**, *35*, 1611.
- (54) Zurwerra, D.; Gertsch, J.; Altmann, K. H. *Org. Lett.* **2010**, *12*, 2302.
- (55) Margrey, K. A.; Chinn, A. J.; Laws, S. W.; Pike, R. D.; Scheerer, J. R. *Org. Lett.* **2012**, *14*, 2458.
- (56) Petriguet, J.; Boudhar, A.; Blond, G.; Suffert, J. *Angew. Chem. Int. Ed.* **2011**, *50*, 3285.
- (57) Uenishi, J.; Ohmi, M.; Ueda, A. *Tetrahedron Asymm.* **2005**, *16*, 1299.
- (58) Paczkowski, R.; Maichle-Mossmer, C.; Maier, M. E. *Org. Lett.* **2000**, *2*, 3967.
- (59) House, H. O.; Lee, L. F. *J. Org. Chem.* **1976**, *41*, 863.
- (60) Lagisetti, C.; Yermolina, M. V.; Sharma, L. K.; Palacios, G.; Prigaro, B. J.; Webb, T. R. *ACS. Chem. Biol.* **2014**, *9*, 643.
- (61) Fukahori, Y.; Takayama, Y.; Imaoka, T.; Iwamoto, O.; Nagasawa, K. *Chem.-Asian J.* **2013**, *8*, 244.

- (62) Fox, R. J.; Lalic, G.; Bergman, R. G. *J. Am. Chem. Soc.* **2007**, *129*, 14144.
- (63) Spino, C.; Barriault, N. *J. Org. Chem.* **1999**, *64*, 5292.
- (64) Roulland, E.; Monneret, C.; Florent, J. C.; Bennejean, C.; Renard, P.; Leonce, S. *J. Org. Chem.* **2002**, *67*, 4399.
- (65) Liu, J.; He, X. F.; Wang, G. H.; Merino, E. F.; Yang, S. P.; Zhu, R. X.; Gan, L. S.; Zhang, H.; Cassera, M. B.; Wang, H. Y.; Kingston, D. G. I.; Yue, J. M. *J. Org. Chem.* **2014**, *79*, 599.
- (66) Trost, B. M.; Machacek, M. R.; Faulk, B. D. *J. Am. Chem. Soc.* **2006**, *128*, 6745.
- (67) Kiyotsuka, Y.; Kobayashi, Y. *J. Org. Chem.* **2009**, *74*, 7489.
- (68) Wulschleger, C. W.; Gertsch, J.; Altmann, K. H. *Org. Lett.* **2010**, *12*, 1120.
- (69) Frankowski, K. J.; Golden, J. E.; Zeng, Y. B.; Lei, Y.; Aubé, J. *J. Am. Chem. Soc.* **2008**, *130*, 6018.

Chapter 4: Second generation synthesis and Bestmann ylide linchpin

4.1 Second generation retrosynthetic analysis

The difficulty with protecting C19 in the C16-C20 fragment (**141**, **146**), and the problem of oxidizing the hydroxy group at C15 to an aldehyde led to the development of a new reaction plan. The second generation strategy relied on a linchpin strategy to construct the dienolate, which involves the use of Bestmann ylide.¹ The fragments to be used in the linchpin reaction, C3-C8 aldehyde (**126**) and the C16-C20 alcohol (*viz.* **141** and **146**) were already prepared (**Scheme 4.1**). The strategy for side-arm attachment, ring-closing and pyran formation stayed the same, namely aza-aldol reaction, metathesis and alkynylation followed by *O*-Michael reaction. In previous zampanolide (**19**) and dactylolide (**20**) syntheses, the dienolate moiety is commonly synthesized by a sequence of a Wittig-type reaction to construct the C2-C3 alkene and esterification between a carboxylic acid at C1 and an alcohol at C19.²⁻⁶ The proposed linchpin approach is more efficient, as it not only reduces the number of steps, but also



Scheme 4.1: Second generation retrosynthetic analysis.

removes the need for protection at C19. The scope of this three-component Bestmann ylide reaction more generally in the synthesis of $\alpha,\beta,\gamma,\delta$ -unsaturated esters was also studied.

4.2 Bestmann ylide

(Triphenylphosphoranylidene)ketene, $\text{Ph}_3\text{P}=\text{C}=\text{C}=\text{O}$, also known as Bestmann ylide (**178**) is capable of, *inter alia*, three-component reactions to form α,β -unsaturated esters from alcohols and aldehydes.¹ First reported in 1966, it initially attracted attention due to its unique structure, namely the 145.5° angle of the $\text{C}=\text{C}=\text{P}$ moiety and the unusually short $\text{C}=\text{C}$ bond (1.210 \AA).^{7,8} Bestmann ylide (**178**) has surprising stability, and can be stored under inert atmosphere at room temperature for months. This stability is attributed to resonance stabilization (**Figure 4.1**). Two zwitterionic resonance structures of the uncharged phosphorane (**I**) exist. The phosphonium ylide (**II**) can have bent conformation which better represents the Wittig-type reactivity and is the source of the 145.5° angle of the $\text{C}=\text{C}=\text{P}$ moiety (insert, **Figure 4.1**), while the charge-segregated alkyne (**III**) can explain the unusually short $\text{C}=\text{C}$ bond.

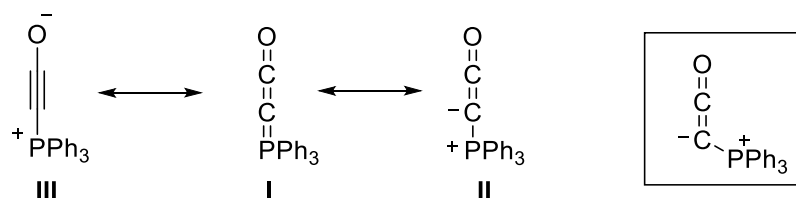
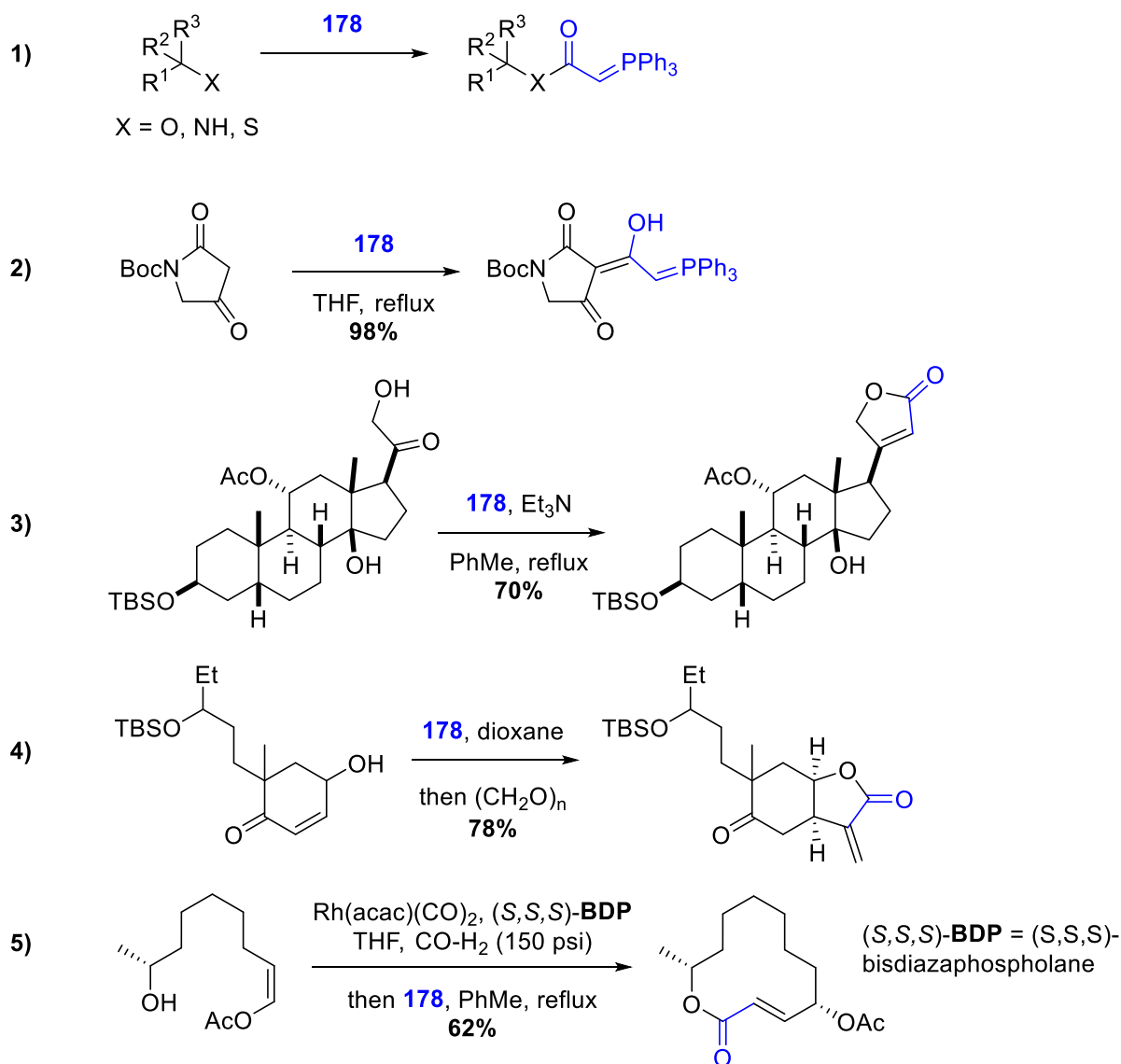


Figure 4.1: Resonance structures of Bestmann ylide (**178**).

Its utility was subsequently explored with pioneering work by Bestmann and co-workers,⁹⁻¹¹ lending the name Bestmann ylide to this versatile and readily obtainable reagent.^{1,12,13} Studies revealed that the ylide can react with alcohols, amines and thiols to form α -phosphoranylidene esters, amides and thioesters, providing diverse isolable Wittig reagents that can be used in subsequent transformations (**Scheme 4.2**, equation 1).⁹⁻¹² The use of a β -ketoamide in this type of reaction has also been explored (equation 2).¹⁴ Furthermore, if the α -phosphoranylidene ester or amide is formed in the presence of an aldehyde, ketone or ester, an additional *in situ* Wittig reaction step can occur.¹⁵⁻²¹ In a similar way, intramolecular couplings with Bestmann ylide (**178**) have enabled direct lactone (equation 3)²² and lactam synthesis,¹⁶⁻¹⁸ including the

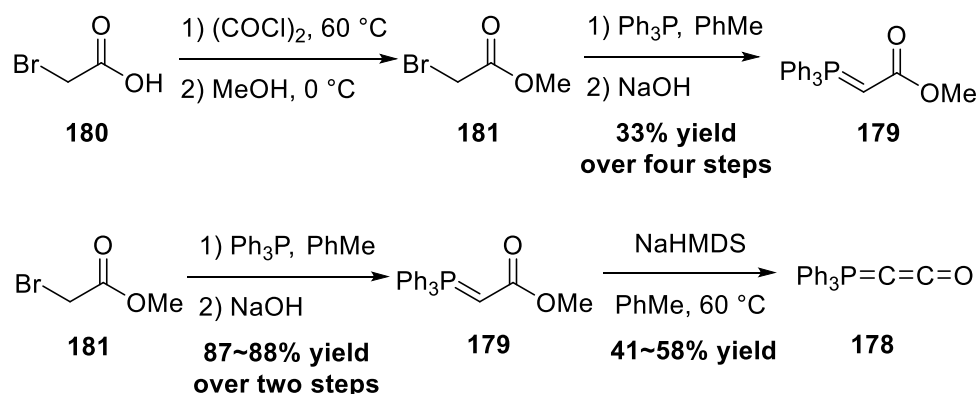
preparation of macrolactones.^{19,21} Such Bestmann ylide cascade reactions can allow good compatibility with other reaction conditions, forming longer cascades. An extension of this methodology by the Taylor group to γ -hydroxyenone substrates allows preparation of α -alkylidene- γ -butyrolactones through tandem acylation and Michael addition, followed by a Wittig reaction (equation 4).^{23,24} Burke and Risi performed a one-pot hydroformylation–macrocyclization cascade, where the aldehyde resulting from enantioselective hydroformylation reacted with Bestmann ylide (**178**) to complete this macrolactone ring (equation 5). The intermolecular Bestmann ylide cascade leads to amides, esters and thioesters through three-component couplings.^{17,19} In the examples above, the **178** is a bifunctional two-carbon linchpin containing two sites: one for nucleophilic attack and the other for subsequent



Scheme 4.2: Examples of the Bestmann ylide (**178**) in synthesis.

Wittig reaction. Unlike the linchpins discussed in **section 1.7**, Bestmann ylide (**178**) partakes in cascades that proceed in a one-pot manner, which optimizes the efficiency of the synthetic linchpin. Although the utility of Bestmann ylide (**178**) in the synthesis of acyclic α,β -unsaturated esters and dienamides has already been reported,^{16,19,25} its application to the synthesis of $\alpha,\beta,\gamma,\delta$ -unsaturated esters (i.e. dienates) remains uncharted. Because Wittig reactions are known to readily occur with α,β -unsaturated aldehydes, this Bestmann ylide cascade should proceed with ease.

As reported by Schobert, Bestmann ylide (**178**) can be prepared by deprotonation of methyl (triphenylphosphoranylidene)acetate (**179**) with the strong non-nucleophilic base sodium bis(trimethylsilyl)amide (NaHMDS).¹³ The phosphorane **179** is commercially available, but can also be prepared following a sequence starting from bromoacetic acid (**180**) (**Scheme 4.3**).²⁶ The acid **180** was methylated to methyl bromoacetate (**181**) after activation with oxalyl chloride, which can readily convert to the desired **179** *via* a phosphonium bromide salt. The four steps only reached a combined yield of 33%, while the substitution and ylidene formation steps have an good yield of 87~88%. Both bromoacetic acid (**180**) and methyl bromoacetate (**181**) are commercially available; the small cost difference between them encouraged the preparation of **179** from **181**. The phosphorane **179** was subjected to deprotonation by NaHMDS. Schobert prepared NaHMDS from sodium amide and bis(trimethylsilyl)amine *in situ* prior to the addition of **179**. However, because of the toxicity and potentially explosive nature of sodium amide, NaHMDS solution was purchased from a commercial source (Sigma-Aldrich). Schobert reported Bestmann ylide (**178**) as a “very pale yellow, flaky powder”, but with careful recrystallization, creamy white needle-shaped crystals were obtained. The better



Scheme 4.3: Preparation of Bestmann ylide (**178**).

crystal quality was compensated by the yields of 41 to 58% of **178** obtained, which are lower than Schobert's yield (**Scheme 4.3**). Interestingly, an attempt to prepare **178** from ethyl (triphenylphosphoranylidene)acetate under the same reaction conditions only returned starting material. This could be a result of the extra steric hindrance from the ethyl group, or reduced acidity of the ylide proton.

The different appearance may explain the slightly lower melting point measured in this work, 164~169 °C, compared to the quoted value 173 °C,¹³ although it could also be merely the discrepancy between melting point apparatus. This sample of Bestmann ylide (**178**) obtained was also characterized by IR, ³¹P NMR and ¹³C NMR spectroscopy, and showed broad agreement with literature (**Table 4.1**). ¹H NMR spectroscopy cannot provide useful information on the identification of **178** due to the paucity of characteristic hydrogens in the molecule, and the ESI-HRMS technique only decomposed the compound. The ¹³C NMR data obtained did not completely match those reported: the α and β -carbon signals, assigned by Schobert at -10.5 ppm ($J = 185.4$ Hz) and 145.6 ppm ($J = 43.0$ Hz), respectively, were not observed, while excess aromatic signals were displayed. The absence of the α and β -carbon signals could be a result of weak peak intensities for those carbonyl and ylide carbons. The excess aromatic signals could be from residue ylide starting material **179**. However, the overall agreement of the data suggested that **178** was made.

Table 4.1: Comparison of the measured Bestmann ylide (**178**) data with literature.

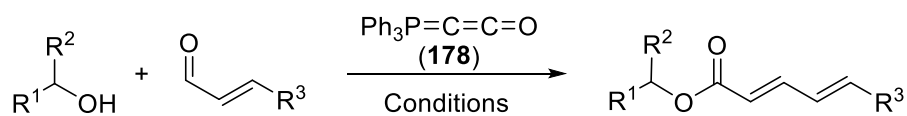
Spectroscopic method	Prepared	Lit. ¹³
IR (C=P)	2097 cm ⁻¹	2090 cm ⁻¹
³¹ P NMR	5.5 ppm	6.0 ppm
m.p.	164~169 °C	173°C
¹³ C NMR	134.99 (d, $J = 3.3$ Hz), 133.31 (d, $J = 10.8$ Hz), 132.07 (d, $J = 10.0$ Hz), 130.39 (d, $J = 13.0$ Hz), 128.48 (d, $J = 12.2$ Hz), 119.3 (d, $J = 88.1$ Hz).	145.6 (d, $J = 43.0$ Hz), 132.3 (s), 132.2 (s), 129.6 (d, $J = 98.5$ Hz), 128.8 (d, $J = 12.9$ Hz), -10.5 (d, $J = 185.4$ Hz)

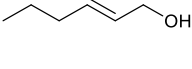
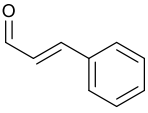
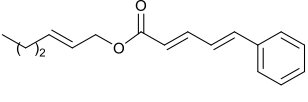
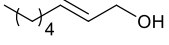
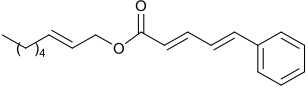
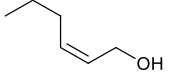
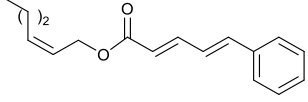
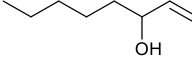
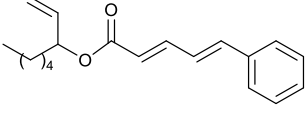
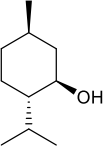
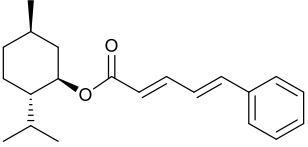
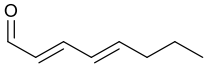
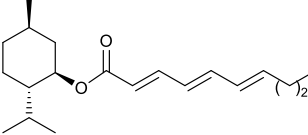
As discussed in Schobert's paper, **178** can be stored for a few months under inert atmosphere. This was corroborated in this work. No change in the quality of **178** was observed for up to six months after preparation. However, longer storage led to gradual decrease in the reactivity. Although no visible change of appearance, IR of the partially decomposed product showed reduced intensity of the characteristic band at 2097 cm⁻¹.

4.3 Scope of the Bestmann ylide cascade in the synthesis of $\alpha,\beta,\gamma,\delta$ -unsaturated esters

The study of the reactions between Bestmann ylide, alcohols and α,β -unsaturated aldehydes began with investigation of the coupling between the linchpin **178**, *E*-hex-2-en-1-ol (**182**) and *E*-cinnamaldehyde (**183**) (Table 4.2, entry 1). Typically, Bestmann ylide reactions are performed at elevated temperature in either high boiling or ether solvents, such as toluene, 1,4-dioxane or THF.^{17-20,23-25} To investigate the necessity for high temperature, the first reaction in this study was initiated at room temperature (19 °C) in toluene and then progressively warmed to reflux (110 °C) while monitoring progress by TLC. It was noted that the Bestmann ylide reagent (**178**) was insoluble up to 80 °C and no reaction was observed until the reaction mixture was heated at reflux. Under these conditions, incomplete consumption of both starting materials was seen after 18 h and the poor conversion was attributed to the instability of Bestmann ylide (**178**) over long periods at elevated temperatures and in the presence of any adventitious nucleophilic source. In response to these observations, the reaction was attempted in THF, a solvent in which the Bestmann ylide readily dissolved, even at room temperature. Upon heating at reflux, this reaction provided better conversion, although the isolated yield of **184** was only marginally improved (entry 2). The poor yields could be due to excessive handling to monitor the reaction. Gratifyingly, the reaction of oct-2-en-1-ol (**185**) with cinnamaldehyde (**183**) was efficient and high yielding, and after a reaction time of just 1.5 hours in high yield (93%) of **186** was obtained (entry 3). Reaction of *Z*-allylic alcohol **187** was run in parallel (entry 4), and likewise produced full conversion and excellent amounts of the product **188** (91% yield), although a longer reaction time was required to achieve this. The *Z*-geometry of the allylic alcohol was retained in **187**, as expected. After this, the secondary allylic alcohol **189** was investigated and a reasonable yield of the product was obtained when the reaction was carried out in THF (entry 5). A comparative reaction in toluene was also performed and found to deliver a better yield of the product **190** after the same length of time

Table 4.2: Coupling reactions of model alcohols and aldehydes with Bestmann ylide (**178**)^a



Entry	Alcohol	Aldehyde	Conditions: solvent, temperature, reaction length	Product	Yield ^b (conversion) ^c
1	 182	 183	Toluene, r.t. to 110 °C 18 h ^d	 184	53% (60%)
2	182	183^e	THF, 68 °C 2 h ^f	184	55% (94%)
3	 185	183	THF, 65 °C 1.5 h	 186	93% (100%)
4	 187	183	THF, 68 °C 6 h ^g	 188	91% (100%)
5	 189	183	THF, 65 °C 4.5 h	 190	61% (100%)
6	189	183	Toluene, 110 °C 5.5 h	190	71% (94%)
7	 191	183	THF, 65 °C 22 h	 192	77% (85%)
8	191	183	Toluene, 110 °C 23 h	192	29% (100%)
9	191	183	Toluene, 110 °C 9.5 h ^g	192	53% (100%)
10	191	 193	Toluene, 110 °C 3 h	 194	67% (90%)
11	191	193	Toluene, 110 °C 4.5 h ^g	194	66% (100%)

^a Unless otherwise stated, reactions were performed on a 0.1 mmol scale using approximately 1:1:1 ratio of alcohol/Bestmann ylide/aldehyde. ^b Isolated yields. ^c Conversion was calculated based on comparison of peak integrations for the limiting reagent (aldehyde) and product in ¹H NMR spectra of the crude product mixture after workup. ^d Reaction was carried out on 0.8 mmol scale. ^e 0.57 equiv. of aldehyde **145** were used. ^f Reaction was carried out on 0.2 mmol scale. ^g Reaction was carried out on 0.3 mmol scale.

(entry 6). The saturated secondary alcohol menthol (**191**), with additional steric encumbrance and stereogenic centres, provided a good yield of the product **192** in THF, despite incomplete conversion after 22 h (entry 7). Disappointingly, full conversion but a poor isolated yield of the product was achieved in toluene after reaction for 23 hours (entry 8). Decreasing the reaction time provided better results (entry 9), indicating that the product may decompose upon prolonged periods at the elevated reflux temperature of toluene. It should be noted that this latter reaction was performed on a larger scale (0.3 mmol rather than 0.1 mmol). The Bestmann ylide reaction with menthol (**191**) and octa-2,4-dienal (**193**) delivered the trienoate product **194** in good yields at both 0.1 and 0.3 mmol scales (entry 10 and 11). Taken together, these results indicate that primary alcohol substrates react effectively in THF, while more hindered secondary alcohols require either longer reaction time or the higher temperature available with toluene. There is also a need for balancing conversion rate and decomposition by adjusting reaction time.

The ¹H NMR spectra of the products all showed characteristic signals for the dienoate β-proton with chemical shift between 7.4 and 7.5 ppm (**Figure 4.2**). Most of them overlap with phenyl signals, apart from in the trienoate **194**, where the β-proton was observed as a doublet of doublets with coupling constants of 15.4 and 11.2 Hz. For all the dienoate products, the *trans*-configuration was confirmed by the coupling constant of the α-protons at about 6.0 ppm (*J* = 14.9~15.6 Hz). The α-protons are always well resolved, thus these signals were used to quantify the conversion rates by comparison with the singlet due to the aldehyde proton of the starting material. The γ- and δ-protons of the dienoates formed from cinnamaldehyde (**183**) are expected to provide signals with doublet of doublets and doublet respectively, but the multiplet observed are heavily distorted. The γ- and δ-protons are in a ABM spin system (Pople's notion), such that the very small difference in their chemical shifts in relation to the coupling constants can result in second order spin couplings, which significantly diverts the intensities of the multiplets from Pascal's triangle.²⁷ The assignments of γ- and δ-protons were confirmed by 2D NMR.

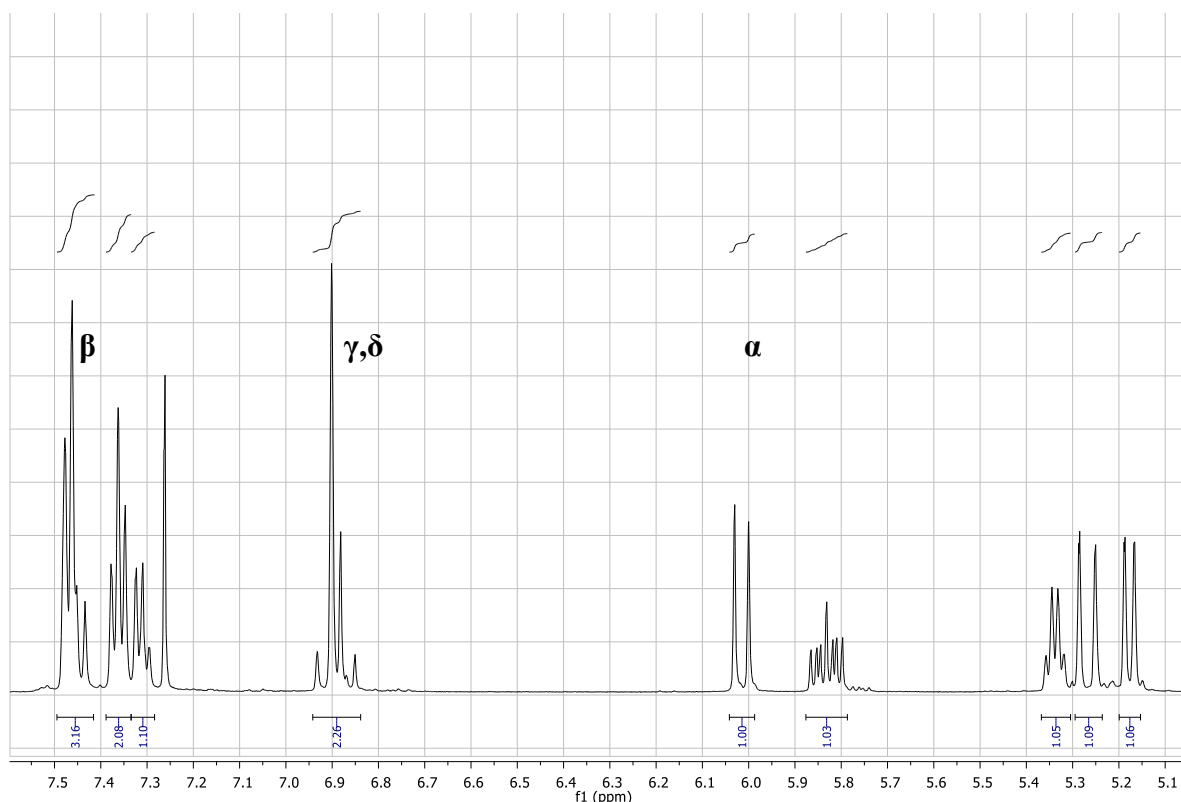


Figure 4.2: Typical multiplets seen for α -, β -, γ - and δ -protons (for **190** as an example).

In the ^1H NMR spectra of products generated from primary alcohols (*viz.* products **184**, **186**, **188**), a small signal at 8.15 ppm (dd, $J = 11\sim 12$ and $15\sim 16$ Hz) was always observed, which integrated up to 10% of the major product (**Figure 4.3**). Product **184** obtained after much handling had the highest percentage of this by-product. This multiplet was also observed in the ^1H NMR spectra of products formed from secondary alcohols, but was barely above the noise level. Analyzing the correlation spectroscopy (COSY) NMR spectrum of **184**, this signal has a correlation to signal at 6.75 ppm (td, $J = 11.5, 1.5$ Hz), which also correlates to a doublet at 5.74 ppm with a J -value of 11.0 Hz. This system is very similar to the major product, but the 11.0 Hz coupling constant of the doublet at 5.74 ppm is much lower than the $15\sim 16$ Hz observed for the major *E,E*-products. Weak signals at alkene, aromatic and oxymethine regions were also observed in the ^{13}C NMR, and showed appropriate HSQC correlations to minor ^1H NMR signals. This minor species could be the *Z,E*-isomer of the desired (major) *E,E*-dienoate. Attempts to separate the two structural isomers by column chromatography were unfruitful and insufficient data was collected for full characterization. Due to the low occurrence of the minor isomer in products generated from secondary alcohols, as required for zampanolide (**19**) synthesis, further separation was not attempted.

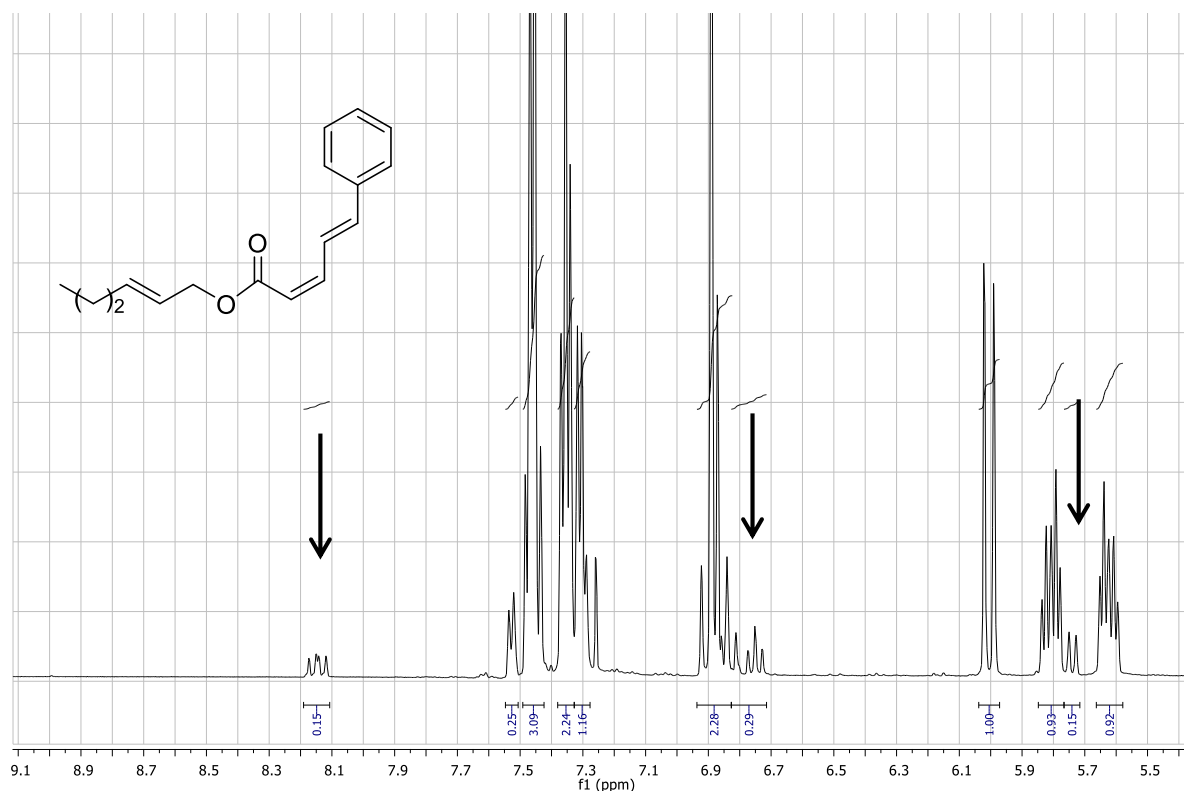
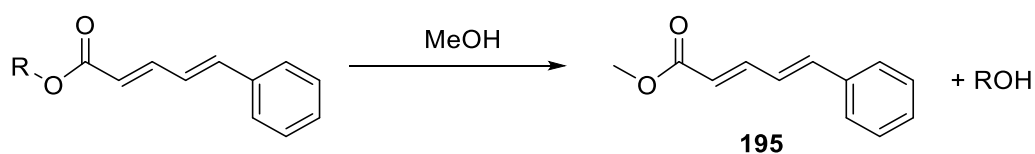


Figure 4.3: Partial ^1H NMR spectrum of *E,E*-dienoate **184** with signals attributed to *Z,E*-isomer indicated.

A singlet peak at 3.78 ppm was also noticed, and the compound was isolated and identified as the methoxy protons of the corresponding methyl ester **195** (Scheme 4.4). This could be due to the presence of methyl phosphoranylidene **179** in the Bestmann ylide (**178**) prepared, and its Wittig reaction with the aldehydes. However, the varying quantity obtained from different reactions indicated that it could instead be a decomposition product resulting from contact of the desired dienolate products with a source of methanol, and transesterification. The source of methanol was unknown at the time, but residual methanol after the preparation of Bestmann ylide (**178**) was suspected. Thus, the **178** prepared was left under high vacuum for prolonged time.

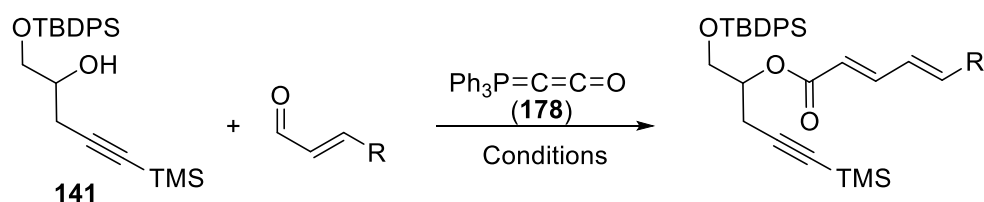


Scheme 4.4: Decomposition of the desired dienolate in the presence of methanol.

4.4 Applying the Bestmann ylide linchpin to macrocycle fragments

After the promising results with simple alcohols, the racemic TBDPS-protected C16–C20 fragment of zampanolide, **141**,^{28,29} was subjected to the Bestmann ylide linchpin reaction with cinnamaldehyde (**183**) in THF and toluene (Table 4.3, entries 1 and 2). In an effort to avoid degradation, the reactions were terminated prior to full conversion, leading to the dienoate product **196** in modest yields and with good recovery of starting material. Unfortunately, it was found that the product was not pure. Apart from the already identified methyl ester degradation product **195**, the purified product contains the desired **196** and a by-product in a ratio between 3:2 and 5:2. Similarly, the reaction of alcohol **141** with hept-2-enal (**197**) afforded the dienoate **198** in equally poor yield and purity (Table 4.3, entries 3).

Table 4.3: Coupling reactions of C16-C20 alcohol fragment **141** and model aldehydes with Bestmann ylide (**178**)^a



Entry	aldehyde	Conditions: solvent, temperature, reaction length	Product	Yield ^b (conversion) ^c
1	183	THF, 68 °C 3.5 h	196	<36% (43%)
2	183	Toluene, 110 °C 2 h	196	<49% (73%)
3	197	Toluene, 110 °C 1 h	198	<41% (50%)

^a Reactions were performed on a 0.1 mmol scale using approximately 1:1:1 ratio of alcohol/Bestmann ylide/aldehyde. ^b Isolated yields. ^c Conversion was calculated based on comparison of peak integrations for the limiting reagent (aldehyde) and product in ¹H NMR spectra of the crude product mixture after workup.

Comparing the ^1H NMR spectra obtained from the crude reaction mixture and the post-column purification species of **196**, the methyl ester decomposition product **195** was only present after purification, which suggested post-reaction decomposition. The source of this decomposition was identified as methanol used to dissolve the product prior to TLC analysis, thus it was switched to dichloromethane, and the situation improved. Separation of the methyl ester **195** from the desired product **196** was not achieved with EtOAc/petroleum ether or Et₂O/petroleum ether elution, but use of CH₂Cl₂/petroleum ether as eluent afforded satisfactory separation. However, the product was still a mixture of two compounds. Examination of the ^1H NMR spectrum revealed great structural similarity between the two products, wherein, apart from the non-resolvable phenyl region, each of the protons in the major compound have a corresponding minor signal with similar peak shape and chemical shift (**Figure 4.4**). Assisted by 2D NMR data, the oxymethine protons were identified as the apparent quintet signals at 5.16 and 4.10 ppm for the major and minor compounds, respectively. The chemical shift of 5.16 ppm is within the expected range of the ester oxymethine in the desired product **196**, while the chemical shift of 4.10 ppm would indicate the absence of the ester functionality. The

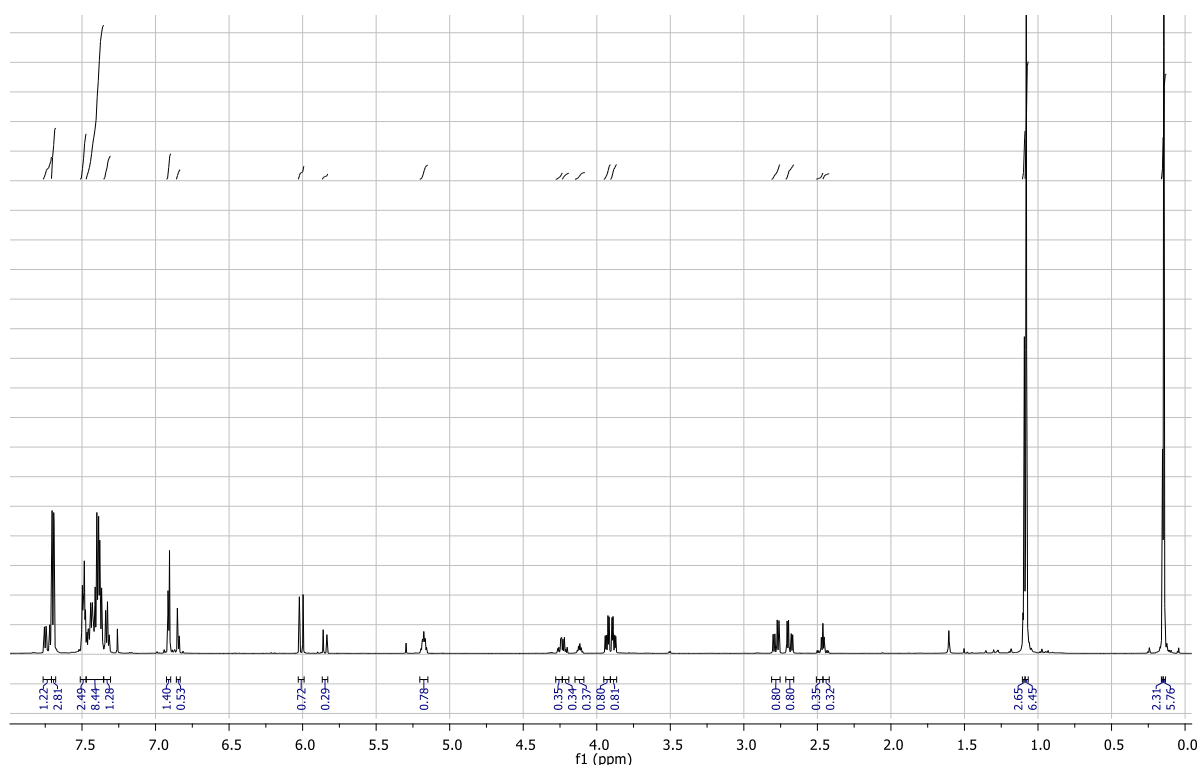


Figure 4.4: ^1H NMR spectrum of the mixture containing **196**.

oxymethylene protons in the minor compound (4.24 and 4.20 ppm) exhibited higher chemical shifts than the equivalent ones in the major compound (3.91 and 3.82 ppm), showing a pair of

signals at, which suggested that the stronger electron withdrawing group was connected to the methylene in the minor compound.

Based on these observations, the mixture might consist of the desired product **196** and its silyl-migrated isomer **199** (Figure 4.5). To confirm this, correlation between H2' and C1 in the major and H1' and C1 in the minor product is needed. However, normal heteronuclear multiple-bond correlation (HMBC) spectroscopy did not detect this three-bond correlation. The classic HMBC is set to detect correlations optimized at about 8 Hz, but three- or four-bond coupling constants can range between 2 and 25 Hz.³⁰ A carbon-proton coupling across an ester functionality (typically 3~4 Hz) can be beyond the detection limit due to incomplete relaxation. Ideally, an HMBC spectrum would show minimal signals from both one-bond carbon-proton and multiple-bond proton-proton correlations, and be able to detect up to five-bond carbon-proton correlations.^{30,31} Great effort has been put into the improvement of HMBC techniques, and several advancements have been reported.³²⁻³⁵ A modified HMBC experiment, namely, constant time inverse-detection gradient accordion rescaled (CIGAR) HMBC spectroscopy³⁶ is one of the most recent development, where the dual-stage low-pass *J*-filter removes a broad range of one-bond proton-carbon couplings, and the complete suppression of proton-proton coupling detection maximises the resolution of the desired multi-bond proton-carbon correlations.³⁶ This CIGAR-HMBC method was applied to the mixture and allowed detection of the three-bond correlations between H2' and C1 in **196** and H1' and C1 in **199**.

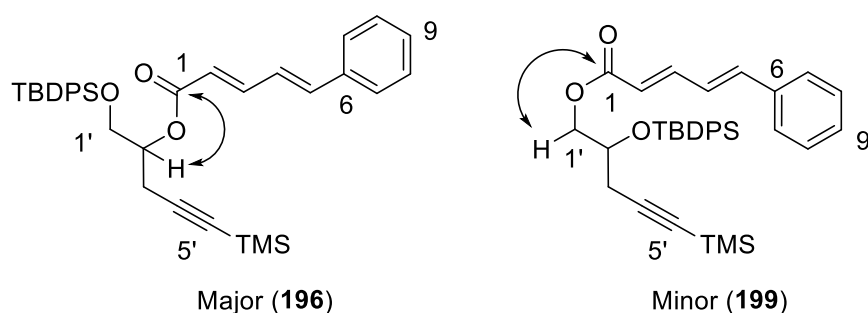
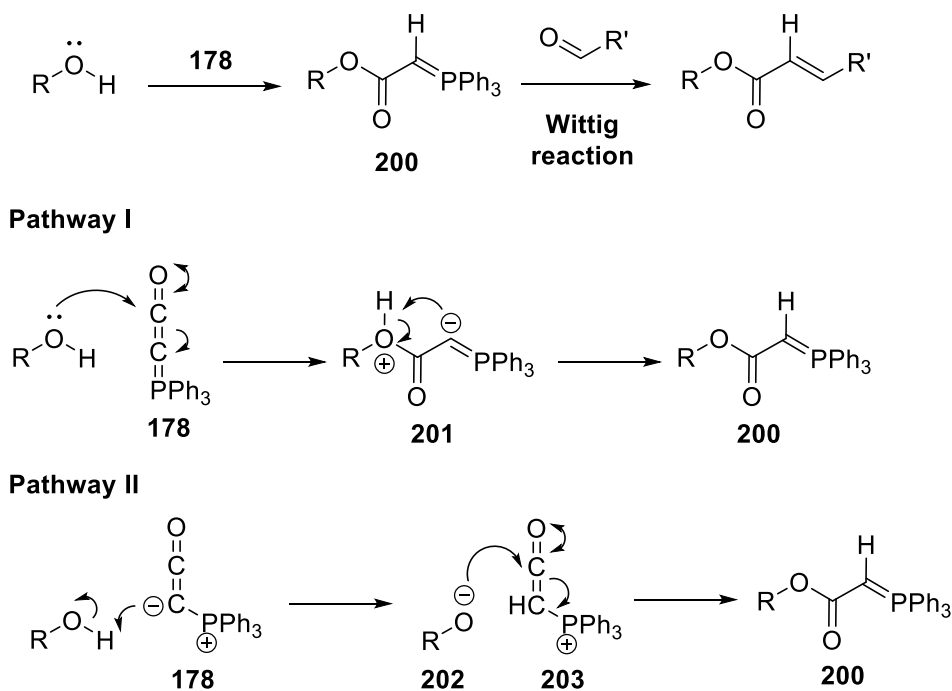


Figure 4.5: CIGAR-HMBC correlations used to confirm the position of the ester functionality in product **196** and **199**.

Silyl groups are known to migrate under basic conditions, and lack of an exogenous base in the simple composition of the reaction mixture suggested that the ylide was serving as the base.

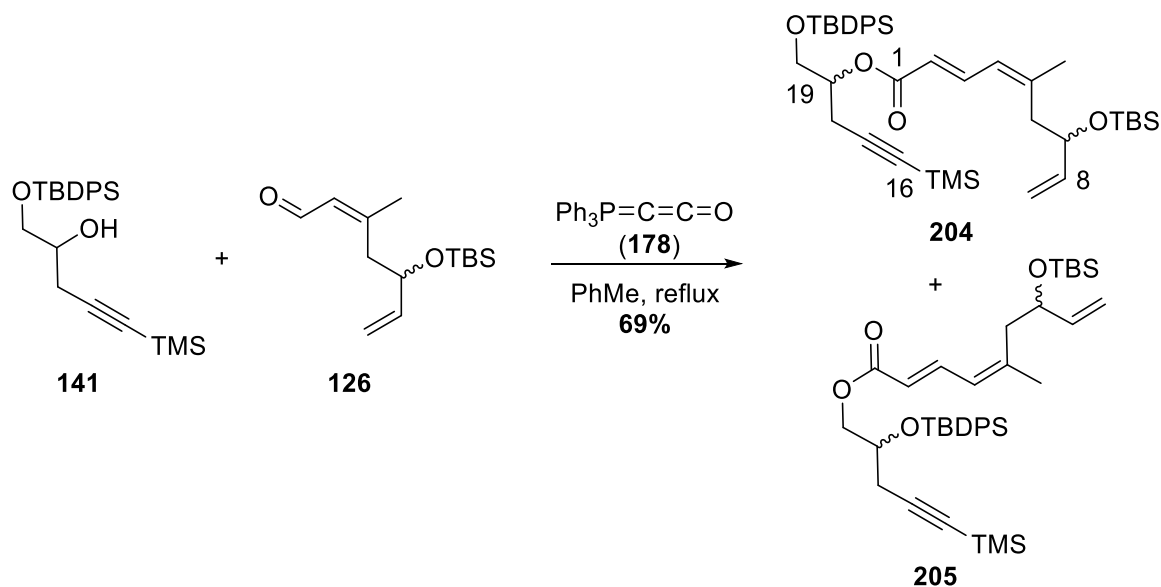
This level of basicity is not expected for Bestmann ylide (**178**) itself, but the migration could also be facilitated by various basic intermediates generated in the cascade. The three component cascade reaction involving **178** is thought to proceed *via* the phosphoranylidene intermediate **200** (Scheme 4.5),^{4,5,9-12} which is isolable in reactions lacking the aldehyde component. There are two possible pathways to form the intermediate **200**: Pathway I shows the case where the hydroxyl would perform the nucleophilic attack directly at the electrophilic



Scheme 4.5: Proposed mechanistic pathways of the ylide–alcohol coupling.

carbon of Bestmann ylide (**178**) to produce **201**, followed by proton transfer, either inter- or intramolecularly, to afford phosphoranylidene **200**; Pathway II involves the deprotonation of the secondary alcohol by **178** first, which produces a stronger alkoxide nucleophile **202** and a better carbonyl electrophile **203** for the subsequent nucleophilic attack. The generation of alkoxide **202** in Pathway II could facilitate the observed silyl migration, and the intermediate **201** in pathway I is potentially basic enough to deprotonate the alcohol starting material to allow the silyl protecting group to migrate. Hydroxyls are not very acidic, with pKa typically around 30 in DMSO. Strong bases such as hydrides, alkaline metals and alkoxides are usually required to deprotonate an alcohol. However, the elevated reaction temperature could have encouraged the deprotonation, and full deprotonation of the alcohol may not be necessary for the silyl to migrate.

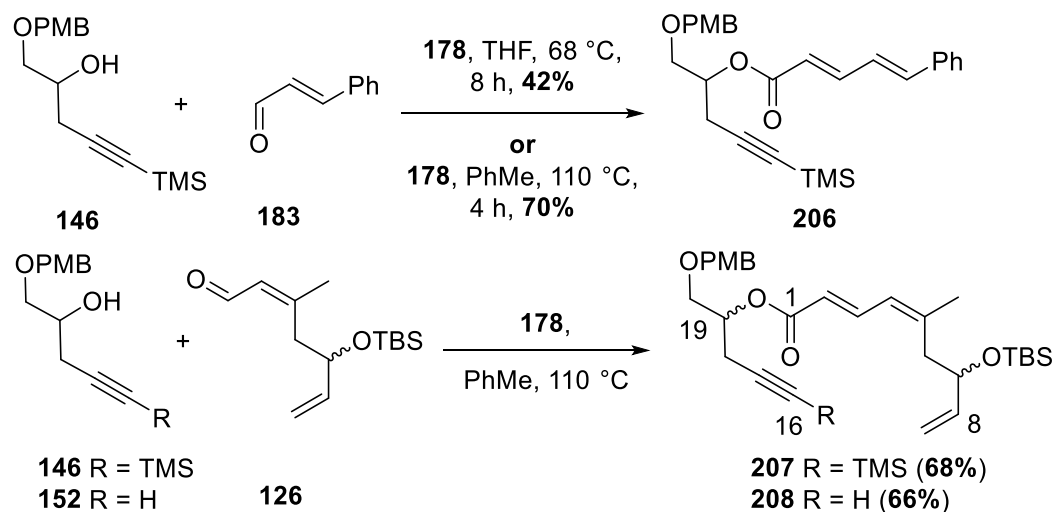
With C3-C8 fragment **126** in hand, a reaction with **178** was performed in toluene using the TBDPS-protected alcohol **141**. A mixture of four isomeric compounds was observed by ^1H and ^{13}C NMR spectroscopy, two diastereomers of **204** and two diastereomers of the silyl migrated product **205** (Scheme 4.6). The diastereomers were not differentiable by ^1H NMR spectroscopy, but four sets of signals were observed in the ^{13}C NMR spectrum. The assignment was supported by the obtained 2D NMR data including CIGAR-HMBC. With the problem of silyl migration seen in all reaction of alcohol **141**, an alternative protection group was required.



Scheme 4.6: Coupling of macrocycle fragments **141** with **126**.

A three-component reaction with the PMB-protected variant **146** was then attempted with cinnamaldehyde **183**. The trial performed in THF did not reach completion after 8 h, and a moderate 42% yield of **206** was achieved, while using toluene as the solvent produced a good 70% yield after 4 h. (Scheme 4.7). The product **206** was obtained with good purity. Employing the alcohol **146** in the reaction with macrocycle fragment **126** led to gratifying yields of products **207**, as a mixture of diastereomers. While the reaction of **146** with aldehyde **126** in THF took 11 h to go to completion (62% isolated yield of **207**), the equivalent reaction in toluene required only 5 h (68% yield). Alcohol **152** was used to test the compatibility of an unprotected alkyne in this linchpin reaction for synthetic ease. To our delight, reaction of aldehyde **126** with alcohol **152** in toluene provided the desired product **208** in a comparable yield (66%) after 5 h. The coupling of enantiopure fragment *S*-**152** with **126** was later carried

out, but only 26% of **19S-208** was obtained with recovered starting material (33%). This is thought to be due to decomposition of the Bestmann ylide (**178**) after months in storage.



Scheme 4.7: Coupling of **146** or **152** with model **183** and macrocycle fragments **126**.

The *E*-configuration of C2-C3 alkene in the *E,Z*-dienoates **207** and **208** was confirmed by the coupling constant of around 15 Hz between the α - and β -protons, as well as the strong through-space correlation of the α -proton to the γ -proton observed by rotating frame Overhauser effect spectroscopy (ROESY) (**Figure 4.5**). Very weak ROESY correlation between α - and β -protons was observed, which is more likely to be due to noise from through-bond interaction. The *Z*-configuration of the γ,δ -alkene was retained as expected, based on strong ROESY correlation of the γ -proton with the singlet attributed to the allylic methyl protons. Correlations between the β -proton and the allylic methylene protons were also clearly seen. The pairs of diastereomers are differentiable in the ^{13}C NMR spectra, with doubled signals between 1.0 and 4.8 Hz apart. The differentiated diastereomeric signals are from carbons around the two stereocentres, C19 and C7, with more differentiation around the C7 centre. The two peaks attributed to C7 in the diastereomers differ by 4.8 Hz, and signals for C6 and C8 are also differentiated. On the other hand, the two signals for C19 only differ by 1.9 Hz and only one peak each was observed for C18 and C20.

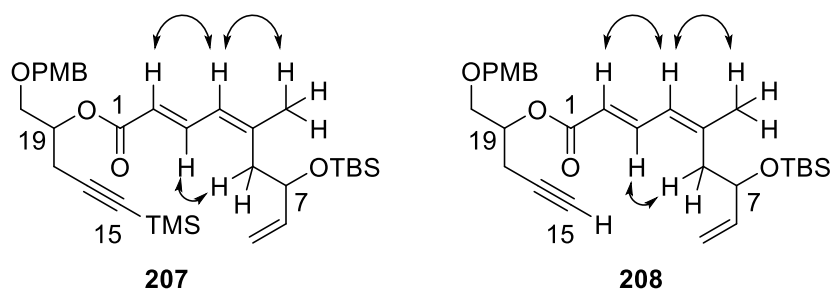


Figure 4.5: ROESY correlations of the diene region in **207** and **208**.

In summary, the scope of the efficient three-component reaction between Bestmann ylide (**178**), an alcohol and an unsaturated aldehyde to deliver $\alpha,\beta,\gamma,\delta$ -unsaturated esters was studied for simple alcohols and aldehydes. This methodology enabled the facile synthesis of *E,Z*-dienoate products **207** and **208**, which represent two-thirds of the dactylolide/zampanolide macrocycle. Terminal alkene **208** is poised to undergo alkynylation at C16 and metathesis at C8.

4.5 Experimental data

General experimental information

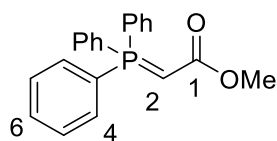
Unless otherwise stated, all reactions were carried out in oven-dried glassware under a positive pressure of nitrogen, delivered via a manifold. Dry tetrahydrofuran and toluene were obtained from a PureSolv MD 5 solvent purification system (Innovative Technology). Analytical grade solvents were used for aqueous work-up and column chromatography (petroleum ether, *n*-hexane, diethyl ether and dichloromethane). Column chromatography was performed on silica gel 60Å (Pure Science, 40–63 micron) with the eluent mixtures as stated in the corresponding procedures. Thin-layer chromatography was performed on silica-coated plastic plates (Macherey-Nagel, POLYGRAM[®] Sil G/UV₂₅₄). UV-active compounds were detected under UV irradiation ($\lambda = 254$ nm), while non-UV-active compounds were visualised with anisaldehyde or potassium permanganate staining solutions.

All other chemicals were purchased from Pure Science, Sigma-Aldrich, Panreac and Bedoukian Research. Infra-red (IR) spectra were collected on an ALPHA FT-IR spectrometer (Bruker) fitted with attenuated total reflectance (ATR). The intensities of signals are defined as: br = broad, s = strong, m = medium, w = weak. Mass spectra were collected on an Agilent

6530 Accurate-Mass Q-TOF LC/MS high-resolution mass spectrometer (HRMS). The specific rotations were collected on an AUTOPOL II automatic polarimeter (Rudolph Research Analytical), and the reported values are an average of 10 measurements and concentrations are reported in g/100 mL.

Nuclear magnetic resonance (NMR) spectra were obtained in deuterated chloroform (CDCl_3) using Varian Inova instruments operating at 500 or 600 MHz for proton, 125 or 150 MHz for carbon, and 120 MHz for phosphorus. Proton and carbon chemical shifts are reported in parts per million (ppm) relative to residual CHCl_3 [$\delta(^1\text{H}) = 7.26$ ppm] and CDCl_3 [$\delta(^{13}\text{C}) = 77.0$ ppm], respectively. Signals are defined as: s = singlet, d = doublet, t = triplet, q = quartet, quin = quintet, sext = sextet, sept = septet, m = multiplet, app. = apparent, obs. = obscured peak. Coupling constants (J) are reported in Hertz (Hz). Assignments were determined by two-dimensional NMR experiments (COSY, HSQC, HMBC, ROESY and CIGAR-HMBC).

Methyl (triphenylphosphoranylidene)acetate (**179**)



To a solution of triphenylphosphine (7.08 g, 27.0 mmol) in toluene (40 mL, 0.67 M), a solution of methyl bromoacetate (**181**, 4.04 g, 26.4 mmol) in toluene (8.0 mL, 3.3 M) was added. The reaction turned cloudy upon the addition, and was stirred at r.t. for 19 h. The solid was collected by filtration to yield a white powder. The powder was dissolved in CH_2Cl_2 (100 mL), and an aqueous NaOH solution (60 mL, 0.43 M) was added. The mixture was shook vigorously for 1 min, and the aqueous layer was separated and extracted with CH_2Cl_2 (3×50 mL). The organic layers were combined and dried over MgSO_4 , and the solvent was removed under reduced pressure to yield the phosphoranylidene **179** as a white powder (7.59 g, 87%).

^1H NMR (500 MHz, CDCl_3): δ 7.66 (dt, $J = 16.9, 8.7$ Hz, 6H, 5-CH), 7.59 – 7.51 (m, 3H, 6-CH), 7.50 – 7.41 (m, 6H, 4-CH), 3.52 (s, 3H, CH_3 , Me), 2.90 (s, 1H, 2-CH).

^{13}C NMR (125 MHz, CDCl_3): δ 133.0 (d, $J = 10.0$ Hz, CH, Ph), 131.9 (d, $J = 2.8$ Hz, CH, Ph), 128.7 (d, $J = 12.7$ Hz, CH, Ph), 50.0 (d, $J = 4.9$ Hz, CH_3 , Me), 29.7 (d, $J = 131.6$ Hz, CH, C2).

^{31}P NMR (120 MHz, CDCl_3): δ 17.6.

M.p.: 163.6 – 164.8 °C (Lit. 162 – 163 °C).³⁷

The signals for C1 and C3 were missing from the ^{13}C NMR data, but ^{31}P NMR and m.p. data agree with those reported previously.³⁷

(Triphenylphosphoranylidene)ketene (**178**)

$$\begin{array}{c} 2 \\ \text{Ph}_3\text{P}=\text{C}=\text{C}=\text{O} \\ 1 \end{array}$$
 To a solution of methyl (triphenylphosphoranylidene)acetate (**179**, 3.00 g, 8.97 mmol) in toluene (30 mL, 0.30 M), a solution of NaHMDS (17 mL, 0.6 M in toluene, 10 mmol) was added. The reaction was heated at 65 °C for 20 h. While still hot, the reaction mixture was filtered through a thin pad of Celite, and the filtrate was concentrated under reduced pressure until white precipitate started to form. After the precipitate was re-dissolved with heating, the solution was cooled down to 4 °C and left to recrystallize overnight. The precipitate was collected by filtration to yield the ylide **178** as cream white needle-shaped crystals (1.43 g, 53%).

^{13}C NMR (125 MHz, CDCl_3): δ 135.0 (d, J = 3.3 Hz), 133.3 (d, J = 10.8 Hz), 132.1 (d, J = 10.0 Hz), 130.4 (d, J = 13.0 Hz), 128.5 (d, J = 12.2 Hz), 119.3 (d, J = 88.1 Hz).

^{31}P NMR (120 MHz, CDCl_3): δ 5.5.

IR (ATR): 2910 (w, C–H), 2093 (s, C=P), 1620 (s, C=O), 1435 (s, C–H), 1347 (s, C–H), 1104 (s, C–O), 743 (s, C–P), 717 (s, C–P), 514 (s, C–H).

M.p.: 163.7 – 168.6 °C (Lit. 173 °C).

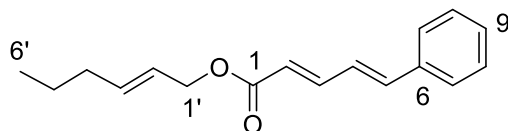
The signals for C1 and C2 were missing from the ^{13}C NMR data, but ^{31}P NMR, IR and m.p. data broadly agree with those reported previously.¹³

General procedure for Bestmann ylide linchpin reaction:

To a mixture of alcohol (1 eq., 0.1–0.3 M) and Bestmann ylide (1 eq.) in solvent (toluene or tetrahydrofuran) heated at reflux, a solution of aldehyde (1 eq., 1.0 M) was added. The reaction was heated at reflux until full consumption of starting material aldehyde was observed by TLC. After cooling to r.t., the reaction was concentrated and purified by silica column chromatography to afford the product as a colourless or pale yellow oil.

(2'E,2E,4E)-Hex-2'-enyl 5-phenylpenta-2,4-dienoate (184)

Formed in 53% yield, 76% BRSM. No detection of (2'E,2Z,4E)-isomer when reaction was carried out to completion with minimum handling.



TLC: $R_f = 0.23$ (20:1 Pet. ether: Et₂O).

¹H NMR (500 MHz, CDCl₃): δ 7.48–7.43 (complex m, 3H, 3-CH & 7-CH), 7.36 (app. t, $J = 7.6$ Hz, 2H, 8-CH), 7.30 (t, $J = 6.9$ Hz, 1H, 9-CH), 6.82–6.93 (complex m, 2H, 4-CH & 5-CH), 6.01 (d, $J = 15.6$ Hz, 1H, 2-CH), 5.81 (dt, $J = 15.4, 6.6$ Hz, 1H, 3'-CH), 5.62 (dt, $J = 15.4, 6.2$ Hz, 1H, 2'-CH), 4.63 (d, $J = 6.6$ Hz, 2H, 1'-CH₂), 2.14 (app. q, $J = 7.1$ Hz, 2H, 4'-CH₂), 1.43 (app. sext, $J = 7.4$ Hz, 2H, 5'-CH₂), 0.92 (t, $J = 7.3$ Hz, 3H, 6'-CH₃).

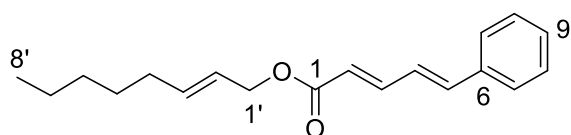
¹³C NMR (125 MHz, CDCl₃): δ 166.8 (C, C=O), 144.7 (CH, C3), 140.4 (CH, C5), 136.3 (CH, C3'), 136.0 (C, C6), 129.0 (CH, C9), 128.8 (CH, C8), 127.2 (CH, C7), 126.2 (CH, C4), 124.0 (CH, C2'), 121.2 (CH, C2), 65.2 (CH₂, C1'), 34.3 (CH₂, C4'), 22.0 (CH₂, C5'), 13.6 (CH₃, C6').

IR (neat) cm⁻¹: 2958 (m, C–H), 2929 (m, C–H), 1706 (s, C=O), 1625 (s, C=C), 1449 (m, C–H), 1236 (s, C–O), 1172 (s, C–O), 997 (m, C–H), 689 (m, C–H).

HRMS (ESI) m/z : found 257.1529, calcd for C₁₇H₂₁O₂ [M+H]⁺ 257.1536 ($\Delta = 2.7$ ppm).

(2'E,2E,4E)-Oct-2'-enyl 5-phenylpenta-2,4-dienoate (186)

Formed in 93% yield, contains 1% of the (2'E,2Z,4E)-isomer as determined by integration of the post-chromatography ¹H NMR spectrum. Key spectral resonances were used to determine the ratio of minor to major isomers as 1:99: 6.01 (d, $J = 15.4$ Hz, 0.99H, 2-CH-major), 8.14 (dd, $J = 15.5, 12.0$ Hz, 0.01H, 3-CH-minor). NMR data are of the major isomer signals obtained from the spectrum of the purified mixture.



TLC: $R_f = 0.08$ (40:1 Pet. ether: Et₂O).

¹H NMR (500 MHz, CDCl₃): δ 7.57–7.50 (complex m, 3H, 3-CH & 7-CH), 7.35 (t, $J = 7.3$ Hz, 2H, 8-CH), 7.31 (t, $J = 7.3$ Hz, 1H, 9-CH), 6.93–6.82 (complex m, 2H, 4-CH & 5-CH), 6.01 (d, $J = 15.4$ Hz, 1H, 2-CH), 5.81 (dt, $J = 15.0, 7.0$ Hz, 1H, 3'-CH), 5.62 (dt, $J = 15.1, 6.6$ Hz, 1H, 2'-CH), 4.62 (d, $J = 6.3$ Hz, 2H, 1'-CH₂), 2.07 (app. q, $J = 7.1$ Hz, 2H, 4'-CH₂), 1.40 (app. quin $J = 7.3$ Hz, 2H, 5'-CH₂), 1.34–1.24 (complex m, 4H, 6'-CH₂ & 7'-CH₂), 0.90 (t, $J = 6.8$ Hz, 3H, 8'-CH₃).

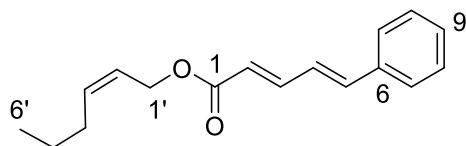
¹³C NMR (125 MHz, CDCl₃): δ 166.8 (C, C1), 144.7 (CH, C3), 140.4 (CH, C4 or C5), 136.6 (CH, C3'), 136.0 (C, C6), 129.0 (CH, C9), 128.8 (CH, C8), 127.2 (CH, C7), 126.2 (CH, C4 or C5), 123.8 (CH, C2'), 121.2 (CH, C2), 65.3 (CH₂, C1'), 32.3 (CH₂, C4'), 31.4 (CH₂, C6'), 28.6 (CH₂, C5'), 22.5 (CH₂, C7'), 14.0 (CH₃, C8').

IR (neat) cm⁻¹: 2956 (m, C–H), 2955 (m, C–H), 1709 (s, br, C=O), 1625 (s, C=C), 1235 (s, C–O), 1129 (s, C–O), 969 (s, C–H), 691 (m, C–H).

HRMS (ESI) m/z : found 307.1666, calcd for C₁₉H₂₄O₂Na [M+Na]⁺ 307.1669 ($\Delta = 0.9$ ppm).

(2'*Z*,2*E*,4*E*)-Hex-2'-enyl 5-phenylpenta-2,4-dienoate (188)

Formed in 91% yield, contains 7% of the (2'*E*,2*Z*,4*E*)-isomer as determined by integration of the post-chromatography ¹H NMR spectrum. Key spectral resonances were used to determine the ratio of major and minor isomers as 93:7: 6.03 (d, $J = 14.9$ Hz, 0.93H, 2-CH-major), 8.15 (dd, $J = 15.7, 11.4$ Hz, 0.07H, 3-CH-minor). NMR data are of the major isomer signals obtained from the spectrum of the purified mixture.



TLC: $R_f = 0.25$ (20:1 Pet. ether: Et₂O).

¹H NMR (500 MHz, CDCl₃): δ 7.49–7.44 (complex m, 3H, 3-CH & 7-CH), 7.36 (app. t, $J = 7.6$ Hz, 2H, 8-CH), 7.30 (t, $J = 6.9$ Hz, 1H, 9-CH), 6.98–6.83 (complex m, 2H, 4-CH & 5-CH), 6.03 (d, $J = 14.9$ Hz, 1H, 2-CH), 5.69 (dt, $J = 11.0, 7.5$ Hz, 1H, 2'-CH), 5.63 (dt, $J = 11.8, 6.4$

Hz, 1H, 3'-CH), 4.76 (d, $J = 7.2$ Hz, 2H, 1'-CH), 2.14 (app. q, $J = 7.2$ Hz, 2H, 4'-CH), 1.45 (app. sext, $J = 7.2$ Hz, 2H, 5'-CH), 0.95 (t, $J = 7.3$ Hz, 3H, 6'-CH).

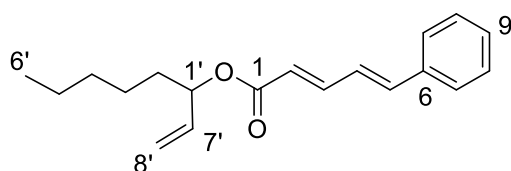
^{13}C NMR (125 MHz, CDCl_3): δ 167.0 (C, C1), 144.7 (CH, C3), 140.5 (CH, C4 or C5), 136.0 (C, C6), 135.2 (CH, C2'), 129.0 (CH, C9), 128.8 (CH, C8), 127.2 (CH, C7), 126.2 (CH, C4 or C5), 123.6 (CH, C3'), 121.1 (CH, C2), 60.4 (CH_2 , C1'), 29.6 (CH_2 , C4'), 22.6 (CH_2 , C5'), 13.7 (CH_3 , C6').

IR (neat) cm^{-1} : 2959 (m, C-H), 2930 (m, C-H), 1707 (s, C=O), 1624 (s, C=C), 1449 (m, C-H), 1234 (s, C-O), 997 (s, C-H), 690 (m, C-H).

HRMS (ESI) m/z : found 257.1527, calcd for $\text{C}_{17}\text{H}_{21}\text{O}_2$ $[\text{M}+\text{H}]^+$ 257.1536 ($\Delta = 3.5$ ppm).

(2*E*,4*E*)-Oct-1'-en-3'-yl 5-phenylpenta-2,4-dienoate (190)

Formed in 61% yield in THF or 71% in toluene, contains 3% of the (2'*E*,2*Z*,4*E*)-isomer as determined by integration of the post-chromatography ^1H NMR spectrum. Key spectral resonances were used to determine the ratio of major and minor as 97:3: 6.02 (d, $J = 14.9$ Hz, 0.1H, 2-CH-major), 8.17 (dd, $J = 15.6, 11.4$ Hz, 0.03H, 3-CH-minor). NMR data are of the major isomer signals obtained from the spectrum of the purified mixture.



TLC: $R_f = 0.16$ (40:1 Pet. ether: Et_2O).

^1H NMR (500 MHz, CDCl_3): δ 7.47 (d, $J = 7.8$ Hz, 2H, 7-CH), 7.46 (dd, $J = 14.9, 8.8$ Hz, 1H, 3-CH), 7.36 (app. t, $J = 7.6$ Hz, 2H, 8-CH), 7.31 (t, $J = 7.2$ Hz, 1H, 9-CH), 6.95–6.84 (complex m, 2H, 4-CH & 5-CH), 6.02 (d, $J = 14.9$ Hz, 1H, 2-CH), 5.83 (ddd, $J = 17.1, 10.6, 6.2$ Hz, 1H, 7'-CH), 5.34 (app. q, $J = 6.6$ Hz, 1H, 1'-CH), 5.27 (dd, $J = 17.3, 1.2$ Hz, 1H, one of 8'- CH_2), 5.18 (dd, $J = 10.5, 1.0$ Hz, 1H, one of 8'- CH_2), 1.74–1.59 (complex m, 2H, 2'- CH_2), 1.39–1.26 (complex m, 6H, 3'- CH_2 & 4'- CH_2 & 5'- CH_2), 0.89 (t, $J = 6.1$ Hz, 3H, 6'- CH_3).

^{13}C NMR (125 MHz, CDCl_3): δ 166.3 (C, C1), 144.6 (CH, C3), 140.4 (CH, C4 or C5), 136.7 (CH, C7'), 136.0 (C, C6), 129.0 (CH, C9), 128.8 (CH, C8), 127.2 (CH, C7), 126.2 (CH, C4 or

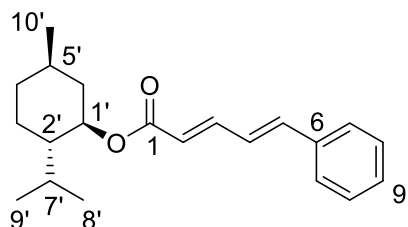
C5), 121.5 (CH, C2), 116.4 (CH₂, C8'), 74.7 (CH, C1'), 34.3 (CH₂, C2'), 31.6 and 24.8 and 22.5 (CH₂, C3' and C4' and C5'), 14.0 (CH₃, C6').

IR (neat) cm⁻¹: 2930 (m, C–H), 2859 (m, C–H), 1706 (s, C=O), 1625 (s, C=C), 1235 (s, C–O), 1130 (s, C–O), 996 (s, C–H), 688 (m, C–H).

HRMS (ESI) *m/z*: found 307.1667, calcd for C₁₉H₂₄O₂Na [M+Na]⁺ 307.1669 (Δ = 0.65 ppm).

(1'*R*,2'*S*,5'*R*,2*E*,4*E*)-2'-*iso*-Propyl-5'-methylcyclohex-1'-yl 5-phenylpenta-2,4-dienoate (192)

Formed in 77% yield in THF or 53% in toluene. No detection of (2'*E*,2*Z*,4*E*)-isomer.



TLC: *R*_f = 0.14 (40:1 Pet. ether: Et₂O).

¹H NMR (500 MHz, CDCl₃): δ 7.46 (d, *J* = 7.8 Hz, 2H, 7-CH), 7.43 (partially obs. ddd, *J* = 15.3, 9.2, 1.0 Hz, 1H, 3-CH), 7.36 (app. t, *J* = 7.6 Hz, 2H, 8-CH), 7.30 (tt, *J* = 7.3, 2.4 Hz, 1H, 9-CH), 6.93–6.83 (complex m, 2H, 4-CH & 5-CH), 5.99 (d, *J* = 15.4 Hz, 1H, 2-CH), 4.79 (td, *J* = 10.9, 4.4 Hz, 1H, 1'-CH), 2.05 (dddd, *J* = 11.9, 4.4, 3.0, 2.0 Hz, 1H, one of 6'-CH₂), 1.91 (septd, *J* = 7.0, 2.7 Hz, 1H, 7'-CH), 1.74–1.66 (complex m, 2H, one of 3'-CH₂ & one of 4'-CH₂), 1.53 (m, 1H, 5'-CH), 1.43 (tt, *J* = 11.7, 2.9 Hz, 1H, 2'-CH), 1.09 (qd, *J* = 13.2, 3.3 Hz, 1H, one of 4'-CH₂), 1.02 (q, *J* = 11.5 Hz, 1H, one of 6'-CH₂), 0.92 (d, *J* = 6.6 Hz, 3H, 10'-CH₃), 0.91 (d, *J* = 7.1 Hz, 3H, 8'-CH₃), 0.94–0.84 (partially obs. m, 1H, one of 3'-CH₂), 0.78 (d, *J* = 7.1 Hz, 3H, 9'-CH₃).

¹³C NMR (125 MHz, CDCl₃): δ 166.6 (C, C1), 144.3 (CH, C3), 140.2 (CH, C4 or C5), 136.1 (C, C6), 129.0 (CH, C9), 128.8 (CH, C8), 127.1 (CH, C7), 126.3 (CH, C4 or C5), 121.9 (CH, C2), 74.1 (CH, C1'), 47.2 (CH, C2'), 41.0 (CH₂, C6'), 34.3 (CH₂, C3'), 31.4 (CH, C5'), 26.3 (CH, C7'), 23.6 (CH₂, C4'), 22.0 (CH₃, C10'), 20.8 (CH₃, C8'), 16.5 (CH₃, C9').

IR (neat) cm^{-1} : 2953 (m, C–H), 2925 (m, C–H), 2868 (m, C–H), 1702 (s, C=O), 1625 (s, C=C), 1237 (s, C–Si), 1131 (s, C–O), 995 (s, C–H), 754 (s, C–Si), 689 (s, C–Si).

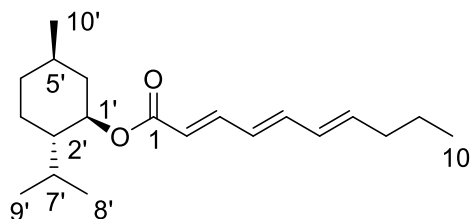
HRMS (ESI) m/z : found 335.1969, calcd for $\text{C}_{21}\text{H}_{28}\text{O}_2\text{Na}$ $[\text{M}+\text{Na}]^+$ 335.1982 ($\Delta = 3.9$ ppm).

Specific rotation: $[\alpha]_{\text{D}}^{22} = -60$ ($c = 0.40$, CH_2Cl_2).

This compound has been reported previously.³⁸ There is close correlation between the IR and ^{13}C NMR data entered above and those in the earlier report. However, the ^1H NMR data quoted previously do not match those obtained. The identity of the sample prepared in this work was supported by NMR and HRMS data, and all NMR assignments were made on the basis of thorough 2D NMR experiments (COSY and HSQC). Therefore, it was suspected that the 90 MHz instrument used in the earlier work did not allow accurate identification of the ^1H NMR signals, and the earlier report does not indicate either HRMS or elemental analytical results.

(1'R,2'S,5'R,2E,4E,6E)- 2'-iso-Propyl-5'-methylcyclohex-1'-yl deca-2,4,6-trienoate (194)

Formed in 67% yield. No detection of (2'E,2Z,4E)-isomer.



TLC: $R_f = 0.14$ (40:1 Pet. ether: Et_2O).

^1H NMR (500 MHz, CDCl_3): δ 7.28 (dd, $J = 15.4, 11.2$ Hz, 1H, 3-CH), 6.53 (dd, $J = 14.9, 10.7$ Hz, 1H, 5-CH), 6.21 (dd, $J = 14.9, 11.2$ Hz, 1H, 4-CH), 6.13 (dd, $J = 15.1, 10.7$ Hz, 1H, 6-CH), 5.92 (dt, $J = 14.9, 7.2$ Hz, 1H, 7-CH), 5.83 (d, $J = 15.4$ Hz, 1H, 2-CH), 4.75 (app. td, $J = 10.9, 4.4$ Hz, 1H, 1'-CH), 2.12 (app. q, $J = 7.3$ Hz, 2H, 8- CH_2), 2.02 (br d, $J = 12.2$ Hz, 1H, one of 6'- CH_2), 1.88 (septd, $J = 6.8, 2.3$ Hz, 1H, 7'-CH), 1.65–1.71 (complex m, 2H, one of 3'- CH_2 & one of 4'-CH), 1.50 (partially obs. m, 1H, 5'- CH_2), 1.44 (m, 2H, 9- CH_2), 1.40 (partially obs. m, 1H, 2'-CH), 1.07 (app. qd, $J = 12.9, 2.9$ Hz, 1H, one of 4'- CH_2), 0.99 (app. q, $J = 11.5$ Hz, 1H, one of 6'- CH_2), 0.91 (t, $J = 7.3$ Hz, 3H, 10- CH_3), 0.90 (d, $J = 6.1$ Hz, 3H,

10'-CH₃), 0.89 (d, J = 6.8 Hz, 3H, 8'-CH₃), 0.87 (partially obs. m, 1H, one of 3'-CH₂), 0.76 (d, J = 7.1 Hz, 3H, 9'-CH₃).

¹³C NMR (125 MHz, CDCl₃): δ 166.8 (C, C1), 144.6 (CH, C3), 141.0 (CH, C5), 140.2 (CH, C7), 130.0 (CH, C6), 127.8 (CH, C4), 120.5 (CH, C2), 73.9 (CH, C1'), 47.2 (CH, C2'), 41.0 (CH₂, C6'), 35.0 (CH₂, C8), 34.3 (CH₂, C3'), 31.4 (CH, C5'), 26.3 (CH, C7'), 23.6 (CH₂, C4'), 22.2 (CH₂, C9), 22.0 (CH₃, C10'), 20.7 (CH₃, C8'), 16.4 (CH₂, C9'), 13.7 (CH₃, C10).

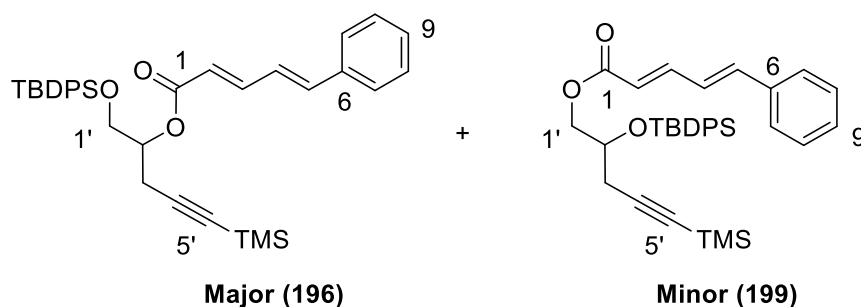
IR (neat) cm⁻¹: 2955 (s, C-H), 2930 (s, C-H), 2869 (s, C-H), 1694 (s, C=O), 1615 (s, C=C), 1456 (m, C-H), 1342 (m, C-H), 1133 (s, C-O), 1007 (s, C-H).

HRMS (ESI) m/z : found 305.2486, calcd for C₂₀H₃₃O₂ [M+H]⁺ 305.2475 (Δ = 3.6 ppm).

Specific rotation: $[\alpha]_D^{22}$ = -26 (c = 0.42, CH₂Cl₂).

Mixture of (2*E*,4*E*)-[1'-(*tert*-butyldiphenylsilyloxy)-5'-trimethylsilyl]pent-4'-yn-2'-yl 5-phenylpenta-2,4-dienoate (196**) and the silyl migrated product (2*E*,4*E*)-[2'-(*tert*-butyldiphenylsilyloxy)-5'-trimethylsilyl]pent-4'-yn-1'-yl 5-phenylpenta-2,4-dienoate (**199**) (3:2)**

The isomers were formed in a combined 36% yield in THF or 49% in toluene.



TLC: R_f = 0.14 (36:1 Pet. ether: Et₂O).

¹H NMR (500 MHz, CDCl₃): δ 7.75–7.67 (complex m, 4H, CH, Ph), 7.55–7.30 (complex m, 11H, CH, Ph), 7.47 (obs. m, 0.6H, 3-CH-**196**), 7.32 (obs. m, 0.4H, 3-CH-**199**), 6.94–6.79 (complex m, 2H, 4-CH & 5-CH), 5.99 (d, J = 15.3 Hz, 0.6H, 2-CH-**196**), 5.83 (d, J = 15.6 Hz, 0.4H, 2-CH-**199**), 5.16 (app. quin, J = 5.6 Hz, 0.6H, 2'-CH-**196**), 4.23 (dd, J = 11.4, 4.4 Hz, 0.4H, one of 1'-CH₂-**199**), 4.20 (dd, J = 11.2, 5.9 Hz, 0.4H, one of 1'-CH₂-**199**), 4.10 (app. quin, J = 5.3 Hz, 0.4H, 2'-CH-**199**), 3.91 (dd, J = 11.2, 5.0 Hz, 0.6H, one of 1'-CH₂-**196**), 3.86 (dd,

$J = 10.9, 4.1$ Hz, 0.6H, one of 1'-CH₂-**196**), 2.77 (dd, $J = 16.7, 7.0$ Hz, 0.6H, one of 3'-CH₂-**196**), 2.67 (dd, $J = 16.7, 5.9$ Hz, 0.6H, one of 3'-CH₂-**196**), 2.47 (dd, $J = 17.0, 6.5$ Hz, 0.4H, one of 3'-CH₂-**199**), 2.43 (dd, $J = 17.0, 5.1$ Hz, 0.4H, one of 3'-CH₂-**199**), 1.08 (s, 2.7H, CH₃, *t*Bu-**199**), 1.06 (s, 5.4H, CH₃, *t*Bu-**196**), 0.14 (s, 2.7H, CH₃, Me-**199**), 0.13 (s, 5.4H, CH₃, Me-**196**).

¹³C NMR (125 MHz, CDCl₃): δ 166.6 (C, C1-**199**), 166.1 (C, C1-**196**), 145.0 (CH, C3-**196**), 144.8 (CH, C3-**199**), 140.6 (CH, C5/4-**196**), 140.5 (CH, C5/4-**199**), 136.0 (CH, Ph), 135.9 (CH, C6), 135.8 (CH, Ph), 135.54 (CH, Ph), 135.52 (CH, Ph), 133.7 (C, Ph), 133.5 (C, Ph), 133.3 (C, Ph), 129.8 (CH, Ph), 129.7 (CH, Ph), 129.08 (CH, C7-**196**), 129.06 (CH, C7-**199**), 128.8 (CH, C9), 127.70 (CH, Ph), 127.68 (CH, Ph), 127.65 (CH, Ph), 127.59 (CH, Ph), 127.21 (CH, C8-**196**), 127.18 (CH, C8-**199**), 126.22 (CH, C4/5-**196**), 126.18 (CH, C4/5-**199**), 121.1 (CH, C2-**196**), 120.8 (CH, C2-**199**), 102.6 (C, C4'-**199**), 102.1 (C, C4'-**196**), 87.2 (C, C5'-**199**), 86.9 (C, C5'-**196**), 72.1 (CH, C2'-**196**), 69.6 (CH, C2'-**199**), 66.9 (CH₂, C1'-**199**), 63.7 (CH₂, C1'-**196**), 26.9 (CH₃, *t*Bu-**199**), 26.7 (CH₃, *t*Bu-**196**), 25.8 (CH₂, C3'-**199**), 21.9 (CH₂, C3'-**196**), 19.4 (C, *t*Bu-**199**), 19.3 (C, *t*Bu-**199**), -0.01 (CH₃, Me).

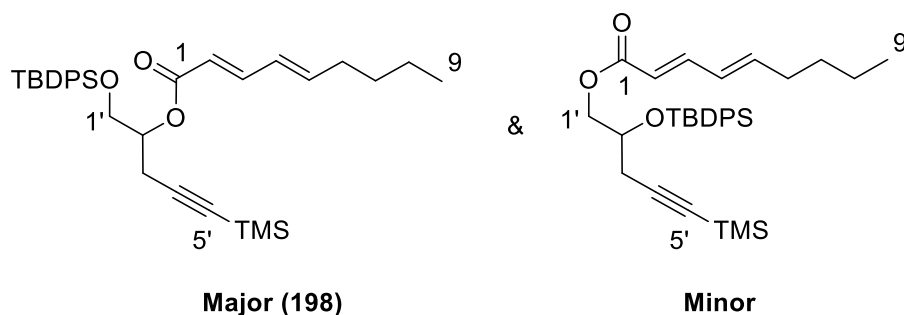
IR (neat) cm⁻¹: 3071 (w, C-H), 2958 (m, C-H), 2857 (m, C-H), 2178 (m, C≡C), 1710 (s, C=O), 1625 (s, C=C), 1235 (s, Si-C), 1112 (s, C-O), 997 (s, C-H), 840 (s, Si-C), 700 (s, Si-C), 504 (s, Si-C).

HRMS (ESI) m/z : found 605.2314, calcd for C₃₅H₄₂O₃Si₂K [M+K]⁺ 605.2304 ($\Delta = 1.7$ ppm).

The three-bond C-H correlations across the esters in both compounds were confirmed by CIGAR-HMBC NMR.

Mixture of (2*E*,4*E*)-[1'-(*tert*-butyldiphenylsilyloxy)-5'-trimethylsilyl]pent-4'-yn-2'-yl nona-2,4-dienoate (198) and the silyl migrated product, (2*E*,4*E*)-[2'-(*tert*-butyldiphenylsilyloxy)-5'-trimethylsilyl]pent-4'-yn-1'-yl nona-2,4-dienoate (2:1)

The isomers were formed in a combined 41% yield.



TLC: $R_f = 0.12$ (36:1 Pet. ether: Et₂O).

¹H NMR (500 MHz, CDCl₃): δ 7.74–7.61 (complex m, 4H, CH, Ph), 7.47–7.32 (complex m, 6H, CH, Ph), 7.28 (dd, $J = 14.7, 10.5$ Hz, 0.67H, 3-CH-**198**), 7.15 (dd, $J = 15.4, 9.8$ Hz, 0.33H, 3-CH-**minor**), 6.23–6.06 (complex m, 2H, 4-CH & 5-CH), 5.78 (d, $J = 15.4$ Hz, 0.67H, 2-CH-**198**), 5.64 (d, $J = 15.1$, 0.33H, 2-CH-**minor**), 5.12 (app. quin, $J = 5.6$ Hz, 0.67H, 2'-CH-**198**), 4.19 (dd, $J = 10.0, 4.2$ Hz, 0.33H, one of 1'-CH₂-**minor**), 4.19 (dd, $J = 10.9, 4.8$ Hz, 0.33H, one of 1'-CH₂-**minor**), 4.07 (app. dt, $J = 10.7, 5.4$ Hz, 0.33H, 2'-CH-**minor**), 3.89 (dd, $J = 11.0, 4.8$ Hz, 0.67H, one of 1'-CH₂-**198**), 3.84 (dd, $J = 10.5, 4.2$ Hz, 0.67H, one of 1'-CH₂-**198**), 2.74 (dd, $J = 16.6, 7.3$ Hz, 0.67H, one of 3'-CH₂-**198**), 2.64 (dd, $J = 16.9, 6.7$ Hz, 0.67H, one of 3'-CH₂-**198**), 2.47 – 2.37 (complex m, 0.66H, 3'-CH₂-**minor**), 2.18 (dt, $J = 13.4, 6.8$ Hz, 2H, 6-CH₂), 1.46–1.39 (complex m, 2H, 7-CH₂), 1.06 (s, 2.97H, CH₃, *t*Bu-**minor**), 1.05 (s, 6.03H, CH₃, *t*Bu-**198**), 0.95–0.89 (complex m, 2H, 8-CH₂), 0.89–0.80 (complex m, 3H, 9-CH₂), 0.13 (s, 2.97H, CH₃, Me-**minor**), 1.03 (s, 6.03H, CH₃, Me-**198**).

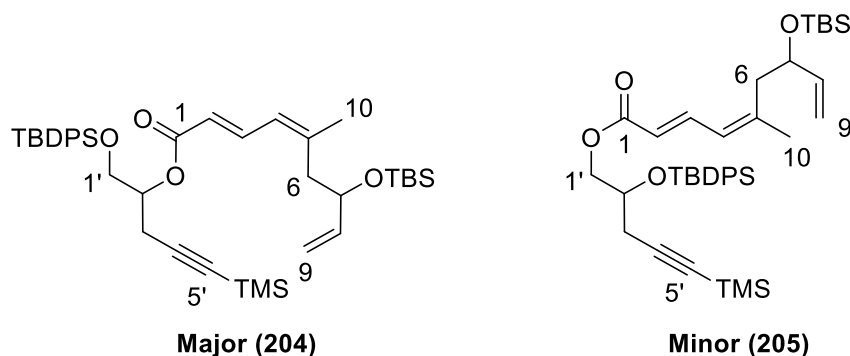
¹³C NMR (125 MHz, CDCl₃): δ 166.9 (C, C1-**minor**), 166.4 (C, C1-**198**), 145.6 (CH, C3-**198**), 145.4 (CH, C3-**minor**), 145.0 (CH, C4-**198**), 144.9 (CH, C4-**minor**), 136.0 (CH, Ph), 135.8 (CH, C5), 135.61 (CH, Ph), 135.55 (CH, Ph), 135.53 (CH, Ph), 135.51 (CH, Ph), 133.3 (C, Ph), 129.8 (CH, Ph), 129.7 (CH, Ph), 128.8 (CH, C9), 127.70 (CH, Ph), 127.70 (CH, Ph), 127.68 (CH, Ph), 127.66 (CH, Ph), 127.62 (CH, CH, C5), 127.58 (CH, Ph), 118.9 (CH, C2-**198**), 118.7 (CH, C2-**minor**), 102.1 (C, C4'), 86.8 (C, C5'), 71.9 (CH, C2'-**198**), 69.6 (CH, C2'-**minor**), 66.8 (CH₂, C1'-**minor**), 63.7 (CH₂, C1'-**198**), 32.70 (CH₂, C6-**198**), 32.68 (CH₂, C6-**minor**), 30.94 (CH₂, C7-**minor**), 30.8 (CH₂, C7-**198**), 26.9 (CH₃, *t*Bu-**minor**), 26.7 (CH₃, *t*Bu-**198**), 22.6 (CH₂, C8), 22.2 (CH₂, C3'), 19.4 (C, *t*Bu-**minor**), 19.3 (C, *t*Bu-**198**), 13.9 (CH₃, C9), -0.02 (CH₃, TMS-**minor**), -0.03 (CH₃, TMS-**198**).

IR (neat) cm^{-1} : 2957 (m, C–H), 2928 (s, C–H), 2857 (m, C–H), 2179 (w, $\text{C}\equiv\text{C}$), 1717 (s, C=O), 1643 (m, C=C), 1249 (s, Si–C), 1137 (s, C–O), 999 (s, C–H), 842 (s, Si–C), 702 (s, Si–C), 506 (s, Si–C).

HRMS (ESI) m/z : found 547.3033, calcd for $\text{C}_{33}\text{H}_{47}\text{O}_3\text{Si}_2$ $[\text{M}+\text{H}]^+$ 547.3058 ($\Delta = 4.6$ ppm).

Mixture of (2*E*,4*Z*)-1'-(*tert*-butyldiphenylsilyloxy)-5'-(trimethylsilyl)pent-4'-yn-2'-yl 7-(*tert*-butyldimethylsilyloxy)-5-methylnona-2,4,8-trienoate (204**) and the silyl migrated product, (2*E*,4*Z*)-2'-(*tert*-butyldiphenylsilyloxy)-5'-(trimethylsilyl)pent-4'-yn-1'-yl 7-(*tert*-butyldimethylsilyloxy)-5-methylnona-2,4,8-trienoate (**205**) (2:1)**

The isomers were formed in a combined 69% yield.



TLC: $R_f = 0.21$ (40:1 Pet. ether: Et_2O).

^1H NMR (500 MHz, CDCl_3): δ 7.75–7.64 (complex m, 4H, CH, Ph), 7.57 (partially obs. ddd, $J = 15.3, 11.6, 3.9$ Hz, 0.67H, 3-CH-**204**), 7.51 (partially obs. ddd, $J = 15.4, 11.7, 3.9$ Hz, 0.33H, 3-CH-**205**), 7.46–7.34 (complex m, 6H, CH, Ph), 6.09 (d, $J = 11.7$ Hz, 0.67H, 4-CH-**204**), 6.04 (d, $J = 11.7$ Hz, 0.33H, 4-CH-**205**), 5.85–5.74 (complex m, 1.67H, 8-CH & 2-CH-**204**), 5.64 (d, $J = 15.1$ Hz, 0.33H, 2-CH-**205**), 5.22–5.10 (complex m, 1.67H, 2'-CH-**204** & one of 9- CH_2), 5.07–5.00 (complex m, 1H, one of 9- CH_2), 4.25 (dt, $J = 6.6, 5.9$ Hz, 1H, 7-CH), 4.18 (dd, $J = 5.1, 1.5$ Hz, 0.66H, 1'- CH_2 -**205**), 4.09–4.04 (complex m, 0.33H, 2'-CH), 3.89 (ddd, $J = 11.0, 4.4, 1.7$ Hz, 0.67H, one of 1'- CH_2 -**204**), 3.84 (ddd, $J = 11.0, 4.4, 1.7$ Hz, 0.67H, one of 1'- CH_2 -**204**), 2.75 (ddd, $J = 16.9, 7.1, 1.5$ Hz, 0.67H, one of 3'- CH_2 -**204**), 2.64 (obs. ddd, $J = 16.9, 5.9, 4.2$ Hz, 0.67H, one of 3'- CH_2 -**204**), 2.60–2.52 (complex m, 1H, one of 6- CH_2), 2.44–2.39 (complex m, 0.66H, 3'- CH_2 -**205**), 2.36 (dd, $J = 13.4, 5.4$ Hz, 1H, one of 6- CH_2), 1.93 (s, 2.0H,

10-CH₃-**204**), 1.92 (s, 1.0H, 10-CH₃-**205**), 1.07 (s, 3.0H, CH₃, *t*Bu, TBDPS-**205**), 1.05 (s, 6.0H, CH₃, *t*Bu, TBDPS-**204**), 0.86 (s, 3.0H, CH₃, *t*Bu, TBS-**205**), 0.86 (s, 6.0H, CH₃, *t*Bu, TBS-**204**), 0.13 (s, 3.0H, CH₃, TMS-**205**), 0.12 (s, 6.0H, CH₃, TMS-**204**), 0.01 (s, 6H, CH₃, Me).

¹³C NMR (125 MHz, CDCl₃): δ 167.15 and 167.14 (C, C1-**205**), 166.68 and 166.65 (C, C1-**204**), 146.54 and 146.51 and 146.46 (C, C5), 141.50 and 141.48 (CH, C3-**204**), 141.30 and 141.29 (CH, C3-**205**), 140.90 and 140.88 and 140.84 (CH, C8), 135.9 (CH, Ph), 135.82 (CH, Ph), 135.81 (CH, Ph), 135.61 (CH, Ph), 135.58 (CH, Ph), 135.54 (CH, Ph), 135.52 (CH, Ph), 135.51 (CH, Ph), 135.50 (CH, Ph), 133.62 (C, Ph), 133.57 (C, Ph), 133.4 (C, Ph), 133.3 (C, Ph), 129.8 (CH, Ph), 129.68 (CH, Ph), 129.66 (CH, Ph), 129.65 (CH, Ph), 129.59 (CH, Ph), 129.32 (CH, Ph), 127.69 (CH, Ph), 127.67 (CH, Ph), 127.64 (CH, Ph), 127.62 (CH, Ph), 127.58 (CH, Ph), 126.11 and 126.06 and 126.04 (CH, C4), 119.02 and 118.96 (CH, C2-**204**), 118.76 and 118.75 (CH, C2-**205**), 114.2 (CH₂, C9), 102.74 and 102.72 (C, C4'-**205**), 102.23 and 102.21 (C, C4'-**204**), 87.01 (C, C5'-**205**), 86.77 and 86.76 (C, C5'-**204**), 72.86 (CH, C7-**205**), 72.84 (CH, C7-**204**), 71.87 and 71.83 (CH, C2'-**204**), 69.53 (CH, C2'-**205**), 66.58 and 66.54 (CH₂, C1'-**205**), 63.72 and 63.69 (CH₂, C1'-**204**), 41.7 (CH₂, C6), 26.9 (CH₃, *t*Bu), 26.74 (CH₃, *t*Bu), 26.72 (CH₃, *t*Bu), 25.82 (CH₃, C10-**204**), 25.68 (CH₃, C10-**205**), 25.66 and 25.65 (CH₂, C3'-**205**), 21.9 (CH₂, C3'-**204**), 19.4 (C, *t*Bu), 19.3 (C, *t*Bu), 18.1 (C, *t*Bu), 1.02 (CH₃, Me), 0.01 (CH₃, Me), 0.00 (CH₃, Me), -0.03 (CH₃, Me).

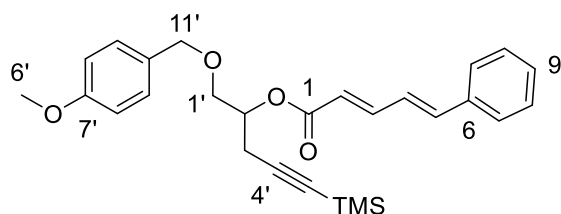
IR (Et₂O film) cm⁻¹: 3072 (w, C-H), 2959 (s, C-H), 2858 (s, C-H), 2179 (m, C≡C), 1716 (m, C=O), 1637 (m, C=C), 1251 (m, C-Si), 1114 (s, Si-O), 776 (m, Si-Me), 702 (s, Si-C).

HRMS (ESI) *m/z*: found 689.3838, calcd for C₄₀H₆₂O₄Si₃ [M+H]⁺ 689.3872 (Δ = 4.8 ppm).

The three-bond C-H correlations across the esters in both compounds were confirmed by CIGAR-HMBC NMR.

(2*E*,4*E*)-[1'-(*para*-Methoxybenzyloxy)-5'-trimethylsilyl]pent-4'-yn-2'-yl 5-phenylpenta-2,4-dienoate (206**)**

Formed in 42% yield in THF or 70% in toluene.



TLC: R_f = 0.28 (80% CH_2Cl_2 in n -hexane).

^1H NMR (500 MHz, CDCl_3): δ 7.51–7.44 (complex m, 3H, 3-CH & 8-CH), 7.37 (app. t, J = 7.1 Hz, 2H, 7-CH), 7.33 (m, 1H, 9-CH), 7.28 (br d, J = 8.8 Hz, 2H, 9'-CH), 6.95–6.84 (complex m, 4H, 8'-CH & 4-CH & 5-CH), 6.02 (d, J = 15.4 Hz, 1H, 2-CH), 5.20 (app. dt, J = 10.5, 5.7 Hz, 1H, 2'-CH), 4.55 (d, J = 11.5 Hz, 1H, one of 11'- CH_2), 4.50 (d, J = 11.7 Hz, 1H, one of 11'- CH_2), 3.80 (s, 3H, 6'- CH_3), 3.72–3.67 (m, 2H, 1'- CH_2), 2.68 (dd, J = 17.1, 7.1 Hz, 1H, one of 3'- CH_2), 2.63 (dd, J = 16.9, 5.9 Hz, 1H, one of 3'- CH_2), 0.14 (s, 9H, CH_3 , TMS).

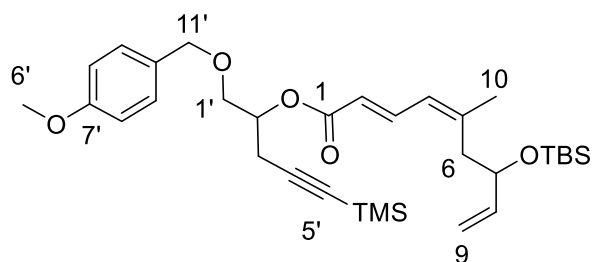
^{13}C NMR (125 MHz, CDCl_3): δ 166.2 (C, C1), 159.2 (C, C7'), 145.2 (CH, C3), 140.7 (CH, C5), 136.0 (C, C6), 130.1 (C, C10'), 129.3 (CH, C9'), 129.1 (CH, C7), 128.8 (CH, C9), 127.2 (CH, C8), 126.2 (CH, C4), 121.0 (CH, C2), 113.8 (CH, C8'), 101.9 (C, C4'), 87.1 (C, C5'), 73.0 (CH_2 , C11'), 70.7 (CH, C2'), 69.4 (CH_2 , C1'), 55.2 (CH_3 , C6'), 22.3 (CH_2 , C3'), 0.00 (CH_3 , TMS).

IR (neat) cm^{-1} : 3028 (w, C–H), 2957 (m, C–H), 2901 (m, C–H), 2178 (m, $\text{C}\equiv\text{C}$), 1709 (s, C=O), 1625 (s, C=C), 1512 (m, C–O), 1245 (s, C–O), 1128 (s, C–O), 840 (s, C–Si), 757 (s, C–Si).

HRMS (ESI) m/z : found 449.2146, calcd for $\text{C}_{27}\text{H}_{33}\text{O}_4\text{Si}$ $[\text{M}+\text{H}]^+$ 449.2143 (Δ = 0.67 ppm).

(2*E*,4*Z*)-1'-(*para*-Methoxybenzyloxy)-5'-(trimethylsilyloxy)pent-4'-yn-2'-yl 7-(*tert*-butyldimethylsilyloxy)-5-methylnona-2,4,8-trienoate (207)

Formed in 68% yield as a single regioisomer, and with 1:1 d.r. based on composition of racemic starting materials.



TLC: R_f = 0.30 (80% CH_2Cl_2 in n -hexane).

^1H NMR (500 MHz, CDCl_3): δ 7.57 (dd, J = 14.9, 11.8 Hz, 1H, 3-CH), 7.26 (d, J = 8.3 Hz, 2H, 9'-CH), 6.87 (d, J = 8.3 Hz, 2H, 8'-CH), 6.07 (d, J = 11.5 Hz, 1H, 4-CH), 5.80 (obs. ddd, J = 16.8, 10.6, 5.7 Hz, 1H, 8-CH), 5.80 (obs. d, J = 15.2 Hz, 1H, 2-CH), 5.23–5.11 (obs. m, 1H, 2'-CH), 5.18 (obs. d, J = 17.2 Hz, 1H, one of 9-CH₂), 5.05 (d, J = 10.3 Hz, 1H, one of 9-CH₂), 4.53 (d, J = 11.5 Hz, 1H, one of 11'-CH₂), 4.48 (d, J = 11.5 Hz, 1H, one of 11'-CH₂), 4.25 (app. q, J = 6.2 Hz, 1H, 7-CH), 3.80 (s, 3H, 6'-CH₃), 3.67 (app. d, J = 4.9 Hz, 2H, 1'-CH₂), 2.69–2.54 (complex m, 3H, 3'-CH₂ & one of 6-CH₂), 2.36 (ddd, J = 13.0, 6.5, 5.5 Hz, 1H, one of 6-CH₂), 1.92 (s, 3H, 10-CH₃), 0.87 (s, 9H, CH₃, *t*Bu), 0.13 (s, 9H, CH₃, TMS), 0.01 (s, 6H, CH₃, Me).

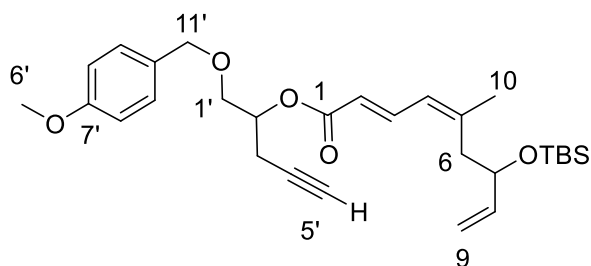
^{13}C NMR (125 MHz, CDCl_3): δ 166.71 and 166.69 (C, C1), 159.2 (C, C7'), 146.58 and 146.56 (C, C5), 141.70 and 141.67 (CH, C3), 140.9 (CH, C8), 130.1 (C, C10'), 129.3 (CH, C9'), 126.09 and 129.07 (CH, C4), 118.89 and 118.87 (CH, C2), 114.2 (CH₂, C9), 113.8 (CH, C8'), 102.0 (C, C4'), 86.92 and 86.90 (C, C5'), 73.00 and 72.99 (CH₂, C11'), 72.86 and 72.82 (CH, C7), 70.48 and 70.47 (CH, C2'), 69.45 and 69.41 (CH₂, C1'), 55.2 (CH₃, C6'), 41.7 (CH₂, C6), 25.83 and 25.82 (CH₃, *t*Bu), 25.64 and 25.62 (CH₃, C10), 22.32 and 22.29 (CH₂, C3'), 18.1 (C, *t*Bu), 0.00 and -0.01 (CH₃, TMS), -4.54 and -4.88 (CH₃, TBS).

IR (neat) cm^{-1} : 2956 (s, C–H), 2857 (m, C–H), 2180 (w, $\text{C}\equiv\text{C}$), 1714 (s, C=O), 1636 (m, C=C), 1513 (m, C=C), 1249 (s, C–O), 1033 (m, C–H), 837 (s, C–Si), 775 (m, C–Si), 760 (m, C–Si).

HRMS (ESI) m/z : found 571.3276, calcd for $\text{C}_{32}\text{H}_{51}\text{O}_5\text{Si}_2$ $[\text{M}+\text{H}]^+$ 571.3270 (Δ = 1.1 ppm).

(2E,4Z)-1'-(*para*-Methoxybenzyloxy)pent-4'-yn-2'-yl 7-(*tert*-butyldimethylsilyloxy)-5-methylnona-2,4,8-trienoate (208)

Formed in 66% yield as a single regioisomer, and with 1:1 d.r. based on composition of racemic starting materials.



TLC: R_f = 0.32 (80% CH_2Cl_2 in n -hexane).

^1H NMR (500 MHz, CDCl_3): δ 7.58 (dd, J = 14.9, 11.7 Hz, 1H, 3-CH), 7.26 (d, J = 8.6 Hz, 2H, 9'-CH), 6.87 (d, J = 8.6 Hz, 2H, 8'-CH), 6.07 (d, J = 11.5 Hz, 1H, 4-CH), 5.80 (obs. ddd, J = 17.1, 10.5, 5.9 Hz, 1H, 8-CH), 5.80 (obs. d, J = 14.9 Hz, 1H, 2-CH), 5.23–5.14 (obs. m, 1H, 2'-CH), 5.18 (obs. d, J = 16.9 Hz, 1H, one of 9-CH₂), 5.05 (d, J = 10.3 Hz, 1H, one of 9-CH₂), 4.53 (d, J = 11.5 Hz, 1H, one of 11'-CH₂), 4.48 (d, J = 11.5 Hz, 1H, one of 11'-CH₂), 4.25 (app. q, J = 5.6 Hz, 1H, 7-CH), 3.80 (s, 3H, 6'-CH₃), 3.71–3.62 (m, 2H, 1'-CH₂), 2.65 (ddd, J = 16.9, 6.6, 2.7 Hz, 1H, one of 3'-CH₂), 2.58 (ddd, J = 16.9, 5.4, 2.5 Hz, 1H, one of 3'-CH₂), 2.61–2.54 (obs. m, 1H, one of 6-CH₂), 2.36 (app. dt, J = 13.1, 4.9 Hz, 1H, one of 6-CH₂), 1.97 (m, 1H, 5'-CH), 1.92 (s, 3H, 10-CH₃), 0.86 (s, 9H, CH₃, *t*Bu), 0.01 (s, 3H, CH₃, Me), 0.00 (s, 3H, CH₃, Me).

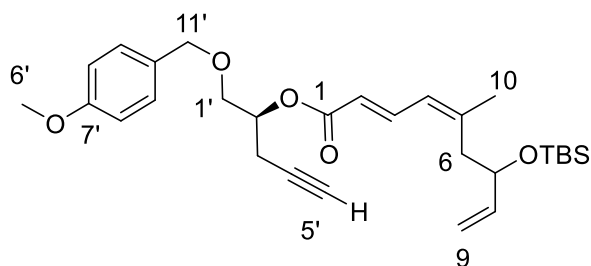
^{13}C NMR (125 MHz, CDCl_3): δ 166.7 (C, C1), 159.2 (C, C7'), 146.81 and 146.78 (C, C5), 141.92 and 141.89 (CH, C3), 140.95 and 140.93 (CH, C8), 130.1 (C, C10'), 129.31 and 129.30 (CH, C9'), 126.07 and 126.05 (CH, C4), 118.71 and 118.68 (CH, C2), 114.2 (CH₂, C9), 113.8 (CH, C8'), 79.6 (C, C4'), 73.0 (CH₂, C11'), 72.81 and 72.77 (CH, C7), 70.33 and 70.30 (CH, C5'), 70.18 and 70.13 (CH, C2'), 69.3 (CH₂, C1'), 55.2 (CH₃, C6'), 41.8 (CH₂, C6), 25.8 (CH₃, *t*Bu), 25.66 and 25.65 (CH₃, C10), 20.97 and 20.95 (CH₂, C3'), 18.1 (C, *t*Bu), -4.54 and -4.88 (CH₃, TBS).

IR (neat) cm^{-1} : 3308 (w, C–H), 2930 (m, C–H), 2857 (s, C–H), 2214 (w, $\text{C}\equiv\text{C}$), 1712 (s, C=O), 1635 (m, C=C), 1612 (m, C=C), 1514 (s, C–H), 1248 (s, C–O), 1033 (m, C–O), 836 (s, C–Si), 776 (s, C–Si).

HRMS (ESI) m/z : found 499.2868, calcd for $\text{C}_{29}\text{H}_{43}\text{O}_5\text{Si}$ $[\text{M}+\text{H}]^+$ 499.2874 (Δ = 1.2 ppm).

(2*E*,4*Z*,2'*S*)-1'-(*para*-Methoxybenzyloxy)pent-4'-yn-2'-yl 7-(*tert*-butyldimethylsilyloxy)-5-methylnona-2,4,8-trienoate (2'*S*-208)

Formed in 26% yield as a single regioisomer, and with 1:1 d.r. based on composition of starting materials.



All spectroscopic data matched those of the racemate **208**.

Specific rotation: $[\alpha]_D^{21} = -2.11$ ($c = 0.18$, CH_2Cl_2).

4.6 References

- (1) Bartlett, M. *Synlett* **2013**, 24, 773.
- (2) Smith, A. B.; Safonov, I. G.; Corbett, R. M. *J. Am. Chem. Soc.* **2001**, 123, 12426.
- (3) Ding, F.; Jennings, M. P. *J. Org. Chem.* **2008**, 73, 5965.
- (4) Uenishi, J.; Iwamoto, T.; Tanaka, J. *Org. Lett.* **2009**, 11, 3262.
- (5) Ghosh, A. K.; Cheng, X. *Org. Lett.* **2011**, 13, 4108.
- (6) Zurwerra, D.; Glaus, F.; Betschart, L.; Schuster, J.; Gertsch, J.; Ganci, W.; Altmann, K. H. *Chem.-Eur. J.* **2012**, 18, 16868.
- (7) Daly, B. J. J.; Wheatley, P. J. *Inorg. Phys. Theor.* **1966**, 1703.
- (8) Matthews, C. N.; Birum, G. H. *Tetrahedron Lett.* **1966**, 7, 5707.
- (9) Bestmann, H. J.; Sandmeier, D. *Chem. Ber.-Recl.* **1980**, 113, 274.
- (10) Bestmann, H. J.; Schobert, R. *Synthesis* **1989**, 419.
- (11) Bestmann, H. J.; Kellermann, W. *Synthesis* **1994**, 1257.
- (12) Bestmann, H. J. *Angew. Chem. Int. Ed.* **1977**, 16, 349.
- (13) Schobert, R. *Org. Synth.* **2005**, 82, 140.

- (14) Schlenk, A.; Diestel, R.; Sasse, F.; Schobert, R. *Chem.-Eur. J.* **2010**, *16*, 2599.
- (15) Jung, M. E.; Yoo, D. *Org. Lett.* **2011**, *13*, 3766.
- (16) Westman, J.; Orrling, K. *Comb. Chem. High T. Scr.* **2002**, *5*, 571.
- (17) Fedoseyenko, D.; Raghuraman, A.; Ko, E.; Burgess, K. *Org. Biomol. Chem.* **2012**, *10*, 921.
- (18) Raghuraman, A.; Ko, E.; Perez, L. M.; Ioerger, T. R.; Burgess, K. *J. Am. Chem. Soc.* **2011**, *133*, 12350.
- (19) Schobert, R.; Siegfried, S.; Gordon, G. J. *J. Chem. Soc. Perk. T. 1* **2001**, 2393.
- (20) Risi, R. M.; Burke, S. D. *Org. Lett.* **2012**, *14*, 1180.
- (21) Bestmann, H. J.; Kellermann, W.; Pecher, B. *Synthesis* **1993**, 149.
- (22) Jung, M. E.; Yoo, D. *Org. Lett.* **2011**, *13*, 2698.
- (23) Kitson, R. R. A.; Taylor, R. J. K.; Wood, J. L. *Org. Lett.* **2009**, *11*, 5338.
- (24) Kitson, R. R. A.; McAllister, G. D.; Taylor, R. J. K. *Tetrahedron Lett.* **2011**, *52*, 561.
- (25) Pachali, S.; Hofmann, C.; Rapp, G.; Schobert, R.; Baro, A.; Frey, W.; Laschat, S. *Eur. J. Org. Chem.* **2009**, 2828.
- (26) Werkhoven, T. M.; van Nispen, R.; Lugtenburg, J. *Eur. J. Org. Chem.* **1999**, 2909.
- (27) Bernstein, H. J.; Pople, J. A.; Schneider, W. G. *Can. J. Chem.* **1957**, *35*, 67.
- (28) Trost, B. M.; Machacek, M. R.; Faulk, B. D. *J. Am. Chem. Soc.* **2006**, *128*, 6745.
- (29) Kuntiyong, P.; Lee, T. H.; Kranemann, C. L.; White, J. D. *Org. Biomol. Chem.* **2012**, *10*, 7884.
- (30) Furrer, J. *Concept. Magnetic Res. A* **2012**, *40A*, 101.
- (31) Furrer, J. *Concept. Magnetic Res. A* **2012**, *40A*, 146.
- (32) Wagner, R.; Berger, S. *Magn. Reson. Chem.* **1998**, *36*, S44.
- (33) Hadden, C. E.; Martin, G. E.; Krishnamurthy, V. V. *J. Magn. Reson.* **1999**, *140*, 274.
- (34) Hurd, R. E. *J. Magn. Reson.* **1990**, *87*, 422.
- (35) Ruizcabello, J.; Vuister, G. W.; Moonen, C. T. W.; Vangelder, P.; Cohen, J. S.; Van Zijl, P. C. M. *J. Magn. Reson.* **1992**, *100*, 282.
- (36) Hadden, C. E.; Martin, G. E.; Krishnamurthy, V. V. *Magn. Reson. Chem.* **2000**, *38*, 143.
- (37) Matveeva, E. D.; Podrugina, T. A.; Grishin, Y. K.; Pavlova, A. S.; Zefirov, N. S. *Russ. J. Org. Chem.* **2007**, *43*, 201.
- (38) Larson, G. L.; Quiroz, F.; Suarez, J. *Synth. Commun.* **1983**, *13*, 833.

Chapter 5: Exploration of late-stage connections

5.1 Formation of *N*-acyl hemiaminal

As discussed in **section 1.4.3**, linear *N*-acyl hemiaminal structures are rare in natural product. Apart from zampanolide (**19**), natural products in the pederin family are often used to demonstrate the occurrence of the *N*-acyl hemiaminal functionality (examples shown in **Figure 5.1**). However, construction of the *N*-acyl hemiaminal in members of the pederin family has been achieved primarily by amide synthesis from carboxylic acids and amines.^{1,2} In the total syntheses of **19**, aza-aldol reactions have been more commonly used (see **section 1.4.3**). Since very few aza-aldol reactions conducted in this fashion were previously published,^{3,4,5} the total synthesis of **19** provided a good basis for exploration of the methodology to form *N*-acyl hemiaminal *via* aza-aldol reaction, especially in complex natural product synthesis.

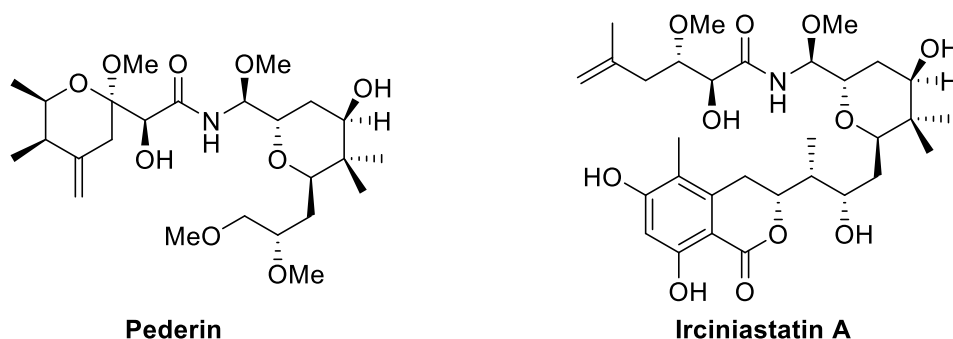
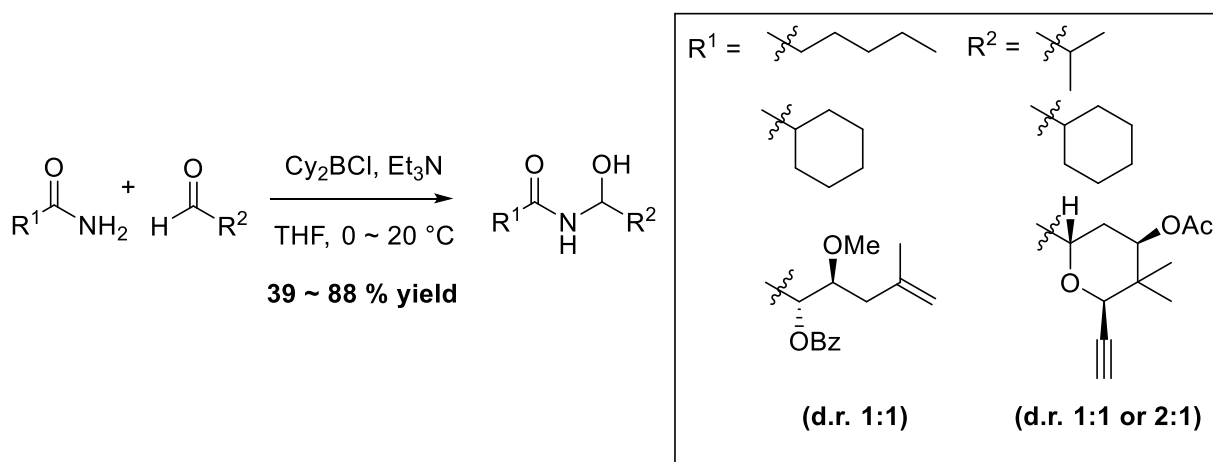


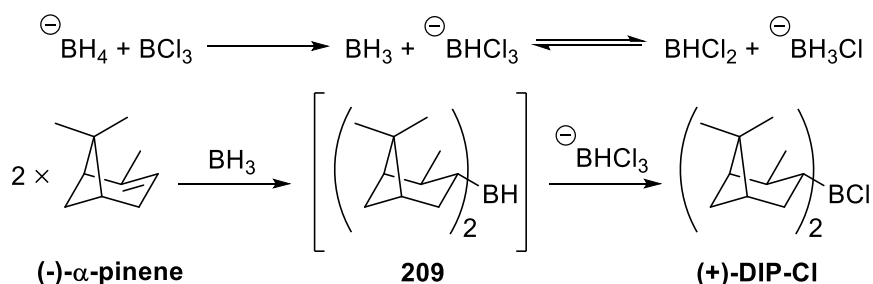
Figure 5.1: Examples of the pederin family.

In the present study, the attachment of the amides to the macrocyclic core was attempted by a boron-catalyzed aza-aldol reaction. A non-stereoselective boron-catalyzed aza-aldol reaction for *N*-acyl hemiaminal formation was reported by Kiren, Shangguan and William in 2007.⁶ In their experiments, a number of chlorodicyclohexylborane (Cy_2BCl)-mediated direct additions of amides to aldehydes were conducted, and moderate to good yields were obtained after a 30 min reaction followed by quenching with a mixture of MeOH, phosphate buffer (pH = 7.40) and H_2O_2 (**Scheme 5.1**).



Scheme 5.1: Kiren's aza-aldol reactions.⁶

Adaption of this type of reaction to use a chiral boron reagent to achieve stereoselectivity was investigated, in particular chlorodiisopinocampheylborane (DIP-chloride). Although DIP-chloride has never been used in aza-aldol reaction, it is well-established to mediate asymmetric aldol reaction.⁷ Both (+)-DIP-chloride and (-)-DIP-chloride were to be tested. (-)-DIP-chloride was purchased, but the high cost encouraged us to also explore the synthesis of DIP-chloride. DIP-chloride can be prepared from the readily available starting material α -pinene following a few well-precedented methods.⁸⁻¹⁰ Reider's convenient method was attempted first (**Scheme 5.2**). In this procedure, BHCl_3 and borane are proposed to form, generated from boron trichloride and excess borohydride *in situ*. The borane or a related entity then reacts with two equivalents of α -pinene to produce the intermediate **209**, which is chlorinated, probably by either BHCl_3 or BCl_3 , to produce DIP-chloride as a solution in 1,2-dimethoxyethane (DME).¹⁰

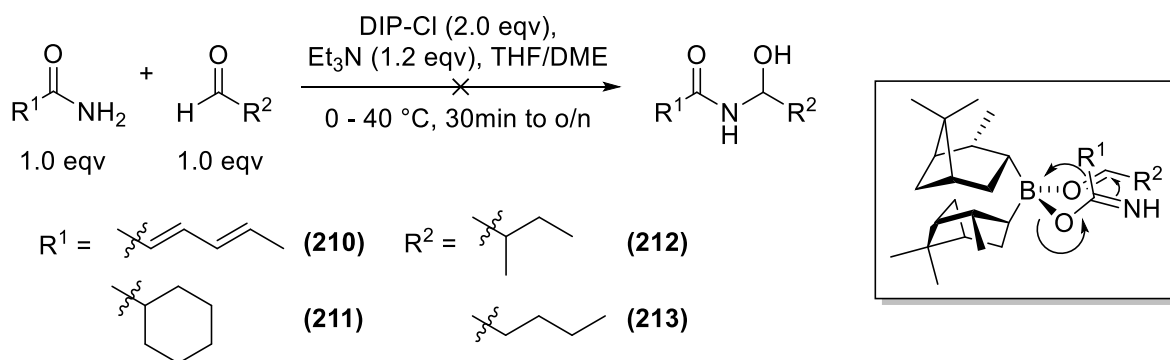


Scheme 5.2: Reider's preparation of (+)-DIP-Cl and proposed mechanism.

In this way, (+)-DIP-chloride was prepared from (-)- α -pinene. The activity of the home-made (+)-DIP-chloride was tested in the reduction of acetophenone, and full conversion was achieved after 5 hours at -23 °C followed by 1 hour at 0 °C. However, the enantioselectivity of the

reagent was not assessed at this time, and the presence of any remaining active borane species in the mixture could reduce the aldehyde starting material in the aza-adol reaction.

The planned DIP-chloride-promoted aza-aldol reaction was first tested in model studies involving simple aldehydes (**Scheme 5.3**), where DIP-chloride, amide and Et₃N were pre-mixed prior to the addition of the aldehyde. With the amine models sorbamide (**210**) and cyclohexylamide (**211**) and aldehyde models 2-methylbutyraldehyde (**212**) and *n*-pentanal (**213**), various reaction conditions were modified, including temperature (0 to 40 °C), time (30 min to overnight) and solvent (THF or DME).



Scheme 5.3: Aza-aldol reaction with DIP-Cl to *N*-acyl hemiaminal.

Model reactions with sorbamide (**210**) and *n*-pentanal (**213**) were carried out in THF, but starting material remained after reacting for up to 60 h at room temperature (**Scheme 5.3**). It was noted that sorbamide (**210**) has very low solubility in THF. Sonication, heating and changing the solvent to DME all failed to produce the required *N*-acyl hemiaminal. Attention was then turned to models similar to Kiren's, cyclohexanecarboxamide (**211**) and 2-methylbutyraldehyde (**212**). In Kiren's procedure, a 30 min reaction at 0 °C was sufficient to carry most of the reactions to completion.⁶ However, in this study, TLC analysis at 30 min showed the presence of both starting materials, and in the ¹H NMR spectrum of the aliquot removed and quenched after 30 min, the signature hemiaminal signal (doublet of doublets at around 5.0 ppm) was not observed. Furthermore, aliquots removed at 15 min intervals during the first hour and then hourly for 3 hours displayed no observable change from the reaction mixture at *t* = 0 min. With commercial (-)-DIP-Cl and an overnight reaction time, aldehyde signal nearly all disappeared and two interesting doublets at around 5.0 ppm with coupling

constants 4.2 and 5.1 Hz were observed (**Figure 5.2**). Unfortunately, this material was lost during column chromatography, and the eluent after flushing the column with ethyl acetate contains mostly isopinocampheol.

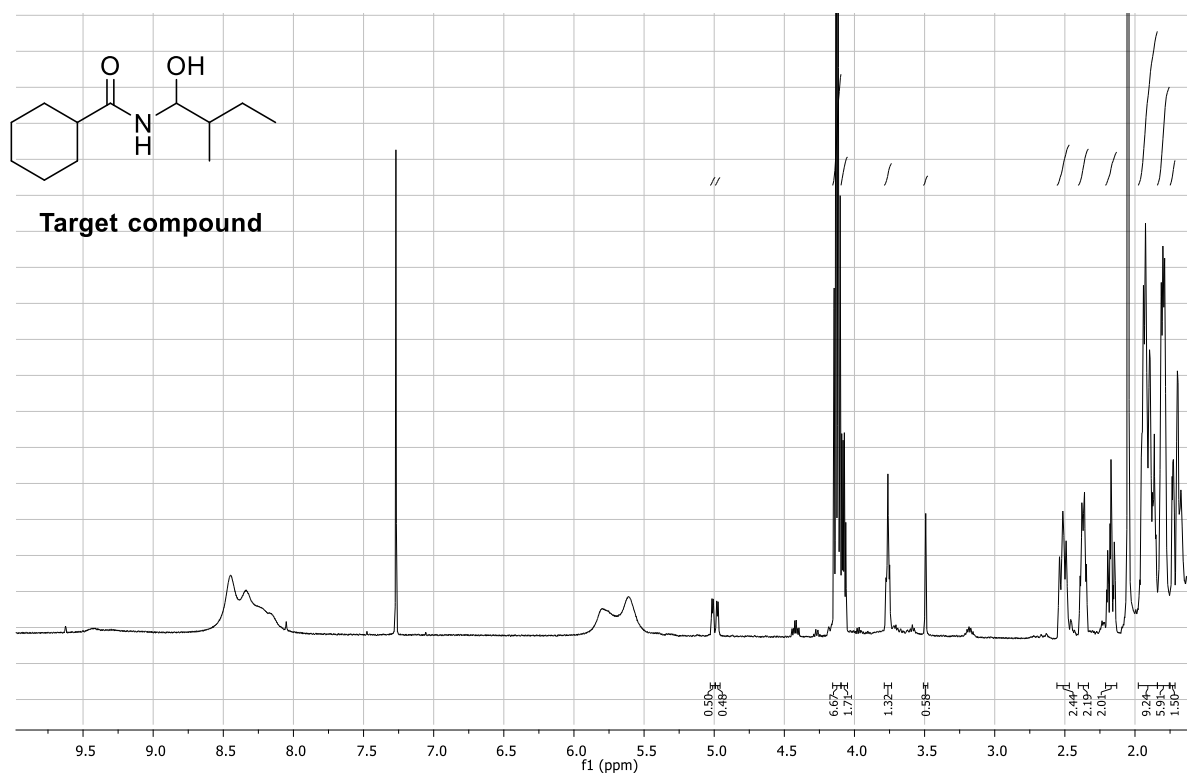


Figure 5.2: ^1H NMR spectrum (500 MHz) of the crude mixture from a model aza-aldol reaction of **211** with **212**.

Although the compound with interesting-looking ^1H NMR signals was lost during column chromatography, further exploration of this reaction was undertaken on substrates **211** and **212**. Interestingly, conducting the work-up with distilled water produced a different result to that obtained with hydrogen peroxide and pH7 buffer. Theoretically, the purpose of hydrogen peroxide is only to facilitate the purification by oxidatively hydrolyzing the boronate ester intermediate to produce boric acid and isopinocampheol. While the result of the hydrogen peroxide work-up was not encouraging, with the water-only work-up, a dd at 5.18 ppm in the ^1H NMR spectrum of the crude mixture with coupling constants of 6.2 and 6.8 Hz was observed. This signal is comparable with the oxymethine signal reported for 1-hydroxyl-1-cyclohexylmethyl hexamide (dd at 5.06 ppm, $J = 7.8, 7.5$ Hz).⁶ After column chromatography, a small amount of a promising-looking product was obtained in impure form (<5~9% yield). The signal at 5.18 ppm appeared as a triplet with J value of 6.1 Hz, and correlated to the signals

at 6.01 and 3.56 ppm, which could be the amide proton and the hydrogen bonded alcohol, respectively (**Figure 5.3**). An aldehyde signal with identical chemical shift (9.74 ppm) to that of aldehyde **212** was observed, which was not present in the ^1H NMR spectrum of the crude reaction mixture before purification. This suggests decomposition of the product on silica, which contradicts Kiren's results. The minor signals near the multiplet at 3.56 ppm could be resulted from other stereoisomers in the mixture. However, full characterization was never achieved, due to decomposition and the low quantity of material hampering efforts to purify it.

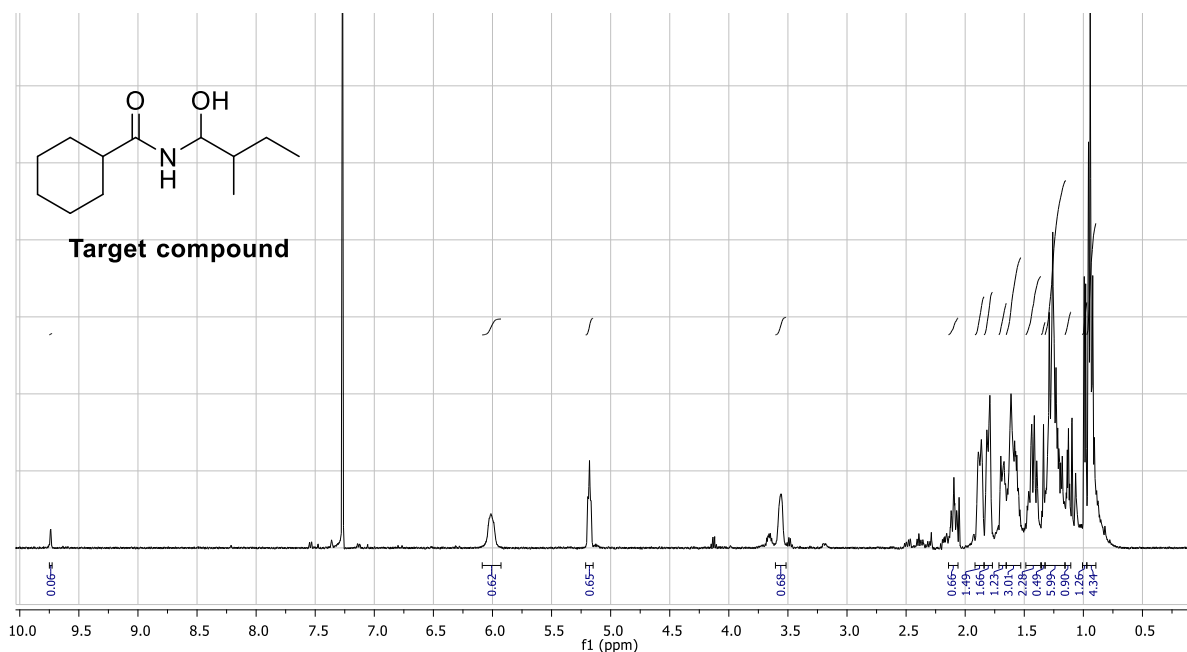


Figure 5.3: ^1H NMR spectrum (500 MHz) of the promising product from model *N*-aldol reaction of **211** with **212**.

A proposal of a hydrogen bonding network in oxygenated *N*-acyl hemiaminals, including zampanolide (**19**) was reported by Porco and Troast (**Figure 5.4**).¹¹ Based on their calculation, this system could contribute to the stability of zampanolide (**19**).¹¹ Porco and Troast also reported that simple *N*-acyl hemiaminals decomposed on the acidic silica gel, and suggested using neutral aluminum oxide for chromatography as a substitute purification method.¹¹

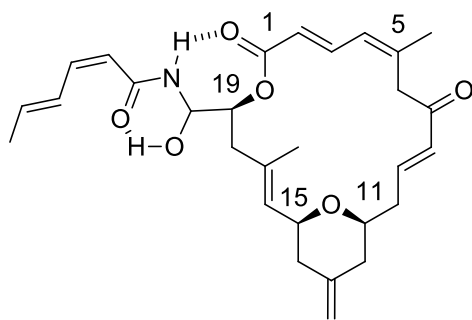
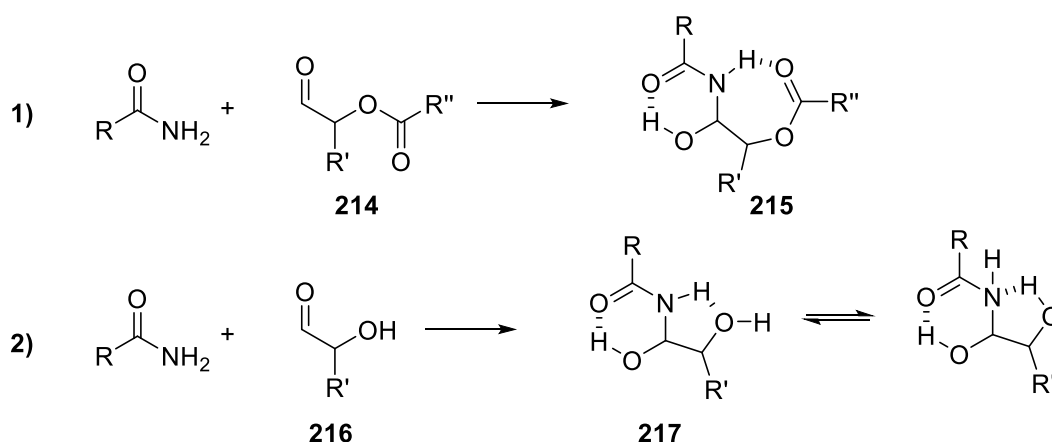


Figure 5.4: Porco's proposed hydrogen bonding network.

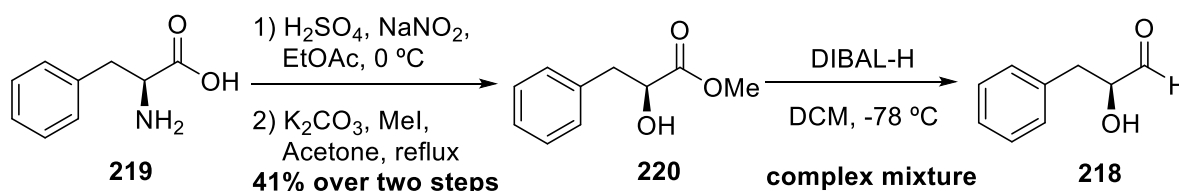
New model substrates were planned to better mimic the structure in (-)-zampanolide (**19**). A couple of aldehyde substrates were proposed that would enable the hydrogen bonding network in product. One is the α -acetoxy aldehyde (**214**), which would lead to a similar *O*-acetylated α -hydroxy-*N*-acyl hemiaminal (**215**) system to that in zampanolide (**19**) (**Scheme 5.4**, eq. 1). However, aldehydes are often accessed by reduction of esters or oxidation of alcohols, so the



Scheme 5.4: Model aldehydes **214** and **216** that enable double hydrogen bonding.

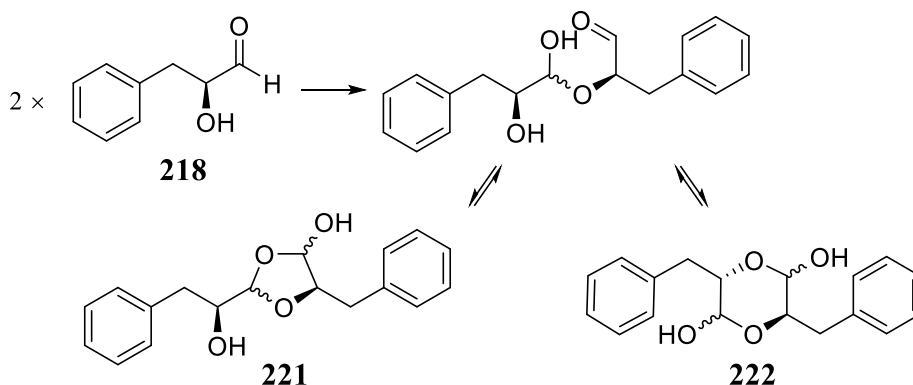
presence of the acetate group would require selective reduction, selective acetylation or other convoluted approaches. Another model is the α -hydroxy aldehyde (**216**), which would produce α -hydroxy-*N*-acyl hemiaminal **217** upon aza-aldol reaction (eq. 2). The α -hydroxy aldehyde model **216** is easier to synthesize, and the product is also capable of forming a hydrogen bonding network, but it would produce a five-membered ring instead of the seven membered ring in the zampanolide system. Both the secondary amide NH and hydroxyl OH in **217** consist of hydrogen bonding donor and acceptor, so an equilibrium was expected, which could improve the stability. Thus, α -hydroxy aldehyde **216** would be tested first.

A suitable aldehyde substrate would ideally meet the following criteria: convenient to prepare; stable and easy to handle; easy to be detected by TLC analysis. (*S*)-2-Hydroxy-3-phenylpropanal (**218**) was chosen for this purpose, which was expected to be stable, UV-active, and available through a three-step preparation from the cheap amino acid (*L*)-phenylalanine (**219**) (**Scheme 5.5**). The first two steps, hydroxylation and methylation proceeded smoothly with moderate yields. The Sandmeyer-type reaction used to convert the amine to an alcohol was related to that previously discussed during the synthesis of the C9-C15 natural fragment in chapter 3, although that was carried out in the presence of bromine at below -5 °C to achieve bromination. In this case, the increased temperature (0 °C) led to the production of the hydroxylated product **220**. The subsequent reduction of methyl ester **220** was incomplete and produced a mixture of inseparable compounds.



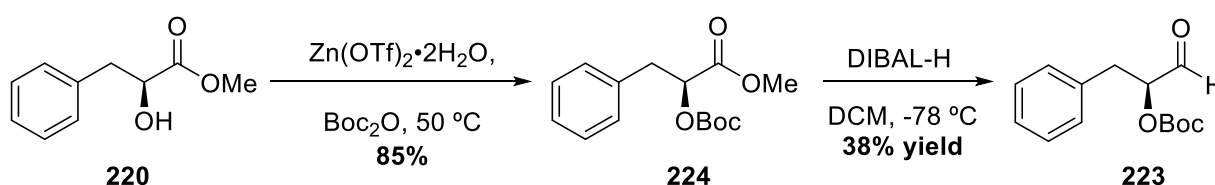
Scheme 5.5: Synthesis of the model aldehyde **218**.

The ^1H NMR spectrum of the inseparable mixture showed a very complicated oxygenated C–H region between 3.5 and 5.5 ppm, with abundant signals. The desired aldehyde signal was also observed, but far weaker than the combined signals in the oxygenated region. This problem was believed to be the result of dimerization of **218** to afford various hemiacetals, which can proceed through two different pathways, resulting in both five- and six-membered heterocycles, **221** and **222**, respectively (**Scheme 5.6**). The existence of multiple stereocenters in this mixture, together with different ring sizes, made the mixture impossible to purify and properly characterize, therefore another model substrate was explored.



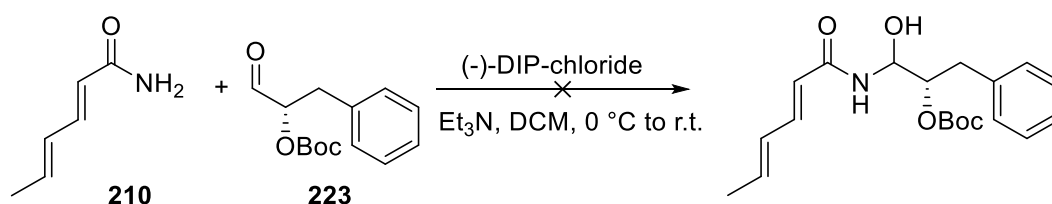
Scheme 5.6: Proposed dimerization of model aldehyde **218**.

Protection of the α -hydroxy group as either an ester or a carbonate was then proposed, as both could serve as a hydrogen bond acceptor in stabilisation of the *N*-acyl hemiaminal. Compared to acetyl protection, a carbonate would be more stable in the reduction of the substrate to afford the aldehyde, and can be easily accessed using the already synthesized intermediate **220**. Therefore, *tert*-butyl carbonate (Boc)-protection was attempted on **220**, and the corresponding aldehyde **223** was produced by DIBAL-H reduction of **224** (Scheme 5.7). The low yield (38%) of this reduction is a result of incomplete reduction, which indicated poor quality of DIBAL-H. Only ^1H NMR and HRMS data were collected to support the characterization of **223**.



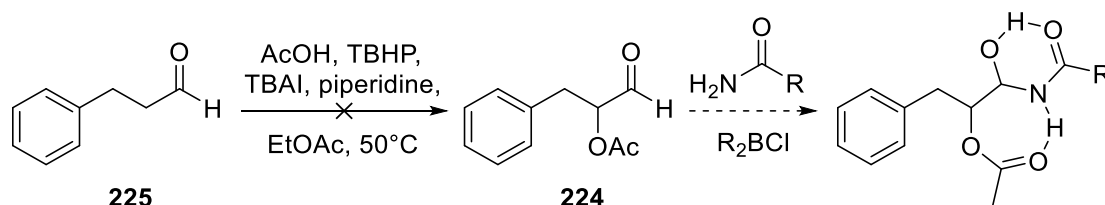
Scheme 5.7: Synthesis of model aldehyde **223**.

A boron reagent-promoted aza-aldol reaction was then tested with substrates **223** and sorbamide (**210**) using commercial (-)-DIP-chloride. Dichloromethane was used as the solvent to achieve good solubility of the aldehyde and amide (Scheme 5.8). Unfortunately, this reaction failed to proceed. After monitoring the reaction for 60 hours, TLC analysis still indicated the presence of the aldehyde, and the crude product mixture contained only the starting materials and pinene-like compounds. This failure might be caused by the bulkiness of the Boc group, which could sterically hinder the reaction.



Scheme 5.8: Aza-aldol reaction of aldehyde **223** and sorbamide (**210**).

The synthesis of the α -acetoxy aldehyde **224** was also investigated, as the relatively small size of the acetyl protecting group would hopefully not cause steric inhibition of the aza-aldol reaction. This acetylated substrate **224** cannot be synthesized *via* the same route as before, because of the difficulty in differentiating the acetoxy from the methyl ester to be reduced. An oxidative addition of acetic acid to 3-phenylpropanal (**225**) was reported to produce the desired α -acetoxy aldehyde **224** using tetrabutylammonium iodide (TBAI) and *tert*-butyl hydroperoxide (TBHP) (Scheme 5.9).¹² The combination of TBAI and TBHP has been found to be useful in a variety of bond forming reactions.¹³ The mechanism of the reaction is believed to go through a radical intermediate, promoted by the active species hypoiodite ($[\text{R}_4\text{N}]^+[\text{IO}]^-$) or iodite ($[\text{R}_4\text{N}]^+[\text{IO}_2]^-$) generated by oxidation of TBAI by TBHP.¹³ However, when this reaction was performed in this work, the product obtained was not the desired **224**.



Scheme 5.9: Proposed substrate **224** for model study of aza-aldol reaction.

The ¹H NMR spectrum of the purified product obtained from this attempted α -oxidation showed a 1:4:10 ratio between aldehyde, phenyl and benzylic signals, which suggested dimerization of starting material **225** (Figure 5.5). However, the signal at 3.59 ppm was thought to be too high field to be the oxymethine signal in the dimerization product **226** *via* an aldol reaction. In addition, the peak at 3.59 ppm correlated to a carbon signal at 34.4 ppm, and thus was not oxygenated. Due to time constraints, the assignment of the unknown by-product and the synthesis of model aldehyde **224** were not pursued further. However, further

investigation of the reaction could be attempted and, if unsuccessful, other procedures for oxidative α -acetoxylation of aldehydes are also available.^{14,15}

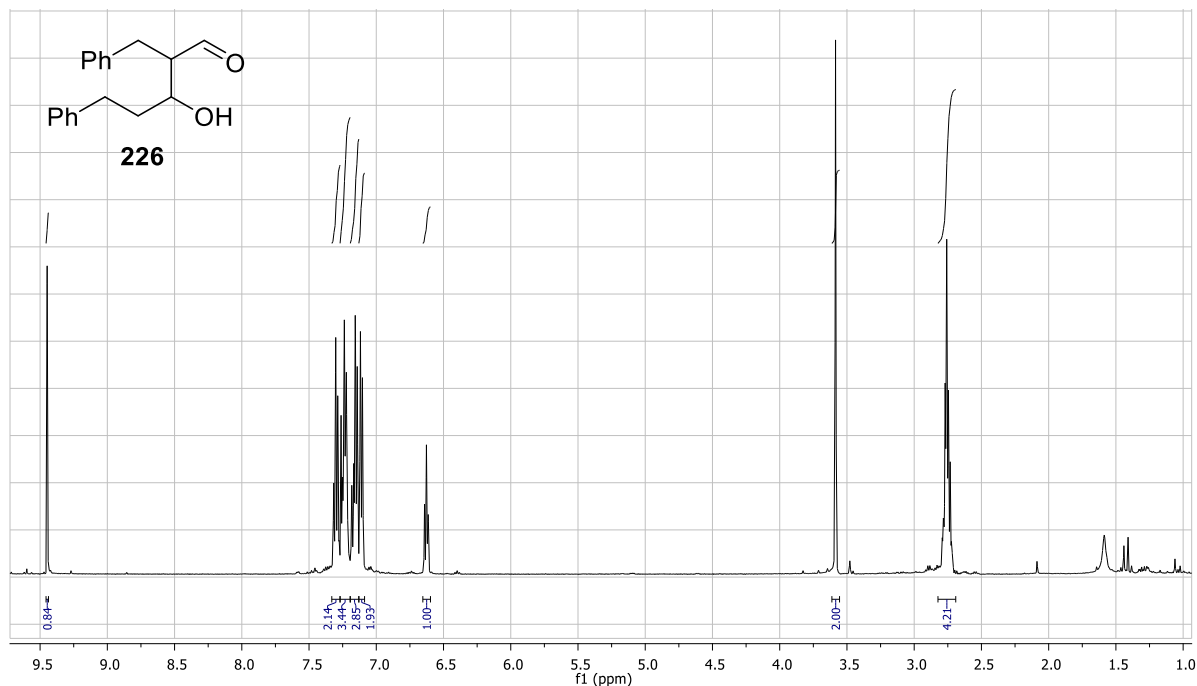
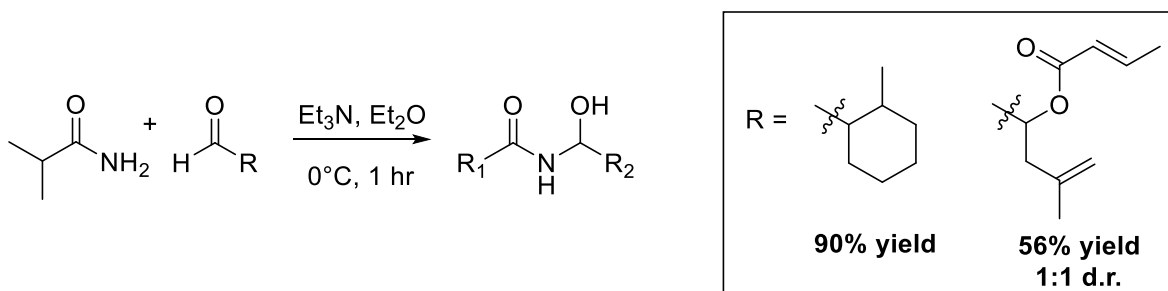


Figure 5.5: ^1H NMR spectrum of the product obtained from the attempted oxidative addition.

After the initial exploration, Ghosh's attempt to use boron reagent-promoted aza-aldol reaction in (-)-zampanolide (**19**) synthesis was published.¹⁶ In the reported work, achiral boron reagent, dicyclohexylboron chloride (Cy_2BCl) was used. A couple of Cy_2BCl -promoted model reactions were successfully carried out (**Scheme 5.10**), but when applying this method to the addition of (*Z,E*)-hex-2,4-dienamide (**45**) to (-)-dactylolide (**20**), decomposition was observed. Thus, the viability of using R_2BCl in the synthesis of the natural product and analogues is questionable.

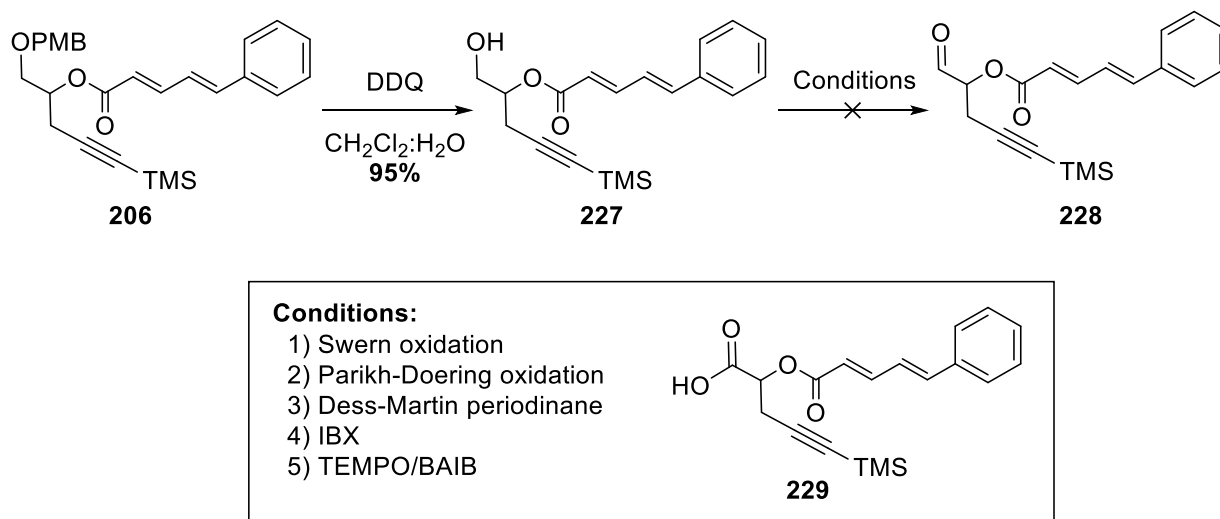


Scheme 5.10: Ghosh's Cy_2BCl -catalyzed aza-aldol model reactions.

5.2 Model study of C20 oxidation

The conversion of the C20-hydroxyl to an aldehyde (**228**) was done exclusively with Dess-Martin periodinane (DMP) in past dactylolide (**20**) and zampanolide (**19**) syntheses.¹⁷⁻²⁴ Product **206** from the model Bestmann ylide cascade was used to test this oxidation of alcohol at C20. The PMB group was deprotected selectively with the well-established oxidative deprotection method of DDQ and H₂O (Scheme 5.11).²⁵ The best yield of **227** (95%) was achieved when the reaction mixture was directly subjected to column chromatography without aqueous work-up. The oxidation of **227** did not go smoothly, so a number of oxidation methods were tested. The precedented DMP and the related oxidant IBX resulted in complicated mixtures, which showed multiple signals in the aldehyde region of the ¹H NMR spectrum, and potentially also contained starting material and structurally similar compounds. At least eight multiplets with various intensities were observed in the oxymethine region (4.8 to 5.4 ppm). Attempts to separate the major aldehyde product by column chromatography failed. Apart from the similar polarity amongst the products, some components also streaked on the TLC plate, typical of carboxylic acids, but DMP and IBX are not known for over-oxidation of alcohols. Swern and Parikh-Doering methods did not promote any oxidation and starting material was recovered. The last method attempted was TEMPO/BAIB oxidation, which is quite different from all the above methods. It proceeds *via* a catalytic cycle, whereby TEMPO goes through a redox sequence assisted by BAIB in order to oxidize the alcohols to aldehydes.²⁶ Unfortunately, TEMPO/BAIB oxidation produced the over-oxidized carboxylic acid **229** quantitatively. After column chromatography, significant line-broadening was observed by ¹H NMR spectroscopy of **229**, which may be a sign of decomposition. Therefore, some characterization data for acid **229** were obtained using the crude product prior to purification. The desired molecular ion [M-H]⁻ was found in large abundance using mass spectrometry, and the broad hydroxy stretch was observed by IR spectroscopy with the carboxylic acid C=O stretch at 1709 cm⁻¹ also evident. In the ¹H NMR spectrum, apart from the disappearance of the oxymethylene signal, very little change was evident in chemical shift and multiplicity. Aldehyde-like compounds were never observed, either by NMR spectroscopy or by TLC analysis during the reaction. The results of these oxidation methods are not very well understood. The hydroxyl group in our substrate **227** may be participating in hydrogen bonding with the ester carbonyl. This interaction may be disturbed in the precursor of dactylolide by the steric hindrance of the ring, but strong enough in the model substrate to interfere with the oxidative reagents. Although the oxidation results

are very discouraging, we are still confident of this late-stage oxidation in the real system, because of the abundant precedence in the literature.

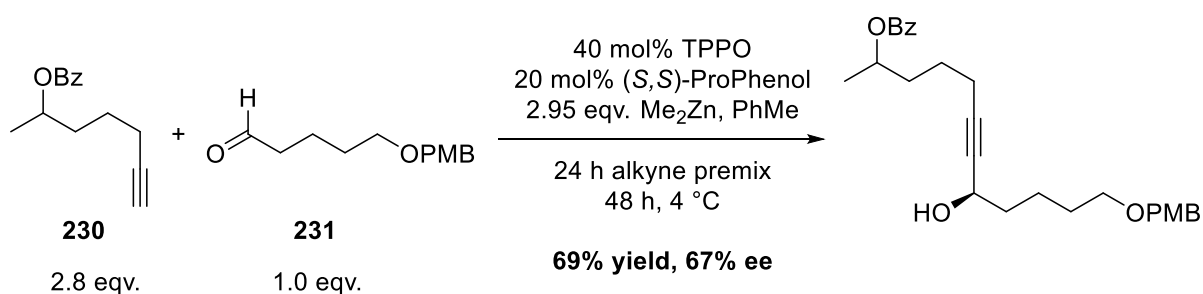


Scheme 5.11: Model oxidation of alcohol at C20.

5.3 Asymmetric alkynylation of aldehydes for C15-C16 connection

Alkynylation of carbonyls has often been used in total syntheses to construct the versatile propargylic alcohol motif, for which metalated alkynylides are commonly used as the nucleophiles. Lithium and magnesium alkynylides are readily formed by treating terminal alkynes with BuLi and alkyl Grignard reagents, respectively, but they are harsh nucleophilic bases and have high reactivity towards a large variety of functional groups, thus are unsuited for reaction with complicated substrates. The formation of zinc alkynides by treating terminal alkynes with Et₂Zn has been known since the mid-1960's,²⁷ and the use of zinc alkynides in the addition to carbonyls was subsequently explored in the past few decades. Although these reactions are slow, the mild reaction conditions and compatibility with a range of functional groups are favored in organic synthesis. With the assistant of chiral catalysts, asymmetric alkynylations can be achieved. A number of methods involving dialkylzinc were developed, including Trost's ProPhenol/Me₂Zn and the BINOL/Ti(IV)/Et₂Zn methods.²⁸

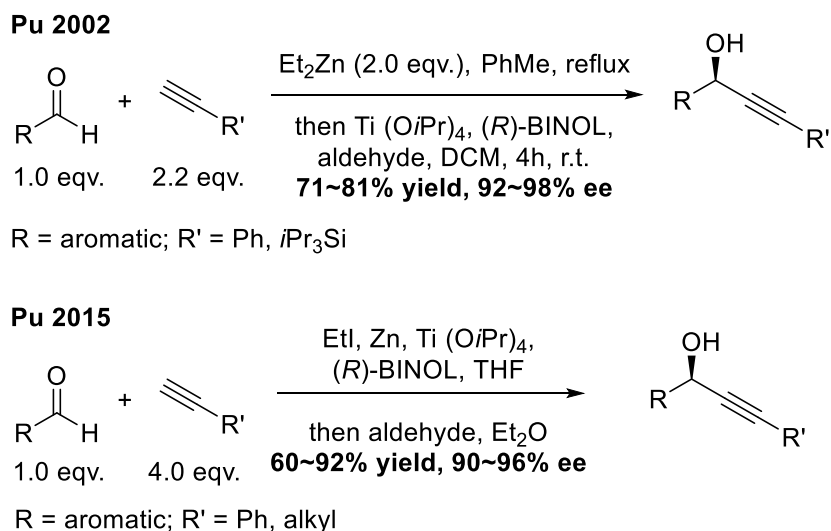
As discussed in **section 1.7**, Trost's ProPhenol-catalyzed alkynylation can achieve excellent yields and ee's between propiolate, aromatic and the sensitive α,β -unsaturated aldehydes (see **Scheme 1.22**).²⁹ The success with propiolate was attributed to the interaction of the Lewis basic carbonyl with ProPhenol-bound zinc. The addition of triphenylphosphine oxide (TPPO) was found to compensate for the absence of a Lewis basic moiety in the alkyne substrates, which further expand the scope to aliphatic alkynes. However, with aliphatic alkynes and enolizable aldehydes such as **230** and **231**, increased catalytic loading and prolonged pre-mixing before the addition of the aldehyde are required to achieve a moderate yield (69%) and enantioselectivity (67% ee) (**Scheme 5.12**).^{29,30}



Scheme 5.12: Prophenol-catalysed alkynylation of aliphatic alkyne **230** and aldehyde **231**.

In the $\text{Et}_2\text{Zn}/\text{Ti(IV)}/\text{BINOL}$ system published by Pu, the alkynylzinc was formed by heating alkyne and diethylzinc in toluene at reflux for 5 hours (**Scheme 5.13**).³¹ At the same time, a very similar procedure was published by Chan, whereby treating an alkyne with dimethylzinc at room temperature in THF for 18 hours afforded the alkynylzinc species.³² The Ti(IV)/BINOL-catalyzed alkyne addition to aldehydes achieved good yields and stereoselectivity in both cases. The reflux condition in Pu's method limits its compatibility with low boiling point and heat sensitive substrates, so Pu and You explored ways to carry out the alkynylzinc formation at room temperature while maintaining high stereoselectivity. Additives such as hexamethylphosphoramide, *N*-methylimidazole and dicyclohexylamine were found to be efficient, and the scope of this method was further extended to aliphatic alkynes and aldehydes at the same time.³³⁻³⁵ Although these above methods are efficient and enantioselective, the use of the highly pyrophoric dialkylzinc introduces environmental and safety hazards, and requires extravagant care to exclude any moisture. Therefore, the formation of Et_2Zn *in situ* was explored by Pu's group. It was found that with the assistance of Ti(OiPr)_4 and BINOL, the alkynylzinc complex can be formed from iodoethane, zinc powder and alkyne

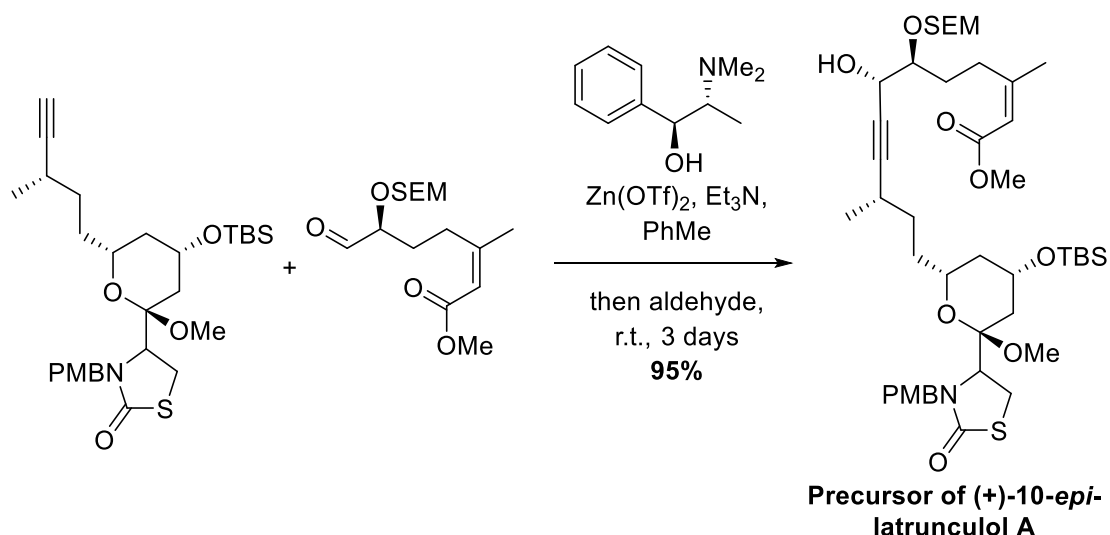
in THF at room temperature, which can then react with aromatic aldehydes in diethylether with high enantioselectivity (**Scheme 5.13**).³⁶ Optimization of this facile alkynylation method by Pu led to conditions involving 4 equivalents of alkyne, 6 equivalents of zinc powder, 12 equivalents of iodoethane and stoichiometric amount of $\text{Ti}(\text{O}i\text{Pr})_4$, thus it is not economical or environmentally friendly. With complex substrates such as those required for zampanolide (**19**) synthesis, further optimization to reduce the amount of reagents, especially the alkyne and $\text{Ti}(\text{O}i\text{Pr})_4$ required, would be prudent.



Scheme 5.13: Pu's development of Ti (IV)/BINOL-catalyzed asymmetric alkynylation.

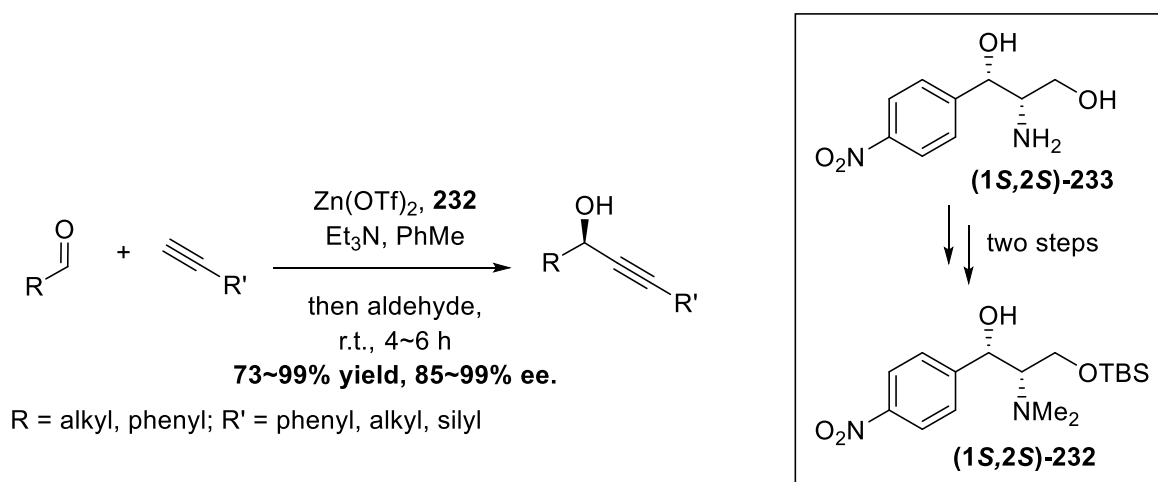
Another efficient way to produce zinc alkynylides was discovered by Carreira.³⁷ With a catalytic amount of zinc triflate and amine base, the zinc alkynylides can readily form from aliphatic, aromatic, mono-silylated and allylic alkynes. The nucleophilic attack of Zinc alkynylides was reported with nitrones, but examples of aldehyde, ketone and imine were also given.³⁷ Further investigation established the use of *N*-methylephedrine as an effective director for asymmetric alkynylation to aldehydes,³⁸ and that the inert atmosphere and exclusion of moisture is not necessary for this method.³⁹ Differing from the methods above, aliphatic aldehydes provide better yields than aromatic aldehydes under Carreira's conditions, because Cannizzaro reactions can occur with aromatic aldehydes.³⁸ Despite this, Carreira's $\text{Zn}(\text{OTf})_2/\text{N}$ -methylephedrine protocol has become the most commonly used asymmetric alkynylation method in natural product synthesis, and good yields and stereoselectivity are often achieved for complicated natural product fragments.⁴⁰⁻⁴³ For example, it was used for a late-stage connection in the synthesis of (+)-10-*epi*-latrunculol, whereby the product was prepared with

the desired configuration in 95% yield (**Scheme 5.14**).⁴³ It was noted during the optimization process that it is essential to thoroughly dry zinc triflate prior to use, which contradicts Carreira's finding that the presence of moisture and oxygen did not interfere with the alkynylation.³⁹



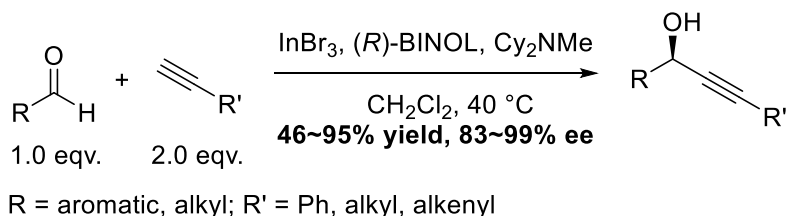
Scheme 5.14: Asymmetric alkynylation in the synthesis of (+)-10-*epi*-latrunculol A.

Unfortunately, ephedrine-derived compounds are strictly controlled substances in New Zealand and, even with a lengthy and costly application process, access is most likely not granted.⁴⁴ An alternative method using zinc alkynylide generated by zinc triflate was reported by Xiong, which involves the use of a different chiral ligand (1*S*,2*S*)-**232** derived from (1*S*,2*S*)-2-amino-1-(4-nitrophenyl)-1,3-propanediol (**233**) (**Scheme 5.15**). Unlike ephedrine-derivatives, the precursor (+) and (-)-**233** are commercially accessible and available in New Zealand. Therefore, this method was tested in the present study. During the literature research, discrepancy was found with methods involving the use of zinc triflate. Apart from the dryness of zinc triflate as mentioned before, the particle size and surface morphology can also affect the outcome of this alkynylation, but insufficient studies have been conducted to fully understand this phenomenon.⁴⁵



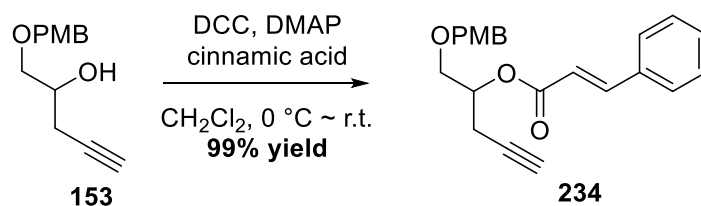
Scheme 5.15: Xiong's Zn(OTf)_2 method using chiral ligand **232**.

Indium (III) has also been used successfully to facilitate asymmetric alkynylation, owing to its dual activating properties for aldehydes and alkynes. Shibasaki has developed a facile asymmetric alkynylation method involving In(III) /BINOL (**Scheme 5.16**).⁴⁶ Good yields and selectivity are obtained, apart from the pairing of an enolizable aldehyde with an aliphatic alkyne. Shibasaki also tested the reaction of benzaldehyde and phenylacetylene in air and found no loss of yield or stereoselectivity.



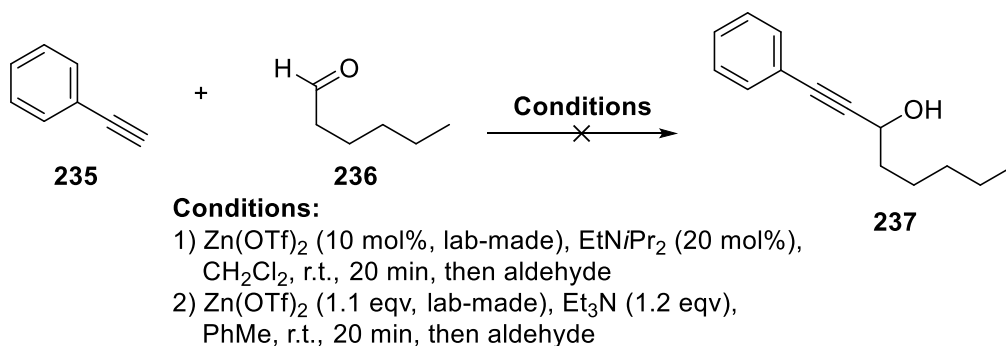
Scheme 5.16: Shibasaki's In(III) /BINOL alkynylation method.

In this study, the alkynylation was tested with model substrate **234** first, which was synthesized *via* Steglich esterification of alcohol **153** and cinnamic acid (**Scheme 5.17**). A few of the literature procedures for asymmetric aldehyde alkynylation were tested, including Carreira's non-stereoselective $\text{Zn(OTf)}_2/\text{EtNiPr}_2$ method³⁷ with either lab-made or commercial zinc triflate, Xiong's Zn(OTf)_2 method with the accessible chiral ligand **232**⁴⁷ and Trost's alkynylation using chiral ligand ProPhenol²⁹.



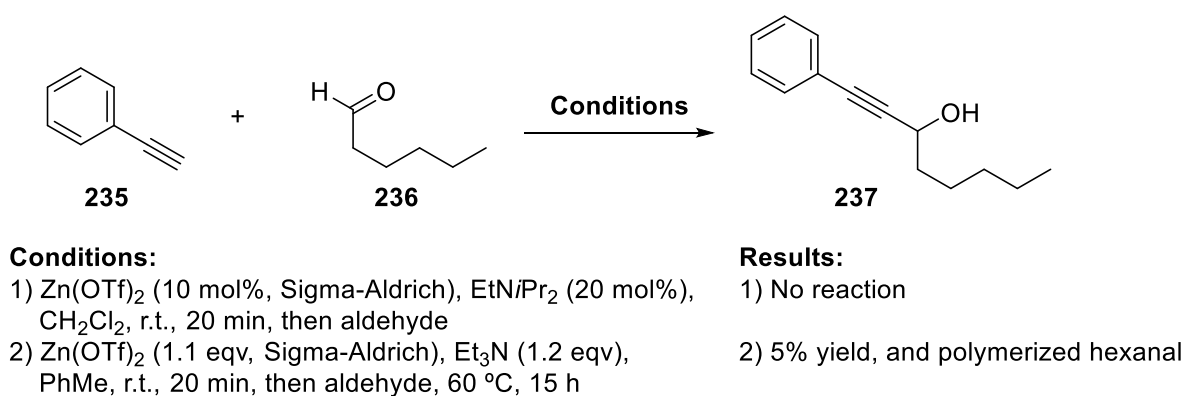
Scheme 5.17: Synthesis of model substrate **234** for alkynylation.

Carreira's three articles describing the alkynylation methods contain three sets of reaction conditions.³⁷⁻³⁹ The non-stereoselective method was first reported for alkyne additions mainly to nitrones with one example of an aldehyde substrate. This method used a catalytic amount of $\text{Zn}(\text{OTf})_2$ (10 mol%) and $i\text{Pr}_2\text{EtN}$ (25 mol%) in dichloromethane.³⁷ The subsequently developed asymmetric alkynylation to aldehydes also used catalytic amount of reagents (20 mol% $\text{Zn}(\text{OTf})_2$, 22 mol% (+)-*N*-methylephedrine, 50 mol% Et_3N), but was carried out in toluene at 60 °C.³⁸ Later, it was found that the reaction can be performed at room temperature in toluene, although its effectiveness was compromised by requiring stoichiometric amounts of $\text{Zn}(\text{OTf})_2$ (1.1 equiv.), (+)-*N*-methylephedrine (1.2 equiv.) and Et_3N (1.2 equiv.).³⁹ Due to the poor availability of (+)-*N*-methylephedrine, the non-stereoselective method was tested first, with catalytic and stoichiometric amounts of reagents on simple substrates phenylacetylene (**235**) and hexanal (**236**) as reported previously, using zinc triflate made by treating activated zinc powder with triflic acid (**Scheme 5.18**).⁴⁸ No reaction was observed. Because discrepancies were present in reports of alkynylation reactions regarding the dryness and particle size of zinc triflate, the prepared zinc triflate was ground and dried under high vacuum at 140 °C overnight, but this did not make any improvement.^{39,45}



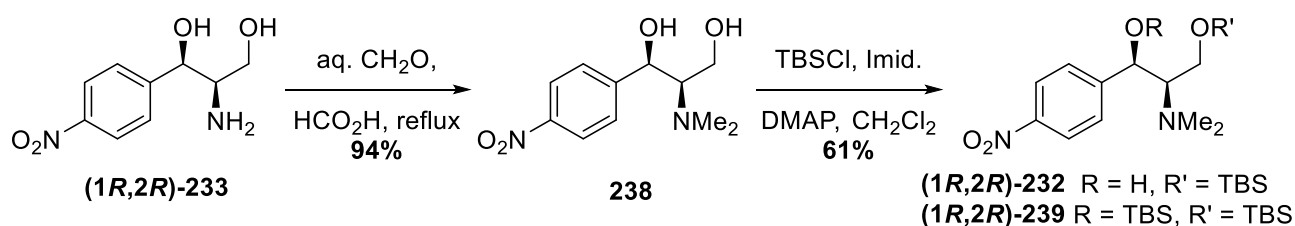
Scheme 5.18: Non-stereoselective alkynylation reactions using lab-made $\text{Zn}(\text{OTf})_2$.

Commercially available zinc triflate was then used in the alkynylation of **235** to **236** (**Scheme 5.19**). The initial experiment with a catalytic amount of zinc triflate and DIPEA in dichloromethane did not produce any product, only starting material was observed by TLC analysis and ^1H NMR spectroscopy after 6 hours at room temperature. Therefore, this mixture was concentrated, re-dissolved in toluene, and additional stoichiometric amounts of zinc triflate and triethylamine were added. After 15 hours at 60 °C, a small amount of the desired propargyl alcohol **237** was isolated (5% yield). The propargylic functionality showed a characteristic proton signal at 4.6 ppm and a carbon signal at 63.0 ppm, which are in agreement with literature values. The major products were the polymerized compounds derived from hexanal (**236**), which is likely to be caused by the concentration process to remove dichloromethane.



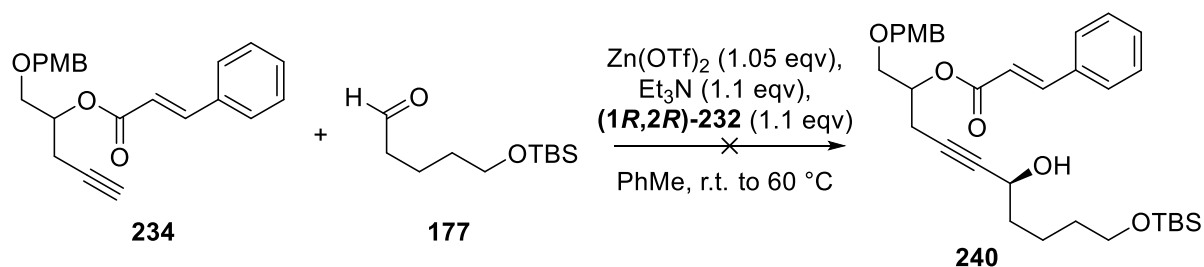
Scheme 5.19: Non-stereoselective alkynylation reactions using commercially available $\text{Zn}(\text{OTf})_2$.

At the same time, the chiral ligand (1*R*,2*R*)-**232** was prepared *via* two steps, *N*-methylation and silyl protection (**Scheme 5.20**).⁴⁷ Because the required configuration in this project is opposite to that of Xiong's report using (1*S*,2*S*)-**232**, (1*R*,2*R*)-**232** was prepared. The methylation of amines with aqueous formaldehyde and formic acid is a well-established method.⁴⁹ During the reaction, the amine of (1*R*,2*R*)-**233** was transformed to an imine or iminium with formaldehyde, which was then reduced by formic acid to form each of the two methyl groups, producing carbon dioxide as the by-product.⁵⁰ This step produced the dimethylated amine **238** in an excellent 94% yield. The following selective mono-silyl protection only reached a moderate 61% yield of (1*R*,2*R*)-**232**. Only 3% of the diprotected product **239** was isolated, and the rest of the mass was thought to be unreacted starting material. A species with higher polarity was observed by TLC analysis, but was not recovered.



Scheme 5.20: Two-step preparation of chiral ligand (1*R*,2*R*)-**232**.

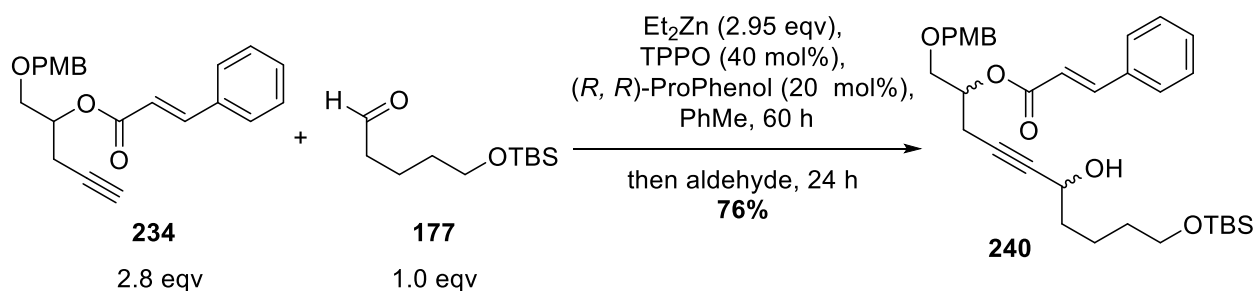
The asymmetric alkynylation using Xiong's chiral ligand (1*R*,2*R*)-**232** was attempted on the model substrates **234** and **177** (Scheme 5.21), despite the poor result obtained with the non-stereoselective alkynylation performed with similar reagents. It has been report that the amino alcohol ligand (1*R*,2*R*)-**232** may be essential for the reactivity as well as the stereoselectivity.⁵¹ With stoichiometric amount of reagents, this reaction was first performed at room temperature. After 14 h, no reaction was observed, thus the reaction mixture was heated up to 60 °C. However, starting material remained after four days at 60 °C. Further investigation is required.



Scheme 5.21: Attempted Xiong's asymmetric alkynylation on model substrates **234** and **177**.

Trost's alkynylation involving the use of ProPhenol was then attempted with substrates **234** and **177** (Scheme 5.22). Due to difficulty in obtaining dimethylzinc, diethylzinc was used instead. Longer premixing of alkyne with diethylzinc, TPPO and (*R,R*)-ProPhenol was applied to compensate for the potentially lower activity of diethylzinc. This air-sensitive reaction was initially carried out as a bench-top reaction under nitrogen atmosphere. All glassware was dried under high vacuum with heating, and the non-volatile reagents were dried under high vacuum. No reaction was observed, possibly due to the presence of adventitious water or air. Therefore, this reaction was next carried out in a glovebox. The alkyne **234** was premixed for 64 h, and the resulting alkynylzinc was allowed to react with the aldehyde **177** for 24 h. To our delight,

the desired product **240** was obtained in high yield (76%) after a single column chromatography operation.



Scheme 5.22: Trost's alkynylation of substrates **234** and **177**.

The product **240** was expected to exist as diastereomers. Kinetic resolution in the alkynylation could conceivably result in a single diastereomer, but the high isolated yield indicated that both stereoisomers of **234** have reacted, as is likely. The signals in the ^1H and ^{13}C NMR spectra showed no differentiation (**Figure 5.6**), and the configuration at the newly formed propargylic alcohol was yet to be determined.

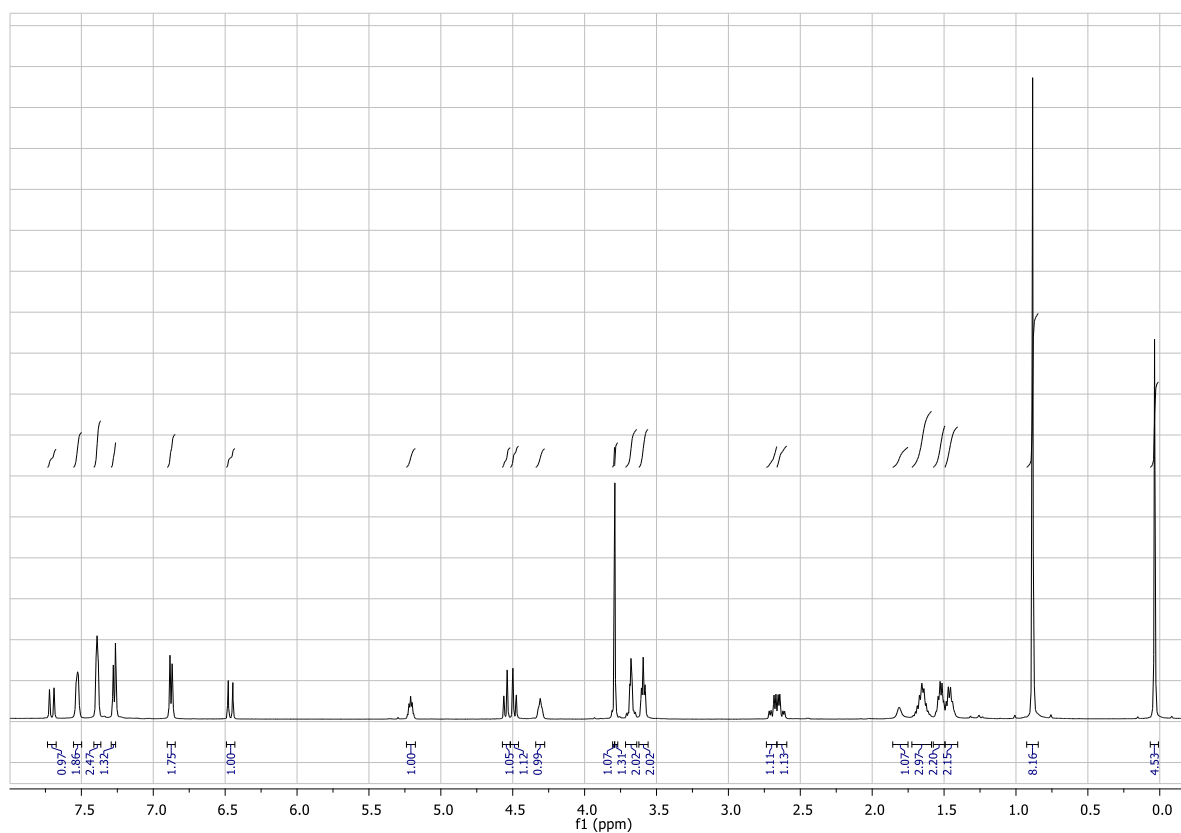


Figure 5.6: ^1H NMR spectrum of propargylic alcohol **240**.

Using chiral derivatizing agents is a convenient NMR-based method to determine the absolute configuration of alcohols.⁴⁵ A commonly used chiral derivatizing agent is α -methoxy- α -trifluoromethylphenylacetic acid (MTPA), also known as Mosher's acid, which reacts with the alcohol to produce its corresponding trifluoromethylphenylmethoxyacetate *via* esterification.^{46,47} As the Mosher model describes, in the lowest energy conformation of the **241**, the electronegative α -CF₃ would be positioned as shown in **Figure 5.7** to avoid the antibonding orbitals of the ester carbonyl, and the H^a would also be eclipsed with the ester carbonyl to minimise steric hindrance. Considering the two configurations of the propargylic alcohol, the H^b protons on the substituent would experience a through-space deshielding or shielding effect from the methoxy or phenyl group on the same side, respectively (**Figure 5.7**).

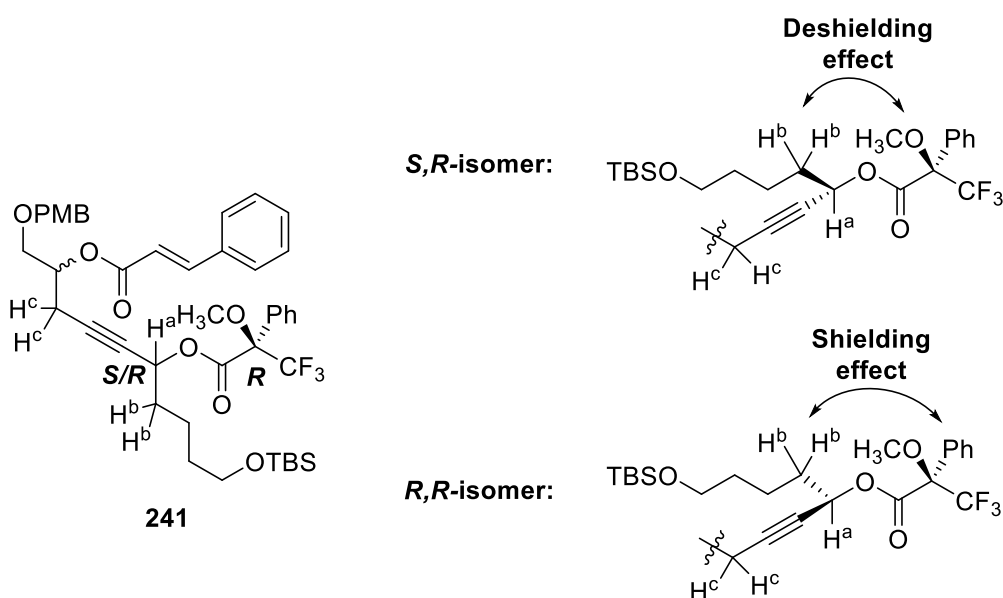
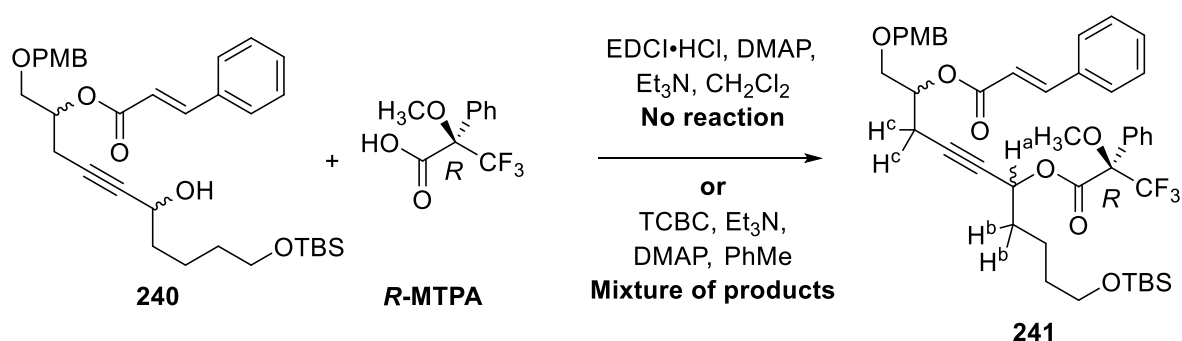


Figure 5.7: Using Mosher's ester method to determine the configuration at the new propargylic centre.

The propargylic protons H^c may also be influenced in the opposite way, but the extended distance would mean a very weak effect. If the product **240** is present as a mixture of the two configurations at the new stereocentre, the ratio of the two isomers can be determined by comparing the integrals of the two pairs of chemical shifts after derivatization of the stereoisomers with either *R*- or *S*-MTPA. However, this will be complicated by the fact that the starting material **234** is racemic. When *R*-MTPA was used, the compound with a shift of H^b signal to lower field would bear the *S*-configuration at the newly formed propargylic centre, and the shift to higher field would indicate *R*-configuration. If the asymmetric alkynylation is entirely stereoselective, the configuration at the new propargylic centre will be determined by

comparing the chemical shift of H^b in the derivatization products from both *S*- and *R*-MTPA (δ_S and δ_R , respectively). The $\Delta\delta^{SR}$ (defined as $\delta_S - \delta_R$) value will be calculated, and a positive value would suggest the *R*-configuration and a negative value the *S*-isomer.

To produce the desired Mosher ester **241**, Steglich esterification with *R*-MTPA was attempted first, but only starting material **240** was observed by TLC analysis and ¹H NMR spectroscopy after 14 hours. Yamaguchi esterification was then attempted, but it did not reach completion after 20 hours. The ¹H NMR spectrum of crude product showed that 25% of the alcohol starting material remained.



Scheme 5.23: Derivatization of **240** with *R*-MTPA.

Two overlapping spots with slightly different R_f was observed on TLC plate, which were thought to be the stereoisomers. Therefore, the products was isolated from column chromatography as two mixtures at 11 mg and 3 mg in weight, and the later contains less of the compound with higher R_f . NMR data were obtained from a 600MHz machine equipped with an indirect detection cold probe to have sufficient resolution to differentiate all of the potential isomers. Six closely related compounds were identified in each mixture, which were sorted into three isomeric pairs according to their intensities, chemical shifts, multiplet pattern and through-bond correlations. The six compounds are likely to be the four stereoisomers of **241** and two by-products. The signals from the pair of by-products were differentiated from the desired stereoisomers of **241** with the assistance of COSY, HSQC and HMBC NMR spectroscopy. Observed in the ¹H and ¹³C NMR spectra, significantly less by-product was present in the 3 mg mixture than the 11 mg, thus the compound with higher R_f was likely to be the by-product. It was also found that the by-products are likely to be a pair of stereoisomers,

and contain the same cinnamate and propargylic systems as the desired products, because most of the signals attributed to those systems overlap with the desired ones (**Figure 5.8**). However, the by-product displayed a distinctively higher chemical shift for the oxymethine proton at the newly formed ester, 5.59 ppm compared to the 5.51 and 5.48 ppm found for the desired products. The ^{13}C NMR signal of the oxymethine was found at 163.1 ppm, which showed HMBC correlation to two singlet peaks in the aromatic region. The two peaks have chemical shifts of 7.30 and 7.31 ppm, close to the aromatic signals reported for 2,4,6-trichlorobenzoyl functionality (7.33 ppm).⁵⁵ Therefore, partial reaction of the alcohol **240** with TCBC, instead of MTPA was suspected. The presence of 2,4,6-trichlorobenzoate by-product **242** was confirmed by HRMS.

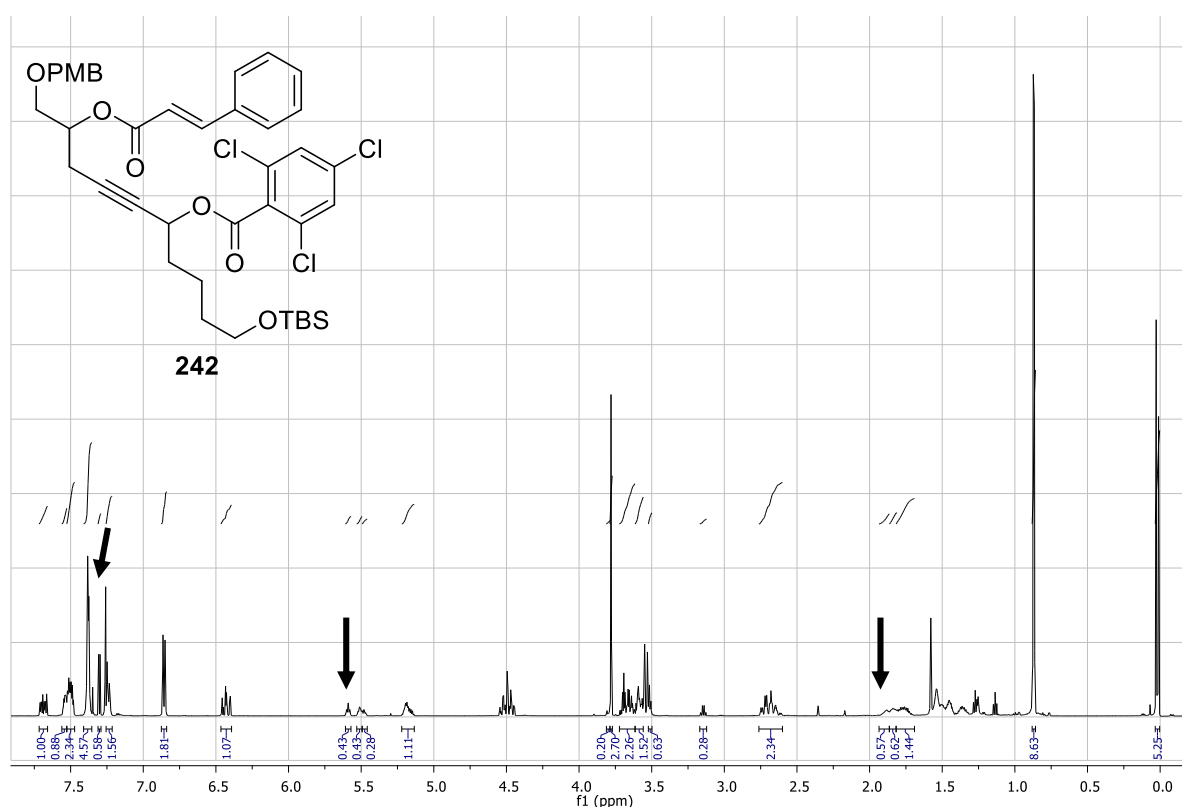
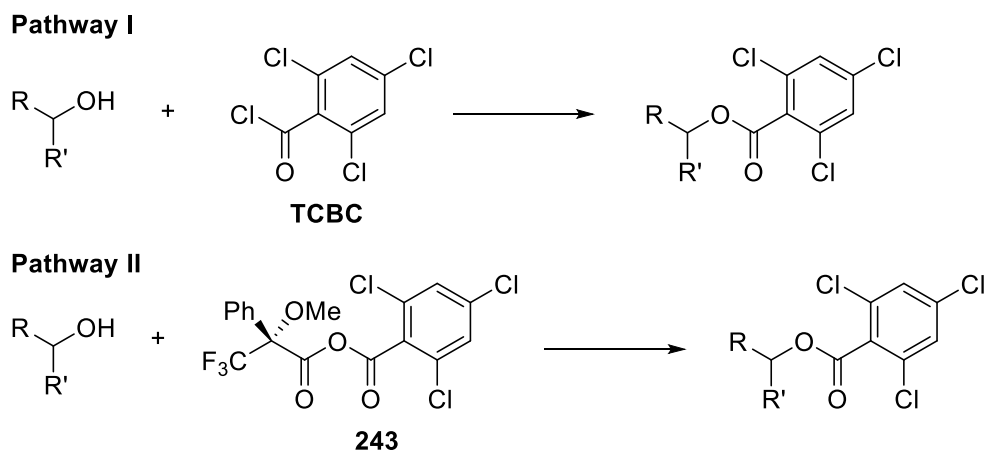


Figure 5.8: ^1H NMR spectrum of the mixture containing **241** and the proposed by-products, with distinctive signals attributed to the by-product **242** indicated.

The formation of **242** could be from direct reaction of alcohol **241** and TCBC. The TCBC was added in excess, and the direct esterification of alcohol and acyl chloride can occur in the presence of base, but high temperature is often required for sterically hindered substrates (**Scheme 5.24**, pathway I).⁵⁶ The attack of **240** at the trichlorophenylcarbonyl in **243** to produce

242 is also possible, because of the high steric hindrance at the MTPA-originated carbonyl (pathway II). Two heteroatom-linked ethyl groups were also identified: one involves a quartet at 3.15 ppm and the triplet at 1.14 ppm; the other one has the distinctive triplet at 1.27 ppm and an obscured multiplet at 3.60 ppm (**Figure 5.8**). The source of the ethyl moieties was thought to be triethylamine, as the chemical shifts were similar to triethylamine hydrochloride (3.16 and 1.43 ppm).⁵⁷ However, due to the lack of additional information in a clean spectrum, no conclusion can be firmly drawn.



Scheme 5.24: Possible pathways for the formation of **242**.

HRMS confirmed the presence of the desired Mosher ester **242**. The observation of four sets of **242** signals in the NMR spectra suggested that both configurations of the propargylic alcohol were formed. Signals of H^b are slightly differentiated for the two groups of stereoisomers (insert C, **Figure 5.9**), and the COSY and HSQC signals were used to define the boundary of multiplets. It is clear that the major pair of signals has a lower chemical shift than the minor pair. According to the discussion before, the major pair of stereoisomers would bear the desired *R*-configuration at the propargylic centre, while the minor pair of stereoisomers would have *S*-configuration. The ratio of the stereoisomers cannot be accurately determined based on the integrals of H^b in the ¹H NMR spectrum, because of the overlapping of the two complex multiplets associated with the major and minor pair of stereoisomers (insert C). Careful examination of the ¹H NMR spectrum led to the decision of using the multiplets at 5.53–5.47 ppm (insert B), and doublets at 6.46–6.39 ppm (insert A), which are the signals for the oxymethine protons next to the cinnamate ester and the α-protons of the cinnamate group. The boundary of the major and minor multiplets at 5.53–5.47 ppm is reasonably defined, while the

doublets at 6.46–6.39 ppm are all partially overlapping, but contain a few well-isolated single peaks which can provide representative ratios for the four constituent compounds. The integrals for both oxymethine and α -protons agreed that the ratio of the major and minor products is consistent in both mixtures, and measured to be 3:2 *R:S*-configuration, which indicates poor stereoselectivity of the method. The ratio was also obtained from the ^1H NMR spectrum of the crude product to better represent the composition of the mixture formed in the reaction, which agreed with the ratio of 3:2, with the *R*-configuration as major. Further optimization of the stereoselectivity will be required.

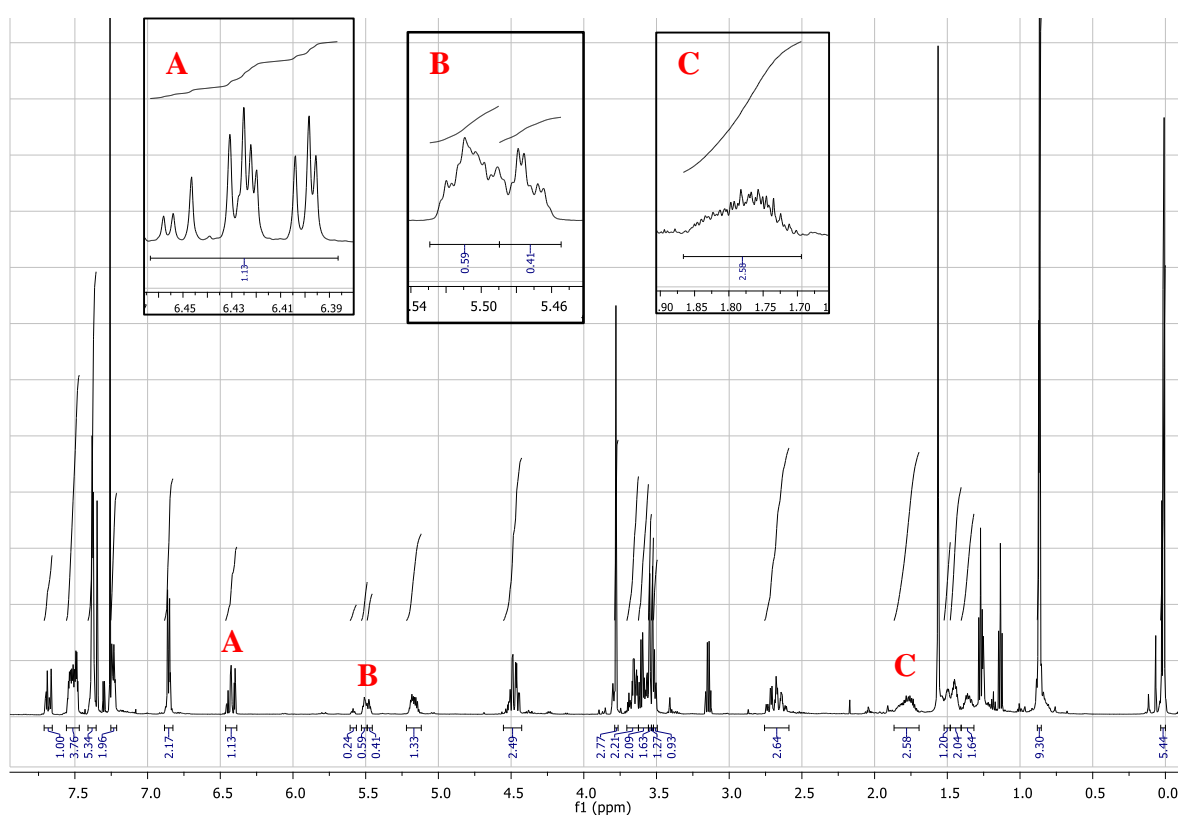
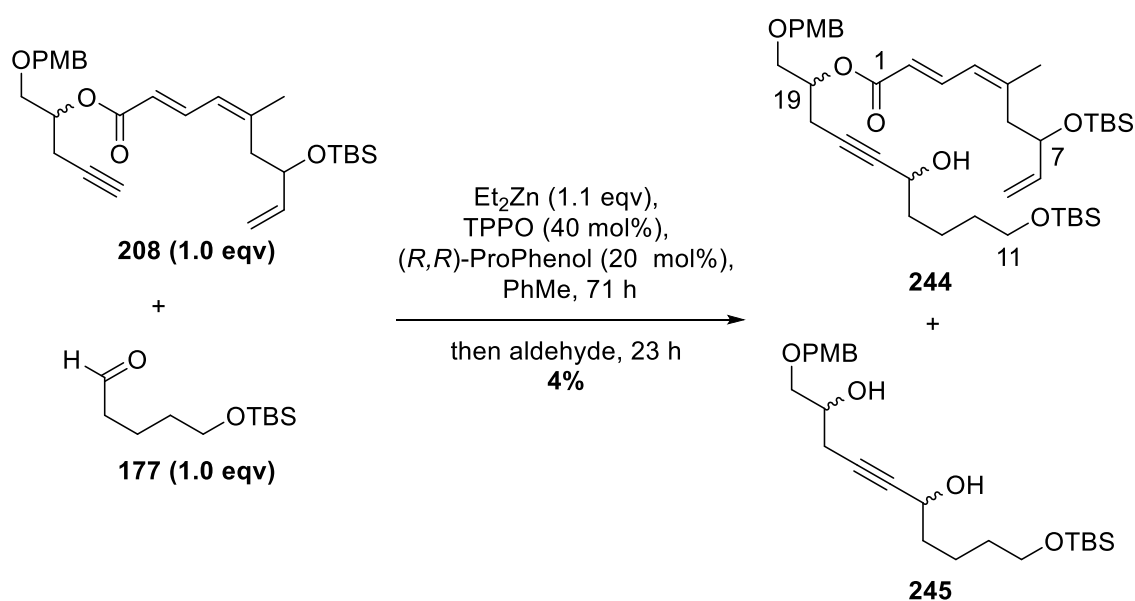


Figure 5.9: ^1H NMR spectrum of the mixture containing **242**, with inserts **A**, **B** and **C** showing expansion of the multiplets at 6.42, 5.50 and 1.80 ppm, respectively.

The viability of subjecting the advanced fragment **208** to Trost's asymmetric alkynylation with analogue aldehyde **177** was also tested, but only 4% of the desired product **244** was obtained, alongside 17% of recovered starting material (**Scheme 5.25**). A substantial amount of the de-esterified product **245** was obtained, which was not purified. The presence of **245** was confirmed by HRMS and comparing ^1H NMR signals with those of a purified and characterized

sample of compound **245** provided by PhD student Geyrhofer. The absence of alkene signals and a signal at 3.96 ppm corresponding to the de-esterified H19 were observed in the ^1H NMR spectrum. Using Pu's alkynylation method involving *in situ* generation of diethylzinc, Geyrhofer had previously isolated mostly the de-esterified product **245**, even with model alkynes similar to **234**. Although Trost's method provided a good yield for model alkyne **234**, the dienoate in fragment **208** was too unstable under the reaction condition. The stereoselectivity of this reaction was expected to be similar as the model system, but substrate influence from the additional stereocenter and the larger substituent could also be a factor. Due to time constraints, Mosher's ester analysis was not performed on **244**.



Scheme 5.25: Use of Trost's alkynylation method with substrates **208** and **177**.

5.4 Summary

In summary, the side arm attachment by a chiral boron reagent-promoted aza-aldol reaction failed to produce the desired product with a simple aldehyde model. However, model substrates that better account for the functionality of the zampanolide macrocycle should be tested in this reaction. If unsuccessful, reliable alternative methods for the aza-aldol reaction can be attempted next. The oxidation of the alcohol group at C20 was briefly tested on a model of zampanolide /dactylolide. Although the well-precedented DMP oxidation led to degradation,

it could be a problem specific to the substrate used, thus substrates better represent dactylolide (**21**) could be investigated.

Alkynylation to form the C15-C16 bond was also investigated. While unsatisfying results were obtained from Carreira's non-stereoselective and Xiong's methods, alkynylation involving ProPhenol and diethylzinc produced an excellent yield with a model alkyne. Although the stereoselectivity of the Et₂Zn/ProPhenol alkynylation is yet to be optimized, it was also tested on the full zampanolide fragment generated from the Bestmann ylide reaction. A small amount of the desired product was isolated, alongside the de-esterified major product. Further optimization of this reaction and its stereoselectivity are underway.

5.5 Experimental data

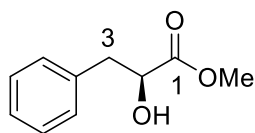
General experimental information

Unless otherwise stated, all reactions were carried out in oven-dried glassware under a positive pressure of nitrogen, delivered via a manifold. Dry tetrahydrofuran, dichloromethane and toluene were obtained from a PureSolv MD 5 solvent purification system (Innovative Technology). Analytical grade solvents were used for aqueous work-up and column chromatography (petroleum ether, ethyl acetate, diethyl ether, methanol and dichloromethane). Column chromatography was performed on silica gel 60 Å (Pure Science, 40–63 micron) with the eluent mixtures as stated in the corresponding procedures. Thin-layer chromatography was performed on silica-coated plastic plates (Macherey-Nagel, POLYGRAM[®] Sil G/UV₂₅₄). All compounds were detected under UV irradiation ($\lambda = 254$ nm), followed by visualization with anisaldehyde staining solutions.

All other chemicals were purchased from Pure Science, Sigma-Aldrich, Panreac, Merk and AK scientific. Infra-red (IR) spectra were collected on an ALPHA FT-IR spectrometer (Bruker) fitted with attenuated total reflectance (ATR). The intensities of signals are defined as: br = broad, s = strong, m = medium, w = weak. Mass spectra were collected on an Agilent 6530 Accurate-Mass Q-TOF LC/MS high-resolution mass spectrometer (HRMS). The specific rotations were collected on an AUTOPOL II automatic polarimeter (Rudolph Research Analytical), and the reported values are an average of 10 measurements and concentrations are reported in g/100 mL.

Nuclear magnetic resonance (NMR) spectra were obtained in deuterated chloroform (CDCl₃) using Varian Inova instruments operating at 500 or 600 MHz for proton and 125 or 150 MHz for carbon. Proton and carbon chemical shifts are reported in parts per million (ppm) relative to residual CHCl₃ [$\delta(^1\text{H}) = 7.26$ ppm] and CDCl₃ [$\delta(^{13}\text{C}) = 77.0$ ppm], respectively. Signals are defined as: s = singlet, d = doublet, t = triplet, q = quartet, quin = quintet, m = multiplet, app. = apparent, obs. = obscured peak. Coupling constants (*J*) are reported in Hertz (Hz). Assignments were determined by two-dimensional NMR experiments (COSY, HSQC, and HMBC).

Methyl 2-hydroxy-3-phenylpropanoate (**220**)



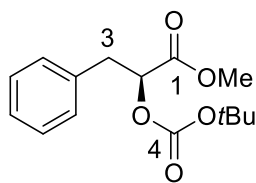
To a solution of (*S*)-phenylalanine (4.00 g, 24.2 mmol) in aqueous H₂SO₄ solution (36.0 mL, 3% V/V in H₂O, 4.66 mmol) at 0 °C, a solution of NaNO₂ (2.51 g, 36.4 mmol) in H₂O (4.8 mL, 7.5 M) was added dropwise over 1 h. After the addition, the reaction was slowly warmed to r.t. and stirred for 16 h. The reaction mixture was extracted with EtOAc (3 × 100 mL), and the organic layers were combined, dried over MgSO₄ and the solvent was removed under reduced pressure to produce 2-hydroxy-3-phenylpropanoic acid as a yellow crystalline material (2.29 g). This yellow solids and K₂CO₃ (2.30 g, 16.6 mmol) were dissolved in acetone (81 mL), and MeI (1.9 mL, 27.8 mmol) was added. This reaction mixture was heated at 50 °C for 4 h. The reaction mixture was concentrated under reduced pressure and dissolved in H₂O (30 mL) and EtOAc (30 mL). The aqueous layer was separated and extracted with EtOAc (3 × 30 mL). The organic layers were combined, dried over MgSO₄ and under reduced pressure to yield **220** as a pale yellow solid (1.58 g, 44% yield from (*S*)-phenylalanine).

¹H NMR (500 MHz, CDCl₃): δ 7.34–7.29 (m, 2H, CH, Ph), 7.26–7.20 (m, 3H, CH, Ph), 4.47 (ddd, *J* = 6.7, 5.6, 4.2 Hz, 1H, 2-CH), 3.79 (s, 3H, CH₃, Me), 3.14 (dd, *J* = 13.9, 4.4 Hz, 1H, one of 3-CH₂), 2.98 (dd, *J* = 13.9, 6.8 Hz, 1H, one of 3-CH₂), 2.70 (d, *J* = 6.1 Hz, 1H, OH).

¹³C NMR (125 MHz, CDCl₃): δ 174.6 (C, C1), 136.3 (C, Ph), 129.5 (CH, Ph), 128.4 (CH, Ph), 126.9 (CH, Ph), 71.2 (CH, C2), 52.5 (CH₃, Me), 40.6 (CH₂, C3).

The data agree with previously reported.⁵⁸

Methyl 2-(*t*-butylcarbonate)-3-phenylpropanoate (**224**)



A mixture of **220** (304 mg, 1.69 mmol), Zn(OAc)₂·2H₂O (37 mg, 0.169 mmol) and Boc₂O (0.43 mL, 407 mg, 1.86 mmol) were stirred at 50 °C for 4 h. Upon cooling, the reaction mixture was diluted with CH₂Cl₂ (10 mL) and H₂O (10 mL). The aqueous layer was separated and extracted with CH₂Cl₂ (2 × 10 mL), the organic layers were combined, dried over MgSO₄ and concentrated under reduced pressure. The crude product was purified by column chromatography (silica, 10:1 pet. ether:EtOAc, R_f = 0.29) to yield the product **224** as a pale yellow solid (397 mg, 85% yield). Only ¹H NMR data was collected when **224** was first prepared. After over three years of storage, some decomposition occurred. The ¹³C NMR, IR and HRMS data were collected on this partially decomposed product, and the desired carbon signals were identified in the mixture by 2D correlations.

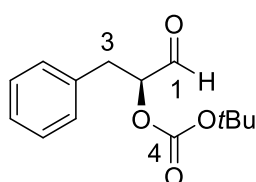
¹H NMR (500 MHz, CDCl₃): δ 7.34–7.28 (m, 2H, CH, Ph), 7.28–7.22 (m, 3H, CH, Ph), 5.10 (dd, *J* = 8.3, 4.4 Hz, 1H, 2-CH), 3.74 (s, 3H, CH₃, Me), 3.19 (dd, *J* = 14.2, 4.1 Hz, 1H, one of 3-CH₂), 3.11 (dd, *J* = 14.0, 8.6 Hz, 1H, one of 3-CH₂), 1.45 (s, 9H, CH₃, *t*Bu).

¹³C NMR (125 MHz, CDCl₃): δ 170.3 (C, C1), 152.8 (C, C4), 135.7 (C, Ph), 129.4 (CH, Ph), 128.5 (CH, Ph), 127.0 (CH, Ph), 83.2 (C, *t*Bu), 75.2 (CH, C2), 52.4 (CH₃, OMe), 37.5 (CH₂, C3), 27.6 (CH₃, *t*Bu).

IR (neat) cm⁻¹: 3031 (w, C–H), 2980 (m, C–H), 1739 (s, C=O), 1604 (w, C–H), 1278 (s, C–O), 1154 (s, C–O), 1103 (s, C–O), 792 (m, C–H), 698 (s, C–H).

HRMS (ESI) *m/z*: found 298.1549, calcd for C₁₅H₂₄O₅N 298.1547 [M+NH₄]⁺ (Δ = 0.7 ppm).

2-(*t*-Butylcarbonate)-3-phenylpropanal (**223**)



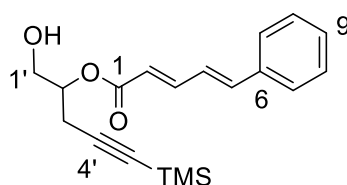
To a solution of ester **224** (63 mg, 0.225 mmol) in CH₂Cl₂ (1.3 mL, 0.17 M) at -78 °C, a solution of DIBAL-H (0.25 mL, 1.0 M in cyclohexane, 0.25 mmol) was added dropwise. The reaction was stirred at -78 °C for 3 h 30 min, and then quenched by the addition of MeOH (0.5 mL) and sat. aq. Rochelle salt (1.0 mL). The mixture was warmed to r.t.. After stirring vigorously for 2 h, the reaction mixture was extracted with EtOAc (3 × 10 mL). The organic layers were combined, dried over MgSO₄ and concentrated under reduced pressure. The crude material was

purified by column chromatography (silica, 10:1 pet. ether:EtOAc, R_f = 0.12) to yield the product **223** as a pale yellow solid (21 mg, 38% yield) and a mixture of starting material and product (31 mg, 4:1 **224**:**223**). Only ^1H NMR and HRMS data were collected.

^1H NMR (500 MHz, CDCl_3): δ 9.61 (s, 1H, 1-CH), 7.35–7.29 (m, 2H, CH, Ph), 7.29–7.20 (m, 3H, CH, Ph), 5.06 (dd, J = 8.0, 5.0 Hz, 1H, 2-CH), 3.18 (dd, J = 14.4, 4.5 Hz, 1H, one of 3- CH_2), 3.04 (dd, J = 14.4, 8.8 Hz, 1H, one of 3- CH_2), 1.46 (s, 9H, CH_3 , *t*Bu).

HRMS (ESI) m/z : found 251.1300, calcd for $\text{C}_{14}\text{H}_{19}\text{O}_4$ $[\text{M}+\text{H}]^+$ 215.1278 (Δ = 1.0 ppm).

(5'-Trimethylsilyl)pent-4'-yn-2'-yl 5-phenylpenta-2,4-dienoate (227)



To a stirred solution of the PMB-ether **206** (131 mg, 0.292 mmol) in CH_2Cl_2 : H_2O (10:1 V/V, 3.9 mL) at r.t., DDQ (79 mg, 0.348 mmol) was added. The reaction mixture was stirred at r.t. for 1 h 30 min. The solvent was removed under reduced pressure. The

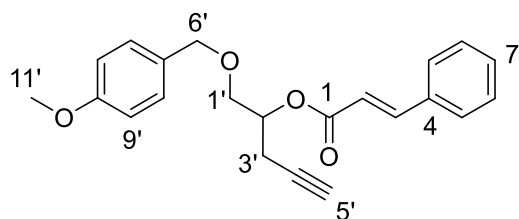
crude product was purified by column chromatography (silica, 5:1 pet. ether:EtOAc, R_f = 0.15) to yield the alcohol **227** as a yellow oil (91 mg, 95% yield).

^1H NMR (500 MHz, CDCl_3) δ 7.51 (dd, J = 16.2, 10.2 Hz, 1H, 2-CH), 7.49 – 7.46 (m, 2H, 7-CH), 7.39 – 7.30 (m, 3H, 8-CH and 9-CH), 6.96 – 6.84 (m, 2H, 4-CH and 5-CH), 6.02 (d, J = 15.3 Hz, 1H, 2'-CH), 5.09 (dtd, J = 7.1, 5.8, 3.6 Hz, 1H, 2-CH), 3.95–3.89 (m, 1H, one of 1'- CH_2), 3.89–3.83 (m, 1H, one of 1'- CH_2), 2.67 (dd, J = 14.9, 4.0 Hz, 1H, one of 3'- CH_2), 2.65 – 2.60 (m, 1H, one of 3'- CH_2), 0.15 (s, 9H, CH_3 , Me).

^{13}C NMR (125 MHz, CDCl_3) δ 166.6 (C, C1), 145.6 (CH, C3), 141.1 (CH, C5), 135.9 (C, C6), 129.2 (CH, C8), 128.8 (CH, C9), 127.3 (CH, C7), 126.0 (CH, C4), 120.5 (CH, C2), 101.4 (C, C4'), 87.6 (C, C5'), 72.8 (CH, C2'), 63.6 (CH_2 , C1'), 22.0 (CH_2 , C3'), -0.05 (CH_3 , Me).

HRMS (ESI) m/z : found 329.1572, calcd for $\text{C}_{19}\text{H}_{25}\text{O}_3\text{Si}$ $[\text{M}+\text{H}]^+$ 329.1567 (Δ = 1.4 ppm).

1'-(*para*-Methoxybenzyloxy)pent-4'-yn-2'-yl 3-phenylprop-2-enoate (234)



To a solution of alcohol **153** (100 mg, 0.454 mmol) in CH₂Cl₂ (1.0 mL, 0.15 M) at r.t., cinnamic acid (75 mg, 0.51 mmol) and DMAP (3 mg, 0.02 mmol) were added. This solution was stirred for 10 min. Upon the addition of DCC (103 mg, 0.499 mmol),

the clear solution turned cloudy. The reaction was stirred for 4 h at r.t., filtered through Celite, and the filtrate was concentrated under reduced pressure. The crude product was purified by column chromatography (silica, 10:1 pet. ether:EtOAc, *R_f* = 0.14) to yield the ester **234** as a colourless oil (158 mg, 99% yield).

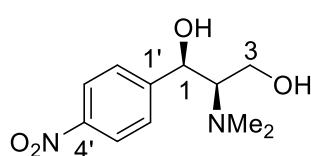
¹H NMR (500 MHz, CDCl₃): δ 7.71 (d, *J* = 16.1 Hz, 1H, 3-CH), 7.53 (d, *J* = 6.2 Hz, 2H, 5-CH), 7.41–7.37 (complex m, 3H, 6-CH & 7-CH), 7.27 (obs. d, *J* = 8.5 Hz, 2H, 8'-CH), 6.88 (d, *J* = 8.5 Hz, 2H, 9'-CH), 6.47 (d, *J* = 15.9 Hz, 1H, 2-CH), 5.23 (app. quin, *J* = 5.4 Hz, 1H, 2'-CH), 4.55 (d, *J* = 11.7 Hz, 1H, one of 6'-CH₂), 4.50 (d, *J* = 11.7 Hz, 1H, one of 6'-CH₂), 3.79 (s, 3H, 11'-CH₃), 3.72 (dd, *J* = 10.5, 5.1 Hz, 1H, one of 1'-CH₂), 3.69 (dd, *J* = 10.7, 4.6 Hz, 1H, one of 1'-CH₂), 2.69 (ddd, *J* = 16.9, 6.6, 2.4 Hz, 1H, one of 3'-CH₂), 2.63 (ddd, *J* = 16.9, 5.9, 2.7 Hz, 1H, one of 3'-CH₂), 2.00 (t, *J* = 2.6 Hz, 1H, 5'-CH).

¹³C NMR (125 MHz, CDCl₃): δ 166.2 (C, C1), 159.3 (C, C10'), 145.4 (CH, C3), 134.3 (C, C4), 130.4 (CH, C7), 129.9 (C, C7'), 129.3 (CH, C8'), 128.9 (CH, C6), 128.1 (CH, C5), 117.8 (CH, C2), 113.8 (CH, C9'), 79.4 (C, C4'), 73.0 (CH₂, C6'), 70.6 (CH, C2'/C5'), 70.5 (CH, C5'/C2'), 69.4 (CH₂, C1'), 55.3 (CH₃, C11'), 21.0 (CH₂, C3').

IR (neat) cm⁻¹: 3290 (m, C–H), 2909 (m, C–H), 2863 (m, C–H), 2120 (w, C≡C), 1709 (s, C=O), 1636 (s, C=C), 1511 (s, C–O), 1245 (s, C–O), 1165 (s, C–O), 710 (s, C–Si).

HRMS (ESI) *m/z*: found 368.1859, calcd for C₂₂H₂₆O₄N [M+NH₄]⁺ 368.1856 (Δ = 0.8 ppm).

(1*R*,2*R*)-2-(*N,N*-Dimethylamino)-1-(4'-nitrophenyl)propane-1,3-diol (238)



(1*R*,2*R*)-2-amino-1-(4'-nitrophenyl)propane-1,3-diol (**233**, 1.00 g, 5.98 mmol), aqueous formaldehyde solution (1.5 mL, 37%) and formic acid (2.0 mL, 98%) were mixed in a flask. The starting material **233** dissolved upon heating, and the solution was heated at

100 °C for 8 h. After cooling to r.t., the yellow solution was neutralized with aqueous NaOH (1N) solution to pH 8 to precipitate out the solid. The aqueous mixture was extracted with CH₂Cl₂ (5 × 50 mL), and the organic layers were combined, dried over MgSO₄ and concentrated under reduced pressure. The yellow oil obtained was then purified by column chromatography (SiO₂, 10:1 CH₂Cl₂:MeOH) to yield the product **238** as yellow crystals (1.06 g, 94%).

¹H NMR (500 MHz, CDCl₃) δ 8.20 (d, *J* = 8.7 Hz, 2H, 3'-CH), 7.60 (d, *J* = 8.7 Hz, 2H, 2'-CH), 4.59 (d, *J* = 9.7 Hz, 1H, 1-CH), 3.61 (d, *J* = 4.7 Hz, 2H, 3-CH₂), 2.59 (dt, *J* = 10.4, 5.2 Hz, 1H, 2-CH), 2.54 (s, 6H, CH₃, Me).

¹³C NMR (125 MHz, CDCl₃): δ 149.9 (C, C4'), 128.0 (CH, C2'), 123.6 (CH, C3'), 71.3 (CH, C2), 69.9 (CH, C1), 57.9 (CH₂, C3), 41.6 (CH₃, Me).

IR (neat) cm⁻¹: 3359 (br, C–O), 2981 (w, C–H), 2917 (m, C–H), 2796 (w, C–H), 1519 (s, C=C), 1348 (s, N–C), 1244 (m, N–C), 1177 (m, N–C), 1059 (s, C–O).

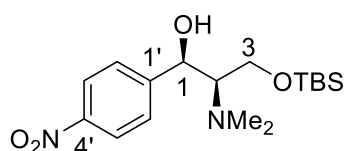
HRMS (ESI) *m/z*: found 241.1183, calcd for C₁₁H₁₇N₂O₄ [M+H]⁺ 241.1183 (Δ = 0.0 ppm).

M.p.: 102.0 – 103.4 °C. (Lit. for (1*S*,2*S*)-isomer: 88.8 – 89.1 °C.)⁴⁷

Specific rotation: [*a*]_D²¹ = -15.4 (*c* = 0.532, CH₂Cl₂). (Lit. for (1*S*,2*S*)-isomer: +25.7 (*c* = 0.505, CH₃OH).)⁴⁷

The carbon signal for C1' was missing, but the overall agreement of the NMR and IR data with those reported for the (1*S*,2*S*)-isomer and the HRMS data suggest that **238** was successfully prepared.⁴⁷ The optical rotation data obtained has opposite sign with the (1*S*,2*S*)-isomer.⁴⁷

(1*R*,2*R*)-3-(*t*-Butyldimethylsilyloxy)-2-(*N,N*-dimethylamino)-1-(4'-nitrophenyl)propan-1-ol (232)



A solution of the diol **238** (1.05 g, 4.37 mmol), TBSCl (676 mg, 4.49 mmol), imidazole (734 mg, 10.8 mmol) and DMAP (5 mg, 0.04 mmol) in CH₂Cl₂ (15 mL) was stirred at r.t. for 15 h. The reaction was diluted with H₂O (10 mL) and basified with aqueous NaOH (1N) to pH 9. The aqueous layer was separated and extracted with CH₂Cl₂ (2 × 20 mL). The organic layers were combined, dried over MgSO₄ and concentrated under reduced pressure. The yellow oil

obtained was then purified by column chromatography (SiO₂, 10:1 pet. ether:EtOAc, R_f = 0.35) to yield the product **232** as a yellow oil (946 mg, 61%).

¹H NMR (500 MHz, CDCl₃) δ 8.18 (d, *J* = 8.6 Hz, 2H, 3'-CH), 7.59 (d, *J* = 8.6 Hz, 2H, 2'-CH), 4.62 (d, *J* = 9.7 Hz, 1H, 1-CH), 3.64 (dd, *J* = 11.3, 2.2 Hz, 1H, one of 3-CH₂), 3.46 (dd, *J* = 11.4, 5.9 Hz, 1H, one of 3-CH₂), 2.48 (s, 6H, CH₃, NMe₂), 2.48–2.45 (obs. m, 1H, 2-CH), 0.86 (s, 9H, *t*Bu, TBS), -0.04 (s, 3H, Me, TBS), -0.05 (s, 3H, Me, TBS).

¹³C NMR (125 MHz, CDCl₃) δ 150.3 (C, C4'), 147.4 (C, C1'), 128.1 (CH, C2'), 123.4 (CH, C3'), 71.4 (CH, C2), 69.1 (CH, C1), 57.1 (CH₂, C3), 41.7 (CH₃, Me), 25.8 (CH₃, *t*Bu, TBS), 18.0 (C, *t*Bu, TBS), -5.8 (CH₃, Me, TBS), -5.8 (CH₃, Me, TBS).

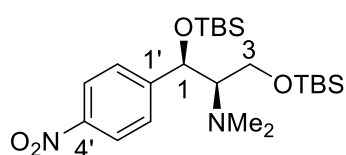
IR (neat) cm⁻¹: 3333 (br, O–H), 2929 (w, C–H), 2857 (m, C–H), 2795 (w, C–H), 1521 (s, C=C), 1346 (s, N–C), 1253 (m, N–C), 1110 (s, C–O), 833 (s, C–H and Si–C), 775 (s, Si–C).

HRMS (ESI) *m/z*: found 355.2054, calcd for C₁₇H₃₀N₂O₄Si [M+H]⁺ 355.2048 (Δ = 1.7 ppm).

Specific rotation: [*a*]_D²³ = +12.6 (*c* = 0.400, CH₂Cl₂). (Lit. for (1*S*,2*S*)-isomer: -15.8 (*c* = 1.09, CHCl₃).)⁴⁷

The NMR and IR data matches those reported for the (1*S*,2*S*)-isomer, and the optical rotation data obtained has opposite sign.⁴⁷

(1*R*,2*R*)-1,3-Bis-(*t*-butyldimethylsilyloxy)-2-*N,N*-dimethylamino-1-(4'-nitrophenyl)propane (239**)**



The di-TBS protected product **239** was a minor product in the TBS protection reaction and was obtained as a yellow oil (62 mg, 3%). R_f (3:1 pet. Ether:EtOAc) = 0.55.

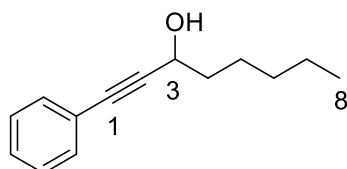
¹H NMR (500 MHz, CDCl₃) δ 8.15 (d, *J* = 7.5 Hz, 2H, 3'-CH), 7.50 (d, *J* = 7.9 Hz, 2H, 2'-CH), 5.01 (d, *J* = 3.7 Hz, 1H, 1-CH), 3.81 (dd, *J* = 9.6, 7.0 Hz, 1H, one of 3-CH₂), 3.63 (dd, *J* = 9.7, 6.4 Hz, 1H, one of 3-CH₂), 2.55 (app. q, *J* = 5.5 Hz, 1H, 2-CH), 2.35 (s, 6H, CH₃, Me), 0.91 (s, 18H, CH₃, *t*Bu, TBS), 0.07 (s, 3H, CH₃, Me, TBS), 0.05 (s, 3H, CH₃, Me, TBS), 0.04 (s, 3H, CH₃, Me, TBS), -0.20 (s, 3H, CH₃, Me, TBS).

¹³C NMR (125 MHz, CDCl₃) δ 151.9 (C, C4'), 146.8 (C, C1'), 127.6 (CH, C2'), 122.8 (CH, C3'), 74.3 (CH, C1), 71.0 (CH, C2), 59.3 (CH₂, C3), 43.5 (CH₃, Me), 25.9 (CH₃, *t*Bu, TBS), 25.8 (CH₃, *t*Bu, TBS), 18.1 (C, *t*Bu, TBS), -4.7 (CH₃, Me, TBS), -5.1 (CH₃, Me, TBS), -5.38 (CH₃, Me, TBS), -5.44 (CH₃, Me, TBS).

IR (neat) cm⁻¹: 2929 (w, C–H), 2857 (m, C–H), 2795 (w, C–H), 1522 (s, C–C), 1388 (s, N–C), 1255 (m, N–C), 1094 (s, C–O), 833 (s, C–H and Si–C), 774 (s, Si–C).

HRMS (ESI) *m/z*: found 469.2917, calcd for C₂₃H₄₅N₂O₄Si₂ [M+H]⁺ 469.2912 (Δ = 1.1 ppm).

1-Phenyloct-1-yn-3-ol (237)

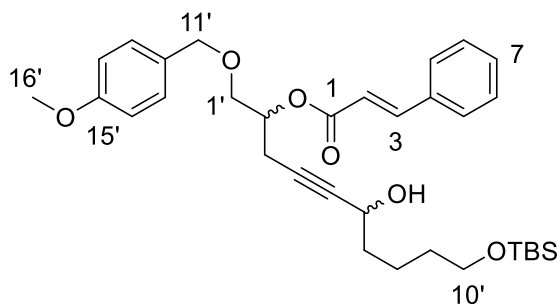


¹H NMR (500 MHz, CDCl₃): δ 7.45–7.40 (m, 2H, Ph), 7.33–7.29 (m, 3H, Ph), 4.60 (app. q, *J* = 6.2 Hz, 1H, 3-CH), 1.88 (d, *J* = 5.8 Hz, 1H, OH), 1.86–1.74 (m, 2H, 4-CH₂), 1.57–1.48 (m, 2H, 5-CH₂), 1.40–1.31 (complex m, 4H, 6-CH₂ and 7-CH₂), 0.91 (t, *J* = 7.0 Hz, 3H, 8-CH₃).

¹³C NMR (125 MHz, CDCl₃): δ 131.7 (CH, Ph), 128.3 (CH, Ph), 128.3 (CH, Ph), 122.7 (C, Ph), 90.2 (C, C2), 84.8 (C, C1), 63.0 (CH, C3), 37.9 (CH₂, C4), 31.5 (CH₂, C6/C7), 24.9 (CH₂, C5), 22.6 (CH₂, C6/C7), 14.0 (CH₃, C8).

These data were consistent with those reported previously.⁵⁹

1'-(*para*-Methoxybenzyloxy)-6'-hydroxy-10'-(*t*-butyldimethylsilyloxy)dec-4'-yn-2'-yl 3-phenylprop-2-enoate (240)



To a solution of alkyne **234** (98 mg, 0.28 mmol), (*R,R*)-ProPhenol (13 mg, 0.020 mmol) and triphenylphosphine oxide (11 mg, 0.040 mmol) in toluene (0.3 mL) at r.t., Et₂Zn (0.30 mL, 1.0 M in hexane, 0.30 mmol) was added dropwise. After the reaction was stirred at r.t. for 64 h, a

solution of aldehyde **177** (38 mg, 0.18 mmol) in toluene (0.3 mL) was added. The reaction was stirred at r.t. for an additional 24 h, and then quenched with sat. aq. NH_4Cl (15 mL). The reaction mixture was extracted with Et_2O (3×20 mL), and the organic layers were combined, dried over MgSO_4 and concentrated under reduced pressure. The crude product was purified by column chromatography (SiO_2 , 5:1 Pet. ether:EtOAc) to yield the product **240** as a colourless, clear oil (76 mg, 76% yield).

^1H NMR (500 MHz, CDCl_3): δ 7.71 (d, $J = 15.9$ Hz, 1H, 3-CH), 7.56–7.50 (m, 2H, 5-CH), 7.41–7.36 (complex m, 3H, 6-CH & 7-CH), 7.27 (obs. d, $J = 7.1$ Hz, 2H, 14'-CH), 6.88 (d, $J = 7.5$ Hz, 2H, 13'-CH), 6.46 (d, $J = 16.0$ Hz, 1H, 2-CH), 5.21 (app. quin, $J = 5.2$ Hz, 1H, 2'-CH), 4.55 (d, $J = 11.9$ Hz, 1H, one of 11'-CH₂), 4.49 (d, $J = 11.7$ Hz, 1H, one of 11'-CH₂), 4.34–4.27 (m, 1H, 6'-CH), 3.79 (s, 3H, CH₃, C16'), 3.72–3.63 (m, 2H, 1'-CH₂), 3.59 (t, $J = 6.2$ Hz, 2H, 10'-CH₂), 2.69 (dd, $J = 16.7, 6.8$ Hz, 1H, one of 3'-CH₂), 2.63 (dd, $J = 16.8, 5.9$ Hz, 1H, one of 3'-CH₂), 1.81 (br. s, 1H, OH), 1.72–1.58 (m, 2H, 7'-CH₂), 1.53 (app. quin, $J = 6.3$ Hz, 2H, 9'-CH₂), 1.46 (app. quin, $J = 6.6$ Hz, 2H, 8'-CH₂), 0.88 (s, 9H, CH₃, *t*Bu, TBS), 0.04 (s, 6H, CH₃, Me, TBS).

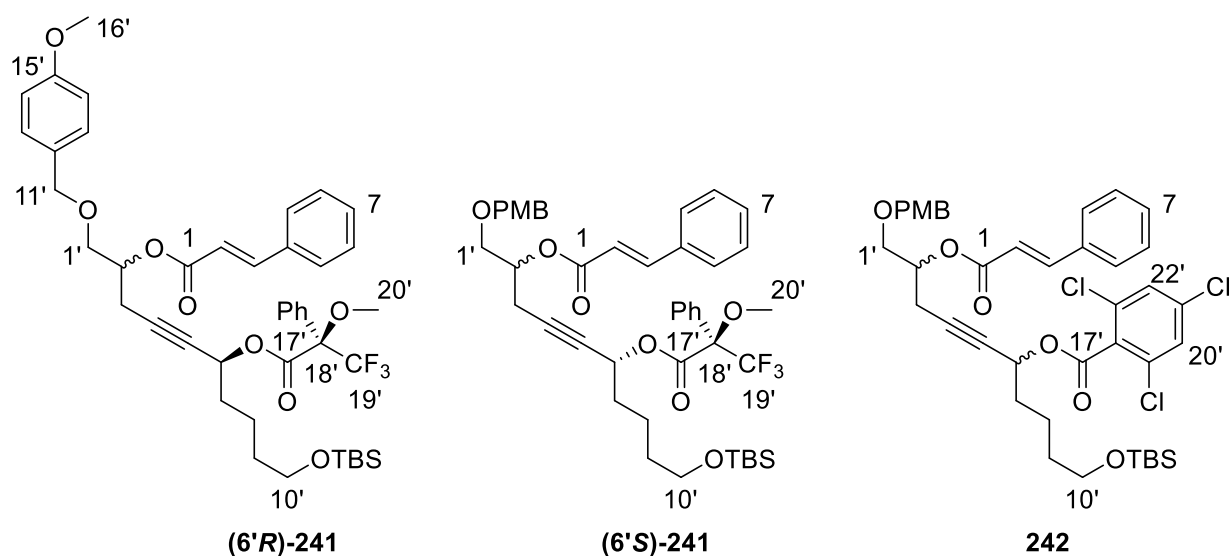
^{13}C NMR (126 MHz, CDCl_3): δ 166.3 (C, C1), 159.3 (C, C15'), 145.4 (CH, C3), 134.3 (C, C4), 130.4 (CH, C7), 129.9 (C, C12'), 129.4 (CH, C14'), 128.9 (CH, C6), 128.1 (CH, C5), 117.8 (CH, C2), 113.8 (CH, C13'), 83.5 (C, C5'), 80.3 (C, C4'), 73.0 (CH₂, C11'), 70.9 (CH, C2'), 69.3 (CH₂, C1'), 63.0 (CH₂, C10'), 62.5 (CH, C6'), 55.3 (CH₃, PMB), 37.7 (CH₂, C7'), 32.4 (CH₂, C9'), 26.0 (CH₃, *t*Bu, TBS), 21.5 (CH₂, C8'), 21.2 (CH₂, C3'), 18.3 (C, *t*Bu, TBS), -5.3 (CH₃, Me, TBS).

IR (neat) cm^{-1} : 3477 (br, O–H), 3190 (w, C–H), 2933 (m, C–H), 2857 (m, C–H), 1712 (s, C=O), 1637 (m, C–C), 1513 (m, C–C), 1388 (m, C–H), 1280 (m, C–H), 1248 (s, C–O), 1171 (s, C–O), 1095 (s, C–O), 1033 (s, C–O), 833 (s, C–Si), 767 (s, C–Si), 682 (C–H).

HRMS (ESI) m/z : found 605.2698, calcd for $\text{C}_{33}\text{H}_{46}\text{O}_6\text{SiK}$ $[\text{M}+\text{K}]^+$ 605.2695 ($\Delta = 0.5$ ppm).

Specific rotation: $[\alpha]_D^{21} = -0.51$ ($c = 1.36$, CH_2Cl_2).

Mosher's ester of alcohol **241** derived from alcohol **240** and **242**



To a solution of (*R*)-methoxy- α -(trifluoromethyl)phenylacetic acid (11 mg, 0.047 mmol) in toluene (0.2 mL, 0.24 M) at r.t., Et₃N (147 μ L, 107 mg, 1.06 mmol) and 2,4,6-trichlorobenzoyl chloride (12 μ L, 19 mg, 0.078 mmol) were added. After stirring at r.t. for 1 h 10 min, a solution of alcohol **240** (17 mg, 0.030 mmol) and DMAP (6 mg, 0.05 mmol) in toluene (0.2 mL) was added dropwise. The reaction was stirred for 20 h at r.t.. The solvent was removed under reduced pressure, and the crude product was purified by column chromatography (SiO₂, 5:1 Pet. ether:EtOAc, *R_f* = 0.33) to yield two fractions consisting of mixtures of isomeric products **241** and by-product **242** as colourless oils (The 11 mg sample contains more by-product **242**, and 3 mg with less **242**).

Table 5.1: Molar ratios of 6'*R*-**241**, 6'*S*-**241** and **242** in the 11 mg and 3 mg samples, calculated based on the ¹H NMR integrals of 2'-CH.

	Molar ratios of isomeric products 241 and by-product 242		
	(6' <i>R</i>)- 241	(6' <i>S</i>)- 241	242
11 mg sample	3	2	3
3 mg sample	3	2	1

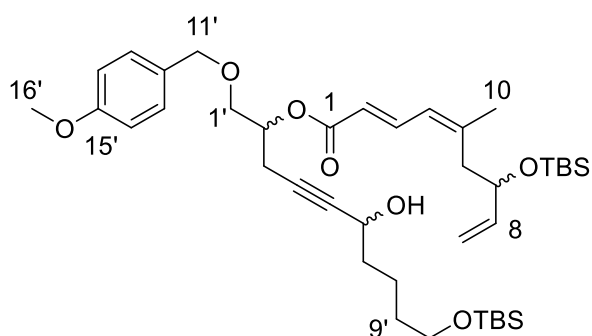
¹H NMR of the 3 mg sample (600 MHz, CDCl₃): δ 7.695 and 7.686 (2 \times d, *J* = 16.1 Hz, 0.17H, 3-CH-**242**), 7.690 and 7.677 (2 \times d, *J* = 16.1 Hz, 0.33H, 3-CH-(6'*S*)-**241**), 7.683 and 7.677 (2 \times d, *J* = 16.1 Hz, 0.50H, 3-CH-(6'*R*)-**241**), 7.56–7.50 (m, 1H, CH, Ph), 7.52–7.47 (m, 2H, CH, Ph), 7.31 (s, 0.17H, 20'/22'-CH-**242**), 7.30 (s, 0.17H, 20'/22'-CH-**242**), 7.41–7.35 (m, 5H, CH,

Ph), 7.27–7.22 2H (m, 1H, CH, Ph), 6.86 (d, $J = 8.6$ Hz, 2H, 13'-CH), 6.445 and 6.441 ($2 \times$ d, $J = 16.0$ Hz, 0.17H, 2-CH-**242**), 6.435 and 6.408 ($2 \times$ d, $J = 16.0$ Hz, 0.33H, 2-CH-(6'S)-**241**), 6.415 and 6.410 ($2 \times$ d, $J = 16.0$ Hz, 0.50H, 2-CH-(6'R)-**241**), 5.59 (t, $J = 6.9$ Hz, 0.17H, 6'-CH-**242**), 5.53–5.49 (m, 0.50H, 6'-CH-(6'R)-**241**), 5.49–5.46 (m, 0.33H, 6'-CH-(6'S)-**241**), 5.22–5.13 (m, 1H, 2'-CH), 4.55–4.43 (m, 2H, 11'-CH₂), 3.78 (s, 3H, 16'-CH₃), 3.55 (s, 1.5H, 20'-CH₃-(6'R)-**241**), 2.53 (s, 1.0H, 20'-CH₃-(6'S)-**241**), 3.72–3.61 (m, 2H, 1'-CH₂), 3.61–3.50 (m, 2H, 10'-CH₂), 2.76–2.60 (m, 2H, 3'-CH₂), 1.93–1.87 (m, 0.34H, 9'-CH₂-**242**), 1.87–1.82 (m, 0.66H, 9'-CH₂-(6'S)-**241**), 1.82–1.69 (m, 1.0H, 9'-CH₂-(6'R)-**241**), 1.57–1.47 (m, 0.34H, 7'-CH₂-**242** and 8'-CH₂-**242**), 1.48–1.40 (m, 3.32H, 7'-CH₂-(6'R) and (6'S)-**241** and 8'-CH₂-(6'R) and (6'S)-**241**), 0.873 and 0.869 and 0.866 (s, 9H, *t*Bu, TBS), 0.027 and 0.018 and 0.011 (s, 6H, Me, TBS)

¹³C NMR (150 MHz, CDCl₃) δ 166.16 and 166.14 (C, C1), 165.71 and 165.70 and 165.64 and 165.63 (C, C17'), 163.7 (CH, C6'), 159.24 and 159.22 (C, C15'), 145.43 and 145.42 and 145.38 (CH, C3-(6'R) and (6'S)-**241**), 145.33 and 145.31 (CH, C3-**242**), 135.04 and 134.40 (C, C18'/C19'/21'-**242**), 134.30 and 134.29 (C, C4-**242**), 134.26 and 134.25 and 134.23 and 134.21 (C, C4-(6'R) and (6'S)-**241**), 132.68 (C, C18'/19'/21'-**242**), 132.42 (C, Ph), 132.32 (C, Ph), 131.98 (C, Ph), 131.76 and 131.75 (C, C18'/C19'/21'-**242**), 130.40 and 130.38 and 130.36 (CH, Ph), 129.93 and 129.89 and 129.87 and 129.85 and 129.84 (C, C12'), 129.60 (CH, Ph), 129.30 (CH, Ph), 128.86 (CH, Ph), 128.37 and 128.35 and 128.34 (CH, Ph), 128.18 and 128.13 and 128.12 (CH, Ph), 127.98 and 127.97 (CH, C20'-**242**), 127.44 and 127.30 (CH, Ph), 117.81 and 117.80 and 117.72 and 117.71 and 117.68 and 117.65 (CH, C2), 113.77 and 113.77 and 113.76 (CH, C13'), 82.39 and 82.38 (C, C4'-(6'R)-**241**), 82.24 and 82.23 (C, C4'-(6'S)-**241**), 82.21 (C, C4'-**242**), 78.73 and 78.72 (C, C5'-**242**), 78.62 and 78.60 (C, C5'-(6'R)-**241**), 78.44 and 78.43 (C, C5'-(6'S)-**241**), 73.04 and 73.02 (CH₂, C11'), 70.61 and 70.59 and 70.51 and 70.49 and 70.48 (CH, C2'), 69.31 and 69.22 and 69.21 and 69.17 and 69.15 (CH₂, C1'), 66.7 (CH, C6'-(6'R) and (6'S)-**241**), 66.37 and 66.34 (CH, C6'-**242**), 62.79 and 62.73 (CH₂, C10'), 55.49 and 55.44 (CH₃, C20'-(6'R) and (6'S)-**241**), 55.2 (CH₃, C16'), 34.58 and 34.41 and 34.39 (CH₂, C9'), 32.15 and 32.10 and 32.02 (CH₂, C7'), 25.94 and 25.92 (CH₃, *t*Bu, TBS), 21.55 and 21.45 and 21.26 and 21.20 (CH₂, C8'), 21.14 and 21.13 and 21.09 and 21.06 (CH₂, C3'), 18.32 and 18.30 (C, *t*Bu, TBS), -5.31 and -5.34 (CH₃, Me, TBS).

HRMS (ESI) m/z : **241** found 800.3815, calcd for C₄₃H₅₇F₃O₈SiN [M+NH₄]⁺ 800.3800 ($\Delta = 1.9$); **242** found 811.1802, calcd for C₄₀H₅₇³⁵Cl₃O₇SiK [M+K]⁺ 811.1788 ($\Delta = 1.8$ ppm).

1'-(*para*-Methoxybenzyloxy)-6'-hydroxy-10'-(*t*-butyldimethylsilyloxy)dec-4'-yn-2'-yl 5-methyl-7-(*t*-butyldimethylsilyloxy)non-2,4,8-trienoate (244**)**



To a solution of **208** (48 mg, 0.096 mmol), (*R,R*)-ProPhenol (12 mg, 0.019 mmol) and TPPO (11 mg, 0.038 mmol) in toluene (0.25 mL) at r.t., a solution of Et₂Zn (0.11 mL, 1.0 M in cyclohexane, 0.11 mmol) was added dropwise. The reaction was stirred for 71 h, and a solution of aldehyde **177** (26 mg, 0.120

mmol) in toluene (0.1 mL) was added dropwise. After stirring for 23 h at r.t., the reaction was quenched with sat. aq. NH₄Cl (10 mL), and extracted with CH₂Cl₂ (3 × 20 mL). The organic layers were combined, dried over MgSO₄ and concentrated under reduced pressure. The crude product was purified by column chromatography (SiO₂, gradient elution: 20:1 then 10:1 then 5:1 Pet. ether:EtOAc, then 100% EtOAc, R_f = 0.15 in 5:1 Pet. ether:EtOAc). Unsatisfactory separation was achieved, and the mixture containing the majority of the desired product isomers (11mg) were further purified by column chromatography (SiO₂, 100% CH₂Cl₂, R_f = 0.06) to yield the product as a colourless, clear oil (3 mg, 4% yield). Evidence of a trace amount of the 2*Z*-isomer of **244** was observed. Due to the complexity of the mixture and the weak signals from the minor compounds, only the signals of the major compound were quoted below.

¹H NMR (600 MHz, CDCl₃): δ 7.57 (dd, *J* = 15.0, 11.5 Hz, 1H, 3-CH), 7.25 (d, *J* = 7.5 Hz, 2H, 14'-CH), 6.87 (d, *J* = 7.2 Hz, 2H, 13'-CH), 6.06 (d, *J* = 11.6 Hz, 1H, 4-CH), 5.86–5.73 (m, 1H, 8-CH), 5.79 (d, *J* = 15.0 Hz, 1H, 2-CH), 5.17 (d, *J* = 17.4 Hz, 1H, one of 9-CH₂), 5.22–5.10 (m, 1H, 2'-CH), 5.04 (d, *J* = 10.3 Hz, 1H, one of 9-CH₂), 4.53 (d, *J* = 11.9 Hz, 1H, one of 11'-CH₂), 4.47 (d, *J* = 11.5 Hz, 1H, one of 11'-CH₂), 4.29 (app. q, *J* = 5.7 Hz, 1H, 6'-CH), 4.24 (app. q, *J* = 6.7 Hz, 1H, 7-CH), 3.80 (s, 3H, 16'-CH₃), 3.69–3.54 (complex m, 4H, 1'-CH₂ and 10'-CH₂), 2.69–2.52 (complex m, 3H, 6-CH₂ and one of 3'-CH₂), 2.40–2.30 (m, 1H, one of 3'-CH₂), 1.91 (s, 3H, 10-CH₃), 1.80–1.29 (complex m, 6H, 7'-CH₂, 8'-CH₂ and 9'-CH₂), 0.94–0.81 (m, 18H, TBS), 0.08– -0.02 (m, 12H, TBS).

¹³C NMR (150 MHz, CDCl₃): δ 166.8 (C, C1), 159.2 (C, C15'), 146.8 (C, C5), 141.9 (CH, C3), 140.89 and 140.87 and 140.85 (CH, C8), 130.0 (C, C12'), 129.3 (CH, C13'), 126.1 (CH, C4), 118.7 (CH, C2), 114.2 (CH₂, C9), 113.7 (CH, C14'), 83.3 (C, C5'), 80.46 and 80.45 (C, C4'), 72.9 (CH₂, C11'), 72.79 and 72.77 (CH, C7), 70.45 and 70.43 (CH, C2'), 69.31 and 69.27 (CH₂,

C1'), 63.0 (CH₂, C10'), 62.5 (CH, C6'), 55.3 (CH₃, C16'), 41.7 (CH₂, C6), 37.7 (CH₂, C7'), 32.4 (CH₂, C9'), 26.0 and 25.8 (CH₃, *t*Bu, TBS), 25.6 and 25.5 (CH₃, C10), 21.5 (CH₂, C8'), 21.2 (CH₂, C3'), 18.4, and 18.3 (C, *t*Bu, TBS), -4.6 and -4.9 and -5.27 and -5.33 (CH₃, Me, TBS).

HRMS (ESI) *m/z*: found 715.4453, calcd for C₄₀H₆₇O₇Si₂ [M+H]⁺ 715.4420 (Δ = 4.6 ppm).

5.5 References

- (1) Mosey, R. A.; Floreancig, P. E. *Nat. Prod. Rep.* **2012**, 29, 980.
- (2) Bielitz, M.; Pietruszka, J. *Angew. Chem. Int. Ed.* **2013**, 52, 10960.
- (3) Halli, J.; Hofman, K.; Beisel, T.; Manolikakes, G. *Eur. J. Org. Chem.* **2015**, 4624.
- (4) Zhang, Y.; Dai, Y.; Li, G.; Cheng, X. *Synlett* **2014**, 25, 2644.
- (5) Bayer, A.; Maier, M. E. *Tetrahedron* **2004**, 60, 6665.
- (6) Kiren, S.; Shangguan, N.; Williams, L. J. *Tetrahedron Lett.* **2007**, 48, 7456.
- (7) Cergol, K. M.; Coster, M. J. *Nature Protocols* **2007**, 2, 2568.
- (8) Brown, H. C.; Ayyangar, N. R.; Zweifel, G. *J. Am. Chem. Soc.* **1964**, 86, 1071.
- (9) Chandrasekharan, J.; Ramachandran, P. V.; Brown, H. C. *J. Org. Chem.* **1985**, 50, 5446.
- (10) Zhao, M. Z.; King, A. O.; Larsen, R. D.; Verhoeven, T. R.; Reider, P. J. *Tetrahedron Lett.* **1997**, 38, 2641.
- (11) Troast, D. M.; Porco, J. A. *Org. Lett.* **2002**, 4, 991.
- (12) Uyanik, M.; Suzuki, D.; Yasui, T.; Ishihara, K. *Angew. Chem. Int. Ed.* **2011**, 50, 5331.
- (13) Wu, X. F.; Gong, J. L.; Qi, X. X. *Org. Biomol. Chem.* **2014**, 12, 5807.
- (14) Kano, T.; Mii, H.; Maruoka, K. *J. Am. Chem. Soc.* **2009**, 131, 3450.
- (15) Gotoh, H.; Hayashi, Y. *Chem. Commun.* **2009**, 3083.
- (16) Ghosh, A. K.; Cheng, X.; Bai, R.; Hamel, E. *Eur. J. Org. Chem.* **2012**, 4130.
- (17) Ding, F.; Jennings, M. P. *Org. Lett.* **2005**, 7, 2321.
- (18) Uenishi, J.; Iwamoto, T.; Tanaka, J. *Org. Lett.* **2009**, 11, 3262.
- (19) Zurwerra, D.; Gertsch, J.; Altmann, K. H. *Org. Lett.* **2010**, 12, 2302.
- (20) Ghosh, A. K.; Cheng, X. *Org. Lett.* **2011**, 13, 4108.
- (21) Zurwerra, D.; Glaus, F.; Betschart, L.; Schuster, J.; Gertsch, J.; Ganci, W.; Altmann, K. H. *Chem.-Eur. J.* **2012**, 18, 16868.

- (22) Sanchez, C. C.; Keck, G. E. *Org. Lett.* **2005**, 7, 3053.
- (23) Louis, I.; Hungerford, N. L.; Humphries, E. J.; McLeod, M. D. *Org. Lett.* **2006**, 8, 1117.
- (24) Yun, S. Y.; Hansen, E. C.; Volchkov, I.; Cho, E. J.; Lo, W. Y.; Lee, D. *Angew. Chem. Int. Ed.* **2010**, 49, 4261.
- (25) Nakajima, N.; Abe, R.; Yonemitsu, O. *Chem. Pharm. Bull.* **1988**, 36, 4244.
- (26) A. E. J. Nooy, A. C. Besemer, H. van Bekkum, *Synthesis* **1996**, 10, 1153.
- (27) Okhlobys.O. Y.; Zakharki.L. I. *J. Organomet. Chem.* **1965**, 3, 257.
- (28) Trost, B. M.; Weiss, A. H. *Adv. Synth. Catal.* **2009**, 351, 963.
- (29) Trost, B. M.; Bartlett, M. J.; Weiss, A. H.; von Wangelin, A. J.; Chan, V. S. *Chem.-Eur. J.* **2012**, 18, 16498.
- (30) Trost, B. M.; Michaelis, D. J.; Malhotra, S. *Org. Lett.* **2013**, 15, 5274.
- (31) Moore, D.; Pu, L. *Org. Lett.* **2002**, 4, 1855.
- (32) Lu, G.; Li, X. S.; Chan, W. L.; Chan, A. S. C. *Chem. Commun.* **2002**, 172.
- (33) Gao, G.; Xie, R. G.; Pu, L. *P. Natl. Acad. Sci. USA* **2004**, 101, 5417.
- (34) Yang, F.; Xi, P. H.; Yang, L.; Lan, J. B.; Xie, R. G.; You, J. S. *J. Org. Chem.* **2007**, 72, 5457.
- (35) Du, Y. H.; Turlington, M.; Zhou, X. A.; Pu, L. *Tetrahedron Lett.* **2010**, 51, 5024.
- (36) Chen, S. Y.; Liu, W. N.; Wu, X. D.; Ying, J.; Yu, X. Q.; Pu, L. *Chem. Commun.* **2015**, 51, 358.
- (37) Frantz, D. E.; Fassler, R.; Carreira, E. M. *J. Am. Chem. Soc.* **1999**, 121, 11245.
- (38) Anand, N. K.; Carreira, E. M. *J. Am. Chem. Soc.* **2001**, 123, 9687.
- (39) Boyall, D.; Frantz, D. E.; Carreira, E. M. *Org. Lett.* **2002**, 4, 2605.
- (40) Archambaud, S.; Legrand, F.; Aphecetche-Julienne, K.; Collet, S.; Guingant, A.; Evain, M. *Eur. J. Org. Chem.* **2010**, 1364.
- (41) Sabitha, G.; Bhikshapathi, M.; Ranjith, N.; Ashwini, N.; Yadav, J. S. *Synthesis* **2011**, 821.
- (42) Mahapatra, S.; Carter, R. G. *J. Am. Chem. Soc.* **2013**, 135, 10792.
- (43) Williams, B. D.; Smith, A. B. *J. Org. Chem.* **2014**, 79, 9284.
- (44) Blundell, D.; New Zealand ministry of health, Ed.; Parliamentary counsel office: **1977**.
- (45) Kirkham, J. E. D.; Courtney, T. D. L.; Lee, V.; Baldwin, J. E. *Tetrahedron* **2005**, 61, 7219.

- (46) Takita, R.; Yakura, K.; Ohshima, T.; Shibasaki, M. *J. Am. Chem. Soc.* **2005**, *127*, 13760.
- (47) Jiang, B.; Chen, Z. L.; Xiong, W. N. *Chem. Commun.* **2002**, 1524.
- (48) Lombard, J.; Romain, S.; Dumas, S.; Chauvin, J.; Collomb, M. N.; Daveloose, D.; Deronzier, A.; Lepretre, J. C. *Eur. J. Inorg. Chem.* **2005**, 3320.
- (49) Pine, S. H.; Sanchez, B. L. *J. Org. Chem.* **1971**, *36*, 829.
- (50) Gibson, H. W. *Chem. Rev.* **1969**, *69*, 673.
- (51) Li, Z.; Upadhyay, V.; DeCamp, A. E.; DiMichele, L.; Reider, P. J. *Synthesis* **1999**, 1453.
- (52) Seco, J. M.; Quinoa, E.; Riguera, R. *Chem. Rev.* **2004**, *104*, 17.
- (53) Dale, J. A.; Dull, D. L.; Mosher, H. S. *J. Org. Chem.* **1969**, *34*, 2543.
- (54) Hoye, T. R.; Jeffrey, C. S.; Shao, F. *Nat. Protoc.* **2007**, *2*, 2451.
- (55) Tran, H. A.; Kitov, P. I.; Paszkiewicz, E.; Sadowska, J. M.; Bundle, D. R. *Org. Biomol. Chem.* **2011**, *9*, 3658.
- (56) Otera, J.; Nishikido, J. *Esterification: Methods, Reactions, and Applications*; John Wiley & Sons: Weinheim, Germany, **2010**.
- (57) Sigma-Aldrich compound data for triethylamine hydrochloride, #90350.
- (58) Fanning, K. N.; Jamieson, A. G.; Sutherland, A. *Org. Biomol. Chem.* **2005**, *3*, 3749.
- (59) Pacheco, M. C.; V, Gouverneur. *Org. Lett.* **2005**, *7*, 1267.

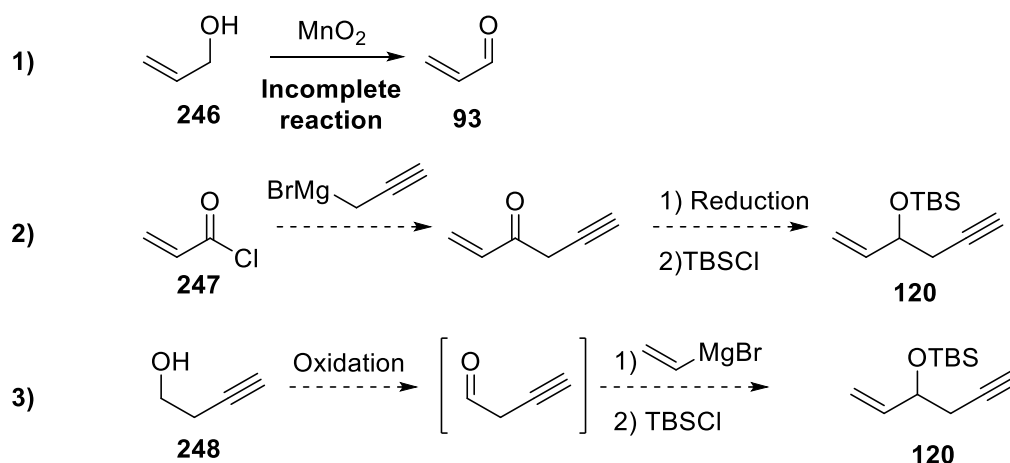
Chapter 6: Summary and Future work

In this project, progress was made towards the synthesis of zampanolide (**19**) and its analogues. According to the first-generation synthetic plan, precursors to fragments C1-C8, C9-C15, C16-C20 and a des-methyl analogue of the C1-C8 fragment were successfully synthesized. However, some difficulties were encountered in advancing the precursors to the desired fragments, namely in protection at the O19 position, incomplete Wittig reaction to construct the C2-C3 alkene and oxidation at C15 of the C9-C15 precursor to aldehyde. The synthesis was then revised, and a more efficient second-generation synthesis utilizing a linchpin approach was developed. This was made possible by the use of Bestmann ylide as a linchpin. This is an expanded application of Bestmann ylide, therefore the scope of the Bestmann ylide reaction to construct $\alpha,\beta,\gamma,\delta$ -unsaturated esters (dienoates) was explored, and it was successfully applied to the coupling of the C3-C8 (**127**) and C15-C20 (**147** and **153**) fragments. Late stage strategies were also tested on model compounds, including the side-arm attachment *via* aza-aldol reaction with chiral boron reagents, oxidation of the C20 alcohol to an aldehyde and C15-C16 alkynylation of aldehydes. Although more research is required, an alkynylation method was found to produce a small amount of the desired product **244**, which established 16 out of the 18 carbons of the macrocycle.

Research to optimize the asymmetric alkynylation is already underway, and the alkynylation product **244** will be transformed to an analogue macrocycle using the methods outlined in chapter 3, or a truncated simplified macrocycle in four steps. An alternative route to the C3-C8 fragment (**127**) is also necessary, due to the scarce supply of the starting material acrolein (**93**).

6.1 Alternatives to the acrolein-dependent C3-C8 fragment

An alternative method for the synthesis of C3-C8 fragment is required, because of the environmental and safety hazards that acrolein (**93**) possesses, and the fact that its supply is now expensive and unreliable. Synthesis of **93** from allyl alcohol (**246**) was briefly attempted (Scheme 6.1, equation 1). To minimise handling of the highly volatile and toxic **93**, oxidation of allyl alcohol (**246**) with MnO_2 in THF was performed in the hope that, after a simple filtration, the acrolein (**93**) solution in THF could be used directly for reaction. However, only a small amount of the allyl alcohol was converted to acrolein (**93**), and an attempt to purify **93** by distillation did not provide satisfying separation from **246**, while loss of product occurred even though the collection vessel was kept at 0 °C.

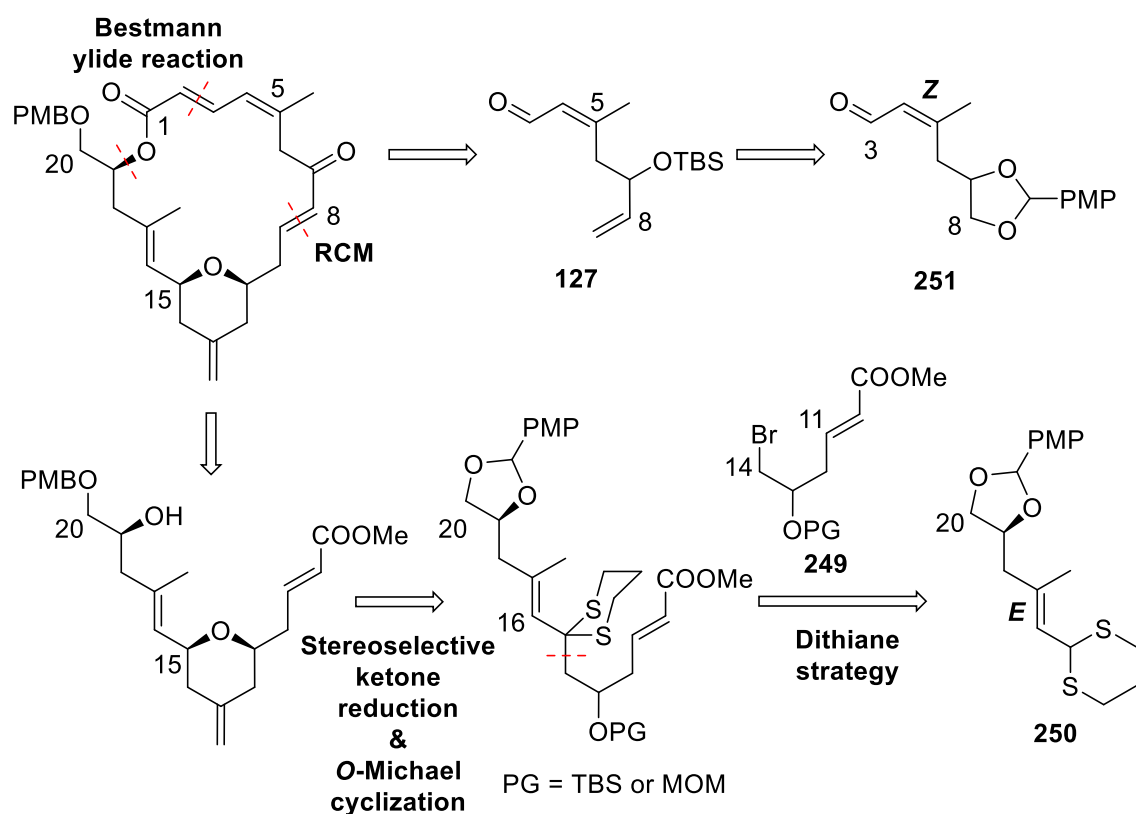


Scheme 6.1: Alternative synthesis of the C3-C8 fragment precursor **120**.

Acryloyl chloride (**247**) was then considered as a starting material, where the chloride can be substituted by a propargyl group. Upon reduction of the ketone and silyl protection, the precursor to C3-C8 fragment, **120**, would be produced (Scheme 6.1, equation 2). One foreseen problem in this sequence is that the reaction of the acyl halide is prone to disubstitution, and reaction conditions to minimise the disubstitution can be hard to find. In addition, no commercial supply and little literature precedence was found on the production of the propargyl Grignard reagent, so it could be hard to obtain. Preparation of **120** from but-3-yn-1-ol (**248**) via a one-pot oxidation and vinyl addition reaction followed by silyl protection was also planned (equation 3). Possible oxidation methods include Swern and TEMPO/BAIB oxidation.

6.2 A new strategy involving a dithiane at C15

Introduced in Chapter 1, dithiane has long been a well-established linchpin, that can be converted to a carbonyl group upon oxidative cleavage. As a protecting group, dithiane allows umpolung-type reactions, where the electrophilic carbon of the carbonyl is converted into a nucleophile. As shown in **Scheme 6.2**, an approach using a dithiane for the C15 position, together with RCM and the Bestmann ylide linchpin, can lead retrosynthetically to fragments C3-C8 (**127**), C10-C14 (**249**) and C15-C20 (**250**). As discussed in section 3.1, a TBS or MOM-protecting group would be used in fragment **249**. The MOM-protected variant of **249** has been previously reported, and the TBS-protected variant can be prepared *via* a similar strategy.¹

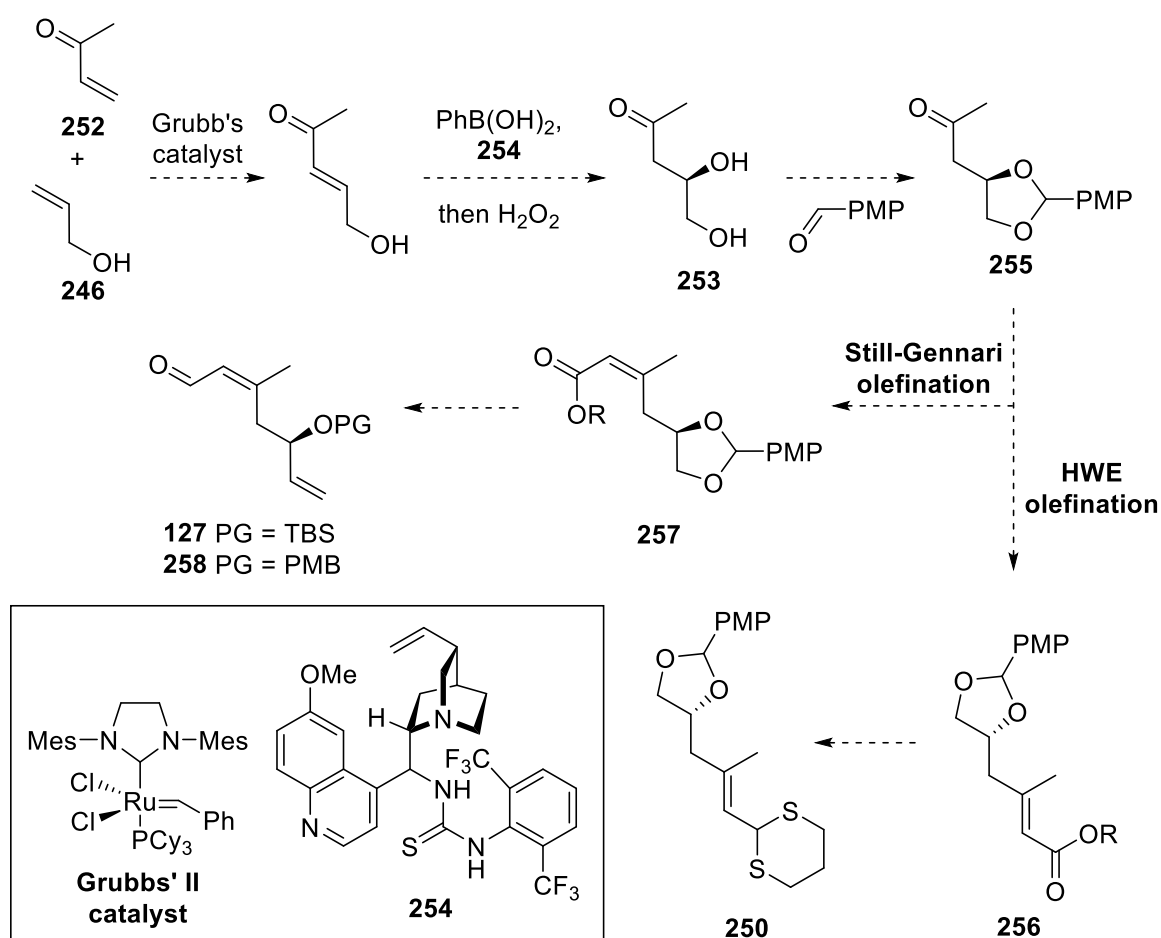


Scheme 6.2: Proposed dithiane approach in retrosynthetic analysis.

Interestingly, the above analysis revealed a symmetry in zampanolide macrocycle, where the C16-C20 fragment (**250**) is structurally similar to an alternative precursor of the C3-C8 fragment, **251**. Therefore, the two fragments **127** and **250** could be synthesized *via* the same route with late stage modification. This convergent synthesis would improve the efficiency of

the synthesis greatly. This strategy cannot be applied using the current precursors to the tetrahydropyran fragments. With the hope this would also lead to an alternative route to fragment C3-C8 (**127**), literature research on the fragment synthesis of this new synthetic plan was carried out.

A divergent synthesis of the C3-C8 and C16-C20 fragments from a common intermediate is theoretically possible. The synthesis can start with a cross-metathesis between the cheap and readily available 3-buten-2-one (**252**) and allyl alcohol (**246**) (**Scheme 6.3**). Grubbs' second generation catalyst can be used for this reaction, because it was reported to promote *E*-selective



Scheme 6.3: Divergent synthesis of fragments **127** and **250**.

cross-metathesis in the presence of unprotected allyl alcohols.² An asymmetric *O*-Michael reaction, achieved by treatment with phenylboronic acid and hydrogen peroxide, can then be carried out to produce diol **253**. This process is facilitated and directed by interaction of the boron reagent with the allylic hydroxyl and chiral amine base **254**.³ After protecting the diol

253 as a PMP-acetal (**255**),⁴ *E*- and *Z*-selective olefination of the ketone **255** can be used to diverge the synthesis to intermediates **256** and **257**. Olefination is a well-explored strategy with a lot of methods available, and can be stereoselective for *Z*- or *E*-alkenes.⁵ The Horner-Wadsworth-Emmons (HWE) olefination is reliable and employs readily available reagents. In general, this olefination favours the formation of *E*-alkenes, and the use of methylmagnesium bromide as the base was reported to improve the *E*-selectivity greatly.⁶ To achieve *Z*-selectivity, Still-Gennari's modification of the HWE olefination using bis(2,2,2-trifluoroethyl) phosphonates can be used.⁷ Both HWE olefination and Still-Gennari's method have been explored mostly on aldehyde substrates. In case that the ketone substrates in this study do not achieve the required stereoselectivity, chromatographic separation of the *E*- and *Z*-products would be employed. The *E*-isomer **256** would need to be reduced to an aldehyde before the dithiane protection to produce the required fragment **250**. The *Z*-isomer **257** can lead to fragment C3-C8 by regioselective acetal ring-opening, oxidation and a Wittig reaction to establish the terminal alkene, followed by conversion of the ester to an aldehyde. Changing the PMB group to a TBS ether would deliver the current C3-C8 fragment **127**, although retaining the PMB group in **258** would also be compatible with the end-game strategy.

Following the procedure described, synthesis of both C3-C8 and C15-C20 fragments can be achieved from a common precursor. The nucleophilic substitution of the bromide **249** by a dithiane anion and the subsequent *O*-Michael addition leads to an alternative route to the pyran fragment. The Bestmann ylide linchpin reaction studied in this thesis and the well-established ring-closing metathesis provide an end-game strategy to complete the synthesis of the zampanolide macrocycle, which is compatible with both the current alkynylation and the proposed dithiane approaches.

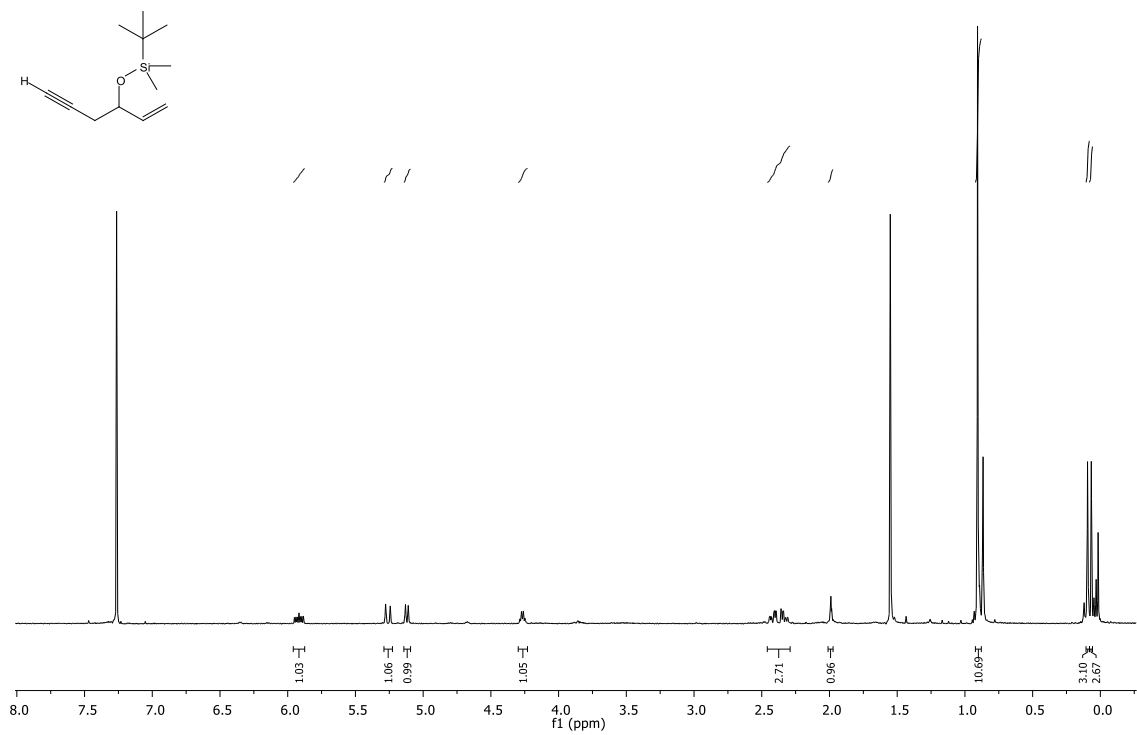
6.3 References

- (1) Lin, W. M.; Zercher, C. K. *J. Org. Chem.* **2007**, 72, 4390.
- (2) Engelhardt, F. C.; Schmitt, M. J.; Taylor, R. E. *Org. Lett.* **2001**, 3, 2209.
- (3) Li de, R.; Murugan, A.; Falck, J. R. *J. Am. Chem. Soc.* **2008**, 130, 46.

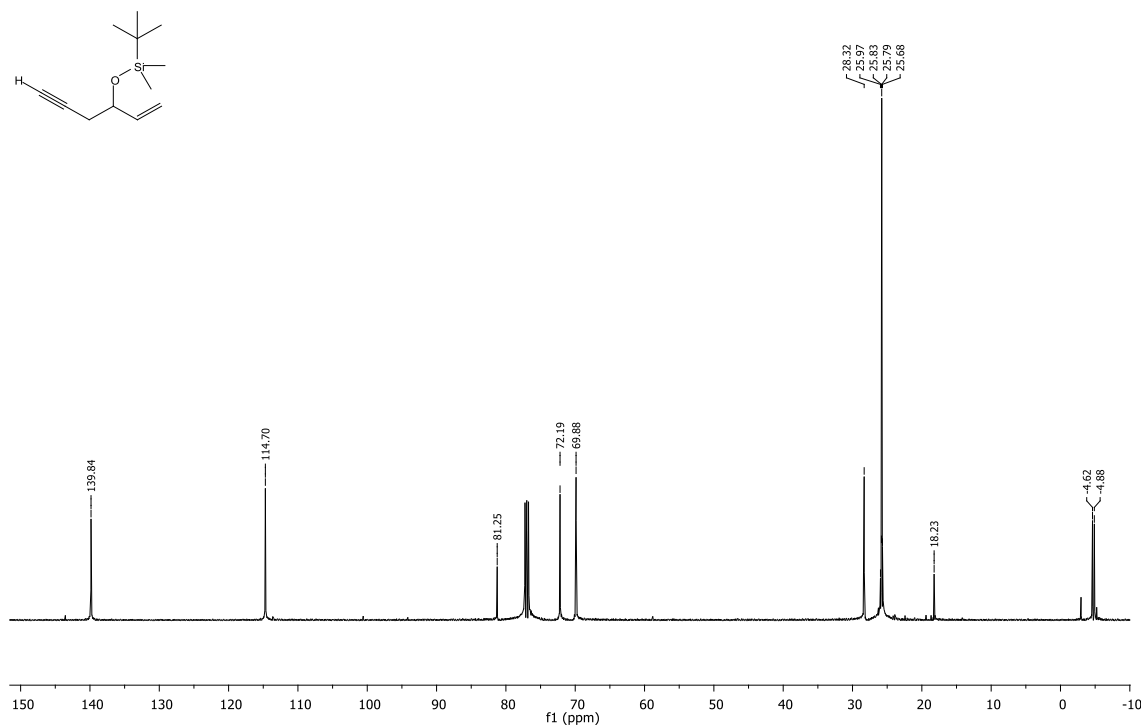
- (4) Wuts, P. G. M.; Greene, T. W. *Greene's protective groups in organic synthesis* 4th ed.; Wiley-Interscience Hoboken, N.J, **2007**.
- (5) Takeda, T. *Modern carbonyl olefination: methods and applications*; WILEY-VCH Verlag GmbH & Co. KGaA: Weinheim, **2004**.
- (6) Claridge, T. D. W.; Davies, S. G.; Lee, J. A.; Nicholson, R. L.; Roberts, P. M.; Russell, A. J.; Smith, A. D.; Toms, S. M. *Org. Lett.* **2008**, *10*, 5437.
- (7) Still, W. C.; Gennari, C. *Tetrahedron Lett.* **1983**, *24*, 4405.

Appendix: NMR spectra

(Hex-1-en-5-yn-3-yloxy)*tert*-butyldimethylsilane (**118**)

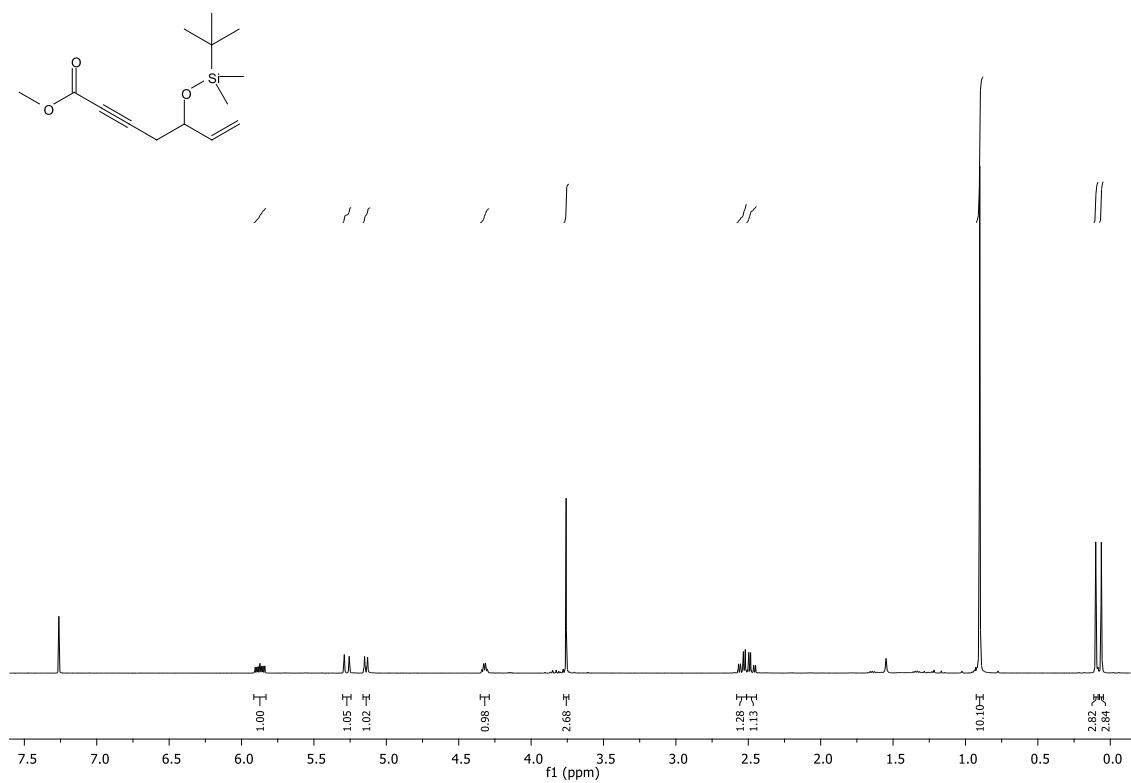


¹H NMR (500 MHz, CDCl₃) spectrum of **118**

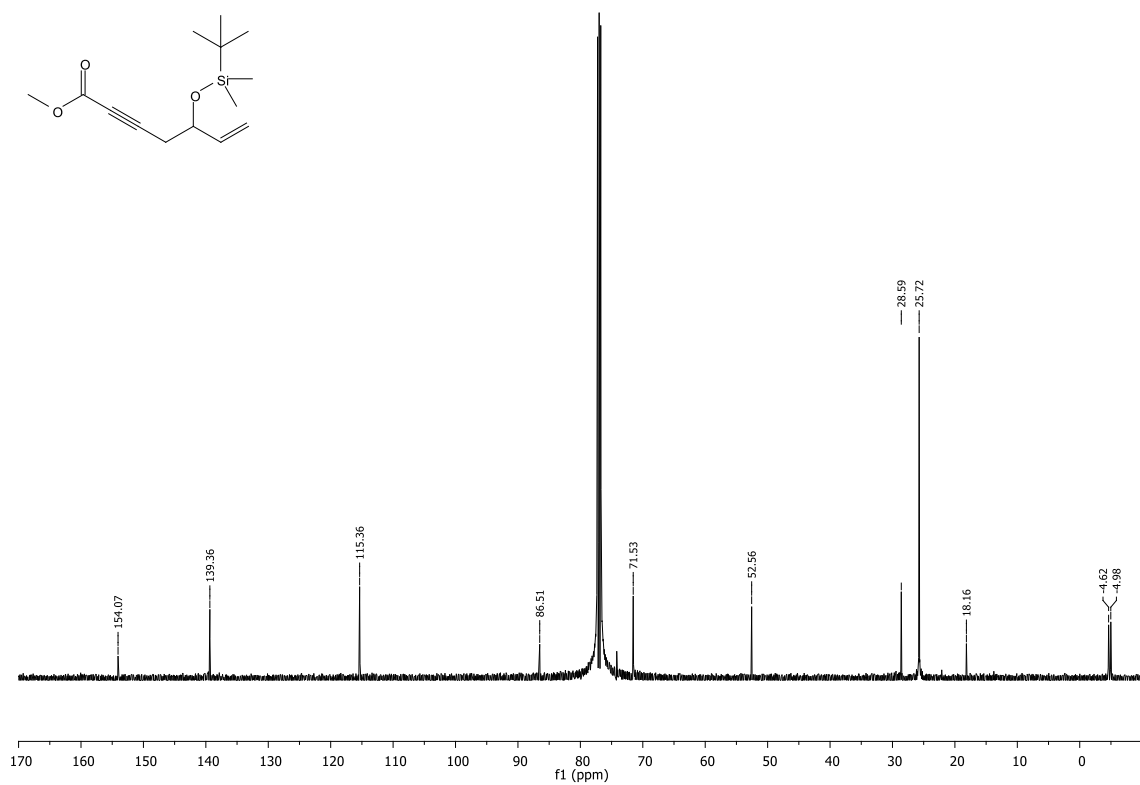


¹³C NMR (125 MHz, CDCl₃) spectrum of **118**

Methyl 5-*tert*-butyldimethylsilyloxy-6-hepten-2-ynoate (119)

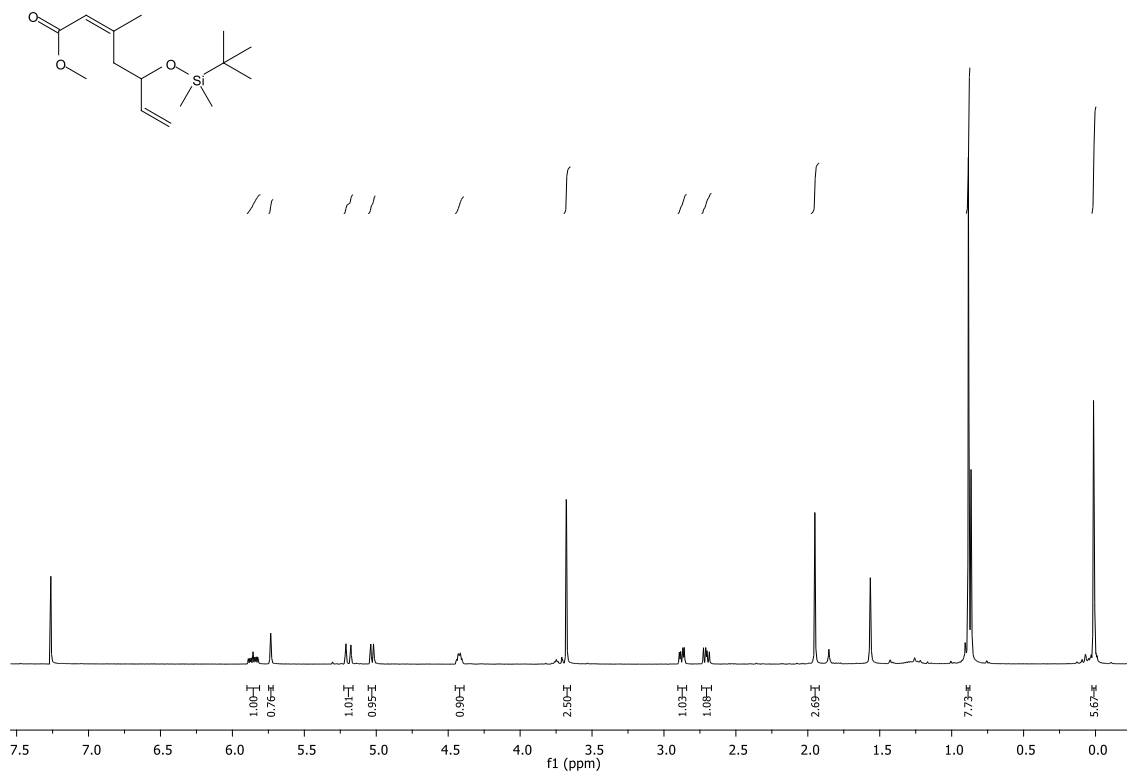


¹H NMR (500 MHz, CDCl₃) spectrum of **119**

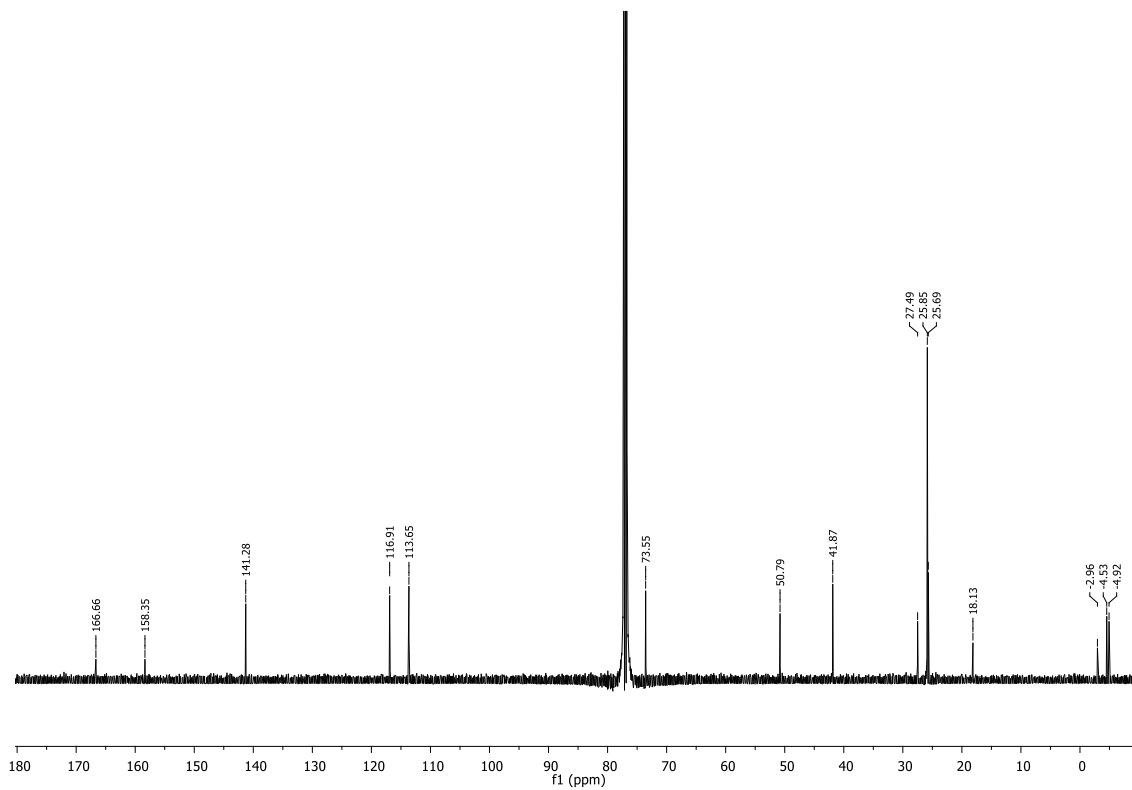


¹³C NMR (125 MHz, CDCl₃) spectrum of **119**

(2Z)-Methyl 5-(*tert*-butyldimethylsilyloxy)-3-methyl-2,6-heptadienoate (125)

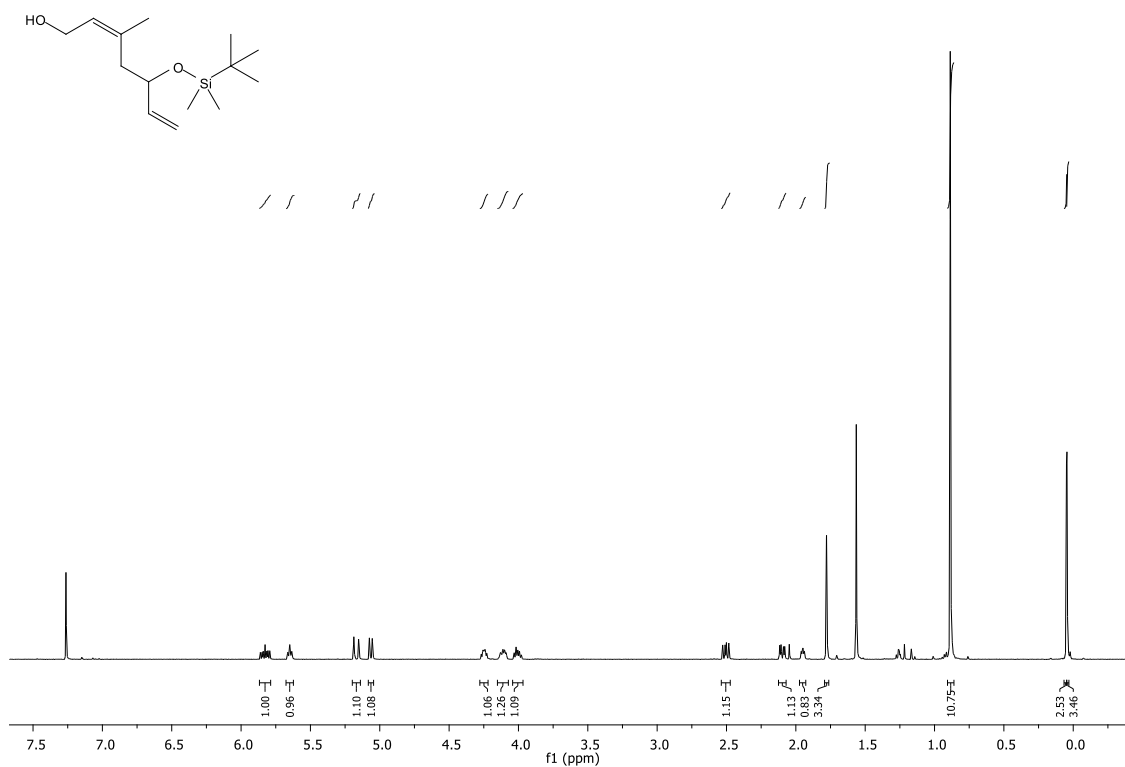


^1H NMR (500 MHz, CDCl_3) spectrum of **125**

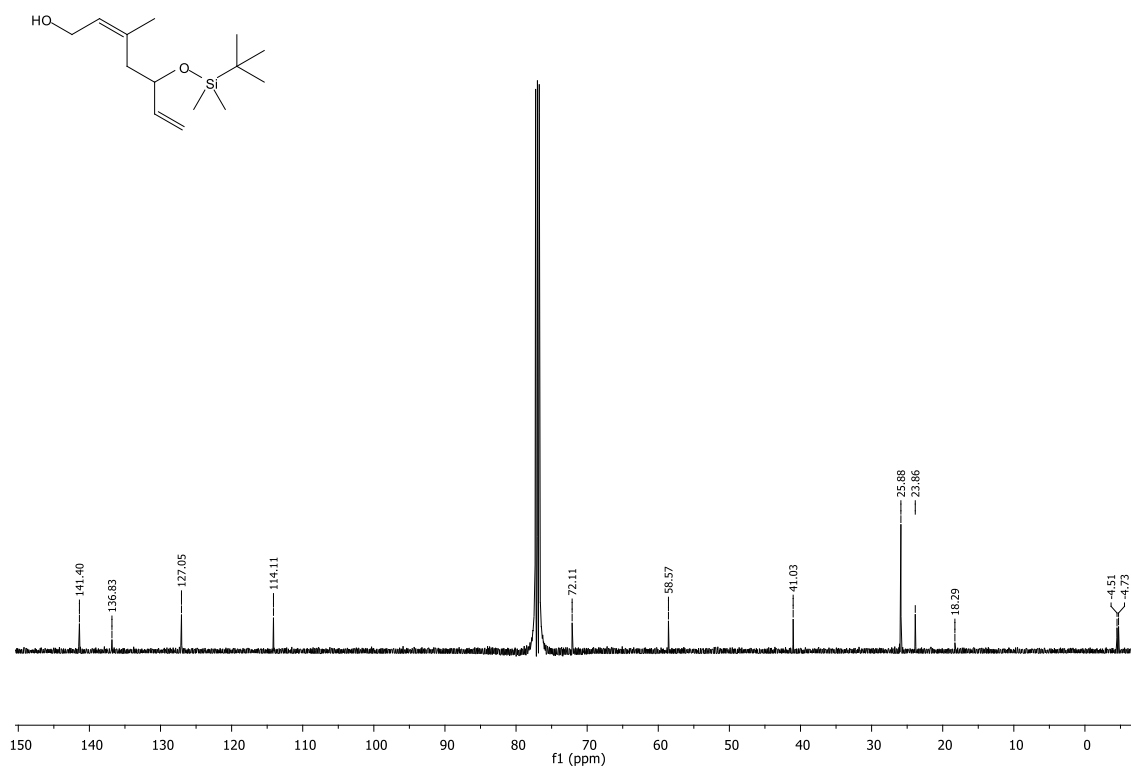


^{13}C NMR (125 MHz, CDCl_3) spectrum of **125**

(2Z)-3-Methyl-5-(*tert*-butyldimethylsilyloxy)hepta-2,6-dien-1-ol (128)

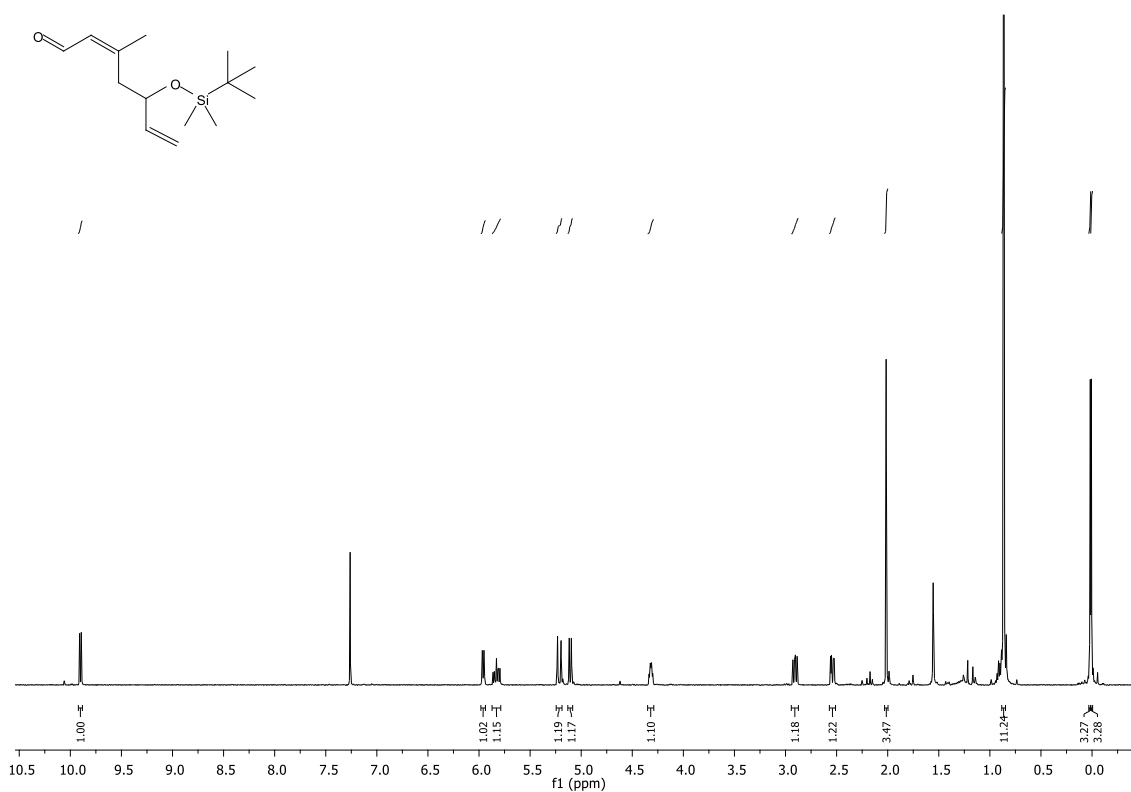


¹H NMR (500 MHz, CDCl₃) spectrum of **128**

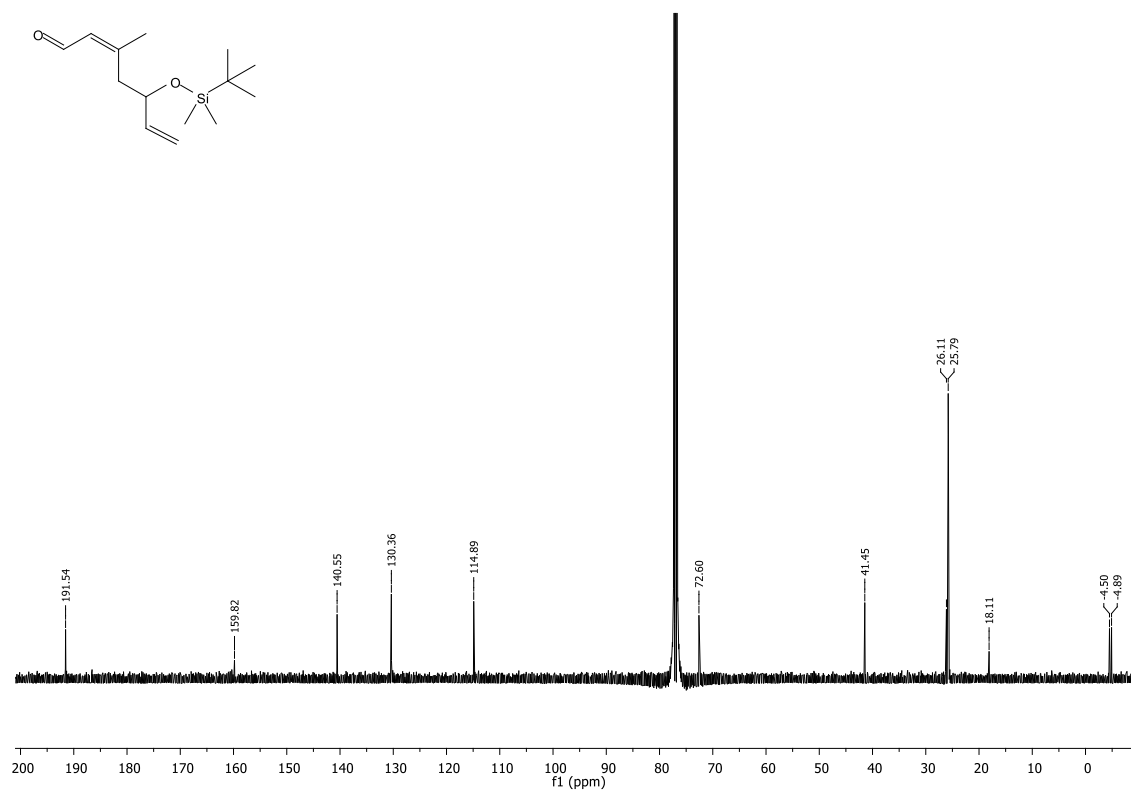


¹³C NMR (125 MHz, CDCl₃) spectrum of **128**

(2Z)-3-Methyl-5-(*tert*-butyldimethylsilyloxy)hepta-2,6-dienal (126)

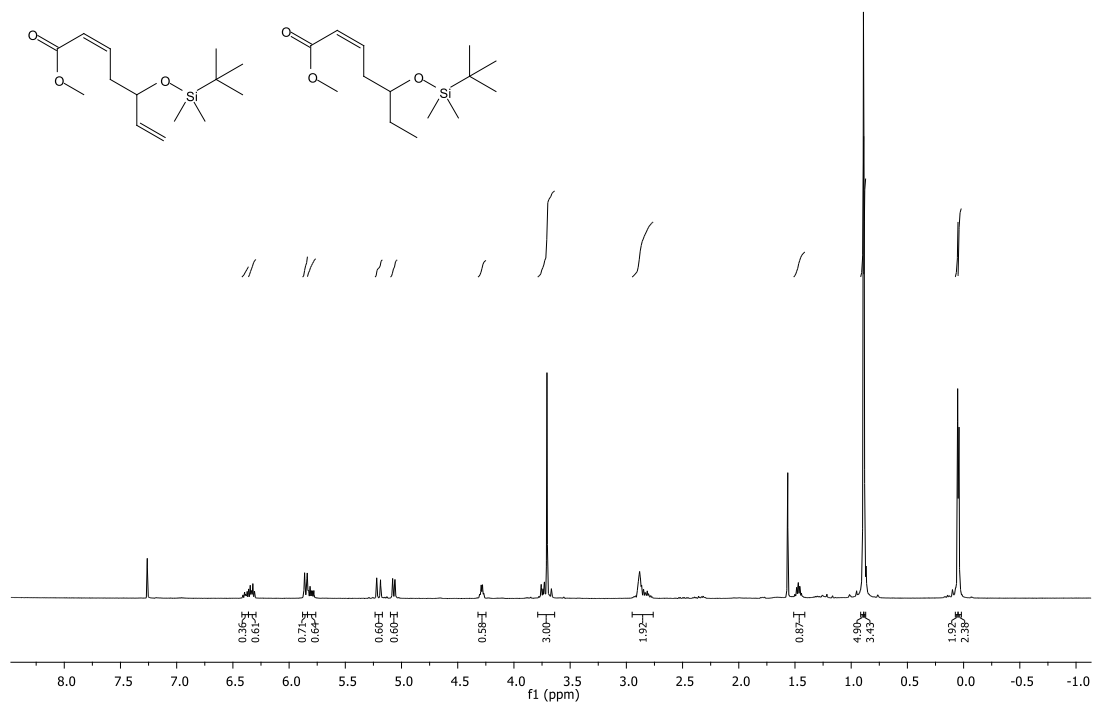


¹H NMR (500 MHz, CDCl₃) spectrum of **126**

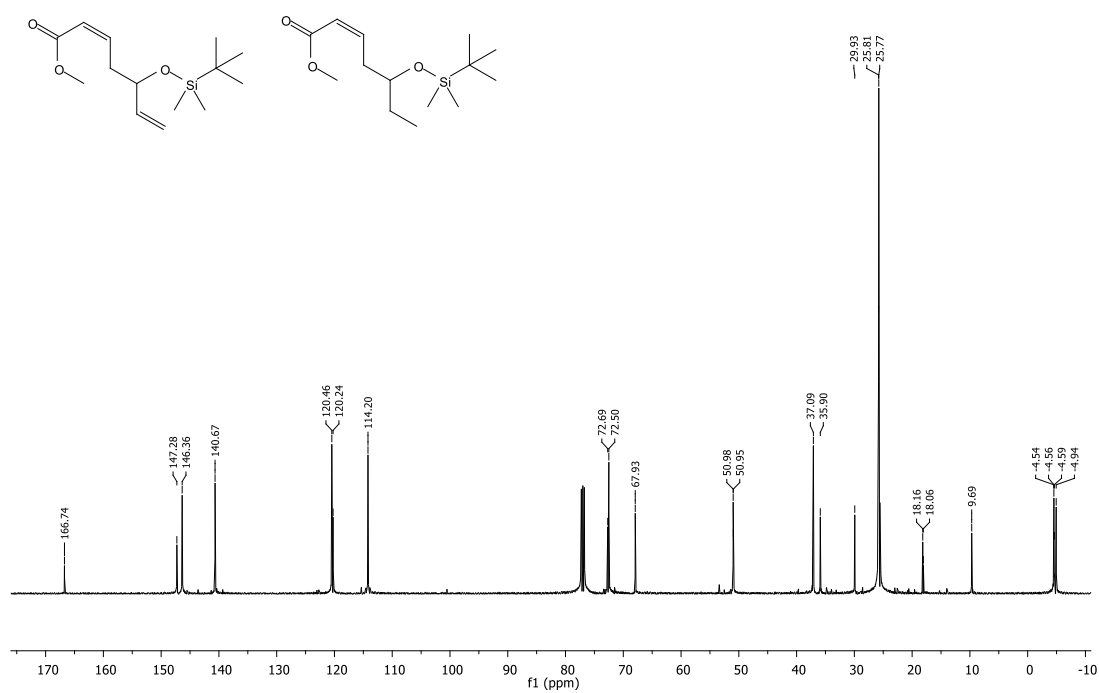


¹³C NMR (125 MHz, CDCl₃) spectrum of **126**

Mixture of (2Z)-methyl 5-(*tert*-butyldimethylsilyloxy)-2,6-heptadienoate (130**) and (2Z)-methyl 5-(*tert*-butyldimethylsilyloxy)-2-heptenoate (**131**) (3:2)**

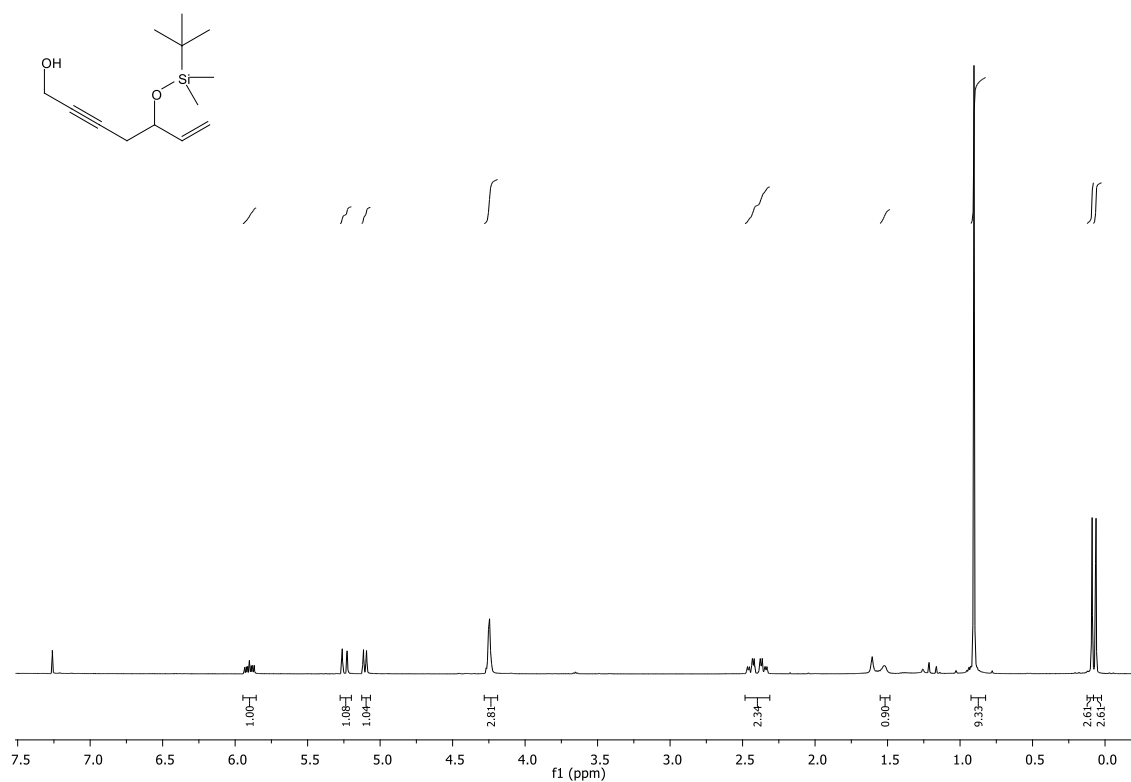


¹H NMR (500 MHz, CDCl₃) spectrum of **130 and **131****

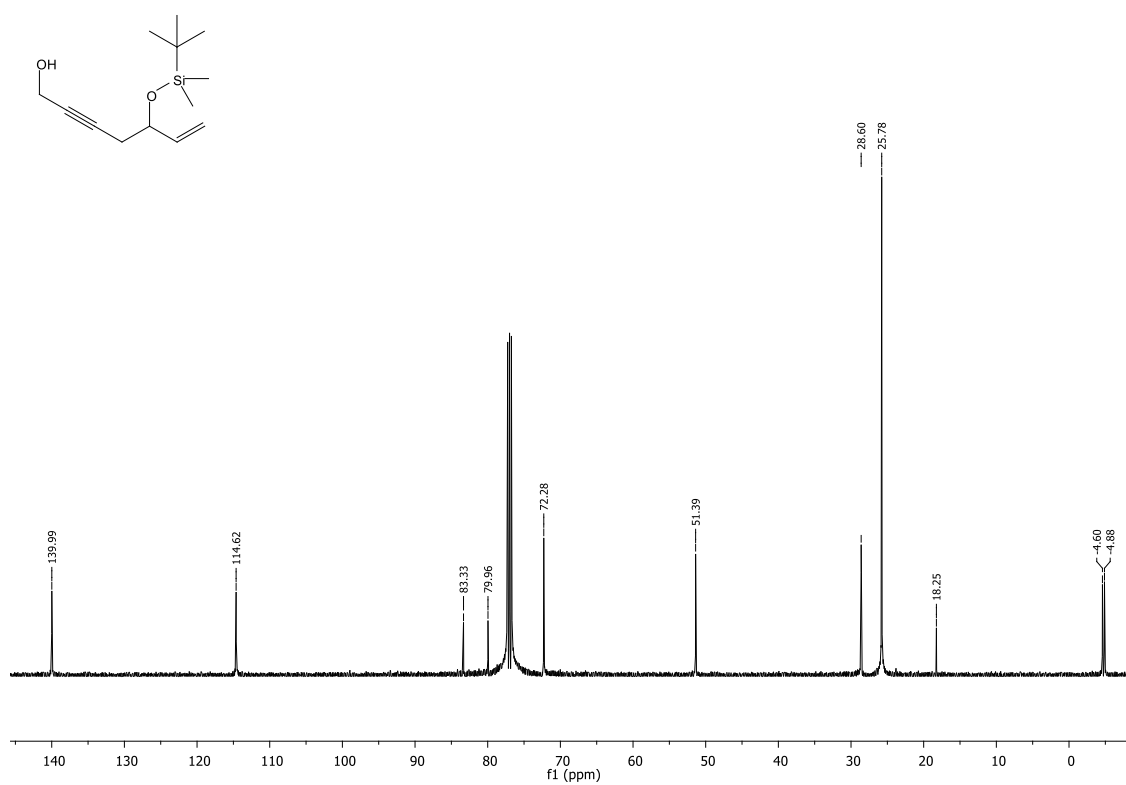


¹³C NMR (125 MHz, CDCl₃) spectrum of **130 and **131****

5-*tert*-Butyldimethylsilyloxy-6-hepten-2-yn-1-ol (132)

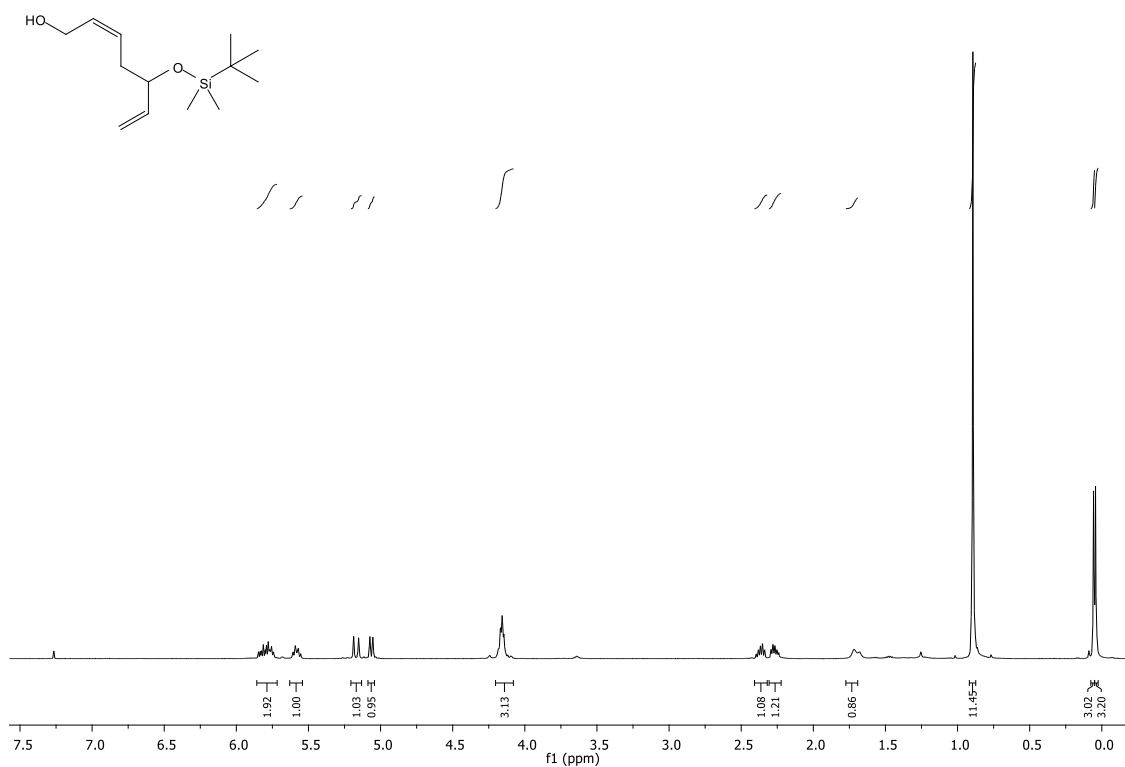


¹H NMR (500 MHz, CDCl₃) spectrum of **132**

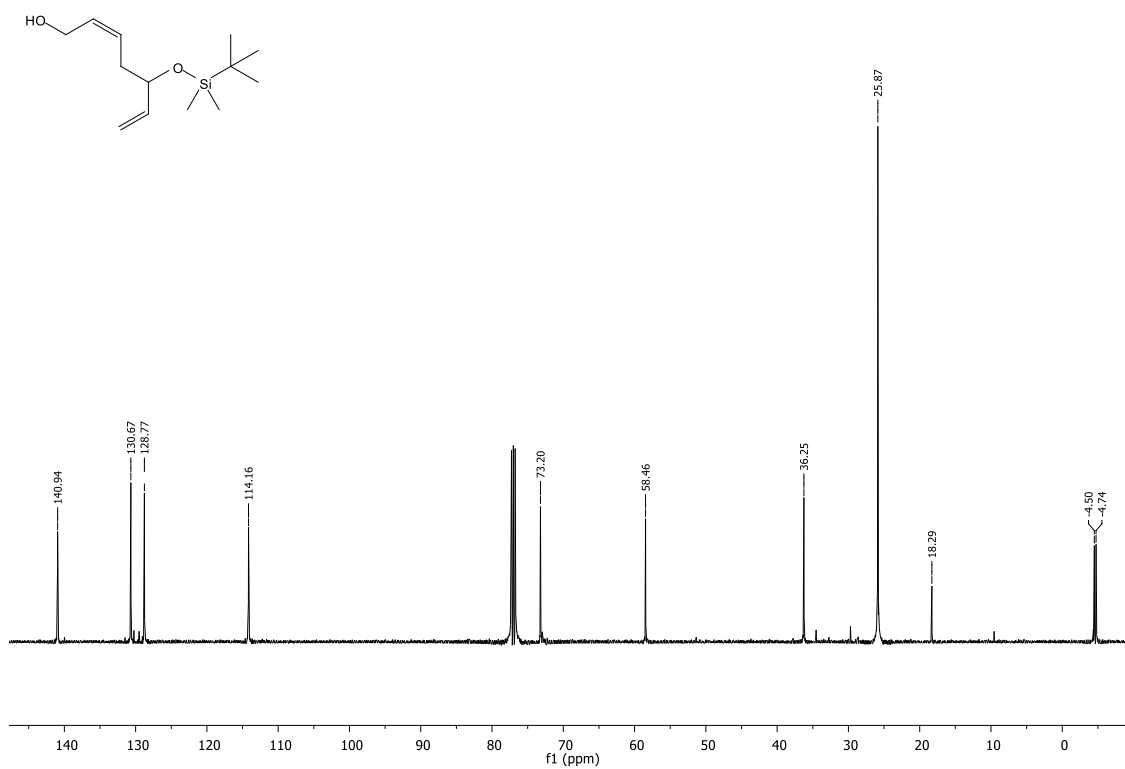


¹³C NMR (125 MHz, CDCl₃) spectrum of **132**

2E-5-(tert-Butyldimethylsilyloxy)hepta-2,6-dien-1-ol (133)

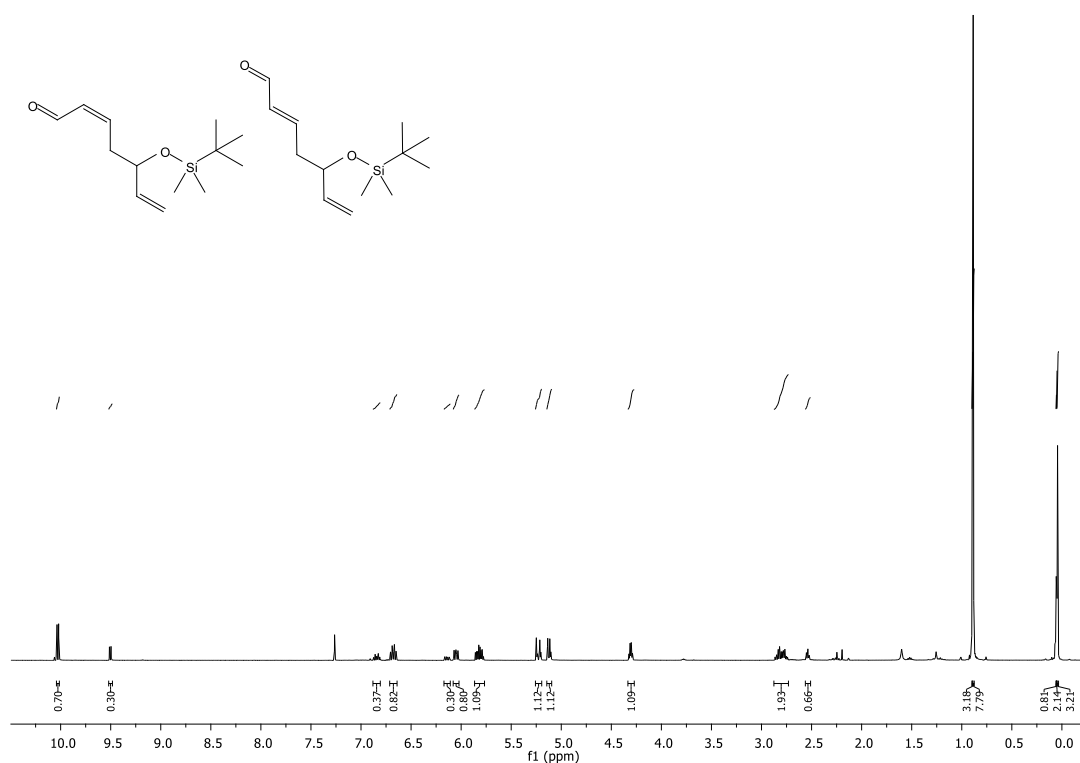


¹H NMR (500 MHz, CDCl₃) spectrum of 133

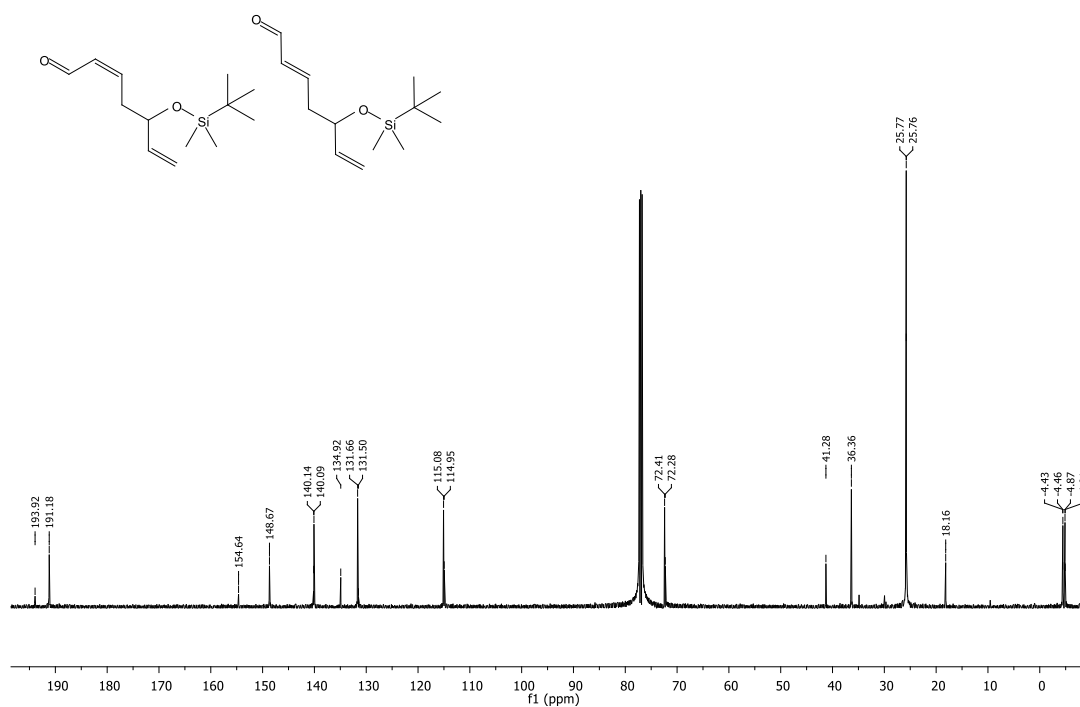


¹³C NMR (125 MHz, CDCl₃) spectrum of 133

Mixture of (2Z)-5-(*tert*-butyldimethylsilyloxy)hepta-2,6-dienal (135) and (2E) 5-(*tert*-butyldimethylsilyloxy)hepta-2,6-dienal (136) (7:3)

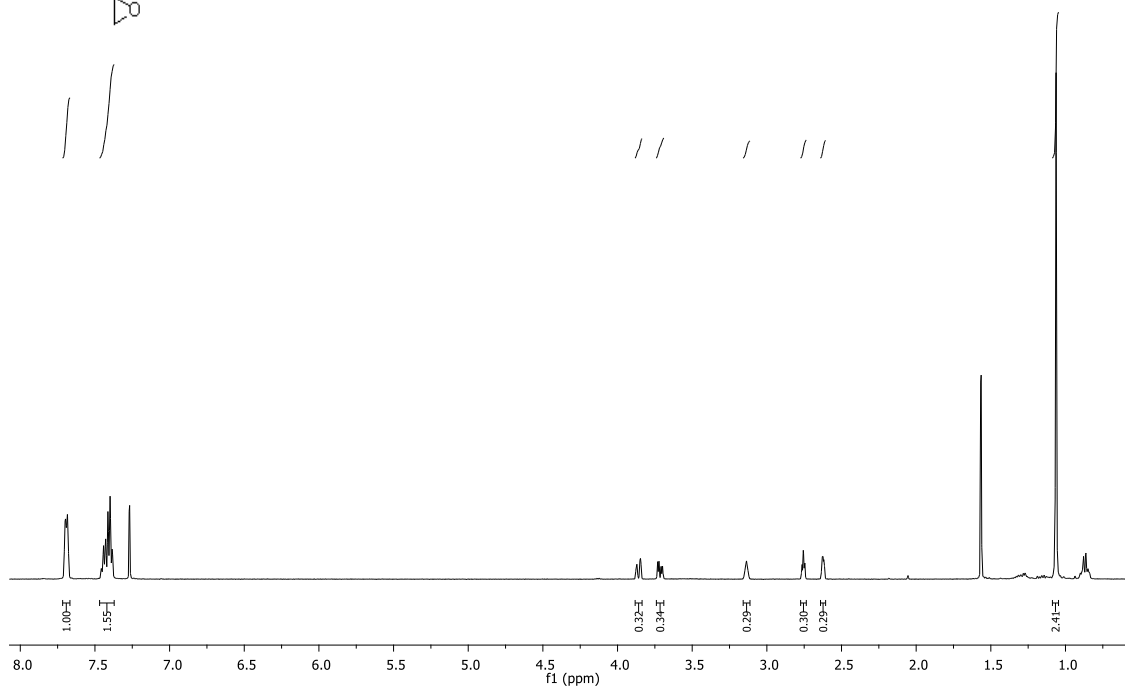
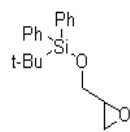


¹H NMR (500 MHz, CDCl₃) spectrum of **135 and **136****

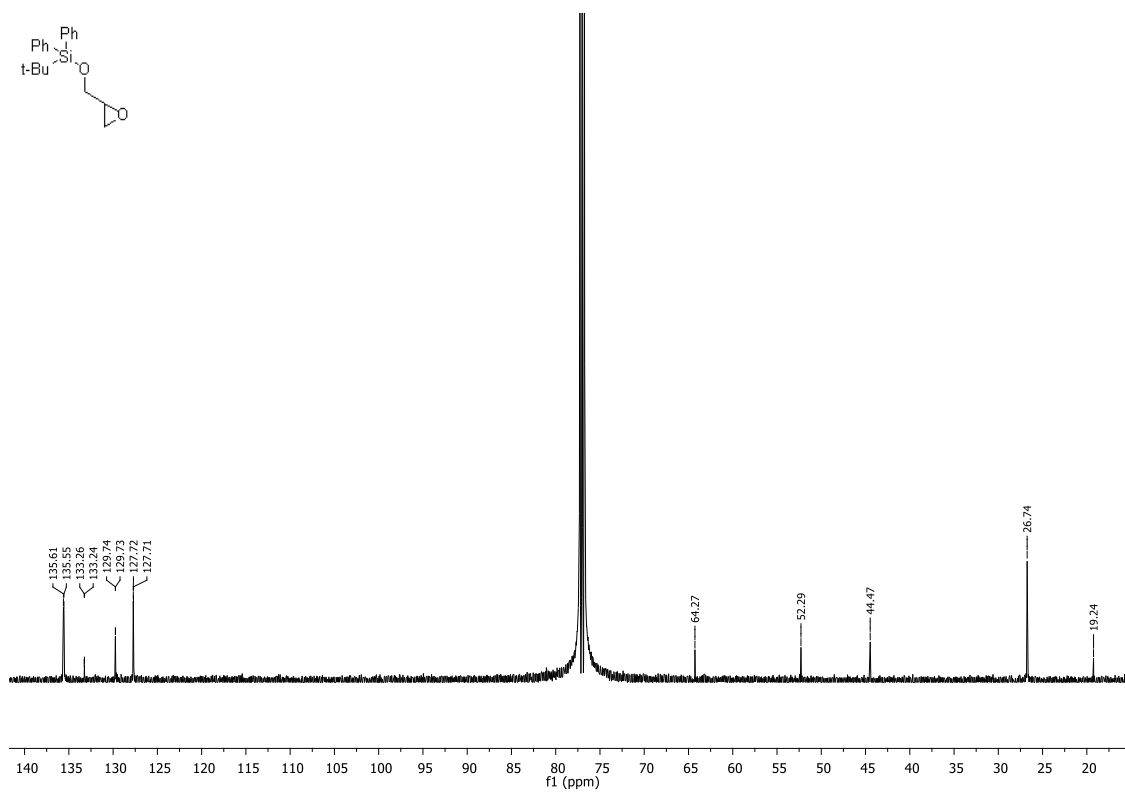


¹³C NMR (125 MHz, CDCl₃) spectrum of **135 and **136****

2-(*tert*-Butyldiphenylsilyloxy)methyloxirane (140**)**

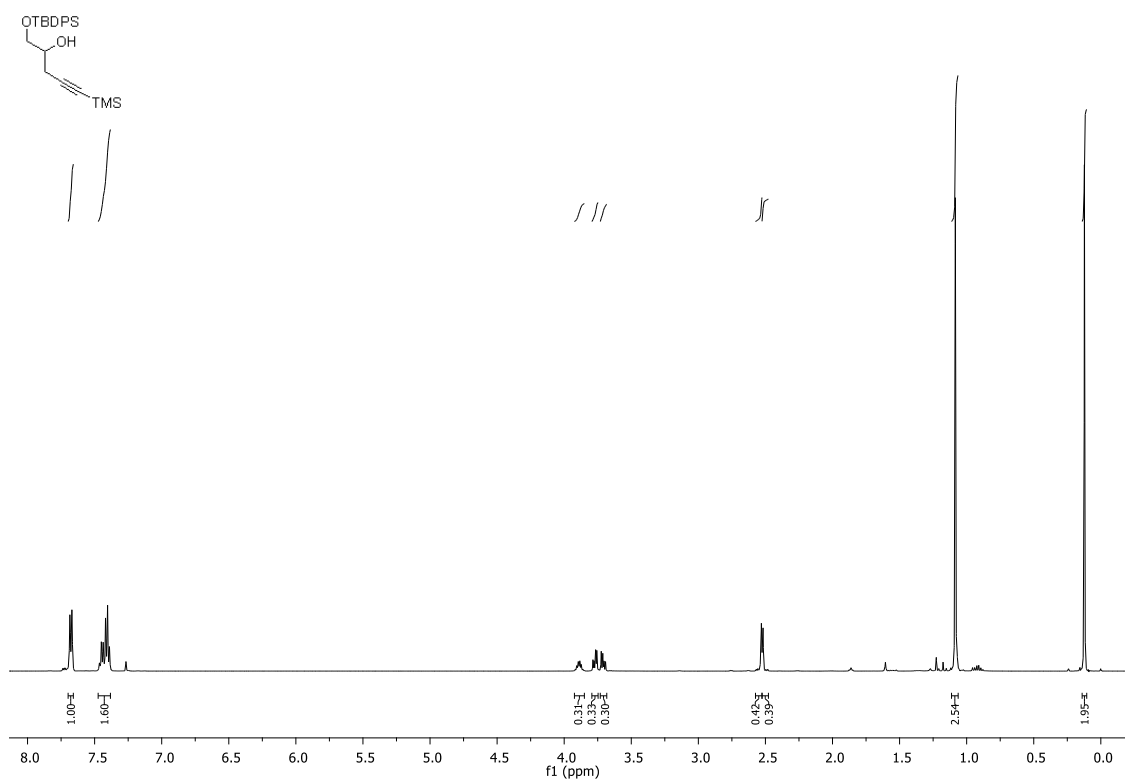


¹H NMR (500 MHz, CDCl₃) spectrum of **140**

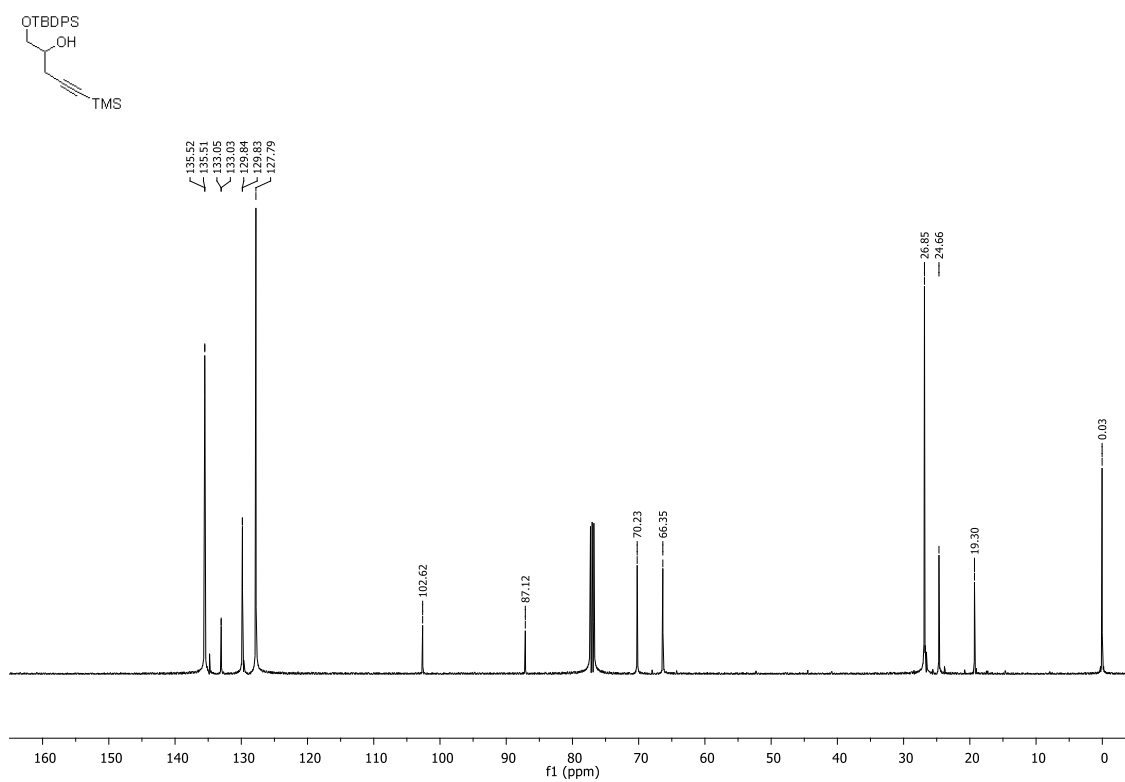


¹³C NMR (125 MHz, CDCl₃) spectrum of **140**

1-(*tert*-Butyldiphenylsilyloxy)-5-trimethylsilyl-4-pentyn-2-ol (141**)**

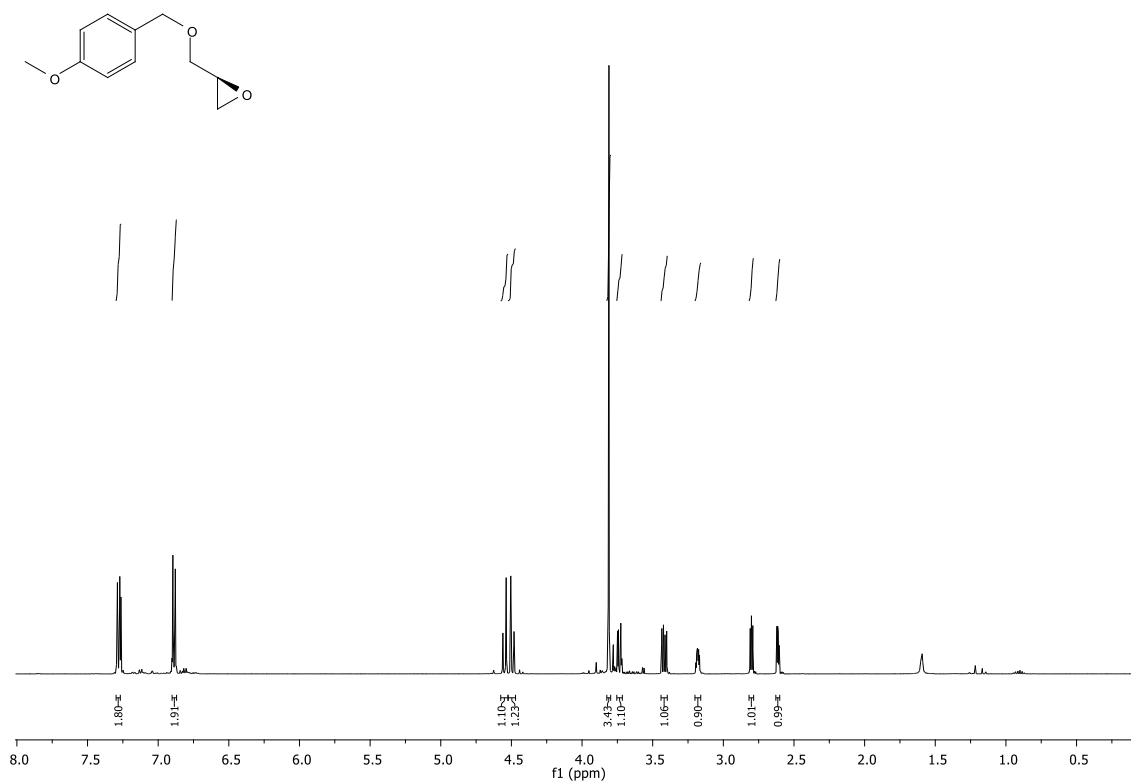


¹H NMR (500 MHz, CDCl₃) spectrum of **141**

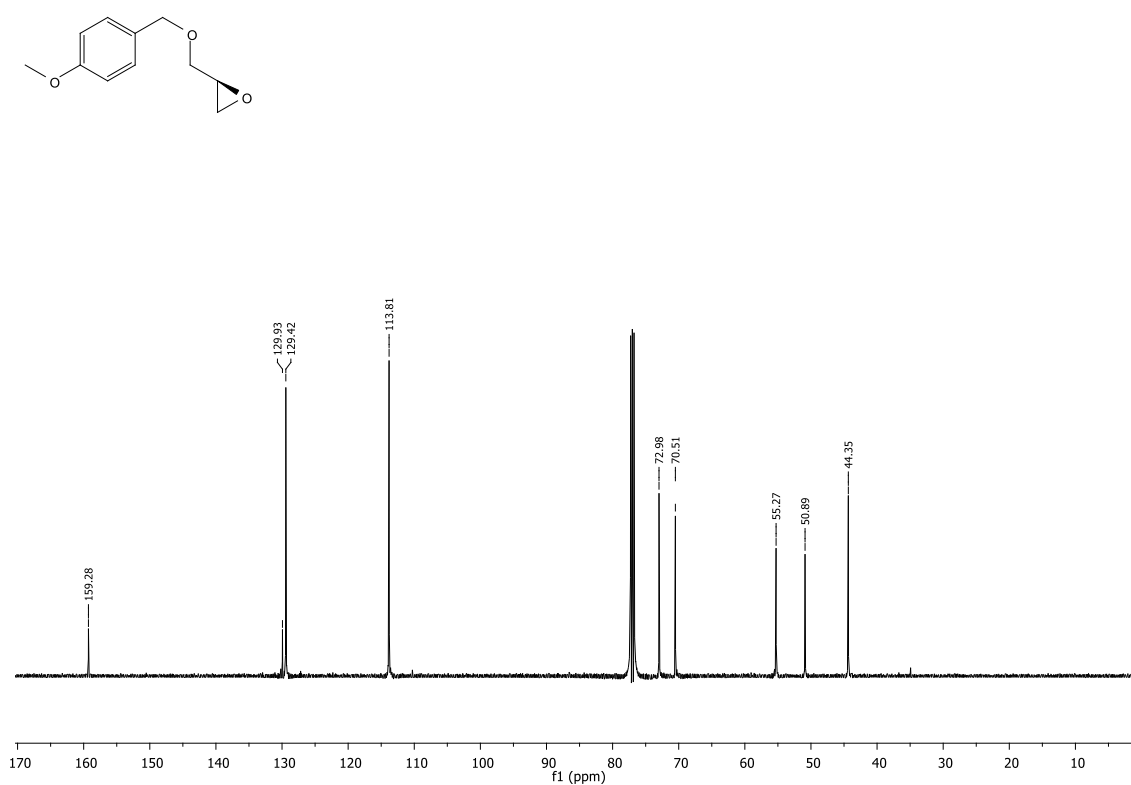


¹³C NMR (125 MHz, CDCl₃) spectrum of **141**

(S)-2-(*para*-Methoxybenzyl)methyloxirane (150**)**

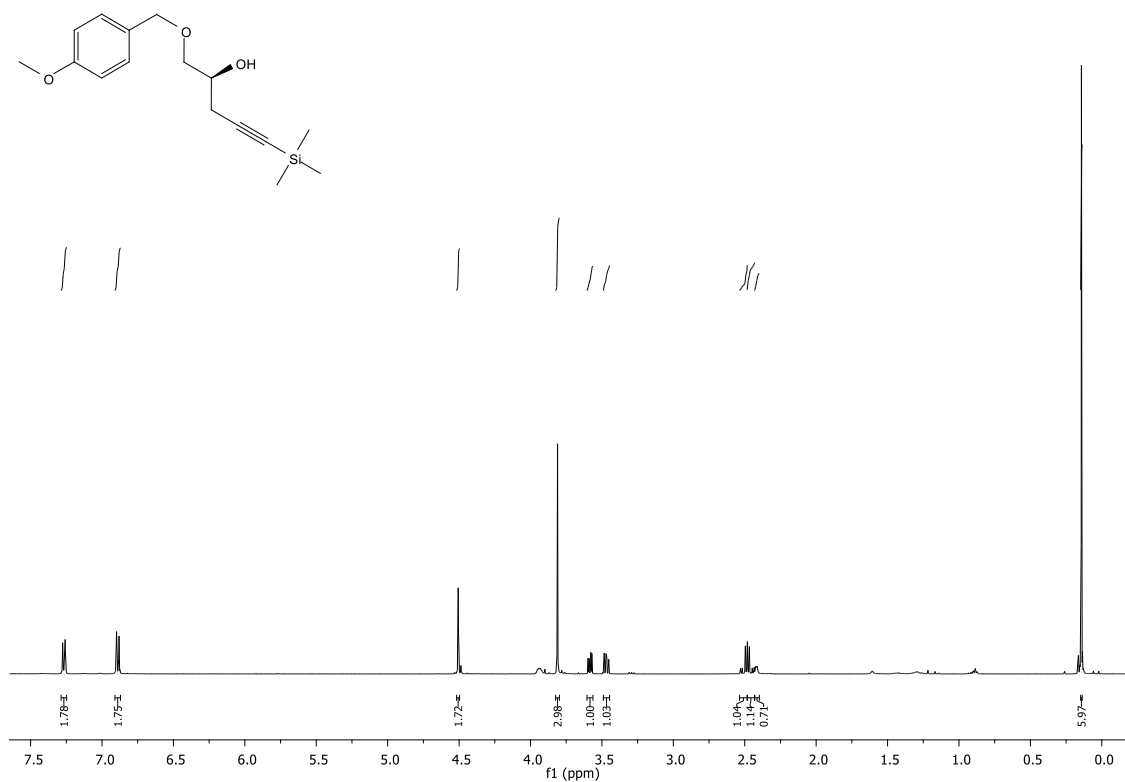


^1H NMR (500 MHz, CDCl_3) spectrum of **150**

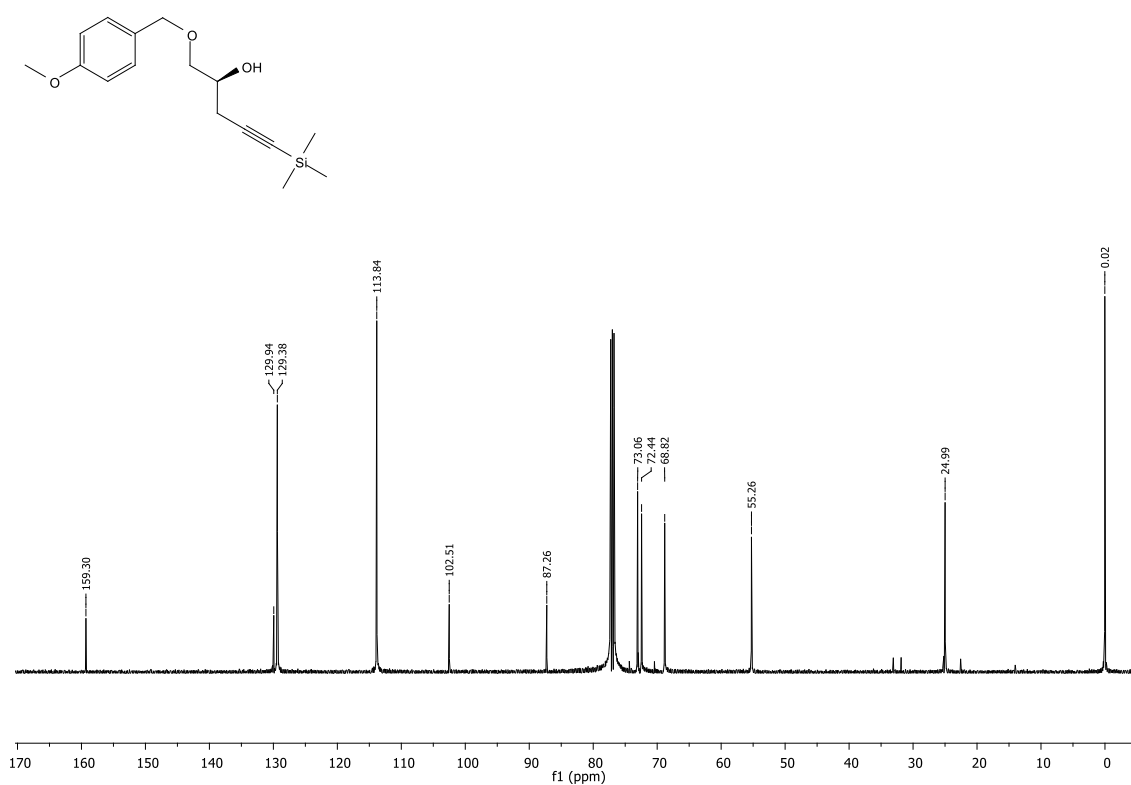


^{13}C NMR (125 MHz, CDCl_3) spectrum of **150**

(S)-1-(*para*-Methoxybenzyl)oxy-5-trimethylsilyl-pentyn-2-ol (146**)**

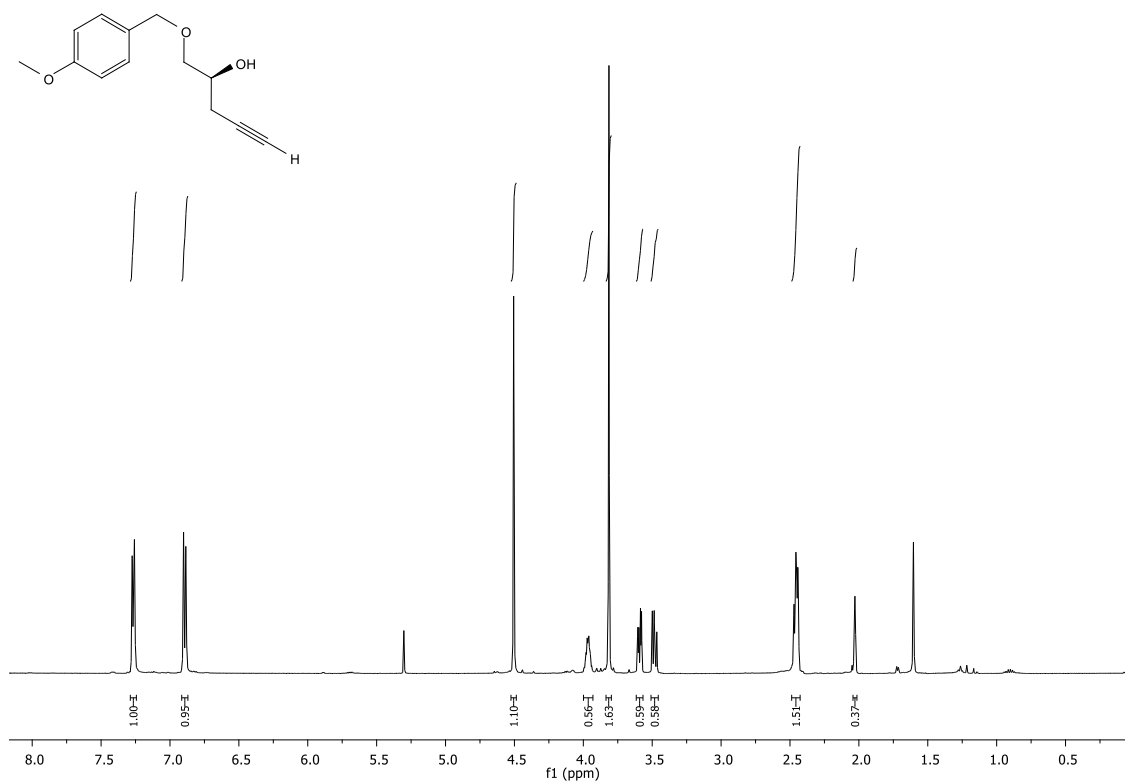


¹H NMR (500 MHz, CDCl₃) spectrum of **146**

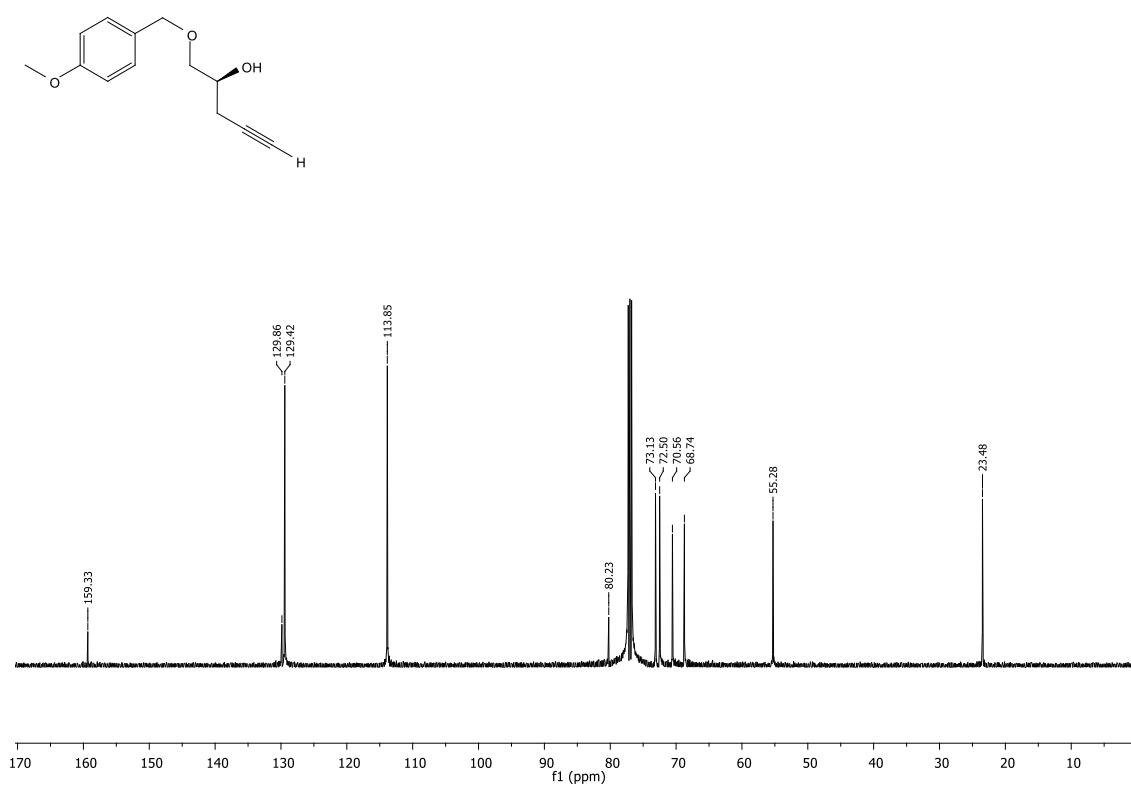


¹³C NMR (125 MHz, CDCl₃) spectrum of **146**

(S)-1-(*para*-Methoxybenzyl)oxy-4-pentyn-2-ol (152**)**

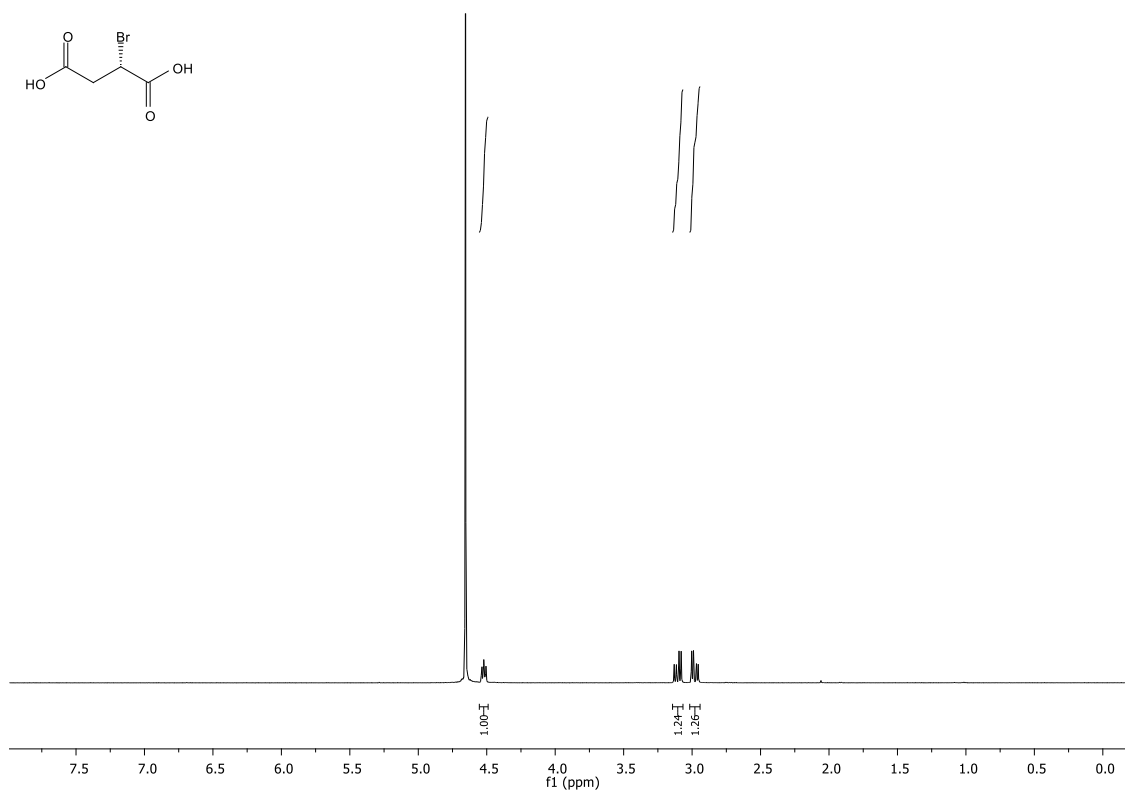


^1H NMR (500 MHz, CDCl_3) spectrum of **152**

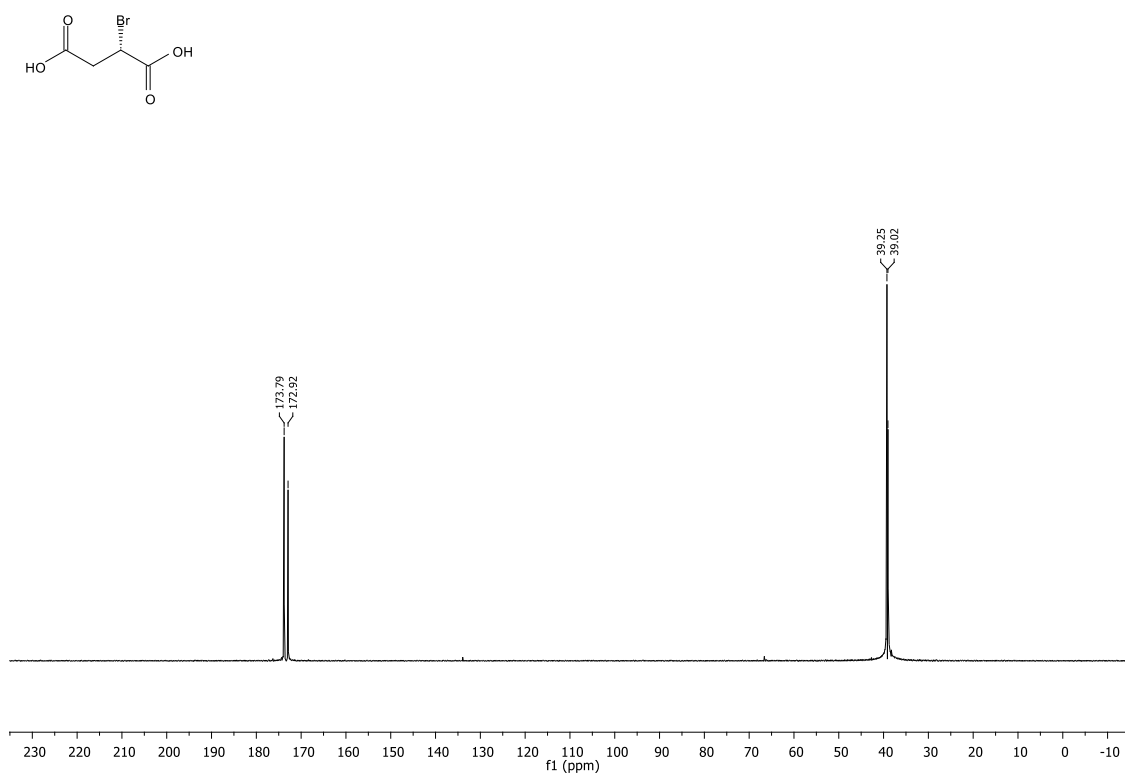


^{13}C NMR (125 MHz, CDCl_3) spectrum of **152**

(S)-Bromosuccinic acid (157)

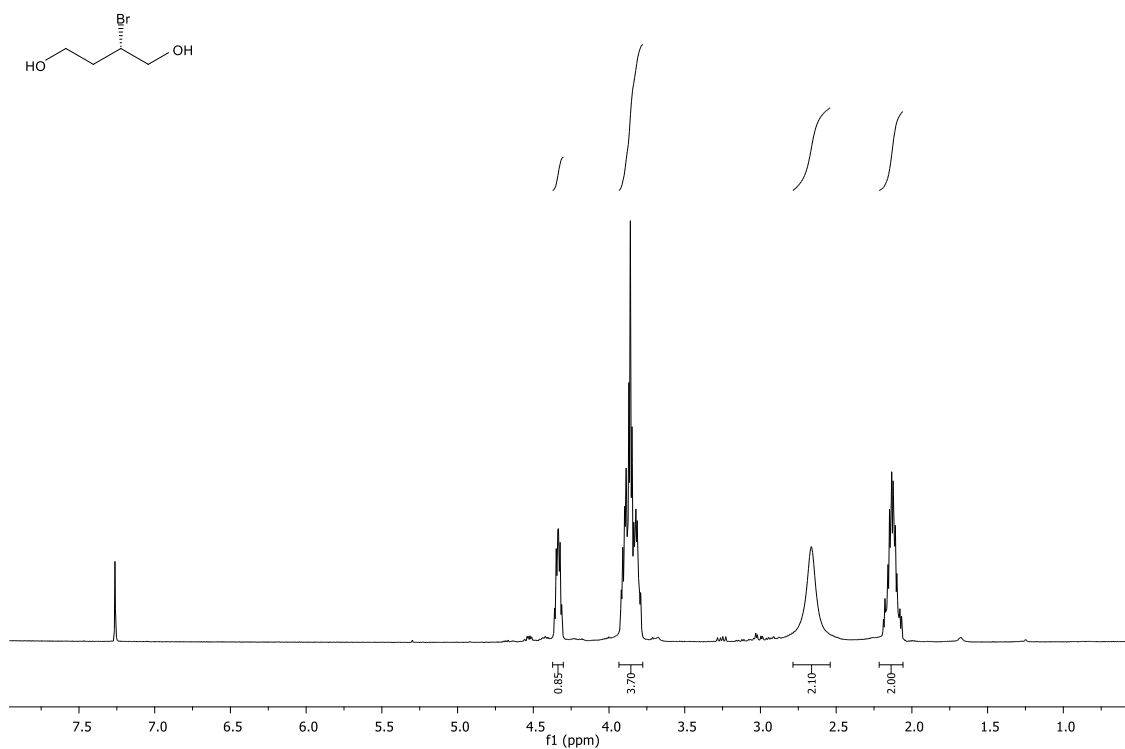


¹H NMR (500 MHz, D₂O) spectrum of **157**

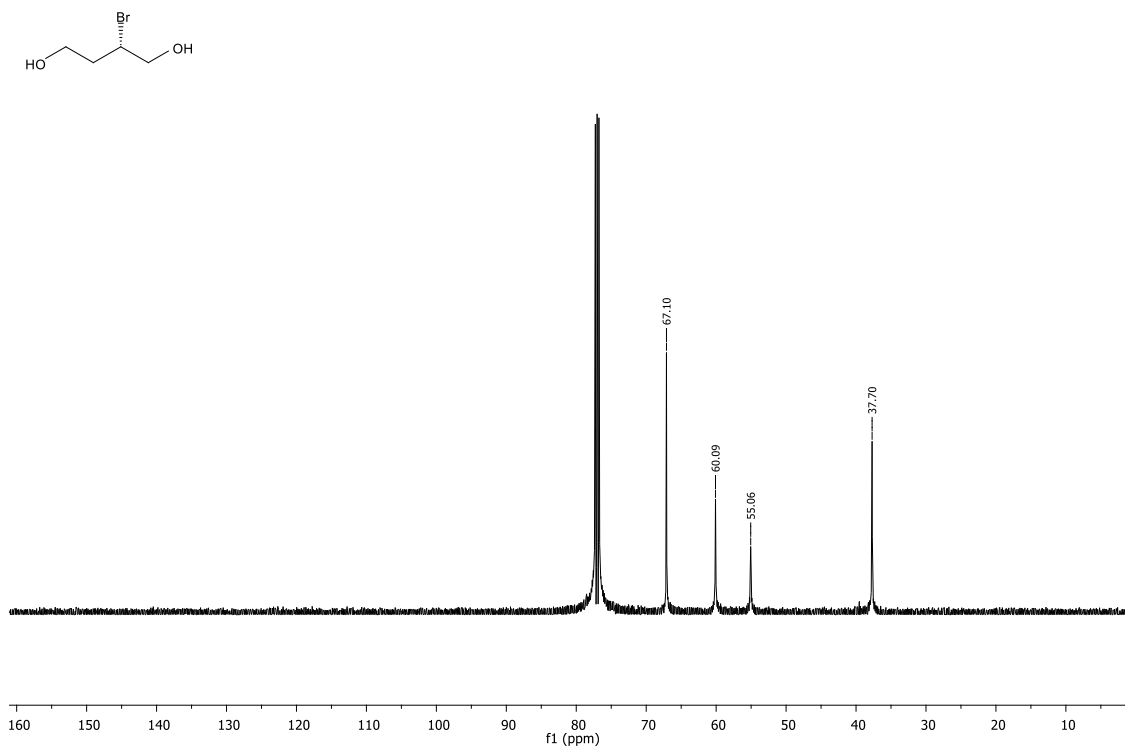


¹³C NMR (125 MHz, D₂O) spectrum of **157**

(S)-2-Bromobutane-1,4-diol (160)

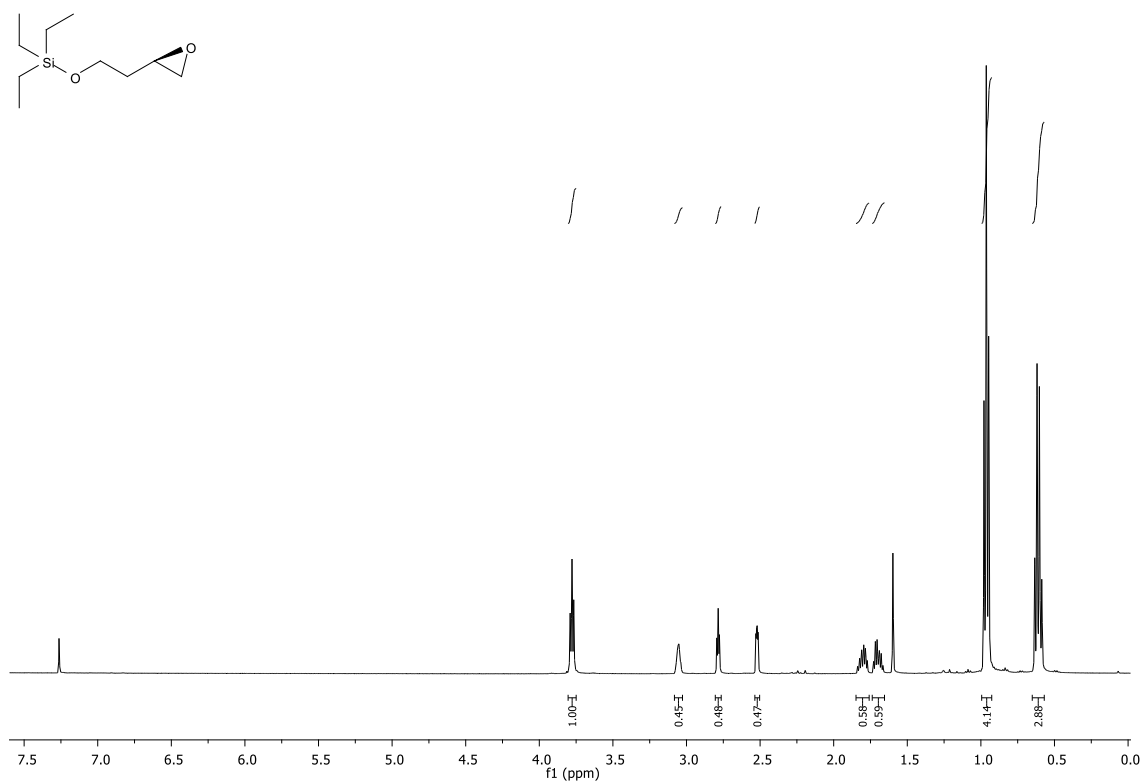


¹H NMR (500 MHz, CDCl₃) spectrum of **160**

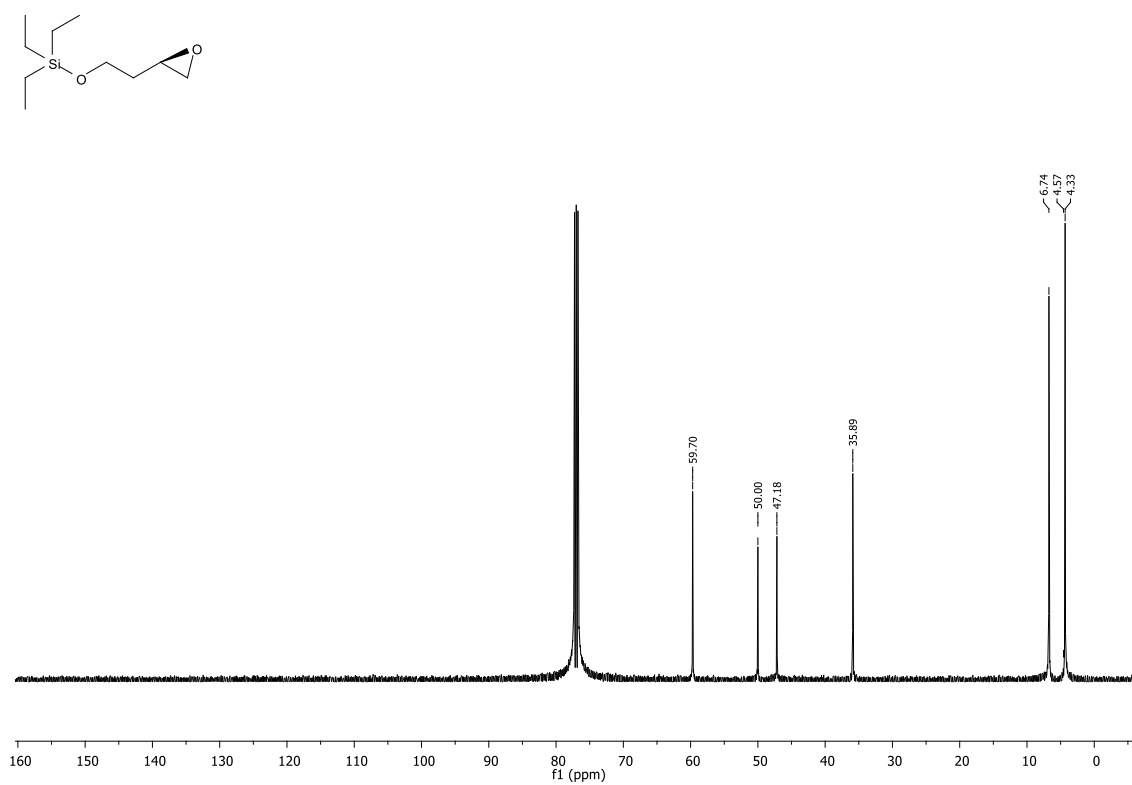


¹³C NMR (125 MHz, CDCl₃) spectrum of **160**

(R)-Triethyl-(2-oxiran-2-yl)ethoxysilane (155)

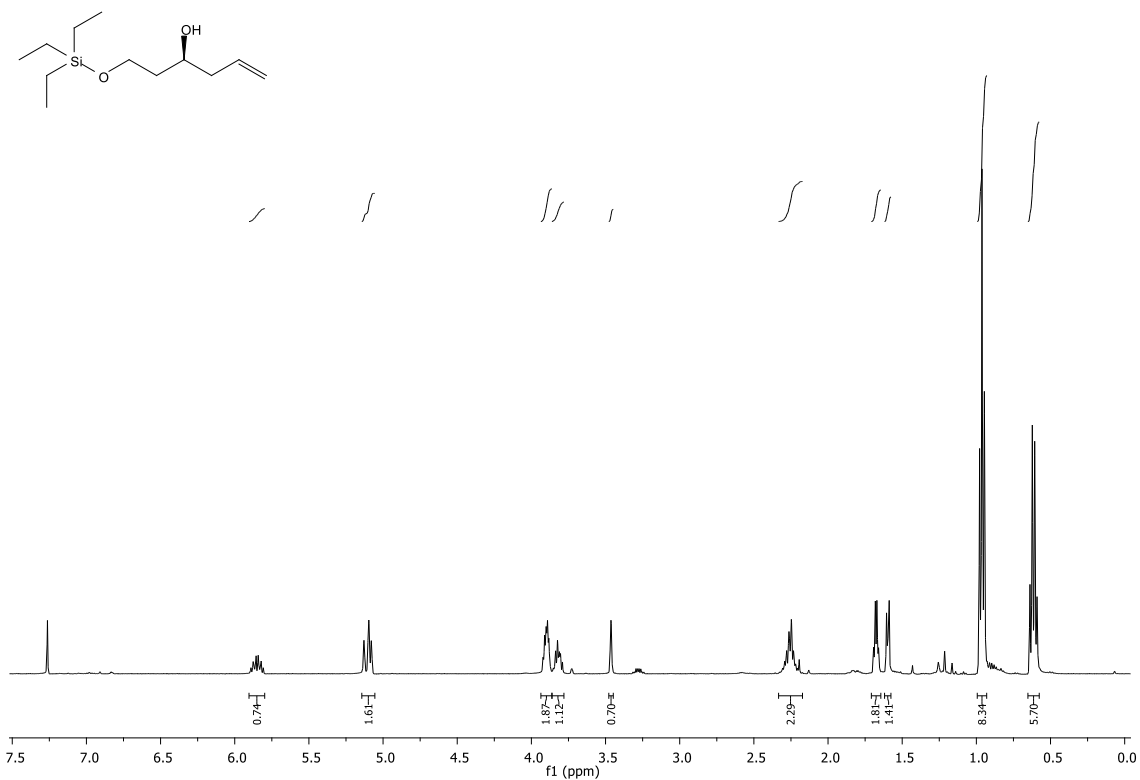


¹H NMR (500 MHz, CDCl₃) spectrum of **155**

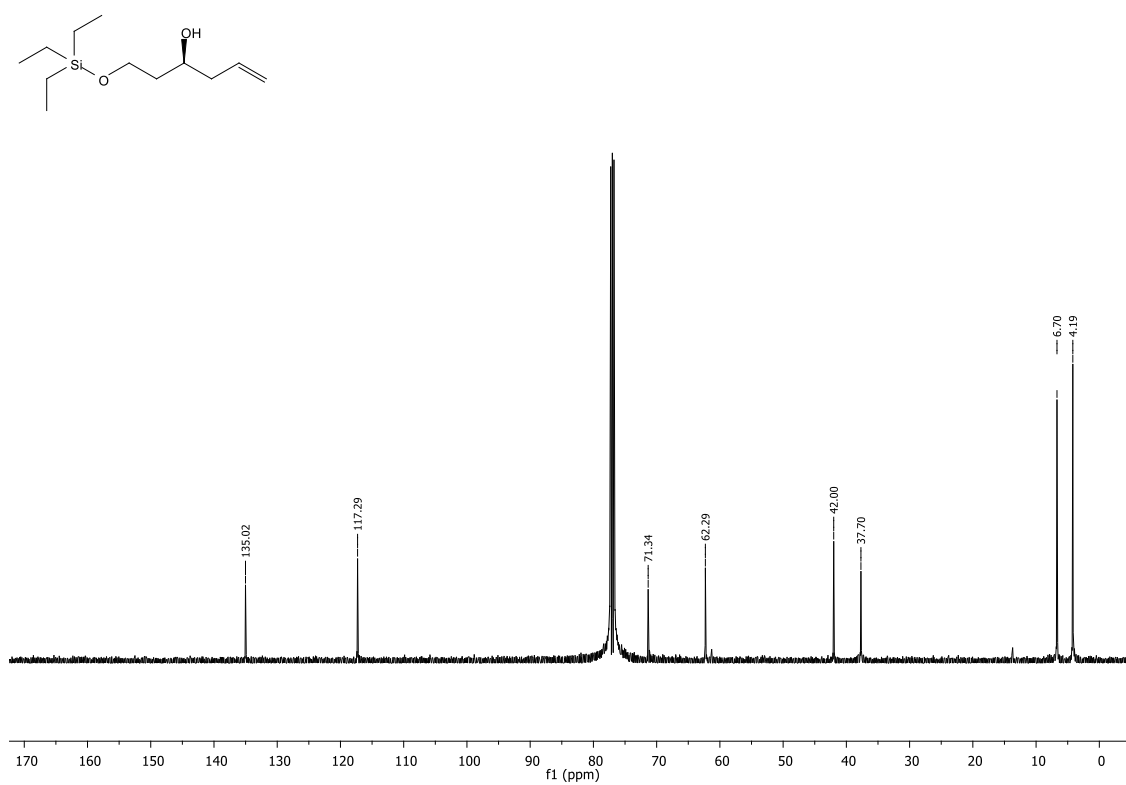


¹³C NMR (125 MHz, CDCl₃) spectrum of **155**

(S)-Triethyl-(3-hydroxy)hex-5-enoxysilane (156)

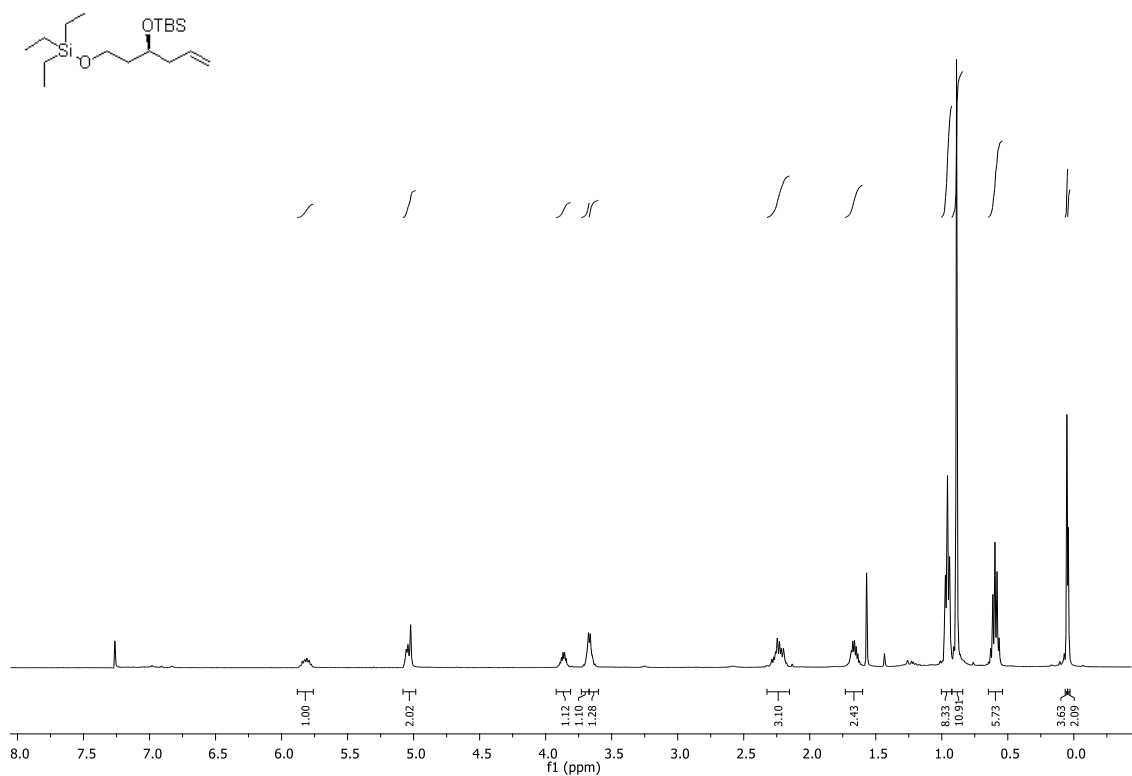


¹H NMR (500 MHz, CDCl₃) spectrum of **156**

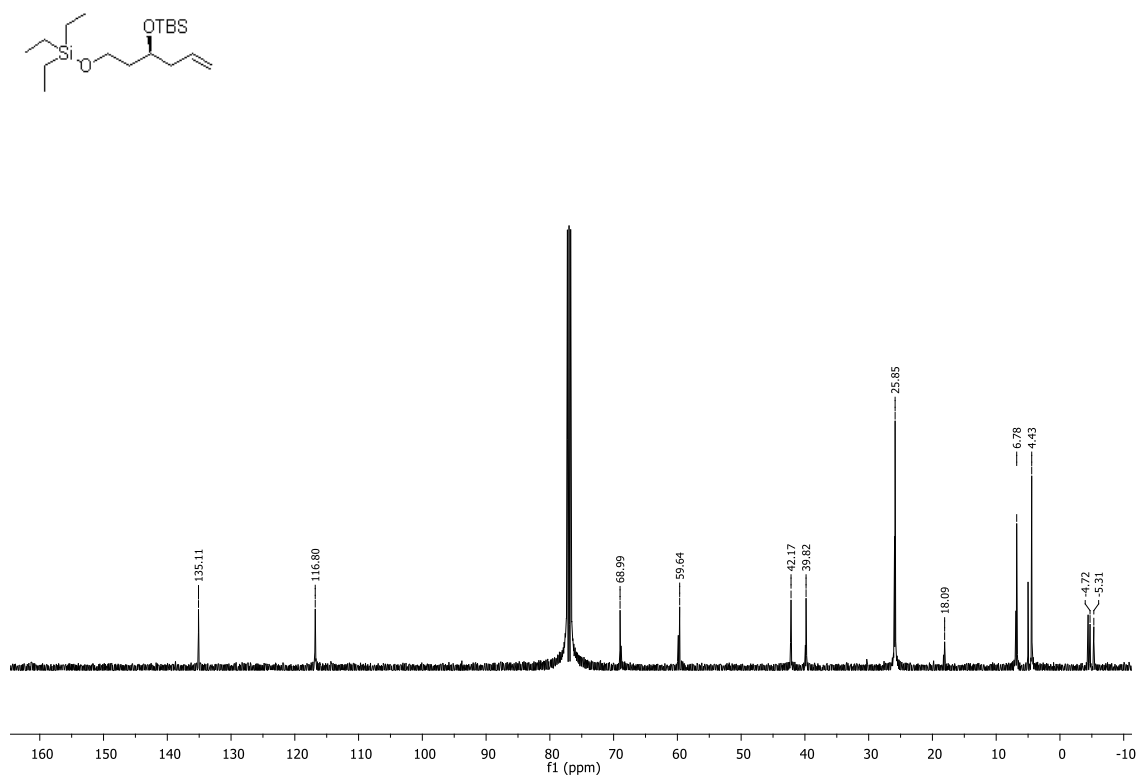


¹³C NMR (125 MHz, CDCl₃) spectrum of **156**

(S)-1-Triethylsilyloxy-(3-*t*-butyldimethylsilyloxy)hex-5-ene (161**)**

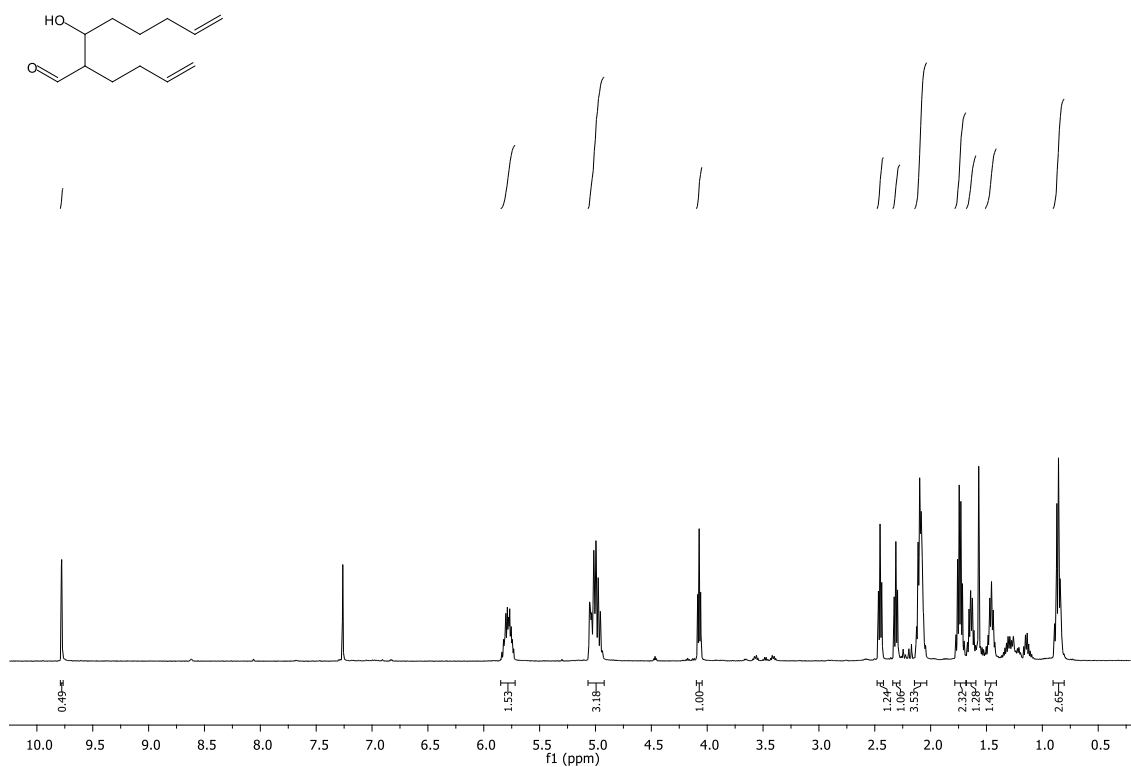


¹H NMR (500 MHz, CDCl₃) spectrum of **161**

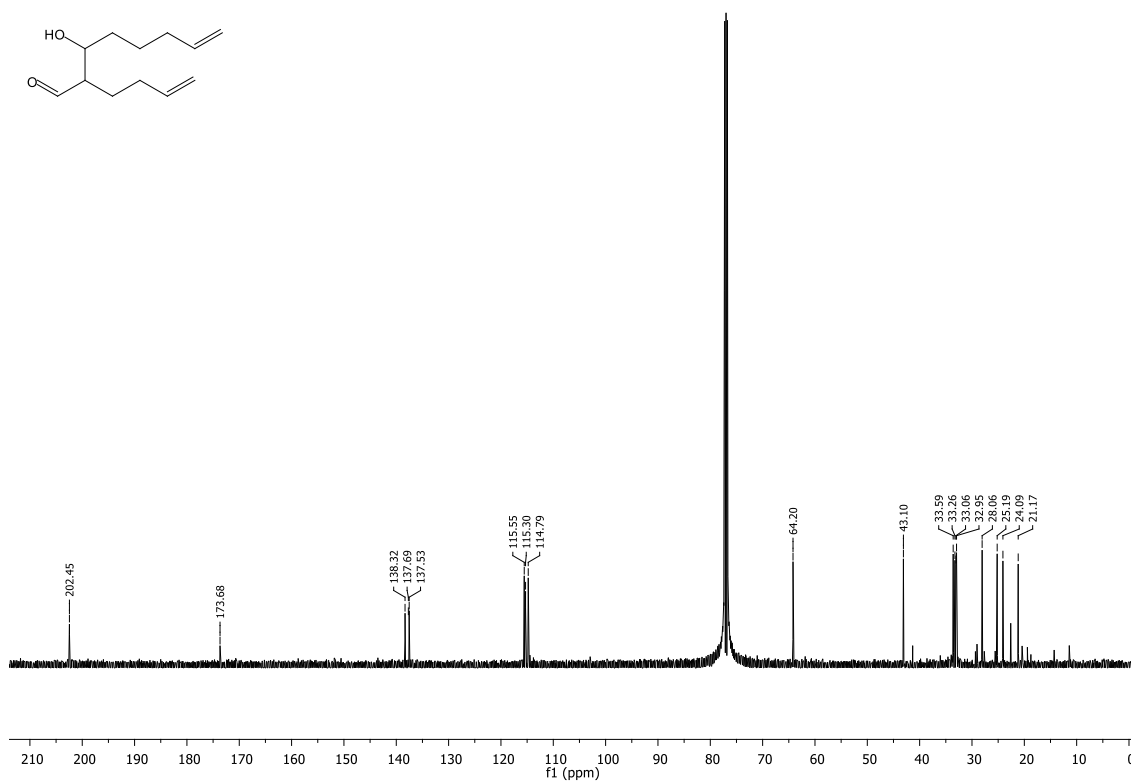


¹³C NMR (125 MHz, CDCl₃) spectrum of **161**

2-(But-3'-enyl)-3-hydroxyoct-7-enal (170, in a mixture)

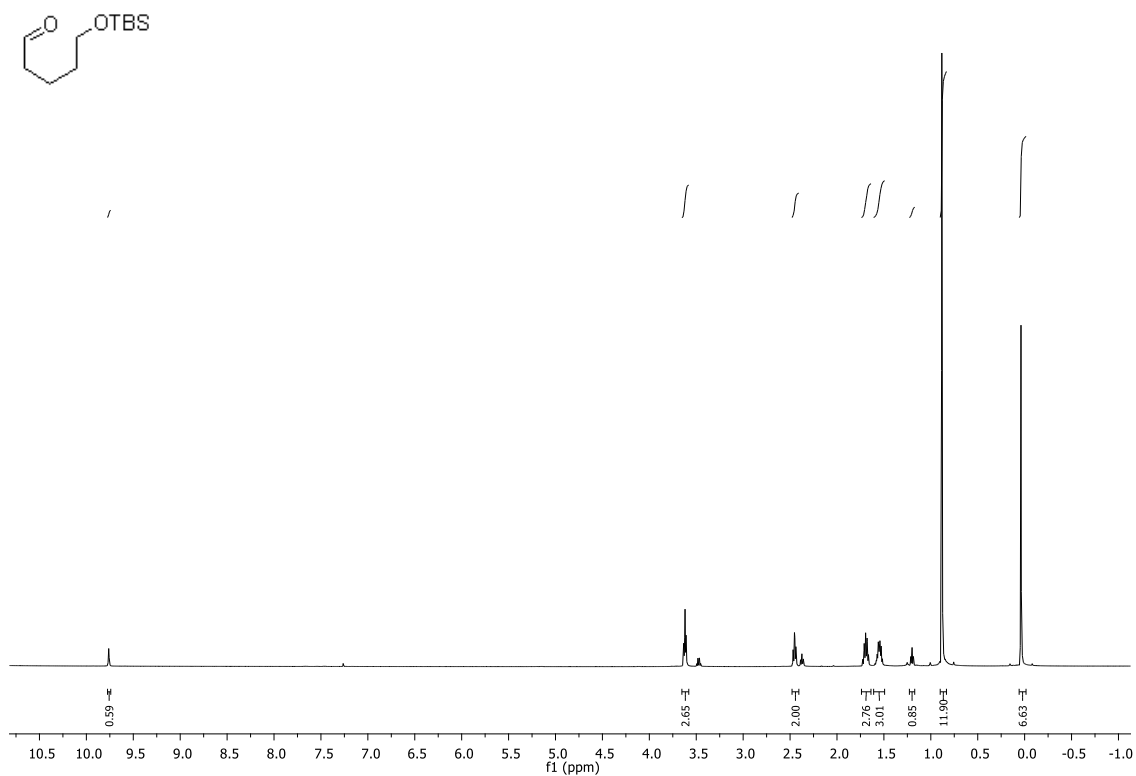


¹H NMR (500 MHz, CDCl₃) spectrum of **170 mixture**

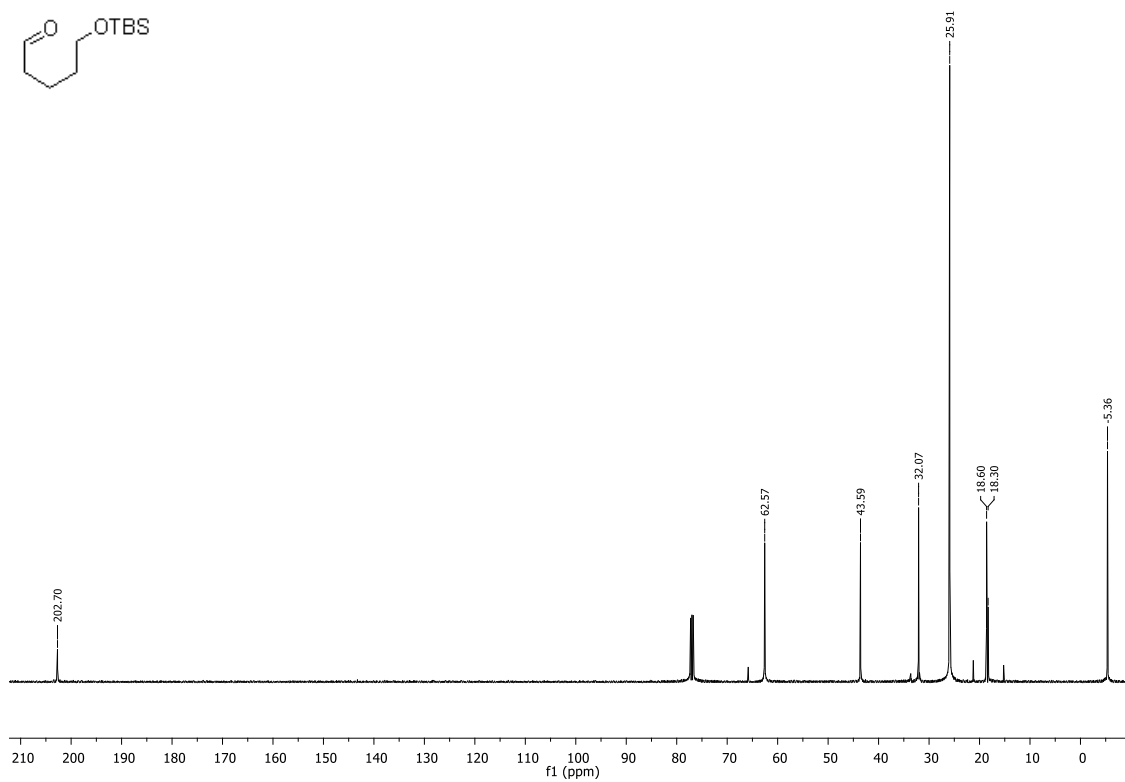


¹³C NMR (125 MHz, CDCl₃) spectrum of **170 mixture**

5-(*t*-Butyldimethylsilyloxy)pentanal (177**)**

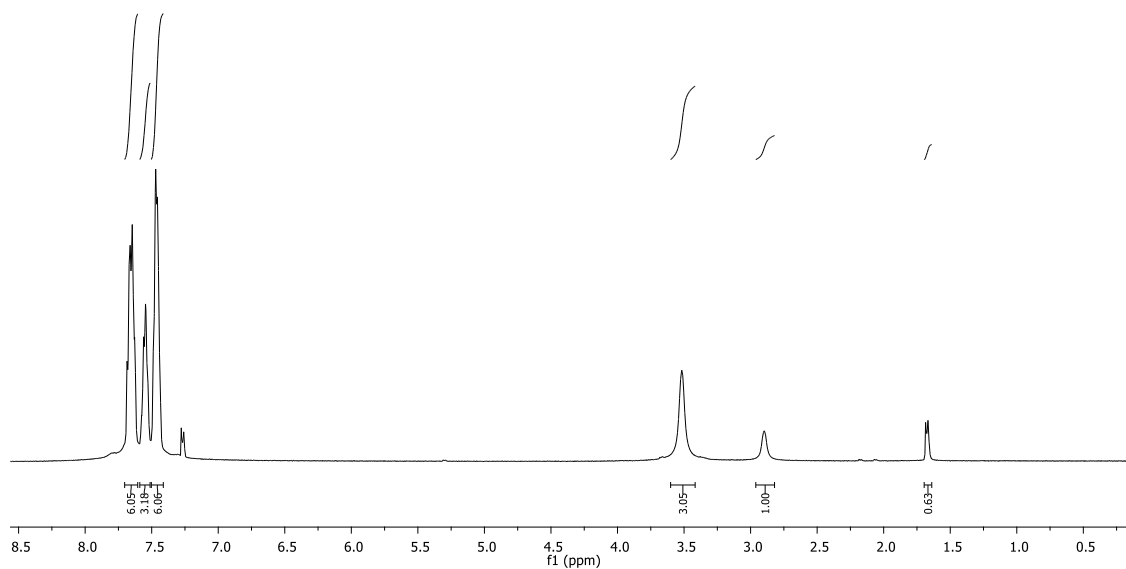
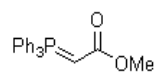


¹H NMR (500 MHz, CDCl₃) spectrum of **177**

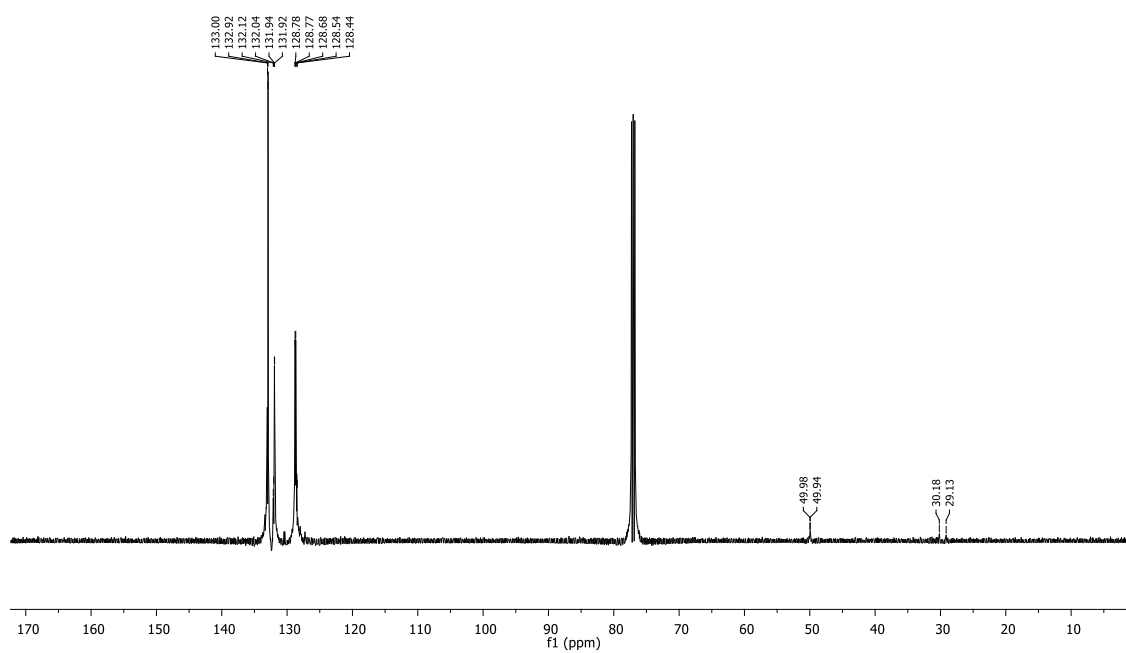
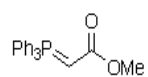


¹³C NMR (125 MHz, CDCl₃) spectrum of **177**

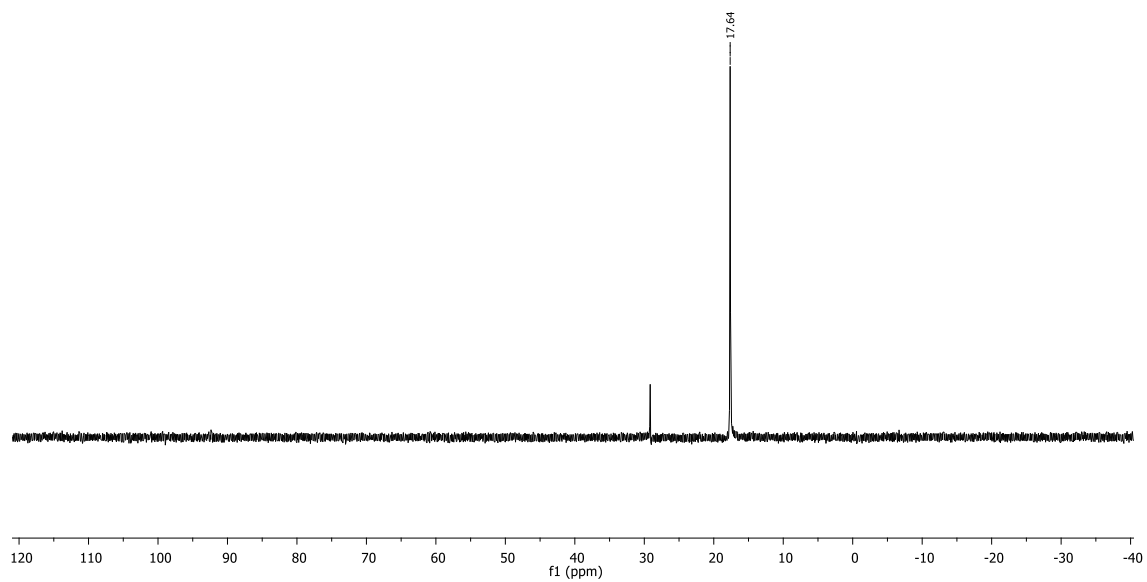
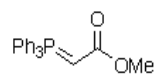
(Triphenylphosphoranylidene)acetate (179**)**



¹H NMR (500 MHz, CDCl₃) spectrum of **179**

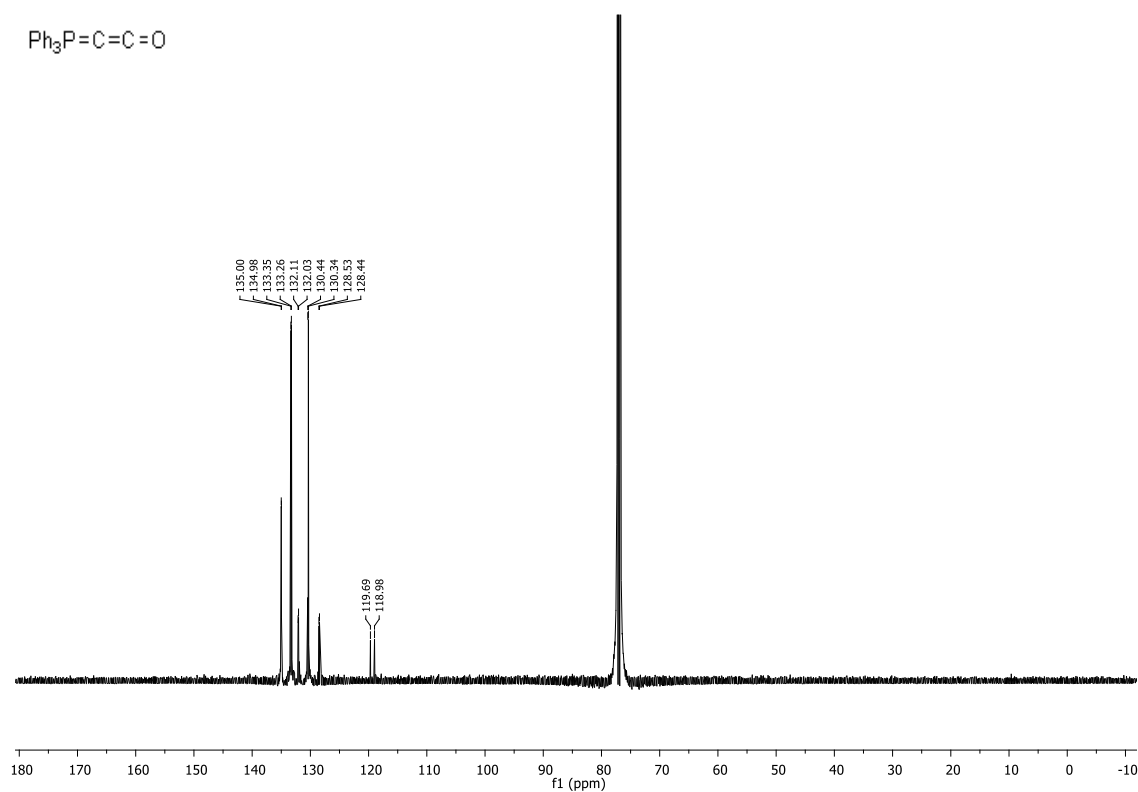
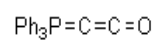


¹³C NMR (125 MHz, CDCl₃) spectrum of **179**

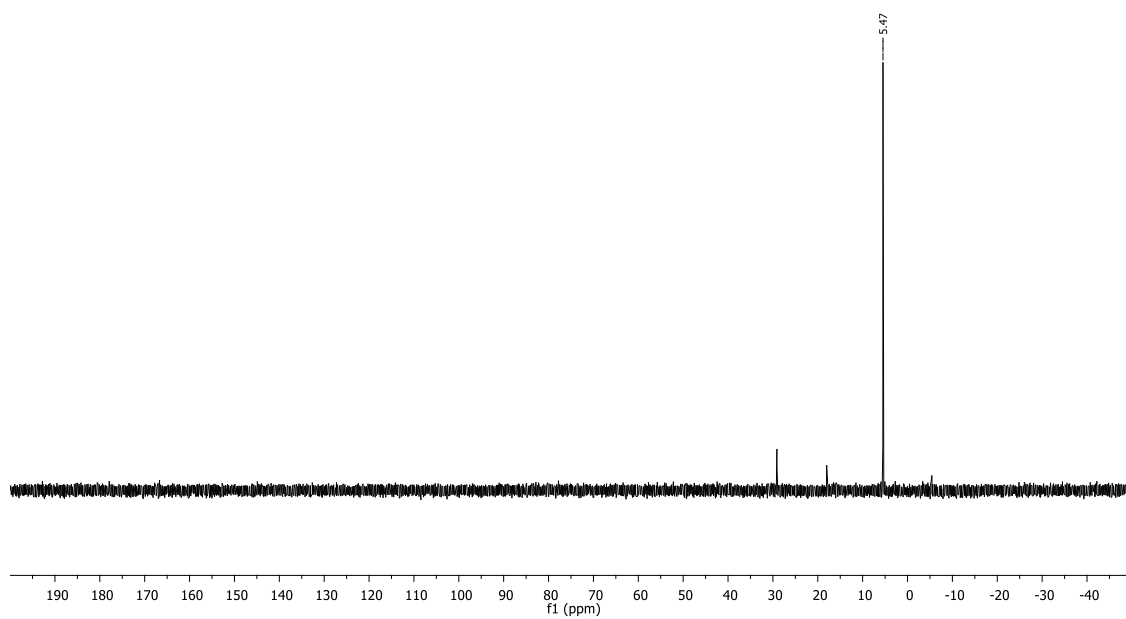
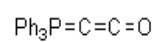


^{31}P NMR (120 MHz, CDCl_3) spectrum of **179**

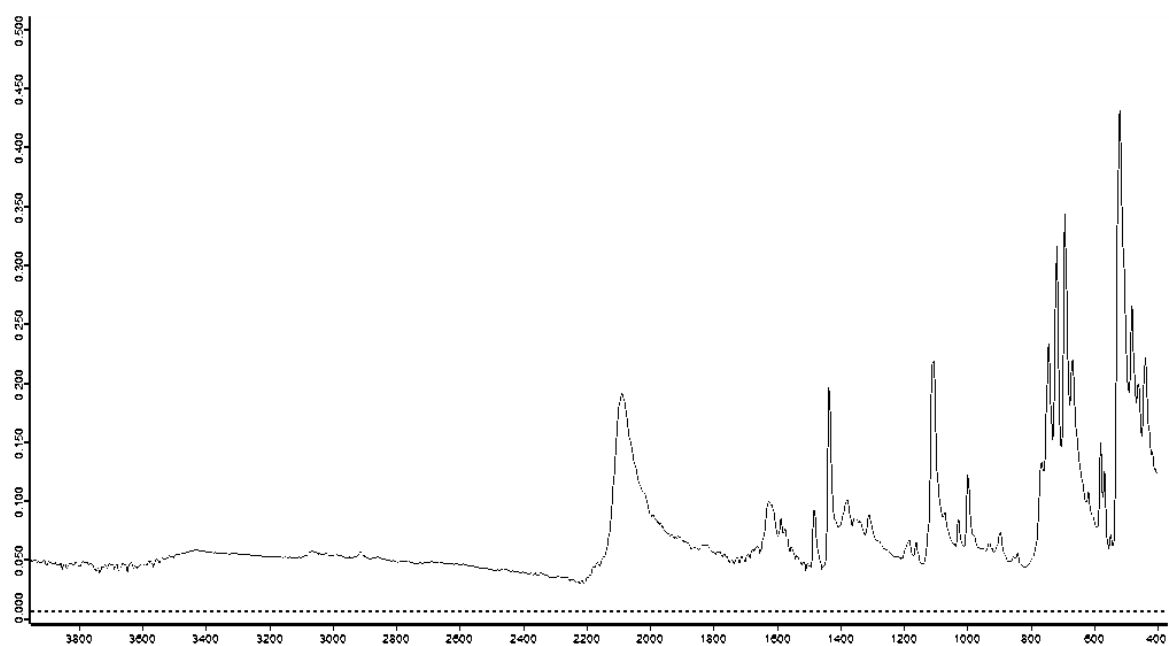
(Triphenylphosphoranylidene)ketene (178)



¹³C NMR (125 MHz, CDCl₃) spectrum of **178**

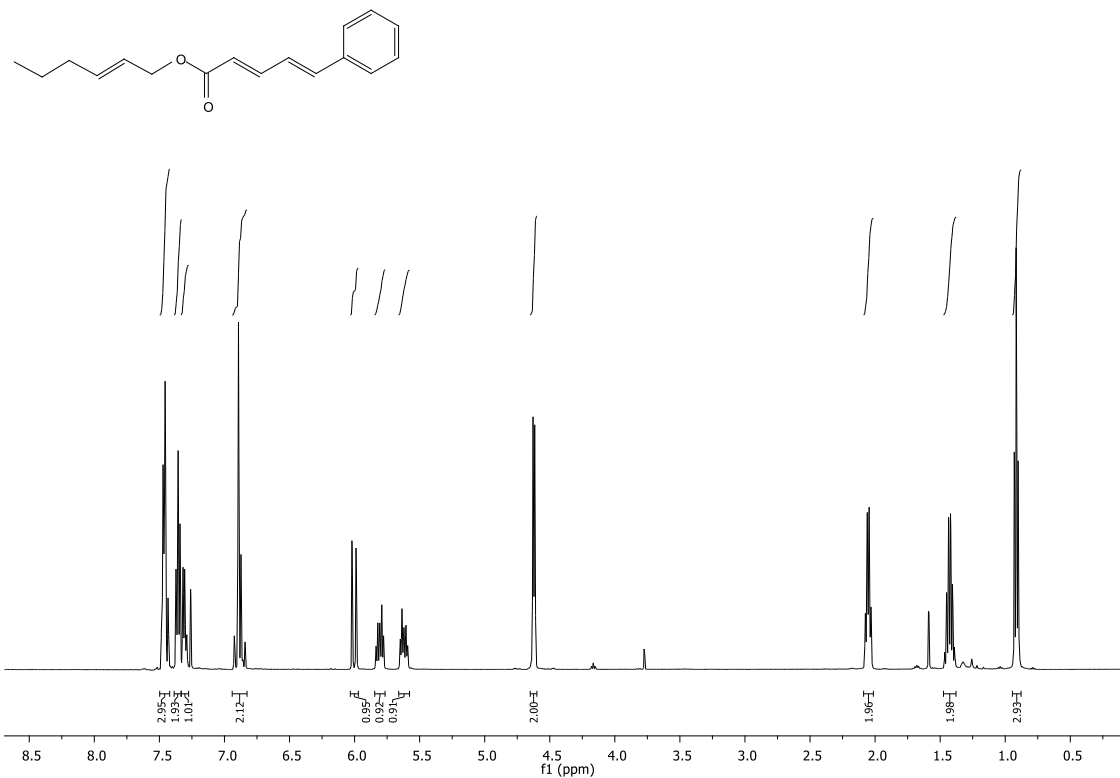


³¹P NMR (120 MHz, CDCl₃) spectrum of **178**

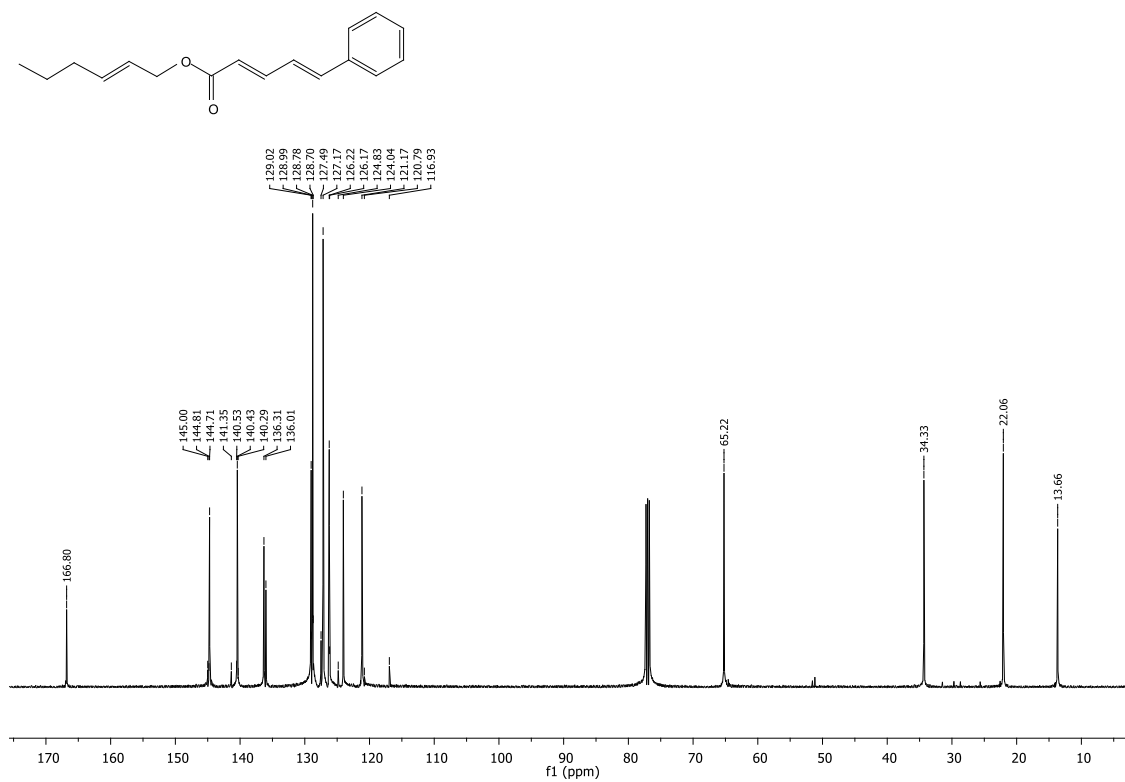


IR (neat) spectrum of 178

(2'E,2E,4E)-Hex-2'-enyl 5-phenylpenta-2,4-dienoate (184)

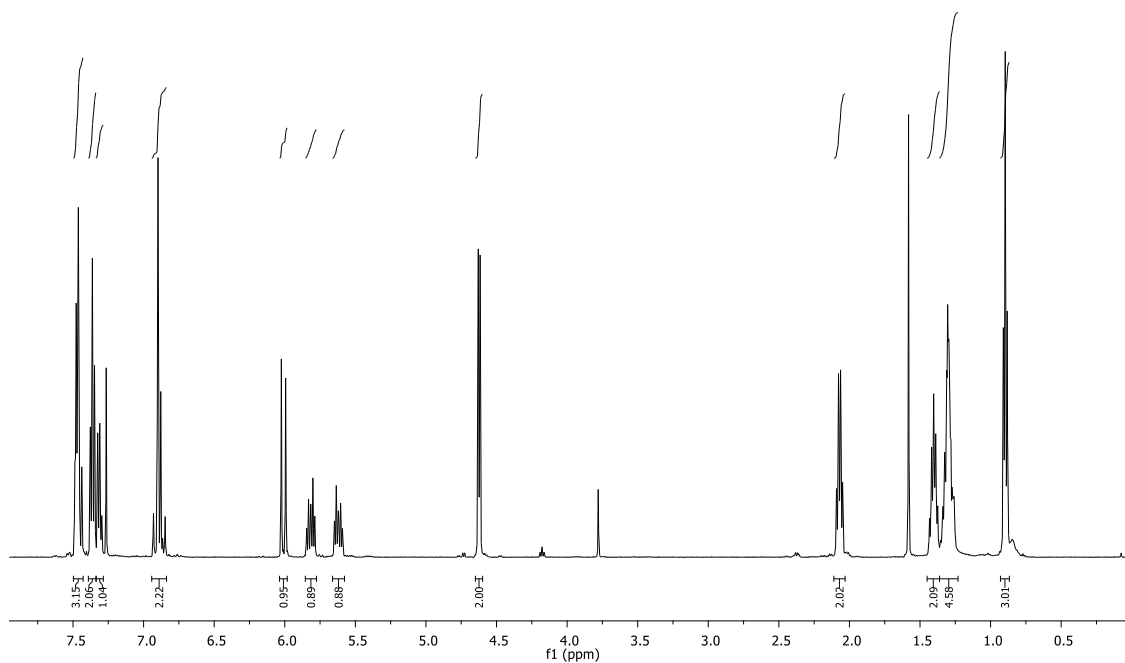
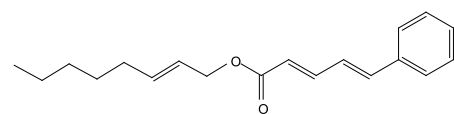


¹H NMR (500 MHz, CDCl₃) spectrum of **184**

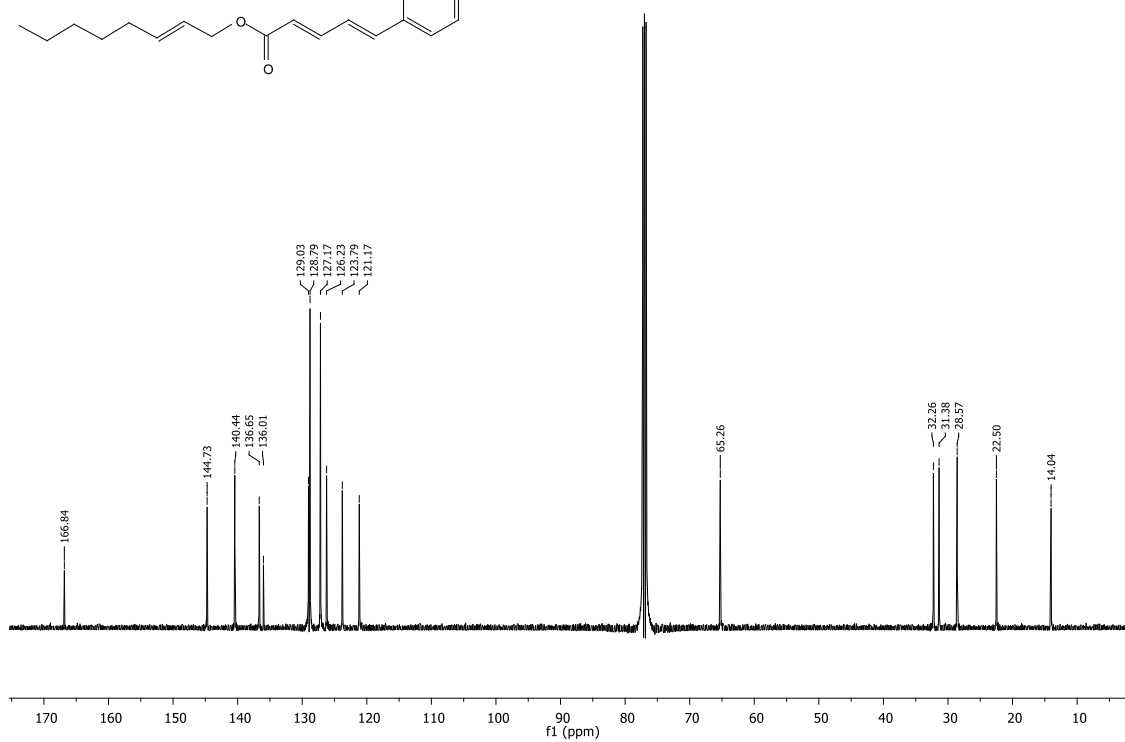
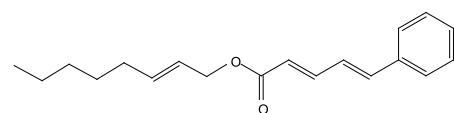


¹³C NMR (125 MHz, CDCl₃) spectrum of **184**

(2'E,2E,4E)-Oct-2'-enyl 5-phenylpenta-2,4-dienoate (186)

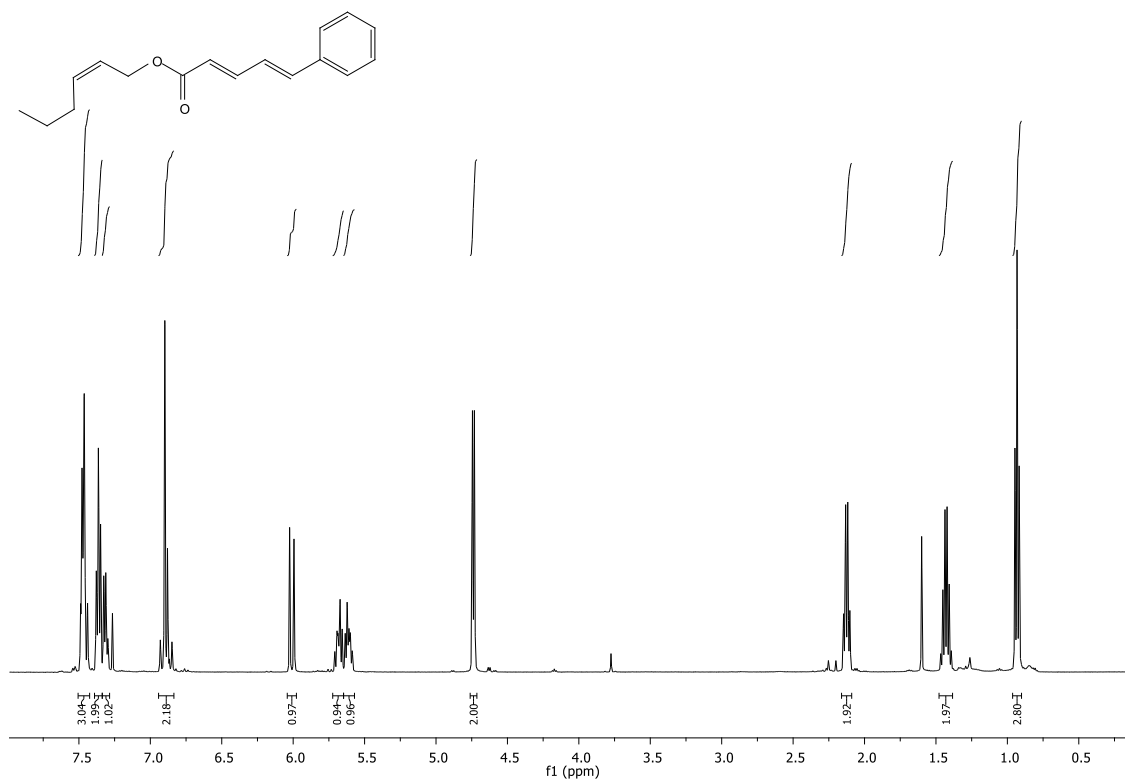


¹H NMR (500 MHz, CDCl₃) spectrum of **186**

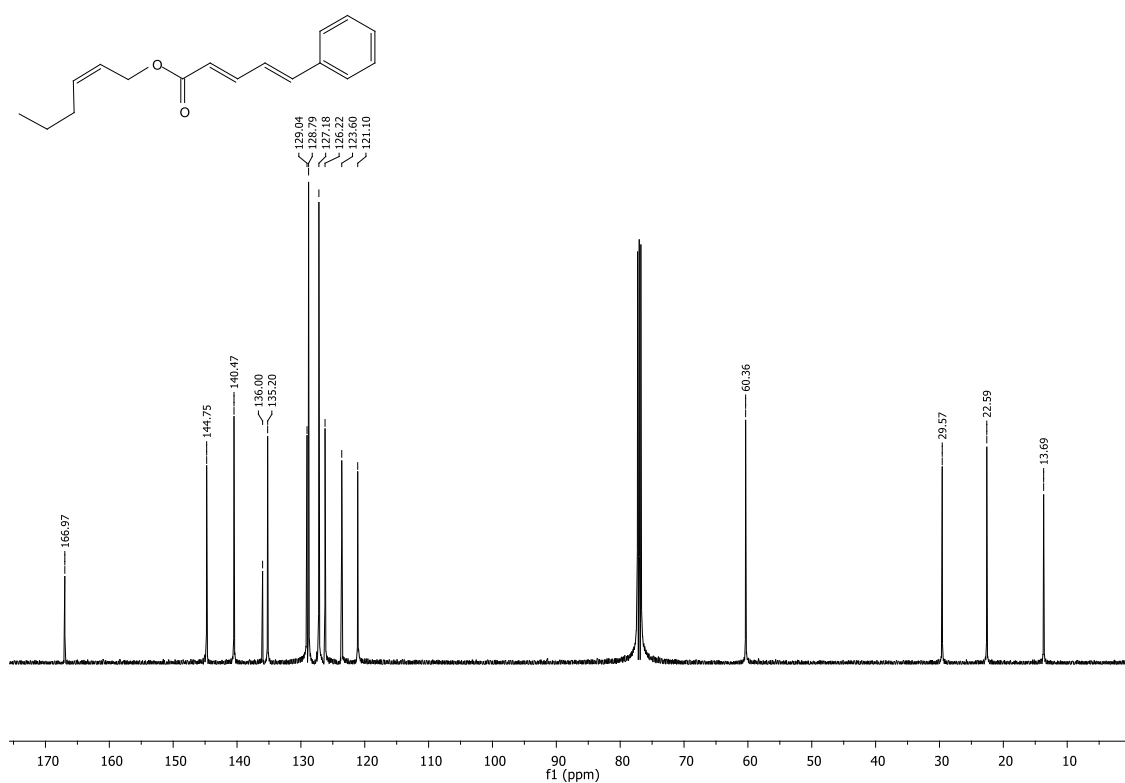


¹³C NMR (125 MHz, CDCl₃) spectrum of **186**

(2'*Z*,2*E*,4*E*)-Hex-2'-enyl 5-phenylpenta-2,4-dienoate (188)

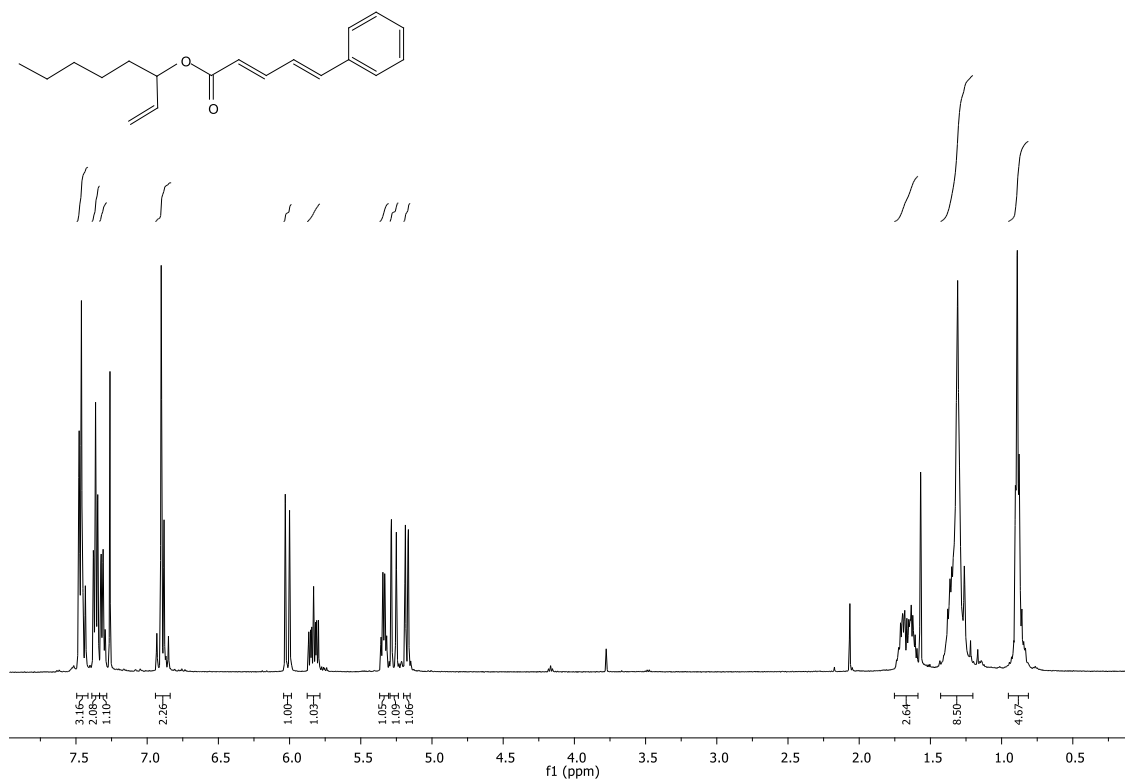


¹H NMR (500 MHz, CDCl₃) spectrum of **188**

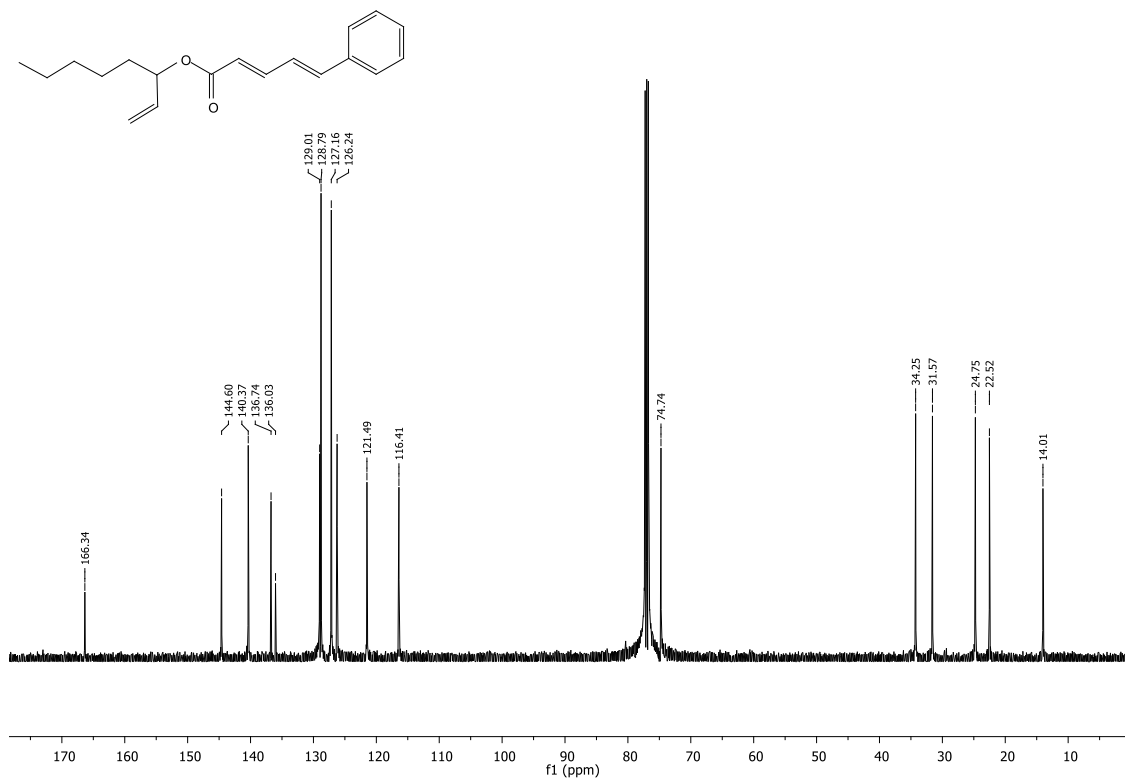


¹³C NMR (125 MHz, CDCl₃) spectrum of **188**

(2E,4E)-Oct-1'-en-3'-yl 5-phenylpenta-2,4-dienoate (190)

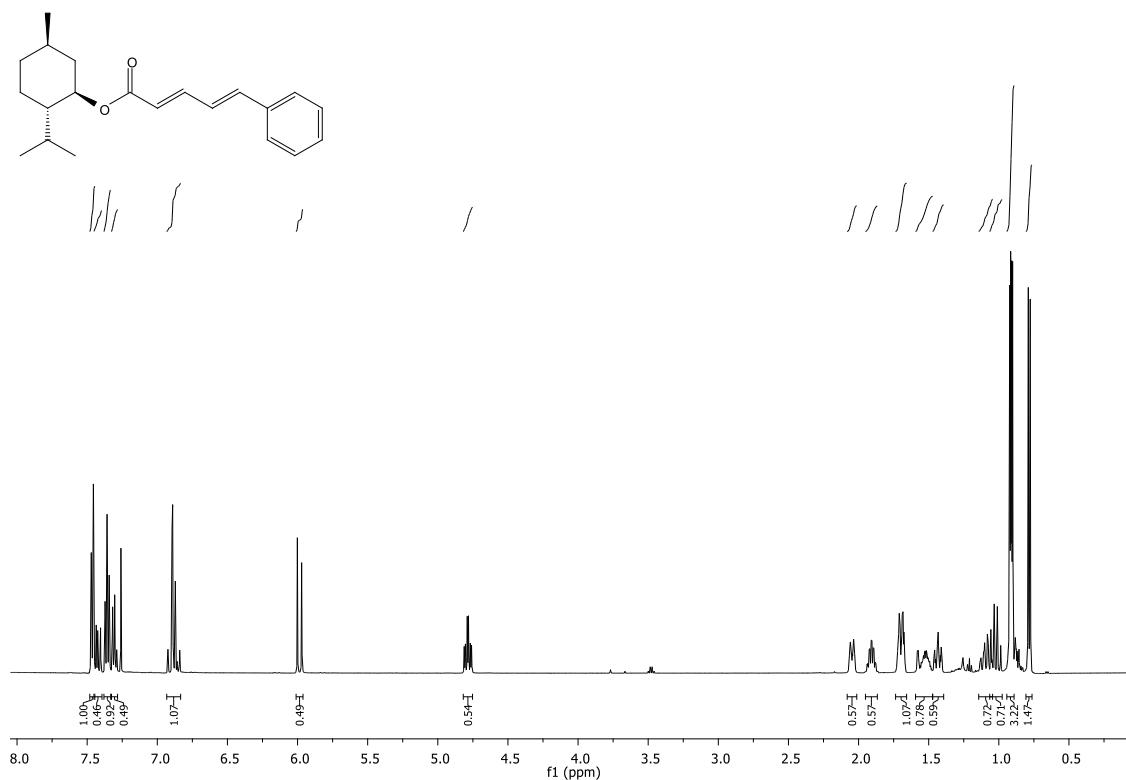


¹H NMR (500 MHz, CDCl₃) spectrum of 190

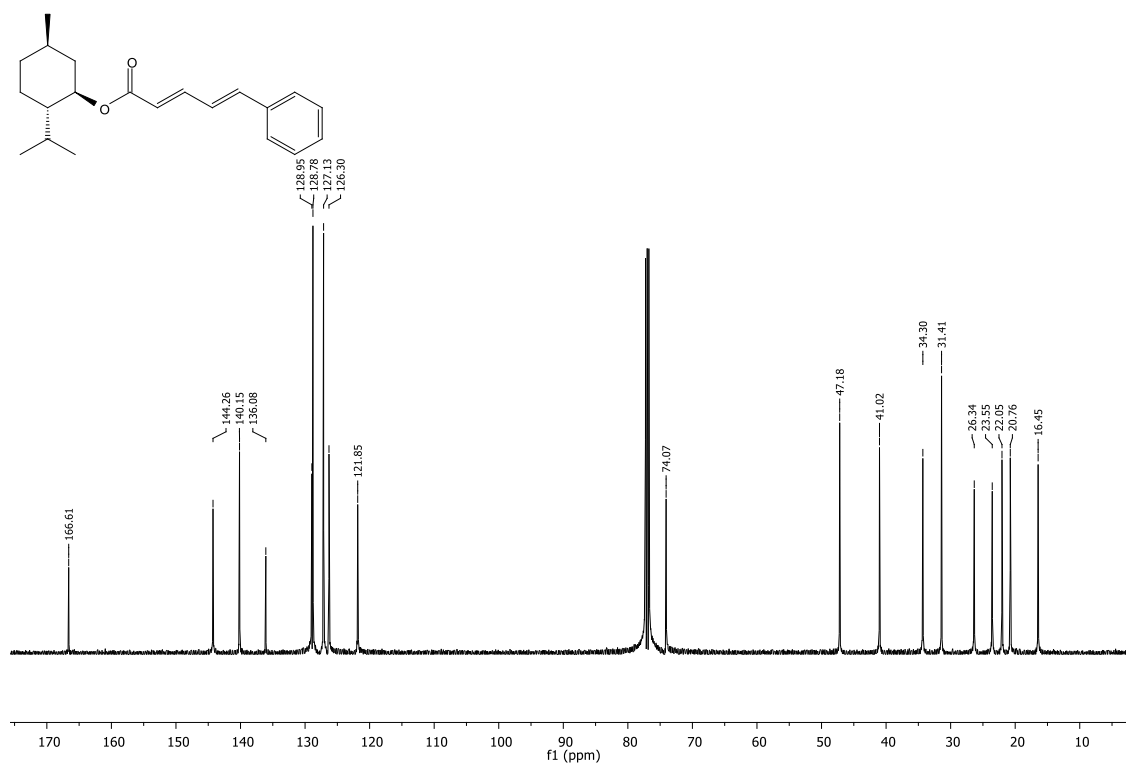


¹³C NMR (125 MHz, CDCl₃) spectrum of 190

(1'*R*,2'*S*,5'*R*,2*E*,4*E*)-2'-*iso*-Propyl-5'-methylcyclohex-1'-yl 5-phenylpenta-2,4-dienoate
(192)

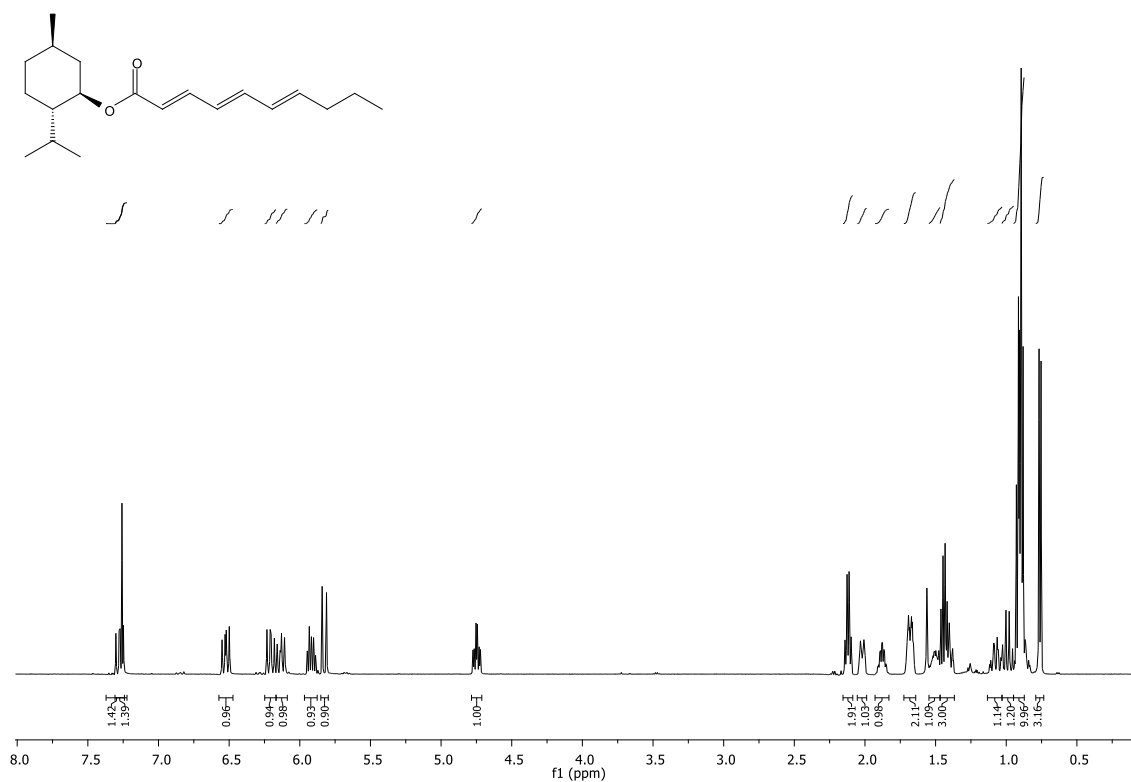


¹H NMR (500 MHz, CDCl₃) spectrum of **192**

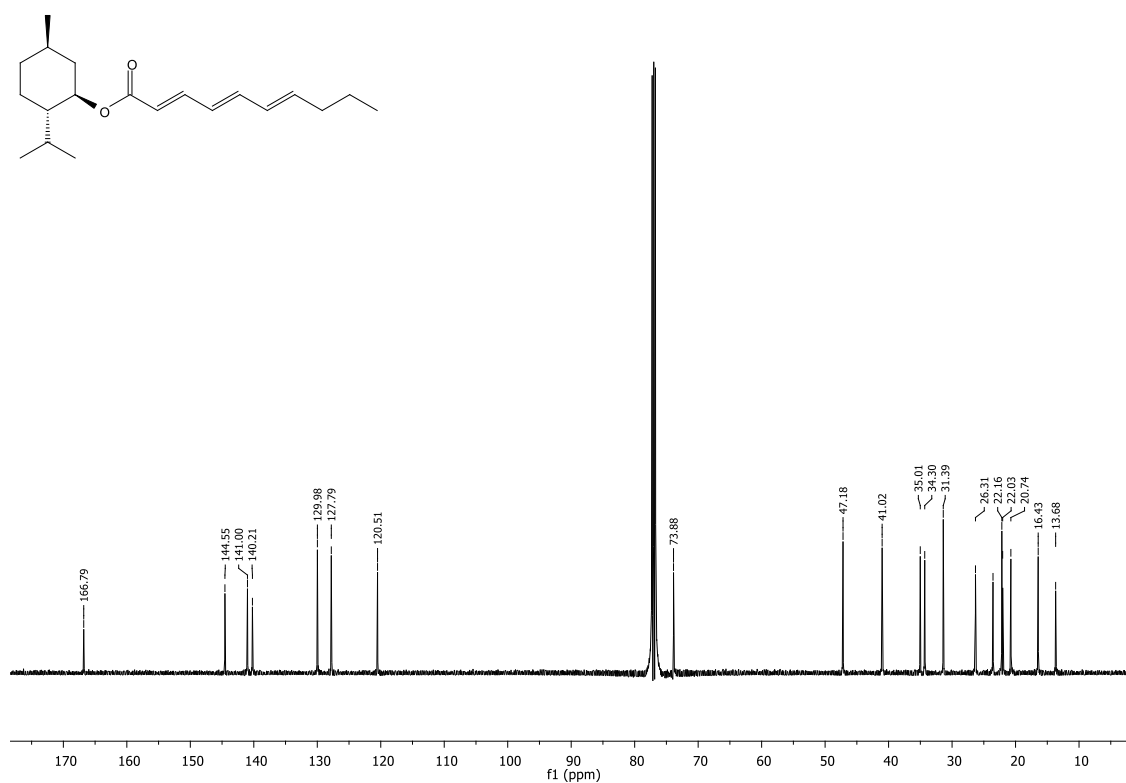


¹³C NMR (125 MHz, CDCl₃) spectrum of **192**

(1'*R*,2'*S*,5'*R*,2*E*,4*E*,6*E*)- 2'-*iso*-Propyl-5'-methylcyclohex-1'-yl deca-2,4,6-trienoate (194**)**

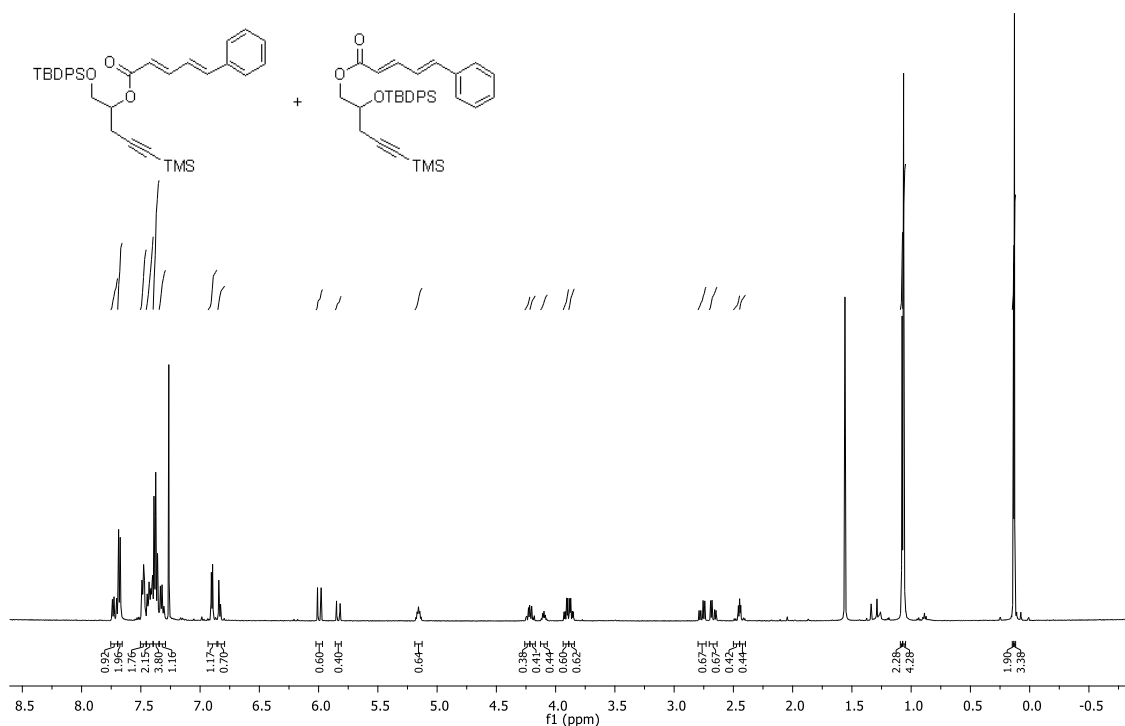


¹H NMR (500 MHz, CDCl₃) spectrum of **194**

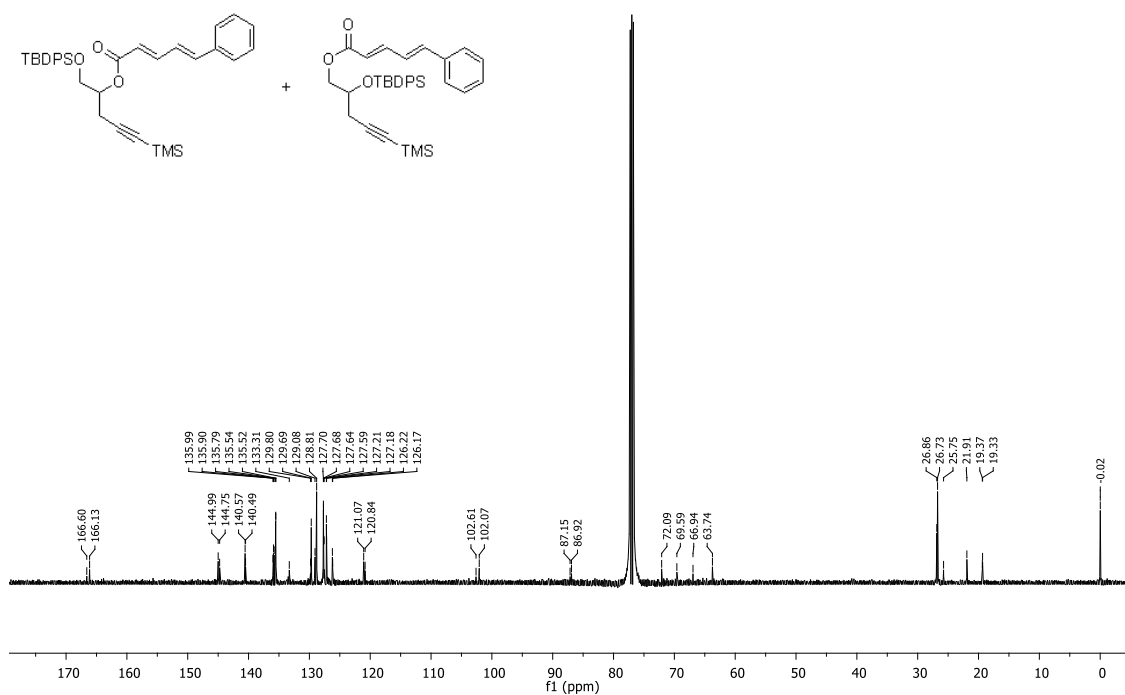


¹³C NMR (125 MHz, CDCl₃) spectrum of **194**

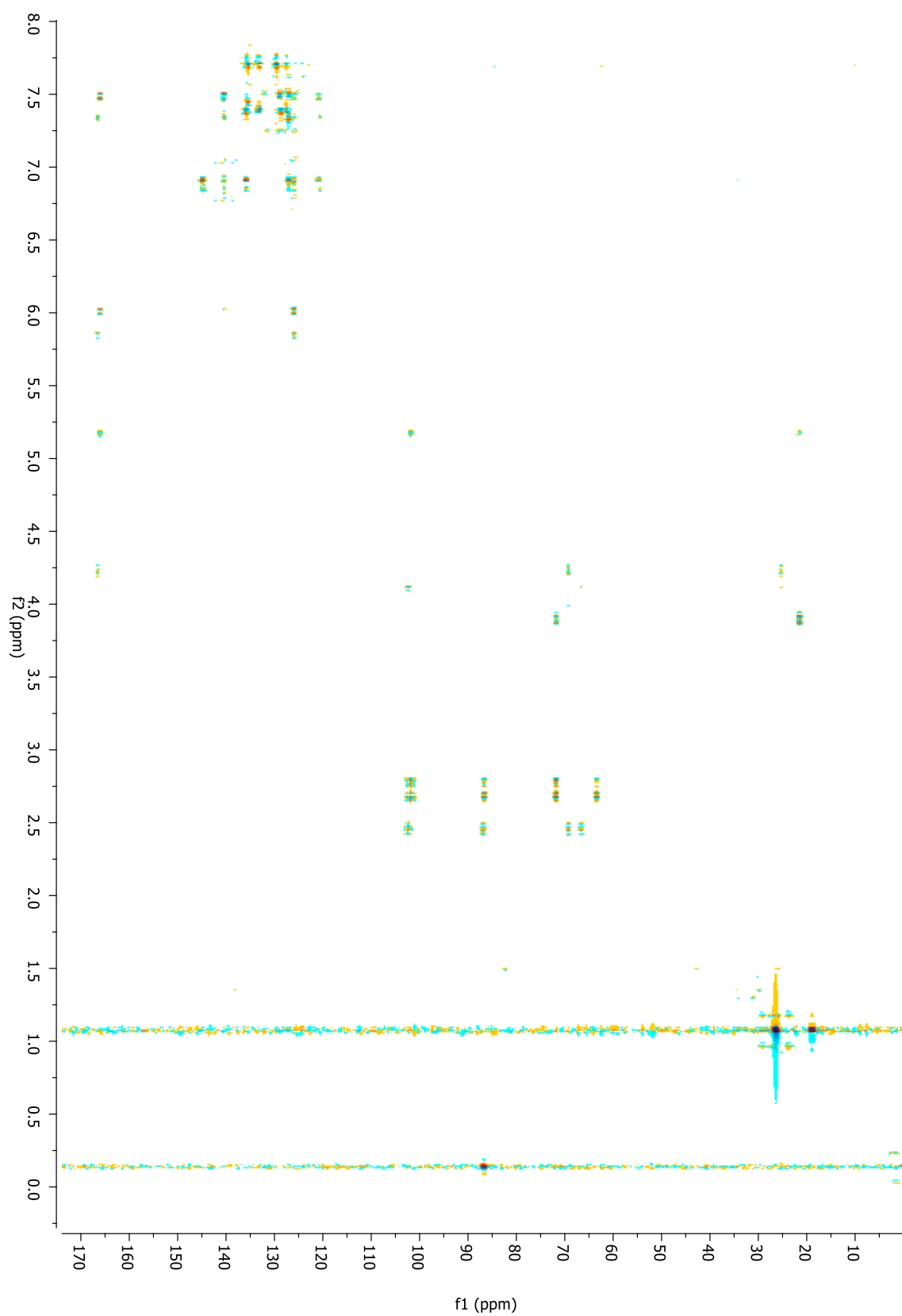
Mixture of (2*E*,4*E*)-[1'-(*tert*-butyldiphenylsilyloxy)-5'-trimethylsilyl]pent-4'-yn-2'-yl 5-phenylpenta-2,4-dienoate (**196**) and the silyl migrated product (2*E*,4*E*)-[2'-(*tert*-butyldiphenylsilyloxy)-5'-trimethylsilyl]pent-4'-yn-1'-yl 5-phenylpenta-2,4-dienoate (**199**)



¹H NMR (500 MHz, CDCl₃) spectrum of **196** and **199**

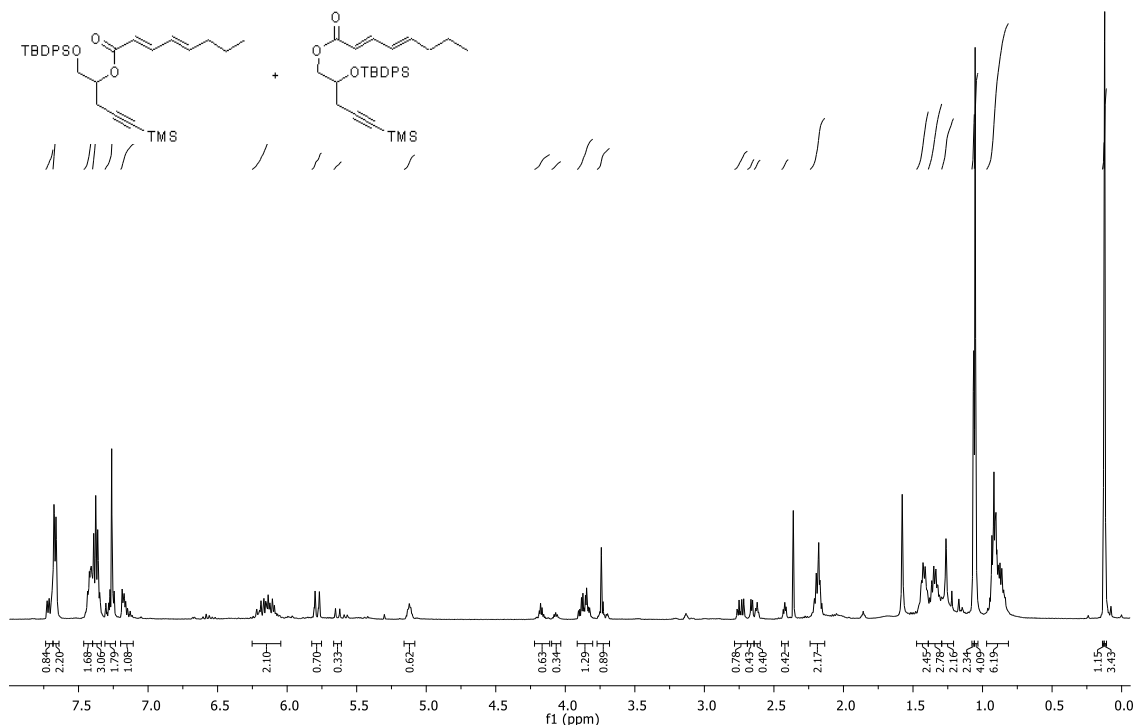


¹³C NMR (125 MHz, CDCl₃) spectrum of **196** and **199**

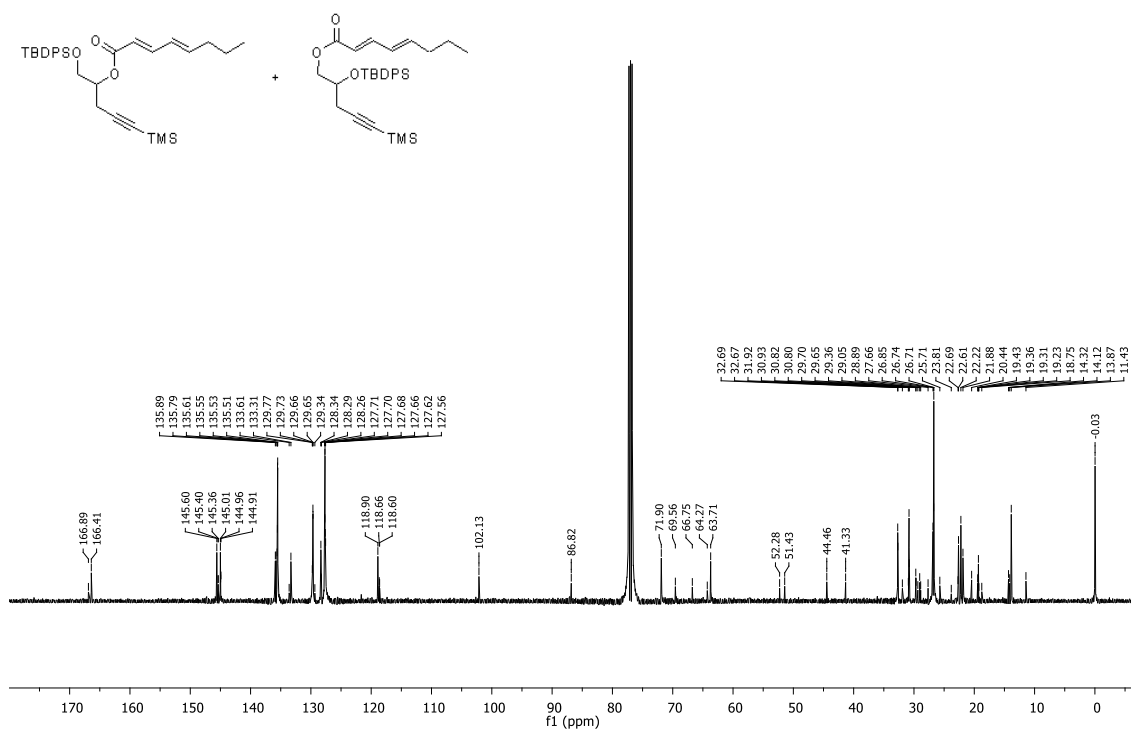


CIGAR-HMBC spectrum of **196** and **199**

Mixture of (2*E*,4*E*)-[1'-(*tert*-butyldiphenylsilyloxy)-5'-trimethylsilyl]pent-4'-yn-2'-yl nona-2,4-dienoate (**198**) and the silyl migrated product, (2*E*,4*E*)-[2'-(*tert*-butyldiphenylsilyloxy)-5'-trimethylsilyl]pent-4'-yn-1'-yl nona-2,4-dienoate

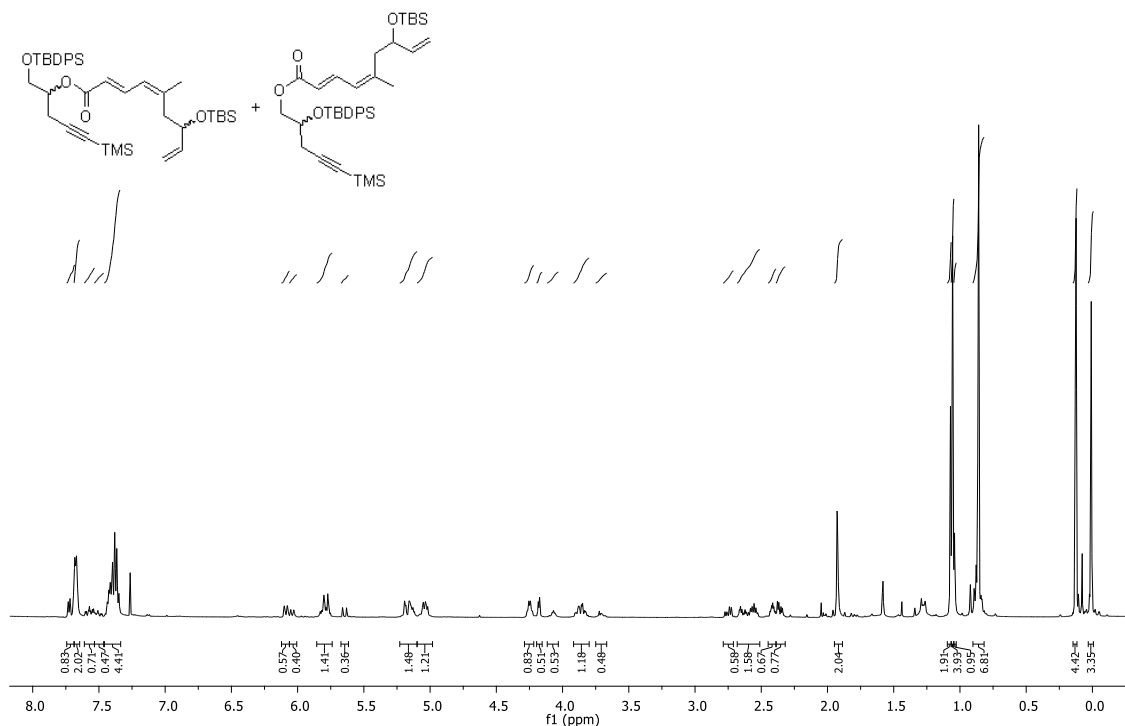


¹H NMR (500 MHz, CDCl₃) spectrum of **198** and silyl migrated product

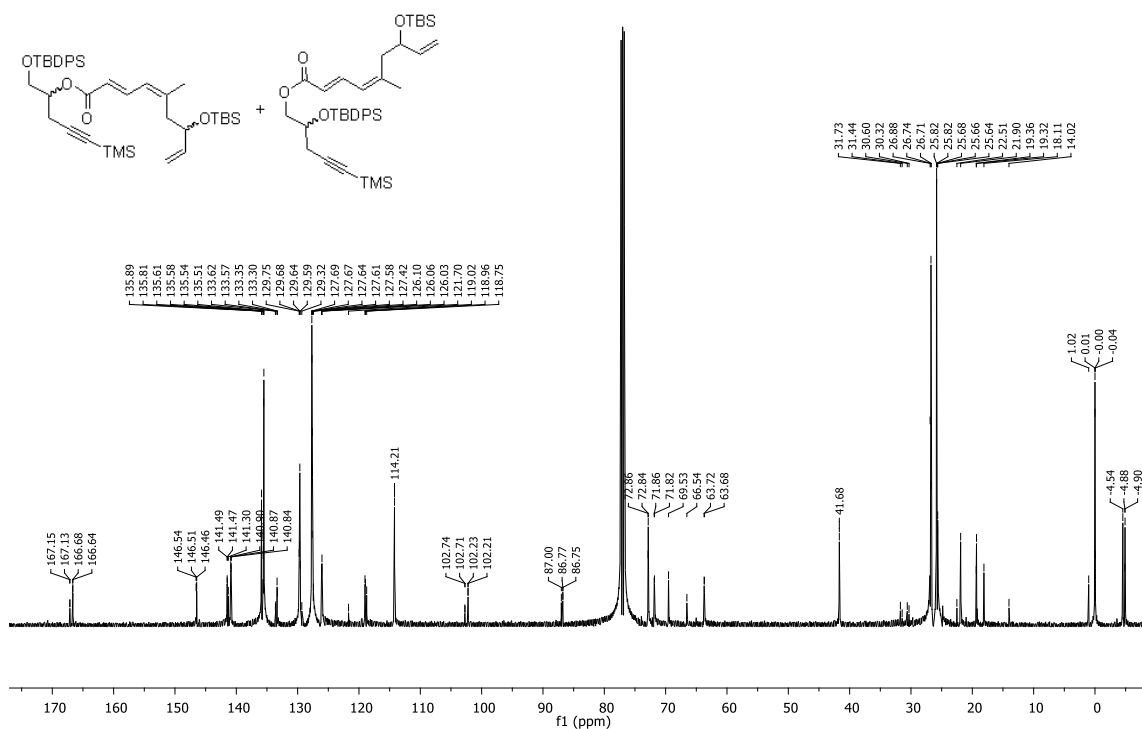


¹³C NMR (125 MHz, CDCl₃) spectrum of **198** and silyl migrated product

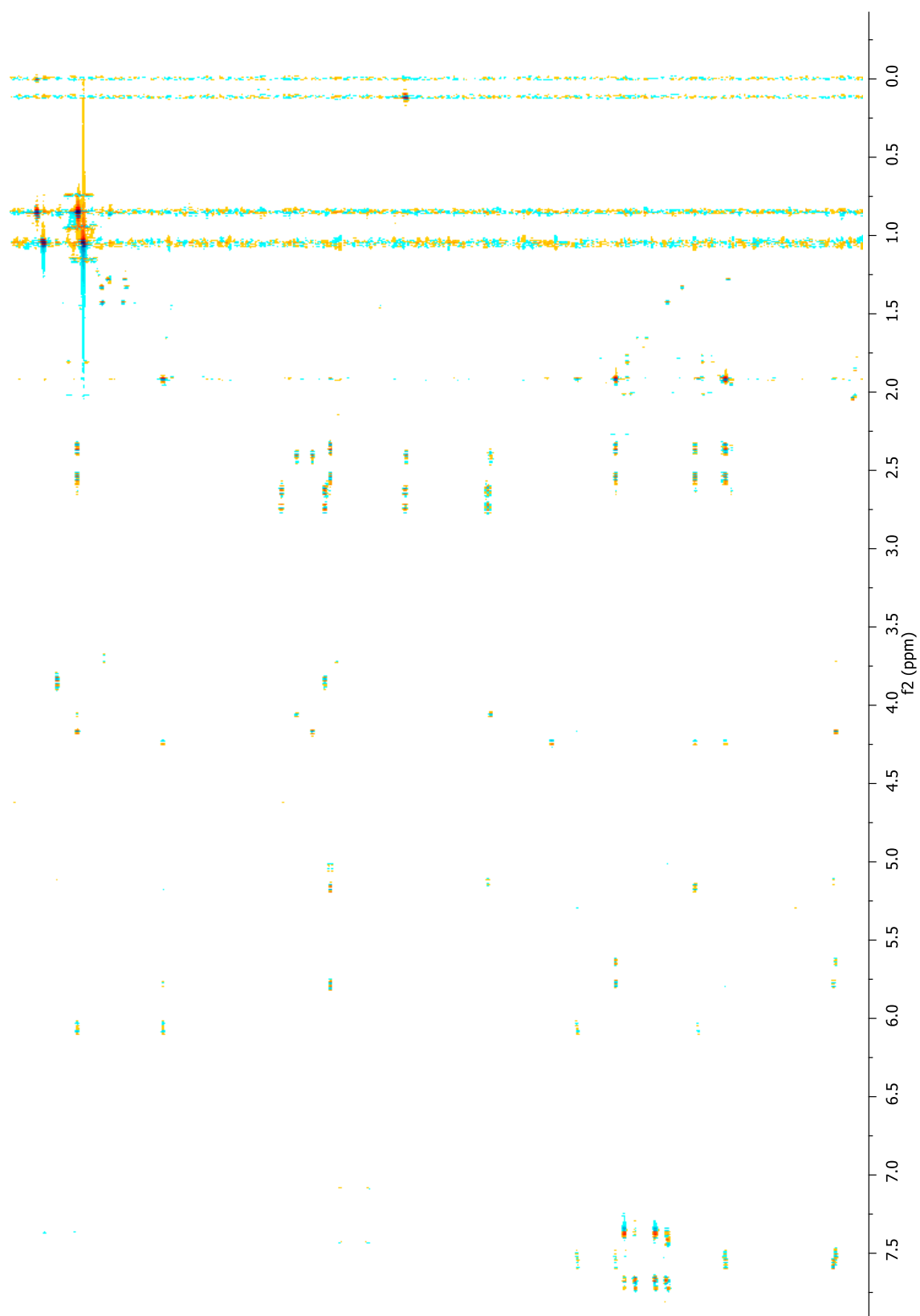
Mixture of (2*E*,4*Z*)-1'-(*tert*-butyldiphenylsilyloxy)-5'-(trimethylsilyl)pent-4'-yn-2'-yl 7-(*tert*-butyldimethylsilyloxy)-5-methylnona-2,4,8-trienoate (**204**) and the silyl migrated product, (2*E*,4*Z*)-2'-(*tert*-butyldiphenylsilyloxy)-5'-(trimethylsilyl)pent-4'-yn-1'-yl 7-(*tert*-butyldimethylsilyloxy)-5-methylnona-2,4,8-trienoate (**205**)



¹H NMR (500 MHz, CDCl₃) spectrum of **204** and **205**

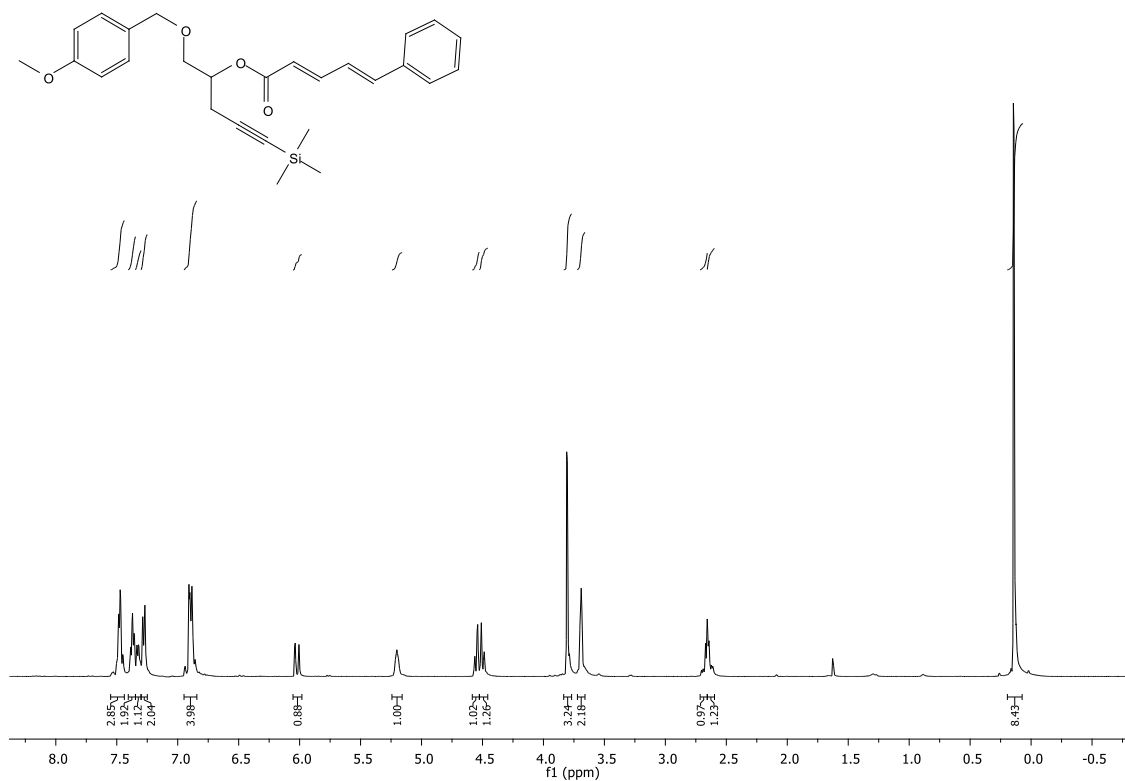


¹³C NMR (125 MHz, CDCl₃) spectrum of **204** and **205**

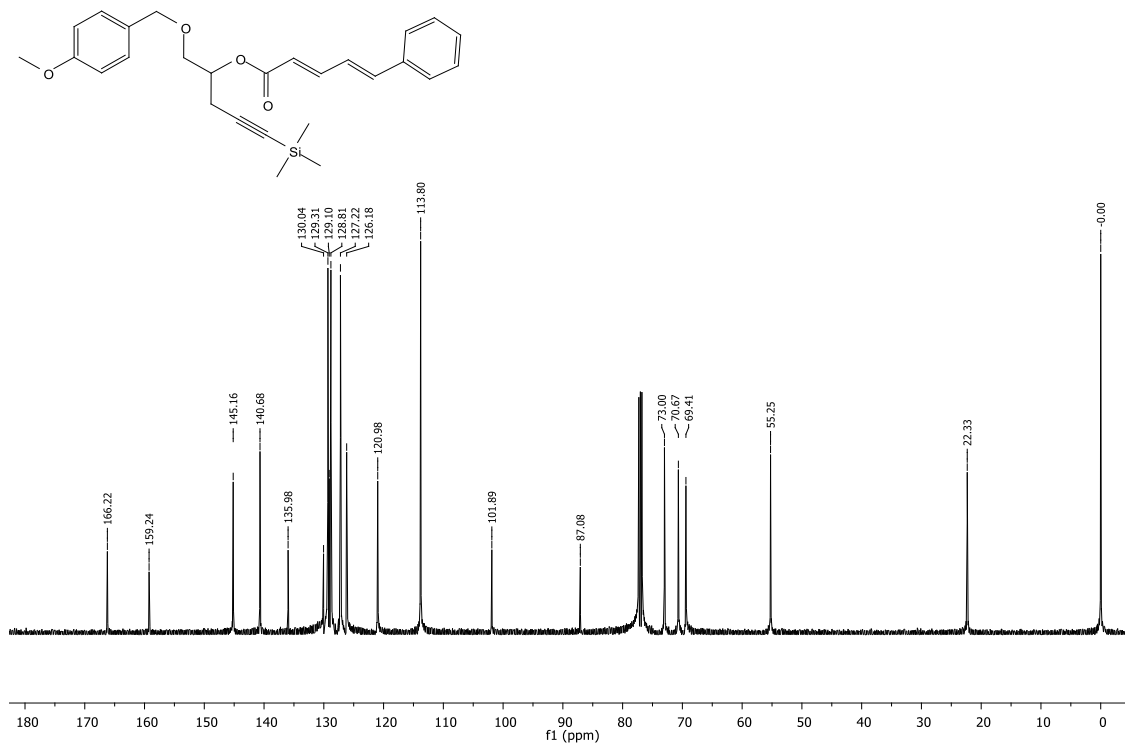


CIGAR-HMBC spectrum of **204** and **205**

(2E,4E)-[1'-(*para*-Methoxybenzyloxy)-5'-trimethylsilyl]pent-4'-yn-2'-yl 5-phenylpenta-2,4-dienoate (206**)**



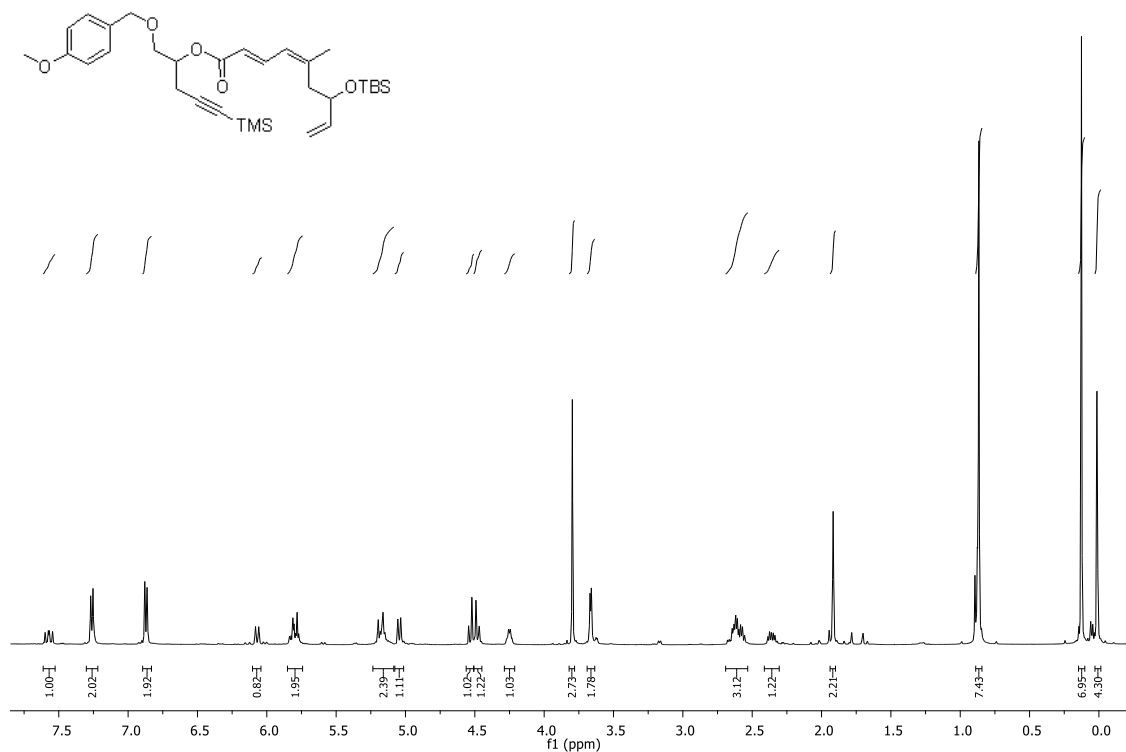
¹H NMR (500 MHz, CDCl₃) spectrum of **206**



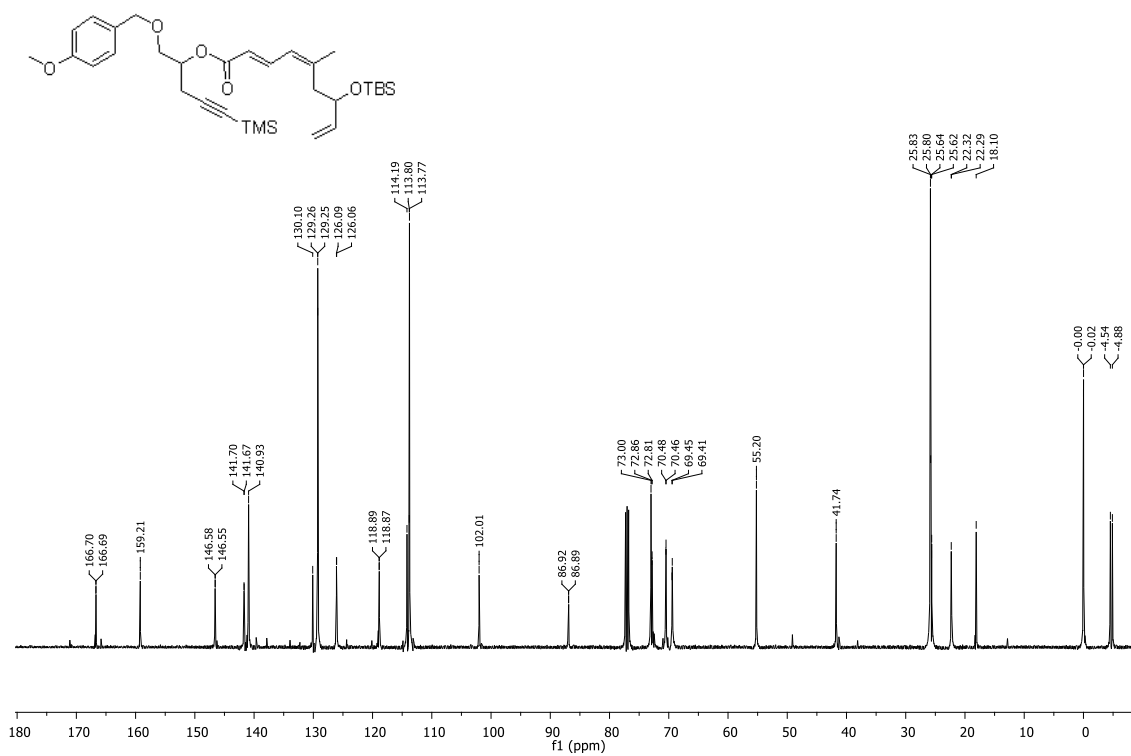
¹³C NMR (125 MHz, CDCl₃) spectrum of **206**

**(2*E*,4*Z*)-1'-(*para*-Methoxybenzyloxy)-5'-(trimethylsilyloxy)pent-4'-yn-2'-yl
butyldimethylsilyloxy)-5-methylnona-2,4,8-trienoate (207)**

7-(*tert*-

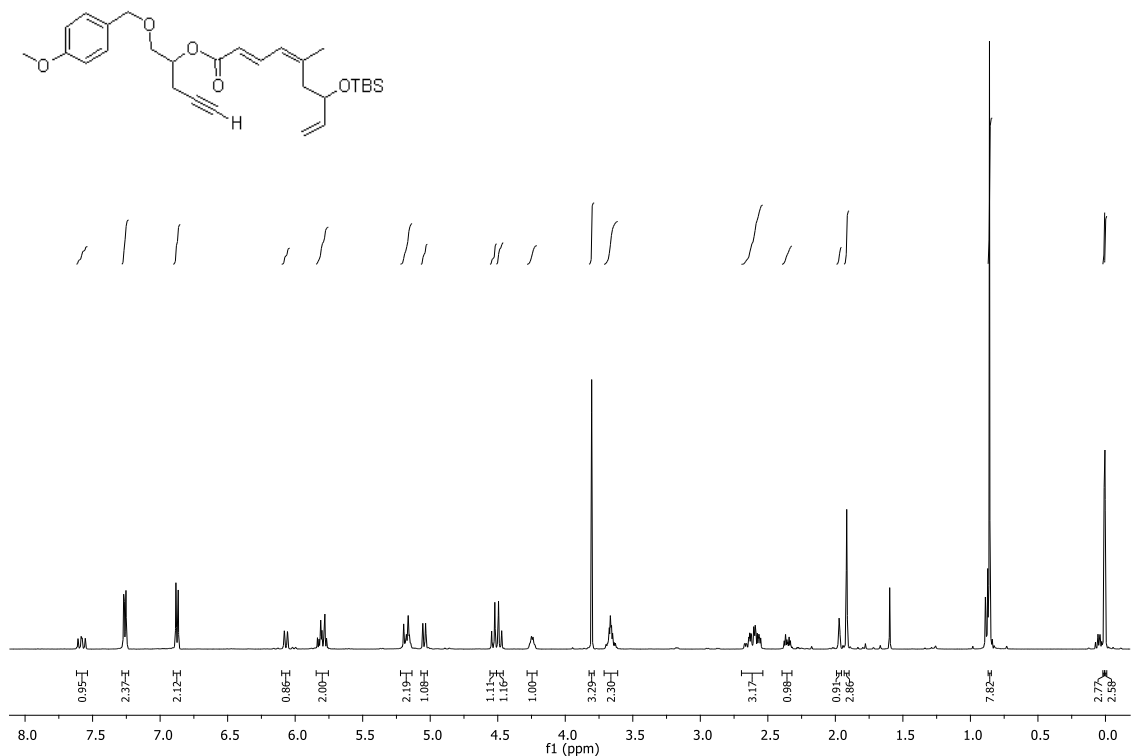


¹H NMR (500 MHz, CDCl₃) spectrum of **207**

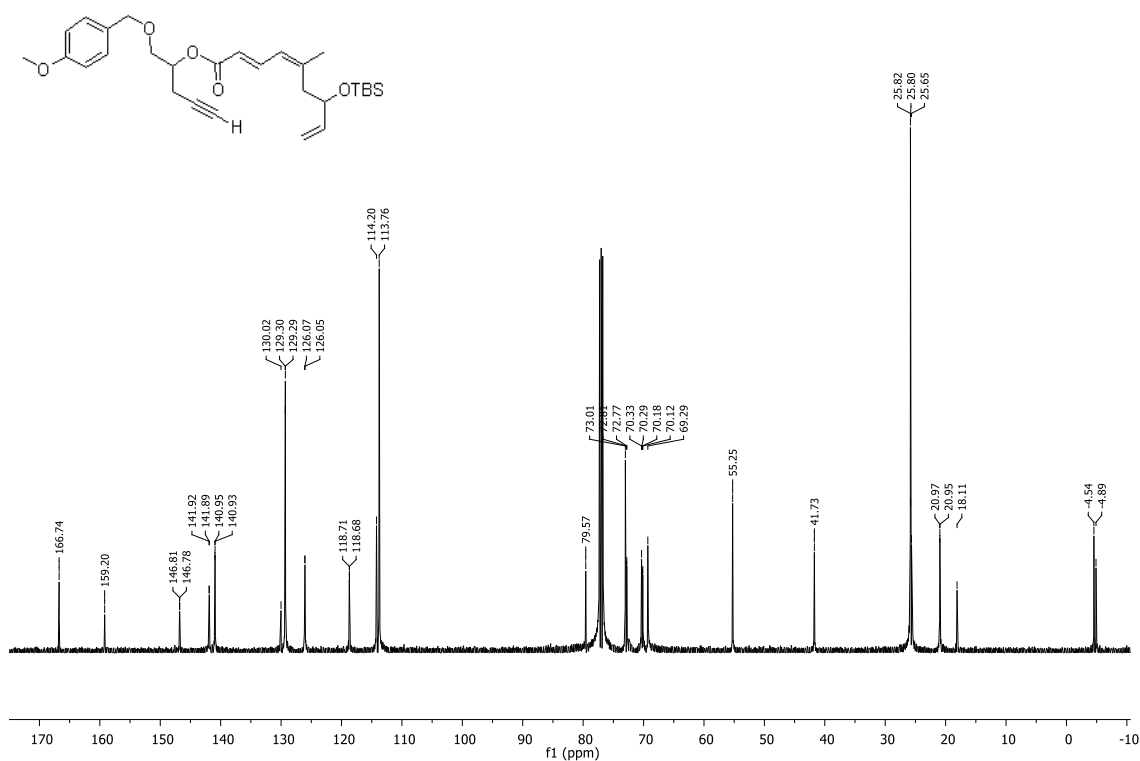


¹³C NMR (125 MHz, CDCl₃) spectrum of **207**

(2*E*,4*Z*)-1'-(*para*-Methoxybenzyloxy)pent-4'-yn-2'-yl 7-(*tert*-butyldimethylsilyloxy)-5-methylnona-2,4,8-trienoate (208)

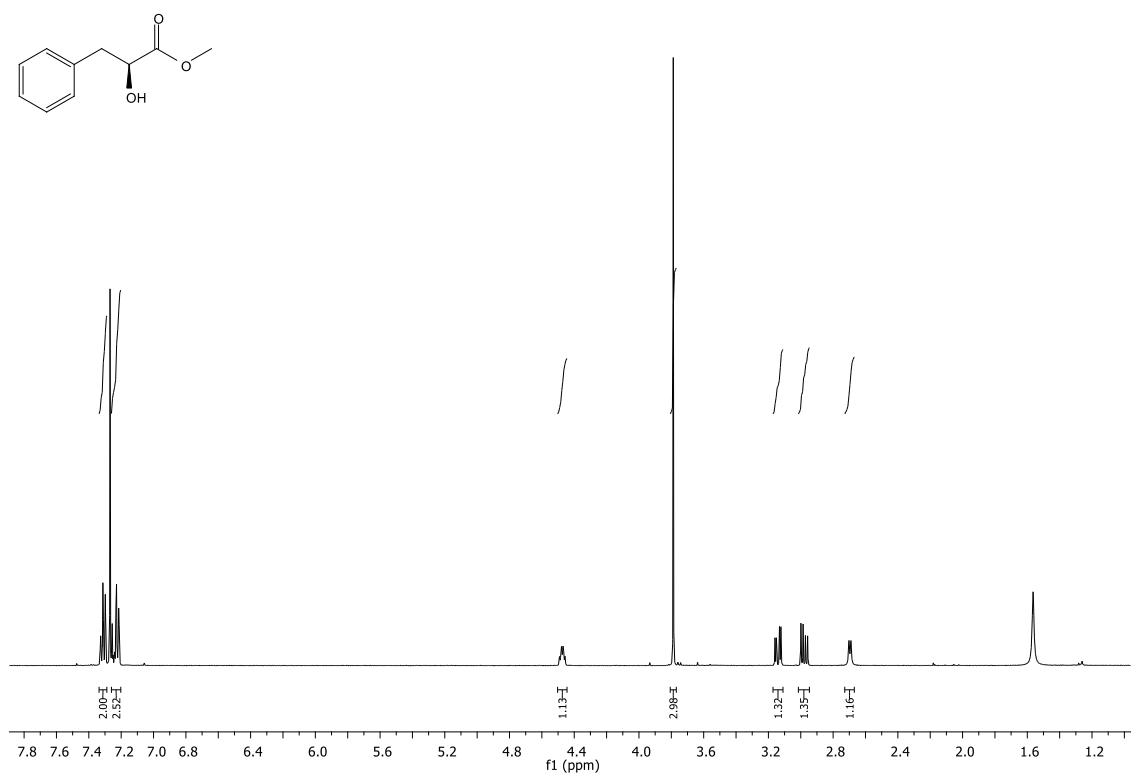


¹H NMR (500 MHz, CDCl₃) spectrum of **208**

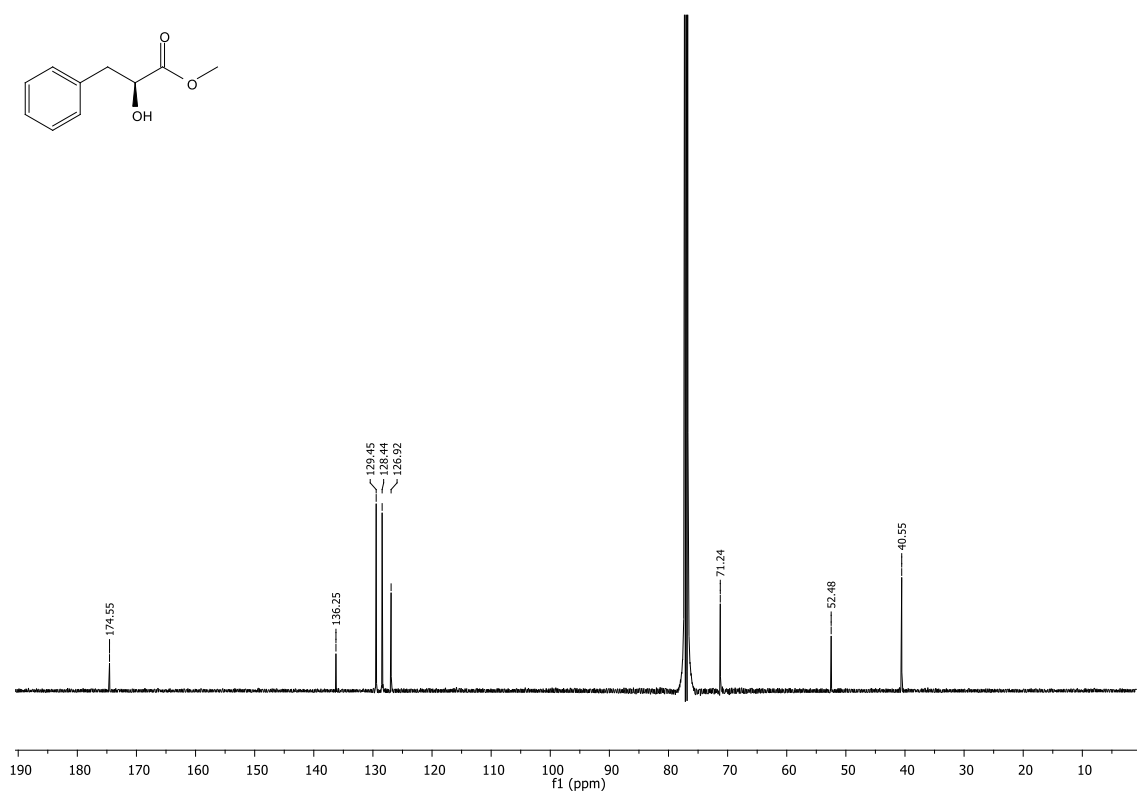


¹³C NMR (125 MHz, CDCl₃) spectrum of **208**

Methyl 2-hydroxy-3-phenylpropanoate (**220**)

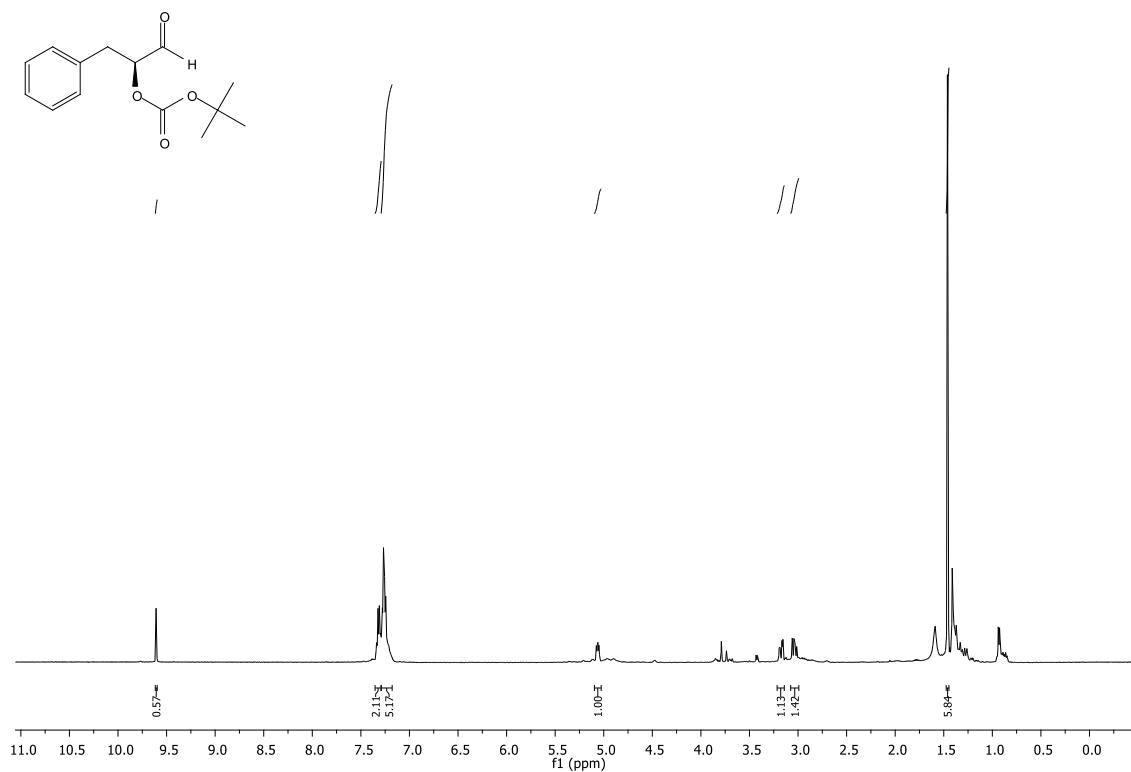


¹H NMR (500 MHz, CDCl₃) spectrum of **220**



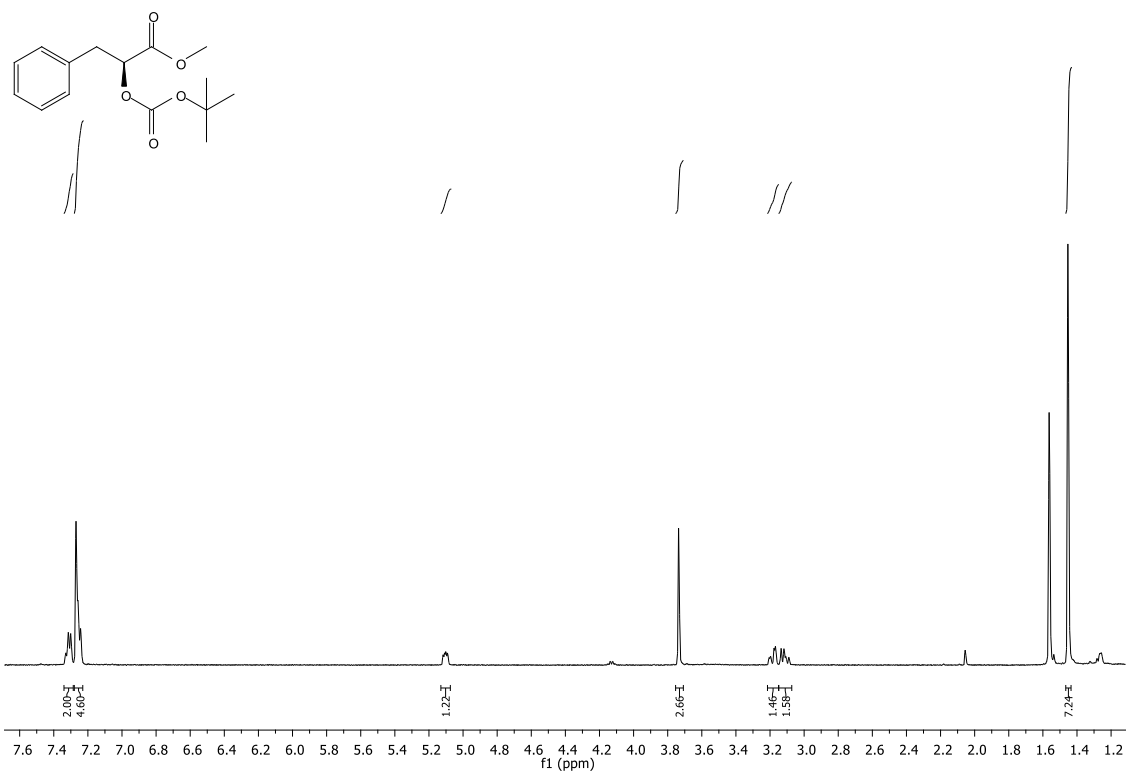
¹³C NMR (125 MHz, CDCl₃) spectrum of **220**

2-(*t*-Butylcarbonate)-3-phenylpropanal (223)

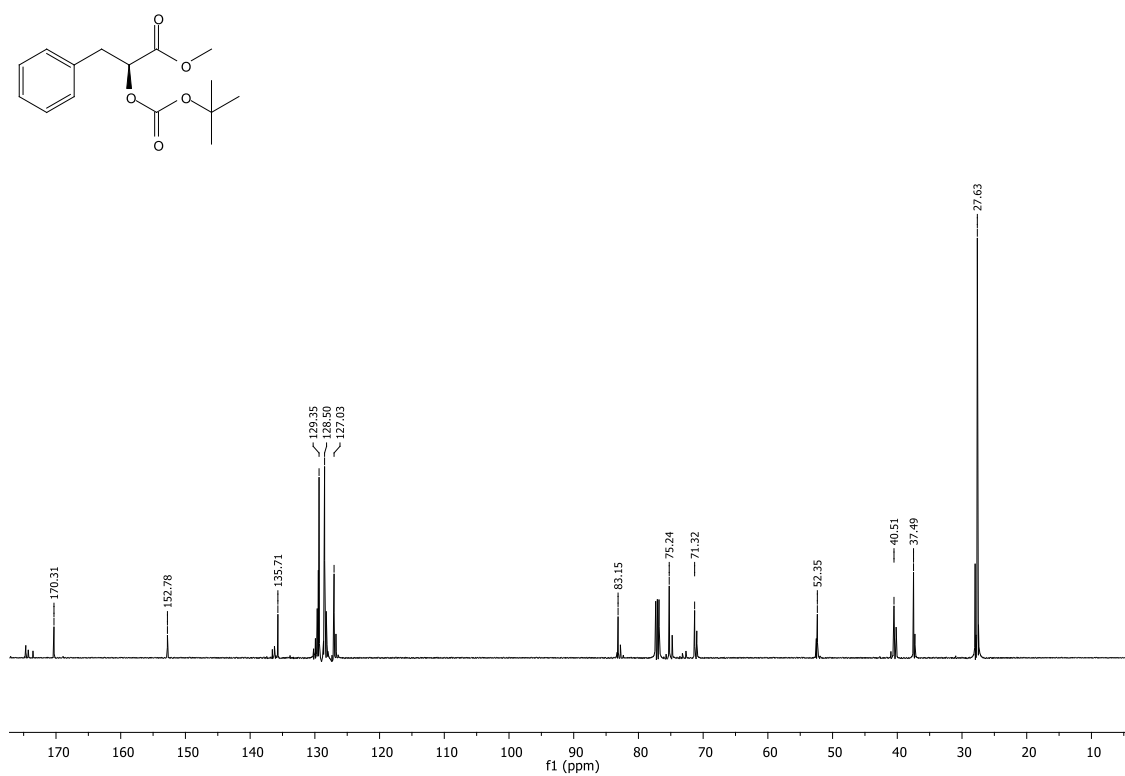


¹H NMR (500 MHz, CDCl₃) spectrum of 223

Methyl 2-(*t*-butylcarbonate)-3-phenylpropanoate (224)

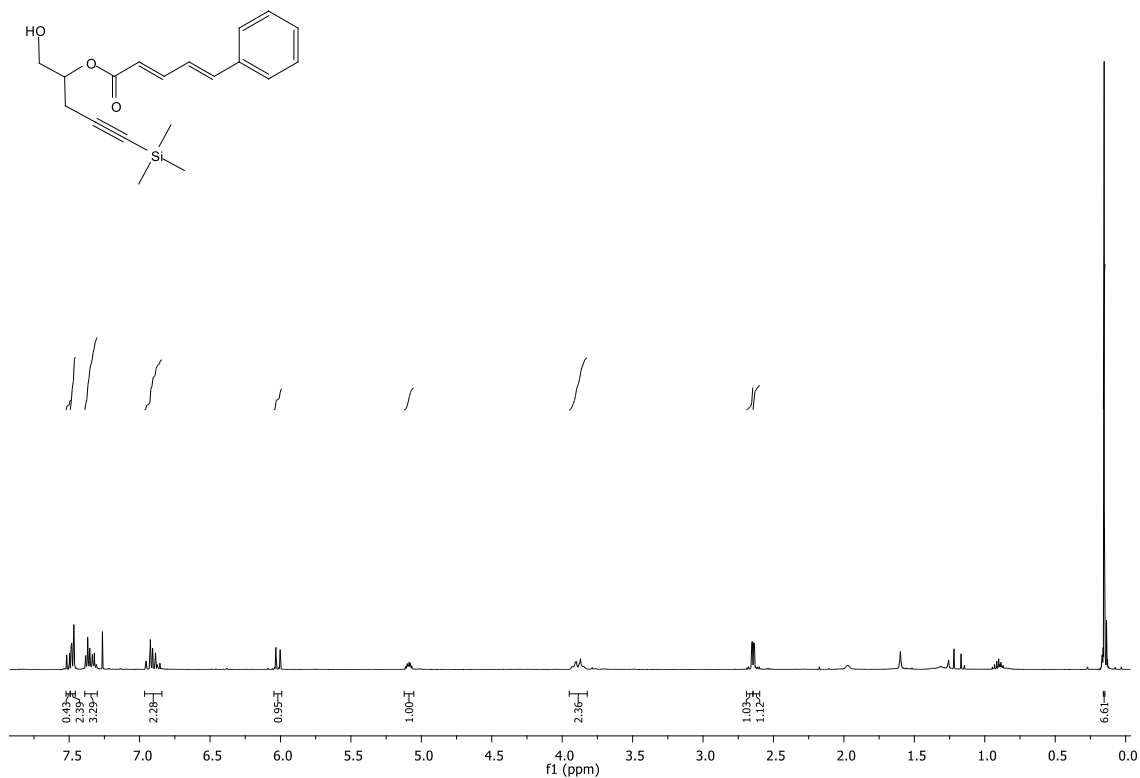


¹H NMR (500 MHz, CDCl₃) spectrum of 224

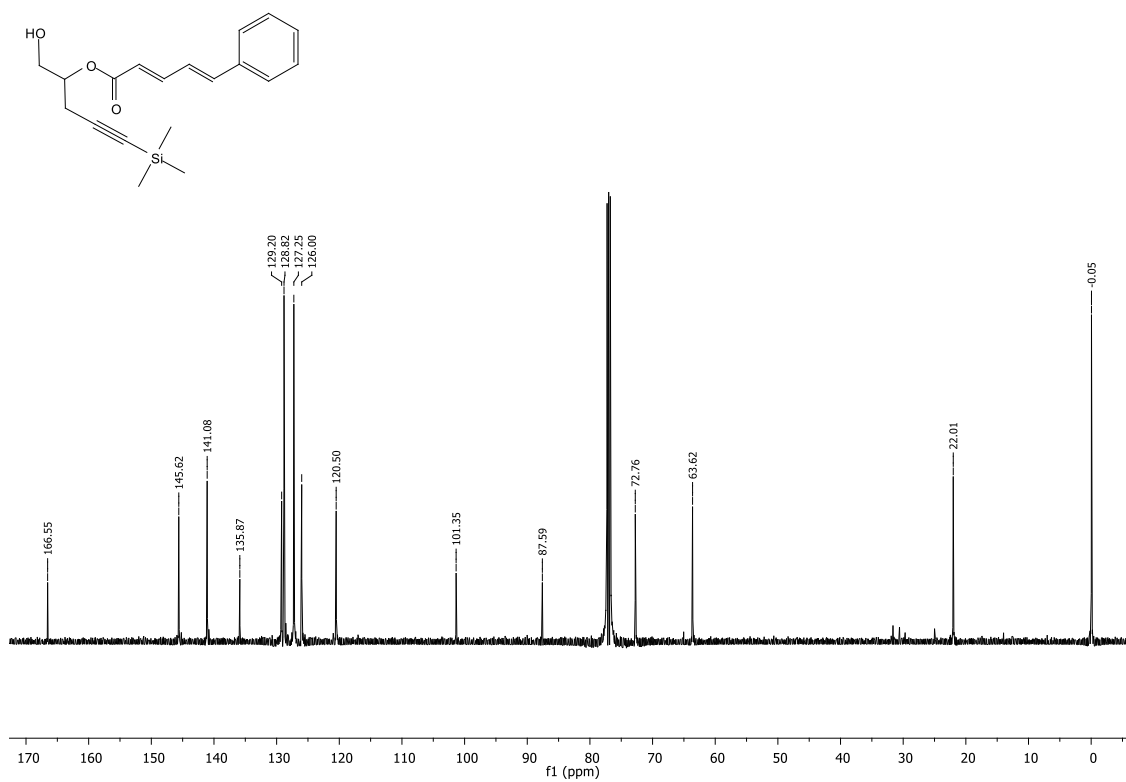


¹³C NMR (125 MHz, CDCl₃) spectrum of 224

(5'-Trimethylsilyl)pent-4'-yn-2'-yl 5-phenylpenta-2,4-dienoate (227)

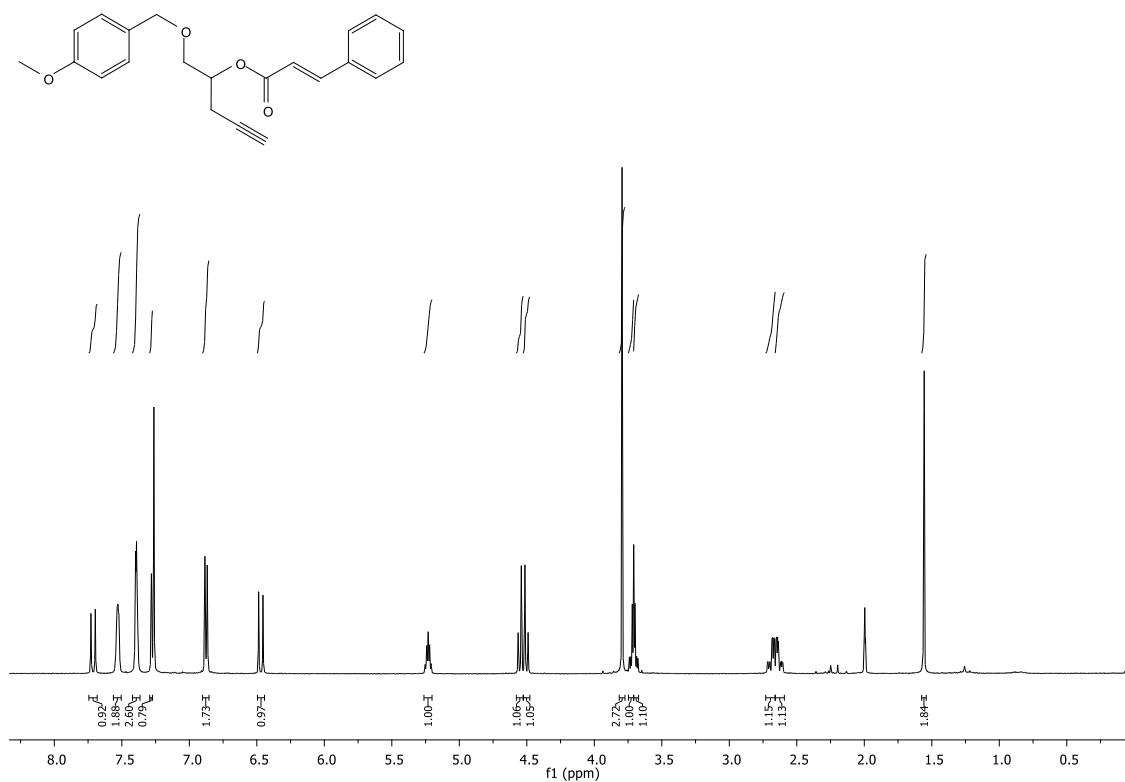


¹H NMR (500 MHz, CDCl₃) spectrum of **227**

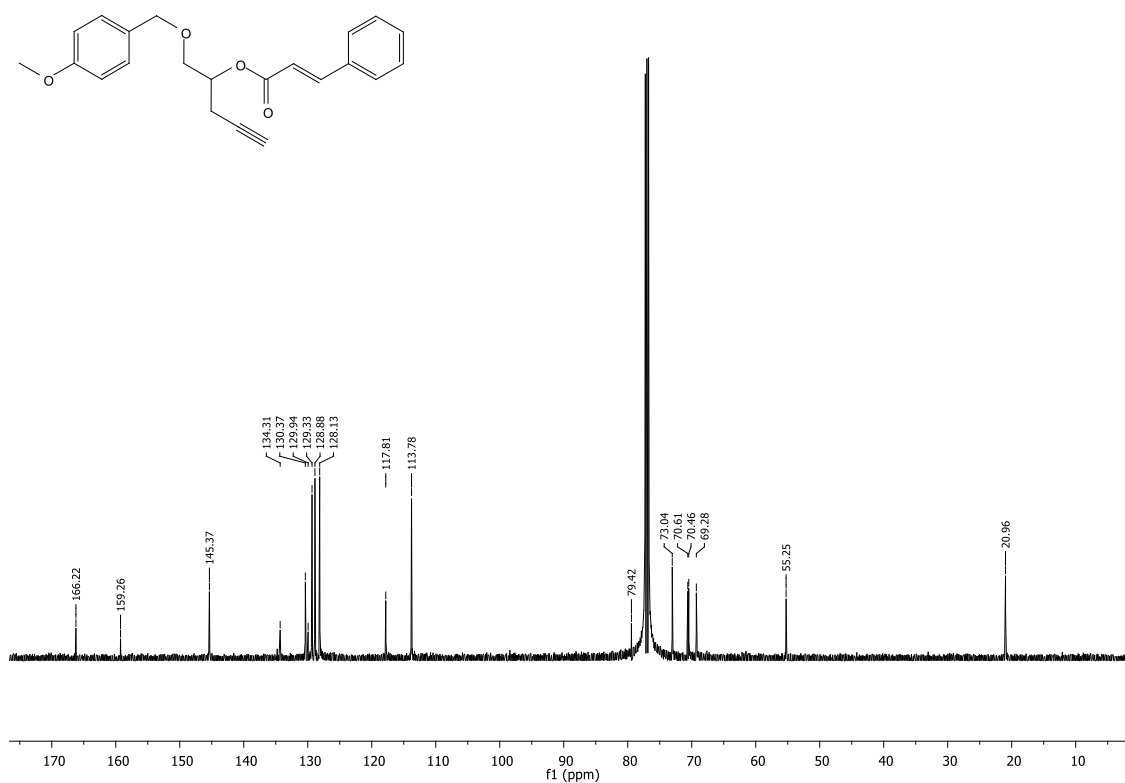


¹³C NMR (125 MHz, CDCl₃) spectrum of **227**

1'-(*para*-Methoxybenzyloxy)pent-4'-yn-2'-yl 3-phenylprop-2-enoate (234)

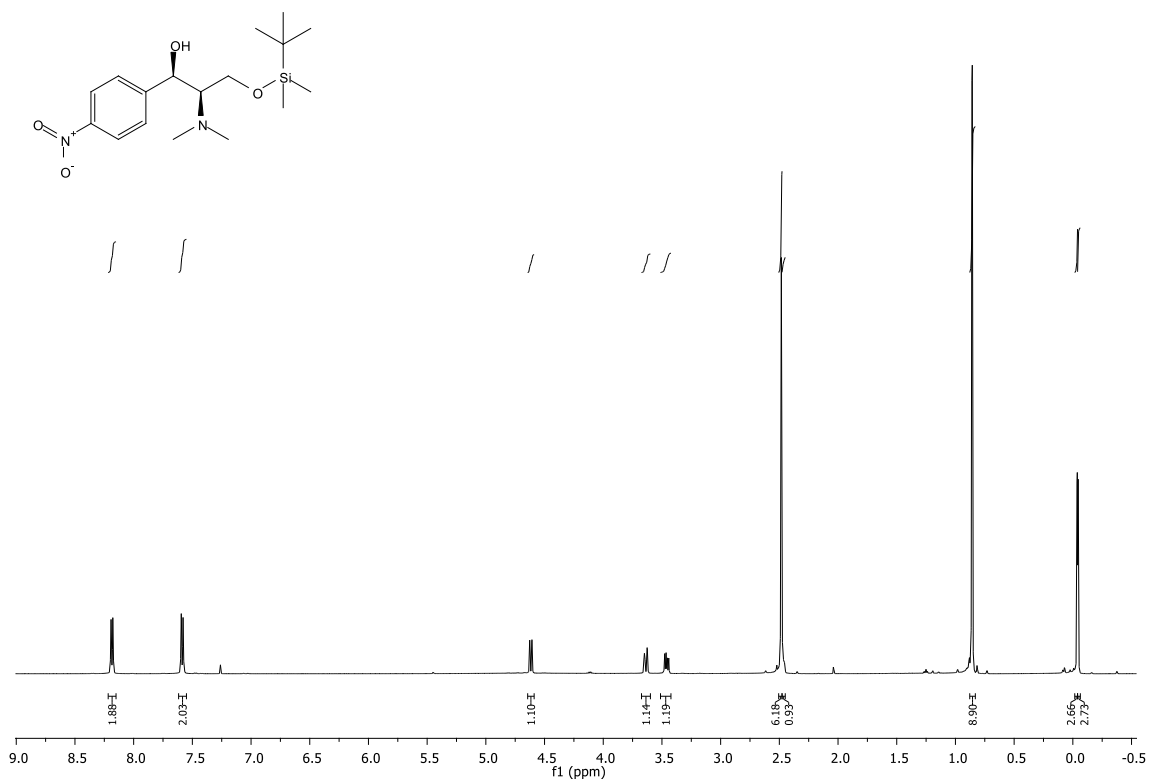


¹H NMR (500 MHz, CDCl₃) spectrum of **234**

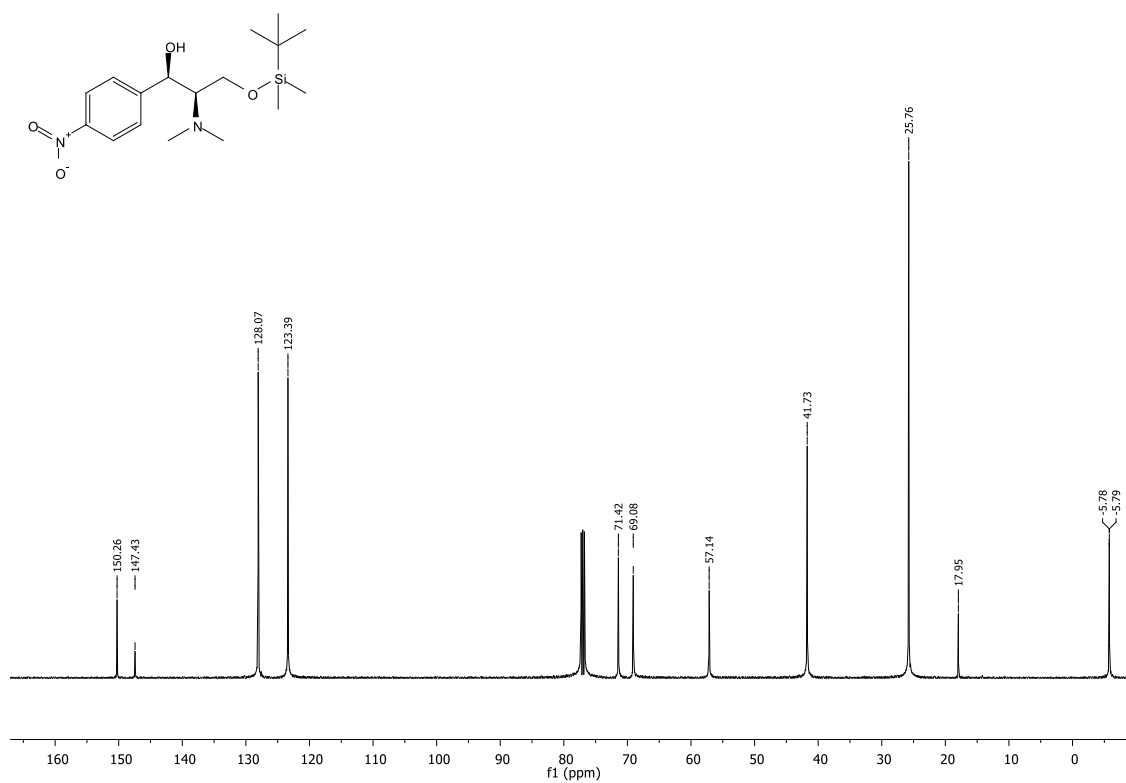


¹³C NMR (125 MHz, CDCl₃) spectrum of **234**

(1*R*,2*R*)-3-(*t*-Butyldimethylsilyloxy)-2-*N,N*-dimethylamino-1-(4'-nitrophenyl)propane-1-ol (232)

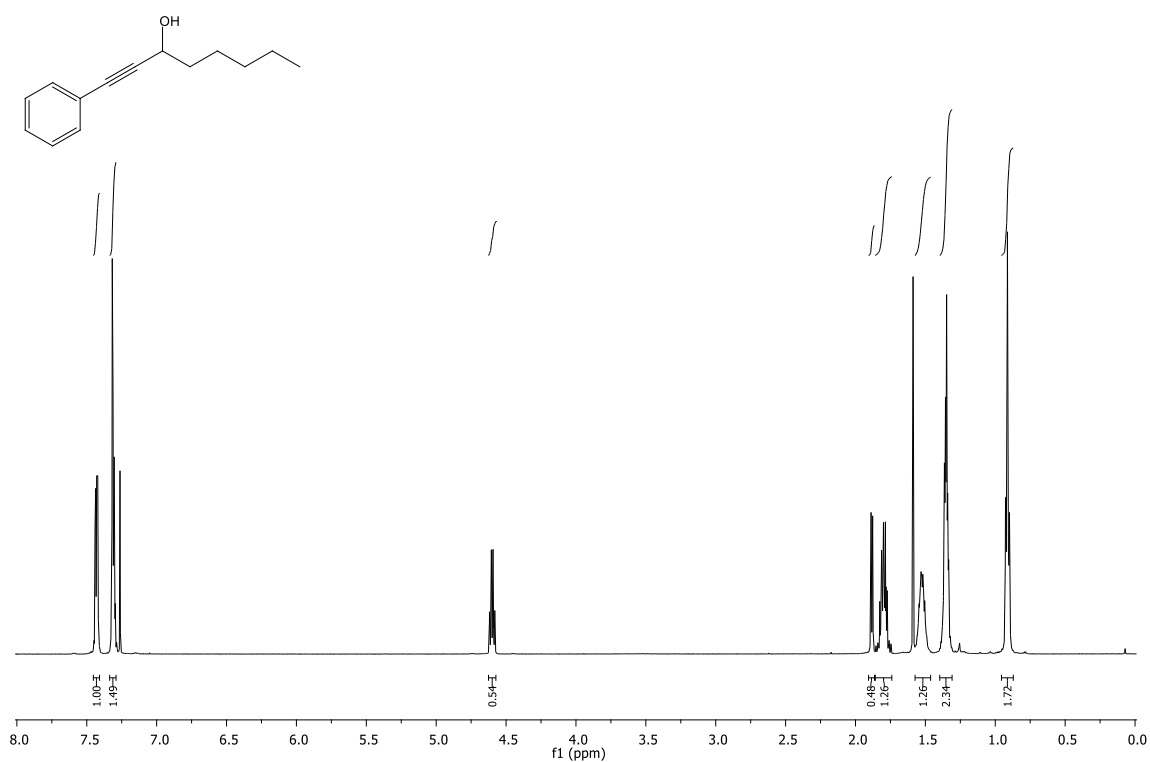


¹H NMR (500 MHz, CDCl₃) spectrum of **232**

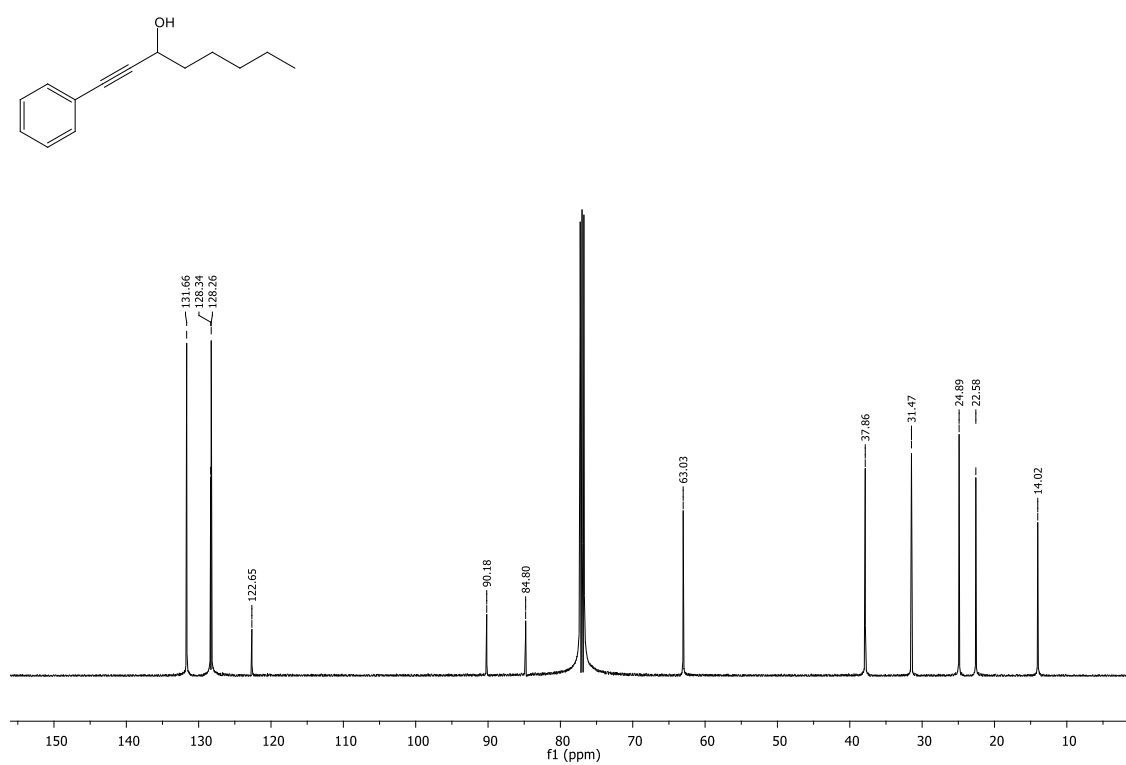


¹³C NMR (125 MHz, CDCl₃) spectrum of **232**

1-Phenyloct-1-yn-3-ol (**237**)

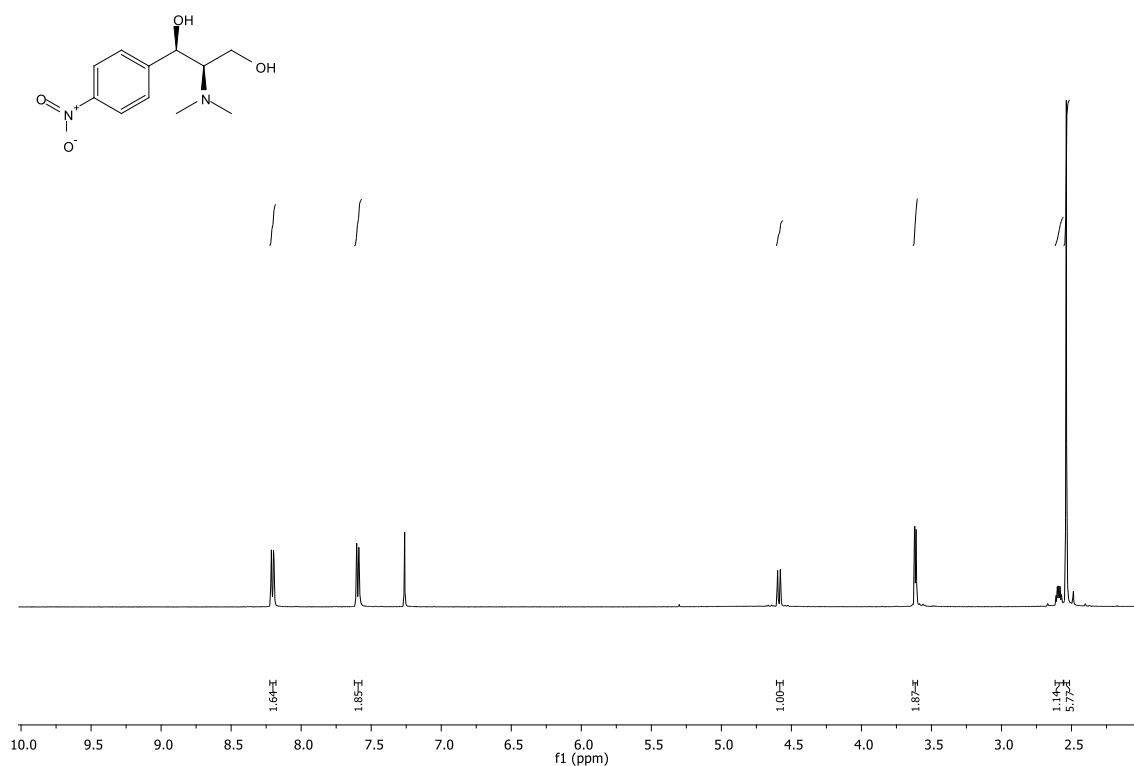


¹H NMR (500 MHz, CDCl₃) spectrum of **237**

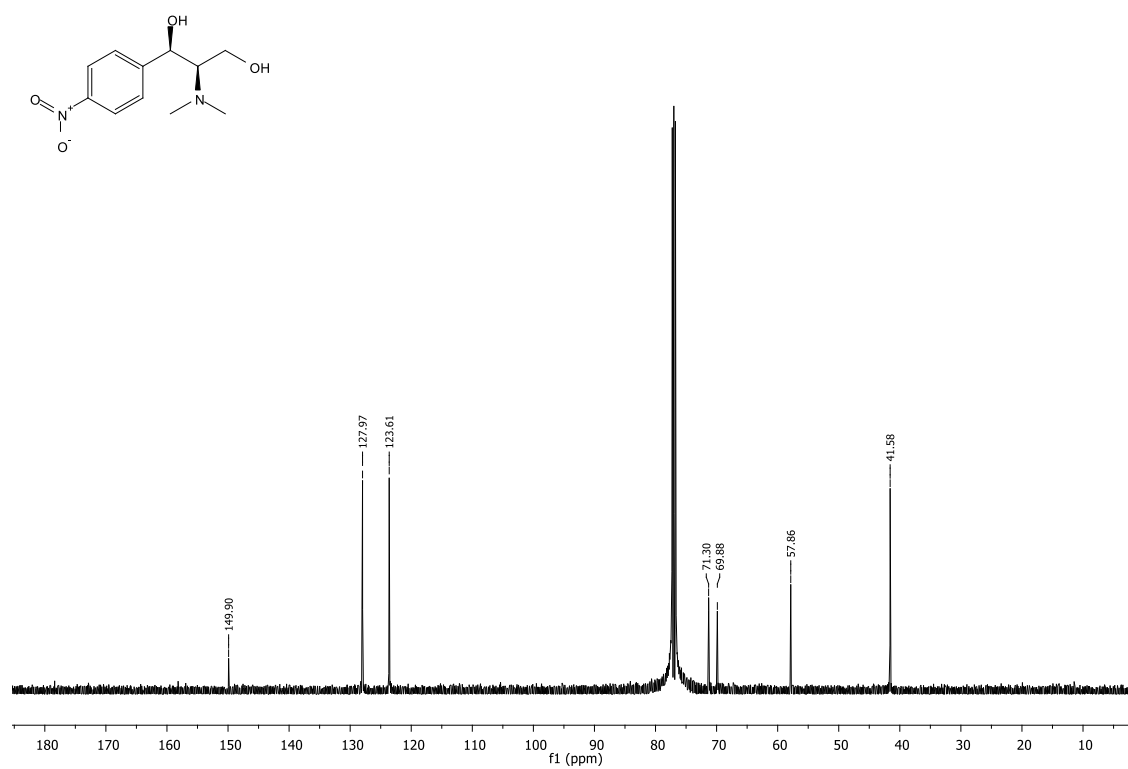


¹³C NMR (125 MHz, CDCl₃) spectrum of **237**

(1*R*,2*R*)-2-*N,N*-Dimethylamino-1-(4'-nitrophenyl)propane-1,3-diol (238)

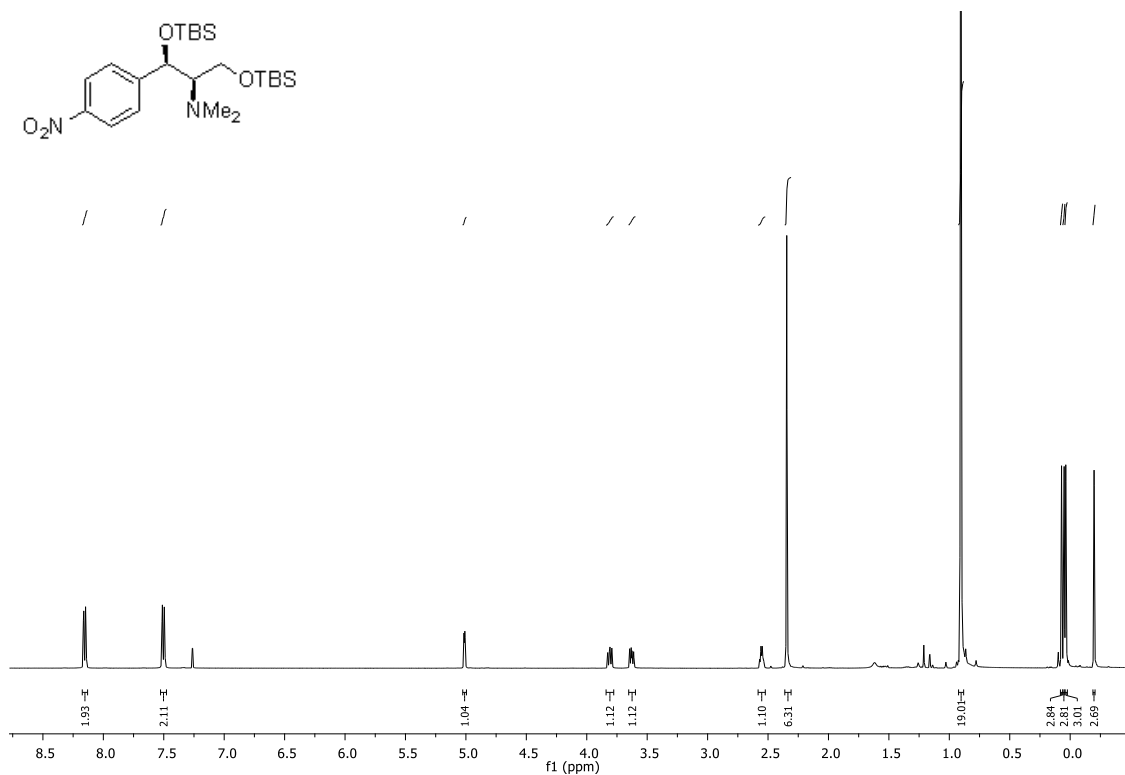


¹H NMR (500 MHz, CDCl₃) spectrum of **238**

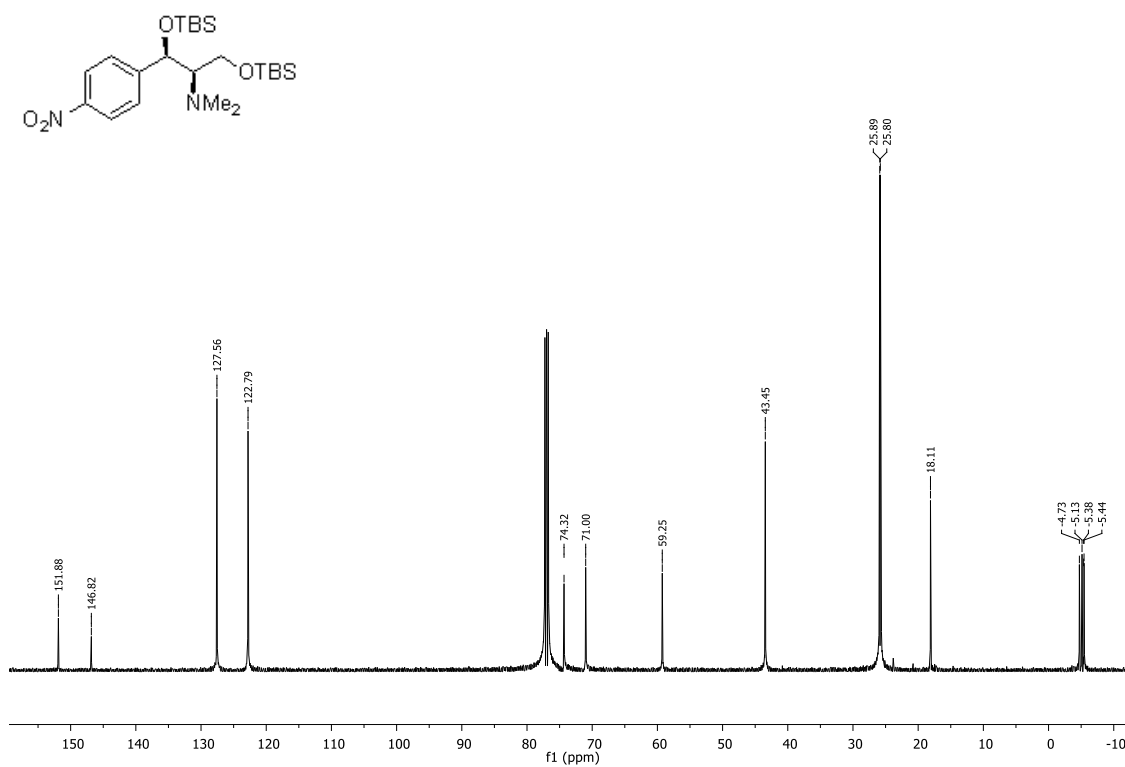


¹³C NMR (125 MHz, CDCl₃) spectrum of **238**

(1*R*,2*R*)-1,3-Bis-(*t*-butyldimethylsilyloxy)-2-*N,N*-dimethylamino-1-(4'-nitrophenyl)propane (239**)**

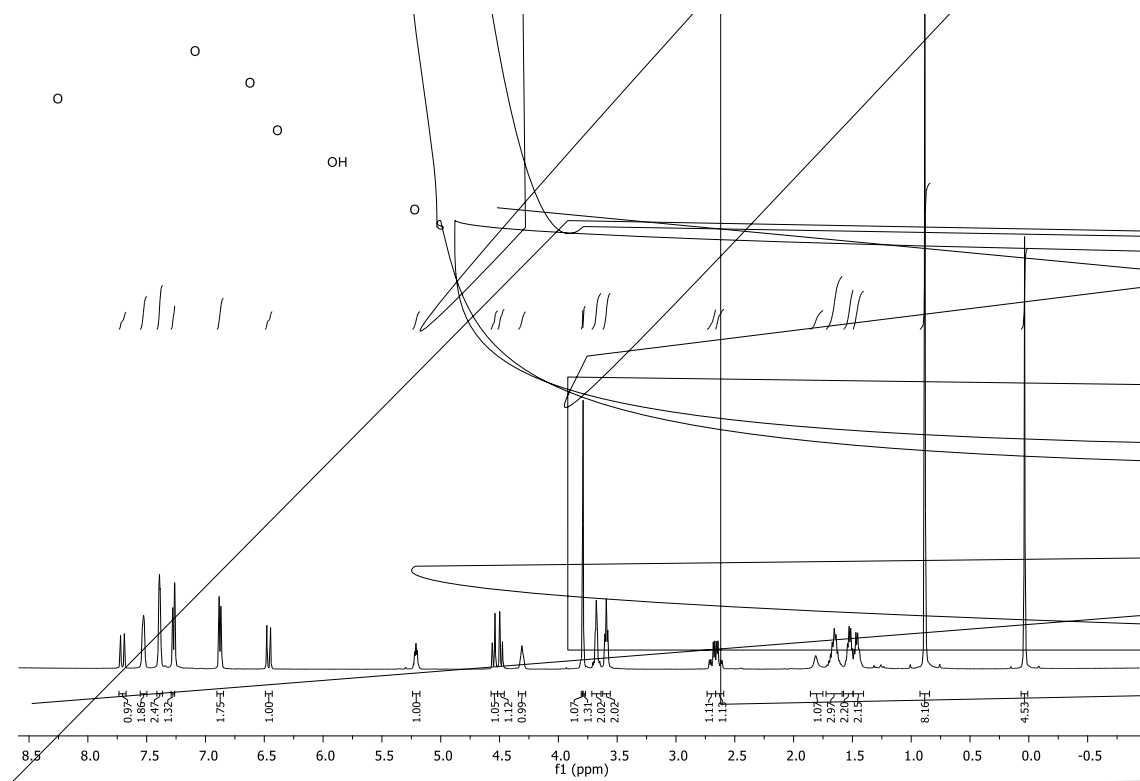


¹H NMR (500 MHz, CDCl₃) spectrum of **239**

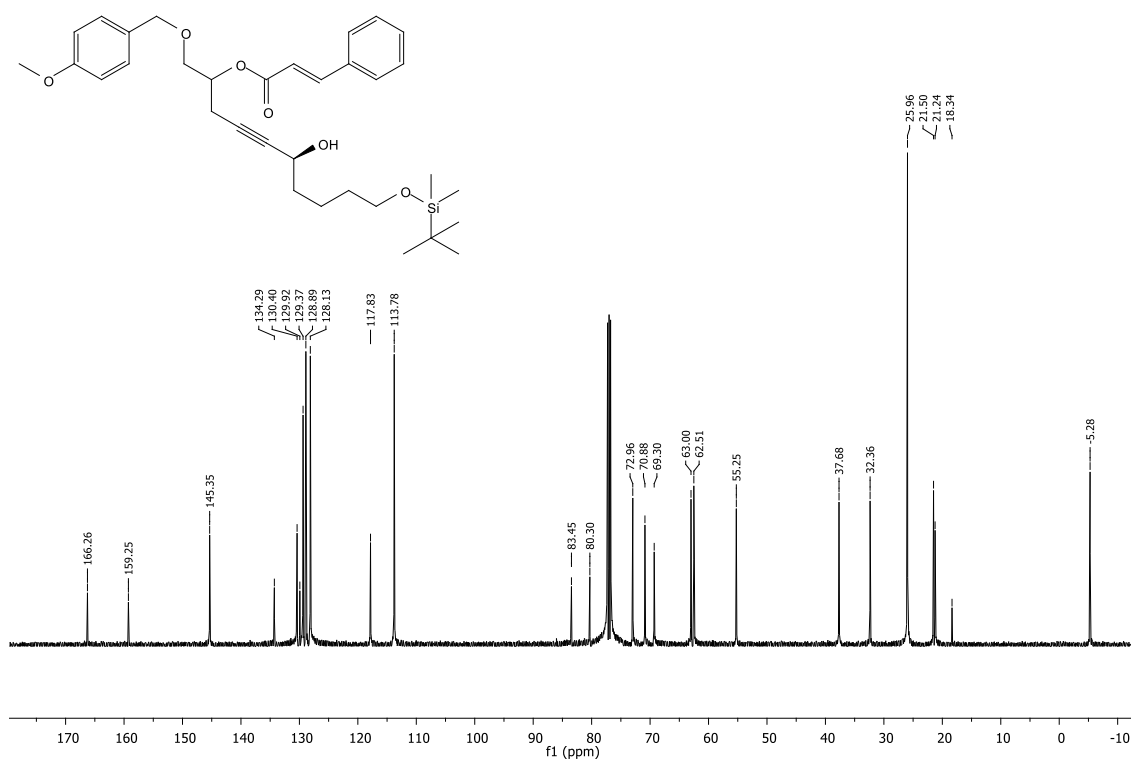


¹³C NMR (125 MHz, CDCl₃) spectrum of **239**

1'-(*para*-Methoxybenzyloxy)-6'-hydroxy-10'-(*t*-butyldimethylsilyloxy)dec-4'-yn-2'-yl 3-phenylprop-2-enoate (240**)**

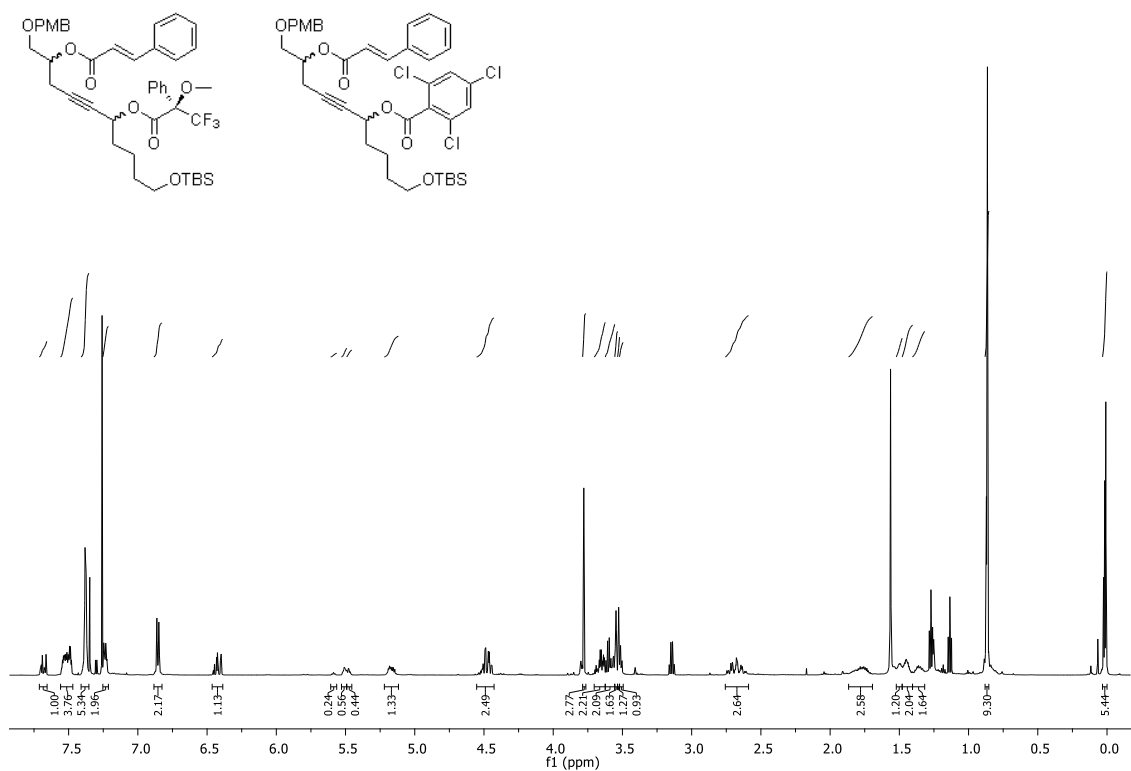


¹H NMR (500 MHz, CDCl₃) spectrum of **240**

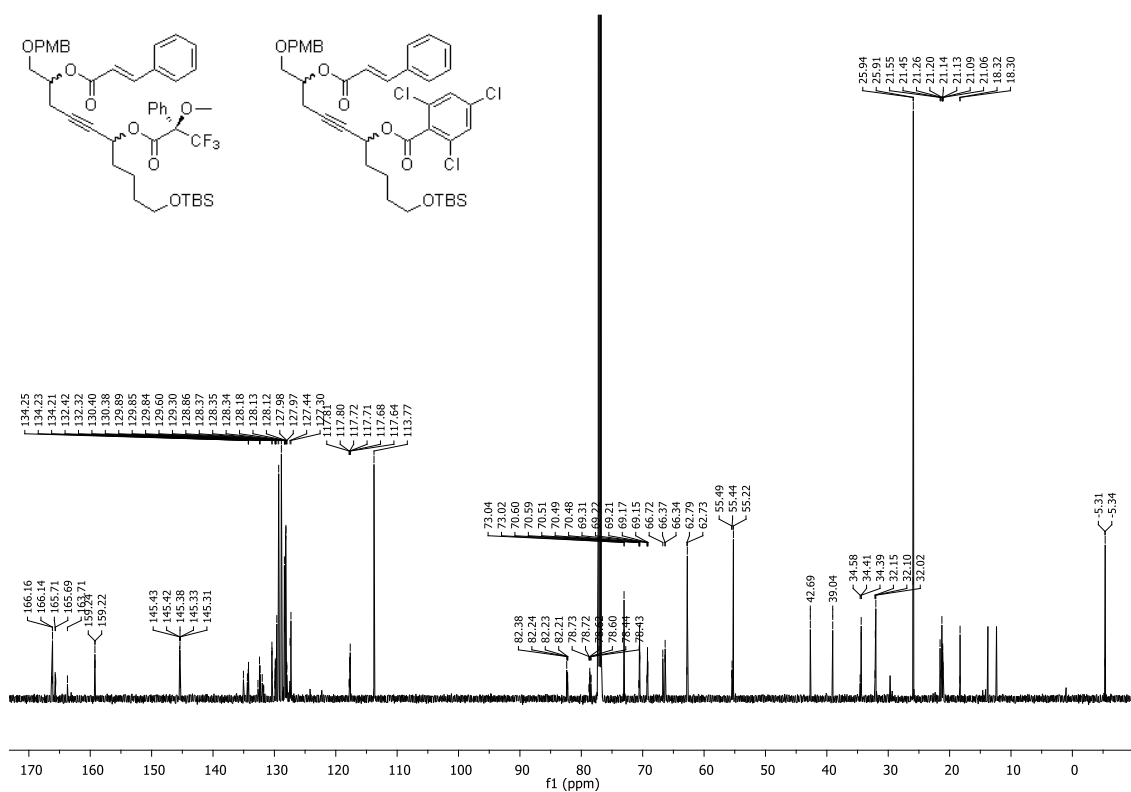


¹³C NMR (125 MHz, CDCl₃) spectrum of **240**

Mosher's ester of alcohol 240 (241)

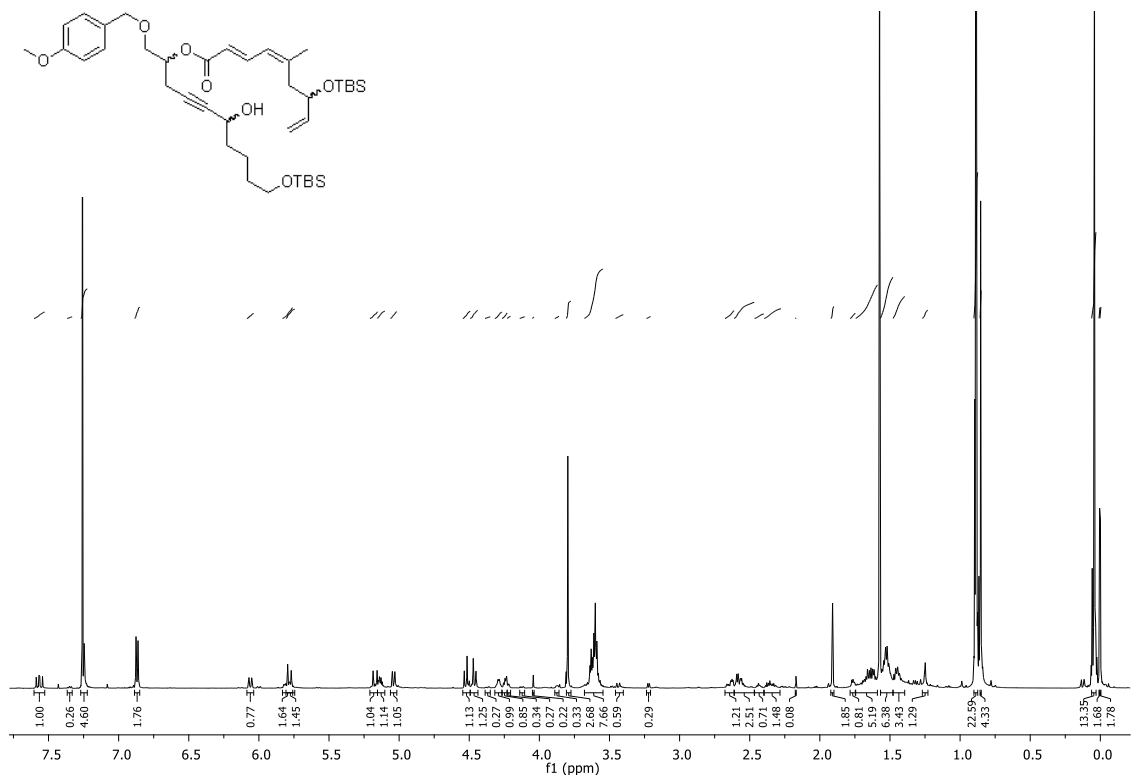


¹H NMR (600 MHz, CDCl₃) spectrum of **241** and **242**

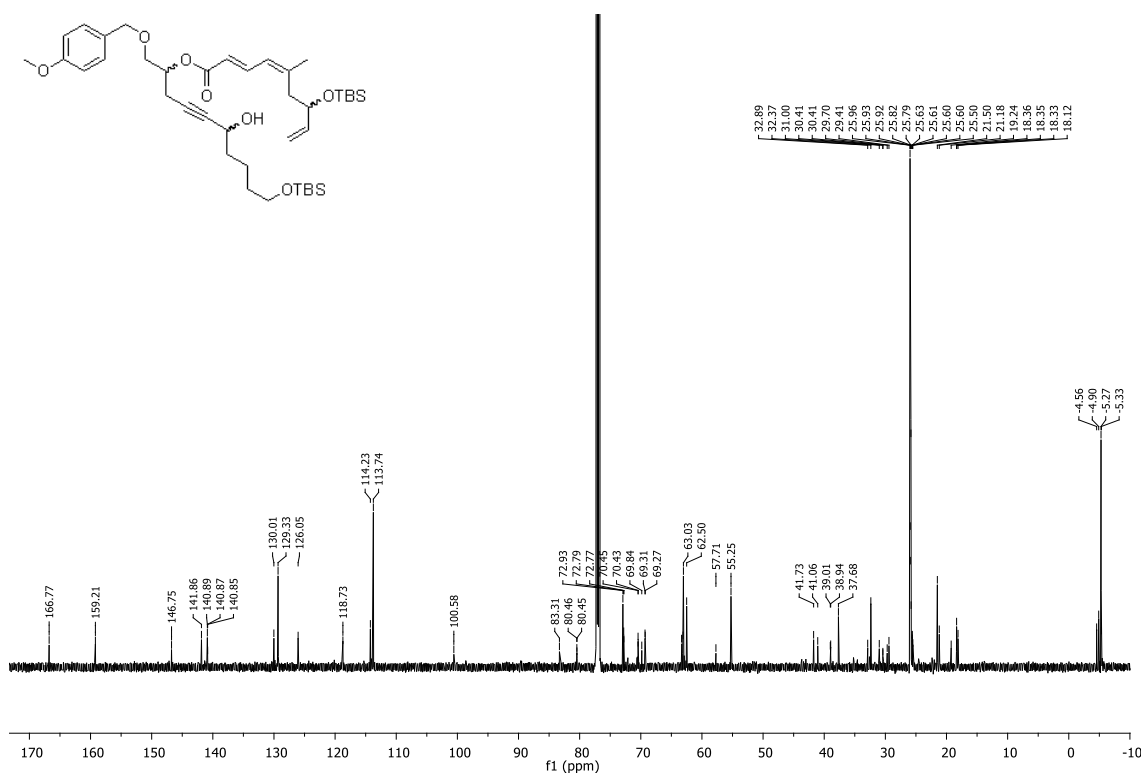


¹³C NMR (150 MHz, CDCl₃) spectrum of **241** and **242**

1'-(*para*-Methoxybenzyloxy)-6'-hydroxy-10'-(*t*-butyldimethylsilyloxy)dec-4'-yn-2'-yl 5-methyl-7-(*t*-butyldimethylsilyloxy)non-2,4,8-trienoate (244)



¹H NMR (600 MHz, CDCl₃) spectrum of 244



¹³C NMR (150 MHz, CDCl₃) spectrum of 244